VOL. 507 MAY 16, 1990
COMPLETE IN ONE ISSUE

13th International Symposium on Column Liquid Chromatography Stockholm, June 25–30, 1989 Part II

JOURNAL OF
CHROMATOGRAPHY
INTERNATIONAL JOURNAL ON CHROMATOGRAPHY, ELECTROPHORESIS AND RELATED METHODS

SYMPOSIUM VOLUMES

ELSEVIER

JOURNAL OF CHROMATOGRAPHY

Scope. The *Journal of Chromatography* publishes papers on all aspects of chromatography, electrophoresis and related methods. Contributions consist mainly of research papers dealing with chromatographic theory, instrumental development and their applications. The section *Biomedical Applications*, which is under separate editorship, deals with the following aspects: developments in and applications of chromatographic and electrophoretic techniques related to clinical diagnosis or alterations during medical treatment; screening and profiling of body fluids or tissues with special reference to metabolic disorders; results from basic medical research with direct consequences in clinical practice; drug level monitoring and pharmacokinetic studies; clinical toxicology; analytical studies in occupational medicine.

Submission of Papers. Papers in English, French and German may be submitted, in three copies. Manuscripts should be submitted to: The Editor of *Journal of Chromatography*, P.O. Box 681, 1000 AR Amsterdam, The Netherlands, or to: The Editor of *Journal of Chromatography, Biomedical Applications*, P.O. Box 681, 1000 AR Amsterdam, The Netherlands. Review articles are invited or proposed by letter to the Editors. An outline of the proposed review should first be forwarded to the Editors for preliminary discussion prior to preparation. Submission of an article is understood to imply that the article is original and unpublished and is not being considered for publication elsewhere. For copyright regulations, see below.

Subscription Orders. Subscription orders should be sent to: Elsevier Science Publishers B.V., P.O. Box 211, 1000 AE Amsterdam, The Netherlands, Tel. 5803 911, Telex 18582 ESPA NL. The *Journal of Chromatography* and the *Biomedical Applications* section can be subscribed to separately.

Publication. The *Journal of Chromatography* (incl. *Biomedical Applications*) has 37 volumes in 1990. The subscription prices for 1990 are:

J. Chromatogr. (incl. *Cum. Indexes, Vols. 451–500*) + *Biomed. Appl.* (Vols. 498–534):
Dfl. 6734.00 plus Dfl. 1036.00 (p.p.h.) (total *ca.* US$ 3885.00)

J. Chromatogr. (incl. *Cum. Indexes, Vols. 451–500*) only (Vols. 498–524):
Dfl. 5616.00 plus Dfl. 756.00 (p.p.h.) (total *ca.* US$ 3186.00)

Biomed. Appl. only (Vols. 525–534):
Dfl. 2080.00 plus Dfl. 280.00 (p.p.h.) (total *ca.* US$ 1180.00).

Our p.p.h. (postage, package and handling) charge includes surface delivery of all issues, except to subscribers in Argentina, Australia, Brasil, Canada, China, Hong Kong, India, Israel, Malaysia, Mexico, New Zealand, Pakistan, Singapore, South Africa, South Korea, Taiwan, Thailand and the U.S.A. who receive all issues by air delivery (S.A.L. — Surface Air Lifted) at no extra cost. For Japan, air delivery requires 50% additional charge; for all other countries airmail and S.A.L. charges are available upon request. Back volumes of the *Journal of Chromatography* (Vols. 1–497) are available at Dfl. 195.00 (plus postage). Claims for missing issues will be honoured, free of charge, within three months after publication of the issue. Customers in the U.S.A. and Canada wishing information on this and other Elsevier journals, please contact Journal Information Center, Elsevier Science Publishing Co. Inc., 655 Avenue of the Americas, New York, NY 10010. Tel. (212) 633-3750.

Abstracts/Contents Lists published in Analytical Abstracts, ASCA, Biochemical Abstracts, Biological Abstracts, Chemical Abstracts, Chemical Titles, Chromatography Abstracts, Clinical Chemistry Lookout, Current Contents/Physical, Chemical & Earth Sciences, Current Contents/Life Sciences, Deep-Sea Research/Part B: Oceanographic Literature Review, Excerpta Medica, Index Medicus, Mass Spectrometry Bulletin, PASCAL-CNRS, Pharmaceutical Abstracts, Referativnyi Zhurnal, Science Citation Index and Trends in Biotechnology.

See inside back cover for Publication Schedule, Information for Authors and information on Advertisements.

0021-9673/90/$3.50

Printed in The Netherlands

For contents see p. VII

Fluka
Chemika-BioChemika

Chemika specialities

ChiraSelect

- **New Quality for chiral reagents and standards for analysis**
- **Guaranteed high enantiomer purity er > 99.5 : 0.5**

Compounds available in the ChiraSelect quality grade have an enantiomer ratio exceeding 99.5 : 0.5 and some compounds even show a guaranteed ratio higher than 99.8 : 0.2! Usually, the chemical purity exceeds 99%.

When buying chiral derivatizing agents and chiral standards without a guaranteed enantiomeric purity, you run the risk employing material of uncertain optical purity. Working with Fluka ChiraSelect reagents gives you the security to use the best reagents available. New compounds fulfilling the *ChiraSelect* criteria will constantly be added to our program. Many chiral compounds in the Fluka program also have the very high enantiomeric purity *er* > 99.5 : 0.5, but have not been assigned the *ChiraSelect* quality grade. These compounds include e.g. many amino acids. The *ChiraSelect* quality grade will be strictly limited to compounds used as chiral derivatizing agents or as chiral standards.

The following compounds are offered in the *ChiraSelect* quality. For the complete catalogue entry of these compounds see our new brochure 'Chiral Compounds' or the new catalogue 1990/91.

21287	**(–)-Camphanic acid chloride**	1 g	sFr. 17.20	5 g	sFr. 68.80	25 g	sFr. 292.60
29002	**(1R,2R)-trans-1,2-Cyclohexanediol**			250 mg	sFr. 23.90	1 g	sFr. 86.–
29003	**(1S,2S)-trans-1,2-Cyclohexanediol**			250 mg	sFr. 23.90	1 g	sFr. 86.–
40764	**(5R,11R)-(+)-2,8-Dimethyl-6H,12H-5,11-methano-dibenzo[b,f][1,5]diazocin, (+)-Tröger's Base**					500 mg	sFr. 65.30
40765	**(5S,11S)-(–)-2,8-Dimethyl-6H,12H-5,11-methano-dibenzo[b,f][1,5]diazocin, (–)-Tröger's Base**					500 mg	sFr. 65.30
23182	**(+)-1-(9-Fluorenyl)ethyl chloroformate > 18 mM in acetone**					10 ml	sFr. 704.80
23183	**(–)-1-(9-Fluorenyl)ethyl chloroformate > 18 mM in acetone**					10 ml	sFr. 704.80
65361	**R(+)-α-Methoxy-α-trifluoromethyl-phenyl-acetic acid**			250 mg	sFr. 47.30	1 g	sFr. 155.30
65369	**S(–)-α-Methoxy-α-trifluoromethyl-phenyl-acetic acid**			250 mg	sFr. 42.00	1 g	sFr. 138.00
65363	**R(–)-α-Methoxy-α-trifluoromethyl-phenyl-acetyl chloride**					500 mg	sFr. 166.40
65365	**S(+)-α-Methoxy-α-trifluoromethyl-phenyl-acetyl chloride**					500 mg	sFr. 151.30
70698	**S(–)-1-(2-Naphthyl)ethanol**					1 g	sFr. 74.60
70710	**R(+)-1-(1-Naphthyl)ethylamine**					1 ml	sFr. 75.–
70712	**S(–)-1-(1-Naphthyl)ethylamine**					1 ml	sFr. 85.–
74865	**R(–)-2-Octanol**	1 ml	sFr. 20.50	5 ml	sFr. 86.–	25 ml	sFr. 367.30
74863	**S(+)-2-Octanol**	1 ml	sFr. 20.50	5 ml	sFr. 86.–	25 ml	sFr. 367.30
76744	**R(+)-1-(Pentafluorophenyl)ethanol**			250 mg	sFr. 34.30	1 g	sFr. 120.–
76746	**S(–)-1-(Pentafluorophenyl)ethanol**			250 mg	sFr. 34.30	1 g	sFr. 120.–
77848	**R(+)-1-Phenylethanol**			1 ml	sFr. 137.70		
77849	**S(–)-1-Phenylethanol**			1 ml	sFr. 137.70		
77879	**R(+)-1-Phenylethylamine er > 99.8 : 0.2**			5 ml	sFr. 26.90	25 ml	sFr. 114.70
77869	**S(–)-1-Phenylethylamine er > 99.8 : 0.2**			5 ml	sFr. 48.20	25 ml	sFr. 200.80
77968	**R(+)-1-Phenylethyl isocyanate**			1 ml	sFr. 43.40	5 ml	sFr. 183.60
77970	**S(–)-1-Phenylethyl isocyanate**			1 ml	sFr. 43.40	5 ml	sFr. 183.60
78922	**R(+)-1-Phenyl-1-propanol**			1 ml	sFr. 109.–	5 ml	sFr. 407.40
78923	**S(–)-1-Phenyl-1-propanol**			1 ml	sFr. 109.–	5 ml	sFr. 407.40

Fluka

Switzerland: Fluka Chemie AG, Industriestrasse 25, CH-9470 Buchs/Switzerland, Telephone 085 6 95 11, Telex 855 282, Telefax 085 6 54 49

France: Fluka S.a.r.l., 27, rue des Trois Frontières, F-68110 Illzach – Ile Napoléon, Boîte Postale 1114, F-68052 Mulhouse Cedex, Téléphone 89 61 75 65, Télex 881 236F, Télécopieur 89 61 77 76
Germany: Fluka Feinchemikalien GmbH, Messerschmittstraße 17, D-7910 Neu-Ulm, Telephone (0731) 70111, Bestellungen zum Ortstarif (0130) 23 41, Telex 712 316 fluka d, Telefax (0731) 75 044
Great Britain: Fluka Chemicals Ltd, Peakdale Road, Glossop, Derbyshire SK13 9XE, Telephone 0457-86 25 18, Linkline 0800-26 23 00, Telex 669960 fluka g, Telefax 0457-85 43 07
USA: Fluka Chemical Corp., 980 South Second Street, Ronkonkoma, New York 11779, Phone 516-467-0980, Toll Free 1-800-358-5287, Telex 96-7807, Fax 516-467-0663

SCIENTIFIC COMPUTING AND AUTOMATION (EUROPE)

Conference (and Exhibition)
12 - 15 June 1990
The MECC, Maastricht, The Netherlands

Come and attend the only inter-disciplinary scientific and automation congress in Europe - bringing together industrial and academic specialists from a wide range of disciplines; scientists from the chemical and pharmaceutical industries, from academia, and the medical community

nature
INTERNATIONAL WEEKLY JOURNAL OF SCIENCE

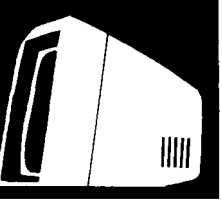

SCIENTIFIC BOARD
Chairman:
Dr. E. Karjalainen
Helsinki University Central Hospital, Helsinki, Finland
Board:
Prof. D.L. Massart
Vrije Universiteit, Brussels, Belgium
Prof. R. Dessy
Virginia Polytechnic Institute and State University Blacksburg VA, USA
Prof. Dr. Chr. Trendelenburg
Städtisches Krankenhaus, Frankfurt, W-Germany
Dr. R. McDowall
Wellcome Research Laboratories, Beckenham, UK
Prof. M. Barbosa
University of Coimbra, Coimbra, Portugal

SCA SHORT COURSES
11/12th June

SCIENTIFIC PROGRAMME

Main session subjects *(and invited speakers)*

- **Chemical Applications for Supercomputers**
  Dr. P. Hopke, Clarkson University, USA
- **Sampling Strategies and Experimental Design**
  Prof. S. Deming, University of Houston, USA
  Prof. D.A. Doornbos, University of Groningen, The Netherlands
- **Scientific Databases**
  Dr. C. Goldstein, National Library of Medicine, USA
- **Expert Systems and Statistical Tools for the Interpretation of Laboratory Data**
  Dr. F. Puppe, University of Karlsruhe, W-Germany
  (Diagnostic Problem Solving: Methods and Tools)
- **Robotics and Discrete Automation in the Laboratory**
  Dr. M. Linder, Mettler, Switzerland
  (Laboratory Automation and Robotics - Quo Vadis?)
- **New Emerging Standards**
  Dr. D. Smith, Molecular Design. USA
  (Information Integration: Distributed Chemical Information Management System)
- **Chemical Monitoring - Multivariate Sensors and Biosensors**
  Prof. PR. Coulet, Lyon, France
  From Chemical Sensors to Bioelectronics: A constant search for improved selectivity, sensitivity and miniaturization.
- **LIMS and Connectivity Strategies for the Laboratory**
  M. Brooks, Excel International, UK
  Dr. D. Mattes, Smith, Kline and Beecham, USA
- **Workstations for the Scientist**
  Dr. C. Wilkins, University of California, USA
  (Synergistic Use of Multi-spectral Data: Missing Pieces of the Workstation Puzzle)
- **Scientific Applications for Neural Networks and Fractals**
  Prof. D.B. Hibbert, University of New South Wales, Australia
  Prof. G. Kateman, University of Nijmegen, The Netherlands
- **Computer Graphics and Image Analysis**
  Prof. J. Encarnacao, Technische Hochschule Darmstadt, W. Germany
- **Europe 1992: Implications for Standards Across Borders**
  J. Noothoven van Goor, AIM Programme, Brussels, Belgium
  (The AIM Programme in Medical Informatics)
- **Validation and Certification**
  Dr. D. Moore, Department of Health, London, UK

Send for your copy of the latest announcement now:

☐ Please send me a copy of the latest announcement for SCA
☐ Please send me further information on exhibiting at SCA

Name: _____

Address: _____

_____

City: _____

Postal Code: _____

Country: _____

Telephone: _____ Fax: _____

Return to: **SCA** - Reunion International - W.G. Plein 475
1054 SH Amsterdam - The Netherlands

JOURNAL OF CHROMATOGRAPHY

VOL. 507 (1990)

JOURNAL *of* CHROMATOGRAPHY

INTERNATIONAL JOURNAL ON CHROMATOGRAPHY,
ELECTROPHORESIS AND RELATED METHODS

SYMPOSIUM VOLUMES

ELSEVIER
AMSTERDAM — OXFORD — NEW YORK — TOKYO

J. Chromatogr., Vol. 507 (1990)

View from the terrace of Fersen (close to the present Stockholm Opera House) in the year 1777 with a part of Stockholm castle in the background to the right. Axel von Fersen (1719–1794) was a politician and field marshal. (After an oil painting of J. Säfvenbom.)

0021-9673/90/$03.50

This issue is printed on acid-free paper.

Printed in The Netherlands

SYMPOSIUM VOLUME

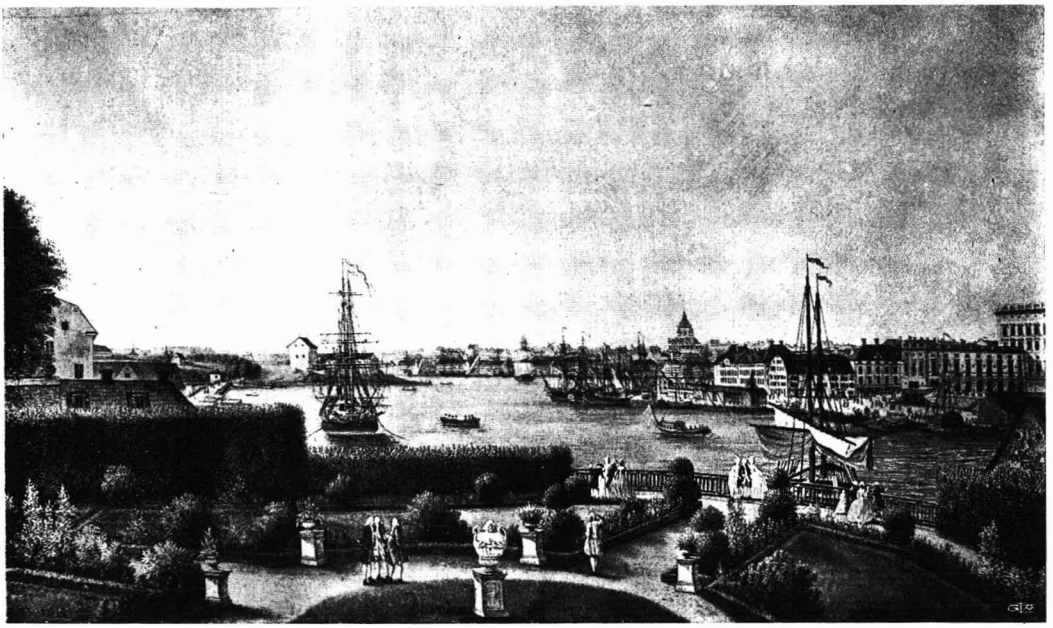

THIRTEENTH INTERNATIONAL SYMPOSIUM ON COLUMN LIQUID CHROMATOGRAPHY

PART II

Stockholm, June 25–30, 1989

Guest Editor

B. D. WESTERLUND

(Uppsala)

The proceedings of the *Thirteenth International Symposium on Column Liquid Chromatography, Stockholm, June 25–30, 1989*, are published in two consecutive volumes of the *Journal of Chromatography*: Vols. 506 and 507. A foreword to the complete proceedings only appears in Vol. 506.

13TH INTERNATIONAL SYMPOSIUM ON COLUMN LIQUID CHROMATOGRAPHY, STOCKHOLM, JUNE 25–30, 1989, PART II

APPLICATIONS

Amino acids, peptides, proteins and polynucleotides

Pharmaceuticals

In articles with more than one author, the name of the author to whom correspondence should be addressed is indicated in the article heading by a 6-pointed asterisk (*)

Journal of Chromatography, 507 (1990) 1–23
Elsevier Science Publishers B.V., Amsterdam — Printed in The Netherlands

CHROMSYMP. 1756

Study of the retention mechanism of proteins in hydrophobic interaction chromatography

XINDU GENG*, LI'AN GUO and JIANHUA CHANG
Laboratory of Modern Separation Science, Department of Chemistry, Northwest University, 710069 Xi'an (China)

SUMMARY

A stoichiometric displacement retention model for proteins based on hydrophobic interaction chromatography (HIC) is presented. Several methods were used to demonstrate that water is the displacing agent in this process. Salt not only affects the molar concentration of water, but also changes the conformation of proteins, hydrophobic interaction forces and the number of water molecules in a series of hydrated protein molecules. An equation that relates the capacity factor of proteins, k', to the water concentration and the stoichiometric displacement factor, Z (the number of water molecules required to displace a protein from ligands) was derived. The intercept of this equation, log I, contains a number of constants that relate to the affinity of protein to the ligands. There is a good linear relationship between log k' and log $[H_2O]$ under different chromatographic conditions. Although Z and log I varied with pH, salt temperature, the plot of log I *vs.* Z was always an excellent straight line, with a slope $j \approx 1.74$, the logarithm of the molar concentration of pure water. Hydrophobic interactions dominate the retention of proteins in HIC at high salt concentrations.

INTRODUCTION

Since Shaltiel and Er-el[1] first described hydrophobic interaction chromatography (HIC), in which agarose gels bonded to alkylamines were used as the stationary phase, this branch of chromatography has developed tremendously. The development of high-performance HIC (HPHIC), in which a rigid material, such as silica gel, is selected as the matrix has made the technique more convenient for the separation and purification of proteins with high biological activity. Chang and Geng[2] recently published a review.

The retention mechanism of proteins on an HIC column has been widely studied. Melander *et al.*[3] presented a thermodynamic model based on the cavity theory of Sinanoglu and Abdulnur[4] for the hydrophobic interaction between a protein and a hydrophobic matrix, and attributed the quantitative relationship between retention of the protein and the concentration of salt in the mobile phase to that between

0021-9673/90/$03.50

retention and the changes in surface tension. Fausnaugh *et al.*[5] and Jennissen and Botzet[6] explained the retention mechanism by an increase in entropy of the mobile phase when the hydrophobic groups are excluded from the polar environment and the interaction of the protein with matrix surface. Jennissen[7,8] suggested that the adsorption of proteins is due to multivalent interaction on the stationary phase. Arakawa[9] and Wyman[10] presented a preferential hydration model.

Although Karger and co-workers[11,12] obtained a linear log–log plot of the capacity factor of proteins, k', *versus* the concentration of a strong eluent (volume fraction) consisting of salt solution, which was very similar to the stoichiometric displacement model of retention (SDM-R) in reversed-phase liquid chromatography (RP-LC), they did not consider the retention mechanism of proteins in HIC.

Zhao *et al.*[13] investigated the influence of salts on the retention of small molecules in RP-LC and concluded that water is a displacing agent during the stoichiometric process of the displacement of solute to water molecules but the concentration unit of water was taken as the molar fraction. Therefore, the stoichiometric displacement factor Z is only a constant related to the real value.

Traditionally, one kind of interaction in one type of chromatography mainly dominates the chromatographic behaviour of solutes, and individual retention mechanisms have been considered on this basis. However, because each ligand bonded on silica or other matrices in HIC contains both polar and apolar groups, the polarities at different locations are unequal. Therefore, there are at least two different kinds of interaction forces between proteins and the stationary phase in HIC. Usually the hydrophobic interaction force is used to describe the interactions between proteins and bonded ligands on the HIC column. According to the definition by Ben-Naim[45], the hydrophobic interaction force is the indirect interaction between the same or different kinds of molecules in an aqueous solution, and it is very difficult to measure it exactly. In addition, except for the direct interaction forces between protein molecules and ligands, the influence of salt on the hydration of proteins and bonded ligands and the conformation of protein molecules make investigations of the retention mechanism of proteins on HIC columns very complicated. Fortunately, based on the recent result[14] that "No matter how different the interactions between adsorbent and solute or solvent molecules are, or how heterogeneous the distribution of these active sites is, the more rational mechanism for adsorption in a liquid–solid system should be stoichiometric displacement for solute adsorption", and the fact that adsorptions for both liquid–solid system in the physical chemistry of surfaces and liquid–solid chromatography were shown to have the same mechanism[15], the retention mechanism of proteins in HIC should also be a stoichiometric displacement process. This paper presents an SDM-R in HIC in which the contributions of salt, protein hydration, conformational changes, *etc.*, to the retention of proteins are considered, which was not the case in RP-LC.

THEORETICAL

When the separations of proteins on an HIC column are carried out with aqueous solutions of salts and the retention mechanism of proteins in HIC is assumed to be a stoichiometric displacement, the first question that needs to be answered is what the displacing agent is, salt, water or both. Strictly, both salt and water should

contribute to the retention of a protein. For convenience, let us assume that only one of them dominates the displacement process. If this is true, the second question that has to be answered is which one should be the displacing agent.

Compared with salt, the polarity of water is lower and stationary phase with moderate polarity in HIC prefers water. On the other hand, as is well known, salts retard the elution of proteins from an HIC column, and the higher the concentration of the salt the stronger is the adsorption of protein on the column. Therefore, it is reasonable to assume that water is the displacing agent. The functions of salt in HIC are very complicated, the most important being as a diluent for water. This will be discussed later.

Proteins in aqueous solutions of salts may hydrate with water[5,6,16,17] stepwise as follows:

$$\begin{aligned} P_0 + H_2O &\rightarrow P_1 \\ P_1 + H_2O &\rightarrow P_2 \\ \vdots \quad &\quad \vdots \quad \vdots \\ P_{n-1} + H_2O &\rightarrow P_n \end{aligned} \tag{1}$$

where P denotes protein, the subscripts, 0–n represent the number of water molecules linking to a protein molecule and n is related to temperature[18], pH[19] and the kinds of proteins and salts[20–22]. The changes in the concentration of water in the usual separations of proteins by HIC are not very great. Therefore, it may be considered that the changes in n are not significant and it can be assumed that the hydrate–protein complexes in the mobile phase exist mainly as one species, P_i ($0 < i < n$). It also appears that a few hydrate–protein species occur in which the number of water molecules linked to the protein molecule are around i. For convenience, their mean value $\bar{m}$ is taken as the following, based on the definition of the mean value of water molecules for a series of hydrated ions[23]:

$$\bar{m} = \frac{[P_1] + 2[P_2] + \ldots + n[P_n]}{[P_0] + [P_1] + [P_2] + \ldots + [P_n]} \tag{2}$$

where the square brackets represent molar concentrations.

A simplified expression of eqn. 2 is

$$P_0 + \bar{m}H_2O \rightleftharpoons P_m \tag{3}$$

The ligands on the surface of the HIC column can also adsorb water and form a hydrated ligand complex:

$$L_0 + rH_2O = L_d \tag{4}$$

where L_0 is the bare ligand, L_d is the hydrated ligand and r is the number of water molecules bonding to a ligand in salt solution.

There are some hydrophobic amino acid residues on the surface of proteins and their distribution may be heterogeneous. As a result, some hydrophobic regions on the surface of a protein may interact with the stationary phase. The stronger the

hydrophobicities of these hydrophobic regions, the greater is the probability of contact with the stationary phase. Consequently, the hydrophilic side of protein molecules is far away from the stationary phase. This is the orientation action of protein molecules during its adsorption process. The orientation action of protein molecules depends mainly on the distributive heterogeneity of hydrophobic regions on the surface of the protein molecules and the chromatographic conditions. When experimental conditions are given, they relate only to the specific kinds of proteins.

Each ligand on the HIC column usually consists of two or three groups with different polarities and the end group of each ligand on the surface is the same. For convenience, assume that each ligand may be considered as a structural unit with a moderate polarity and the moderate hydrophobicity of the HIC column is the total result of these ligands, the distribution of which on the surface of the stationary phase may be considered to be homogeneous.

Compared with the size of the ligand noted above, a molecule of a protein is very large and has many hydrophobic regions, which may make contact with many ligands. Therefore, when protein molecules are adsorbed by an HIC column, the interactions between the stationary phase in HIC and protein molecules may be considered as if the latter had interacted with many of the same particles distributed homogeneously in a salt solution.

For convenience, the assumption in RP-LC is that the conformations of protein molecules in the mobile phase and on the stationary phase are identical[24,25]. However, this assumption is not valid for HIC. Pahlman *et al.*[26] proved that there is a difference by circular dichroism. This difference depends on the kinds of salts and ligands and also the characteristics of the protein[26–30]. This is because the conformation of the protein molecules in mobile phase is only affected by salt and water, whereas on the stationary phase it is influenced by ligands, salts and water molecules. Compared with the mobile phase, the surface of the HIC column is a relatively apolar region where the ligands can interact strongly with the hydrophobic regions on the surface of protein molecules with a three- or four-dimensional structure and draws these hydrophobic regions near the contact area towards the ligands and, as result, increases the contact surface area between the stationary phase and protein molecules. The conformation of the protein molecules in adsorbed state is therefore different from that in the mobile phase. The more apolar are the ligands, the stronger is the drawing force, and the greater are the changes in the conformation of the protein molecules[31–33]. The changes in the conformation of protein molecules also cause changes in the number of water molecules linked to the protein molecules[11,27,28]. From the foregoing discussion, it may be concluded that the conformation of protein molecules in the adsorbed state is different from that in the mobile phase under the elution conditions.

Suppose that both the conversion of the conformations of protein molecules between two states and the conversion between adsorption and desorption are rapid and reversible processes, the displacement of protein by water molecules in an aqueous solution may be given by

$$P_b + ZH_2O \rightleftharpoons P_m + nL_d \tag{5}$$

where P_m is the hydrated protein in the mobile phase, Z is the number of water molecules needed to displace a protein molecule adsorbed on the stationary phase and

n is the number of ligand interactions with a protein molecule. Here we mention again that the difference between P_b and P_m in eqn. 5 is not only with regard to the number of water molecules linked to the protein molecule, but their molecular conformations.

In order to elucidate clearly the physical meanings of each term in the foregoing equations and understand fully all of the changes in the conformations of proteins and the number of water molecules bonding to proteins as the environment around ligands and proteins changes, suppose the retention process of a protein on an HIC column involves the following steps.

(1) When a protein molecule interacts with ligand under vacuum, the conformation of the protein molecule under vacuum, P_0, is different from that in the adsorbed state, P'_a, then,

$$P_{0(\text{vacuum})} \rightleftharpoons P'_{a(\text{adsorbed state})} \tag{6}$$

If the number of ligands interacting with P'_a is assumed to be n_w, then we have

$$P'_a + n_w L_0 \rightleftharpoons P'_b \tag{7}$$

where P'_b represents protein–ligand complex in a vacuum environment.

(2) Suppose equilibrium 6 occurs in a system consisting of pure water, all the ligands, proteins and the conformations of protein molecules in both vacuum and pure water are identical and the proteins, ligand and their complex interact only with water molecules. The hydration process noted above and the reversible process of adsorption and desorption for proteins may be written as

$$P_0 + m_w H_2O \rightleftharpoons P_m^w \tag{8}$$

$$L_0 + r_w H_2O \rightleftharpoons L_d^w \tag{9}$$

$$P'_b + (m_w - b_w - q_w) H_2O \rightleftharpoons P_b^w \tag{10}$$

where P_m^w, P_b^w and L_d^w are hydrated protein, hydrated protein–ligand complex and hydrated ligand in pure water, respectively. When P'_b interacts with water, the number of water molecules bonding to it should be equal to the mean number of water molecules of hydrated protein molecule in pure water, m_w, minus the decreased number of water molecules due to the changes in the conformation of protein molecule b_w and the number of it released, q_w, from the contact surface area between hydrated protein molecule and ligands during the hydration process of protein in the adsorbed state.

When the hydrated ligands adsorb a hydrated protein molecule, r_w and q_w water molecules are released from the interface between the ligands and each protein molecule, respectively. Because the chromatographic process is a reversible adsorption–desorption process, the number of water molecules released from the interface between hydrated ligands and each hydrated protein as adsorption occurs should be equal to the water molecules adsorbed by both as desorption occurs. Suppose desorption of a protein molecule from the stationary phase occurs in two ways: (i) the conformation of the protein molecule remains the same for both the adsorbed state

P_b^w and the desorbed state P_a^w; (ii) the adsorbed and desorbed states at the moment of desorption of the protein vary in their conformations. For the former,

$$P_b^w + (r_w n_w + q_w)H_2O \rightleftharpoons P_a^w + n_w L_d^w \tag{11}$$

and for the latter,

$$P_a^w + b_w H_2O \rightleftharpoons P_m^w \tag{12}$$

Eqn. 12 shows that the desorbed state P_m^w has b_w water molecules more than the adsorbed state P_a^w as water is selected as the mobile phase.

(3) If the mobile phase is an aqueous salt solution, the presence of salt will change both the molar concentration of water in mobile phase and the conformation of the protein[13,26]. The changes in the conformation of protein molecule cause changes in its surface area, and also the contact area and the number of water molecules linked to it[19,27,28]. When a hydrated protein in water P_m^w is transferred into an aqueous salt solution or the usual mobile phase in HIC, a hydrated protein P_m^s in the latter instance will lose m_s water molecules:

$$P_m^w \rightleftharpoons P_m + m_s H_2O \tag{13}$$

In addition, the presence of a salt will influence the number of water molecules linked to each ligand which will be covered by protein molecules:

$$L_d^w \rightleftharpoons L_d + r_s H_2O \tag{14}$$

where L_d^w is the hydrated ligand complex in water, L_d is that in an aqueous salt solution and r_s is the change in the number of water molecules between the two states.

The change in the conformation of protein molecules due to the presence of salt causes a change in the contact surface area, and consequently the change in the number of ligands, n', linked to each protein molecule is

$$P_b^w + (q_s - b_s + rn')H_2O \rightleftharpoons P_b + n' L_d \tag{15}$$

where q_s is the decreased number of water molecules on the contact surface area as salt is added to water and b_s is that due to the conformation difference of each protein molecule in water P_b^w and the aqueous salt solution P_b. The term r denotes the difference between r_w and r_s, *i.e.*, $r = r_w - r_s$. When the mass action law can be used to describe the quantitative relationship for the foregoing eight thermodynamic equilibria (eqns. 6–10 and 13–15) in which the equilibrium constants are K_a, K_b, K_c, K_d, K_e, K_f, K_g and K_h, respectively, then

$$K = \frac{K_h}{K_f K_g^{n_w}} \cdot \frac{K_a K_b K_e}{K_c K_d^{n_w}} \tag{16}$$

or

$$K = \frac{[P_b]}{[P_m][L_d]^{n_w - n'}} [H_2O]^{(r_w n_w + b_w + q_w - q_s + b_s - n'r - r_s n_w - m_s)} \quad (17)$$

suppose

$$r_w - r_s = r \quad (18)$$
$$n_w - n' = n \quad (19)$$
$$r_w n_w + b_w + q_w = Z_{H_2O} \quad (20)$$
$$m_s + r_s n_w + q_s - b_s + rn' = Z_s \quad (21)$$
$$Z_{H_2O} - Z_s = Z \quad (22)$$

where Z denotes the number of water molecules released as a protein molecule is adsorbed by the HIC column, Z_{H_2O} represents the Z value as water is used as the mobile phase and Z_s is the change in the number of water molecules as protein molecules are transferred into an aqueous salt solution from water. For a given chromatographic system, when the salt, ligand and temperature are fixed, Z will be a characteristic constant of a protein.

Combining eqns. 17–22,

$$K = \frac{[P_b]}{[P_m][L_d]^n} [H_2O]^Z \quad (23)$$

Eqn. 23 is an exponential expression of eqn. 5.

In HPLC, the capacity factor of a solute, k', may be related to the partition coefficient, K_p, of the solute in both solid and liquid phases and the phase ratio, φ, of the column:

$$k' = K_p \varphi \quad (24)$$

From eqns. 23 and 24,

$$K_p = \frac{[P_b]}{[P_m]} = \frac{K [L_d]^n}{[H_2O]^z} \quad (25)$$

or

$$k' = K [L_d]^n \varphi / [H_2O]^z \quad (26)$$

When both the temperature and column are given, K and φ are constants. Suppose that the changes in the range of $[H_2O]$ is not too large, the term $[L_d]$, as that in the previous[24], may still be considered as approximately constant.

Assuming

$$I = K [L_d]^n \varphi \quad (27)$$

then combining eqns. 26 and 27,

$$\log k' = \log I - Z \log [H_2O] \quad (28)$$

$$\log I = \log K + n \log [L_d] + \log \varphi \quad (29)$$

Because both $\log I$ and Z in eqn. 28 are constants, eqn. 28 is linear and the plot of $\log k'$ *vs.* $\log [H_2O]$ should be a straight line. Although there are more equilibria in HIC than in RP-LC, eqn. 28 is the same expression as in RP-LC[24]. However, the Z values contain different terms in each instance.

EXPERIMENTAL

Equipment

An LC-6A liquid chromatograph (Shimadzu, Kyoto, Japan) was used, consisting of three pumps (LC-6A), a detector (SPD-6A V, variable-wavelength UV–visible), column oven (CTO-6A), controller system (SCL-6A), data system (CRT-3A) and recorder (R-112). Stainless-steel columns (5–10 cm × 4.1 mm I.D.) were used, packed with a slurry-packing apparatus (Chemico, Japan). A freezing system was set up *in situ*. A ZD-2 pH-meter was obtained from Second Analytical Instrument Co. (Shanghai, China).

Packings

Silica (7 μm, 500 Å) was removed with hydrochloric acid and then linked to two different ligands. Both ligands consist of a modified ether chain with the same ligand density, but the hydrophobicity of the first end-group is weaker than that of the second. The former is named HIC-I (alcohol group) and the latter HIC-II (keto group). The two kinds of columns were used continuously for 8 months without a significant decrease in the column efficiency.

Chemicals

Myoglobin (MYO, horse heart), cytochrome *c* (Cyt-*c*, horse heart, type III), α-chymotrypsinogen-A (α-CTY-A, bovine pancreas, type II) and α-amylase (α-AMY, *Bacillus anthracis*, type II A) were purchased from Sigma (St. Louis, MO, U.S.A.). Bovine serum albumin (BSA), ribonuclease (RNase), lysozyme (Lys), egg white and ovalbumin (OVA) were obtained from the Institute of Biochemicals (Shanghai, China). The other chemicals used were of analytical-reagent grade. Water was re-distilled (quartz).

Procedures

All retentions were determined with isocratic elution with a flow-rate of the mobile phase of 1.0 ml/min and the detection at 280 nm. The temperature of the column was adjusted by the column oven and a freezer. Each concentration was obtained by mixing a salt solution with a high concentration (A) and a low concentration of salt or water (B) by the SCL-6A controller. Before injecting a sample solution, the column was brought to equilibrium with 20 column volumes of new mobile phase. The dead volume of the column was determined as the minimum retention volume of the same protein by using a series of mobile phases with different

concentrations of water, including pure water. The capacity factor of a protein, k', is calculated as

$$k' = (t_R - t_0)/t_0 \tag{30}$$

where t_R is the retention time and t_0 is the dead time.

In order to prevent abnormal retentions of proteins owing to the very low salt concentration[34], the minimum concentration used here was not lower than 0.50 *M*.

The concentration of water $[H_2O]$ is calculated as

$$[H_2O] = \frac{d_A\varphi_A + d_B\varphi_B - W_s}{0.018} \text{ (mol/l)} \tag{31}$$

where d_A and d_B are the densities of solutions A and B, respectively, φ_A and φ_B are the volume fractions (v/v) of solutions A and B, respectively, and W_s is the weight of salt in mixed solution. For example, when a mixture of 40% B (water) and 60% A [3 *M* $(NH_4)_2SO_4$)] as used as the mobile phase at 20°C (d_A = 1.189 g/ml, d_B = 1.000 g/ml, $MW_{(NH_4)_2SO_4}$ = 132.1), the concentration of water is 48.64 *M*.

For different solutions of salts, when the concentration is 1.00 *M*, the corresponding concentration of water and the difference, ΔH_2O, between pure water and the solution are as listed in Table I.

Determination of adsorption isotherm

The method for the determination of the adsorption isotherm used in this paper is according to frontal elution as described by Horváth and co-workers[35,36]. When the equilibrium concentration of proteins in mobile phase is P_m, the concentration of proteins adsorbed on the stationary phase $[P_b]$ is calculated as

$$P_b = P_{b-1} + \frac{([P_m] - [P_{m-1}])(V_F - V_D)}{V_{sp}} \text{ (mg/ml)} \tag{32}$$

where $[P_m]$ and $[P_{m-1}]$ are two different equilibrium concentrations of protein in mobile phase, P_{b-1} is the concentration of proteins adsorbed on the stationary phase when the equilibrium concentration of proteins in the mobile phase is P_{m-1}, V_F is the frontal retention volume, V_D is the dead volume of the system including column hold-up volume and V_{sp} is the volume of the packing in the column. The correlation coefficient, *C*, for linear regression analysis was taken to four digits. When *C* was greater than 0.99995, it was simply rounded to 1.000.

TABLE I

MOLAR CONCENTRATIONS OF WATER AND ITS CHANGES IN 1.00 *M* SALT SOLUTIONS

Parameter	*Na_2SO_4*	*$(NH_4)_2SO_4$*	*NaCl*	*KCl*	*NaBr*	*NH_4Cl*
M_{H_2O}	54.02	52.16	54.45	53.88	54.09	53.39
ΔH_2O	1.54	3.40	1.11	1.68	1.47	2.17

RESULTS AND DISCUSSION

Linear plot of log k' vs. log [H_2O]

In accordance with eqn. 28, the plot of log k' *vs.* log [H_2O] should be linear. So long as the displacement between a protein and water molecules is reversible and stoichiometric, this linear relationship should exist in all cases. Fig. 1a–d show these cases for (a) the different salts, (b) temperature changes, (c) two kinds of columns and (d) various pH values, the other experimental conditions remaining fixed in each instance. All the correlation coefficients, C, for linear regression analysis are larger than 0.99. Hence the experimental results fitted the expected values well.

Compared with a few popular models or plots in HIC, as shown in Fig. 2a–d, the linear relationships are straight lines in all instances: (a) SDM-R in this work; (b) ln k' *vs.* m (m = molar concentration of salt) by Horváth and co-workers[3,37]; (c) log k' *vs.* log ($1/X_{[H_2O]}$) by Zhao *et al.*[13] (X_{H_2O} = molar fraction of water); and (d) log k' *vs.* log φ_B (φ_B = volume fraction of strong eluent for gradient elution) by Karger and co-workers[11,12]. We selected eight kinds of proteins and measured their k' values

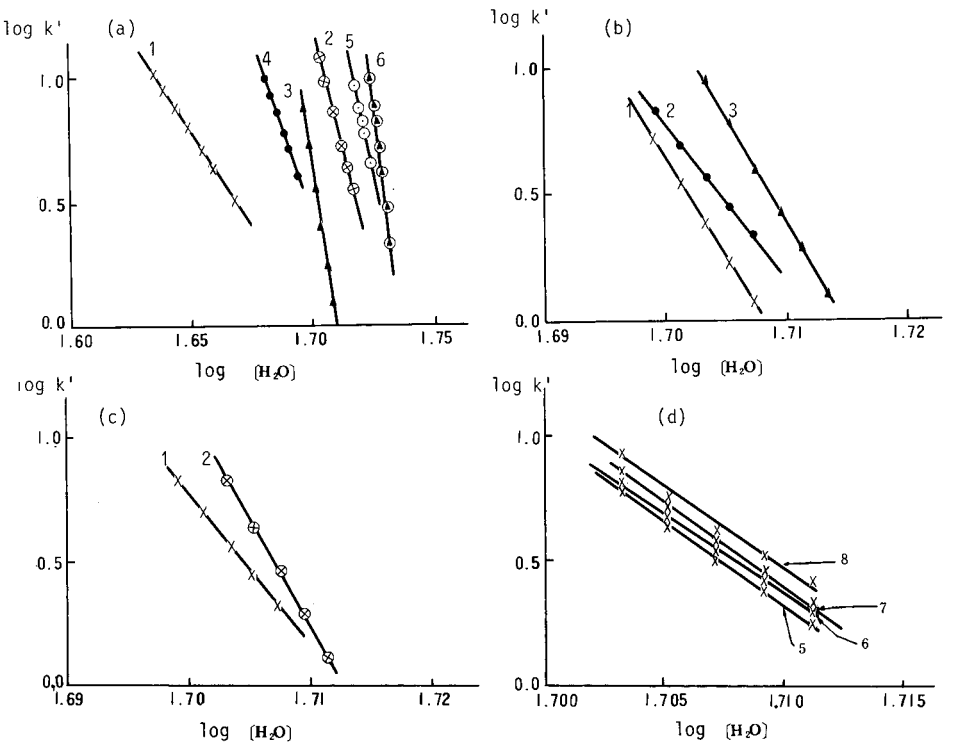

Fig. 1. Plot of log k' *vs.* log [H_2O] for lysozyme with different chromatographic conditions. (a) Lysozyme with various aqueous salt solutions. HIC-I column, 30°C, pH = 7. 1 = NH_4Cl; 2 = KCl; 3 = $(NH_4)_2SO_4$; 4 = NaBr; 5 = NaCl; 6 = Na_2SO_4. (b) Lysozyme at different temperatures. HIC-I column, $(NH_4)_2SO_4$–0.01 *M* KH_2PO_4, pH = 7. 1 = 10°C; 2 = 30°C; 3 = 50°C. (c) Lysozyme with different columns. $(NH_4)_2SO_4$–0.01 *M* KH_2PO_4, pH = 7, 30°C. 1 = HIC-I column; 2 = HIC-II column. (d) Lysozyme at pH values 5, 6, 7 and 8, as indicated. HIC-I column, 30°C, $(NH_4)_2SO_4$–0.01 *M* KH_2PO_4.

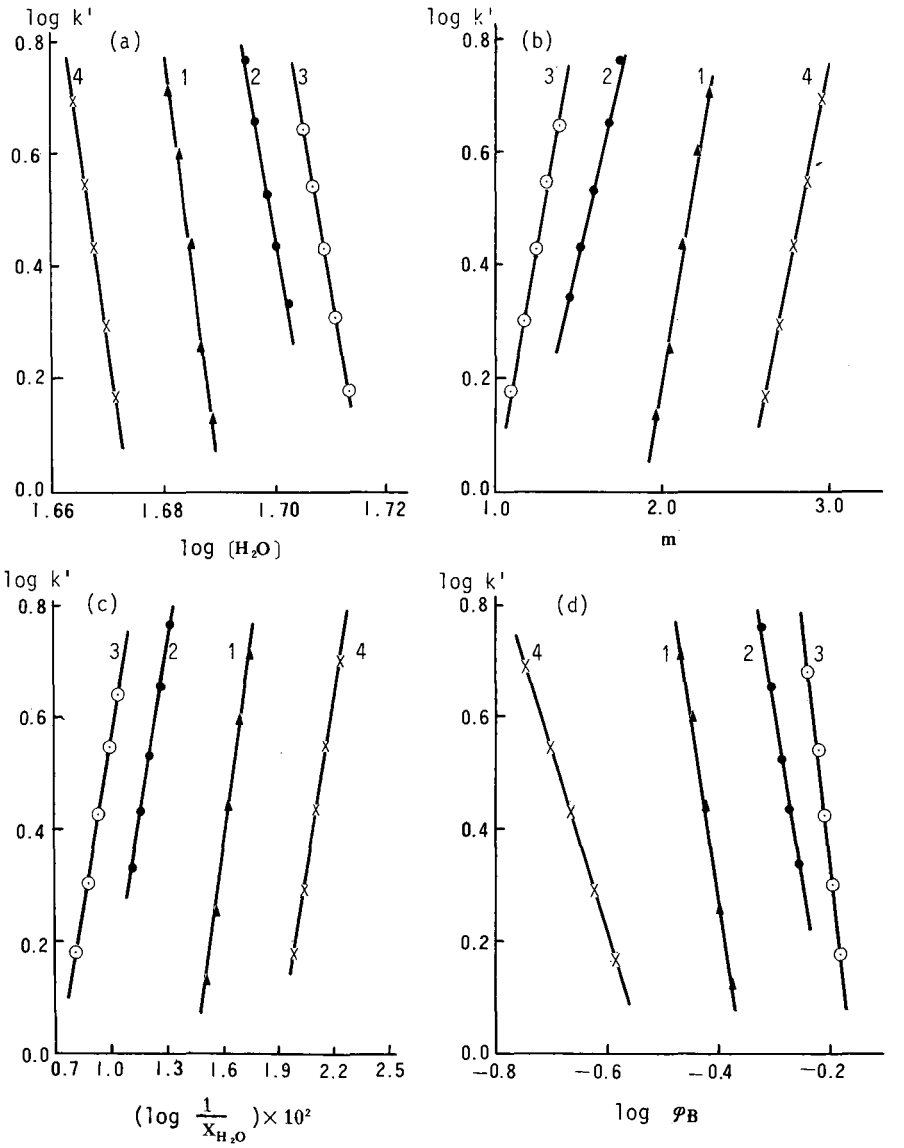

Fig. 2. Comparisons of four models or plots in HIC. (a) SDM-R in this work; (b) plots of log k' *vs.* m, from Melander *et al.*[3]; (c) plots of log k' *vs.* log $(1/X_{H_2O})$, from Zhao *et al.*[13]; (d) plots of log k' *vs.* log φ_B, from Karger and co-workers[11,12]. 1 = RNase; 2 = Lys; 3 = α-AMY; 4 = Cyt-*c*. HIC-I column, 0°C, $(NH_4)_2SO_4$–0.01 *M* KH_2PO_4, pH 7.

under the same experimental conditions. The same k' values were calculated with the foregoing four models (a–d). All the C values were larger than 0.99 and the agreement between the experimental and theoretical data may be considered to be satisfactory. Although such agreement is the most important criterion for evaluating a model, it is not the sole one, and the elucidation of some discrepancies with each of the above models needs detailed investigation.

Linear parameters log I and Z

When the intercepts are plotted against the slopes for each model or plot considered above, as shown in Fig. 3a–d, there is a good linear relationship only for the model presented in this paper (see Fig. 3a) with $C = 0.9998$. From previous studies[38–41] this linear relationship also exists in RP-LC for small molecules:

$$\log I = jZ + \log \varphi \tag{33}$$

where j is a constant related to the affinity of the solvent for the stationary phase in RP-LC and is independent of the kind of solute and temperatures changes[40]. The term

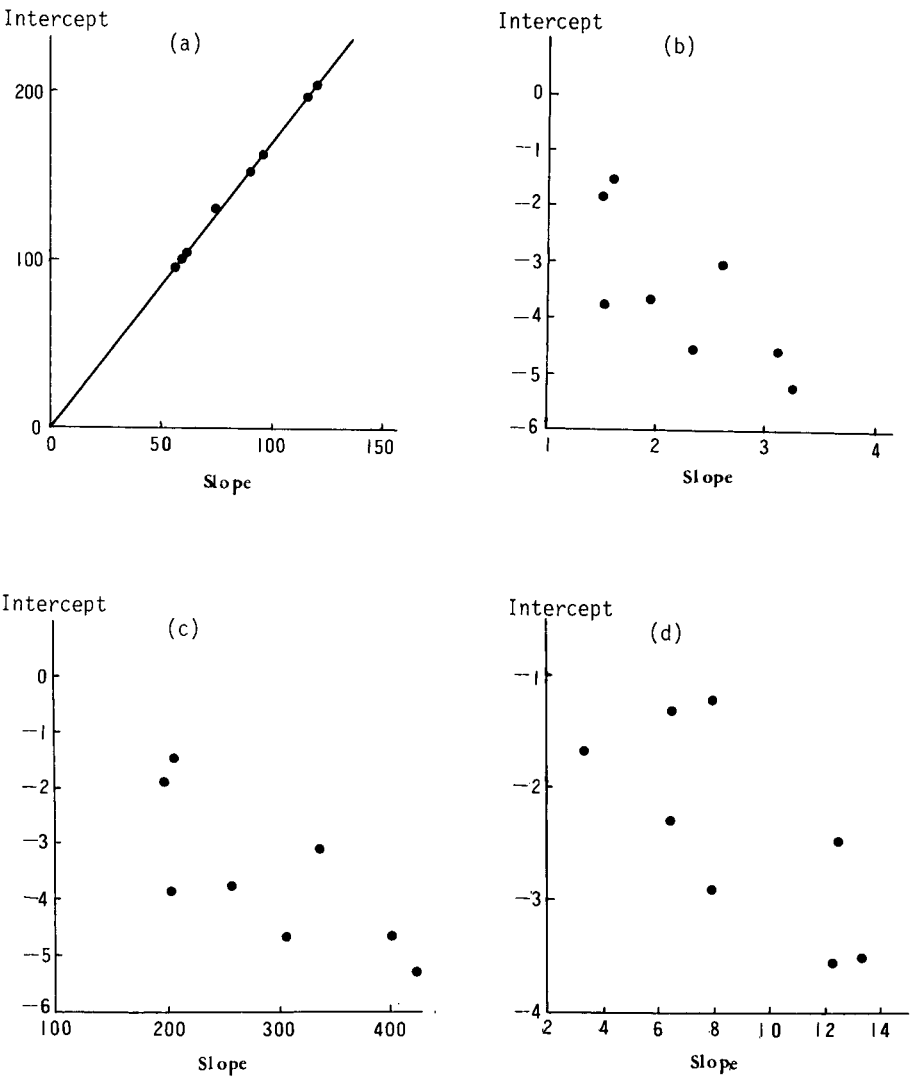

Fig. 3. Comparisons of plots of intercepts *vs.* slopes for each plot in Fig. 2. (a)–(d) as in Fig. 2.

φ is the phase ratio, which is defined from the point of view of thermodynamics[40], considering the value of the capacity factor of solute k' when the free energy of the solute in the displacement process equals to zero.

In order to confirm the applicability of this model, three different experimental conditions were selected to test eqn. 33 and these plots are shown in Fig. 4a–c. Although each log I or Z value for different cases is variable, each obeys the linear

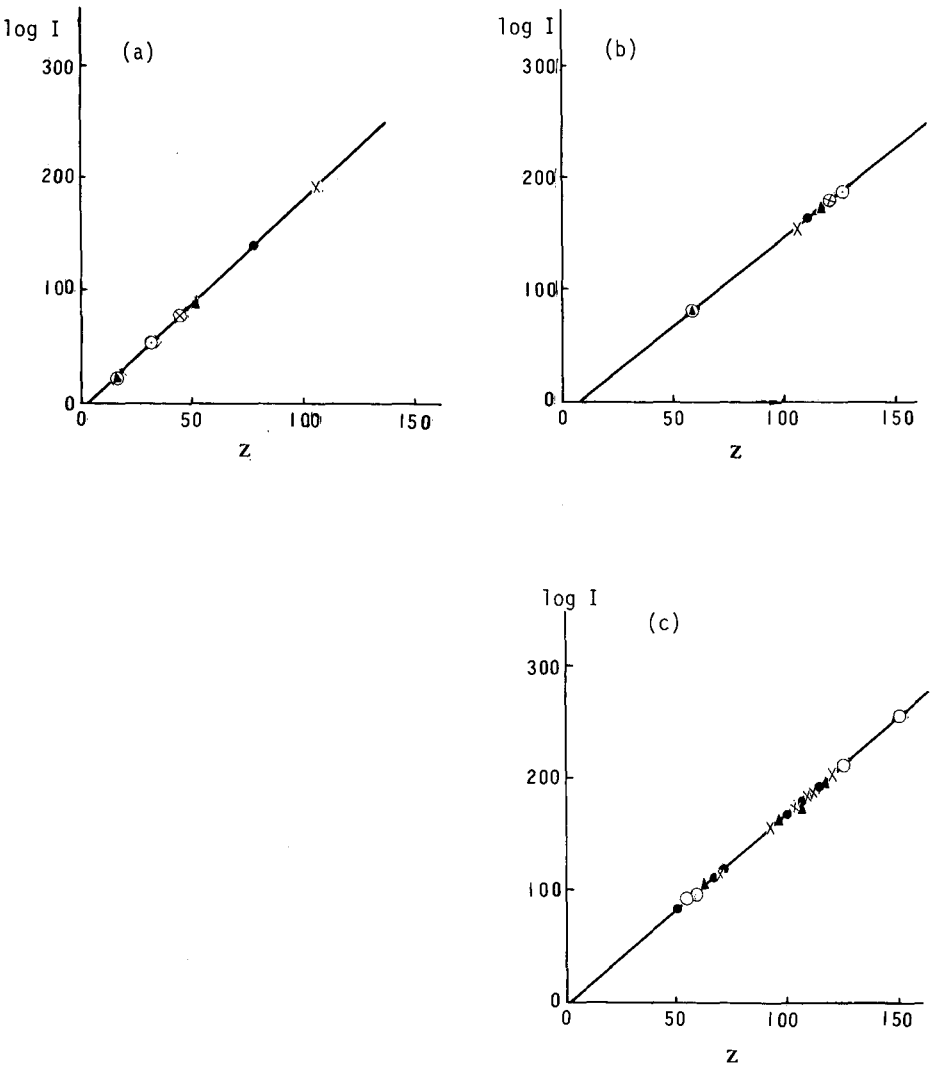

Fig. 4. Plots of log I *vs.* Z for the different cases. (a) Different mobile phases. Experimental conditions as in Fig. 1a. (b) Different temperatures. Experimental conditions as in Fig. 1b, but the temperatures are 0, 10, 20, 30, 40 and 50°C. (c) Different pH values. HIC-I column; $(NH_4)_2SO_4$–10 mM KH_2PO_4; seven kinds of proteins: Lys, Cyt-*c*, α-CTY-A, RNase, MYO, BSA and OVA, 30°C. pH: × = 5; ● = 6; ▲ = 7; ○ = 8.

relationship in eqn. 33. Further, we found that all 44 C values for these kinds of plots are larger than 0.9970 and, except for five C values which are less than 0.9990 and one equal to 0.9990, the other 38 C values are larger than 0.9995. Of the five cases where C was less than 0.9990, four involve temperature changes with the same protein.

Although the SDM-R was proved to be valid for normal-phase chromatography (NPC)[39], *i.e.*, eqn. 28 can be used to explain the quantitative relationship between k' and the concentration of strong solvent in the mobile phase, as shown in Fig. 5d, eqn. 33 is usually not valid as the selective force between silica and the solute predominates over the chromatographic behaviour. The linear plots in RP-LC have been tested and shown to be valid for small molecules (Fig. 5a) but not to be valid for

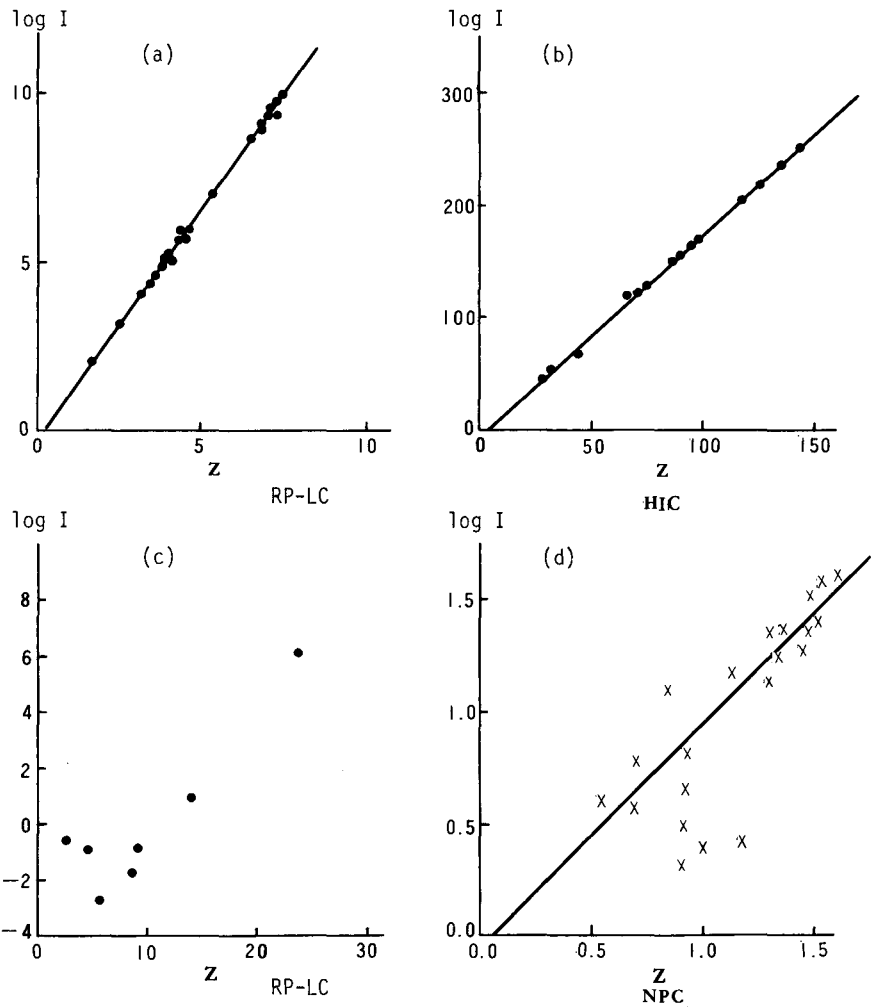

Fig. 5. Plot of log I *vs.* Z. (a) Small apolar solutes in RP-LC (original k' values were taken from ref. 38). (b) Proteins in HIC in this work. pH = 7, 30°C, four proteins (Lys, OVA, α-CTY-A and α-AMY) and four salt solutions [$(NH_4)_2SO_4$, NaCl, NH_4Cl and KCl]. (c) Proteins in RP-LC (data taken from ref. 24). (d) Small non-homologous solutes in NPC (ref. 39).

proteins (Fig. 5c), because the non-selective force controls the retention of small apolar or polar molecules. Fig. 5b shows this in HIC. Compared with both NPC and RP-LC, in accordance with Fig. 5a–d, it may be concluded that HIC is closer to RP-LC for solutes with small molecules and it seems that non-selective forces predominate over the interactions between the bonded phase and protein molecules in HIC or the hydrophobic interaction force has the characteristics of a non-selective force. Further, the stoichiometric displacement of protein molecules to water molecules is a very similar process to that of the displacement of small molecules including apolar and polar small molecules to organic solvent molecules in RP-LC. If this conjecture is reasonable, the method of investigating the retention mechanism of small apolar molecules on RP-LC columns may be applied to that of protein molecules on an HIC column.

The statistical result for j values from the experiments is a constant 1.74 whereas the j values on the HIC-I column (alcohol group) and the HIC-II column (keto group) are 1.77. These results are reasonable. The difference in j values between the two columns is only 0.03, but it is significant statistically. This result is consistent with the j value being a constant independent of the kinds of proteins and salts, pH and temperature but dependent on the type of column.

The most reasonable values of j should be the constant for the affinity of 1 mol of water to the HIC column without any influence of salts. When pure water is used as the mobile phase, the foregoing experimental conditions may be satisfactory. Inserting eqn. 33 for $\log I$ into eqn. 28, we obtain

$$\log k' = Z(j - \log [H_2O]) + \log \varphi \tag{34}$$

From eqn. 34 we know that, provided that

$$j = \log [H_2O] \tag{35}$$

then

$$\log k' = \log \varphi$$

In other words, the retention of protein in this case is due not to the protein itself but to pure water. If the retention mechanism of proteins in HIC as a stoichiometric displacement process between the protein and water molecules is true, then the logarithm of the molar concentration of pure water should be the most reliable value of j in an HIC system for the reasons discussed above. Table II gives the experimental and theoretical j values in HIC. In order to confirm the reliability of the foregoing conjectures, some j values from the experiments and expected values in RP-LC published in the literature are also given in Table II. The experimental and theoretical j values agree well.

Log k' and Ostwald absorption coefficient

It was pointed out above that we may use the method for the investigation of the chromatographic behaviour of small molecule in RP-LC to study that of protein molecules in HIC. Some workers have correlated the relationship between the k' values

TABLE II

COMPARISONS OF j AND THE LOGARITHM OF THE CONCENTRATIONS OF THE PURE DISPLACING AGENTS IN HIC AND RP-LC

Mobile phase	*Displacing agent*	*M (pure)*	*Log M*	*j*	*Ref.*
Methanol–water	Methanol	24.75	1.39	1.44	40
				1.42	40
				1.40	40
				1.38	38
				1.41	40
				1.35	39
2-Propanol–water	2-Propanol	13.06	1.17	1.14	40
THF[a]–water	THF[a]	10.23	1.01	1.03	40
ACN[b]–water	ACN[b]	19.07	1.28	1.29	40
				0.94	40
Salt–water	Water	55.56	1.74	1.74	

[a] Tetrahydrofuran.
[b] Acetonitrile.

of solutes in RP-LC and their partition coefficients in liquid–liquid extraction. The influence of salts on the k' values of proteins in HIC is of interest. The Ostwald absorption coefficients, γ_s, of methane or argon in water or solutions of salts in water and other solvents[42] have been considered as a criterion to describe the effects of salts on the free energy of transfer of a solute between two phases. In other words, γ_s can be used to explain quantitatively the influences of each salting-out effect on the partition coefficient of methane or argon. Some γ_s values are listed in Table III. The term k' in HIC has the same function of elucidating the energy of transfer of proteins between two phases. The γ_s value represents the interactions among molecules in an electrolyte solution. For the apolar solute methane, the interactions should be the hydrophobic interaction force. If the same salt solution used to investigate the γ_s value is used as the mobile phase in HIC, and the ligands on the HIC column are considered to be equivalent to a mechanically held moderately apolar liquid phase in liquid–liquid extraction, then the interactions among protein and ligand molecules can also be

TABLE III

OSTWALD ABSORPTION COEFFICIENT FOR METHANE IN VARIOUS SALT SOLUTIONS

Conditions: 25°C and 1 atm. From ref. 42.

Salt solution	$\gamma_s \times 10^3$
1 *M* NaCl	24.2
1 *M* KCl	24.9
1 *M* NH_4Cl	27.9
Pure H_2O	34.1

considered to be the same as the interactions between an organic liquid and argon. Provided that the kinds and concentrations of salts in both the aqueous solution for measuring γ_s and the mobile phase for measuring k' in HIC are the same, k' and γ_s should have a parallel relationship, because the same interaction force should show the same characteristics[37,43]. We found that there is a linear relationship between the log k' values of some proteins in HIC and log γ_s for methane in 1.00 *M* solutions of NaCl, NH_4Cl and KCl (results not shown). The linear relationship between log k' and log γ_s explains why the hydrophobic force mainly dominates the chromatographic behaviour of proteins in HIC.

Adsorption isotherm

The study of the adsorption isotherm of a solute on a stationary phase in RP-LC is an important tool for investigating the retention mechanism of a solute under the same chromatographic conditions and is receiving increasing attention. In a previous paper[14] it was concluded that the quantitative relationship between the concentration of a solute on the stationary phase and the equilibrium concentration in solute may be expressed as:

$$\log K_p = \beta_C + (q/Z) \log (1/[P_m]) \tag{36}$$

or

$$\log [P_b] = \beta_C + (nr/Z) \log [P_m] \tag{37}$$

where K_p is the partition coefficient of the solute in both phases, β_C contains a number of constants related to the affinity of the solute to the adsorbent, $[P_m]$ is the equilibrium concentration of solute in mobile phase, $[P_b]$ is the concentration of solute on the adsorbent and n, q, r and Z have the same meanings as before. The term q is the number of water molecules displaced from the contact surface area of the protein when it adsorbs to a HIC support.

Both eqns. 36 and 37 are expressions of the stoichiometric displacement model of adsorption (SDM-A) for solutes[14] and eqn. 37 is equivalent to the Freundlich empirical equation mathematically. In other words, the Freundlich empirical equation can be derived by SDM and gives the exact physical meaning of each term. Further, if an adsorption isotherm for a solute in a liquid–solid system belongs to the Freundlich type, its adsorption mechanism can be shown to be a stoichiometric displacement of solute to solvent molecules. Although Jennisson[8,44] reported that the adsorption isotherms of phosphorylase kinase on alkylamine–Sepharose derivatives obtained by a static method are of the Freundlich type, the results obtained by the static method are still far from valid for a complicated chromatographic system.

Horváth and co-workers[35,36] presented a dynamic method with frontal elution for measuring the adsorption isotherms of solutes. Their results should be much closer to real chromatographic conditions. We used their dynamic method for the HIC system, column–lysozyme–$(NH_4)_2SO_4$–KH_2PO_4 (pH 7.0), to obtain the Freundlich-type isotherm as shown in Fig. 6. The results demonstrate that the retention mechanism of proteins in HIC obeys the SDM-R.

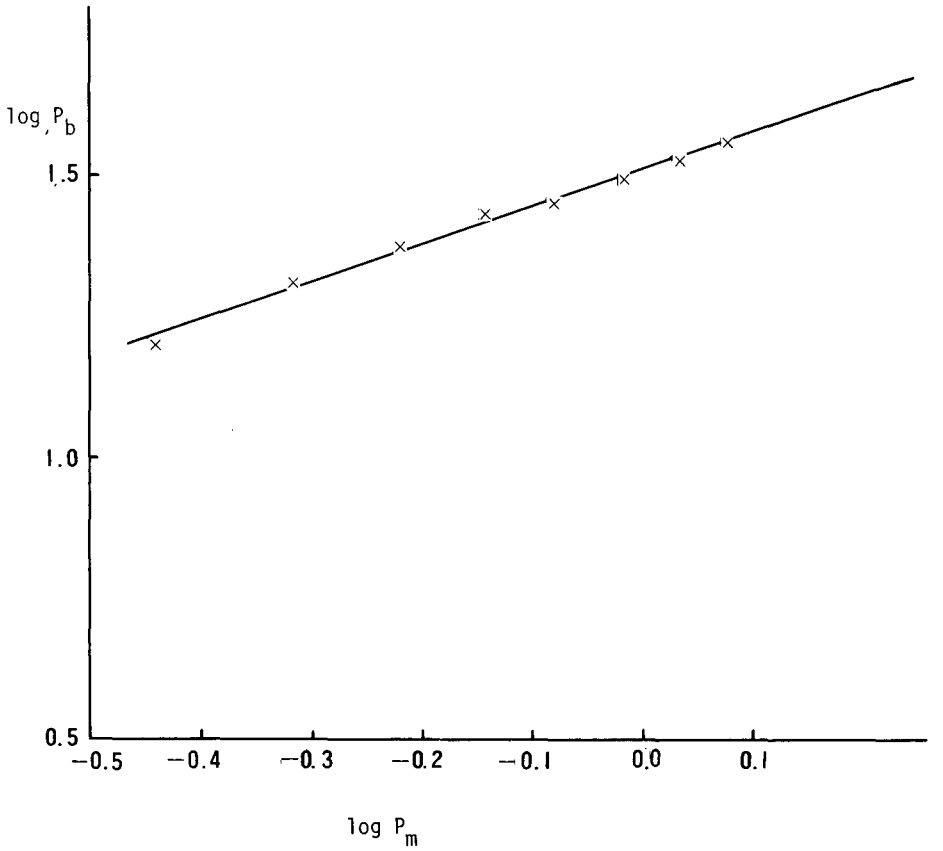

Fig. 6. Adsorption isotherm of lysozyme on HIC-I column (room temperature). $(NH_4)_2SO_4$–0.01 *M* KH_2PO_4, pH 7.

Functions of salts

As pointed out under Theoretical, the most important role of salt is as a diluent. According to Table I, the ability to act as a diluent for salts of concentration 1.00 *M* decreases in the order $(NH_4)_2SO_4$ > NH_4Cl > KCl > Na_2SO_4 > NaBr > NaCl. This order shows that the larger the changes in the concentration of water or ΔH_2O (also shown in Table I), the broader is the potential range of gradient elution in HIC, or the better is the mobile phase. From Table I it may be concluded that ammonium sulphate is the best diluent for making mobile phases in HIC. As discussed under Theoretical, the adsorption ability of proteins on an HIC column depends on the kind of salts and may be measured with log *I*. The adsorption of a particular protein decreased in the order Na_2SO_4 > $(NH_4)_2SO_4$ > NaCl > KCl > NaBr > NH_4Cl, as shown in Table IV.

The effect of salts on the adsorption ability may be attributed to the values of log *I*. As shown in eqns. 23 and 29, salts will affect the thermodynamic equilibrium constants *K* and the concentration of water $[L_d]$ on the surface of an HIC packing in addition to the number, *n*, of water molecules released from this surface. This involves

TABLE IV

VALUES OF Z AND LOG I FOR SDM-R ON AN HIC-I COLUMN WITH DIFFERENT SALT SOLUTIONS

Conditions: 30°C, pH = 7.00.

Salt	*Lys*		*OVA*		*α-CTY-A*		*α-AMY*	
	Z	*Log I*	*Z*	*Log I*	*Z*	*Log I*	*Z*	*Log I*
Na_2SO_4	110.1	192.1	–	–	263.9	459.1	369.0	641.4
$(NH_4)_2SO_4$	79.9	136.4	118.3	202.1	104.7	180.0	118.3	203.6
NaCl	50.1	87.0	50.1	86.0	89.4	154.6	64.8	111.6
KCl	45.1	78.0	45.1	77.8	66.6	114.6	67.4	115.6
NaBr	31.1	53.4	29.5	50.6	39.4	67.3	–	–
NH_4Cl	16.4	27.8	17.6	29.8	25.3	43.0	–	–

the kinds of HIC packings and proteins and also the composition of the mobile phase. When a chromatographic system is given, it depends only on the kind of protein.

The effect of salts on the conformation of protein molecules and various hydrations, such as ligands, proteins and some protein complexes, may cause a change in the total Z values, as shown in eqns. 18–22.

As shown in eqn. 21, Z includes many terms, and so far, we do not have the ability to measure all of them. However, from eqn. 28 the Z value may be measured accurately and some Z and log I values are listed in Table IV. The decrease in the order of Z values for a particular protein is $Na_2SO_4 > (NH_4)_2SO_4 > NaCl > KCl > NaBr > NH_4Cl$. This order is identical with that for the adsorption ability discussed above, and eqn. 32 already proves it theoretically.

In Summary, the effect of salts on the retention of proteins in HIC includes changes in the concentration of water, hydrophobicity (or adsorption affinity) and the conformation of protein molecules in addition to the hydration of ligands, protein molecules and ligand-protein complexes, *i.e.*, salts may affect each term on the right-hand side of eqn. 28, log I, Z and $[H_2O]$.

CONCLUSIONS

We believe that the most rational retention mechanism of proteins in hydrophobic interaction chromatography is a stoichiometric displacement process between protein and solvent molecules, with water as displacing agent. The adsorption of a protein molecule should be accompanied by the release of a stoichiometric number of water molecules to the solution from the interface between the protein molecule and the HIC ligands.

The mathematical model expressing the stoichiometric displacement process of retention may be described by saying that the logarithm of the capacity factor of the protein is proportional to the logarithm of the concentration of water in the mobile phase.

The stoichiometric number of water molecules Z displaced by one protein molecule is believed to involve in many factors, such as the characteristics of the

ligands, proteins, salts, many kinds of hydrations and the conformations of protein molecules.

The parameter for measuring the adsorption ability of proteins on HIC columns, log I, also measures the hydrophobic interactions between ligands and protein molecules.

The excellent linear relationship between Z and log I shows that HIC is closer to RP-LC or, more exactly, closer to the RP-LC of small molecules. The method of investigating the contribution of hydrophobic interaction forces to the retention of proteins in HIC by following the method used to study the relationship of the Ostwald absorbent coefficient in the same solutions of salts is valid and parallel relationships were found between log k' and log γ_s for 1.00 M solutions of various salts.

The functions of salts in HIC are believed to be as diluents and as reagents to change the affinity of proteins to ligands and the conformation of protein molecules, and also various hydrations such as of ligands, protein molecules and a series of protein complexes.

The adsorption isotherm of proteins on an HIC column was demonstrated to be of the Freundlich type by a dynamic chromatographic method, and showing again that the adsorption mechanism of proteins on an HIC column is a stoichiometric displacement process.

ACKNOWLEDGEMENTS

This work was supported by grants from the National Natural Science Foundation of China and the Excellent Young Professor Foundation of the State Education Committee of China.

SYMBOLS

b_w	changed number of water molecules linked to a protein molecule due to its different conformations between the adsorbed and desorbed states in pure water.
b_s	changed number of water molecules linked to a protein molecule due to its different conformations in the adsorbed state between pure water and salt solution.
C	correlation coefficient for linear regression analysis.
d_A, d_B	densities of eluates A and B for gradient elution, respectively.
I	contains a number of constants related to the affinity of a protein to the HIC column.
j	constant related to the affinity of water to the HIC column.
K	general equilibrium constant of the stoichiometric displacement process.
K_a, K_b, K_c, K_d, K_e, K_f, K_g	individual equilibrium constants during the displacement process.
K_p	partition coefficient of a protein between two phases.
k'	capacity factor.

L_0	bare ligands.
L_d, L_d^w	hydrated ligands in salt solution and pure water, respectively.
m	molar concentration of salt.
$\bar{m}$, m_w	mean numbers of water molecules linked to a protein molecule in salt solution and pure water, respectively.
m_s	changed number of water molecules linked to a protein molecule between pure water and salt solution, *i.e.*, $m_s = m_w - \bar{m}$.
n, n_w	numbers of ligands bonded to a protein molecule in salt solution and pure water, respectively.
n'	changed number of water molecules linked to a protein molecule between pure water and salt solution, *i.e.*, $n = n_w - n'$.
P_0	bare protein.
P'_a, P_a^w	protein at the moment it just desorbs from ligands and their molecular conformations are in an unstable state in vacuum and pure water, respectively.
P_b, P'_b, P_b^w	proteins in the adsorbed state in salt solution, vacuum and pure water, respectively.
P_m, P_m^w	hydrated proteins in salt solution and pure water, respectively.
P_{b-1}	concentration of proteins adsorbed on the stationary phase when the equilibrium concentration of protein in the mobile phase is P_{m-1}.
P_{m-1}	equilibrium concentration of protein in salt solution.
q	number of water molecules displaced from the contact surface area of the protein when it adsorbs to a HIC support.
q_w, q_s	changed numbers of water molecules on the surface of a protein molecule linked to ligands in the presence of pure water and salt solution, respectively.
r, r_w	numbers of water molecules bound to a ligand in the presence of salt solution and pure water, respectively.
r_s	changed number of water molecules bonded to a ligand when salt is added into pure water, *i.e.*, $r = r_w - r_s$.
t_0	dead time.
t_R	retention time.
V_D	dead volume of a system including the column hold-up volume.
V_F	retention volume of frontal elution.
V_{sp}	volume of adsorbent in a chromatographic column.
W_s	weight of salt in solution.
X_{H_2O}	molar fraction of water.
Z, Z_{H_2O}	total numbers of water molecules released from the interface between the protein molecule and the HIC column in the salt solution and pure water, respectively.

Z_s	change in the number of water molecules when protein molecules are transferred from water into an aqueous salt solution.
β_C	contains a number of constants related to the affinity of the solute to the absorbent (see eqns. 36 and 37).
φ	phase ratio of a column.
φ_A, φ_B	volume fractions of solutions A and B in a mixed solution, respectively.
γ_s	Ostwald absorption coefficient.

REFERENCES

1 S. Shaltiel and Z. Er-el, *Proc. Natl. Acad. Sci. U.S.A.*, 70 (1973) 778.
2 J. Chang and X. Geng, *J. Northwest Univ., Nature Sci.*, 4 (1989) 103.
3 W. R. Melander, D. Corradini and Cs. Horváth, *J. Chromatogr.*, 317 (1984) 67.
4 O. Sinanoglu and S. Abdulnur, *Fed. Proc. Fed. Am. Soc. Exp. Biol.*, 24 (1965) 12.
5 J. L. Fausnaugh, L. A. Kennedy and F. E. Regnier, *J. Chromatogr.*, 317 (1984) 141.
6 H. P. Jennissen and G. Botzet, *Int. J. Biol. Macromol.*, 1 (1979) 171.
7 H. P. Jennissen, *J. Solid-Phase Biochem.*, 4 (1979) 151.
8 H. P. Jennissen, *J. Chromatogr.*, 159 (1978) 71.
9 T. Arakawa, *Arch. Biochem. Biophys.*, 248 (1986) 101.
10 J. Wyman, *Adv. Protein Chem.*, 10 (1964) 223.
11 S. L. Wu, K. Benedek and B. L. Karger, *J. Chromatogr.*, 359 (1986) 3.
12 S. L. Wu, A. Figueroa and B. L. Karger, *J. Chromatogr.*, 371 (1986) 3.
13 J. Zhao, Y. Xu and X. Geng, *J. Northwest Univ., Nature Sci.*, 2 (1986) 25.
14 X. Geng and Y. Shi, *Sci. China, Ser. B*, 32 (1989) 11.
15 X. Geng, paper presented at the *12th International Symposium on Column Liquid Chromatography, Washington, DC, June 19–24, 1988.*
16 D. R. Robinson and W. P. Jencks, *J. Am. Chem. Soc.*, 87 (1965) 2470.
17 W. Norde, *Adv. Colloid Interface Sci.*, 25 (1986) 267.
18 J. C. Lee and S. N. Timasheff, *J. Biol. Chem.*, 256 (1981) 7193.
19 K. Gekko and S. N. Timasheff, *Biochemistry*, 20 (1981) 4667.
20 H. S. Frank and M. W. Evans, *J. Chem. Phys.*, 13 (1945) 507.
21 W. Kauzmann, *Adv. Protein Chem.*, 14 (1959) 1.
22 T. G. Cooper, *The Tools of Biochemistry*, Wiley-Interscience, New York, 1977, p. 370.
23 L. Xucha and S. Kotrly, in D. Betteridge (Editor), *Solution Equilibria in Analytical Chemistry*, Reinhold, London, 1972.
24 X. Geng and F. E. Regnier, *J. Chromatogr.*, 296 (1984) 15.
25 Cs. Horváth, W. Melander and L. R. Snyder, *J. Chromatogr.*, 125 (1976) 129.
26 S. Påhlman, J. Rosengren and S. Hjertén, *J. Chromatogr.*, 131 (1977) 99.
27 T. Arakawa and S. N. Timasheff, *Biochemistry*, 21 (1982) 6545.
28 T. Arakawa and S. N. Timasheff, *Biochemistry*, 23 (1984) 5912.
29 T. Arakawa and S. N. Timasheff, *Biochemistry*, 23 (1984) 5924.
30 J. L. Fausnaugh, E. P. Fannkoch, S. Gupta and F. E. Regnier, *Anal. Biochem.*, 137 (1984) 464.
31 F. E. Regnier, *Chromatographia*, 24 (1987) 241.
32 T. Ueda, Y. Yasui and Y. Ishida, *Chromatographia*, 24 (1987) 427.
33 K. Benedek, *J. Chromatogr.*, 458 (1988) 93.
34 R. A. Barford, T. F. Kumosinski, N. Parris and A. E. White, *J. Chromatogr.*, 458 (1988) 57.
35 J. Jacobson, J. Frenz and Cs. Horváth, *J. Chromatogr.*, 316 (1984) 53.
36 J. Huang and Cs. Horváth, *J. Chromatogr.*, 406 (1987) 275.
37 W. R. Melander and Cs. Horváth, *Arch. Biochem. Biophys.*, 183 (1977) 200.
38 X. Geng and F. E. Regnier, *J. Chromatogr.*, 332 (1985) 147.
39 Z. Song and X. Geng, *Acta Chim. Sin.*, 48 (1990) 237.
40 X. Geng, *J. Chromatogr.*, submitted for publication.

41 X. Geng and Y. Shi, paper presented at the *12th International Symposium on Column Liquid Chromatography, Washington, DC, June 19–24, 1988.*
42 A. Ben-Naim and M. Yaacobi, *J. Phys. Chem.*, 78 (1974) 170.
43 X. Geng, *Introduction of Modern Separation Science*, Northwest University Publisher, Xi'an, 1990.
44 H. P. Jennissen, *Biochemistry*, 15 (1976) 5683.
45 A. Ben-Naim, *Hydrophobic Interaction*, Plenum, New York, 1980.

Journal of Chromatography, 507 (1990) 25–31
Elsevier Science Publishers B.V., Amsterdam — Printed in The Netherlands

CHROMSYMP. 1733

High-performance size-exclusion chromatography and molar mass measurement by low-angle laser light scattering of recombinant yeast-derived human hepatitis B virus surface antigen vaccine particles

YOSHIKO SATO
Institute for Protein Research, Osaka University, Suita, Osaka 565 (Japan)
NOBUYOSHI ISHIKAWA
Kanonji Institute, Research Foundation for Microbial Diseases of Osaka University, Kanonji, Kagawa 768 (Japan)
and
TOSHIO TAKAGI*
Institute for Protein Research, Osaka University, Suita, Osaka 565 (Japan)

SUMMARY

Two kinds of recombinant yeast-derived human hepatitis B virus surface antigens (HBsAg) for use as vaccines were analysed by high-performance size-exclusion chromatography using a TSK-GEL G6000PWXL column. One consisted of the surface antigen, a glycosylated polypeptide with of about 230 amino acid residues identical with that of human hepatitis B virus in addition to lipids derived from the yeast cell. The other differed in that it consisted of a polypeptide with an additional peptide of nine amino acid residues corresponding to the pre-S2 region. Elution from the column was monitored with a low-angle laser light-scattering detector and also UV and refractive index detectors. The results obtained indicate that both of the antigen particles gave a single symmetrical peak in the elution curves, the molar masses of the particles were 5040 and 4640 kg/mol for the former and the latter, respectively, and the particle size was homogeneous for both of the HBsAg particles. The present approach seems suitable for the characterization of such antigen particles, which will be widely used as vaccines.

INTRODUCTION

Hepatitis type B virus is a widespread disease affecting an estimated 200 million persons throughout the world. An antigenic particle discovered in a human serum in the 1960s was named Australian antigen, and was eventually shown to be hepatitis B virus surface antigen (HBsAg). The antigen turned out to be a particle with a complex composition consisting of glycosylated protein polypeptides and lipids with

0021-9673/90/$03.50

a diameter of about 22 nm as determined by electron microscopy. The HBsAg was purified from sera of carriers of hepatitis B virus, and treated with heat and formaldehyde to produce a hepatitis B vaccine. Limitation of supply and danger of infection were the major demerits of the use of the natural HBsAg particle as a vaccine. Development of the gene engineering technique triggered efforts to develop of a vaccine free from such disadvantages. The production of HBsAg in the form of a particle similar to the natural one was reported by Miyanohara *et al.*[1] using yeast as the host. Recently the vaccine thus prepared became commercially available.

One of our research groups has also succeeded in the production of HBsAg using yeast as the host[2]. Two kinds of the antigens were produced. One containing a protein polypeptide with an amino acid sequence identical with that of the natural HBsAg and the other having a different protein polypeptide in that it had an elongation on the N-terminus consisting of nine additional amino acid residues corresponding to the pre-S2 region. The engineered HBsAg particles can be intensively studied without fear of the infection pertinent to the natural counterpart. The detailed characterization of the yeast-derived HBsAg will also be useful as a test of studies that should be carried out for any such antigen particles produced for various virus diseases. This paper reports the results obtained by characterization of the engineered HBsAg particle by high-performance size-exclusion chromatography (HPSEC) and monitoring of its elution by the low-angle laser light-scattering (LALLS) technique. This study forms part a series of efforts to apply the light-scattering technique to the physico-chemical characterization of biological macromolecules and particles[3].

EXPERIMENTAL

Yeast cells in which HBsAg genome was cloned were cultured in Burkholder medium and were broken by high-pressure homogeneizer. The extract was purified by adsorption–desorption and centrifugation. Further purification was carried out by two subsequent density-gradient centrifugations using sucrose in the first and potassium bromide in the second gradient former. Fractions active with respect to the HBsAg activity were collected and dialysed against 5 m*M* sodium phosphate buffer (pH 7.6) containing 0.02% gelatin. The final concentration was estimated to be 94.4 μg/ml according to the Lowry method using bovine serum albumin as the standard.

For a single high-performance liquid chromatographic (HPLC) analysis according to our procedure, 100 μl of solution containing 30 μg of the vaccine were required. This solution was concentrated prior to HPLC by ultrafiltration using a Centricon-30 tube (Amicon). The gelatin of low molecular weight added for stabilization during storage could be removed by filtration.

The columns were equilibrated and eluted with 0.1 *M* sodium phosphate buffer (pH 6.9) containing 0.02% sodium azide at 25°C. HPLC analysis was carried out at a flow-rate of 0.30 ml/min at room temperature (25°C). In the initial phase of the study, a tandem arrangement of TSK-GEL G6000PWXL and TSK-GEL G4000SW columns in addition to a guard column (Tosoh) was used. The SW column was specially selected for lipoprotein analysis. Most of the later experiments were carried out without the G4000SW column. For application of standard proteins, the column(s) was replaced with a TSK-GEL G3000SWXL column.

Elution was monitored with three detectors connected in series in the following

sequence: a UV absorption photometer (UV detector), a low-angle laser light-scattering photometer (LS detector) and a precision differential refractometer (RI detector). The outputs of these three detectors were used to calculate the molar masses of the HBsAg particles.

RESULTS

Fig. 1 is a schematic diagram of the measuring system used. Fig. 2 shows a typical example of triple sets of elution curves obtained using this measuring system for the two kinds of engineered HBsAg particle. The retention time corresponding to the void volume of the series of columns was 26.5 min as determined by the frontal elution of dextran T500 (Pharmacia). It should be noted that the scattering detector, which is extremely sensitive to the presence of large particles, detected nothing at the retention time corresponding to the void volume. The particle was eluted as a single symmetrical but broad peak at 35 min for both types of HBsAg particles. No protein was eluted behind the peak of the HBsAg particles, despite the deliberate use of the special G4000SW column with a low affinity for lipoproteins in the initial phase of the experiments.

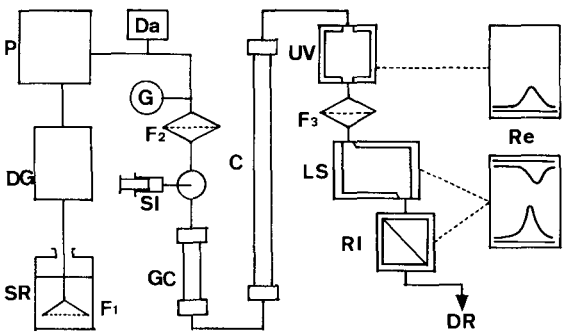

Fig. 1. Schematic diagram of instrumentation. SR = Solvent reservoir; F_1 = sintered stainless-steel filter (Umetani Seiki, Model SFY); DG = degasser (Erma Optical Works, Model ERC-3310); P = dual pump (Tosoh, CCPD); Da = bellows-type damper (Umetani Seiki, Model S-100) with a helically coiled stainless-steel tube (2 m × 0.1 mm I.D.) on the downstream side; G = pressure gauge with safety device to shut down the pump when the pressure exceeds a predetermined value (Umetani Seiki); F_2 = sintered stainless-steel filter (Umetai Seiki, Model SLF); SI = sample injector with a sample loop of 100-μl internal capacity; GC = guard column (Tosoh, TSK-GEL GPWXL, 4.0 cm × 6.0 mm I.D.); C = column (Tosoh, TSK-GEL G6000PWXL, 30 cm × 7.8 mm I.D.); UV = UV detector (Tosoh UV-8000); F_3 = ultrafilter with pore size 0.5 μm (Millipore, Type FHLP 01300); LS = low-angle laser light-scattering photometer (Tosoh, LS-8000); RI = RI detector (Tosoh, RI-8011); Re = two double-pen recorders.

In Fig. 2, retention time was that recorded by the scattering detector. Traces from the other two detectors were corrected for displacements due to the difference in pen positions and the location of the detectors along the flow-line. The displacements were calculated using proteins such as bovine serum albumin and *E. coli* β-galactosidase. The peak positions were identical, irrespective of the method of detection, as expected for a sample without size distribution.

The three detectors give outputs, hereafter denoted by (UV), (LS) and (RI),

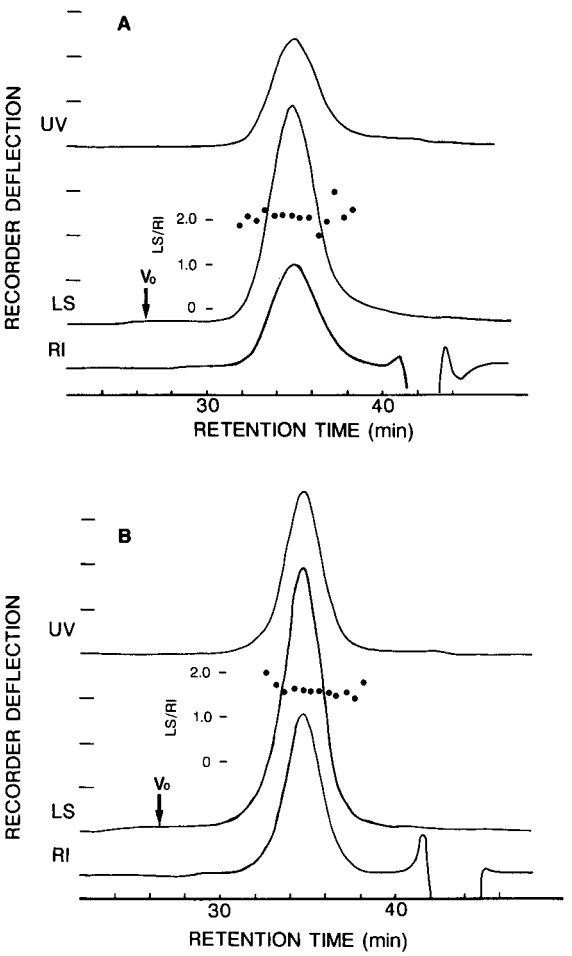

Fig. 2. Elution patterns of the HBsAg vaccine particles obtained using the measuring system shown in Fig. 1 (A) Pre S(+); (B) Pre S(−). The amounts of samples were 39 and 42 μg for A and B, respectively. UV, LS and RI indicate traces given by the respective detectors. The sensitivity setting for these detectors were 0.32, 4 and 2, respectively, for both A and B. As the RI detector is set at the next to the highest sensitivity, the room temperature must be well thermostated in order to obtain a flat baseline. V_0 indicates the retention time corresponding to the void volume detected by the LS detector. ● = (LS)/(RI) ratio.

reflecting changes in UV absorption, light scattering and refractive index. The molar mass (M_r) of a particle the size of which is small enough compared with the wavelength of the light (633 nm) can be determined according to the following equations[3],

$$M_r = K_1 \frac{(\mathrm{LS})}{(\mathrm{d}n/\mathrm{d}c)\ (\mathrm{RI})} \tag{1}$$

or

$$M_r = K_2 \frac{(\mathrm{UV})\ (\mathrm{LS})}{E_1^{1\%}{}_{\mathrm{cm}}\ (\mathrm{RI})^2} \tag{2}$$

where (dn/dc) is the specific refractive index increment and $E_1^{1\%}{}_{cm}$ is the extinction coefficient.

Fig. 2 includes a plot of the (LS)/(RI) ratio that is flat over most of the peak. The (RI)/(UV) ratio also gave a similar flat plot for each of the types of the vaccine particles. This constancy of the (RI)/(UV) ratio strongly suggests that the composition of the HBsAg particle with respect to protein, lipid and carbohydrate is homogeneous. The result does not exclude the possibility that the sample is heterogeneous with respect to composition but homogeneous with respect to size. However, this possibility can be excluded, because the particle was shown to give a narrow band in density gradient centrifugation. If the content of the two major components, protein and lipid, which have markedly different densities were present in different proportions, the sample should not behave in this manner. The sample can be therefore concluded to be homogeneous with respect to the value of the specific refractive index, and hence the flat plot of (LS)/(RI) shown in Fig. 2 is a strong indication that the particles are homogeneous with respect to molar mass according to eqn. 1. The plot of $(UV)/(LS)/(RI)^2$ (not shown) was, however, less flat. This is an inevitable consequence of the serial arrangement of the three detectors, which adversely affects the solute distribution and thus the conformity of the three elution curves.

The specific refractive index increment in eqn. 1 was calculated to be 0.164 ml/g for the Pre S(+) vaccine particle from the weighted average [protein, 53%; lipids, 36%; sugars, 11% (w/w)] of the refractive index increments of the components, assumed to be 0.187, 0.134 and 0.148 ml/g, respectively. For the Pre S(−) particle, no data are available for its composition and the same value as that for the Pre S(+) particle was tentatively assumed. This might be allowed as a first approximation, because the (RI)/(UV) ratio for the Pre S(−) particle was the same as that for the Pre S(+) particle.

Using the value of (dn/dc), the molar masses of the Pre S(+) and Pre S(−) HBsAg particles were calculated to be 5040 ± 480 and 4640 ± 240 kg/mol ($n=3$), respectively, according to eqn. 1. The scale of concentration in the value of (dn/dc) is the weight of the total vaccine particle, and the molar mass thus obtained by light-scattering measurements is the total molar mass of the particle.

On the other hand, the molar mass can also be obtained by using eqn. 2. The extinction coefficient was obtained by the procedure proposed by Edelhoch[4], in which the extinction coefficient on the basis of concentration expressed in terms of g/dl can be calculated from the equation

$$E_1^{1\%}{}_{cm} = (10/M_W)(N_{Trp} \cdot 5690 + N_{Tyr} \cdot 1280) \quad (3)$$

where M_W is molar mass of the Pre S(+) surface atigen protein, N_{Trp} and N_{Tyr} are the contents in residue numbers of tryptophan and tyrosine, respectively, in the Pre S(+)surface antigen protein molecule and 5690 and 1280 are the extinction coefficients of tryptophan and tyrosine residues, respectively. Although eqn. 2 is for a denatured protein in 6 *M* guanidine hydrochloride, the same values can be safely assumed for a native protein without correction, as a first approximation. The Pre S(+) surface antigen protein molecule contains thirteen tryptophan and five tyrosine residues. The extinction coefficient, $E_1^{1\%}{}_{cm}$ in eqn. 3, was found to be 30.9 dl/g · cm. The value for the Pre S(−) surface antigen protein was calculated to be 32.1 dl/g · cm, taking the absence of the Pre S peptide into consideration.

Using the values of the extinction coefficients the molar masses of the Pre S(+) and Pre S(−) vaccine particles were calculated to be 3030 ± 380 and 2440 ± 150 kg/mol ($n=3$), respectively, according to eqn. 2. The scale of concentration in the value of (dn/dc) is the weight of the protein moiety of the respective vaccine particle, and the molar mass thus obtained by light-scattering measurements is the molar mass of the protein moiety.

DISCUSSION

In serum from a patient or carrier of human hepatitis B, a small particle with a diameter of about 22 nm can be observed and has been found consist of the surface antigen of hepatitis B virus particle (HBsAg). The HBaAg particle described here is a particle equivalent to the above natural particle, produced by yeast according to the gene engineering technique. It is interesting that the engineered yeast produces a particle similar to that produced by human cell invaded by hepatitis B virus. Physico-chemical characterization of the egineered particle seemed to provide useful information for the utilization of the particle as a vaccine against hepatitis B, and the present study was started with this motivation.

Electron microscopic observations suggested that there is limited distribution in their sizes[2]. The present results however, strongly indicate that the vaccine particles, both Pre S(+) and Pre S(−) types, are homogeneous with respect to their molar masses and sizes. The molar masses of the Pre S(+) and Pre S(−) HBsAg particles were calculated to be 5040 and 4640 kg/mol, respectively and those of the protein moiety 3030 and 2440 kg/mol, respectively. These values indicate that the Pre S(+) and Pre S(−) particles are composed of 116 and 102 copies of the HBsAg proteins, respectively. The Pre S(+) particle was calculated to be 9 and 24% larger in its molar mass than the Pre S(−) type particle with respect to the total particle and protein moiety, respectively. These figures should not show such a difference if their compositions with respect to molar ratios were the same. Both are, however, significantly larger than the increase expected solely from the presence of the additional nonapeptides. This point needs further careful study and is under further investigation using the dynamic light-scattering technique. The effect of the presence of such an additional peptide or even protein on the nature of such a protein–lipid vaccine particle is worthy of further detailed investigation, because such particles seem to be excellent vehicles for covalently bound biologically active components.

As shown in Fig. 2, the ratios of the outputs of the detectors, such as (LS)/(RI), were constant in the peak region except at the edges. The peaks were unexpectedly broad, however, for the HBsAg particles giving a broad peak. Rechromatography gave a single peak at the same position as in the initial run whether the sample was collected in the front or in the rear region. Application of a sample such as dextran T500 with a skewed molar mass distribution gave an asymmetric peak.

The present results show that particles of large size without a molar mass distribution give a wide peak in the elution curve. It is not yet clear whether a pure molecular sieve effect of the column is responsible for this broadening, or other effects due to the large size of the particle involved. We are currently comparing the elution behavior of other particles of comparable molecular size with that of the vaccine particles.

This study has shown that the engineered vaccine of particle nature against human hepatitis B can be successfully applied to the HPSEC columns and the eluate monitored by a measuring system provided with detectors for molar mass determination. Based on these results, further physico-chemical characterization of the HBsAg particles is now in progress. These studies should be of use in providing examples for the physico-chemical characterization of future vaccine particles for application against various viral diseases.

ACKNOWLEDGEMENTS

We thank Dr. Kohnosuke Fukai of the Research Foundation for Microbial Diseases of Osaka University for his continued encouragement. We also thank Dr. Yoshio Kato of Tosoh for providing the special SW column.

REFERENCES

1 A. Miyanohara, A. Toh-e, C. Nozaki, F. Hamada, N. Ohtomo and K. Matsubara, *Proc. Natl. Acad. Sci. U.S.A.*, 80 (1983) 1–5.
2 A. Takamizawa, H. Fujita, S. Manabe, H. Gohda, N. Isikawa, T. Suzuki, S. Murakami, S. Yoshida, T. Ishikawa, M. Kato, I. Yosida, T. Konobe, K. Takaku and K. Fukai, *Kiso-to-Rinsho (Clin. Rep.)*, 23 (1989) 813–824.
3 T. Takagi, in H. Parvez *et al.* (Editors), *Progress in HPLC: Gel Permeation and Ion-Exchange Chromatography of Proteins and Peptides*, Vol. 1, VNU Science, Amsterdam, 1985, Ch. 3, pp. 27–41.
4 H. Edelhoch, *Biochemistry*, 6 (1967) 1948–1954.

Journal of Chromatography, 507 (1990) 33–44
Elsevier Science Publishers B.V., Amsterdam — Printed in The Netherlands

CHROMSYMP. 1710

High-performance liquid chromatography of amino acids, peptides and proteins

CI[a]. Identification and characterisation of coulombic interactive regions on sperm whale myoglobin by high-performance anion-exchange chromatography and computer-graphic analysis

A. N. HODDER
Department of Biochemistry and Centre for Bioprocess Technology, Monash University, Clayton, Victoria 3168 (Australia)
K. J. MACHIN
St. Vincent's Institute of Medical Research, Princes St., Fitzroy, Victoria 3065 (Australia)
and
M. I. AGUILAR and M. T. W. HEARN*
Department of Biochemistry and Centre for Bioprocess Technology, Monash University, Clayton, Victoria 3168 (Australia)

SUMMARY

A combination of high-performance liquid chromatographic and computer-graphic analysis of the electrostatic interactive surface of sperm whale myoglobin has allowed the putative anion-exchange binding domains to be identified and characterised. These studies have established the existence of four regions of high electrostatic potential in terms of negatively charged amino acid side chain groups. These binding sites are comprised of seven glutamic acid residues, two aspartic acid residues and two propionic acid groups located on the heme moiety which are arranged in a continuous topographic band around one section of the myoglobin surface. The number of charged groups in these interactive patches correlated with the range of experimentally determined Z_c values under different elution conditions of varying gradient time, flow-rate and displacer salt. The changes in Z_c values observed under some chromatographic conditions have been interpreted in terms of the conformational reorientation of the myoglobin molecule as it interacts with the charged stationary phase surface.

[a] For Part C, see ref. 8.

0021-9673/90/$03.50

INTRODUCTION

Recent advances in the development of retention models to describe the interactive properties of proteins separated by high-performance liquid chromatography have demonstrated a complex dependence of chromatographic behaviour on protein three-dimensional structure[1,2]. In particular, the ability of the stationary phase to act as a topographic probe for the surface of a protein solute has provided significant insight into the factors which control the mechanistic basis of protein–surface interactions. For example, protein retention in high-performance ion-exchange chromatography (HPIEC) arises from complex electrostatic interactions between the protein solute and the coulombic sorbent and is dependent on both the number and distribution of charged sites on the protein surface. As demonstrated in various recent studies[3–7], over a limited range of displacing salt concentration, c, the dependence of protein retention of log k' (capacity factor) on log $(1/c)$ can be approximated by the following linear relationship

$$\log k' = \log K + Z_c \log (1/c) \quad (1)$$

where K is an ion-exchange distribution coefficient obtained by extrapolation of plots of log k' versus log $(1/c)$. According to the stoichiometric displacement model[3], the Z_c term, which is the slope of these plots, represents the number of charges involved in the binding of the protein to the stationary phase surface. In anion-exchange chromatography, the magnitude of Z_c is dependent on the buffer pH[3,4], the salt or buffer concentration[5], the type of displacer salt[6,7] and the mode of elution[6]. This variation in Z_c is therefore associated with changes in the interactive surface structure, or the ionotope of the protein. The ability to predict the number of surface regions of high electrostatic potential and to determine the relative interactive or ionotopic dominance of these sites under a particular set of chromatographic conditions would clearly provide significant insight into protein retention behaviour. In an associated study[8], we have characterised the anion-exchange binding site on hen egg white lysozyme (HEWL) in terms of the relative distribution of charged regions on the protein surface through correlation of chromatographic properties and X-ray crystallographic data. Furthermore, variations in the range of Z_c values were interpreted in terms of conformational flexibility of the HEWL molecule during the retention process. The present paper reports the results of a similar analysis of the anion-exchange chromatographic properties and crystallographic data of sperm whale myoglobin (SWM). Regions of negative charge arising from spatially or sequentially juxtaposed glutamic acid and aspartic acid residues were located and analysed in terms of their charge density and surface accessibility, and the data utilised in the development of a model for the interaction of SWM with the positively-charged anion-exchange support surface.

MATERIALS AND METHODS

High-performance anion-exchange chromatography

All chromatographic experiments were performed with a Pharmacia (Uppsala, Sweden) fast-protein liquid chromatography (FPLC) system as previously described[5].

Computer-assisted molecular modelling

Protein-molecular modelling studies were carried out with a Silicon Graphics (Mountain View, CA, U.S.A.) Iris 3120 computer system.

RESULTS AND DISCUSSION

Myoglobin is a single polypeptide chain comprised of 153 amino acid residues, the primary structure of which is shown in Fig. 1. Compared to many globular proteins the myoglobin molecule is unique in terms of its high α-helix content. X-ray crystallographic[9] studies indicate that *ca.* 75% of the amino acid residues are arranged in segments of right-handed α-helices. These helical arrangments lead to a compact and roughly spheroidal molecule with dimensions 45 × 35 × 25 Å. In terms of the anatomy and taxonomy of proteins, myoglobin is representative of the Greek key helix bundle sub-group of proteins characterised by an antiparallel arrangement of α-helical domains[10]. Most polar amino acid residues are located on the surface of the protein while the interior is largely comprised of non-polar residues.

Myoglobin functions as an oxygen-storing protein in skeletal muscle cells. This is achieved by the formation of a complex between oxygen and the prosthetic heme group of the protein. The iron-containing heme group is planar and located in a small pocket between two α-helices, termed the E- and F-helices[9]. The iron atom, located at the centre of the heme, is bound at the fifth coordination site to the imidazole nitrogen of histidine 93 while oxygen complexes at the sixth coordination site. While two polar propionic acid groups of the heme are orientated at the surface of the protein, the heme moiety is predominantly buried within the myoglobin structure.

Myoglobin has an isoelectric point (pI_{SWM}) of 7.68. In anion exchange chromatographic systems where the buffer pH is greater than pI_{SWM}, SWM will carry an overall net negative charge, due to the ionisation of glutamic acid (Glu) and aspartic acid (Asp) residues. Myoglobin contains 21 acidic residues which contribute to the surface charge of the protein which could all potentially interact with a positively charged stationary phase surface. While there will be several areas of surface negative charges, the interaction of SWM-related proteins with charged surfaces will, however, be mediated through regions of highest electrostatic potential in terms of negative charge density. In chromatographic systems, the charge stoichiometry of this interaction, which depends on the degree of protein ionisation and the extent of salt–charge interactions in the dominant ionotope, is quantitated by the parameter Z_c. Table I shows the experimentally determined Z_c values representing the number of charged

```
        *         *         *         *         *         *
VLSEGEWQLVLHVWAKVEADVAGHGQDILIRLFKSHPETLEKFDRFKHLKTEAEMKASED
        *         *         *         *         *         *
LKKHGVTVLTALGAILKKKGHHEAELKPLAQSHATKHKIPIKYLEFISEAIIHVLHSRHP
        *         *         *
GDFGADAQGAMNKALELFRKDIAAKYKELGYQG
```

Fig. 1. Primary structure of sperm whale myoglobin. The asterisks denote every tenth residue.

TABLE I

Z_c VALUES FOR MYOGLOBIN AT pH 9.60

Salt	Z_c		
	Elution mode		
	Varied gradient time, constant flow-rate	*Varied flow-rate, constant gradient time*	*Constant flow-rate, isocratic elution*
LiCl	17.75 ± 3.23	6.72 ± 3.11	0.82 ± 0.13
LiBr	1.96 ± 0.66	4.11 ± 0.44	–[a]
NaF	5.49 ± 1.71	1.46 ± 0.14	2.36 ± 0.65
NaCl	4.61 ± 1.57	5.09 ± 0.80	2.76 ± 0.31
NaBr	1.43 ± 0.02	3.48 ± 0.59	2.36 ± 0.69
KF	1.98 ± 0.27	1.32 ± 0.12	–[a]
KCl	4.54 ± 0.75	1.47 ± 0.15	1.43 ± 0.14
KBr	4.84 ± 0.75	6.03 ± 2.26	–[a]

[a] Not eluted with this salt.

interactions between SWM and the positively charged Mono-Q column. These data were derived under elution conditions of pH 9.6 with a variety of alkali metal halide salts as the displacer salt. The Z_c values obtained under these elution conditions, where all acidic amino acid side chain groups will be ionised, were generally in the range between 1 and 6. This result suggests that only a portion of the negatively charged amino acid side chain groups are involved in the interactive process.

Computer simulation of the three-dimensional structure for SWM was therefore carried out to search for clusters of surface accessible glutamic acid (Glu) and aspartic acid (Asp) residues. Initial inspection of the X-ray crystallographic data revealed a complex surface distribution of negative and positive charges as shown in Figs. 2 and 3, respectively. Aspartic acid and glutamic acid residues are shown in red and yellow while pink and blue areas represent the positively charged lysine (Lys) and arginine (Arg) residues, respectively. Because of spatial constraints associated with the protein–ligand interaction four areas on the SWM surface were considered to have the potential to act as anion-exchange binding sites. Generally, it is anticipated that surface interactive patches occur as a result of either sequentially-linked amino acids or via topographic arrangements involving through-space alignment of acidic residues. The patches of negative charge identified on the SWM surface all arise from non-sequential juxtaposition of the Glu and Asp residues.

The first interactive site is shown in Fig. 4, where Glu 105 and Glu 109 located in the G-helix, and Glu 136 in the H-helix, were found to be in close spatial proximity. Another potential anion-exchange binding site located nearby and at the top of the molecule in Fig. 4 incorporates Glu 36, Glu 41 which are both located in the C-helix and Asp 44 in the non-helical CD region. The remaining two sites which are potentially involved in the anion-exchange binding process both incorporate the heme prosthetic group. Fig. 5 shows a view into the cleft containing the heme group where the depth of the picture has been reduced by Z-clipping (a function of the graphics software) to allow clear observation of the potential interactive sites. The surface-

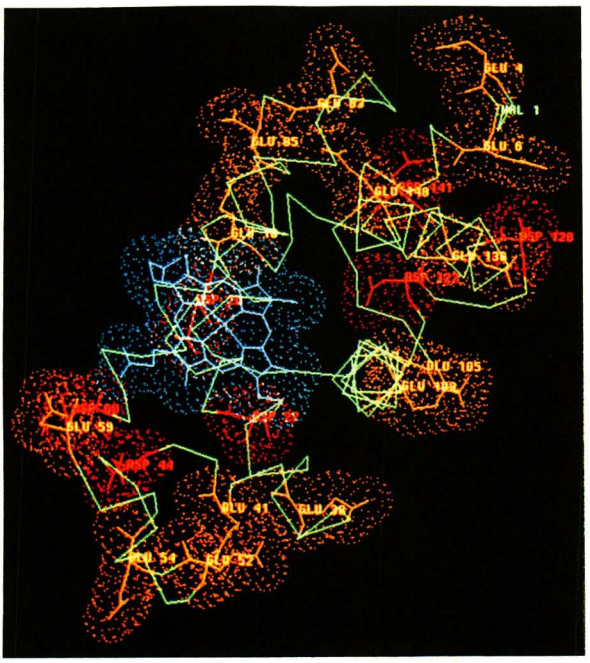

Fig. 2. Computer-graphic simulation of the X-ray crystal structure of SWM showing the location of aspartic acid (red) and glutamic acid (yellow) residues. The prosthetic heme group is shown in blue. Picture produced by a computer program written by A. M. Lesk and K. D. Hardman[22].

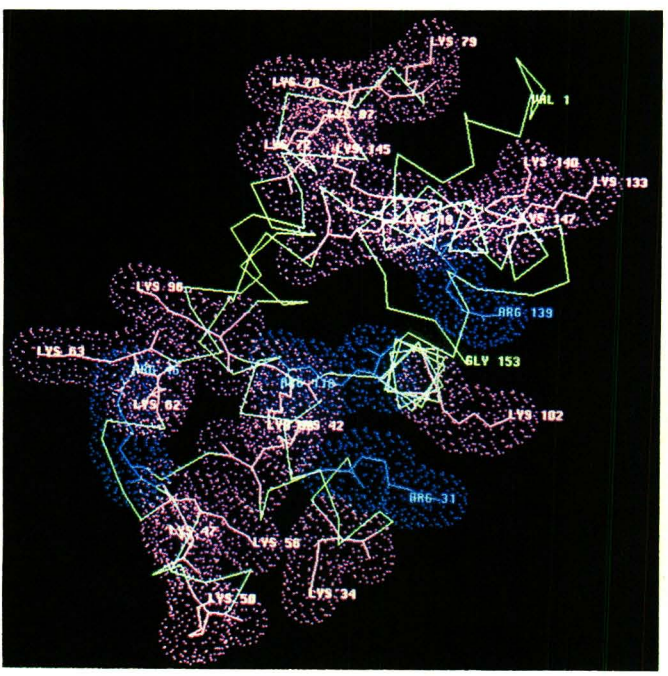

Fig. 3. Computer-graphic simulation of the X-ray crystal structure of SWM indicating the location of lysine (pink) and arginine (blue) residues. Picture produced by a computer program written by Lesk and Hardman[22].

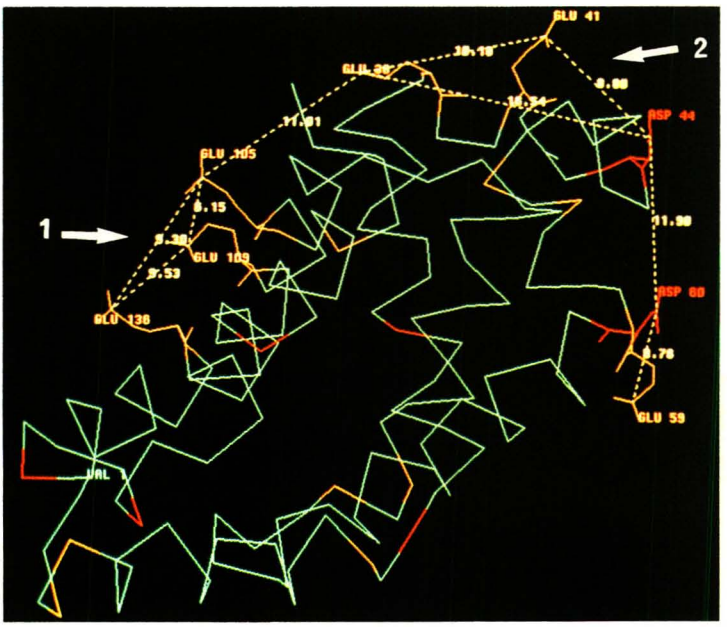

Fig. 4. Computer-graphic representation of the orientation of negatively charged groups located around the heme-derived propionic acid side chains. Contour lines were drawn to obtain the distances between the Glu 105, 109 and 136 in site 1 and Glu 41, 36 and Asp 44 in site 2. The charge densities of these triangles are listed in Table II. Picture produced by a computer program written by Lesk and Hardman[22].

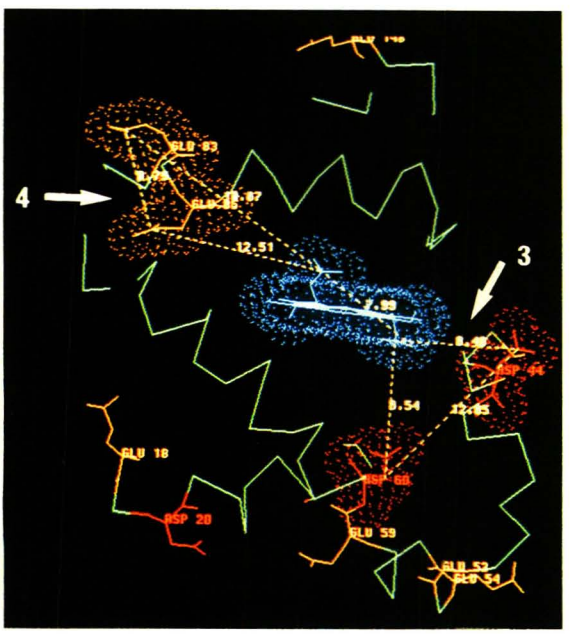

Fig. 5. Computer-graphic analysis of the distances between Asp 44, 60 and one heme propionic acid group (site 3) and Glu 83, 85 and a second heme propionic acid group (site 4). The resulting charge density values are listed in Table II. The spatial depth of the picture has been reduced by Z-clipping to facilitate visual analysis. Picture produced by a computer program written by Lesk and Hardman[22].

accessible propionic acid side-chains of the porphyrin ring have a *trans*-configuration. At high pH both propionic acid groups will be negatively charged and have the potential to participate in electrostatic interactions. The close spatial proximity of Asp 60, 44 and Glu 83, 85 to the propionic acid groups generates one if not two areas that have the potential to participate in the anion-exchange binding process.

Protein–surface interactions in anion-exchange chromatography will be mediated through the negatively charged regions of highest electrostatic potential. The ranking of these areas in terms of the magnitude and direction of the charge vector will provide further information on the relative significance of these four regions in terms of their role in the approach and orientation of the protein solute to the stationary phase in the intitial stages of adsorption. The charge density of the four potential interactive sites was therefore determined to assess the relative influence of each site in both steering the molecule toward the support surface and its position in the interactive hierarchy. In Figs. 4 and 5 the distances between proximal negatively charged groups are illustrated. Sites 1 and 2 are shown in Fig. 4 while sites 3 and 4 incorporating the heme group are shown in Fig. 5. Estimates of the charge density (charge per unit area) were calculated using the areas obtained for the dotted contours of each binding site and the resultant values are shown in Table II. Site 1, which encompasses Glu 105, 109 and 136 has the highest charge density, namely 0.37 charge/10 $Å^2$. This information indicates that these charged residues located in the G- and H-helices will under conditions of near equilibrium be important in steering the myoglobin molecule from the bulk solvent toward the stationary phase via attractive, electrostatic forces.

While the regions of high electrostatic potential will dominate the interaction of the protein solute with the anion-exchange sorbent, the relative spatial disposition of neighbouring positive and even neutral groups will also play an important role in the approach and orientation of the protein solute at the stationary phase surface. The alignment of SWM shown in Fig. 2 was rotated to allow the influence of neighbouring positively charged groups to be assessed. This indicated that the site 1 residues comprising Glu 105, 109 and 136 project from the protein surface to form an unobstructed region of negative charge. However, in site 2, comprised of Glu 36, 41 and Asp 44, the positively charged Lys 42 was found to project out of the plane directly between residues 38 and 44. As a consequence, this residue will sterically interfere with the binding process and significantly inhibit the approach and orientation of this potential binding site to the anion-exchange support surface.

TABLE II

CHARGE DENSITY FOR POTENTIAL BINDING SITES ON SPERM WHALE MYOGLOBIN

Location: Site 1 = Glu 105, 109 and 136; site 2 = Glu 41, 36 and Asp 44; site 3 = Asp 44, 60 and heme propionic acid; site 4 = Glu 83, 85 and heme propionic acid.

Site	*Charge (per 10 $Å^2$)*
1	0.37
2	0.26
3	0.25
4	0.21

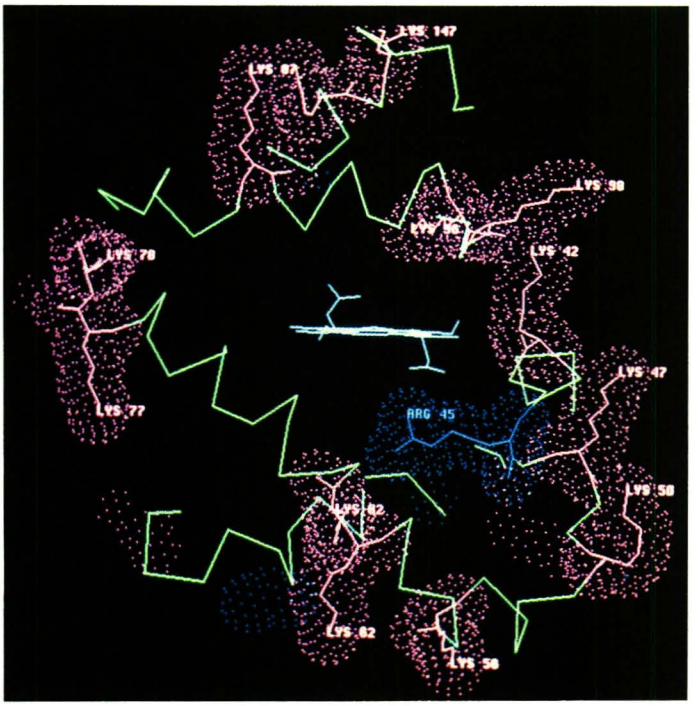

Fig. 6. Computer-graphic representation of the distribution of positively charged lysine (pink) and arginine (blue) residues in the anion-exchange binding sites 3 and 4. The spatial depth of the picture has been reduced by Z-clipping to facilitate visual analysis. Picture produced by a computer program written by Lesk and Hardman[22].

In Fig. 6, the distribution of the positively charged Lys and Arg residues around sites 3 and 4 is shown from the same viewpoint as depicted in Fig. 5. The general distribution of positive charge in this area does not directly interfere with the potential binding sites shown in Fig. 5. However, Arg 45 is located between Asp 44 and 60 and is orientated toward the lower propionic acid groups as shown in Fig. 6. In the X-ray crystal structure, Arg 45 is reported[11] to be salt-linked to this particular acid group. During binding to the anion-exchanger it is possible that electrostatic repulsion will reorientate Arg 45 away from the propionic acid side-chain to permit increased electrostatic interaction between site 3 and the stationary phase.

Close inspection of Fig. 4 also reveals that the four areas identified as anion-exchange binding sites are arranged in a continuous topographic band around a specific region on the myoglobin molecule. If the native structure is maintained, then steric restrictions will prevent all of these residues interacting with the support surface at the same time. However, a wide range of Z_c values was obtained for myoglobin eluted by various neutral salts and elution modes at buffer pH 9.6, which suggests that the molecule is undergoing some degree of conformational reorientation or unfolding at the surface of the sorbent. Inspection of the Z_c values for each of the three different elution modes (Table I) indicates that neutral salts significantly influence the size of

the anion-exchange binding site on myoglobin. Neutral salts can influence the structure of macromolecules via complicated changes to the layer of hydration and electrostatic potential at the protein surface. The small fluctuations in Z_c values observed for different salts (*i.e.*, when Z_c values remain between 1 and 3) may indicate small movements in the structural subunits or domains, which influence the degree of electrostatic interaction between residues of a single binding site and the stationary phase. Studies on the structural dynamics of myoglobin[12] indicate that this conformational equilibrium is possible as the α-helices in this protein do not only move as rigid units but may also experience rippling or breathing modes. Larger changes in the magnitude of Z_c values will indicate the occurrence of more extensive structural reorientations resulting in an increased number of residues interacting with the stationary phase surface. For example, the change from NaF to NaCl, with varied flow elution, resulted in the Z_c value increasing from *ca.* 1.5 to 5.1, respectively. If binding sites 1 to 4 are involved in the retention process then some unfolding will be necessary to permit five negatively charged residues to interact simultaneously with the support surface.

In Table I the magnitude of the Z_c value is also observed to change significantly with variation in the mode of elution. For example, the elution of SWM by NaF resulted in Z_c values of *ca.* 5.5, 1.5 and 2.4 for the varied gradient time, varied flow-rate and isocratic modes of elution. Consequently, the rate of change of the displacer salt concentration not only determines the column residence time for the protein but also affects the dynamic geometry of the protein molecule[13]. The fluctuations in Z_c observed between each elution mode in Table I could therefore reflect the preferential solute–stationary phase interaction through different binding sites on the surface of SWM.

Inspection of Fig. 1 reveals that there are 21 Glu and Asp residues in the primary sequence of SWM, while there are 11 residues implicated in anion-exchange binding sites 1–4. Although the Z_c values shown in Table I vary from *ca.* 1 to 18, the majority of values fall between 1 and 6. If the three-dimensional structure of SWM as it interacts with the stationary phase surface, is approximated by the X-ray crystal structure, then allowing for some steric restrictions, the range of Z_c values of 1–6 in Table I indicates that only a proportion of these sites will be involved in the binding process. However, when myoglobin is eluted with LiCl, under varied gradient time conditions, the Z_c value (*i.e.*, $Z_c = 17.75$) approaches the total number of Glu and Asp residues present in this protein. This result almost certainly reflects the situation where the majority of Glu and Asp groups have electrostatically bound to the stationary phase during elution. Such an event would require the total unfolding of the myoglobin molecule. One mechanism through which this apparent surface-mediated phenomenon may occur is via the initial binding of the "steering" residues in site 1 to the stationary phase. The molecule could then unfold in a rolling manner as adjacent sites (*i.e.*, 1 to 4) progressively bind as a preferred sequence of events. This phenomenon, shown schematically in Fig. 7, is analogous to the unrolling of a carpet, and would permit an increased number of electrostatic interactions to arise from the geometrical flattening of the myoglobin molecule.

The physicochemical processes which underly the interaction of proteins with chromatographic surfaces are analogous to the environmental and structural factors which control cellular biorecognition processes such as hormone–receptor and antibody–antigen reactions. The surface structures of a number of proteins have been

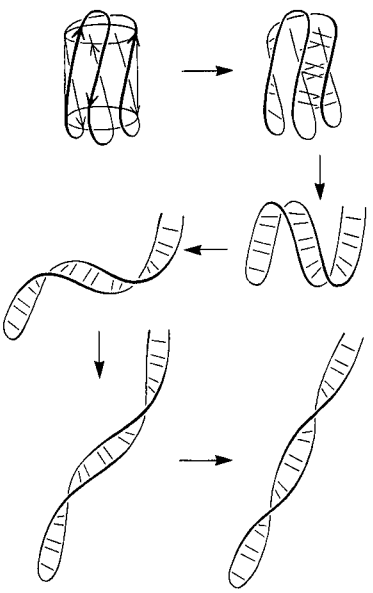

Fig. 7. Schematic representation of the conformational unravelling of the helical domains of SWM.

probed in considerable detail by immunochemical techniques. In particular, a variety of antigenic determinants (epitopes) have been mapped on SWM using anti-myoglobin antibodies and T-cell clones. Up to nine continuous epitopes, comprising sequentially linked amino acid residues, have been identified immunologically by recognition of a variety of peptides derived from the digestion of the native protein[14–18]. Furthermore, monoclonal antibodies to SWM have also been shown to recognise determinants that differ from the continuous epitopes. These differences were attributed to the variation in conformation associated with topographically —rather than sequentially— linked residues on the protein surface involved in antibody binding. Similarly, two further antigenic determinants on the G- and H-amphipathic helices in myoglobin have been defined by reactivity with T-cell clones[19–21]. The factors which predispose particular amino acid residues to be antigenic or immunogenic are not fully known or understood. While it is generally considered that accessibility of surface amino acid residues is a major contributing factor, the precise physicochemical requirements of the epitope structure, such as the number of hydrophobic, hydrophilic and neutral residues, have not yet been determined. In Table III the amino acid residues identified in each antigenic determinant of SWM are compared to the residues predicted to constitute electrostatic interactive ionotopes at the surface of SWM. Most significantly, all the residues that define the anion-exchange binding sites are also located within the known B-cell and T-cell epitopes. Moreover, the fourteen epitopes listed in Table III all contain charged residues (*i.e.*, Glu, Asp, Lys or Arg) and eleven of these epitopes contain Glu or Asp groups.

It is apparent from these observations that the distribution and surface accessibility of Glu and Asp residues play an important role in the overall antigenicity of myoglobin. The results of the present study therefore demonstrate that the correla-

TABLE III

COMPARISON OF THE POTENTIAL ANION-EXCHANGE BINDING SITES TO THE KNOWN ANTIGENIC DETERMINANTS ON SPERM WHALE MYOGLOBIN

Residues	
Anion-exchange sites	*Antigenic sites*
	B-cell continuous epitopes[14–18]
1 = 105, 109 and 136	1–6, 15–22, 22–55, 56–62,
2 = 36, 41 and 44	72–89, 94–99, 113–119,
3 = 44, 60 and heme propionic acid	121–127 and 145–151
4 = 83, 85 and heme propionic acid	
	B-cell topographic epitopes[19]
	Mab 1 = 4 and 79
	Mab 2 = 83, 144 and 145
	Mab 3 = 140, ?
	T-cell epitopes[20–21]
	clone 1.2, 9.27 = 102–118
	clone 14.5 = 132–153

tion between anion-exchange chromatographic data and X-ray structural data can be used to partially define and characterise immunologically active amino acid residues on SWM. These studies also document further an experimental approach pertinent to the characterisation of protein–surface reactivity in biological systems via detailed topographic mapping of protein-interactive surfaces through a combined analysis of chromatographic data derived from electrostatic, hydrophobic or related modes of protein–ligand interactions.

ACKNOWLEDGEMENTS

Research grants to M.T.W.H. from the National Health and Medical Research Council, the Australian Research Council and the Monash University Research Fund Committee are gratefully acknowledged.

REFERENCES

1 M. T. W. Hearn and M. I. Aguilar, in Z. Deyl, (Editor), *Separation Methods*, Elsevier, Amsterdam, 1988, p. 107.
2 F. E. Regnier, *Science (Washington, D.C.)* 238 (1987) 319.
3 W. Kopaciewicz, M. A. Rounds, J. Fausnaugh and F. E. Regnier, *J. Chromatogr.*, 266 (1983) 3.
4 M. T. W. Hearn, A. N. Hodder, P. G. Stanton and M. I. Aguilar, *Chromatographia*, 24 (1987) 769.
5 M. T. W. Hearn, A. N. Hodder and M. I. Aguilar, *J. Chromatogr.*, 458 (1988) 27.
6 W. Kopaciewicz and F. E. Regnier, *Anal. Biochem.*, 133 (1983) 251.
5 M. T. W. Hearn, A. N. Hodder and M. I. Aguilar, *J. Chromatogr.*, 443 (1988) 97.
8 M. T. W. Hearn, A. N. Hodder and M. I. Aguilar, *J. Chromatogr.*, submitted for publication.
9 J. C. Kendrew, R. E. Dickerson, B. E. Stradberg, R. G. Hart, D. R. Davies, D. C. Phillips and V. C. Shore, *Nature (London)*, 185 (1960) 422.
10 J. S. Richardson, *Adv. Protein Chem.*, 24 (1981) 167.
11 J. C. Kendrew, *Brookhaven Symp. Biol.*, 15 (1962) 216.
12 H. Frauenfelder, G. A. Petsko and D. Tsernoglou, *Nature (London)*, 280 (1979) 558.
13 A. N. Hodder, M. I. Aguilar and M. T. W. Hearn, *J. Chromatogr.*, 476 (1989) 391.

14 M. Z. Atassi, *Eur. J. Biochem.*, 145 (1984) 1.
15 H. E. Schmitz, H. Atassi and M. Z. Atassi, *Mol. Immunol.*, 19 (1982) 1699.
16 C. R. Young, H. E. Schmitz and M. Z. Atassi, *Mol. Immunol.*, 20 (1983) 567.
17 H. E. Schmitz, H. Atassi and M. Z. Atassi, *Immun. Commun.*, 12 (1983) 161.
18 S. J. Leach, *Biopolymers*, 22 (1983) 425.
19 J. A. Berzofsky, G. K. Buckenmeyer, G. Hicks, F. R. N. Gurd, R. J. Feldmann and J. Minna, *J. Biol. Chem.*, 257 (1982) 3189.
20 H. Z. Streicher, I. J. Berkower, M. Busch, F. R. N. Gurd and J. A. Berzofsky, *Proc. Natl. Acad. Sci., U.S.A.*, 81 (1984) 6831.
21 K. B. Cease, I. Berkower, J. York-Jolley and J. A. Berzofsky, *J. Exp. Med.*, 164 (1986) 1779.
22 A. M. Lesk and K. D. Hardman, *Science (Washington, D.C.)*, 216 (1982) 539.

Journal of Chromatography, 507 (1990) 45–49
Elsevier Science Publishers B.V., Amsterdam — Printed in The Netherlands

CHROMSYMP. 1692

Modification of the selectivity of a reversed-phase high-performance liquid chromatographic system by binding sodium dodecyl sulphate to peptides

L. DALLA LIBERA
CNR Unit for Muscle Biology and Physiopathology, Institute of General Pathology, University of Padova, Via Trieste 75, 35100 Padova (Italy)

SUMMARY

Cytochrome *c* and myoglobin were subjected to sodium dodecyl sulphate (SDS) polyacrylamide gel electrophoresis, electroeluted from the gel and fragmentated with cyanogen bromide. High-performance liquid chromatographic (HPLC) separation of the peptide mixtures obtained was improved when using a gradient of acetonitrile containing phosphates in comparison with a gradient containing trifluoroacetic acid. This finding may be useful for the HPLC analysis of peptides derived from SDS–protein complexes.

INTRODUCTION

Polyacrylamide gels are widely used media for the analytical separation of proteins and peptides. Although these procedures are generaly thought of as analytical techniques, they also provide a powerful preparative technique for small amounts of protein if the protein can be removed from the gel once the protein positions have been located[1]. It should be noted that for many proteins, particularly large hydrophobic proteins, polyacrylamide gel electrophoresis in the presence of sodium dodecyl sulphate (SDS-PAGE) is an easy method for the final stage of the purification procedure. Interestingly, the recovered protein is suitable for chemical and enzymatic fragmentations. The peptides derived can be separated and purified by reversed-phase liquid chromatography, in order to obtain information about the primary sequence of a given protein[2].

By reversed-phase chromatography and C_{18} column, we have analysed the cyanogen bromide fragments derived from proteins purified by SDS-PAGE and then electroeluted. Employing the most widely used mobile phase system, *i.e.*, a gradient of a water–acetonitrile mixture in the presence of low concentrations of trifluoroacetic acid (TFA), we observed that peptides displayed long retention times and were very poorly separated. In this paper we present a method that overcomes these difficulties, allowing a better resolution of the peaks.

0021-9673/90/$03.50

EXPERIMENTAL

Reagents

Water was distilled from glass and filtered through a 0.45-μm Millipore filter. Potassium phosphate buffer (analytical-reagent grade) was obtained from Merck (Darmstadt, F.R.G.), TFA from BDH (Poole, U.K.), acetonitrile from Carlo Erba (Milan, Italy) and cyanogen bromide from Fluka (Buchs, Switzerland).

Protein preparation and cyanogen bromide treatment

Myoglobin and cytochrome *c* (horse heart) were obtained from Sigma (St. Louis, MO, U.S.A.) and Boehringer (Mannheim, F.R.G.), respectively. About 10 mg of each protein were subjected to preparative SDS-PAGE on 15% polyacrylamide gel, as described previously[1]. After equilibration in electroelution buffer, the portion of the gel containing each protein was electroeluted in a ISCO (Lincoln, NE, U.S.A.), apparatus and lyophilized. In some experiments SDS was removed from proteins by ion-pair extraction[3]. The lyophilized proteins were dissolved in 70% formic acid and cleaved at methionyl residues with cyanogen bromide[2]. After recovery, the resulting mixtures of peptides were dried under a stream of nitrogen and dissolved in 70% formic acid.

Apparatus

A Perkin-Elmer (Norwalk, CT, U.S.A.) high-performance liquid chromatographic (HPLC) system was used as described previously[4]. A Bakerbond TM C_{18} (15 μm) wide-pore (330 Å) column (25 cm × 0.46 cm I.D.) was obtained from Baker (Phillisburg, NJ, U.S.A.). A guard column obtained from Upchruch (Oak Harbour, WA, U.S.A.) was always used to protect the main column.

HPLC method

All chromatografic runs were carried out at room temperature af a flow-rate of 1.0 ml/min. Peptide elution was accomplished by the application of a binary gradient from 0 to 50% acetonitrile containing either 0.1% (w/v) TFA or potassium phosphate buffer (pH 5.9) as indicated in the legends of the figures.

RESULTS AND DISCUSSION

The cyanogen bromide fragments derived from proteins electroeluted from polyacrylamide gels were analysed by reversed-phase HPLC on a C_{18} column using two different mobile phase modifiers, TFA and phosphate buffer. Significant differences in the peptide elution profiles are evident when different separation conditions are used, as illustrated in Fig. 1.

When the elution is performed with a mobile phase containing 0.1% TFA (Fig. 1a and b), the separations are poor and several peptides are strongly retained by the column. On replacing TFA by 20 m*M* phosphate buffer, not only a marked reduction in retention times of the peptides but also an improvement in their separation are obtained (Fig. 1c and d).

It is well known that salts in the mobile phase may be corrosive towards the steel of the pumps and of the chromatographic column. Moreover, low concentra-

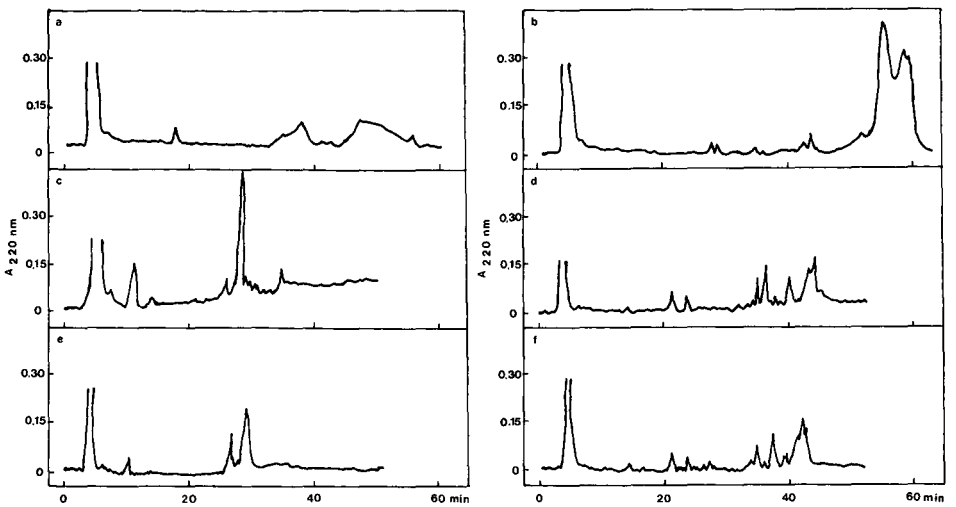

Fig. 1. Separation by HPLC of cyanogen bromide fragments of proteins electroeluted from acrylamide gels. The protein fragments were applied to a Bakerbond TM C_{18} wide-pore (330 Å) column (25 × 0.46 mm I.D.) and eluted with a 50-min linear gradient from 0 to 50% acetonitrile. Temperature, ambient; flow-rate, 1.0 ml/min. Mobile phase additives: (a), (b) 0.1% TFA (w/v); (c), (d) 20 m*M* potassium phosphate buffer (pH 5.9); (e), (f) 5 m*M* potassium phosphate (pH 5.9). (a), (c), (e) Cytochrome *c*; (b), (d), (f) myoglobin.

tions of salts in the chromatographic system make it easier to perform further analyses of the collected peptides, such as amino acid analysis. We therefore tested the quality of the separation obtained by the use of a mobile phase containing 5 m*M* phosphate buffer. These separations are very similar to but not identical with those resulting from 20 m*M* phosphate in that they are characterized by a lower quality (compare Fig. 1c and d with e and f). Nevertheless, it is worth stressing that the addition of such a small amount of buffer (5 m*M*) still produces separations that are better than those obtained with 0.1% TFA (compare Fig. 1a and b with e and f).

The profile obtained from an electroeluted protein is different form that typical of a non-electrophoresed protein, *i.e.*, in the absence of SDS. As an example, one can compare the cyanogen bromide digestion profile of the electroeluted form of cytochrome c (Fig. 1a) with that of the non-electrophoresed form of cytochrome c (Fig. 2a), obtained using a gradient of acetronitrile containing TFA in both instances.

The loss of separation observed in the elution pattern of fragments derived from electroeluted proteins could be related to the presence SDS bound to the peptides. To test this possibility, we performed the cyanogen bromide digestion of cytochrome *c* subjected to electroelution and then to removal of SDS by ion-pair extraction, as described elsewhere[3]. The chromatographic profile is shown in Fig. 2b. It is evident that the separation of fragments performed with TFA as mobile phase modifier is poorer than that of non-electroeluted cytochrome *c* (Fig. 2a); however the quality of the separation is better than that obtained for electroeluted protein which contains SDS (Fig. 1a).

Electrophoretic purification is a very powerful technique that allows the separation of small amounts of very pure proteins. It is also known that the SDS used in

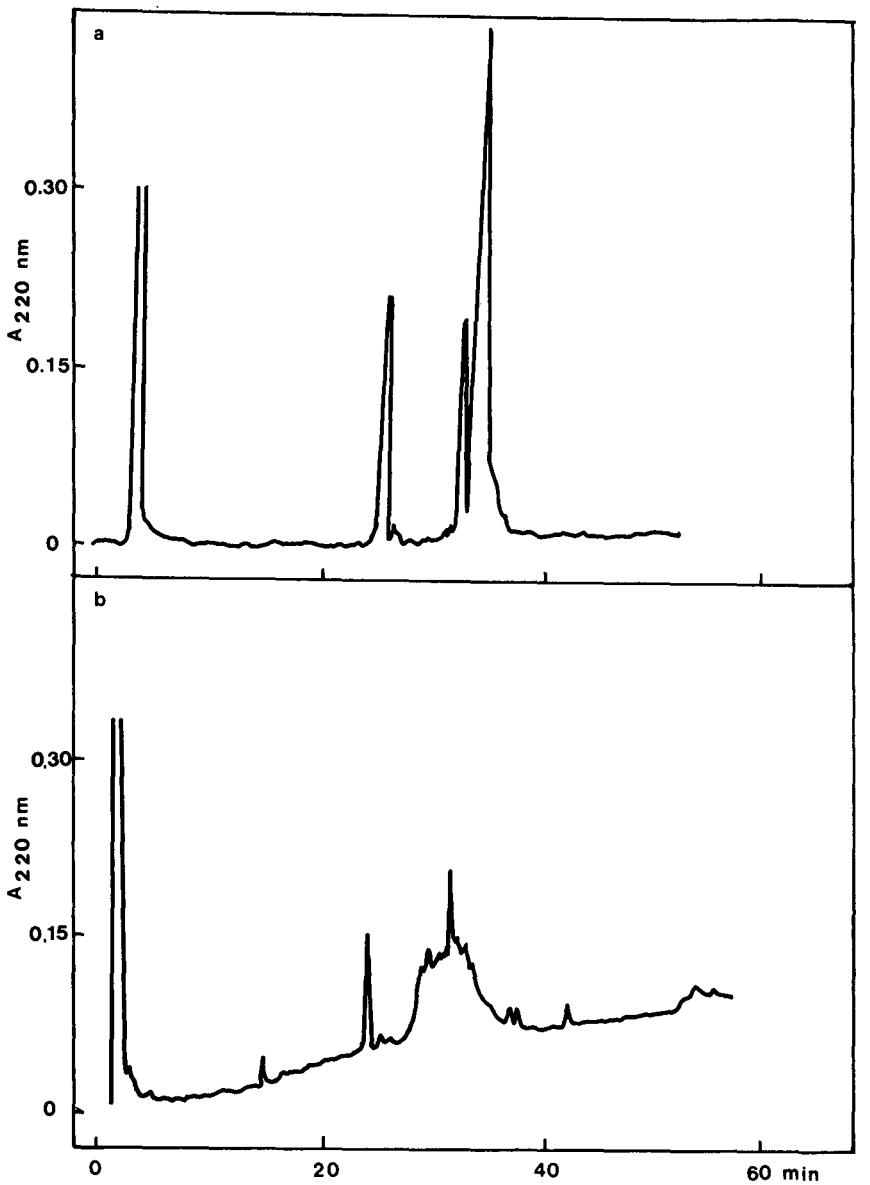

Fig. 2. Separation by HPLC of cyanogen bromide fragments of cytochrome *c*. Column and gradient as in Fig. 1, with acetonitrile containing 0.1% (w/v) TFA. (a) Cytochrome *c* not subjected to SDS-PAGE and electroelution; (b) cytochrome *c* subjected to SDS-PAGE electroelution and then removal of SDS.

the electrophoretic run binds tightly to most proteins. Several procedures have been described for the removal of SDS from electroeluted proteins, but have the disadvantage that losses are frequently encountered when only small amounts of samples are used.

We have observed that a mobile phase containing the most popular modifier, TFA[5], does not produce satisfactory separations of the fragments derived from cyanogen bromide cleavage, probably owing to the presence of SDS bound to the peptides. However, for the same peptides, we have found that the addition of millimolar amounts of phosphate buffer to the mobile phase reduces the retention times and improves the separation. This is not surprising, bearing in mind that phosphate in a variety of forms has found wide application as an additive in mobile phases used in the analysis of amino acids, peptides and proteins by HPLC (see ref. 6 for a review). Interestingly, the peptides so obtained are in a form suitable for gas-phase sequence analysis[2].

ACKNOWLEDGEMENTS

The skillful technical assistance of Mr. S. Belluco is gratefully acknowledge. The author is particularly indebted to Drs. U. Carraro and I. Mussini for helpful suggestions.

REFERENCES

1 L. Dalla Libera, R. Betto, R. Lodolo and U. Carraro, *J. Muscle Res. Cell Motil.*, 5 (1984) 411–426.
2 J. H. Collins, J. L. Theibert and L. Dalla Libera, *Biosci. Rep.*, 6 (1986) 655–661.
3 W. A. Konigsberg and L. Henderson, *Methods Enzymol.*, 91 (1983) 254–259.
4 L. Dalla Libera, R. Betto and D. Biral, *J. Chromatogr.*, 264 (1983) 164–169.
5 F. E. Regnier, *Science*, 222 (1983) 245–252.
6 C. A. Bishop, in W. S. Hancock (Editor), *Handbook of HPLC for the Separation of Amino acids, Peptides and Proteins*, Vol. I, CRC Press, Boca Raton, FL, 1984, 153–159.

Journal of Chromatography, 507 (1990) 51–57
Elsevier Science Publishers B.V., Amsterdam — Printed in The Netherlands

CHROMSYMP. 1704

Development and validation of a high-performance liquid chromatographic method for the determination of desmosines in tissues

E. GUIDA, M. CODINI, C. A. PALMERINI and C. FINI
Dipartimento di Medicina Sperimentale e Scienze Biochimiche, Università di Perugia, Via del Giochetto, 06100 Perugia (Italy)
C. LUCARELLI
Istituto Superiore di Sanità, Rome (Italy)
and
A. FLORIDI*
Dipartimento di Medicina Sperimentale e Scienze Biochimiche, Università di Perugia, Via del Giochetto, 06100 Perugia (Italy)

SUMMARY

The development and the validation of a general strategy for the simple and accurate analysis of desmosines (isodesmosine and desmosine) in tissues coupled with the determination of collagen (as hydroxyproline) is described. The method is based on simplified sample (*i.e.*, lung) pretreatment which involves, in a PTFE screw-capped Pyrex tube, homogenization, collagen estraction with hot 5% trichloroacetic acid and hydrolysis of the elastin-containing residue with 6 *M* hydrochloric acid, followed by cellulose minicolumn purification of desmosines from the hydrolysates, dansyl chloride pre-column derivatization of the purified desmosines and reversed-phase high-performance liquid chromatographic (HPLC) analysis of the dansyl derivatives using a Spherisorb ODS-2 column, an on-column enrichment sample device and a linear gradient of organic modifier (acetonitrile) in phosphate buffer. The simple sample pretreatment, the optimized chromatographic conditions and the short HPLC analysis time (less than 15 min) allow the accurate and rapid determination of desmosine and isodesmosine, thus permitting the determination of elastin in several kinds of tissues with a minimum of sample manipulation.

INTRODUCTION

Structural and metabolic studies on elastin, a protein present in most types of connective tissues, need a suitable method for the determination of desmosine and isodesmosine (DID), the major cross-linking amino acids of elastin. The accurate determination of these cross-linking markers allows the determination of the elastin content in tissues, obviating laborious extraction procedures.

0021-9673/90/$03.50

On the other hand, several problems regarding DID determination make their analysis difficult, as indicated by the high number of methods developed. Conventional ion-exchange chromatography[1–3], thin-layer chromatography[4,5] and immunoassays[6–9] have been employed to determine DID; more recently, high-performance liquid chromatography (HPLC) with[10,11] and without[12–15] precolumn derivatization has been used for the determination of these cross-linkers in pure elastin[10,11] or in tissue hydrolysates[12–14]. Immuno- and conventional ion-exchange chromatographic assays, and also HPLC without precolumn derivatization, often require a multi-step sample manipulation prior to analysis, or they lack specificity and sensitivity or involve time-consuming chromatographic analysis. More success has been achieved with reversed-phase chromatography by using precolumn derivatization with dansyl chloride (DNS-Cl)[10] or naphthalenedialdehyde–cyanide[11]; however, the method was limited to the determination of desmosines in a pure elastin sample, not in tissues.

In this paper, we report a general strategy for the determination of DID in tissues. The method is based on a DNS-Cl precolumn derivatization of the cross-linkers purified by cellulose minicolumns from tissue hydrolysates and a rapid separation and determination of the derivatives by reversed-phase HPLC with a precolumn sample enrichment device. Owing to the concentration and purification pretreatment of the samples and the precolumn enrichment chromatographic system, the method allows the determination of DID in the picomole range, thus permitting the determination of elastin in tissue samples of low elastin content, such as foetal lungs.

EXPERIMENTAL

Chemicals

Crystalline DNS-Cl and a standard mixture of free amino acids were purchased from Sigma (St. Louis, MO, U.S.A.). Pure desmosine, isodesmosine and elastin from bovine ligamentum nuchae were supplied by Elastin Products (Pacific, MO, U.S.A.). Potassium dihydrogenphosphate, hydrochloric acid, acetic acid, potassium hydroxide, sodium hydrogencarbonate and *n*-butanol were analytical-reagent grade products from Merck (Darmstadt, F.R.G.). Cellulose powder (Watman CF-1) was obtained from W. & R. Balston (Maidstone, U.K.). HPLC-gradé acetonitrile, acetone and water were obtained from Inalco (Milan, Italy).

Standards

Stock solutions of desmosine and isodesmosine were prepared in 0.01 *M* hydrochloric acid. The concentration of DID solutions was adjusted to 2 μmol/ml by spectrophotometric determination using $\varepsilon = 4900$ at 268 nm for desmosine and $\varepsilon = 7850$ at 278 nm for isodesmosine[16]. Aliquots (0.1 ml) of cross-linker solutions and of standard mixture of amino acids (2.5 μmol/ml) were diluted to 2 ml with 6 *M* hydrochloric acid and processed according to the cellulose minicolumn method[17]. The aqueous eluate from the cellulose column was lyophilized and the residue dissolved in 2 ml of 0.01 *M* hydrochloric acid. This solution was used as a working standard solution for the chromatographic calibration.

Tissue samples

Aorta and liver samples from a 120-g rat were removed, rinsed in 0.9% sodium chloride solution, stripped of adhering tissue, weighed, cut into small pieces, poured into a PTFE screw-capped Pyrex tube, frozen, lyophilized and then dried at 40°C under vacuum and weighed again. Rabbit foetuses of 30-days gestational age were used as a source of foetal lungs; the organs were removed from the thorax and treated as the aorta sample.

Dried tissue samples (usually 50–100 mg) were homogenized in water (1:5, w/v) with a Polytron PT$_x$ 10-35 homogenizer using a PT 10/TS probe (Brinkman Instruments, Westbury, NY, U.S.A.). The homogenate was mixed with an equal volume of 10% (w/v) cold trichloroacetic acid (TCA) solution and centrifuged at 9000 *g* at 4°C for 10 min. The supernatant was discarded and the residue was treated with 5 ml of 5% TCA at 90°C for 30 min in order to extract collagen[18]. After centrifugation, the TCA extract can be saved and used for the determination of collagen (as hydroxyproline) according to the procedure described previously[19]. The TCA-extracted residue was washed with acetone by centrifugation and dried at 60°C under vacuum. The dried material was suspended in 2 ml of 6 *M* hydrochloric acid; after flushing with nitrogen, the tube was sealed and the sample was hydrolysed for 48 h at 120°C. Isodesmosine and desmosine were isolated in almost pure form from the hydrolysate sample using a cellulose minicolumn[16]. Cellulose eluate was lyophilized and the residue dissolved in 0.01 *M* hydrochloric acid. Precolumn derivatization of desmosines was carried out according to a slight modification of Gray's method[20]. Typically, 100 μl of 0.5 *M* sodium hydrogencarbonate in HPLC-grade water and 100 μl of 20 m*M* DNS-Cl in acetone were added to 100 μl of the sample or of the working standard solution in a screw-capped glass tube. After 40 min at 65°C in the dark, the derivatization mixture was diluted to 1 ml with the mobile phase. Sodium hydrogencarbonate and DNS-Cl solutions were always freshly prepared. Volumes of 25–250 μl of derivatization mixture were injected into the chromatograph.

Elastine sample

A 2-mg amount of elastin was dissolved in 2 ml of 6 *M* hydrochloric acid in a Pyrex tube. After flushing with nitrogen, the tube was flame-sealed and the sample hydrolysed at 120°C for 48 h. The hydrolysed sample was processed and derivatized as described above for the tissue samples.

High-performance liquid chromatography

Chromatographic separations were performed using an HPLC apparatus including two Model 2150 pumps and a Model 2152 controller (LKB, Bromma, Sweden), a Model 440 absorbance detector equipped with a 254-nm interference filter (Waters Assoc., Milford, MA, U.S.A.), a Model 910 injection valve (Negretti & Zambra, Southampton, U.K.), the loop being replaced with a Guard-Pak C_{18} module (Waters Assoc.), used as a pre-column and as an on-column enrichment sample device. A Spherisorb ODS-2, 5-μm particle size, column (150 × 4 mm I.D.) was used. Chromatographic profiles and peak areas were determined by using a Model 3390 A integrator (Hewlett-Packard Italiana, Rome, Italy).

Chromatographic analysis was performed with binary gradient elution as described below. Mobile phase A was a mixture of 25 m*M* potassium dihydrogen-

phosphate–25 m*M* acetic acid and acetonitrile (85:15, v/v); mobile phase B was the same mixture but in the proportions 40:60 (v/v); the mobile phases were degassed under reduced pressure and the pH adjusted to 7.2 with 2 *M* potassium hydroxide solution. The column was first equilibrated with mobile phase A at room temperature and a flow-rate of 1.2 ml/min for 8 min. At the beginning of the analysis, with the injection valve in the load position, 25–250 μl of the sample were injected into the Guard-Pak C_{18} cartridge through the needle port by using a Model 750 500-μl Hamilton syringe; then the C_{18} cartridge was washed with 1 ml of mobile phase A by means of a syringe and finally the valve handle was rotated to the inject position to bring mobile phase A from the pump to the opposite end of the Guard-Pak module and to determine the sample to be flushed into analytical column. Elution was carried out with a linear gradient from 25% to 45% B in 20 min. At the end of the chromatography, the column was washed with mobile phase B for 5 min and then conditioned with mobile phase A for 8 min.

Quantification was performed by external calibration. The concentration of the analyte was determined by comparison of the peak area with that of a known standard. A calibration graph was obtained by applying aliquots of working standard solutions containing scalar amounts of DID from 30 to 1500 pmol to the column. Recovery experiments were carried out by adding known amounts of DID to dried aliquots of foetal rabbit lung and processing the samples through the acid hydrolysis and cellulose minicolumn steps. To evaluate the precision of the method, within-run and between-run coefficients of variation (C.V.) were calculated according to Godel *et al.*[21].

RESULTS AND DISCUSSION

Tissue sample treatment

Elastin, together with collagen, is the main component of connective tissue, which ensures the functional integrity of many anatomical systems. The indirect determination of this protein may be performed by the determination of specific amino acids, which are markers for elastin. Thus the determination of desmosines in tissue hydrolysates provides a measure of the elastin content. However, owing to the low concentration of desmosines in tissue samples, a reliable determination of these markers cannot be performed directly in acid hydrolysates of tissue samples by HPLC. Cellulose minicolumn treatment can be used for a simple purification and concentration of DID from acid hydrolysates of samples containing elastin. The purified DID sample can be analysed by reversed-phase HPLC with precolumn derivatization, without serious interferences.

HPLC with pre-column derivatization

Several reagents have been proposed for the precolumn derivatization of amino acid molecules, e.g. *o*-phthaldialdehyde (OPA)[22], DNS-Cl[23], dimethylaminoazobenzenesulphonyl chloride (DABS-Cl)[24], phenyl isothiocyanate (PITC)[25] and 7-chloro-4-nitrobenz-2-oxa-1,3-diazole (NBD-Cl)[26]. Each of these reagents can be considered as a good candidate for the precolumn derivatization of the desmosines, owing to the presence of four amino groups in their molecules. Nevertheless, only DNS-Cl holds promise of being a suitable reagent for DID derivatization; OPA and PITC, as reported previously[10], DABS-Cl and NBD-Cl, as checked by us (unpublished results), were found to be inadequate.

The HPLC method here presented is dedicated to the determination of DID, purified from tissue hydrolysates, following a simplified gradient programme. Fig. 1 shows the appearance of the DNS derivative of standard DID on the HPLC trace. The profile relates to the injection of 90 pmol of derivatized DID in 100 μl of the reaction mixture. Isodesmosine and desmosine are not separated following this HPLC procedure; as the molar extinction of the derivatives of desmosine and isodesmosine are equivalent[10], the lack of separation of DID is not a drawback with respect to the total determination of the linkers for elastin determination. As can be seen from Fig. 1, by using the column-switching device, the peak at the beginning of the chromatogram, which corresponds to excess of reagent and to the main side-products of the reaction, is small, considering the high sensitivity of the detector and the large volume of sample injected. In addition to the peak of the analyte of interest, other small peaks are detectable in the chromatographic profile, with lower retention times; the major small peak is DNS-NH_2 but the nature of the remaining components is unknown. Analysis is complete in less than 15 min with the solvent gradient chosen. Attempts to perform HPLC under isocratic conditions gave poor results, particularly for biological samples.

Calibration graphs for 30–1500 pmol of DNS-DID in the column showed good linearity of peak-area response *vs.* amount of analyte injected, with a correlation coefficient of 0.998. The limit of detection of DID was 3 pmol, which gave a signal-to-noise ratio of 3 at attenuation $\times 1$.

Fig. 2 shows typical chromatograms for DID in (a) elastin hydrolysate, (b) rat aorta, (c) foetal rabbit lung and (d) from adult rat liver. The DID peak shows almost complete separation from interfering peaks present in purified samples. Chromatogram (a) corresponds to the analysis of 10 μg of pure elastin and the other chromatograms to 1–2 mg of the processed dried sample.

Recovery experiments gave satisfactory results. With standard additions of DID to dried samples, the mean recovery was 87 $\pm$ 3% (S.D., n = 11). Recovery experiments were also performed to demonstrate the linearity between the amount of DID measured and the amount of tissue analysed. Analysis of a larger number (n = 11) of samples from a pool of dried foetal rabbit lungs demonstrates that the DID level found is linearly proportional (r = 0.997) to the amount of tissue between 50 and 250

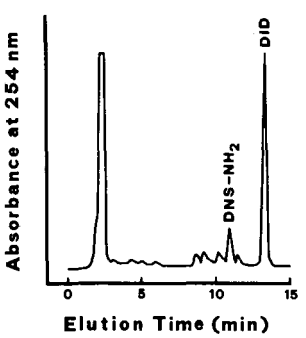

Fig. 1. HPLC of standard DID derivatized according to the procedure described under Experimental. The analyte peak correspond to an injected amount of 90 pmol of DID in 0.1 ml of derivatization mixture. Integrator attenuation $\times 3$; other conditions are described in the text.

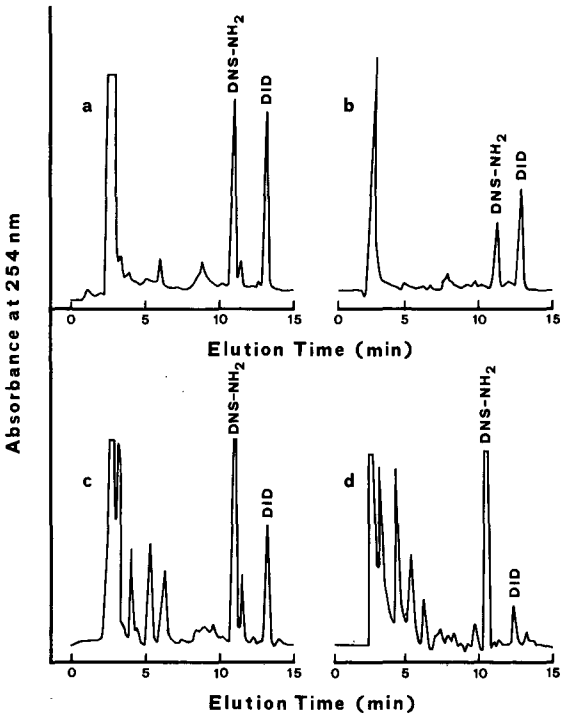

Fig. 2. Representative chromatograms of derivatized samples from (a) elastin, (b) rat aorta, (c) foetal rabbit lung and (d) rat liver. Concentrations of DID: (a) 35 pmol/mg of elastin, (b) 9 nmol/mg of dried sample tissue, (c) 81 pmol/mg of dried sample tissue and (d) 15 pmol/mg of dried sample tissue. Integrator attenuation ×3; other conditions are described in the text.

mg. As little as 50 mg of dried lung sample is sufficient to give routinely reliable results. The within-run reproducibility (C.V.) of the procedure, performed by repeated injections ($n = 11$) of the same sample with a 50 pmol injected amount of DID, was 2.8%. The between-run precision (C.V.), obtained from analyses of aliquots of the same sample carried out on five subsequent days, was 6.2%. In addition, when separate aliquots ($n = 7$) of a pool of dried foetal rabbit lungs were processed and analysed by HPLC, the procedure showed a C.V. of 5.2%.

The procedure described here has been used to assay DID in pure elastin and in foetal rabbit lungs. To measure the DID content in elastin, five separate samples of protein were hydrolysed and processed according to the present procedure. A mean value of 37 ± 1.1 nmol/mg was found, which is comparable to those reported elsewhere[10,11]. Determinations of DID in five samples of foetal lungs (30 days of gestation) gave a mean cross-linker value of 8.5 ± 1.5 nmol per 100 mg of dried sample.

The isolation of desmosines from tissue samples and their determination are technically difficult. Although several efficient HPLC systems are available for the assay of DID in pure elastin, many problems arise in the determination of these cross-linkers in tussue samples. The most important step in the present procedure is the effective purification and concentration of the compound of interest, which permits the HPLC determination of DID to be performed.

REFERENCES

1 M. Ledvina and F. Bartos, *J. Chromatogr.*, 31 (1967) 56.
2 B. C. Starcher, *J. Chromatogr.*, 38 (1968) 293.
3 C. G. Zarcadas, J. A. Rochemont, G. C. Zarkadas, C. N. Karátzas and A. D. Khalili, *Anal. Biochem.*,160 (1987) 251.
4 S. Keller, G. M. Turino and I. Mandl, *Connect. Tissue Res.*, 8 (1981) 251.
5 S. Keller, A. K. Ghosh, A. K. Ghosh, G. M. Turino and I. Mandl, *J. Chromatogr.*, 305 (1984) 461.
6 G. S. King, V. S. Mohan and B. C. Starcher, *Connect. Tissue Res.*, 1 (1980) 263.
7 S. Harel, A. Janoff, S. Y. Yu, A. Hurewitz and E. H. Bergofsky, *Am. Rev. Resp. Dis.*, 122 (1980) 769.
8 S. J. M. Skinner, J.-C. Schellenberg and G. C. Liggins, *Connect. Tissue Res.*, 11 (1983) 113.
9 Z. Gunja-Smith, *Anal. Biochem.*, 147 (1985) 258.
10 A. Negro, S. Garbisa, L. Gotte and M. Spina, *Anal. Biochem.*, 160 (1987) 39.
11 S. M. Lunte, T. Mohabbat, O. S. Wong and T. Kuwana, *Anal. Biochem.*, 178 (1989) 202.
12 B. Fabris, R. Ferrera, M. Glembourt, P. J. Crombie and C. Franzblau, *Anal. Biochem.*, 114 (1981) 71.
13 N. T. Soskel, *Anal. Biochem.*, 160 (1987) 98.
14 H. P. Covault, T. Lubrano, A. A. Dietz and H. M. Rubinstein, *Clin. Chem.*, 7 (1982) 1465.
15 Y. Yamaguchi, J. Haginaka, M. Kunitomo, H. Yasuda and Y. Bando, *J. Chromatogr.*, 422 (1987) 53.
16 J. Thomas, D. F. Eldsen and S. M. Partridge, *Nature (London)*, 299 (1963) 651.
17 S. J. M. Skinner, *J. Chromatogr.*, 229 (1982) 200.
18 S. M. Fitch, M. L. R. Harkness and R. D. Harkness, *Nature (London)*, 176 (1955) 163.
19 C. A. Palmerini, A. Vedovelli, A. Morelli, C. Fini and A. Floridi, *J. Liq. Chromatogr.*, 8 (1985) 1853.
20 W. R. Gray, *Methods Enzymol.*, 25 (1972) 121.
21 H. Godel, T. Graser, P. Pfaender and P. Fürst, *J. Chromatogr.*, 297 (1984) 49.
22 B. N. Jones and J. P. Gilligan, *J. Chromatogr.*, 266 (1983) 471.
23 C. De Jong, G. J. Hughes, E. Van Wieringen and K. J. Wilson, *J. Chromatogr.*, 241 (1982) 345.
24 R. Knecht and J.-Y. Chang, *Anal. Chem.*, 58 (1986) 2375.
25 R. L. Heinrikson and S. C. Meredith, *Anal. Biochem.*, 136 (1984) 65.
26 M. Roth, *Clin. Chim. Acta*, 83 (1978) 273.

Journal of Chromatography, 507 (1990) 59–66
Elsevier Science Publishers B.V., Amsterdam — Printed in The Netherlands

CHROMSYMP. 1766

High-performance liquid chromatographic study of the reduction of protected oxytocein by sodium in liquid ammonia

A. PÉTER*, F. LUKÁCS and K. BURGER
Department of Inorganic and Analytical Chemistry, A. József University, P.O. Box 440, 6701 Szeged (Hungary)
and
I. SCHŐN, M. LŐW and L. KISFALUDY
Gedeon Richter Chemical Works, P.O. Box 27, 1475 Budapest (Hungary)

SUMMARY

A combined high-performance liquid chromatographic (HPLC)–electrochemical method was developed to investigate the mechanism of reduction of protected oxytocein by metallic sodium in liquid ammonia. The changes in the redox potential and conductivity of protected oxytocein solution provided information on the stoichiometry of the reduction. HPLC methods elaborated for the identification and selective determination of the reaction intermediates and products were used to analyse the compounds formed. This combined procedure revealed the reaction path of the reduction processes and permitted optimization of the experimental conditions to increase the yield of oxytocin.

INTRODUCTION

Reductions by alkali metals in liquid ammonia have long been used in peptide chemistry to cleave tosyl and benzyl protecting groups[1]. The protected oxytocein investigated in this work contained one benzyloxycarbonyl (Z) and two benzyl (Bzl) groups: Z–Cys(Bzl)–Tyr–Ile–Gln–Asn–Cys(Bzl)–Pro–Leu–Gly–NH_2.

Different stoichiometries have been reported for the reduction of the benzyl group[2–5], the N-benzyloxycarbonyl group[5–7] and organic sulphides (*e.g.*, in cysteine)[8]. The application of this reduction for oxytocin production is based on empirical prescriptions, but the oxytocin yield does not exceed 55–60%.

In previous work[9], we applied a method that had been developed to measure the redox potentials and conductivities of model substances in liquid ammonia in the course of "titration" with a solution of metallic sodium. Data relating to redox potential and conductivity changes during "titration" provided information on the stoichiometry of the reduction of protected oxytocein, but not on the products, mechanism or degree of reaction.

0021-9673/90/$03.50

The degree of reduction has been observed to depend on, among other factors, the presence of proton donor molecules in organic substance–metallic sodium systems[8,10]. This phenomenon was explained in terms of the acidic behaviour and buffer action of proton donors. The proton donor molecules most often used are alcohols[10]. In this work we chose urea as proton donor; it acts as a dibasic acid in liquid ammonia[11] and has a pK_a of 12.9[12].

The direct product of reduction of protected oxytocein in liquid ammonia is not oxytocin, but the sodium salt of oxytocein. Oxytocin is formed in a further oxidation step in water.

High-performance liquid chromatography (HPLC) was found to be the most useful method for characterizing the reaction intermediates and products and for determining the mechanism of oxytocin synthesis. Several HPLC systems have been reported for the determination of oxytocin[13–30], but none of them was suitable for the separation of oxytocein and oxytocin.

We set out to investigate the steps of the oxytocin synthesis and to optimize the reaction conditions with the aim of increasing the oxytocin yield. HPLC methods were elaborated for these investigations.

EXPERIMENTAL

Apparatus

A glass apparatus was constructed for the quantitative characterization of reactions with metallic sodium in liquid ammonia[9]. In the "titration" process with sodium, the changes in redox potential and conductivity were recorded.

HPLC separations

Experiments were carried out with Model 2150 (LKB, Bromma, Sweden) and Liquochrom OE 330 (Labor-MIM, Budapest, Hungary) liquid chromatographs connected with LKB 2138 Uvicord S and UV 308 detectors. Rheodyne loop injectors (10 μl) were used for sample introduction. Prepacked Hypersyl ODS (10 μm) columns (250 × 4.6 mm I.D.) (Bio Separation Technology, Budapest, Hungary) were also used.

Materials

Protected oxytocein and oxytocin were obtained from Gedeon Richter (Budapest, Hungary) and urea and toluene from Reanal (Budapest, Hungary). Diphenylethane was prepared by the usual method.

The organic solvents used were of HPLC grade (E. Merck, Darmstadt, F.R.G.). Buffers and salt solutions were prepared from Merck, BDH (Poole, U.K.) or Fluka (Buchs, Switzerland) reagents, using water doubly distilled from a glass apparatus and further purified by pumping through 10-μm filters.

RESULTS AND DISCUSSION

Fig. 1 shows the potentiometric and conductimetric titration curves of protected oxytocein with standard sodium solution in the presence and absence of urea. As can be seen from the potentiometric curves, the reduction requires about 7 equiv. of sodium in both instances. The presence of urea does not change the stoichiometry of reduction.

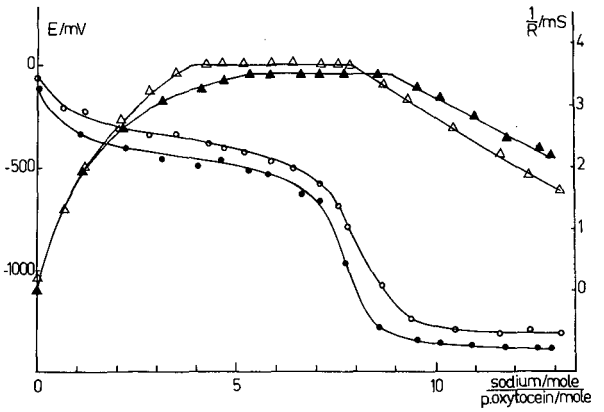

Fig. 1. Potentiometric (○, ●) and conductometric (△, ▲) titration curves of protected oxytocein in the absence (○, △) and presence (●, ▲) of urea. Concentration of protected oxytocein, $6 \cdot 10^{-3}$ mol dm^{-3}; concentration of urea, $3.6 \cdot 10^{-2}$ mol dm^{-3}.

To determine the reduction products, the reaction was stopped at different molar ratios of sodium to peptide, the ammonia was removed by evaporation and the product was dissolved in water (or in methanol for analysis of aromatic compounds), suitably oxidized and analysed by HPLC.

In the reduction of protected oxytocein with sodium, toluene and the sodium salt of oxytocein are first formed. The formation of toluene may reflect the splitting off of benzyl and N-benzyloxycarbonyl groups via a two-electron step mechanism. The formation of diphenylethane, indicating reduction via a one-electron step, is negligible.

The sodium salt of oxytocein was oxidized to oxytocin in a careful oxidation step. The degree of oxidation was followed by HPLC on the basis of the difference in polarity between oxytocein and oxytocin (the latter is less polar).

The eluent system applied to resolve oxytocin from oxytocein was acetonitrile–0.01 *M* phosphate buffer (pH = 2.2) (25:75) containing 0.1 *M* sodium perchlorate. The capacity factors (k') were 3.0 for oxytocein and 3.4 for oxytocin (Fig. 2).

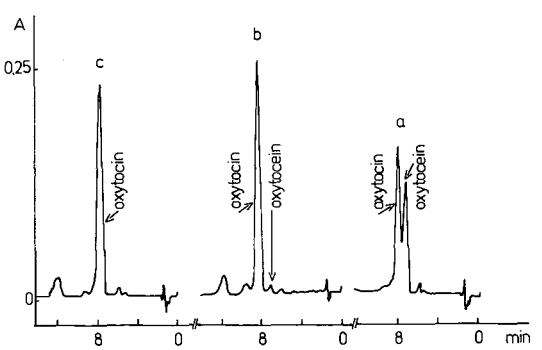

Fig. 2. Chromatograms of reduction products of protected oxytocein in various stages of oxidation. Eluent, acetonitrile–0.01 *M* KH_2PO_4 (pH 2.2) (25:75); detection, UV, 220 nm; concentration of protected oxytocein in liquid ammonia, $6 \cdot 10^{-3}$ mol dm^{-3}; molar ratio of sodium to protected oxytocein, 7.06; molar ratio of urea to protected oxytocein, 6.0; stirring time in air, (a) 20, (b) 70 and (c) 120 min.

TABLE I

OXYTOCIN YIELD ON OXIDATION AT pH 6.8

Procedure	*Temperature (K)*	*Concentration of protected oxytocin in liquid ammonia (mol dm^{-3})*															
		3 · 10^{-3}						*6 · 10^{-3}*						*12 · 10^{-3}*			
		Concentration of urea in liquid ammonia (mol dm^{-3})															
		0		*18 · 10^{-3}*		*72 · 10^{-3}*		*0*		*36 · 10^{-3}*		*72 · 10^{-3}*		*0*		*72 · 10^{-3}*	
		r[a]	*Yield (%)*	*r*	*Yield (%)*	*r*	*Yield (%)*	*r*	*Yield (%)*	*r*	*Yield (%)*	*r*	*Yield (%)*	*r*	*Yield (%)*	*r*	*Yield (%)*
Addition of sodium																	
By "titration"	228	7.29	77	8.02	80	8.33	87	7.32	67	7.52	78			7.27	64	7.52	76
		8.45	79											7.75	62	7.89	74
In solid form	228	6.76	83	7.06	86	7.50	89	7.75	65			7.32	85	7.46	57	7.26	75
		6.98	83	8.47	76			7.76	67								
	240	7.12	82	7.57	79									6.80	64	7.34	71
		7.53	78	8.31	79									7.48	69	7.68	76
		7.65	78	8.50	76												

[a] r = Molar ratio of sodium to protected oxytocin in liquid ammonia.

Optimization of oxytocin production

The yield of oxytocin depends on the efficiency of the reduction and oxidation stages.

To optimize the reduction stage, first the optimum molar ratio of sodium to protected oxytocein was determined which was found to be about 7–8 (Fig. 3). At lower ratios unreacted protected oxytocein remained in the system, decreasing the yield. The protected oxytocein does not dissolve in water, only in hot dimethylformamide, and therefore it does not appear in HPLC analysis. Above the ratio of 7–8 the excess of sodium splits the peptide bonds. Peaks in the chromatograms characterizing smaller peptides increase with increasing sodium concentration.

To determine the dependence of the oxytocin yield on the concentration of protected oxytocein, three concentrations were studied, $12 \cdot 10^{-3}$, $6 \cdot 10^{-3}$ and $3 \cdot 10^{-3}$ mol dm^{-3}. Tables I and II show that a decrease in the protected oxytocein concentration leads to an increased oxytocin yield. This may be due either to suppression of the side-reactions or to the dissociation of the weakly acidic groups on protected oxytocein with dilution, leading to an increase in the proton concentration, favouring reduction.

The effect of the proton donor urea was investigated at various urea and protected oxytocein concentrations. At a constant protected oxytocein concentration of $12 \cdot 10^{-3}$ mol dm^{-3}, variation of the concentration ratio of urea to protected oxytocein between 3 and 12 revealed that the optimum ratio was about 6.

At a protected oxytocein concentration of $3 \cdot 10^{-3}$ mol dm^{-3}, no influence of urea was observed (Fig. 3b); at concentrations of $6 \cdot 10^{-3}$ and $12 \cdot 10^{-3}$ mol dm^{-3}, the oxytocin yield in the presence of urea was higher, the increase reaching 10–15% (Fig. 3a and Tables I and II).

For practical reasons, the influence of temperature was examined only at 228 and 240 K. The results did not reflect a temperature effect.

The results of the "titration" of the peptide with metallic sodium dissolved in liquid ammonia were compared with those for the reactions between solid sodium and

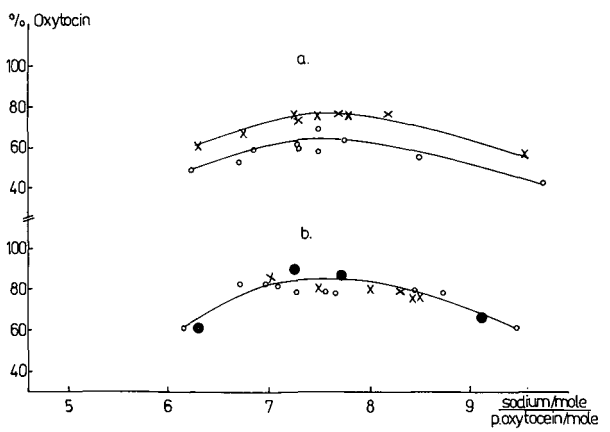

Fig. 3. Plots of oxytocin yield (%) *versus* molar ratio of sodium to protected oxytocein in the absence and presence of urea. pH = 6.8. Initial concentration of protected oxytocein in liquid ammonia: (a) $12 \cdot 10^{-3}$ and (b) $3 \cdot 10^{-3}$ mol dm^{-3}. Ratio of urea to protected oxytocein: ○ = 0; × = 6; ● = 24.

TABLE II

OXYTOCIN YIELD ON OXIDATION AT pH 11.9

Procedure	*Temperature (K)*	*Concentration of protected oxytocein in liquid ammonia (mol dm^{-3})*															
		3 · 10^{-3}						*6 · 10^{-3}*						*12 · 10^{-3}*			
		Concentration of urea in liquid ammonia (mol dm^{-3})															
		0		*18 · 10^{-3}*		*72 · 10^{-3}*		*0*		*36 · 10^{-3}*		*72 · 10^{-3}*		*0*		*72 · 10^{-3}*	
		r[a]	*Yield (%)*	*r*	*Yield (%)*	*r*	*Yield (%)*	*r*	*Yield (%)*	*r*	*Yield (%)*	*r*	*Yield (%)*	*r*	*Yield (%)*	*r*	*Yield (%)*
Addition of sodium																	
By "titration"	228	7.29	86	8.02	99	8.33	99	7.32	80	7.52	78			7.27	74	7.52	83
		8.45	90					7.90	75	7.90	75			7.75	71	8.17	83
In solid form	228	6.76	90	7.06	97	7.50	96	7.75	70			7.32	91	7.46	70	7.26	86
		6.98	95	8.47	88			7.76	69								
	240	7.12	95	7.57	87									6.80	75	7.34	86
		7.53	87	8.31	90									7.48	75	7.68	78
		7.65	90	8.50	91												

[a] r = Molar ratio of sodium to protected oxytocein in liquid ammonia.

peptide solution (Tables I and II). No significant difference in oxytocin yield was observed under the conditions studied.

To optimize the oxidation stage in oxytocin synthesis, the kinetics of oxidation were investigated. The product of sodium reduction, the solid sodium salt of oxytocein, was dissolved in water to give different concentrations. The pH of these oxytocein solutions was adjusted to 11.9 or 6.8 and the solutions were allowed to stand in open beakers in contact with air. At fixed intervals, samples were taken from the solutions and the oxytocein and oxytocin contents were determined by HPLC.

The $3 \cdot 10^{-3}$ mol dm^{-3} oxytocein solution was oxidized more slowly than the $7.5 \cdot 10^{-4}$ mol dm^{-3} solution; it reached its maximum value 2–6 h later. This may be due to the high ratio of oxytocein to oxygen in solution, because the oxygen concentration was lower than the concentration of oxytocein and oxygen was replaced by diffusion only. When the replacement of oxygen was enhanced by stirring the solution, the rate of oxidation increased. On the other hand, the concentration of oxytocin started to decrease after reaching a maximum value. This phenomenon may be explained by oligomerization and degradation of the peptide being favoured in concentrated solution, as reflected in the chromatograms by some peaks after the oxytocin peak, these peaks increasing in time.

In some experiments, hydrogen peroxide was used instead of oxygen as the oxidant. The oxidation with hydrogen peroxide must be performed carefully, as too fast an addition or overaddition decreases the yield of oxytocin.

When oxidation was carried out in basic solution, the chromatograms contained higher peaks at the position of oxytocin, indicating a higher yield. Biological activity measurements confirmed the results of HPLC measurements.

REFERENCES

1 I. Schön, *Chem. Rev.*, 84 (1984) 287.
2 R. H. Siffered and V. du Vigneaud, *J. Biol. Chem.*, 108 (1935) 735.
3 W. I. Patterson and V. du Vigneaud, *J. Biol. Chem.*, 111 (1935) 393.
4 I. Schön, T. Szirtes and T. Überhard, *J. Chem. Soc., Chem. Commun.*, (1982) 639.
5 I. Schön, T. Szirtes, T. Überhard, A. Rill, A. Csehi and B. Hegedüs, *Int. J. Pept. Protein Res.*, 22 (1983) 92.
6 E. Wünsch (Editor), *Synthese von Peptide (Houben–Weyl Methoden der Organischen Chemie*, Vol. 15), Georg Thieme, Stuttgart, 1974.
7 S. Bajusz and K. Medzihradszky, in G. T. Young (Editor), *Peptides*, Pergamon Press, Oxford, 1962, p. 49.
8 W. L. Jolly and D. J. Hallada, in T. C. Waddington (Editor), *Non-Aqueous Solvent Systems*, Academic Press, London, New York, 1965, Ch. 1, pp. 1–45.
9 F. Lukács, A. Péter, G. Sipos-Nagy, K. Burger, M. Löw, I. Schön and L. Kisfaludy, *Inorg. Chim. Acta*, 157 (1989) 121.
10 A. J. Birch and G. S. Rao, *Adv. Org. Chem.*, 8 (1972) 1.
11 G. W. Watt, D. M. Soluards and W. R. McBride, *J. Am. Chem. Soc.*, 77 (1955) 5835.
12 M. Herlem, *Bull. Soc. Chim. Fr.*, (1967) 1687.
13 F. Maxl and K. Krummen, *Pharm. Acta Helv.*, 53 (1978) 207.
14 B. Larsen, B. L. Fox, M. F. Burke and V. J. Hruby, *Int. J. Pept. Protein Res.*, 13 (1979) 12.
15 M. J. O'Hare and E. C. Nice, *J. Chromatogr.*, 171 (1979) 209.
16 K. Krummen, *Pharm. Technol. Inst.*, 2 (1979) 37.
17 K. Krummen, F. Maxl and F. Nachtman, *Pharm. Technol. Inst.*, 3 (1979) 77.
18 K. Krummen, *J. Liq. Chromatogr.*, 3 (1980) 1243.
19 R. A. Pask-Hughes, P. H. Corran and D. H. Calam, *J. Chromatogr.*, 214 (1981) 307.

20 M. T. W. Hearn and B. Grego, *J. Chromatogr.*, 203 (1981) 349.
21 M. Gazdag and G. Szepesi, *J. Chromatogr.*, 218 (1981) 603.
22 C. T. Wehr, K. Correia and S. R. Abbott, *J. Chromatogr. Sci.*, 20 (1982) 114.
23 M. T. W. Hearn and B. Grego, *J. Chromatogr.*, 255 (1983) 125.
24 H. Mabuchi and H. Nakahashi, *J. Chromatogr.*, 213 (1981) 275.
25 H. Mabuchi and J. Nakahashi, *J. Chromatogr.*, 233 (1982) 107.
26 C. A. Browne, H. P. J. Benett and S. Solomon, *Anal. Biochem.*, 224 (1982) 201.
27 K. A. Cohen, *J. Chromatogr.*, 282 (1983) 423.
28 M. W. White, *J. Chromatogr.*, 262 (1983) 420.
29 K. Hermann, R. E. Lang, T. Unger, C. Bayer and D. Ganten, *J. Chromatogr.*, 312 (1984) 273.
30 M. Andre, *J. Chromatogr.*, 351 (1986) 341.

Journal of Chromatography, 507 (1990) 67–77
Elsevier Science Publishers B.V., Amsterdam — Printed in The Netherlands

CHROMSYMP. 1676

Fully automated amino acid analysis for protein and peptide hydrolysates by precolumn derivatization with 9-fluorenyl methylchloroformate and 1-aminoadamantane

BARBRO GUSTAVSSON and INGVAR BETNÉR*
Pharmacia LKB Biotechnology, Box 305, S-161 26 Bromma (Sweden)

SUMMARY

A fully automated precolumn derivatization method for the determination of primary and secondary amino acids using reversed-phase chromatography is described. The derivatization reagent 9-fluorenyl methylchloroformate is used, together with 1-aminoadamantane for reaction with excess of reagent. The derivatization procedure is described in detail. Reproducibility data are presented and compared between the manual and the fully automated methods. Optimization strategies for separation, and differences in detection between fluorescence and UV methods are discussed. Analytical data for protein and peptide hydrolysates are compared with their sequenced data.

INTRODUCTION

9-Fluorenyl methylchloroformate (FMOC) was introduced as a precolumn derivatization reagent in high-performance liquid chromatographic (HPLC) amino acid analysis in 1983[1]. FMOC forms derivatives for both primary and secondary amino acids. The derivatives are highly fluorescent, and are rapidly formed within less than 1 min in a buffered aqueous solution. The derivatized amino acids and the reagent itself have almost identical excitation and emission spectra, and therefore the excess of reagent has to be removed before injection, so that the detection of some amino acids is not affected. This could be done by pentane extraction[1] or by derivatizing the excess of reagent with a hydrophobic amine[2]. In this paper, we describe a fully automated derivatization method based on the hydrophobic amine approach.

An advantage with the hydrophobic amine method, using 1-aminoadamantane (ADAM), is that the risk of partial extraction of the hydrophobic amino acids into the organic phase is eliminated. This problem has been discussed in several reports[1,3–5]. Our experience is that when derivatizing amino acids at a concentration of 20 pmol per amino acid or less, the pentane extraction transfers 50–75% of the more hydrophobic amino acids (histidine, ornithine, lysine) into the organic phase. This will adversely effect the reproducibility of the analysis for these amino acids. The

0021-9673/90/$03.50

objective of this study was to develop a reliable amino acid analysis method. To meet this objective, we developed a fully automated derivatization method with a few sample preparation steps as possible, in order to make it easy to use in routine amino acid analysis.

EXPERIMENTAL

HPLC system

The chromatographic system was a two-pump gradient system. AminoSys (Pharmacia–LKB, Bromma, Sweden) and consisted of Model 2248 HPLC pumps, a Model 2248-300 dynamic high-pressure mixer, a Model 2156 solvent conditioner, a Model 2146 HPLCmanager PC control system in combination with Nelson evaluation software on an IBM AT computer, a Model 2157-020 autosampler (the automated method with an experimental modification of the autosampler; the modification consisted of an external mixmotor and software changes), a Model 2144 fluorescence detector, a Model 2141 variable-wavelength monitor and a Model 2155 column oven.

Chemicals

Solvents were of HPLC grade and chemicals were of the highest purity available, all from E. Merck (Darmstadt, F.R.G.), except FMOC from Sigma (St. Louis, MO, U.S.A.), ADAM · HCl from Serva (Heidelberg, F.R.G.) and amino acid standards from Pharmacia LKB Biochrom Ltd. (Cambridge, U.K.) or Pierce (Rockford, IL, U.S.A.).

Mobile phase

A stock solution of 100 m*M* sodium acetate buffer was prepared by adding acetic acid to water and adjusting the pH to 4.4 with 30% sodium hydroxide solution. The buffer was filtered through a 0.45-μm filter. Eluent A was sodium acetate buffer (100 m*M*, pH 4.4)–tetrahydrofuran–acetonitrile (75:15:10) and eluent B was acetonitrile–tetrahydrofuran (85:15), with the following gradient profile: 0–2.5 min, 0% B; 2.5–6.6 min, 7% B; 6.6–8.3 min, 14% B; 8.3–8.4 min, 21% B; 8.4–10 min, 21% B; 10.0–10.1 min, 17% B; 10.1–20.0 min, 19% B; 20–29 min, 55% B; 29–30 min, 100% B. The flow-rate was 1.5 ml/min.

Column

The stationary phase was Kromasil C_8, 5 μm (EKA Nobel, Surte, Sweden) in a 250 × 4 mm I.D. column. The column temperature was 45°C.

Derivatization procedure

A 10-μl volume of sample was pipetted into a clean autosampler vial and 10 μl of borate buffer (0.5 *M* boric acid solution adjusted to pH 7.7 with 30% sodium hydroxide solution) were added. After vortexing, 20 μl of FMOC (1 m*M*) in acetone were added and vortex mixed immediately. After incubation for 45 s, 20 μl of ADAM (40 m*M*) in water–acetone (1:3, v/v) were added and the mixture was vortex mixed. After incubation for at least 45 s, 5–10 μl were injected for HPLC analysis. The procedure was used either in the manual mode by using ordinary pipettes or in the automated mode by utilizing the modified autosampler.

Hydrolysis procedure

The hydrolysis vessel was supplied by Ciba Corning Diagnostics (Essex, U.K.). Solutions of proteins and peptides were added to the sample tubes and were dried in a Speed Vac vacuum centrifuge (Savant Instrument, Farmingdale, NY, U.S.A.) for 20 min and then placed in the hydrolysis vessel. The vessel was flushed with nitrogen and 2 ml of 6 *M* hydrochloric acid were transferred into the bottom of the vessel. The vessel was evacuated and purged with nitrogen. The hydrolysis was carried out at 110°C for 23 h. After cooling, the vessel was opened and the samples were dried in a vacuum centrifuge for 20 min. The contents were redissolved in 0.01 *M* hydrochloric acid or water (HPLC grade).

RESULTS AND DISCUSSION

Derivatization buffer

As we have observed precipitations of borate and FMOC, we modified the acetone to water ratio given in the earlier published method[3]. The pH was optimized for this modified derivatization system; pH 7.7 was choosen so that the area of the FMOC hydrolysis product (FMOC-OH) was minimized, but still gave a good response for all amino acids (Fig. 1).

FMOC reaction

The FMOC stock solution concentration (1 m*M*) gave a linear response between 0.25 and 35 pmol per amino acid for the method with respect to fluorescence

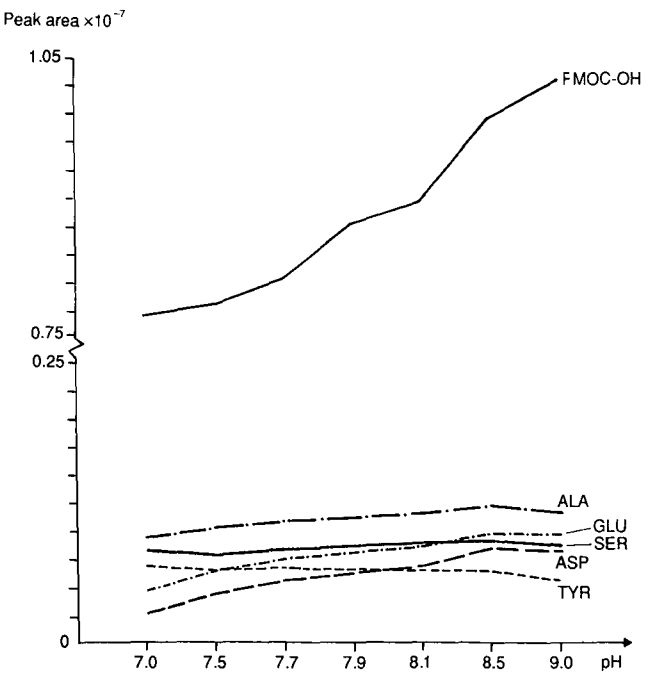

Fig. 1. Effect of derivatization pH on peak area.

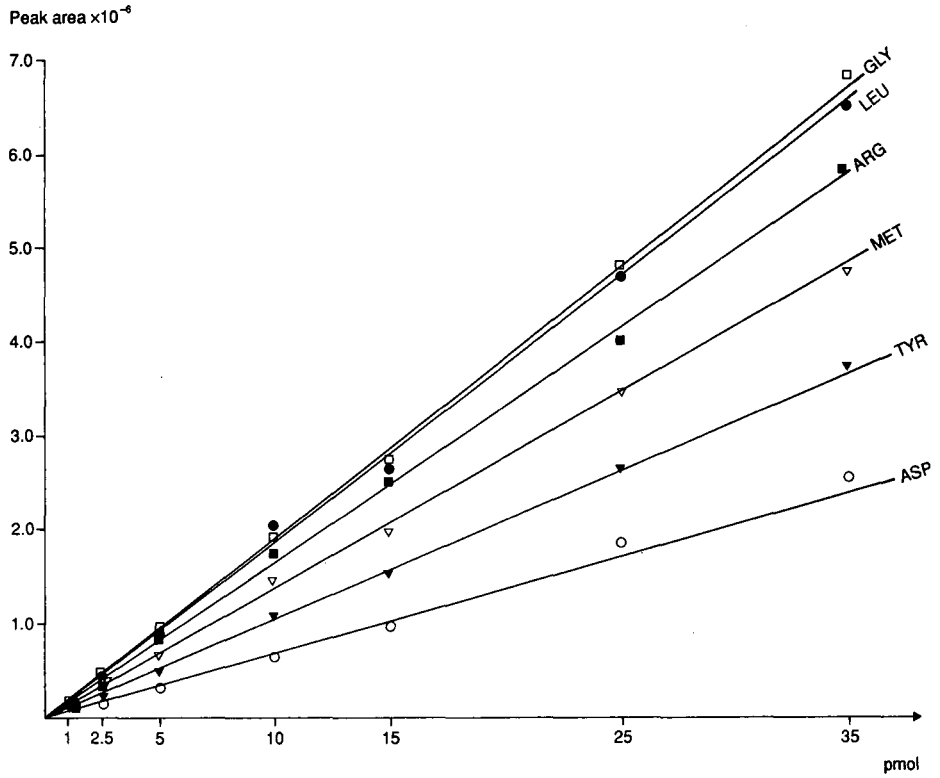

Fig. 2. Linearity of the automated method with respect to fluorescence.

(Fig. 2). This FMOC concentration gave an optimum response for all amino acids[3]. The optimum reaction time for the FMOC derivatization was 45 s for all amino acids. Most amino acids were fully derivatized after 30 s, but the acidic amino acids (aspartic acid, glutamic acid) needed a longer reaction time.

Stability of derivatives

Stability of the FMOC derivatives was measured at both 22°C (room temperature) and 6°C by injecting a constant volume from a single derivatization of a protein hydrolysate standard every hour for 24 h. One derivative that showed a significant breakdown at ambient temperature was di-derivatized histidine (49.4%), which was converted to the mono-derivatized form. Cysteine also showed a decrease in response (26.0%). These effects were reduced when thermostating the vials in the autosampler at 6°C. The relative standard deviation of the peak area for the different amino acids was between 1.7 and 5.1% except for di-derivatized histdine (20%). This shows that the stability of the derivatives is sufficient to be able to use the method in a manual derivatization mode, if the vials are stored at 6°C during analysis, except for unstable histidine.

Influence of ADAM

The concentration ratio of ADAM to FMOC in the reaction mixture was 40:1.

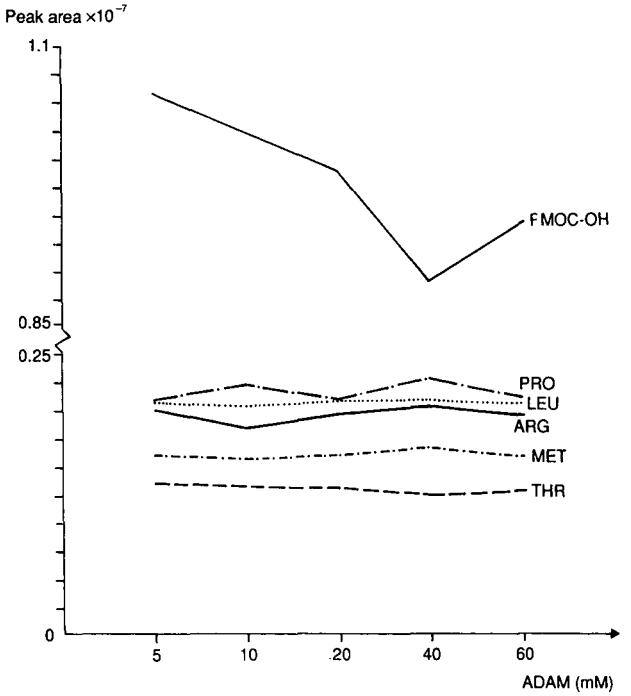

Fig. 3. Effect of ADAM concentration on peak area.

With this ratio, the interference with the remaining FMOC-OH peak and the more hydrophobic amino acids was kept to the minimum. The response of the amino acid derivatives was independent of the ADAM concentration within the tested concentration range (Fig. 3).

Reproducibility of manual and automated methods

The reproducibility of the manual and automated derivatization methods was measured by analysing ten different derivatizations from the same protein hydrolysate standard sample.

As we have observed the risks of introducing contaminants in the pipetting steps during a manual derivatiation, and introducing volume errors when pipetting small volumes with commercially available automatic pipettes, we aimed to make the derivatization steps fully automated by using an autosampler. The automation should make the method more reliable, as the number of manual pipetting steps is reduced. The instability of the histidine derivative will also not be a limiting step.

A comparison of the relative standard deviations of peak areas between the manual derivatization method and the fully automated method is shown in Table I. To be able to achieve reproducible results, all chemicals and reagents must be freshly prepared and the highest purity available[3].

Stationary phase

Instability of the silica matrix is still a common problem associated with re-

TABLE I

RELATIVE STANDARD DEVIATION FOR PEAK AREA: COMPARISON BETWEEN MANUAL AND AUTOMATIC DERIVATIZATION

Amino acid	*R.S.D. (%) (n = 10)*			*R.S.D. (%) (n = 10)*	
	Automatic	*Manual*		*Automatic*	*Manual*
Arginine (Arg)	2.04	4.76	Tyrosine (Tyr)	2.79	4.16
Serine (Ser)	1.72	4.01	Methionine (Met)	2.19	4.01
Aspartic acid (Asp)	4.69	4.81	Valine (Val)	4.11	5.19
Glutamic acid (Glu)	4.81	4.72	Phenylalanine (Phe)	2.91	5.26
Threonine (Thr)	2.59	4.39	Isoleucine (Ile)	2.45	4.17
Glycine (Gly)	3.18	3.32	Leucine (Leu)	2.07	4.38
Alanine (Ala)	2.36	4.26	Histidine (His)	4.71	8.35
Proline (Pro)	2.53	3.19	Lysine (Lys)	2.42	4.86

versed-phase chromatography. We have observed an increase in retention of arginine compared with other amino acids as the column ages[3]. This cannot be compensated for with the mobile phase used in routine analysis. Therefore, a new column matrix was choosen for this study. This column gave satisfactory results, especially for stability of the retention times of basic amino acids.

Mobile phase

The mobile phase system was optimized for a baseline separation of all the amino acids in a protein hydrolysate with the column matrix choosen in this study. For mobile phase optimization, pH, temperature, organic modifiers and ionic strength were investigated.

A decrease in pH increased the retention of all amino acids. Methionine was eluted together with the FMOC-OH peak and cystine together with leucine. The retention times of the FMOC-OH and ammonia peaks were only slightly affected by the pH of the eluent. When the pH was increased, serine and aspartic acid were not fully resolved, and valine eluted together with the FMOC-OH peak; pH 4.4 gave the best selectivity for this separation.

The use of an acetonitrile gradient was not sufficient to separate some of the hydrophilic amino acids. Therefore, another organic modifier, tetrahydrofuran (THF), was introduced into the mobile phase system. The optimized gradient profile was necessary in order to elute methionine before the FMOC-OH peak.

The ionic strength of the elution buffer mostly affected the peak shape of cystine. An increase in the ionic strength of the buffer reduced the interaction of cystine with the matrix; 100 m*M* acetate was sufficient to separate cystine as a sharp peak.

Reproducibility of the retention time for the optimized separation system was excellent; the relative standard deviation was between 0.1 and 0.7%. The column temperature was maintained at 45°C. A separation of a protein hydrolysate standard is shown in Fig. 4.

Detection and analysis

The FMOC derivatization gave highly fluorescent adducts which were detected

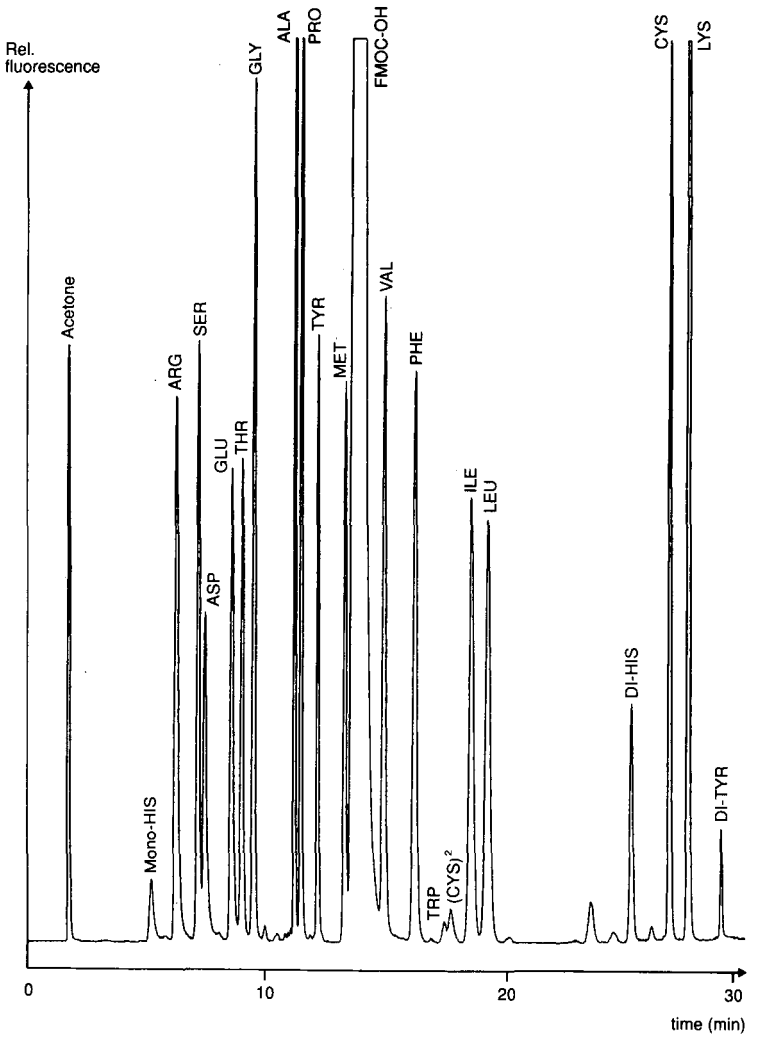

Fig. 4. Separation of protein hydrolysate standard; 10 pmol per amino acid. Fluorescence detection, λ_{ex} 263 nm, and λ_{em} 313 nm. Injection volume, 5 μl.

TABLE II

RELATIVE RESPONSE OF PEAK AREA RELATED TO Ala FOR FMOC DERIVATIVES, DETECTED BY UV AND FLUORESCENCE METHODS

Amino acid	*UV*	*Fluorescence*	*Amino acid*	*UV*	*Fluorescence*
Mono-His	0.44	0.66	Met	0.96	0.93
Arg	0.79	1.08	Val	1.10	1.27
Ser	0.69	0.88	Phe	1.14	1.39
Asp	0.11	0.31	Cys[2] (cystine)	0.63	N.D.
Glu	0.46	0.50	Trp	1.41	0.05
Thr	0.66	0.80	Ile	1.10	1.36
Gly	1.25	1.44	Leu	1.02	1.22
Ala	1.00	1.00	Di-His	0.67	0.19
Pro	1.28	1.43	Cys (cysteine)	1.49	1.51
Tyr	1.30	0.89	Lys	1.93	2.15

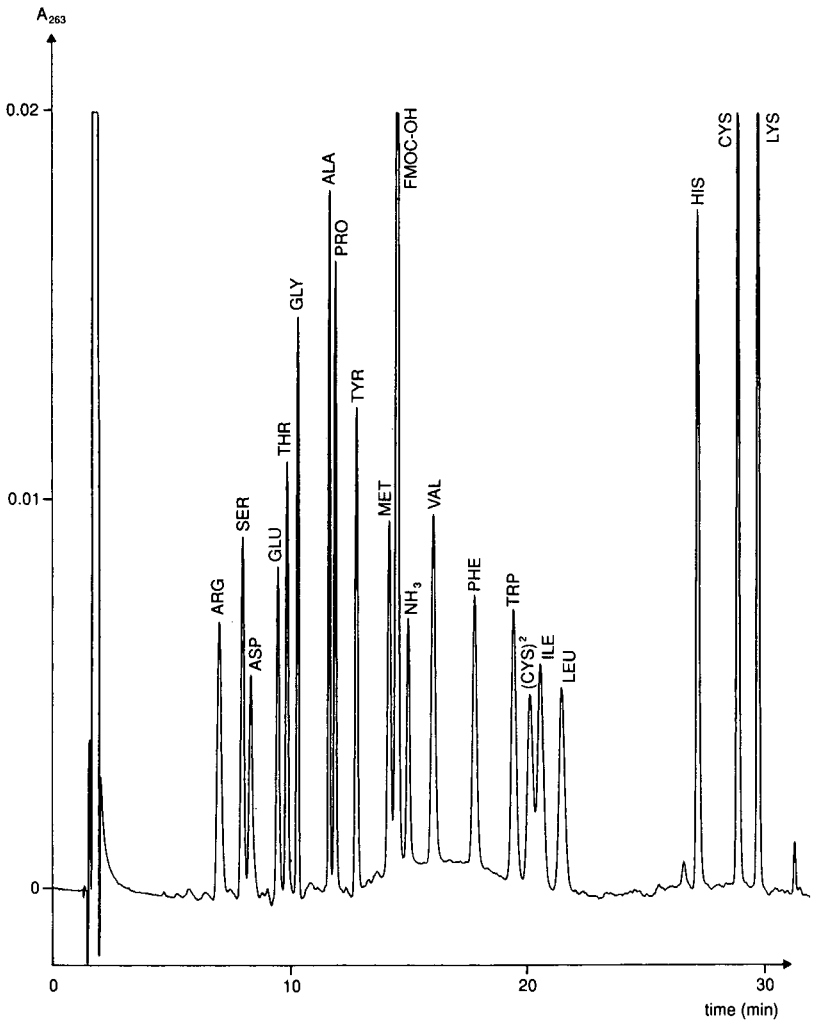

Fig. 5. Separation of protein hydrolysate standard; 200 pmol per amino acid. UV detection at 263 nm. Injection volume, 6 μl.

with excitation at 263 nm and emission at 313 nm[3]. In this study, we used a filter fluorescence detector with an interference filter at 265 nm, with a band-with of 8 nm. A Schott WG 305 cut-off filter was used in combination with a Schott UG11 block filter in order to obtain the highest possible signal-to-noise ratio (S/N). With this combination the detection limit (S/N = 3) was 40 fmol for alanine. However, the highest sensitivity routinely obtainable was about 100 fmol, because of the contamination of amino acids in a standard laboratory environment[3].

Owing to intramolecular quenching in fluorescence, the response for some amino acids, *e.g.*, cystine and tryptophan, was low. To investigate this fully, the response

TABLE III

AMINO ACID COMPOSITION OF LYSOZYME, RPI-1 AND SM-5

Comparison of sequenced data with FMOC analysis and dedicated amino acid analyser.

Amino acid	*Lysozyme*		*Synthetic peptide RPI-1*			*Synthetic peptide SM-5*		
	Seq.	*FMOC*	*Seq.*	*FMOC*	*Nin-hydrin*	*Seq.*	*FMOC*	*Nin-hydrin*
Arg	11	11.1	1	1.0	1.0			
Ser	10	8.7						
Asp[a]	21	18.3				7	7.2	6.4
Glu[b]	5	4.6	2	2.1	1.9	5	6.2	4.9
Thr	8	6.4	1	1.0	1.0	3	2.9	2.6
Gly	11	11.4				2	1.9	2.4
Ala	12	11.8	2	1.6	2.3	3	3.0	3.0
Pro	2	2.1	1	1.0	1.0	1	1.0	1.0
Tyr	3	2.8				1	0.7	0.6
Met	2	0.5						
Val	6	5.1				1	1.0	1.0
Phe	3	2.9	1	0.9	1.0			
Trp	6	N.D.						
Ile	6	5.9	1	1.0	1.0	1	1.0	0.9
Leu	8	8.2	1	1.0	1.0	5	4.9	4.6
His	1	0.6				1	1.0	1.0
Cys[c]	8	0.2						
Lys	6	5.6				4	3.6	3.6

[a] Aspartic acid + aspargine
[b] Glutamic acid + glutamine.
[c] Cysteine.

factors for these amino acids relative to alanine were compared with the same chromatogram with UV detection at 263 nm, using a variable-wavelength monitor (Table II and Fig. 5).

A hydrolysate of lysozyme was analysed using the automated FMOC method, and a comparison with its sequenced data is shown in Table III.

Hydrolysates from the synthetic ten-residue peptide Retroviral Protease Inhibitor, RPI-1 (Fig. 6), and a 35-residue peptide SM-5 were also analysed using the automated FMOC method. The results were compared both with their sequenced data and with the results obtained with a Model 4151 Alpha Plus ninhydrin post-column derivatization dedicated amino acid analyser (Pharmacia LKB Biochrom Ltd., Cambridge, U.K. (Table III).

The results for cysteine, tryptophan and methionine were low, owing to degradation in the hydrolysis method used in this analysis[6]. No precautions for the protection of labile amino acids were made in this hydrolysis method. Oxidation of the sample prior to hydrolysis would be an alternative[7]. With this gradient, cysteic acid and methionine sulphone are eluted at 3.2 and 7.5 min, respectively.

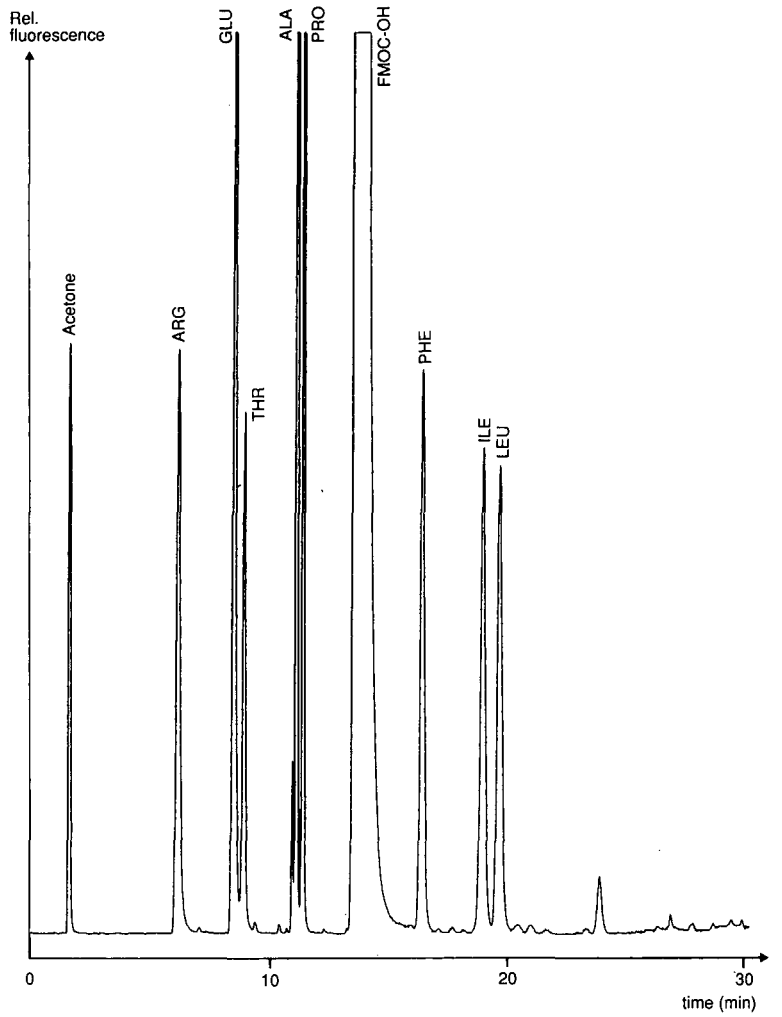

Fig. 6. Chromatogram of the synthetic ten-residue peptide Retroviral Protease Inhibitor (RPI-1) hydrolysate. Fluorescence detection, λ_{ex} 263 nm, λ_{em} 313 nm. Injection volume, 6 μl.

CONCLUSIONS

The fully automated FMOC–ADAM approach fulfils the need for a reliable method for the routine determination of protein and peptide hydrolysates at levels of less than 10 pmol per amino acid. Absolute control over the different steps in the derivatization procedure is necessary in order to achieve reproducible results.

ACKNOWLEDGEMENTS

We thank Dr. Nouri Baldar for providing peptide and protein hydrolysates and

ninhydrin analysis data. Synthesized peptides were gifts from Dr. Sherri Dolan and Dr. Don Whitney.

REFERENCES

1 S. Einarsson, B. Josefsson and S. Lagerkvist, *J. Chromatogr.*, 282 (1983) 609–618.
2 I. Betnér and P. Földi, *Chromatographia*, 22 (1986) 381–387.
3 I. Betnér and P. Földi, *LC · GC Mag. Liq. Gas Chromatogr.*, 6 (1988) 832–840.
4 S. Einarsson, *J. Chromatogr.*, 348 (1985) 213–220.
5 H. Godel, *Thesis*, University of Hohenheim, Stuttgart, 1986.
6 A. S. Inglis, *Methods Enzymol.*, 91 (1983) 26–36.
7 V. C. Mason, M. Rudemo and S. Bech-Anderson, *Z. Tierphysiol. Tierernähr. Futtermittelkd.*, 43 (1980) 35.

Journal of Chromatography, 507 (1990) 79–84
Elsevier Science Publishers B.V., Amsterdam — Printed in The Netherlands

CHROMSYMP. 1715

High-performance liquid chromatographic determination of an arginine-containing octapeptide antagonist of vasopressin in human plasma by means of a selective post-column reaction with fluorescence detection

VENKATA K. BOPPANA and GERALD R. RHODES*
Department of Drug Metabolism, Smith Kline and French Laboratories, P.O. Box 1539, King of Prussia, PA 19406-0939 (U.S.A.)

SUMMARY

A novel high-performance liquid chromatographic method was developed for the determination in plasma samples of the synthetic octapeptide SK&F 105494 {O-ethyl-D-tyrosyl-L-phenylalanyl-L-valyl-L-asparaginyl-5-[1-(carboxymethyl)cyclohexyl]-L-norvalyl-L-arginyl-D-arginamide, cyclic (5–1) peptide}, an active aquaretic agent which significantly increases water excretion in experimental animal models through competitive antagonism of renal epithelial vasopressin receptors. The method involves isolation of Sk&F 105494 from plasma samples by solid phase extraction prior to chromatographic analysis. Following chromatographic separation, in-line fluorescence detection was accomplished via a selective-post-column reaction of the guanidino group of the arginine moiety of the peptide with alkaline ninhydrin to generate a highly fluorescent product. Optimization of the post-column reaction conditions and the use of high-performance liquid chromatography columns of reduced internal diameter (2.1 mm), resulted in an on-column detection limit of 50 pg (45 fmol). The limit of sensitivity in plasma was 0.5 ng/ml. The assay was linear over the range 0.5–100 ng/ml. Precision and accuracy were within 11% across the calibration range. The assay was shown to be suitable to study the pharmacokinetics of SK&F 105494 in human subjects and animals. In addition, the methodology developed has general applicability in the detection of arginine-containing peptides in biological matrices.

INTRODUCTION

The increasing interest in developing pharmacological agents based upon synthetic analogues of naturally occurring peptides necessitates the development of sensitive and specific analytical methodology for their measurement in biological matrices. SK&F 105494 {O-ethyl-D-tyrosyl-L-phenylalanyl-L-asparaginyl-5-[1-(carboxymethyl)cyclohexyl]-L-norvalyl-L-arginyl-D-arginamide, cyclic (5–1) peptide; Fig.

0021-9673/90/$03.50

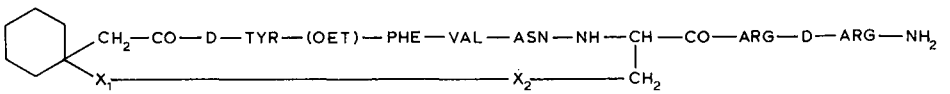

PEPTIDE	SK & F #	X_1	X_2
I	105494	CH_2	CH_2
II	104146	S	S

Fig. 1. Chemical structures of SK&F 105494 (I) and SK&F 104146 (II).

1, I}, a synthetic octapeptide analogue of vasopressin (AVP), is a parenterally active aquaretic agent which significantly increases water excretion in experimental animal models[1]. The compound selectively blocks renal water reabsorption via competitive antagonism of renal epithelial vasopressin (V2) receptors and is currently undergoing clinical trials. The peptide is highly potent and administered in low doses (5–10 μg/kg). The anticipated sensitivity requirement of 1 ng/ml in plasma made the development of analytical methodology for this compound a difficult problem due to a lack of a native chromophoric or common derivatizable functional group in the molecule. Although I has a blocked carboxy and amino terminus and generally non-reactive amino acid residues, the guanidino group in the arginine moiety of the peptide provided a potentially useful site for selective chemical modification to improve the detectability of I and develop a high-performance liquid chromatography (HPLC) assay with fluorescence detection.

Previous reports concerning HPLC analysis of arginine-containing peptides with fluorescence detection via pre- and post-column derivatization[2–5] have suffered from a lack of routine applicability or sensitivity in measuring such peptides at physiological levels. This report describes a novel, rapid, selective and highly sensitive HPLC method for the quantification of I in plasma. The approach involved isolation of the peptide from plasma samples by solid phase extraction and quantitative analysis by HPLC using a selective post-column reaction. Selective detection using the arginine moiety was accomplished through a post-column reaction of the guanidino side chain with ninhydrin under basic conditions to generate a fluorescent product which was measured at high sensitivity with an in-line fluorometer. The use of HPLC columns of reduced internal diameter and careful optimization of the post-column reaction conditions resulted in an on-column limit of detection of 50 pg (45 fmol, signal-to-noise ratio = 3) for this peptide. The methodology developed has general applicability in the analysis of arginine-containing peptides and peptide drugs.

EXPERIMENTAL

Materials

SK&F 104146 (Fig. 1, II) was used as the internal standard. I and II (purity > 98%) were obtained from Peptide Chemistry, Smith Kline and French Laboratories (Swedeland, PA, U.S.A.). HPLC-grade water (Ultrapure Water Systems, Durban, NC, U.S.A.) was used in the preparation of solutions, buffers and in the mobile phase. Monochloroacetic acid and sodium hydroxide were purchased from Mallinckrodt (Paris, KY, U.S.A.). HPLC-grade methanol and disodium ethylenediaminetetraacetic

acid (disodium EDTA, 99.5%) were purchased from EM Science (Cherry Hill, NJ, U.S.A.). Ninhydrin and trifluoroacetic acid (TFA, 99%) were obtained from Pierce (Rockford, IL, U.S.A.). All other chemicals were reagent grade and obtained from local sources.

Weak cation-exchange (carboxymethylhydrogen form, CBA) solid-phase extraction columns (1 ml) were purchased from Analytichem International (Harbor City, CA, U.S.A.).

Monochloroacetate buffer, pH 3.2, was prepared by dissolving monochloroacetic acid (5.7 g), sodium hydroxide (2.0 g) and disodium EDTA (0.2 g) in 1 l of deionized water to give a molarity of approximately 65 m*M*.

Extraction procedure

An aliquot of plasma (1 ml), containing I as standard or as an unknown, was mixed with 50 μl of methanol–water (50:50, v/v) solution of the internal standard II (1 μg/ml). A CBA column was conditioned by successive washings with 1 ml of 1% TFA in methanol, 1 ml of methanol and 2 ml of water. The plasma sample was applied to the column, the sample tube was rinsed with 1 ml of water and the washings were also transferred to the column. The column was washed successively with 1 ml of 1% TFA in water, 2 ml of water and 2 ml of methanol. The sample was then eluted with 2 ml of 1% TFA in methanol and collected into a 75 × 10 mm borosilicate tube. The eluate was evaporated under a gentle stream of nitrogen at 40°C and the residue was reconstituted in 100 μl of methanol–monochloroacetate buffer (50:50, v/v) and transferred to an autosampler vial. Volumes of 5–50 μl were injected into the HPLC system for analysis.

HPLC

The HPLC system consisted of a Hitachi 665A-12 high-pressure gradient semi-micro solvent delivery system (EM Science), a post-column reactor module (PCRS Model 520, ABI Analytical, Ramsey, NJ, U.S.A.) and a Hitachi F-1000 fluorescence detector (EM Science). Chromatographic separations were carried out on a 25 cm × 2.1 mm I.D., 5-μm octyl silica column (Ultrasphere, Beckman, Palo Alto, CA, U.S.A.), maintained at 60°C, at a flow-rate of 300 μl/min. The initial mobile phase composition was monochloroacetate buffer (pH 3.2)–methanol (45:55, v/v). Following injection, the methanol concentration was raised to 70% over a period of 10 min, held for 5 min and cycled back to initial conditions in 2 min. The system was equilibrated at the initial mobile phase composition for 13 min before injecting the next sample. Mobile phase eluents were filtered through a 0.2-μm Nylon-66 filter and degassed before use. Samples were injected by using an HPLC autosampler (WISP, Model 710B, Waters Associates, Milford, MA, U.S.A.). The post-column reactor module contains two independently heated zones which are used, in this case, as a column heating chamber and a reaction coil heating block. Two additional pumps (Model 114, Beckman) were utilized to deliver the sodium hydroxide (0.4 *M*) and ninhydrin reagent (0.05% w/v) solutions, at flow-rates of 150 and 50 μl/min, respectively, to the post-column reactor where they were mixed with the column effluent utilizing low dead volume mixers. The optimization of the ninhydrin post-column reaction for arginine-containing peptides has been described previously[6]. Following formation of the fluorescent reaction product, detection was accomplished

by utilizing excitation at 390 nm while monitoring the fluorescence emission with a 470-nm cut-off filter. Although the emission maximum for the fluorescent product is 500 nm, utilization of a 470-nm cut-off filter enhanced the fluorescence signal without sacrificing the specificity. The chromatographic data were collected with an automated laboratory system (CIS, Beckman, Waldwick, NJ, U.S.A.).

Standard curves

To establish calibration curves, three standard solutions of I [10, 1 and 0.1 μg/ml in water–methanol (50:50, v/v)] were used to prepare a series of 1-ml plasma samples at concentrations of 0, 1, 2, 5, 10, 20, 50 and 100 ng/ml. These samples were processed by the extraction procedure described above to generate an eight-point standard curve. The peak height ratios of I and the internal standard were weighed by $1/y$ (based on analysis of residual plots) and plotted against the concentrations of I. Linear regression analysis gave a calibration line that was used to calculate the concentration of I in unknown samples and seeded control samples. Standard solutions were stable for two months stored at 4°C.

RESULTS AND DISCUSSION

Application of the HPLC methodology described here provided a highly sensitive and specific assay for I in plasma samples. In large part, the specificity of the method was due to the selectivity of the post-column reaction chemistry. Although the structure is not presently known, under the strongly basic conditions used here (pH 12) ninhydrin gives a fluorescent product with the guanidino moiety of arginine but not with other common peptide functional groups, including primary amines. Injection of a variety of other peptides lacking arginine resulted in a lack of fluorescence response. Additional specificity was obtained through the use of weak cation-exchange rather than reversed-phase solid phase extraction of the peptide from plasma samples. Moreover, the product formed in the post-column reaction has excellent fluorescence properties in reversed-phase HPLC allowing detection of I at low femtomole levels.

Recovery and stability

The recovery of I and the internal standard from plasma was estimated with five determinations by comparing the peak height obtained with processed samples to that obtained by direct injection of an amount of standard equivalent to 100% recovery. At 75 ng/ml, a mean plasma recovery of 75.6 ± 3.7% was obtained for I. The recovery of the internal standard, II, from plasma, determined at a concentration of 50 ng/ml, was 77.5 ± 4.3%. In addition, I and internal standard were found to be stable in the final extract at room temperature for at least 24 h. Samples reanalyzed up to 24 h later showed no significant variation in peak height. Consequently, injection of prepared samples can be performed on the next day without observable quantitative changes.

Sensitivity, selectivity and linearity

By utilizing a 2.1-mm I.D. HPLC column, the on-column limit of detection (signal-to-noise ratio = 3) was 50 pg. Under the conditions used in this assay, the lowest concentration of I that could be determined quantitatively in 1-ml plasma samples without interference was 0.5 ng, which corresponded to an injected amount of

TABLE I

SUMMARY OF THREE-DAY ASSAY VALIDATION STUDY

Five replicates at three concentrations were analyzed on each of three successive days. At 2.5, 25 and 75 ng/ml, the within-day precision (mean of the daily coefficients of variation) was 10.26, 6.53 and 3.83%, respectively, the between-day precision (coefficient of variation of the daily means) 5.63, 4.59 and 1.87%, respectively and the mean accuracy 95.6, 100.6 and 102.6, respectively. S.D. = Standard deviation; C.V. = coefficient of variation.

Sample (N = 5)	*Day 1*	*Day 2*	*Day 3*
2.5 ng/ml			
Mean	2.24	2.43	2.50
S.D.	0.22	0.15	0.37
C.V. (%)	9.80	6.17	14.80
Accuracy	89.60	97.20	100.00
25 ng/ml			
Mean	26.38	24.99	24.09
S.D.	1.03	2.17	1.72
C.V. (%)	3.80	8.70	7.10
Accuracy	105.50	99.90	96.40
75 ng/ml			
Mean	77.99	77.65	75.34
S.D.	2.15	2.86	3.76
C.V. (%)	2.80	3.70	5.00
Accuracy	103.90	103.50	100.50

I of approximately 250 pg. Calibration curves obtained were linear over the range of 0.5–100 ng/ml of I. In this range, no interferences either from endogenous substances or from the known metabolites of I were observed. Weighed $(1/y)$ linear regression analysis of standard curves provided the equation $y = 0.03311x - 0.004373$ and a correlation coefficient greater than 0.99. Standard curves obtained over five successive days provided a composite curve with a correlation coefficient of 0.998. The precision, as measured by the relative standard deviations at each of the seven seeded concentrations, was within 11% across the calibration range. The average concentration back-calculated from the composite curve was within 10% of the seeded value at each concentration.

Accuracy and precision

The accuracy and precision of the assay were within 11% across the calibration range. Table I summarizes the results obtained from a three-day validation study in which five replicate-seeded standards at three concentrations, 2.5, 25 and 75 ng/ml, were analyzed each day by this methodology. The mean accuracy of the assay at these concentrations ranged from 95.6 to 102.6%, whereas the within-day precision, indicated by the mean of the daily coefficients of variation, varied from 3.83 to 10.26%. The reproducibility of the assay was high with between-day precision, indicated by the coefficients of variation of the daily means, ranging from 1.87 to 5.63%.

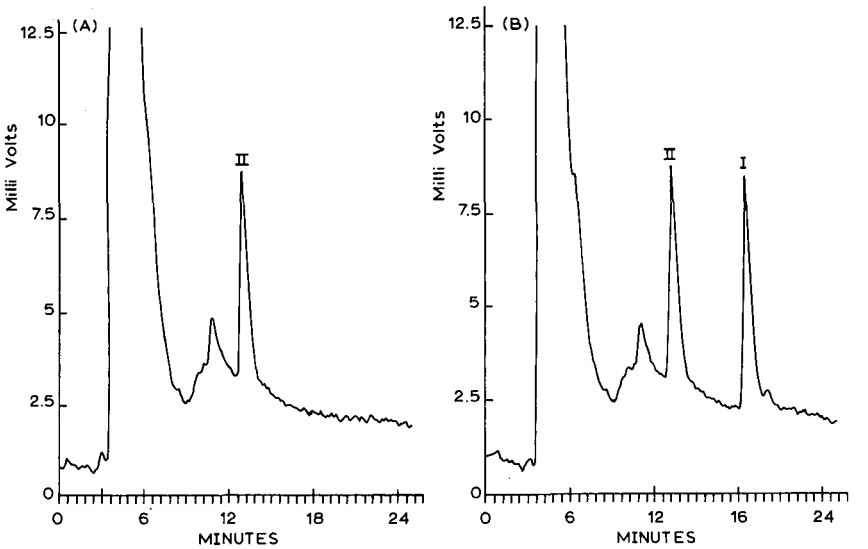

Fig. 2. Chromatograms of plasma extracts from a human subject before (A) and 2 h after (B) intravenous administration of 10 μg/kg of I. The concentration of I was 21.9 ng/ml.

Application of the procedure to plasma samples

Typical results obtained from the analysis of human plasma samples are shown in Fig. 2, which displays HPLC chromatograms of processed samples of drug-free human plasma and a plasma sample obtained from a human subject following an intravenous dose of I. The chromatography is highly reproducible and provides a retention time for I and internal standard of 18.6 and 14.0 min, respectively. To date the procedure has been used successfully in the analysis of biological samples from clinical and pre-clinical studies. The assay methodology developed was sufficiently sensitive for use in the study of the pharmacokinetics of I in humans and animal species.

In conclusion, a novel HPLC assay with fluorescence detection for an arginine-containing synthetic octapeptide antagonist of vasopressin, I, has been developed that is capable of measuring as low as 0.5 ng of I in 1 ml of plasma. The assay has excellent linearity, accuracy and precision over the range 0.5–100 ng/ml and has been shown to be suitable for pharmacokinetic studies of I. In addition, with slight modifications in HPLC conditions, the approach described here has general applicability in the detection of arginine-containing peptides, especially those without other easily modifiable functional groups.

REFERENCES

1 D. P. Brooks, P. F. Koster, C. B. Albrightson-Winslow, F. L. Stassen, W. Huffman and L. B. Kinter, *J. Pharmacol. Exp. Ther.* 245 (1988) 211.
2 M. Kai, T. Miyazaki, Y. Sakamoto and Y. Ohkura, *J. Chromatogr.*, 322 (1985) 473.
3 M. Ohno, M. Kai and Y. Ohkura, *J. Chromatogr.*, 392 (1987) 309.
4 Y. Hiraga, K. Shirono, S. Oh-Ishi, S. Sakakibara and T. Kinoshita, *Bunseki Kagaku*, 33 (1984) E279.
5 Y. Hiraga and T. Kinoshita, *J. Chromatogr.*, 226 (1981) 43.
6 G. R. Rhodes and V. K. Boppana, *J. Chromatogr.*, 444 (1988) 123.

Journal of Chromatography, 507 (1990) 85–93
Elsevier Science Publishers B.V., Amsterdam — Printed in The Netherlands

CHROMSYMP. 1801

Characterization of a reversed-phase high-performance liquid chromatographic system for the determination of blood amino acids

GIUSEPPE BUZZIGOLI, LAURA LANZONE, DEMETRIO CIOCIARO, SILVIA FRASCERRA, MAURIZIO CERRI, ANGELO SCANDROGLIO, ROBERTO COLDANI and ELEUTERIO FERRANNINI*

Metabolism Unit of the CNR Institute of Clinical Physiology and 2nd Medical Clinic, University of Pisa, Via Savi 8, 56100 Pisa (Italy)

SUMMARY

High-performance liquid chromatography was used to separate physiological amino acids in perchloric acid supernatants of blood samples. Precolumn derivatization with phenyl isothiocyanate was carried out, starting with 20 μl of supernatant; 2–10 μl were injected into a 30-cm Pico Tag column, which was eluted with a gradient of two eluents in 64 min. Stock amino acid solutions prepared in water, hydrochloric acid or perchloric acid showed comparable recoveries on serial dilution (parallelism test). The recovery of crystalline amino acids added to blood in amounts ranging from normal to six times normal was generally satisfactory. The within-assay relative standard deviations were $< 5\%$ for many amino acids. The performance of the system was less than satisfactory for cysteine and methionine. Glutamine and asparagine are interconverted into glutamate and aspartate, respectively, in a time-dependent fashion; a separate measurement of one member of the pair is therefore required in order to assay the other starting from the sum of both chromatographic peaks. The method is suitable for the relatively rapid, sensitive and accurate measurement of blood amino acids in perchloric acid supernatants (in which other relevant metabolites are customarily assayed) over a wide range of physiological concentrations, on very small amounts of sample.

INTRODUCTION

In metabolic studies, the determination of blood amino acid concentrations, together with those of other metabolites (*e.g.*, glucose, lactate, pyruvate, β-hydroxybutyrate, glycerol) is often important[1]. Physiological amino acids can be assayed in plasma, serum or whole blood[2]. Although plasma values are more prevalent in the literature[3], whole-blood measurements are of prime interest because red blood cells actively participate in amino acid exchange between blood and tissues. Therefore,

0021-9673/90/$03.50

when assessing the role of an organ in amino acid metabolism with the use of the net balance technique, flow-rates and blood arteriovenous amino acid concentration gradients should be used to determine the true net organ balance[4,5]. Moreover, most of the metabolites of interest in physiological studies are also measured in whole blood. Obtaining measurements of amino acids and intermediate metabolites in the same pool therefore presents an obvious advantage. Metabolites are generally unstable at room temperature, and correct processing (including deproteinization) of blood samples is critical[6]. It should also be considered that experiments are often of long duration and, customarily, many blood samples are obtained at timed intervals. For this reason, important factors for amino acid analysis in metabolism studies are, in addition to reproducibility and sensitivity, the use of micro-methods (many parameters to be measured in the same sample) with a high level of automation (many samples to be assayed).

The classical approach to amino acid analysis is separation on a sulphonate cation-exchange resin, followed by derivatization with ninhydrin and spectrophotometric detection[7]. These methods are adequate but generally time consuming; further, they require substantial amounts of sample. The use of reversed-phase high-performance liquid chromatography (HPLC) permits amino acid determinations in a relatively short time, on small samples and with good sensitivity and specificity[8,9]. In this work, we selected a method that employs precolumn derivatization with phenyl isothiocyanate[10,11] and adapted it to blood samples deproteinized with chilled perchloric acid.

EXPERIMENTAL

Materials

Acetonitrile and methanol (LiChrosolv) were obtained from Merck (Darmstadt, F.R.G.). Sodium acetate trihydrate, disodium hydrogenphosphate, sodium dihydrogenphosphate, phosphoric acid, perchloric acid (PCA), ethylenediaminetetraacetic acid, disodium salt (EDTA) and hydrochloric acid (HCl) were of analytical-reagent grade, purchased from Merck (Darmstadt, F.R.G.). Triethylamine (TEA) and phenyl isothiocianate (PITC) were obtained from Pierce (Rockville, IL, U.S.A.). High-purity water was obtained by a Milli-Q purification system (Millipore, Bedford, MA, U.S.A.), which was fed with a supply of previously deionized reversed-osmosis-purified water. Basic (product N A-6282), neutral and acid (product N A-6407) physiological amino acid standard solutions were obtained from Sigma (St. Louis, MO, U.S.A.). These standards were mixed at the time of derivatization and used for calibration. Moreover, a set of standards (20, 50, 100, 286, 400 and 667 μM) was prepared by diluting Sigma standard solutions in water, and another set (20, 50, 100, 200, 400, 600 and 800 μM) by diluting the same Sigma standards in 0.1 M HCl or 0.5 M PCA. Individual crystalline amino acids (reference substances for chromatography obtained from Merck) were used to prepare three physiological standards in 0.5 M PCA. First, concentrated stock solutions in 0.1 M HCl of 20 single amino acids were made. Then, a six times normal physiological standard (6N) in 0.5 M PCA was obtained by means of appropriate dilutions (each amino acid was brought up to six times the basal, post-absorptive value of normal humans). In the same way, three times normal (3N) and normal (N) physiological standards were prepared (to cover a wide

range of possible final concentrations in actual blood samples in PCA). Derivatization tubes were Pirex brand (Corning, Corning, NY, U.S.A.); vacuum vials were purchased from Waters Assoc. (Milford, MA, U.S.A.).

Sample preparation and derivatization

Blood samples were deproteinized immediately after drawing blood by adding an equal volume of chilled 1 *M* PCA (the final sample concentration was therfore *ca.* 0.5 *M* PCA). The samples were spun at 1500 *g* at 4°C for 20 min in a refrigerated centrifuge. Appropriate aliquots of the supernatants were passed through 0.45-μm HV Millipore filters obtained from Waters Assoc. Volumes of 20 μl were used for derivatization, and dried under vacuum (*ca.* 80 mTorr for 30 min) by using a Pico Tag work station (Waters Assoc.). Dried residues were reconstituted with 20 μl of 1 *M* sodium acetate–methanol–TEA (2:2:1) solution. Samples were re-dried (*ca.* 80 mTorr for 15 min), and reconstituted in 20 μl of derivatization solution [methanol–water–TEA–PITC (7:1:1:1)]. A period of 20 min at room temperature was allowed for the reaction of PITC with amino groups (to produce phenylthiocarbamyl amino acid residues). The samples were then dried again until a constant vacuum of 60 mTorr was obtained (*ca.* 90 min). Finally, the dried samples were reconstituted with 200 μl of phosphate buffer (pH 7.40). After vortex mixing and sonicating for a few seconds, the samples were injected. The same derivatization scheme was applied to standard solutions.

Chromatographic system

The system utilized was purchased from Waters Assoc. and consisted of two M510 solvent-delivery pumps driven by an M680 automated gradient system controller. A Pico Tag column (30 cm × 3.9 mm I.D.) was employed. The column temperature was maintained at 46 ± 1°C by means of a column heater with a temperature control module. An M441 fixed-wavelength UV detector set at 254 nm was connected to a M745 recorder/integrator. Samples were injected in volumes ranging from 2 to 10 μl using an M712 Wisp autoinjector equipped with a Wisp cooling unit (samples were kept at 4°C). The mobile phase consisted of a gradient of two eluents, kept under a blanket of helium. Eluent A was an aqueous buffer of 0.07 *M* sodium acetate containing 2.5% acetonitrile and 1 ppm EDTA titrated to pH 6.50 with 10% glacial acetic acid. Eluent B was an organic phase consisting of acetonitrile–water–methanol (45:40:15). The gradient employed in the separation started with eluent B rising from 3 to 34% in *ca.* 64 min. After a washing step of 10 min with 100% B, the column was re-equilibrated for 20 min with 100% A. A constant flow-rate of 1 ml/min was maintained throughout.

Assay procedure

Each daily derivatization set consisted of ten unknown samples, two Sigma standards containing 38 amino acids, and two N "physiological" standards. The unknown samples were run after two perfect blanks, one Sigma (125 μmol/l) and one N physiological standard. The run was terminated with another Sigma and another N physiological standard. Peak reading was done by means of a one-point calibration external standard (Sigma). The control of the procedure in terms of accuracy and precision was obtained through the N physiological standards[12].

RESULTS

The separation of an N physiological standard in 0.5 *M* PCA is shown in Fig. 1. A typical separation of an amino acid calibration standard (125 pmol injected) is shown in Fig. 2. A representative separation of a blood sample is shown in Fig. 3. Data on the between-assay precision of the retention times are given in Table I.

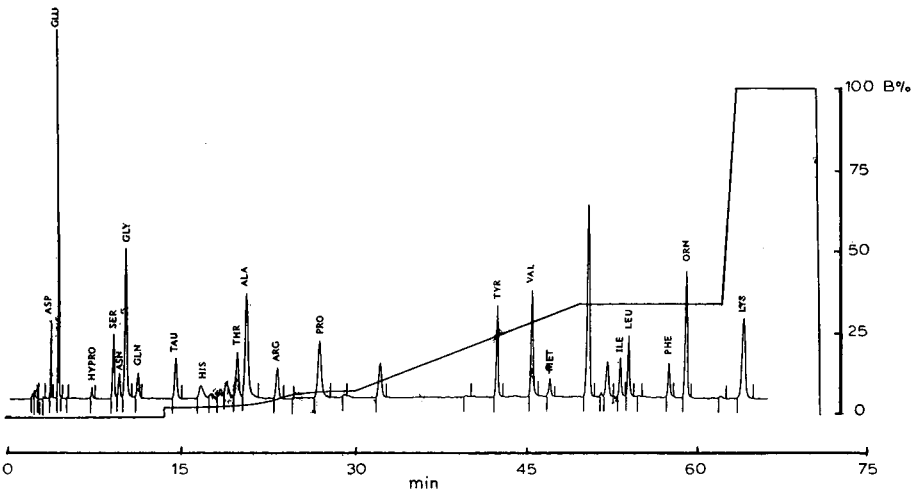

Fig. 1. Elution pattern of a mixture of physiological amino acids dissolved in 0.5 *M* PCA at concentrations close to those found in the blood of normal fasting subjects. Twenty amino acids were separated by using a gradient of two eluents: eluent A (aqueous buffer of 0.07 *M* sodium acetate containing 2.5% acetonitrile and 1 ppm EDTA titrated to pH 6.50 with glacial acetic acid) and eluent B [acetonitrile–methanol–water (45:40:15)]. The gradient is indicated as a percentage of eluent B. Flow-rate was constant at 1 ml/min.

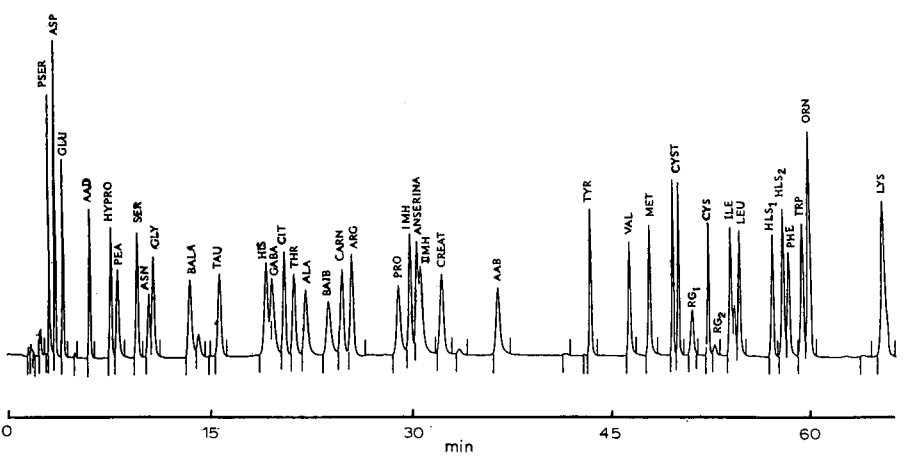

Fig. 2. Separation of 38 amino acids in a Sigma standard (125 pmol injected). Elution conditions as in Fig. 1.

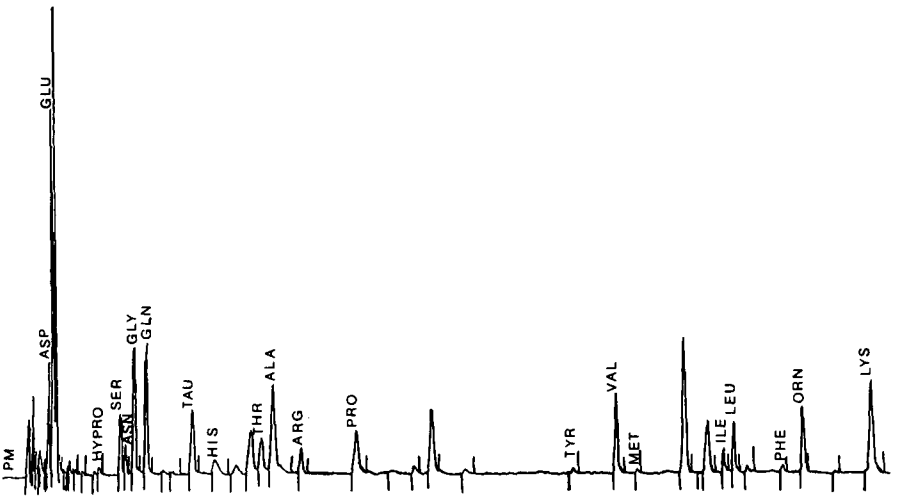

Fig. 3. Elution pattern of a blood sample obtained from a healthy subject after an overnight fast. Elution conditions as in Fig. 1.

TABLE I

RETENTION TIMES FOR VARIOUS AMINO ACIDS

Data from 30 chromatographic runs. C.V. = coefficient of variation.

Amino acid	*Retention time (min)*		*Amino acid*	*Retention time (min)*	
	Mean ± S.D.	*C.V. (%)*		*Mean ± S.D.*	*C.V. (%)*
Aspartic acid	3.48 ± 0.09	2.5	Alanine	20.93 ± 0.52	2.5
Glutamic acid	4.02 ± 0.12	3.0	Arginine	23.78 ± 1.05	4.4
Hydroxyproline	7.19 ± 0.20	2.8	Proline	27.25 ± 0.69	2.5
Serine	9.12 ± 0.21	2.3	Tyrosine	42.55 ± 0.30	0.7
Asparagine	9.67 ± 0.32	3.3	Valine	45.61 ± 0.25	0.6
Glycine	10.22 ± 0.26	2.5	Methionine	47.20 ± 0.24	0.5
Taurine	14.69 ± 0.38	2.6	Isoleucine	53.26 ± 0.28	0.5
Histidine	17.16 ± 1.06	6.2	Leucine	53.92 ± 0.28	0.5
GABA	17.71 ± 0.66	3.7	Phenylalanine	57.34 ± 0.43	0.8
Citrulline	18.48 ± 0.80	4.4	Ornitine	58.84 ± 0.50	0.9
Threonine	20.04 ± 0.52	2.6	Lysine	63.52 ± 0.95	1.5

Linearity of response in water, 0.1 M HCl and 0.5 M PCA

The use of an external standard prepared in 0.1 *M* HCl to be used against blood samples deproteinized with 0.5 *M* PCA made it necessary to check that the results were not affected by the use of different solvents. Using the solutions previously desribed, seventeen principal amino acids were measured in water, 0.1 *M* HCl or 0.5 *M* PCA (three measurements for each concentration point). No significant difference was found in either the intercepts or the regression coefficients between the three solvents: the correlation coefficients ranged from 0.963 (valine) to 0.999 (methionine) in water,

from 0.982 (phenylalanine) to 0.995 (glutamine) in 0.1 *M* HCl and from 0.977 (alanine) to 0.994 (isoleucine) in 0.5 *M* PCA. There were two exceptions. For cysteine, when run in either 0.1 *M* HCl or 0.5 *M* PCA, the slopes (0.418 and 0.379, respectively) were almost one third of those of the other amino acids, with intercepts of different sign, even though the correlation coefficients were almost identical (0.9413 and 0.9411, respectively). Methionine, on the other hand, had a very good pattern of recovery in water, with $r = 0.9985$, slope = 0.919, and an intercept not significantly different from zero; in 0.1 *M* HCl, these figures were $r = 0.9028$, slope = 0.692, with a positive intercept, and in 0.5 *M* PCA, $r = 0.891$, slope = 0.487, with a negative intercept.

Recovery under physiological conditions

Physiological amino acid standards (N, 3N and 6N) in 0.5 *M* PCA were run at least in quadruplicate for every concentration point to evaluate the recovery under conditions mimicking normal and pathological states (Table II). The recovery was also tested by adding the N physiological standard to a blood sample and then measuring the overall recovery (Table III). In addition, to determine the differential recovery along the chromatogram (the run takes *ca.* 64 min), hydroxyproline (retention time, $t_R = 7.19$ min), alanine ($t_R = 20.43$ min) and ornitine ($t_R = 58.84$ min) were added as crystalline amino acids to an unknown blood sample and their recoveries measured. The recoveries were 96, 102 and 87%, respectively.

TABLE II

RECOVERY OF VARIOUS AMINO ACIDS FROM PHYSIOLOGICAL STANDARDS IN 0.5 *M* PERCHLORIC ACID

Table entries are percent recoveries from standards having normal, 3 × normal, and 6 × normal amino acid concentrations.

Amino acid	*Recoveries (%)*	*Amino acid*	*Recoveries (%)*
Aspartic acid	69, 71, 73	Proline	93, 93, 97
Glutamic acid	93, 95, 97	Tyrosine	96, 122, 124
Hydroxyproline	91, 93, 94	Valine	93, 93, 96
Serine	96, 88, 93	Isoleucine	95, 93, 93
Glycine	94, 95, 101	Leucine	84, 99, 82
Taurine	97, 96, 100	Phenylalanine	92, 89, 93
Histidine	86, 84, 89	Ornitine	93, 89, 96
Threonine	92, 86, 91	Lysine	93, 99, 95
Alanine	91, 87, 93	γ-Aminobutyric acid	100, 102, 91
Arginine	86, 86, 91	Citrulline	94, 96, 103

Within-run and between-run precision

Forty duplicate unknowns were used to estimate the within-assay standard deviation (Table IV). The between-assay precision was determined from the N physiological standards included in every run. The results for 40 runs over a period of 6 months are given in Table IV.

TABLE III

RECOVERY OF VARIOUS AMINO ACIDS ADDED TO BLOOD SAMPLES

Amino acid	*Recovery (%)*	*Amino acid*	*Recovery (%)*
Aspartic acid	85	Arginine	104
Glutamic acid	107	Proline	101
Hydroxyproline	110	Tyrosine	97
Serine	102	Valine	102
Asparagine	104	Methionine	106
Glycine	109	Isoleucine	93
Taurine	101	Leucine	102
Histidine	102	Phenylalanine	98
Threonine	97	Ornitine	99
Alanine	100	Lysine	103

TABLE IV

WITHIN-ASSAY AND BETWEEN-ASSAY PRECISION

Amino acid	*Within-assay*			*Between-assay*		
	Mean	*S.D.*	*C.V.*	*Mean*	*S.D.*	*C.V.*
	(μM)		*(%)*	*(μM)*		*(%)*
Aspartic acid	74	5	6.7	43	4	9.6
Glutamic acid	618	14	2.2	298	31	10.3
Hydroxyproline	12	3	25.2	26	14.0	
Serine	101	3	2.9	95	11	11.1
Asparagine	77	3	4.2	63	8	12.8
Glycine	251	8	3.2	325	25	7.8
Glutamine	1845	19	1.0	–	–	–
Histidine	63	9	14.6	52	8	15.4
Taurine	178	4	2.4	103	10	9.7
Threonine	89	8	9.4	126	15	11.5
Alanine	264	12	4.4	324	32	10.0
Arginine	52	2	4.2	72	7	9.8
Proline	156	5	3.4	206	16	7.7
Tyrosine	47	3	5.7	170	26	15.5
Valine	165	4	2.1	211	17	7.8
Methionine	11	2	20.5	40	6	15.2
Cysteine	331	13	4.0	–	–	–
Isoleucine	65	7	11.1	81	11	13.6
Leucine	80	3	4.0	106	12	11.5
Phenylalanine	38	5	12.8	72	8	10.6
Ornitine	62	2	3.4	137	16	11.5
Lysine	114	3	2.6	139	16	11.4

Stability and conservation of standards and samples

The stock standard solutions, when stored in PCA at −20°C, presented problems depending on the solvent used for dilution. In particular, tryptophan, cysteine and hydroxylysine disappeared over a short period of time, whereas tyrosine and phenylalanine were prone to degradation. It was possible to demonstrate that this

problem is related to the use of PCA on account of its acidic and oxidizing power. Once derivatized, samples are stable for at least 1 month if stored under vacuum at −20°C. When reconstituted in phosphate buffer (pH 7.4) after derivatization, samples are stable for at least 1 week if the autoinjector is used, because they stay protected and refrigerated. When stored at −20°C, no appreciable variations were observed over a 2-week period.

DISCUSSION

The method described is able to assay most physiological amino acids in an acidic supernatant with satisfactory accuracy, recovery and precision. The assay time (a total of 90 min for a complete run and subsequent column reconditioning) and sample volume (10 μl) are favourable. The stability of the sample after derivatization is satisfactory if a refrigerated autoinjector is used; the stability of samples reconstituted in phosphate buffer is also favourable.

There are several unresolved problems. First, it is impossible to measure tryptophan, which is unstable in 0.5 *M* PCA. Second, cysteine is lost from stored samples and methionine is assayed with insufficient accuracy. It is possible that pretreatment of samples with antioxidants will stabilize these two amino acids; however, this may distort the elution pattern of other amino acids. Third, in samples stored at −20°C, glutamine and asparagine are converted into glutamate and aspartate, respectively, in a time-dependent fashion. We attempted to overcome this problem by neutralizing samples with chilled potassium hydroxide immediately after deproteinization with PCA. Under these neutral pH conditions, glutamine and asparagine were in fact assayed, but aspartate and glutamate eluted with the eluent front and were lost. Therefore, this method is accurate only for the sums glutamine + glatamate and asparagine + aspartate. To obtain actual values, separate measurements of asparagine and glutamine (or aspartate and glutamate) by an enzymatic spectrophotometric method should be made; the values can then be subtracted from the sums determined by HPLC to obtain the concentration of the other member of the pair. In general, prompt treatment of blood samples with the deproteinizing agent and adequate storage of the resulting supernatants seem to be critical factors for the accuracy of the method. In fact, delayed deproteinization of plasma samples has been shown to change amino acid concentrations after only 30 min at room temperature[13]. Further, even storage at −20°C appears to lead to a decrease in the measurable levels of glutamine/glutamate and asparagine/aspartate[14]. We are currently evaluating the effect of storing immediately PCA-deproteinized supernatants at −20°C *vs.* −70°C.

The recovery and reproducibility data presented here refer to HPLC analyses run in the absence of internal standards. The results show that most physiological amino acids are assayed with a precision of $\leqslant 5\%$. Hydroxyproline and phenylalanine have a relative standard deviation of $> 10\%$, possibly on account of their low blood concentration. The pattern of dispersion of retention times (Table I) indicates that the inclusion of multiple internal standards may be necessary to improve the reproducibility of this chromatographic system. The recovery experiments (Tables II and III), however, suggest that variable recovery during the HPLC run may not be a major source of scatter. In a separate series of experiments, we found that the relative standard deviations for almost all amino acids decrease to 2–3% when quadruplicate

injections are made of the same sample after derivatization. This result indicates that at least half of the variability of the method may derive from the derivatization step. Accordingly, any internal standards would most suitably be added to the PCA solution before addition of blood specimens. We are currently testing the possibility of improving the precision of the method in this way.

In conclusion, the HPLC method described here demonstrates that blood amino acids can be assayed in PCA supernatants with high sensitivity and good accuracy, using very small volumes of material and in relatively short time. Precolumn derivatization of PCA supernatants remains a time-consuming (*ca.* 3 h) step, and a probable source of imprecision. Improvement of the precision seems to be feasible. Ultimately, nevertheless, the detection of small arteriovenous differences for some amino acids must rely on replicate measurements, visual selection of chromatographic peaks and statistical treatment of outlying observations.

REFERENCES

1 C. R. Scriver and L. E. Rosenberg, *Amino Acid Metabolism and its Disorders*, Saunders, Philadelphia, London, Toronto, 1973.
2 J. P. Greenstein and M. Vinitz, *Chemistry of Amino Acids*, Wiley, New York, London, Sydney, 1961.
3 H. J. Bremmer, M. Duran, J. P. Kamerling, H. Przyremble and S. D. Wadman, *Disturbance of Amino Acid Metabolism. Clinical Chemistry and Diagnosis*, Urban and Schwartzenberg, Baltimore, 1981.
4 P. Felig, J. Wahren and L. Raf, *Proc. Natl. Acad. Sci. USA*, 70 (1973) 1775.
5 E. Ferrannini, E. J. Barrett, S. Bevilacqua, R. Jacob, M. Walesky, R. S. Sherwin and R. A. De Fronzo, *Am. J. Physiol.*, 250 (1986) E686.
6 E. Ferrannini, S. Bevilacqua, L. Lanzone, R. Bonadonna, L. S. Brandi, M. Oleggini, C. Boni, G. Buzzigoli, D. Ciociaro, L. Luzi and R. A. De Fronzo, *Diab. Nutr. Metab.*, 3 (1988) 175.
7 S. Moore, D. H. Spackman and W. H. Stein, *Anal. Chem.*, 30 (1958) 1185.
8 R. Pfeifer, R. Karol, J. Korpi, R. Burgoyne and D. McCourt, *Am. Lab.*, March (1983) 77.
9 G. A. Qureshi, L. Fohlin and J. Bergstrom, *J. Chromatogr.*, 297 (1984) 91.
10 B. A. Bidlingmeyer, S. A. Cohen and T. L. Tarvin, *J. Chromatogr.*, 336 (1984) 93.
11 R. J. Early and R. O. Ball, *J. Anal. Pur.*, 2 (1987) 47.
12 W. J. Youden. *Statistical Methods for Chemists*, Wiley, New York, 1951.
13 G. A. Qureshi and A. R. Qureshi, *J. Chromatogr.*, in press.
14 K. Olek, S. Uhlhaas, P. Wardenbach and M. Yamaguchi, *J. Clin. Chem. Clin. Biochem.*, 17 (1979) 599.

Journal of Chromatography, 507 (1990) 95–101
Elsevier Science Publishers B.V., Amsterdam — Printed in The Netherlands

CHROMSYMP. 1778

Separation of free amino acids by reversed-phase ion-pair chromatography with column switching and isocratic elution

MITSUKO HIRUKAWA
Gasukuro Kogyo Inc., 237-2 Sayamagahara, Iruma 358 (Japan)
MASAKO MAEDA and AKIO TSUJI
Showa University, Pharmaceutical Department, Hatanodai, Shinagawa-ku, Tokyo 142 (Japan)
and
TOSHIHIKO HANAI*
International Institute of Technological Analysis, Health Research Foundation, Institute Pasteur de Kyoto 5F, Hyakumanben, Kyoto 606 (Japan)

SUMMARY

Free amino acids (FAA) were separated by reversed-phase ion-pair liquid chromatography using a column-switching technique with isocratic elution. The eluted FAA were monitored by fluorescence detection using *o*-phthalaldehyde reagent. A 5-μm phenyl-bonded silica gel column (5 cm × 4.6 mm I.D.) was used for the hydrophobic and basic amino acids, which were separated within 20 min. A 5-μm octadecyl-bonded silica gel column (25 cm × 4.6 mm I.D.) was used for polar acidic and small amino acids, which were separated within 11 min. The system was applied to the FAA analysis of hydrolysate of bovine serum albumin.

INTRODUCTION

The chromatographic determination of amino acids is frequently used in many fields, and shortening of the analysis time is required. Reversed-phase ion-pair chromatography (RP-IPC) has been demonstrated to give more rapid and efficient separations of ionizable compounds than ion-exchange liquid chromatography (IEC)[1]. Free amino acids (FAA) were separated by RP-IPC with copper(II) ion. A column-switching technique with a combination of different alkyl-bonded silica gel columns under isocratic elution made it easy to achieve a rapid separation of a mixture of FAA[2]. However, the sensitivity was not satisfactory for application of the system to the determination of amino acids in biological samples.

o-Phthalaldehyde (OPA) reagent reacts with primary amines and amino acids in alkaline medium in the presence of a reducing agent such as 2-mercaptoethanol[3]. The post-column method was applied to IEC[4]. The OPA reagent in combination with sodium hypochlorite (NaOCl) oxidation made it possible to detect imino acids such as proline[5,6], and N-acetyl-L-cysteine was more suitable than mercaptoethanol be-

0021-9673/90/$03.50

cause of the stable thio-substituted isoindole derivative[7,8]. The OPA post-column detection method has been widely employed in reversed-phase liquid chromatography[9–21] for highly sensitive detection.

In this work, a column-switching technique and a post-column reaction detection system using OPA were combined for the rapid determination of FAA by RP-IPC.

EXPERIMENTAL

The liquid chromatograph consisted of an ERC-3310 degasser from ERMA (Tokyo, Japan) two Model 576 HPLC pumps and a Model FA-1040 flow-injection analysis pump from Gasukuro Kogyo (Tokyo, Japan), a Model F-1000 fluorescence detector from Hitachi (Tokyo, Japan) a Model 7125 injector, a Model 7000 six-way valve and a Model 7040 four-way valve from Rheodyne (Cotati, CA, U.S.A.) and a Sysmac PO time sequencer from Omron (Osaka, Japan). The six- and four-way valves were operated by Model 5701 pneumatic actuators (Rheodyne).

An octadecyl-bonded (ODS), an octyl-bonded (C_8) and a phenyl-bonded (Ph) silica gel (Inertsil ODS-2, C_8 and Ph respectively) and a diethyl-bonded silica gel (C_4) were obtained from Gasukuro Kogyo. These columns were 250 and 50 mm × 4.6 mm I.D. and were thermostated at 40 or 45°C. The eluent was prepared by dissolving appropriate amounts of a given sodium hexane- (C_6), heptane- (C_7) and octanesulphonate (C_8) and dodecyl sulphate (SDS) together with sodium chloride and an organic solvent (methanol, acetonitrile or ethanol) in phosphate buffer. OPA–N-acetyl-L-cysteine (N-AcCys) reagent was prepared by dissolving of 1.6 g of OPA and 2.0 g of N-AcCys in 10 ml of methanol and diluting with 1 l of 0.2 *M* sodium borate buffer, prepared by dissolving 24.6 g of boric acid and 15.2 g of sodium hydroxide in 2 l of doubly distilled water. Sodium hypochlorite solution was prepared by diluting 0.4 ml of commercial Antiformin (5% aqueous NaOCl solution) in 0.2 *M* sodium borate buffer[8].

All reagents were purchased from Wako (Osaka, Japan) and amino acids from Ajinomoto (Tokyo, Japan).

Protein hydrolysis was effected by the following method[8]. The protein sample (*ca.* 100 μg) [bovine serum albumin, crystallized four times, from ICN Pharmaceuticals (Cleveland, OH, U.S.A.)] was dissolved in 50 μl of 6 *M* hydrochloric acid in a Reacti-Vial, and the vial was placed in an oven at 150°C for 2 h. After hydrolysis, the vial was cooled. The hydrolysate were evaporated to dryness in a desiccator over potassium hydroxide pellets, then the residue was dissolved in 200 μl of the eluent.

RESULTS AND DISCUSSION

The effects of several factors on the retention behaviour of amino acids in RP-IPC was examined, *viz.*, alkyl chain length of the ion-pair (IP) reagent, concentration of IP reagent and organic modifier, pH, column temperature, phosphate and sodium ion concentrations in the eluent and selectivity of bonded phases of the silica gel packings.

First, the retention behaviour of polar acidic and small amino acids (Asp, Ser, Glu, Gly, Thr, Ala, Pro and Cys) was examined, because of their very weak retention in RP-IPC. These polar amino acids were more strongly retained as a result of forming

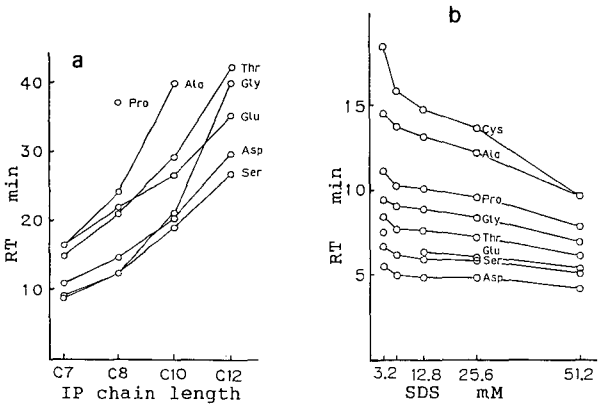

Fig. 1. Effect of (a) ion-pair reagent and (b) concentration. C7, C8, C10 = heptane-, octane- and decane-sulphonate respectively; C12 = dodecylsulphate. Column, Inertsil ODS-2 (250 mm × 4.6 mm I.D.); detector, UV (200 nm); flow-rate, 1.0 ml/min; column temperature, (a) 20°C and (b) 45°C; eluents, see text. RT = Retention time.

more hydrophobic ion pairs with a longer alkyl chain IP reagent, as shown in Fig. 1a where the eluent was 0.05 *M* sodium phosphate buffer (pH 2.0) with 6.4 m*M* IP reagent added. However, no simple behaviour was observed for the amino acids, and the alkyl chain length of IP reagent was potentially effective on the retention of glycine. Their retention became constant with more than 6.4 m*M* of SDS, as shown in Fig. 1b where the eluent was a combination of 0.05 *M* sodium phosphate buffer containing SDS (pH 2.7) and 16% methanol containing SDS. The column was easily re-equilibrated with highly concentrated IP reagent solution. Therefore, 25.6 m*M* SDS solution was selected as giving a good separation and shorter equilibration time.

Increasing the organic modifier concentration shortened the retention time, and this effect was readily observed on the retention of relatively hydrophobic amino acids such as proline. However, no specificity was observed between methanol and acetonitrile (ACN) as shown in Fig. 2.

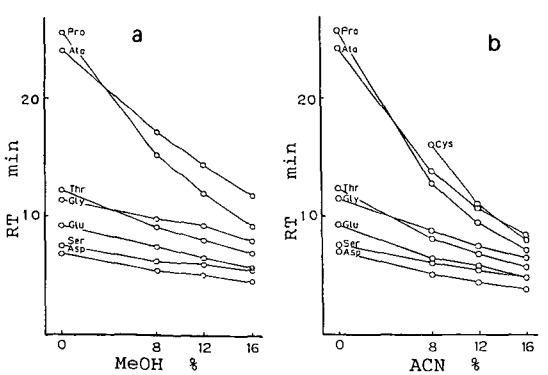

Fig. 2. Effect of organic modifier, methanol (MeOH) and acetonitrile (ACN) on the retention parameters of various amino acids. Eluent, 0.05 *M* sodium phosphate buffer containing 25.6 m*M* SDS (pH 2.7) plus methanol or ACN containing 25.6 m*M* SDS; column temperature, 45°C; other conditions as in Fig. 1.

The pH was the most sensitive factor in the separation of amino acids. After examining its effect with eluents of pH 2.0–5.0, pH 2.7 was selected as giving the best separation of polar amino acids. The concentration of sodium phosphate buffer was an important factor in shortening the retention time, but was not critical for separating less retained amino acids (Fig. 3a). The effect of sodium chloride concentration was examined on an ODS column. After injection of amino acids on to a column equilibrated with a conditioning eluent [0.05 *M* sodium phosphate buffer containing 25.6 m*M* SDS (pH 2.7) plus 12% methanol containing 25.6 m*M* SDS], these amino acids were eluted with a separation eluent [0.05 *M* sodium phosphate buffer (pH 2.7) containing 5% ethanol and ACN and some sodium chloride]. As seen in Fig. 3b, an increase in sodium chloride concentration had a greater effect on both the retention time and elution order, especially for basic amino acids. An increase in column temperature shortened the retention times. The retention times on bonded-phases from C_4 to ODS groups increased with increase in the alkyl chain length. However, the lifetime of the C_4 phase was too short to make separation system. The separation of acidic amino acids required an ODS column, and that of valine and methionine was achieved on a Ph column.

A column-switching system was established from the above results. As shown in Fig. 4, two switching valves and one fluorescence detector were used instead of one switching valve and two ultraviolet absorption detectors as in a previous study[2].

The time sequence is given in Table I. After injection on to a Ph column, the sample was separated into polar acidic and small (less retained) and hydrophobic and basic (retained) amino acids. The less retained amino acids were transferred to an ODS column by eluent 2 from pump 2. Eluent 2 was 0.05 *M* sodium phosphate buffer containing 25.6 m*M* SDS (pH 2.7) plus 12% methanol and 0.094 *M* sodium chloride. The flow-rate was 1.0 ml/min (process I). The ODS column was removed from the line at the first column switch 3.5 min after injection. The retained amino acids were first separated on the Ph column by eluent 1 from pump 1. Eluent 1 was 0.05 *M*

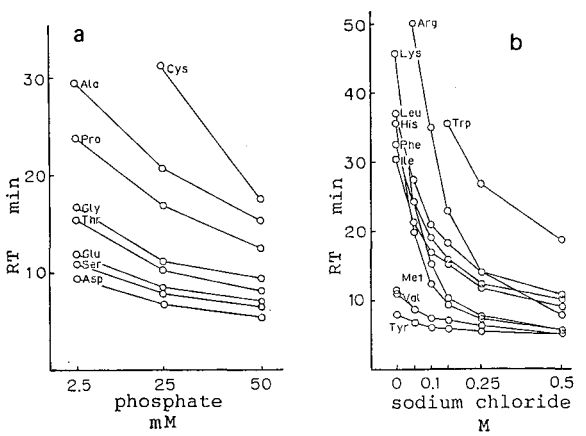

Fig. 3. Effect of phosphate and sodium ion concentration on retention of amino acids. (a) Eluent, sodium phosphate buffer (pH 2.7) plus 12% methanol and 25.6 m*M* SDS; other conditions as in Fig. 1. (b) Column, Inertsil ODS-2 (50 mm × 4.6 mm I.D.); flow-rate, 1.0 ml/min; column temperature, 45°C; eluent, see text.

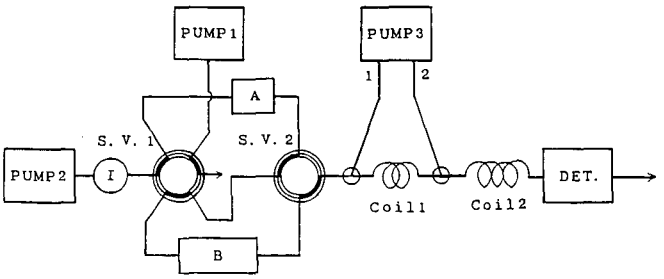

Fig. 4. Flow diagram of column-switching system. Column A, Inertsil Ph (50 mm × 4.6 mm I.D.); column B, Inertsil ODS-2 (250 mm × 4.6 mm I.D.); DET, fluorescence detector (excitation at 340 nm, emission at 450 nm); PUMP 1 and 2, HPLC pumps; PUMP 3-1, NaOCl reagent pump, flow-rate 0.9 ml/min; PUMP 3-2, OPA reagent pump, flow-rate 0.9 ml/min; coil 1, 60 cm × 0.5 mm I.D.; coil 2, 600 cm × 0.5 mm I.D., column and reaction coil temperature, 40°C; I, injector; S.V.1 and 2, six- and four-way switching valves. Eluent and reaction reagents, see text.

sodium phosphate buffer (pH 2.7) containing 6.5% ethanol, 6.5% ACN and 0.11 *M* sodium chloride. The flow-rate was 1.0 ml/min (process II).

After 23.5 min, less retained amino acids were separated on the ODS column by eulent 2, and the separation was completed within 34.5 min (process III). Finally, the Ph column was reconditioned with eluent 2 and the ODS column was recombined at 37.5 min, ready for the next injection.

The selection of the sodium chloride concentration in eluents 1 and 2 was important because an imbalance in the sodium chloride concentration in two eluents made the baseline shift when column switching was operated and quantitative analysis became difficult. Therefore, eluent 1 contained 0.11 *M* and eluent 2 contained 0.094 *M* sodium chloride in this system.

The effluent was first mixed with NaOCl reagent from pump 3-1, then mixed with OPA reagent from pump 3-2. The reation products were monitored by a fluorescence detector excitation at 340 nm and emission at 450 nm).

These four process were repeated for each separation. A standard amino acid mixture was chromatographed by the above system and a chromatogram is shown in Fig. 5a. Seventeen amino acids were successively separated within 35 min. If two fluorescence detectors were used, separation in 25 min was possible. The retention time of tryptophan was very long and when this compound is present it is better to

TABLE I

OPERATION OF THE SEPARATION OF FREE AMINO ACIDS BY COLUMN SWITCHING

Inj. = injection point; I–IV = column-switching points; Ph and ODS = phenyl- and octadecyl-bonded columns; eluents 1 and 2, see text.

Parameter	*Process*				
	Inj.	*I*	*II*	*III*	*IV*
Time (min)		0	3.5	23.5	34.5
Separation column	Ph + ODS		PH	ODS	Ph
Eluent		2	1	2	2

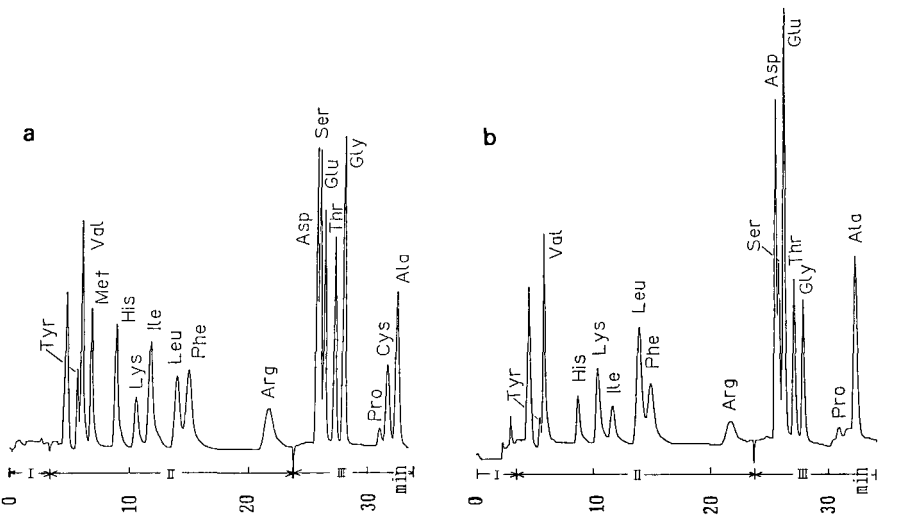

Fig. 5. Chromatograms of (a) standard amino acids and (b) amino acids in a hydrolysate of bovine serum albumin.

add one more column-switching stage in the above system. Further, this system was applied to the analysis of hydrolysate of bovine serum albumin, and a chromatogram is shown in Fig. 5b. The composition of amino acids analysed by this system was satisfactorily correlated with that calculated from the structure in the literature[22], and

TABLE II

REPRODUCIBILITIES OF RETENTION TIME AND PEAK HEIGHT

Experimental conditions: see Fig. 4. Amounts of amino acids: 100 pmol each.

Amino acid	*Variation (± %)*	
	Retention time	*Peak height*
Tyr	0.07	5.27
Val	0.06	1.77
Met	0.08	0.46
His	0.11	1.25
Lys	0.15	2.81
Ile	0.08	1.03
Leu	0.14	5.01
Phe	0.11	1.58
Arg	0.19	15.1
Asp	0.04	2.18
Ser	0.02	1.91
Glu	0.02	2.92
Thr	0.003	1.22
Gly	0.002	1.22
Pro	0.06	4.23
Cys	0.04	1.00
Ala	0.03	0.83

the correlation coefficient was 0.96. The correlation coefficient between this result and that measured by liquid chromatography[8] was 0.97.

The reproducibilities of the retention time and peak height were examined by manual five injections of a mixture of 100 pmol each of various amino acids, and the results are given in Table II. The reproducibility of the retention time was fairly good; the variation was less than ±0.2%. The peak-height variation was less than ±5%, except for arginine. The retention time of arginine was relatively long, and the integrator could not be well adjusted.

The sensitivity for amino acids having shorter retention times was 2–5 pmol and that for those having longer retention time was 3–9 pmol; that for proline was 20 pmol (signal-to-noise ratio = 3). Their calibration graphs were linear up to 500 pmol.

CONCLUSION

Seventeen free amino acids were separated within 35 min by RP-IPC using a column-switching technique. This system can be applied to the analysis of FAA in hydrolysate samples by applying post-column reaction detection with OPA–N-Ac-Cys. This study demonstrated the possibility of further development of a faster separation system by using two fluorescence detectors and packings of smaller particle size.

REFERENCES

1 K.-G. Wahlund and K. Groningsson, *Acta Pharm. Suec.*, 7 (1970) 615.
2 M. Hirukawa and T. Hanai, *J. Liq. Chromatogr.*, 11 (1988) 1741.
3 M. Roth, *Anal. Chem.*, 43 (1971) 880.
4 M. Roth and A. Hampai, *J. Chromatogr.*, 83 (1973) 353.
5 P. A. St. John, *Aminco Lab. News*, 31, No. 1 (1975) 1.
6 Y. Ishida, T. Fujita and K. Asai, *J. Chromatogr.*, 204 (1981) 143.
7 T. Kinoshita and N. Nimura, *Jpn./Pat.*, 147079/83, 1983.
8 N. Nimura and T. Kinoshita, *J. Chromatogr.*, 352 (1986) 169.
9 R. S. Deelder, M. G. F. Kroll, A. J. B. Beeren and J. H. M. Van den Berg, *J. Chromatogr.*, 149 (1978) 669.
10 R. S. Deelder, H. A. J. Linssen, A. P. Konijnendijk and J. L. M. Van de Venne, *J. Chromatogr.*, 185 (1979) 241.
11 M. K. Radjai and R. T. Hatch, *J. Chromatogr.*, 196 (1980) 319.
12 T. Hayashi, H. Tsuchiya and H. Naruse, *J. Chromatogr.*, 274 (1983) 318.
13 N. Seiler and B. Knodgen, *J. Chromatogr.*, 341 (1985) 11.
14 T. A. Walker and D. J. Pietrzyk, *J. Liq. Chromatogr.*, 8 (1985) 2047.
15 S. Allenmark, S. Bergström and L. Enerbäck, *Anal. Biochem.*, 144 (1985) 98.
16 T. Hayashi, M. Komaki, H. Tsuchiya, F. Matsuda and H. Naruse, *Bunseki Kagaku*, 35 (1986) 949.
17 T. A. Walker and D. J. Pietrzyk, *J. Liq. Chromatogr.*, 10 (1987) 161.
18 P. G. Rigas, S. J. Arvanitis and D. J. Pietrzyk, *J. Liq. Chromatogr.*, 10 (1987) 2891.
19 W. Buchberger and K. Winsauer, *Anal. Chim. Acta*, 196 (1987) 251.
20 J. Haginaka and J. Wakai, *J. Chromatogr.*, 396 (1987) 297.
21 J. Haginaka and J. Wakai, *Anal. Biochem.*, 171 (1988) 398.
22 Japanese Biochemical Society, *Seikagaku Deita Bukku*, Vol. 1, Tokyokagakudojin, Tokyo, 1979, p. 303.

Journal of Chromatography, 507 (1990) 103–111
Elsevier Science Publishers B.V., Amsterdam — Printed in The Netherlands

CHROMSYMP. 1729

Rapid and sensitive determination of nucleoside H-phosphonates and inorganic H-phosphonates by high-performance liquid chromatography coupled with flow-injection analysis

YOSHINOBU BABA[a],*
Chemical Laboratory, Faculty of Education, Oita University, Dannoharu, 700, Oita 870-11 (Japan)
MITSUTOMO TSUHAKO
Kobe Women's College of Pharmacy, Kitamachi, Motoyama, Higashinadaku, Kobe 658 (Japan)
and
NORIMASA YOZA
Department of Chemistry, Faculty of Science, Kyushu University, Hakozaki, Higashiku, Fukuoka 812 (Japan)

SUMMARY

A coupled high-performance liquid chromatographic (HPLC) and flow-injection analysis (FIA) system was developed for the separation and detection of H-phosphonates. The H-phosphonates are separated by HPLC in the anion-exchange mode and then introduced into an on-line FIA system. In the FIA system, H-phosphonate esters and anhydrides (P–O–P bonds) are hydrolysed and oxidized to orthophosphate, the resulting orthophosphate is converted into the heteropoly blue complex and the latter is monitored spectrophotometrically at 830 nm. The system is sensitive and easy to use. The detection limit is 10^{-6} *M* for inorganic, sugar and nucleoside H-phosphonates. The reproducibility of the peak areas was less than 1% (relative standard deviation) for all H-phosphonates.

INTRODUCTION

Nucleoside H-phosphonates are useful synthetic intermediates for the rapid synthesis of DNA and RNA[1–3]. H-phosphonates have also been widely applied in the synthesis of "biophosphates", such as phospholipid and nucleoside polyphosphates[4–9]. Few analytical methods, however, have been developed for the sensitive determination of H-phosphonates[10–15]. The development of an analytical method for

[a] Present address: Kobe Women's College of Pharmacy, Kitamachi, Motoyama, Higashinadaku, Kobe 658, Japan.

0021-9673/90/$03.50

H-phosphonates would open up new possibilities for characterizing the mechanisms of their synthetic reactions and designing methods for their preparation.

In this study, we developed a coupled high-performance liquid chromatographic (HPLC) and flow-injection analysis (FIA)[10–12] system, the latter being used for post-column reaction detection for the sensitive determination of H-phosphonate. Sodium hydrogensulphite[13–15] and an acidic solution containing molybdenum(V) and molybdenum(VI)[16,17] were used as an oxidizing agent and a chromogenic agent, respectively. In the post-column reaction detector, H-phosphonate is oxidized to orthophosphate and then the resulting orthophosphate is converted into a heteropoly blue complex which is detectable by spectrophotometry at 830 nm.

EXPERIMENTAL

Chemicals

Unless stated otherwise, guaranteed reagents from Wako (Osaka, Japan) and Yamasa Shoyu (Chiba, Japan) were used without further purification. The structures

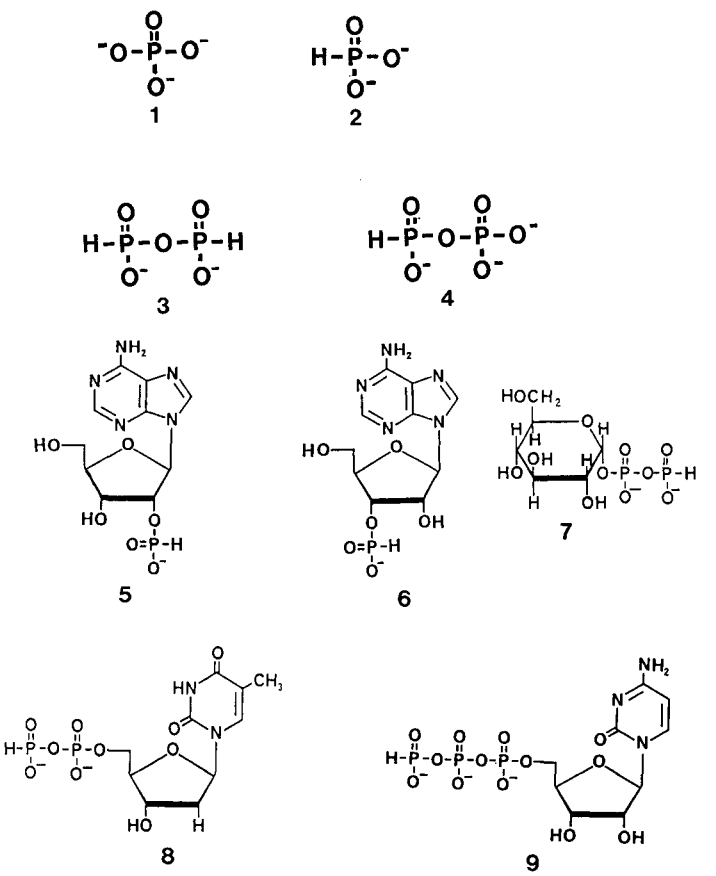

Fig. 1. Structures of orthophosphate (**1**), inorganic H-phosphonates (**2–4**), nucleoside H-phosphonates (**5,6,8,9**) and sugar H-phosphonate (**7**). Sodium salts of these compounds, which are illustrated as ionic forms, were used.

of H-phosphonate samples used are shown in Fig. 1. Disodium diphosphonate (**3**)[8], diphosphate(III, V) (**4**)[18], sugar H-phosphonate (**7**)[7] and nucleoside H-phosphonates (**5, 6, 8, 9**)[8,9] were prepared according to the literature. Water was purified with a Milli-Q system (Millipore, Bedford, MA, U.S.A.).

Reagents and eluents

Chromogenic reagent. An acidic solution containing molybdenum(V) and molybdenum(VI) was used as a chromogenic reagent for the determination of H-phosphonates. Such reagent is called a molybdenum(V)–molybdenum(VI) or Mo(V)–Mo(VI) reagent. The reagent was prepared as follows[16,17]. About 5.3 g of ammonium molybdate, $(NH_4)_6Mo_7O_{24} \cdot 4H_2O$, were dissolved in *ca.* 700 ml of Milli-Q water. After the dissolution of molybdate [Mo(VI)], 100 ml of concentrated sulphuric acid (*ca.* 18 *M*) were slowly added. Metallic zinc (sandy, 0.65 g) was then added to the acidic Mo(VI) solution. Some of the Mo(VI) was reduced to Mo(V) after complete dissolution of zinc. The solution was diluted to 1 l with Milli-Q water to give an orange Mo(V)–Mo(VI) reagent solution.

Oxidizing reagent. Sodium hydrogensulphite solution was used to oxidize the H-phosphonate group to phosphate, which is detectable by the Mo(V)–Mo(VI) reagent. A sulphite solution was prepared daily by dissolving 52 g of sodium hydrogensulphite in Milli-Q water and dilution to 500 ml.

Eluents. The eluents for the separation of H-phosphonates were composed of appropriate concentrations of potassium chloride and 0.1% (w/v) Na_4EDTA. The addition of EDTA is essential to prevent the distortion of chromatographic peaks, probably due to the hydrolysis of phosphoric anhydride bonds (P–O–P bonds) during the chromatographic process[19].

Equipment

The HPLC–FIA system is shown in Fig. 2. The HPLC system consisted of a Jasco 880-PU HPLC pump (P_A), an injection valve (S) (Sanuki SV1-5U7) and the separation column (250 mm × 4.0 mm I.D.) packed with an anion exchanger (TSKgel SAX, d_p = 10 μm; Tosoh). The FIA system consisted of a Sanuki FIA pump (2P2M-4027) with two channels (P_B and P_C), a six-way loop-valve injector (L) (Sanuki SVM-6M2), two detectors (D_A, Jasco UVIDEC-100-IV UV detector; D_B, Soma S-3250 spectrophotometric), two PTFE coils (RC, reaction coil, 20 m × 0.5 mm I.D.; BC, back-pressure coil, 1.5 m × 0.25 mm I.D.) and a thermostated reaction bath (Taiyo TAH-1).

Eluent (P_A), chromogenic reagent (P_B) and Milli-Q water (P_C) were pumped into the analytical lines at flow-rates of 1.0, 0.8 and 0.2 ml/min, respectively. The oxidizing reagent was introduced into the water stream via a six-way loop-valve injector (L), becuase the sulphite solution tended to corrode the stainless-steel pumping system. Sample solution (100 μl) was introduced with an injection valve (S) into the eluent stream. The separations were performed on the separation column. The effluent was introduced into the FIA system. Separated phosphonate species were mixed with chromogenic and oxidizing reagents, and then the UV absorption of nucleotide was monitored at 260 nm (D_A). Although the UV detector is located after the mixing point in Fig. 2, it can be located before the mixing point. The mixed solution was carried through a 20-m reaction coil maintained at 140°C, during which time (*ca.* 120 s)

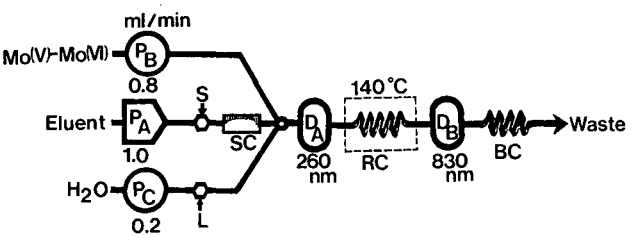

Fig. 2. HPLC–FIA system. P_A = HPLC pump (1.0 ml/min); P_B and P_C = FIA pumps with two pumping channels (0.8 and 0.2 ml/min); S = sample injector; L = sulphite injector; SC = separation column (TSK gel SAX anion exchanger, 250 mm × 4.0 mm I.D.); D_A = UV detector; RC = reaction coil (PTFE, 20 m × 0.5 mm I.D.); D_B = spectrophotometric detector; BC = back-pressure coil (PTFE, 1.5 m × 0.25 mm I.D.). The dashed line shows the reaction bath (Taiyo TAH-1), in which the reaction coil is tightly wound on a thermostated aluminium block kept at 140°C.

H-phosphonate esters and anhydrides were hydrolysed to orthophosphate and H-phosphonate, H-phosphonate was subsequently oxidized to orthophosphate and the resulting orthophosphate was allowed to react with the chromogenic reagent to form a heteropoly blue complex, The absorption of the blue complex at 830 nm was monitored by the spectrophotometer (D_B). The back-pressure coil (BC) at the exit of the spectrophotometer (D_B) prevented baseline noise due to gas bubbling even at temperatures as high as 140°C.

RESULTS AND DISCUSSION

FIA for post-column reaction detection

H-phosphonates injected into the HPLC–FIA system (Fig. 2) are separated by HPLC and detected in the on-line FIA system. The following three reactions occurred simultaneously in the FIA system: (1) hydrolysis of phosphoric (or phosphonic) ester and anhydride linkages catalysed by sulphuric acid (eqn. 1); (2) oxidation of H-phosphonate to orthophosphate with sulphite (eqn. 2); and (3) colour development of orthophosphate by Mo(V)–Mo(VI) reagent (eqn. 3). The oxidation of phosphonate with sulphite is well known[20–22], but its reaction mechanism is too complicated to be expressed by a simple equation.

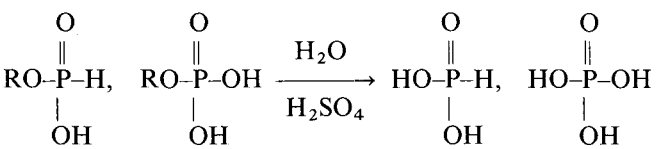

(1)

R = alkyl or phosphoric group

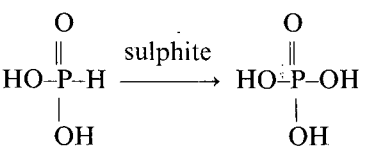

(2)

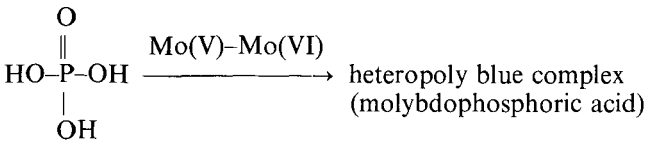

(3)

To examine the extent of oxidation of H-phosphonate, inorganic orthophosphate (**1**) or inorganic phosphonate (**2**), the sample was introduced into the system (Fig. 2) without the separation column. Fig. 3 indicates that oxidation of phosphonate is quantitative in the 120-s residence time in the reaction coil, *i.e.*, the peak height at each concentration of phosphonate with sulphite is the same as that of each equimolar amount of orthophosphate, whereas no peak of phosphonate was detected without sulphite.

Fig. 3 also demonstrates that the differentiation of phosphate and phosphonate was easily achieved by use of the system, because both phosphate and phosphonate were detected in the presence of sulphite, whereas only phosphate was detected in the absence of sulphite.

The calibration graph for phosphonate with sulphite showed good linearity (correlation coefficient = 0.999) and the relative standard deviation of measurement was less than 1%. The detection limit was found to be *ca.* 10^{-6} *M* for phosphonate.

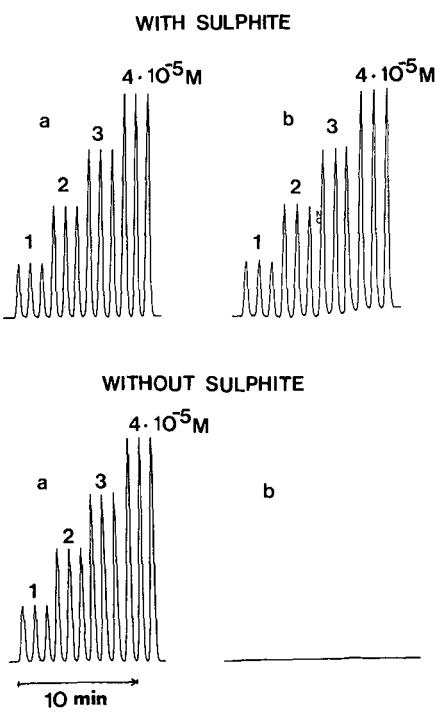

Fig. 3. FIA calibration profiles of (a) orthophosphate and (b) phosphonate with and without sulphite solution. The concentration of each sample increases from left to right, *i.e.*, from $1 \cdot 10^{-5}$ to $4 \cdot 10^{-5}$ *M*. Each sample was injected in triplicate. The anion-exchange column was not connected.

With orthophosphate detection, almost the same linearity, reproducibility and sensitivity were observed.

Analysis of inorganic H-phosphonates

Some inorganic phosphates and H-phosphonates were separated and detected using the HPLC–FIA system as shown in Figs. 4 and 5. Orthophosphate (**1**) and phosphonate (**2**) were almost separated (Fig. 4). The solid line in Fig. 4b represents the sum of the absorbances due to phosphate and phosphonate units measured in the presence of sulphite, and the dotted line represents the absorbance due to the phosphate unit measured in the absence of sulphite. The peak of orthophosphate was observed in both cases (solid and dotted lines) but that of posphonate only in the presence of sulphite (solid line). No peak was detected by the UV detector, as shown in Fig. 4a.

Fig. 5 shows the elution profile of the products and the reactants for the phosphonylation of orthophosphate (**1**) with inorganic diphosphonate (Fig. 7b). We recently found that diphosphonate (**3**). The reaction gave phosphonate (**2**) and diphosphate(III, V) (**4**) as products. Diphosphonate (**3**) was detected only with sulphite, because diphosphonate was the dimer of phosphonate as illustrated in Fig. 1. Diphosphate(III, V) (**4**), which is an anhydride of phosphate and phosphonate, is detected in both instances, as shown in Fig. 5b. The ratio of phosphate to phosphonate groups for **4** was calculated to be 1.0, which is expected from the structure in Fig. 1. Differentiation of phosphate and phosphonate by use of the HPLC–FIA system gave useful information for the establishment of the chemical structure.

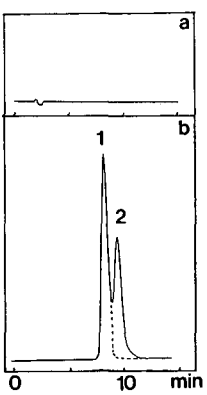

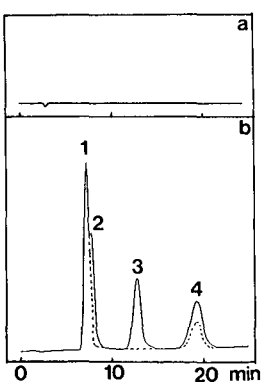

Fig. 4. Elution profiles of orthophosphate (**1**) and phosphonate (**2**). Eluent: 0.10 *M* KCl + 0.1% Na_4EDTA (pH 10). Wavelength: (a) 260 nm and (b) 830 nm. The solid line in (b) indicates total phosphate and phosphonate units with sulphite and the dotted line only the phosphate unit without sulphite. Peak numbers correspond to the compound numbers in Fig. 1.

Fig. 5. Elution profiles for orthophosphate (**1**) phosphonylated by diphosphonate (**3**) at pH 6 and 60°C for 10 h. **2** = Phosphonate;**4** = diposphate(III,V). Eluent: 0.15 *M* KCl + 0.1% Na_4EDTA. Wavelength and meaning of the solid and dotted lines in (b) as in Fig. 4. Peak numbers correspond to the compound numbers in Fig. 1.

Analysis of sugar and nucleoside H-phosphonates

Figs. 6–9 illustrate the separation and detection of some nucleoside and sugar H-phosphonates. Such H-phosphonates (**5–9** in Fig. 1) are all prepared by the reaction of nucleoside[6,8,9], sugar phosphate[7,8] and nucleotides[6,8,9] with diphosphonate (**3**).

Nucleoside 2′- and 3′-H-phosphonates (**5** and **6**), which are used as valuable intermediates in the synthesis of DNA, are almost separated, as shown in Fig. 6a, in which the UV absorption of each compound is detected. With sulphite (Fig. 6b), nucleoside 2′-H-phosphonate is separated and detected but 3′-H-phosphonate is overlapped with the peak of diphosphonate. No peaks were observed without sulphite (dotted line in Fig. 6b).

Glucose 1-monophosphate (GlclP) and phosphonylated GlclP (**7**) were detected with sulphite, as shown in Fig. 7b. Peaks of GlclP and **7** also appeared without sulphite (dotted line in Fig. 7b) owing to the detection of phosphate groups on both compounds. Sugar phosphate and H-phosphonate, which could not be detected by UV absorption as sown in Fig. 7a, were easily analysed by use of the HPLC–FIA system. The ratio of phosphate to posphonate groups on **7** was found to be *ca.* 1.0 by differentiation of the peak areas of phosphate and phosphonate (**3**) reacts with nucleoside monophospates[8] or diphosphates[9] to form a new class of H-phosphonate analogues of nucleoside polyphosphates (**8** and **9** in Fig. 1). Examples of the separation of such compounds are shown in Figs. 8 and 9.

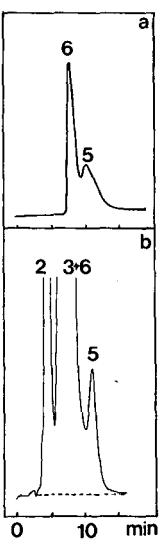

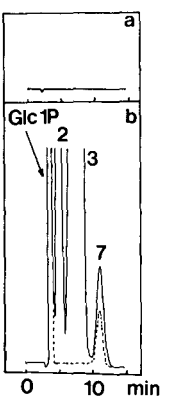

Fig 6. Elution profiles for adenosine phosphonylated by diphosphonate (**3**) at pH 10 and 20°C for 30 min. **2** = Phosphonate; **5** = adenosine 2′-H-phosphonate; **6** = adenosine 3′-H-phosphonate. Adenosine has disappeared after 30-min incubation with diphosphonate. Eluent: 0.15 *M* KCl + 0.1% Na_4EDTA. Wavelength and meaning of the solid and the dotted lines in (b) as in Fig. 4. Peak numbers correspond to the compound numbers in Fig. 1.

Fig. 7. Elution profiles for glucose 1-phosphate (GlclP) phosphonylated by diphosphonate (**3**) at pH 6 and 70°C for 60 min. **2** = Phosphonate; **7** = phosphonylated GlclP. Eluent: 0.2 *M* KCl + 0.1% Na_4EDTA. Wavelength and meaning of the solid and the dotted lines in (b) as in Fig. 4. Peak numbers correspond to the compound numbers in Fig. 1.

The H-phosphonate analogue (**8**) of dTDP, dTMP, phosphonate (**2**) and diphosphonate (**3**) were resolved completely, as shown in Fig. 8b. The H-phosphonate analogue (**8**) of dTDP was found to involve nucleoside, phosphate and phosphonate groups from the differentiaton of such groups by means of the HPLC–FIA system as shown in Fig. 8a and b. The ratio of phosphate to phosphonate was confirmed to be *ca.* 1.0.

Fig. 9 shows that all components are separated almost completely. The H-phosphonate analogue of CTP (**9** in Fig. 9) also involves nucleoside, phospate, and phosphonate groups, in addition to **8** as described above. The ratio of phosphate to phosphonate, however, is estimated to be *ca.* 2, because **9** has a triphosphate group composed of the phosphate groups and a phosphonate group.

In conclusion, these applications of the HPLC–FIA system clearly demonstrate its potential for the sensitive detection of inorganic, sugar and nucleoside H-phosphonates. Several phospates and H-phosphonates of biological importance were easily separated and detected. The system would be applicable to the simultaneous separation of complex mixtures of inorganic phosphates, inorganic H-phosphonates, biophosphates and "bioH-phosphonates". Such complex mixtures are obtained when a nucleotide reacts with a sugar phosphate, *e.g.*, uridine 5′-triphosphate reacts with GlclP to give uridine 5′-diphosphoglucose (UDPG) and inorganic diphosphate (pyrophosphate)[23,24].

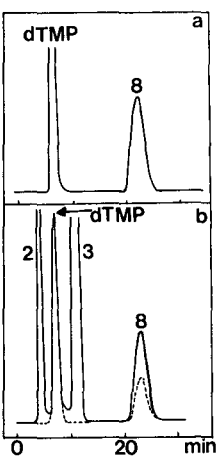

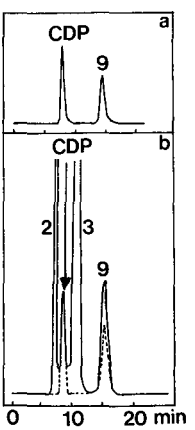

Fig. 8. Elution profles for thymidine 5′-monophosphate (dTMP) phosphonylated by diphosphonate (**3**) at pH 6 and 80°C for 4 h. **2** = Phosphonate; **8** = phosphonylated dTMP. Eluent: 0.2 *M* KCl + 0.1% Na_4EDTA. Wavelength and meaning of the solid and the dotted lines in (b) as in Fig. 4. Peak numbers correspond to the compound numbers in Fig. 1.

Fig. 9. Elution profiles for cytidine 5′-diphosphate (CDP) phosphonylated by diphosphonate (**3**) at pH 6 and 70°C for 50 min. **2** = Phosphonate; **9** = phosphonylated CDP. Eluent: 0.3 *M* KCl + 0.1% Na_4EDTA. Wavelength and meaning of the solid and the dotted lines in (b) as in Fig. 4. Peak numbers correspond to the compound numbers in Fig. 1.

ACKNOWLEDGEMENTS

The authors express their appreciation to Mr. Yoshisuke Yamamoto, Miss Mika Onoe and Miss Tomoko Sumiyama for technical assistance.

REFERENCES

1 P. J. Garegg, T. Regberg, J. Stawinski and R. Strömberg, *Chem Scr.*, 25 (1985) 280 and 26 (1986) 59.
2 P. J. Garegg, I. Lindh, T. Regberg, J. Stawinski and R. Strömberg, *Tetrahedron Lett.*, 27 (1986) 4051 and 4055.
3 B. C. Froehler and M. D. Matteucci, *Tetrahedron Lett.*, 27 (1986) 469.
4 I. Lindh and J. Stawinski, *Nucleic Acids Res. Symp. Ser.*, No 18 (1987) 189.
5 B. C. Froehler, *Tetrahedron Lett.*, 27 (1986) 5575.
6 Y. Baba, Y. Yamamoto, N. Yoza and S. Ohashi, *Nucleic Acids Res. Symp. Ser.*, No. 17 (1986) 69.
7 Y. Baba, M. Onoe, T. Sumiyama, M. Tsuhako, N. Yoza and S. Ohashi, *Chem. Lett.*, 1987 (1987) 1389.
8 Y. Yamamoto, Y. Baba, M. Mizokuchi, M. Onoe, T. Sumiyama, M. Tsuhako, N. Yoza and S. Ohashi, *Bull. Chem. Soc. Jpn.*, 61 (1988) 3217.
9 Y. Baba, T. Sumiyama, M. Tsuhako and N. Yoza, *Bull. Chem. Soc. Jpn.*, 62 (1989) 1587.
10 M. Valcarcel and M. D. Luque de Castro, *J. Chromatogr.*, 393 (1987) 3.
11 J. Růžička and E. H. Hansen, *Flow Injection Analysis,* Wiley, New York, 2nd ed., 1988.
12 Y. Baba, in Y. Takashima and N. Yoza (Editors), *Flow Injection Analysis,* Hirokawa, Tokyo, 1989, Ch. 5.
13 H. Hirai, N. Yoza and S. Ohashi, *J. Chromatogr.*, 206 (1981) 501.
14 Y. Baba, N. Yoza and S. Ohashi, *J. Chromatogr.*, 295 (1984) 153.
15 Y. Baba, N. Yoza and S. Ohashi, *J. Chromatogr.*, 318 (1985) 319.
16 Y. Baba, N. Yoza and S. Ohashi, *J. Chromatogr.*, 348 (1985) 27.
17 Y. Baba, Y. Yamamoto, N. Yoza and S. Ohashi, *Bunseki Kagaku,* 34 (1985) 692.
18 Y. Baba, *Thesis,* Kyushu University, Fukuoka, 1986.
19 T. Nakamura, T. Yano, T. Nunokawa and S. Ohashi, *J. Chromatogr.*, 161 (1978) 421.
20 F. Wöhler, *Justus Liebig Ann. Chem.*, 39 (1841) 252.
21 *Gmelin's Handbuch, Schwefel B-II,* Verlag Chemie, Weinheim, 1960, p. 544.
22 N. Yoza and S. Ohashi, *Bull. Chem. Soc. Jpn.*, 37 (1964) 37.
23 H. Hirano, Y. Baba, N. Yoza and S. Ohashi, *Chem. Lett.*, 1986 (1986) 633.
24 N. Yoza, H. Hirano, Y. Baba and S. Ohashi, *Phosphorus Sulfur*, 30 (1987) 605.

Journal of Chromatography, 507 (1990) 113–123
Elsevier Science Publishers B.V., Amsterdam — Printed in The Netherlands

CHROMSYMP. 1748

Analysis of oligonucleotides by capillary gel electrophoresis

ARAN PAULUS[a] and J. I. OHMS*
Research Department, Spinco Division, Beckman Instruments, Inc., Palo Alto, CA 94304 (U.S.A.)

SUMMARY

Analysis of oligonucleotides with gel-filled capillary columns is a fast, efficient and automated way to check their purity. Gel-filled columns were optimized to separate oligonucleotides which were 20–50 nucleotides in length. The influence of sample size on resolution is discussed. A comparison between capillary gel electrophoresis and slab gel electrophoresis in terms of analysis time per sample is made. In addition to homopolymeric samples, the separation of heteropolymeric oligonucleotides with one nucleotide difference in size is presented and suggests the possibility of using capillary gel electrophoresis as a tool for DNA sequencing.

INTRODUCTION

The pharmaceutical industry is currently undergoing a major shift in the way new drugs are designed. Whereas in the past, small organic molecules, *e.g.*, molecules with a molecular weight below 1000, made up the vast majority of all drugs, present and future efforts seem to be directed toward peptides and proteins[1]. In this context, biotechnology is rapidly becoming an important part of the pharmaceutical industry. The primary information is stored in the DNA of bacterial or mammalian cells and translated within the cell into the desired protein drug. The demands on analytical methods for biopolymers in general, and proteins, oligonucleotides and DNA in particular, change in parallel with the growth of biotechnology. A new analytical field, which has been termed "analytical biotechnology", is emerging[2].

Analytical biotechnology is, in essence, analytical chemistry dealing with biopolymers. The traditional questions such as structural elucidation, quantitation in a physiological environment, potency, safety and stability are altered by the nature of the samples. The structural elucidation of biopolymers requires information about the sequence of known monomers. Although the sequence determines the primary structure, and therefore the identity of biomolecules, secondary, tertiary and quaternary structure have considerable influence on their activity. The sensitivity in analytical biotechnology must be in the pico- to femtomole range to detect the minute

[a] Present address: Ciba-Geigy AG, CH-4002 Basel, Switzerland.

0021-9673/90/$03.50

quantities of molecules of interest in the biochemical environment, while the industrial biotechnology environment requires speed, quantitation and automation.

Capillary electrophoresis (CE) is a relatively new analytical technique with the potential of becoming a standard method for analysis of biochemical samples[3–5]. It offers speed, ease, accuracy of quantitation, automation and is compatible with physiological samples.

As with high-performance liquid chromatography (HPLC), the term CE indicates the type of instrumentation and covers several separation modes[6,7]. The most popular techniques today are capillary zone electrophoresis (CZE)[8–14], micellar electrokinetic capillary chromatography (MECC)[15–18], capillary electroendosmotic chromatography[6,7] and capillary gel electrophoresis[19–22]. Gel electrophoresis in the slab configuration is a major separation tool for biochemical samples. Therefore, capillary gel electrophoresis has drawn considerable interest in the biochemical community, since it offers the possibility of transferring routine electrophoretic techniques to the automated capillary format.

Synthetic oligonucleotides are used extensively in biochemistry and molecular biology as probes for gene isolation and diagnostics, as primers for DNA sequencing, site-directed mutagenesis experiments and template amplification, and as linkers and adapters for cloning and gene alteration. In general, purity should not be crucial because only complementary strands will hybridize, but in amplification experiments contaminating oligomers may also be enhanced. Nevertheless, an easy, fast and reliable method for purity assessment of small oligonucleotides is needed to exclude impurities as a possible source of error in biological and biochemical experiments.

Recently, the separation of oligonucleotides on ion-exchange columns has been improved[23,24]. The development of new stationary phases allows the separation of oligonucleotides of up to 70 bases. Because the separation mechanism depends on apparent charge differences, the resolution of larger oligonucleotides becomes increasingly difficult. The same argument holds in CZE where small oligonucleotides can easily be separated by open tube methods. However, no separation could be observed with oligonucleotides of more than thirteen nucleotides. Adding metal ions and sodium dodecyl sulfate (SDS) extended the separation range to about 20 nucleotides[17].

Since the separation mechanism in column chromatography is not based on size differences, these methods offer no alternative to the resolving power of slab gels, where oligonucleotides of 600 bases can be separated by a one-nucleotide difference. However, the slab gel approach has the disadvantages of being slow, difficult to quantitate, and consists of many time-consuming manual steps. Capillary gel electrophoresis has the potential to combine the resolution power of slab gels with the automation and speed of the capillary instrument[25]. In this paper we examine the separation of various oligonucleotide samples with gel-filled capillaries.

EXPERIMENTAL

Apparatus

The CE system used in this work was similar to those described in the literature[3–5]. It consisted of a fused-silica capillary, a power supply, a detection unit and a data collection system. The fused-silica capillary (Polymicro Technologies,

Phoenix, AZ, U.S.A.), has the dimensions 75-μm inner diameter (I.D.), 360-μm outer diameter (O.D.).

A programmable Spellman power supply UHA 120 W (0–60 kV) (Spellman High Voltage Electronics, Plainview, NY, U.S.A.) was interfaced with a HP series 300 computer system and a HP 3852 data acquisition system (Hewlett-Packard, Palo Alto, CA, U.S.A.). A BASIC program was written to control the power supply during injection and run times and to collect and store the data from the detector output and current readings. The same software also allowed for simple plot and integration routines.

The detector, a Kratos 783 absorbance detector (Applied Biosystems, Ramsey, NJ, U.S.A.), was modified in-house for on-column detection. The HPLC flow cell was replaced by a round disc with a 3-mm hole in the middle upon which grooved apertures of various dimensions were mounted. The capillary was fixed over the aperture with an adhesive. Both ends of the capillary were placed outside the detector housing in 3-ml buffer reservoirs. This arrangement resulted in a minimum length of 30 cm and an effective length (distance from injection point to detection point) of 15 cm, but for convenience a capillary length of 40 cm (20-cm effective length) was used in all experiments. The light reaching the reference cell was reduced by covering it with an aperture having a 50 × 50 μm hole. The average noise level of the detector was determined to be $300 \cdot 10^{-6}$ a.u.

Chemicals

The buffer components, tris-(hydroxymethyl)-aminomethane (Tris), boric acid and urea, the acrylamide–cross-linker mixture (29:1) and the starter of the polymerization reaction, ammonium persulfate (APS) and N,N,N′,N′-tetramethylethylenediamine (TEMED) were electrophoresis-grade and purchased from Schwarz/Mann Biotech (Cleveland, OH, U.S.A.). Methacryloxypropyltrimethoxysilane was supplied by Petrarch (Bristol, PA, U.S.A.); polyethylene glycol (PEG) 20 000 was obtained from Fluka (Ronkonkoma, NY, U.S.A.); methanol and water were HPLC-grade.

The oligodeoxythymidylic acids pd(T)12–18, pd(T)19–24 and pd(T)25–30 were purchased from Pharmacia (Piscataway, NJ, U.S.A.). Stock solutions of 0.05 A_{260} units per μl or 2 μg/μl were stored at −20°C and diluted by ten for injection. (By convention, one A_{260} unit equals 40 μg of oligomer.) The ladder-type polydeoxythymidylic acids pd(T)10–50 and the heterooligomeric nucleotides used in this study were synthesized with a Beckman System 1 Plus DNA Synthesizer. Reduction of the nucleoside phosphoramidite reagent concentration was automatically programmed at desired synthetic base additions to increase synthesis failure and enhance a given oligomeric size[26].

Procedure

A stock solution of buffer, consisting of 50 m*M* Tris, 50 m*M* boric acid, 3% PEG[27], and 7 *M* urea, was used for the preparation of the gel columns and as the running buffer. All buffer solutions were filtered through a nylon 66 filter unit of 0.2-μm pore size (Schleicher and Schüll, Keene, NH, U.S.A.). To provide an optical detection window, about 2 mm of the polyimide coating were removed with an electrically-heated wire in the middle of an appropriate piece of fused silica, normally about 50 cm long. The capillary was flushed with 1 *M* hydrochloric acid, 1 *M* sodium

hydroxide and methanol, respectively. A mixture of methanol and methacryloxypropyltrimethoxysilane (50:50, v/v) was injected into the capillary and left there for at least 3 h[28,29]. Then 750 mg of the acrylamide–cross-linker mixture were dissolved in 10 ml buffer solution, resulting in a 7.5% polyacrylamide gel. A 10% (w/v) solution of both APS and TEMED was prepared. Depending on the polymerization time, 2–5 μl of each was used to start the polymerization of 1 ml of the monomer solution. The unpolymerized solution was injected into the capillary and left overnight for full polymerization.

Sample injections were made electrophoretically by switching the cathodic buffer reservoir with a sample vial and applying voltage for a predetermined time. Typical injection conditions were 3–10 s at 1000–2000 V for aqueous solutions of the samples. Fields ranging from 250–450 V/cm were applied (40-cm capillary, 10–18 kV), resulting in a current of 3–7 μA. During operation, the capillary was actively cooled at room temperature with a fan.

Slab gels were prepared with 10% T and 5% C[a] in 0.1 *M* Tris-borate buffer with 2 m*M* EDTA, pH 8.3. The 0.5-mm thick gels were electrophoresed at 1000 V or 55 V/cm for 5 h. Radiolabelling of the oligomers and their detection on photographic film following separation were done according to standard procedures[30].

RESULTS AND DISCUSSION

Separation of homopolymeric oligonucleotides

In contrast to earlier reports[22], where the separations of deoxypolyadenylic acids were carried out on 5% gels, a monomer concentration of 7.5% was used in this work. The electropherogram of the separation of deoxypolythymidylic acids with 12–30 bases (Fig. 1) reveals that the mixture was composed of three different component size groups, each one having a distinct peak pattern. The component containing 12 to 18 nucleotides shows a Gaussian distribution, but for the other two component groups, the relative amount of each oligonucleotide decreases with increasing nucleotide number. The pattern recognition allows an easy check of column performance and resolution.

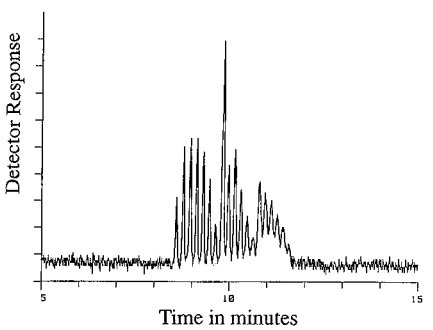

Fig. 1. Separation of deoxypolythymidylic acid pd(T)12–30. Separation conditions: capillary 75 μm I.D., 360 μm O.D., length 40 cm, effective length 20 cm; buffer 50 m*M* Tris, 50 m*M* boric acid, 7 *M* urea; column 7.5% T, 3.3% C; field 375 V/cm; current 5.6 μA; injection 4000 Vs; detection 260 nm UV on-column.

[a] %T = [g acrylamide + g N,N′-methylene bisacrylamide(Bis)]/100 ml solution; %C = g Bis/% T.

In order to check the performance of the gel columns, we synthesized homopolymeric oligonucleotide samples of an exact size by solid phase methods. The sample was a homopolymer to exclude any mobility differences, *e.g.*, the separation mechanism should depend solely on size differences and have an easily recognizable pattern. The synthesis of an oligodeoxythymidylic acid pd(T)50 was carried out in a way that, starting from cycle 15, the repetitive yield of each fifth nucleotide addition was decreased. In this manner, a sample with a ladder-type pattern was obtained. Fig. 2 shows the capillary electropherogram of this sample and the comparable slab gel pattern. Beside the major peak for the pd(T)50, passing the detector at 26 min, seven peaks representing pd(T)15, pd(T)20, pd(T)25, pd(T)30, pd(T)35, pd(T)40 and pd(T)45 can be distinguished. Between pd(T)30 and pd(T)35, and between pd(T)35 and pd(T)40, there are four peaks observed just above the noise level of the detector that originate from the failure rate at each cycle. The migration times increase linearly with the nucleotide number, indicating a separation correlated with size differences for the 15–50 nucleotide chain length. The slab gel electropherogram shows corroboration of the gel-filled capillary pattern. Capillary electrophoresis with gel-filled capillaries, therefore, suggests a more readily quantifiable check of the purity of an oligonucleotide sample.

Influence of sample size

Using the same separation conditions and the same capillary as in Fig. 2, the capillary column was overloaded by injecting the test sample for 10 s at 5000 V. The resolving power of the column decreases dramatically: only the major peaks can be detected with a distorted and split peak shape and it is not possible to observe the failure sequences (see Fig. 3). These results point out an additional factor relative to

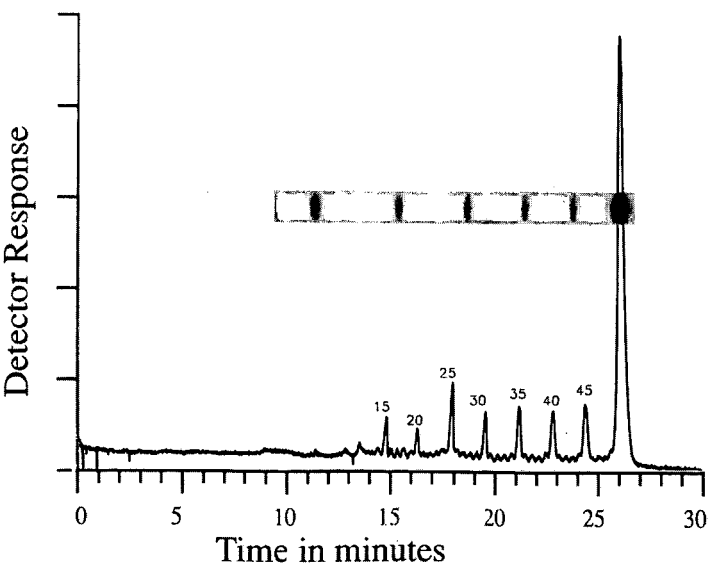

Fig. 2. Separation of deoxypolythymidylic acids pd(T)10–50. Field 250 V/cm; current 5.8 μA; injection 4000 Vs; other conditions same as Fig. 1. Slab gel electrophoresis conditions, see text.

sample injection onto capillaries. It is customary to inject samples dissolved in water or solvents lower in ionic strength than the electrolyte to enhance sample detection by means of zone sharpening. Much of the peak distortion and loss of resolution shown in Fig. 3 may be due to the fact that the sample solvent was water and it was injected into an electrolyte containing 7 *M* urea. The chaotropic effect of urea in the electrolyte is probably inversely related to the size of the aqueous sample slug.

Rose and Jorgenson[31] derived an equation to calculate the volume and quantity of a sample injected electrophoretically onto a capillary column. They used open-tube capillaries and had to correct the electrophoretic mobility for the electroosmotic flow-rates of the system. Since no effective bulk fluid flow is observed when injecting a neutral marker in a gel-filled column, the equation of Rose and Jorgenson simplifies to

$$Q = \frac{\mu_{ep} \pi r^2 V_i t_i}{L} C$$

where Q is the quantity of sample injected, μ_{ep} the apparent electrophoretic mobility, r the radius of the capillary tube, V_i the injection voltage, t_i the injection time, L the overall length of the capillary and C the sample concentration.

However, this equation must be modified to determine the amount injected into gel-filled capillaries. The gel presents several unique factors, some of which are difficult to quantify: the electrolyte displacement by the gel or interstitial space, the geometric obstruction factor[7] pertinent to the solute, and the volume fraction of the electrolyte components. While an estimate of the interstitial space for a gel formulation in a capillary is difficult, it is expected that the volume fraction of 7 *M* urea in the electrolyte solution would be approximately 0.3. These factors are collected as a single term of α of this argument:

$$Q = \frac{\mu_{ep} V_i t_i}{L} C \pi r^2 (1 - \alpha)$$

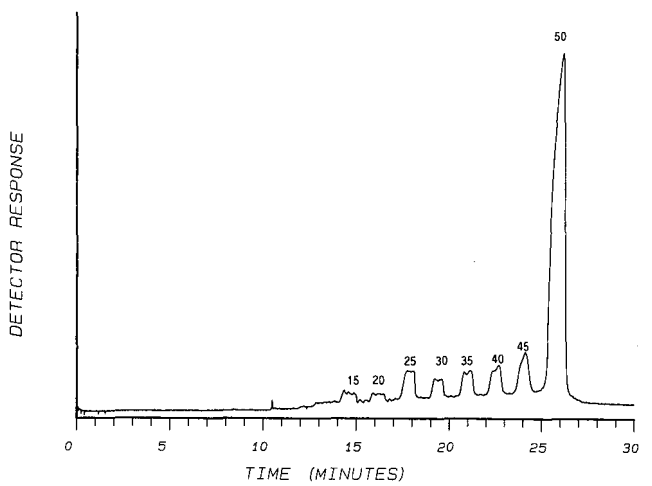

Fig. 3. Same sample and conditions as used in Fig. 2, except injection at 50 000 Vs.

Since these factors were not quantified in this work, only a relative comparison of injections on the same capillary can be made from the mathematical product of the electrical potential or voltage (V) and injection time (t_i) in s. These two product values are 4000 and 50 000 Vs, respectively, or a ratio of 12.5. As stated above, the higher sample loading resulted in a decreased resolution. Therefore, the sample dynamic range for the separation of oligonucleotides is probably less than 10 with the UV detector used in this work. This demonstrates the need for more sensitive detection principles such as fluorescence[32] or radioactivity[33].

Separation of heterooligonucleotides

In order to examine the usefulness of gel-filled capillaries for the separation of heterooligonucleotides, we synthesized a series of four oligonucleotides, two complementary strands with 29 and 30 nucleotides each. The sequence of the 30-mer and its complementary 30-mer strand were the same as the corresponding 29-mers plus an additional nucleotide. Thus, the 29-mer hybridizes with the complementary 29-mer and with one of the 30-mers, whereas hybridization with the second 30-mer is not possible because their sequences are the same.

In Fig. 4, the electropherograms for the 29- and 30-mers are plotted in one diagram. As expected, each separation shows one major component plus a number of smaller failure sequences with higher mobilities than the main product. The samples were used after synthesis without any further purification. Slab gel electrophoresis shows, in general, a smeared spot for impure oligonucleotide samples. Capillary electrophoresis with gel columns can, therefore, be used to check the purity of an oligonucleotide sample.

It is apparent from Fig. 4 that the separation of the failure sequences is not as regularly spaced as with homopolymeric oligonucleotides. This is expected in view of the size difference between the purine and the pyrimidine nucleotides. Nevertheless,

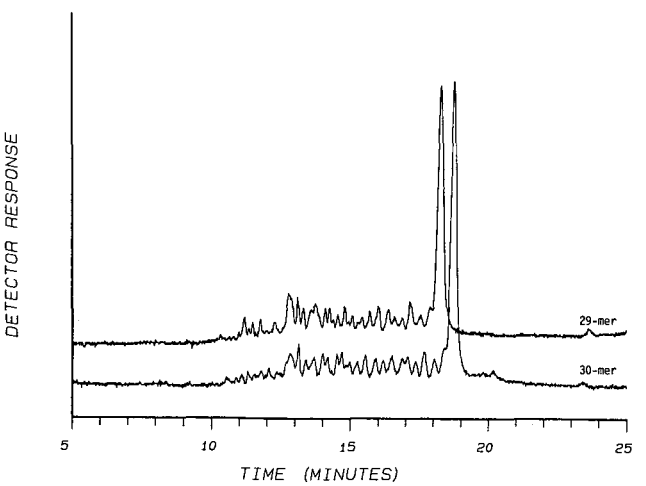

Fig. 4. Separation of crude synthetic oligonucleotides, upper trace, 29-mer: 5'ATGACAGAATACAAG CTTGTGGTGGTGGG3'; lower trace, 30-mer: 5'ATGACAGAATACAAGCTTGTGGTGGTGGGC3'. Each sample was injected separately. Field 250 V/cm; current 4.8 μA; injection 4000 Vs; other conditions same as Fig. 1.

Fig. 4 indicates that the separation of the 29- and the 30-mers is possible with this system. It should be noted that an absolute comparison of migration times cannot be made for the experiments described here. Since this CE system was not equipped with an adequate temperature control unit, current changes from 7 to 4 μA were seen over the course of 5 to 10 h of repeated operation. Also, as seen by inspection of the capillary under a microscope, bubbles formed at the injection end of the gel-filled capillary. Therefore, the capillary was cut by a few mm when the current dropped below 3 μA. After cutting the capillary, the current readings went back to former values and the separation power of the capillary was restored.

For the reasons stated above, single-base resolution of heterooligonucleotides can only be proven by injection of a mixture of oligonucleotides, differing by one nucleotide in length. Fig. 5 shows the result of this experiment. Because the 29- and the 30-mers were mixed and the absolute concentration of oligonucleotide in the sample volume decreased by a factor of two, the amount injected is too small for detection of the failure sequences. But the 29- and the 30-mers show baseline resolution. This experiment confirms that capillary electrophoresis has the potential for DNA sequencing[34]. Extending the separation range of gel-filled capillary columns to base numbers of several hundred and using Sanger-type sequencing mixtures will require a more sensitive fluorescence detector for CE, as well as certain improvements in the instrument (temperature control) and optimization of gel columns.

The use of 7 *M* urea in both the capillary and the buffer inhibits hybridization of complementary single-stranded oligonucleotides. With homopolymeric, non-complementary samples, hybridization does not occur. However, hybridization may occur if the complementary 29-mer and 30-mer are mixed in water at room temperature, rather than in urea and above the melting point of the double-stranded DNA fragment. In Fig. 6, the electrophoretic separation reveals three different species: two peaks between 18 and 19 min corresponding to the 29- and 30-mer and an additional peak at 20 min.

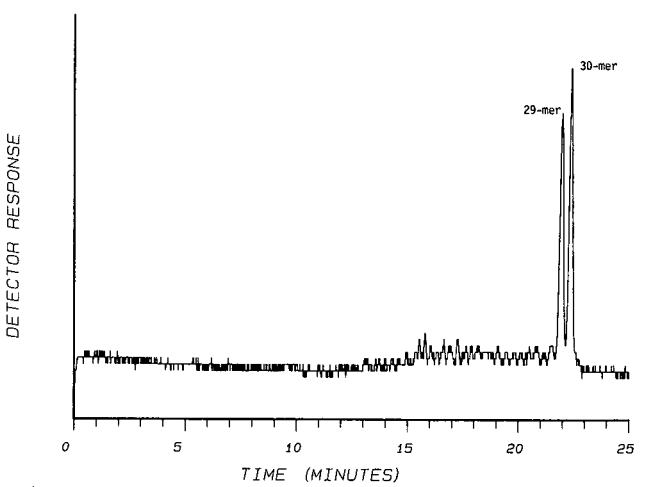

Fig. 5. Separation of a mixture of the two oligonucleotides described in legend to Fig. 4 under the same conditions.

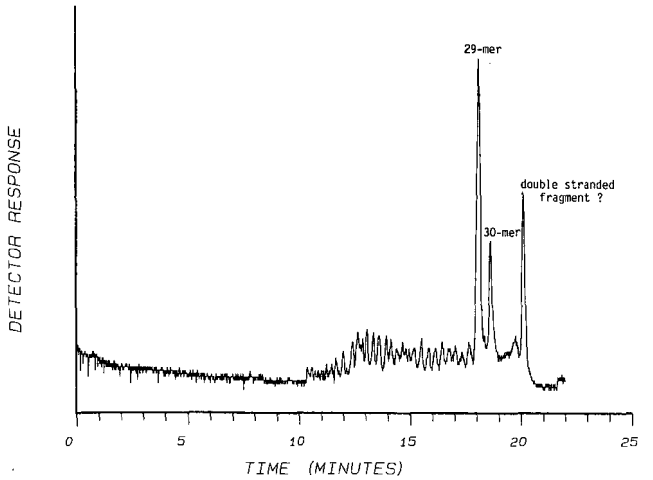

Fig. 6. Separation of a mixture of two crude, synthetic oligonucleotides, 29-mer: 5'GCCCACCACCAC AAGCTTGTATTCTGTCA3', and 30-mer: 5'ATGACAGAATACAAGCTTGTGGTGGTGGGC3'. Separation conditions were the same as described in legend to Fig. 4.

It can be speculated that even if the separation medium contains urea, this is not sufficient to break up all hydrogen bonds in the double-stranded DNA. The appearance of a third peak depends on the time that the sample was left to hybridize. It is expected that there is approximately 8% decrease in renaturation rate for each mole increase in concentration[35]. The separation shown in Fig. 6 was obtained by injecting the sample 10 min after mixing. If the same mixture is injected 40 min after mixing, the peak at 20 min increases in height, whereas the peak for the 30-mer at 18.7 min decreases. After 70 min, only two peaks can be observed. This would be expected, since one oligomer is present in excess of the other. After hybridization, the mixture consists of a double-stranded DNA fragment and a single-stranded, unhybridized oligonucleotide. If the separation time is sufficiently short compared to the hybridization time, it may be possible to measure the hybridization kinetics under different conditions by this method. The analysis time can be shortened by increasing the field strength in one of two ways: by an increase in the voltage drop at a constant capillary length or by a decrease in the capillary length at a constant voltage.

Comparison of slab gel electrophoresis and capillary gel electrophoresis for the separation of oligonucleotides

When comparing capillary gel or column electrophoresis to slab gel or open-bed electrophoresis, two variations of the same basic separation technique are contrasted. In general, the advantages of a column-operated technique are on-line sample detection, easy quantitation and automation and the separation medium can be reused for a number of runs. The disadvantage of this technique is that only one sample at a time can be analyzed. In contrast, several samples can be analyzed at the same time with slab gels.

To compare analysis times of the two techniques, the run time per sample has to be determined. In capillary gel electrophoresis, run times are typically 30 min or less.

No additional time is needed for detection and data reduction; sample preparation is the only manual step and accounts for 2 min per sample. On a slab gel, 18 samples can be loaded on one plate. Total estimated analysis time for slab gel electrophoresis consists of 2 h for gel preparation and casting, 5 h of run time, 1 h of gel transfer time to the photographic plate and film development, and 16 h of autoradiogram development. The total analysis time is 24 h, or 80 min per sample, more than double the time required with CE instrumentation. Also, technician time adds up to 3 h total, or 10 min per sample, and is considerably more than with CE.

CONCLUSIONS

Capillary gel electrophoresis can be used to check the purity of a synthetic oligonucleotide. The separation by CE is completed within 10 to 30 min and is much faster than slab gel electrophoresis. A comparison of the analysis time for both techniques is made. When the differences in mobilities are taken into account, the method also gives easy and accurate quantitation, which should be useful to optimize synthesis programs using an automated DNA synthesizer. The columns in this work were stable and were used for 50 consecutive injections (more than 20 h of run time).

Single-nucleotide resolution can also be achieved with oligonucleotides composed of an arbitrary sequence. CE with gel-filled columns seems to be an alternative to slab gel electrophoresis to obtain sequence information from DNA fragments. Further developments in column design are directed to the resolution of longer oligonucleotides with nucleotide numbers between 100 and 500.

ACKNOWLEDGEMENTS

We gratefully acknowledge the considerable and expert technical assistance of Theresa Cash in the synthesis of the oligonucleotides used in these studies. We thank Nebojsa Avdalovic for suggesting the sequence of the 29- and 30-nucleotide heterooligomers.

REFERENCES

1 D. Blohm, C. Bollschweiler and H. Hillen, *Angew. Chem., Int. Ed. Engl.*, 27 (1988) 207.
2 R. L. Garnick, N. J. Soll and P. A. Papa, *Anal. Chem.*, 60 (1988) 2546.
3 J. W. Jorgenson and K. D. Lukacs, *Science (Washington, D.C.)*, 222 (1983) 266.
4 A. G. Ewing, R. A. Wallingford and T. M. Olefirowicz, *Anal. Chem.*, 61 (1989) 292A.
5 M. J. Gordon, X. Huang, S. J. Pentoney and R. N. Zare, *Science (Washington, D.C.)*, 242 (1988) 224.
6 J. H. Knox and I. H. Grant, *Chromatographia*, 24 (1987) 135.
7 J. H. Knox, *Chromatographia*, 26 (1988) 329.
8 J. W. Jorgenson and K. D. Lukacs, *Anal. Chem.*, 53 (1981) 1298.
9 S. Hjerten, *J. Chromatogr.*, 270 (1983) 1.
10 E. Gassman, J. E. Kuo and R. N. Zare, *Science (Washington, D.C.)*, 230 (1985) 813.
11 S. Hjerten, *J. Chromatogr.*, 347 (1985) 191.
12 H. H. Lauer and D. McManigill, *Anal. Chem.*, 58 (1986) 166.
13 H. Lüdi, E. Gassman, H. Grossenbacher and W. Märki, *Anal. Chim. Acta*, 213 (1988) 215.
14 P. D. Grossman, J. C. Colburn, H. H. Lauer, R. G. Nielson, R. M. Riggin, G. S. Sittampalam and E. C. Rikard, *Anal. Chem.*, 61 (1989) 1186.
15 S. Terabe, K. Otsuka, K. Ichikawa, A. Tsuchiya and T. Ando, *Anal. Chem.*, 56 (1984) 113.
16 S. Terabe, K. Otsuka and T. Ando, *Anal. Chem.*, 57 (1987) 834.

17 A. S. Cohen, S. Terabe, J. A. Smith and B. L. Karger, *Anal. Chem.*, 59 (1987) 1021.
18 A. T. Balchunas and M. J. Sepaniak, *Anal. Chem.*, 60 (1988) 617.
19 A. S. Cohen and B. L. Karger, *J. Chromatogr.*, 397 (1987) 409.
20 A. S. Cohen, A. Paulus and B. L. Karger, *Chromatographia*, 24 (1987) 15.
21 A. Guttman, A. Paulus, A. S. Cohen, N. Grinberg and B. L. Karger, *J. Chromatogr.*, 448 (1988) 41.
22 A. Guttman, A. Paulus, A. S. Cohen, B. L. Karger, H. Rodriquez and W. S. Hancock, in C. Schaefer-Nielson (Editor), *Electrophoresis '88, Proceedings of the 6th Meeting of the International Electrophoresis Society*, VCH, Weinheim, 1988, pp. 151–159.
23 Y. Kato, T. Kitamura, A. Mitsui, Y. Yamasaki, T. Hashimoto, T. Murotsu, S. Fukushige and K. Matsubara, *J. Chromatogr.*, 447 (1988) 212.
24 A. Y. Tsygankov, Y. A. Motorin, A. D. Wolfson, D. B. Kirpotin and A. F. Orlovsky, *J. Chromatogr.*, 465 (1989) 325.
25 A. S. Cohen, D. R. Najarian, A. Paulus, A. Guttman, J. A. Smith and B. L. Karger, *Proc. Natl. Acad. Sci. U.S.A.*, 85 (1989) 9660.
26 J. I. Ohms, J. H. Burns, Jr., K. Wert and S. Beaucage, *Fed. Proc.*, 45 (1986) 1945.
27 A. S. Cohen and B. L. Karger, *U.S. Pat.*, 4 865 707 (Sept. 12, 1989).
28 S. Hjerten, *J. Chromatogr.*, 347 (1985) 191.
29 B. J. Radola, *Electrophoresis*, 1 (1980) 43.
30 A. T. Andrews, *Electrophoresis*, Oxford University Press, Oxford, 2nd ed., 1987.
31 D. J. Rose and J. W. Jorgenson, *Anal. Chem.*, 60 (1988) 642.
32 Y. G. Cheng and N. J. Dovichi, *Science (Washington, D.C.)*, 242 (1988) 562.
33 S. L. Pentoney, Jr., R. N. Zare and J. F. Quint, *J. Chromatogr.*, 480 (1989) 259.
34 A. S. Cohen, A. Guttman and B. L. Karger, *First International Symposium on HPCE, Boston, April 11–13, 1989*, Abstract No. M-L-8.
35 J. R. Hutton, *Nucleic Acids Res.*, 4 (1977) 3537.

Journal of Chromatography, 507 (1990) 125–140
Elsevier Science Publishers B.V., Amsterdam — Printed in The Netherlands

CHROMSYMP. 1678

Comparison of high-performance liquid chromatography, supercritical fluid chromatography and capillary zone electrophoresis in drug analysis

W. STEUER*, I. GRANT and F. ERNI[a]
Analytical Research and Development, Pharma Division, Sandoz Ltd., Basle (Switzerland)

SUMMARY

High-performance liquid chromatography (HPLC), supercritical fluid chromatography (SFC) and capillary zone electrophoresis (CZE) are compared with respect to their usefulness in drug analysis. Factors discussed include efficiency, performance, sensitivity, optimization parameters, method development time, sample preparation, technical difficulties, orthogonality of the information obtained and the possible application to various substance groups. It is concluded that HPLC can be applied successfully in virtually all areas of pharmaceutical analysis. CZE has a promising future in the analysis of drugs and in the field of biotechnological analysis, where a high number of plates is required together with a short analysis time. Nevertheless improvements in detection are still necessary for most applications. SFC is particularly suitable for moderately polar compounds or substances for which mass-sensitive detection is required. SFC and CZE can be considered as complementary to HPLC owing to the orthogonality of the acquired data, and as a result more information can be obtained from the analysis.

INTRODUCTION

High-performance liquid chromatography (HPLC) is a well established method for the purity control and assay of drugs in galenical forms or in biological matrices. Over the last 4 years, the use of supercritical fluid chromatography (SFC) has greatly increased. At present, in addition to non-polar compounds, strongly polar substances and large molecules can be separated. Recently, SFC[1] has been extended to include applications involving ionic compounds. During the last few years, capillary zone electrophoresis (CZE), a high-efficiency separation technique, has attracted considerable attention, mainly for the separation of proteins. However, there has been comparatively little interest in the analysis of pharmaceuticals.

This paper compares the utility of HPLC, SFC and CZE in drug analysis. The advantages and limitations of each technique are discussed, in most instances, on the basis of our own experience in the laboratory. Most of the example separations using

0021-9673/90/$03.50

SFC and CZE were carried out using laboratory-constructed apparatus, which has been described elsewhere[1,2].

Drug analysis can be divided into the following subgroups: drug substance analysis, stability investigations of galenical forms, analysis of excipients, determination of drugs in biological fluids and biotechnological analysis. Each of these subgroups possesses an additional profile of requirements in terms of efficiency, performance, selectivity, sensitivity and sample preparation, which must be taken into account when deciding on the suitability of a separation method.

EVALUATION CRITERIA

This comparative study is based on the following evaluation criteria: efficiency (N); performance (N/t) (N = number of plates; t = time); sensitivity; parameters available for modification of selectivity; method development time; sample preparation; and orthogonality of information.

Efficiency and performance

Davis and Giddings[3] and Martin *et al.*[4] demonstrated, using a statistical method, that a very high peak capacity is necessary in order to obtain, with 90% probability, a baseline separation of a small number of components in a single experiment. For the separation of eight compounds more than half a million plates would be necessary[5]. This indicates that in many analytical problems a high number of plates is desirable. Table I compares the necessary analysis times in HPLC, SFC and CZE for the separation of a given number of species with a given number of plates. A limiting pressure drop of 300 bar was assumed for the chromatographic techniques. In chromatography the optimum particle diameter for a given set of conditions can be determined from the kinetic optimization procedure of Knox and Saleem[6]. For SFC and HPLC the calculated optimum particle diameters range from 0.3 to 7.6 μm. In all instances the most appropriate commercially available particle size was used, which means that for N = 1000–50 000 optimum kinetic conditions are not possible (see Appendix). For N > 50 000 the required times were calculated under kinetically optimized conditions. In HPLC the maximum available pressure of 300 bar can be used for bringing about the flow of the mobile phase. In SFC, however, a post-column

TABLE I

ANALYSIS TIMES REQUIRED FOR HPLC, SFC AND CZE

Assumptions: ΔP = 300 bar; coefficients for the Knox hv curve were taken as; A = 1.0, B = 2.0, C = 0.1, which leads to h_{min} = 2.4 and v_{min} = 2.7; for the calculation of diffusion coefficients of pharmaceutical compounds, a typical value for the effective hydrodynamic radius of 4 Å was assumed.

No. of components	N	*Times required (s)*			
		HPLC (20°C)	*HPLC (90°C)*	*SFC*	*CZE*
5	1000	4.2	1.1	0.8	–
10	10 000	56	15.2	10.6	–
20	50 000	480	140	95	60
50	500 000	32 000	10 300	7100	600

restrictor must be employed to maintain the desired fluid density at the column outlet, which often means an outlet pressure of 200 bar. Hence, two thirds of the available pressure is consumed merely to sustain the supercritical conditions, leaving only 100 bar for generation of fluid flow. The separation of drug substances by SFC requires, owing to their often polar nature, high fluid densities and the use of polar modifiers[7]. Taking this into consideration, a diffusion coefficient of $0.3 \cdot 10^{-4}$ cm^2 s^{-1} and a viscosity of $7.2 \cdot 10^{-2}$ cP were calculated[8] and used together with a maximum pressure drop of 100 bar in the calculations for SFC. Ideally, the efficiency of CZE increases indefinitely as the analysis time is reduced[9]. However, when factors such as wall adsorption and ohmic heating are taken into account, diffusion-limited efficiency can be realised in only a few instances. In our experience, typical efficiencies of 500 000 plates per metre are attained with an electric field gradient of 30 kV m^{-1} and an ionic strength of 0.030 mol dm^{-3}. If the electric field gradient is held constant while varying the column length, the retention time and the plate number will be directly proportional to the column length, at least to a first approximation. Instrumental difficulties, namely extra-column broadening, impose a practical limit of no less than about 10 cm for the column length. Hence capillary zone electrophoresis with a desired plate number of less than 50 000 cannot be considered practical.

Table I demonstrates that HPLC should be used when a small number of components have to be separated in a short time. This is a typical requirement for the stability analysis of galenical forms. When a high number of plates is required, SFC and CZE are to be preferred. Calculations using the values estimated above show that SFC has a three times greater performance than HPLC. However, if HPLC is carried out at high temperatures[10], performances approaching those of SFC can be obtained. For the determination of drug purity, where often 10–15 peaks have to be separated, in some instances SFC may be a useful alternative to HPLC. CZE is the most appropriate technique for the separation of very complex mixtures, where more than 100 000 plates

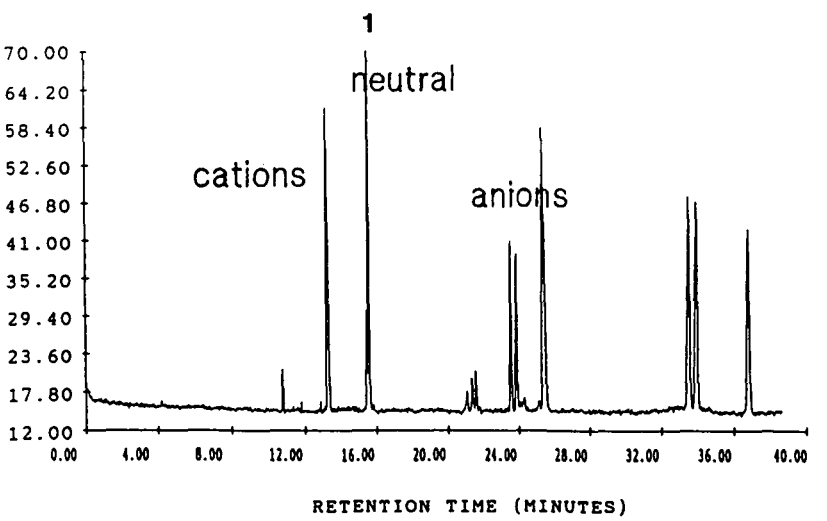

Fig. 1. Analysis of a stressed pharmaceutical alkaloid (1) by CZE. Applied voltage, 25 kV; buffer, water–acetonitrile (60:40)–30 m*M* Na_2HPO_4; capillary, 90 cm × 50 μm I.D.

are required (Fig. 1). Typical examples are the purity control of drugs and biotechnological analyses such as the separation of protein digests (Fig. 9).

Sensitivity

The sensitivity of a separation method depends on both the loading capacity of the system and the nature of the available detectors. In addition to concentration-dependent detectors such as UV absorbance and fluorescence types, the mass-sensitive flame-ionization detector can be implemented in SFC, provided that the addition of modifiers to the carbon dioxide can be avoided. Unfortunately, this is seldom the case for polar drugs. In contrast to HPLC and SFC, CZE can only be used in a miniaturized form, resulting in constraints in terms of loading capacity and sensitivity. It should be emphasized that for absorbance and fluoresence detection it is the concentration sensitivity and not the minimum detectable amount that is relevant in drug analysis.

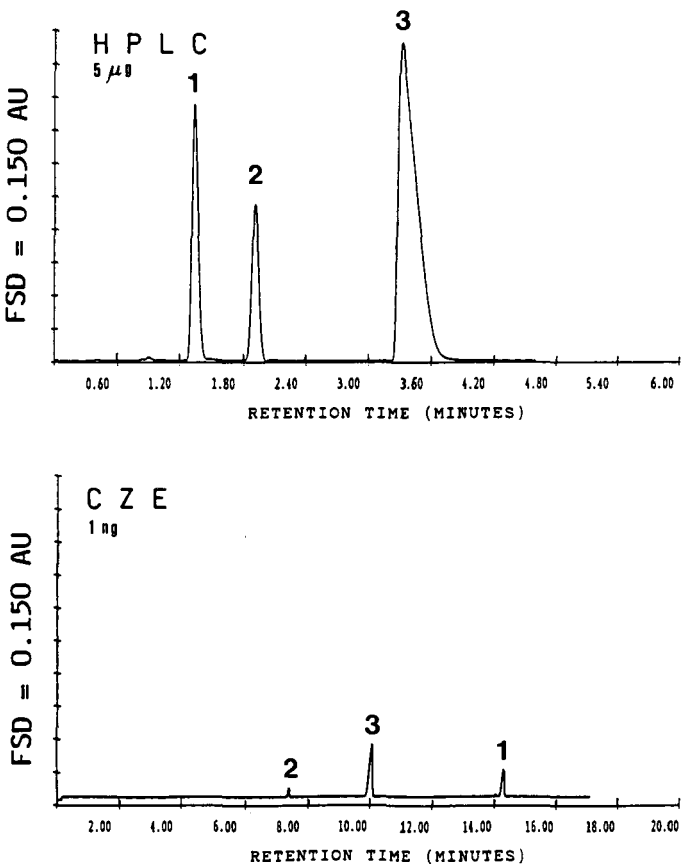

Fig. 2. Sensitivity comparison for HPLC and CZE; separation of spirapril and its degradation products. HPLC: column, Brownlee RP-18, 5 µm, 100 mm × 4.6 mm I.D.; eluent, acetonitrile–water (50:50)–0.5 m*M* tetramethylammonium hydroxide, adjusted to pH 2; temperature, 70°C; UV detection at 217 nm. CZE: UV detection at 214 nm; buffer, acetonitrile–10 m*M* disodium tetraborate (15:85), adjusted to pH 11.7 with sodium hydroxide; capillary, 90 cm × 50 µm I.D.; applied voltage, 25 kV ($i = 14$ µA).

The latter can often be deceptive in capillary SFC and CZE. When working with packed conventional columns, UV detection in SFC and HPLC is comparable in terms of sensitivity and loading capacity, although the noise level may be greater in SFC owing to density-related refractive index changes in the highly compressible supercritical fluid. UV detection in capillary SFC demands an on-line detection technique[11,12], with detector volumes of less than 100 nl and optical path lengths of less than 250 μm, resulting in a sensitivity loss, relative to HPLC, of a factor 40.

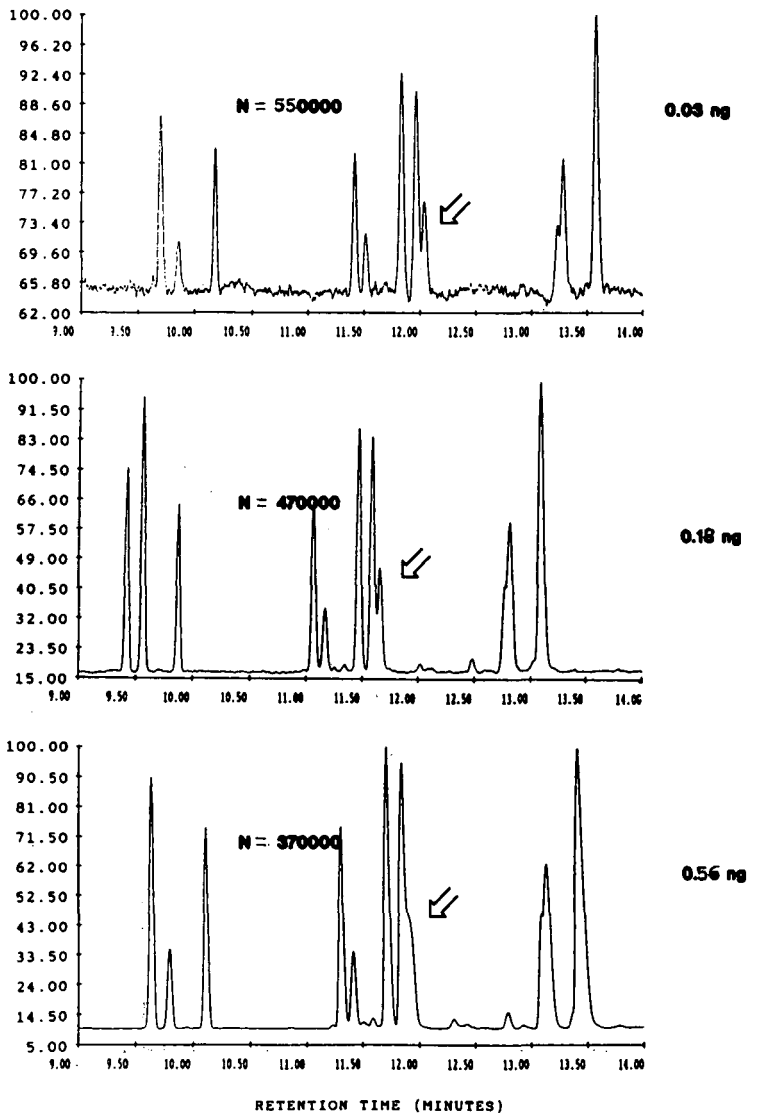

Fig. 3. Loading capacity study for the separation of terbinafine and its by-products by CZE. UV detection at 214 nm; volume injected held constant; buffer, 60% acetonitrile in 12 m*M* KH_2PO_4–12 m*M* Na_2HPO_4, adjusted to pH 2.4 with phosphoric acid; capillary, 90 cm × 50 μm I.D.; applied voltage, 30 kV ($i = 14$ μA).

From our experience with the separation of spirapril an angiotensin converting enzyme inhibitor co-developed by Sandoz and Schering-Plough and its degradation products (Fig. 2), it can be concluded that the concentration sensitivity in HPLC is at least ten times better than that in CZE. In both instances the same sample concentration was injected (1 mg/ml). As shown in Fig. 3, for the separation of terbinafine and its by-products, the poor sensitivity of CZE cannot be totally compensated for by an increase in the amount injected. In our study of the loading capacity in CZE, the efficiency was observed to decrease by a factor of four following a 100-fold increase in the sample concentration (Fig. 4), which leads to an unacceptable loss of resolution. Additionally, the signal-to-noise ratio does not increase linearly with the amount injected because of the additional peak broadening, which results in a less than linear increase in peak height. From the above, it is clear that, in addition to the optimization of selectivity, the amount injected can also be optimized, subject to resolution requirements. The loading capacity can be increased by increasing the ionic strength, but the applied voltage then has to be reduced, which results in a longer analysis time. In general, it can be concluded that CZE has a limited application in trace analysis, where one component is usually present in a large excess.

Parameters available for modification of selectivity

The number of parameters and the extent to which they influence selectivity are indications of the optimization potential of the separation technique. However, it does not imply that the method that has the most available parameters influencing

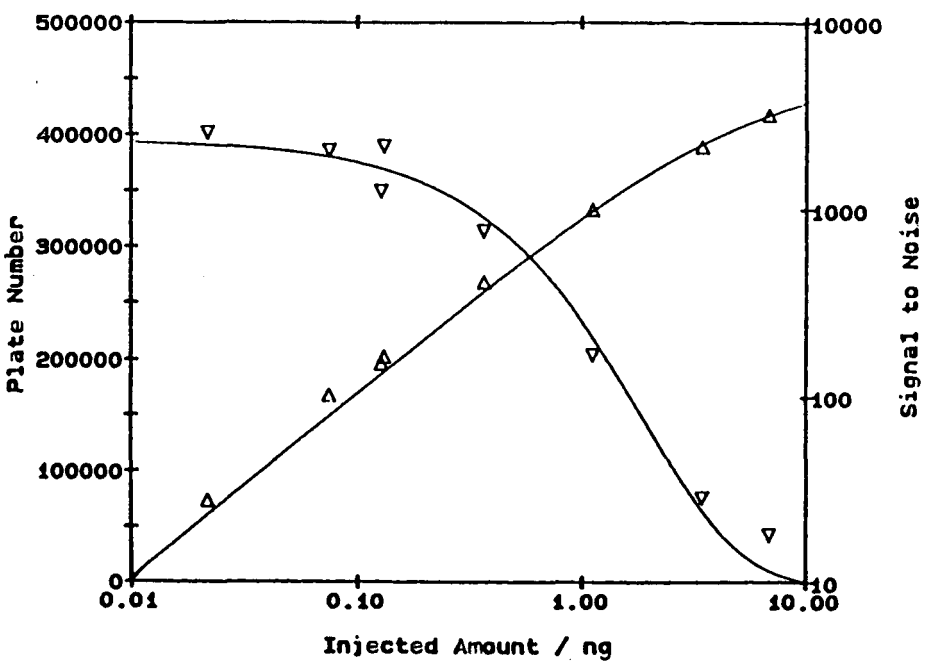

Fig. 4. Effect of amount injected on efficiency and signal-to-noise ratio in the CZE of terbinafine with constant injection volume. Conditions as in Fig. 3. ▽ = Number of theoretical plates; △ = signal-to-noise ratio.

TABLE II

USEFULNESS OF PARAMETERS INFLUENCING THE SELECTIVITY

Scale from 0 to 10, where 10 = most significant effect.

Parameter	*HPLC*	*SFC (packed)*	*CZE*
Stationary phase	10	5	0
pH	10	1	10
Ionic strength	7	2	1
Modifier	10	5	4
Ion pairing agent	5	5	5
Pressure	0	10	0
Temperature	1	4	0
Gradients	8	9	0
Total	51	41	20

selectivity can be optimized in the shortest time. Table II compares the parameters that may be capable of modifying the selectivity. The parameters are evaluated according to their relative significance for each technique; the number 10 indicates that the parameter is of the greatest importance on a scale from 0 to 10 and 0 indicates that the effect of changing the parameter is negligible. The greatest advantage of HPLC over SFC is that a large number of stationary phases and mobile phases are available with a wide range of polarities. Organic modifier gradients can be run in HPLC and SFC but not, so far, in CZE. In SFC the density can be used to change the selectivity rapidly and very effectively. This effect can be exploited by the use of pressure gradients, which can even be combined with organic modifier gradients allowing the simultaneous separation of polar and non-polar species (Fig. 5). Hence the lack of efficiency in HPLC and SFC, compared with that of CZE, can be compensated for, to a certain extent. In CZE the most important factor for bringing about selectivity changes is the pH. In pure CZE the electrolyte must possess, at least to a certain extent, an aqueous character, which limits the choice of buffer composition[13]. The separation of neutral substances can be achieved only through the use of micellar solutions[14]. In electrically driven chromatography (electrochromatography)[15], the selectivity can also be influenced by the choice of the stationary and mobile phases as in HPLC. Based on Table II, HPLC is the most versatile method. The fact that SFC possesses more possibilities for selectivity modification than CZE must not be overestimated in drug analysis, as it should be taken into account that compounds such as strongly basic amines and large peptides cannot be considered for analysis by SFC owing to the limited polarity range of the mobile phase.

Method development time

The time required to develop a separation method depends mainly on the time required for column equilibration, the performance (N/t) and the efficiency (N). CZE shows the most promise in this area because of its very high performace and efficiency

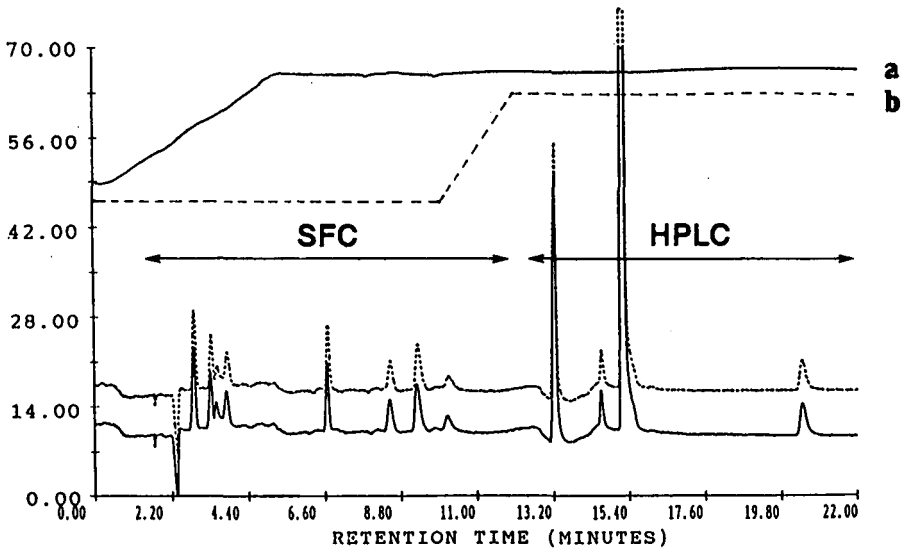

Fig. 5. Combined pressure and modifier gradient in SFC. Column, Brownlee diol-phase, 5 μm, 500 mm × 4 mm I.D.; eluent, carbon dioxide–methanol–20 m*M* dimethyloctylamine; UV detection at 220 nm. (a) Pressure gradient 183–322 bar; (b) modifier gradient 8–25%.

(Fig. 1) compared with SFC and HPLC. SFC offers a higher performance than HPLC and often shorter equilibration times[7,16], because following changes of the supercritical fluid density a stable system is rapidly obtained. From the above it can be concluded that HPLC requires the longest method development time.

Sample preparation

The sample preparation should be minimal and should not be influenced by the separation step. The separation should not be sensitive to the nature of the extraction solvent or to the presence of matrix components. On-line sample pretreatment procedures such as column switching should be available. Because, in most instances, the extraction of drugs from their galenical forms requires the use of a polar solvent, the subsequent separation step should not be affected by its presence, *i.e.*, the eluent should have at least the same eluotropic strength as the extraction solvent. When comparing HPLC, SFC and CZE, only reversed-phase HPLC comes close to fulfilling these requirements. In this instance only minimum constraints are imposed on the extraction solvent and it may even contain large amounts of water. The choice of extraction solvent in SFC is, in contrast, severely restricted. Polar modifiers containing water would cause spurious artefacts or at the very least a loss of efficiency. Therefore, SFC is often not suitable when polar solvents must be used for the extraction of polar substances from an aqueous excipient matrix, or from biological matrices. This problem can be alleviated by the use of an on-line extraction set-up, in which the eluent is also used as the extraction solvent[17], or by column switching, permitting the replacement of the polar solvent. These problems are less severe in capillary SFC.

In CZE, the sample solvent and the electrophoresis buffer are preferably the same, otherwise disturbances of the electric field or precipitation of the extracted components could occur. The problem can be avoided by preventing electroosmosis and using electromigration as the injection principle, although care must be taken to ensure that the analytes are ionized in the sample solvent. When the separation requires buffers that are vastly different from the extraction solvents, such as extreme pH values, or pure water, the extraction may be disturbed. This is demonstrated for the

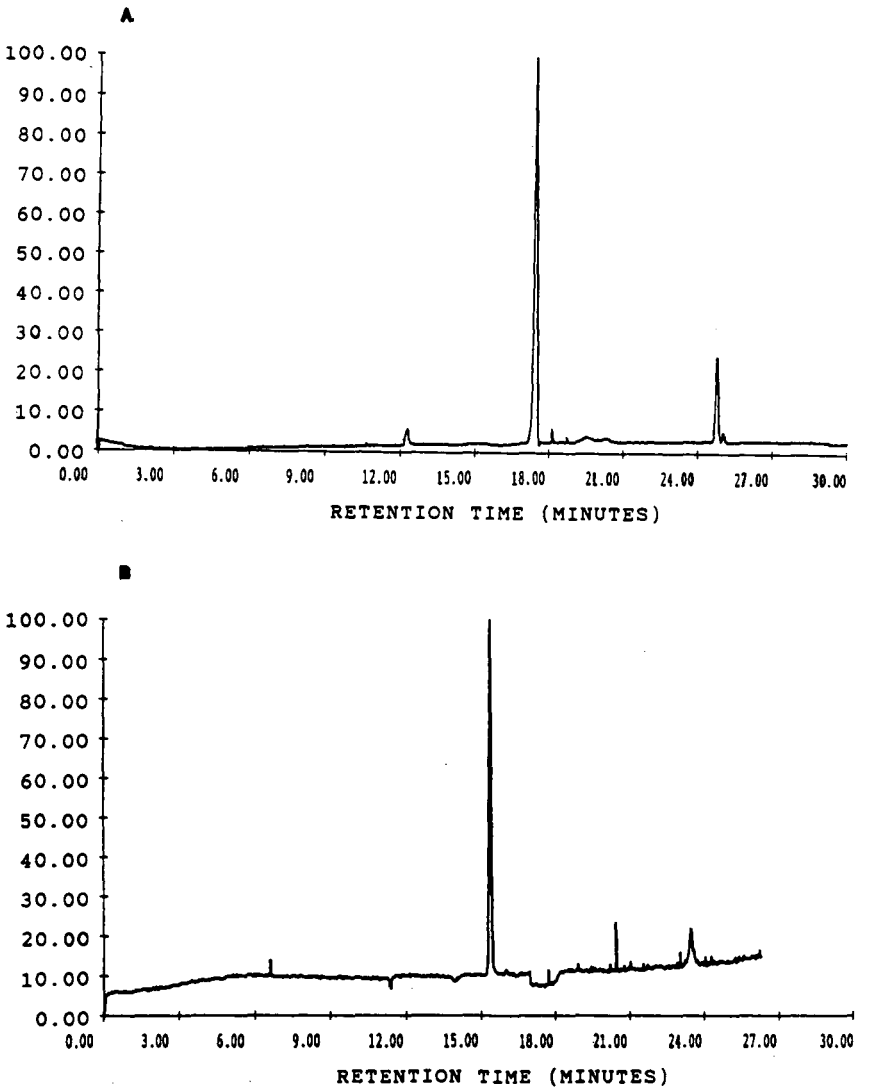

Fig. 6. Interaction between the preparation of the sample and the subsequent separation step. Extraction of spirapril from dosage forms: (A) CZE, buffer of pH 11.7; (B) standard HPLC procedure. Extraction buffer for HPLC, acetonitrile–water (50:50); buffer for CZE, see Fig. 2. HPLC buffer causes disturbances of the electric field.

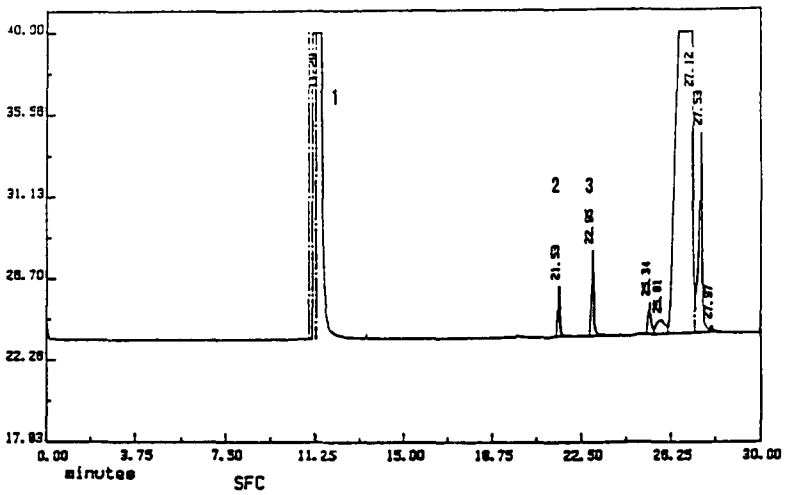

Fig. 7. Determination of cetyl alcohol in cetyl palmitate by capillary SFC. Cyano column, 10 m × 50 μm I.D.; film thickness, 0.25 μm; density gradient, 0.2 → 0.5 g/ml; FID. Peaks: 1 = methylene chloride; 2 = cetyl alcohol; 3 = stearyl alcohol (internal standard).

extraction of spirapril and its degradation products from the capsule mixture (Fig. 6). At the necessary pH of 12 the excipients were partly dissolved as colloids, which hindered the centrifugation. In most instances these problems are less critical in CZE than in SFC.

Technical feasibility

During the last decade, HPLC with packed columns has been developed to a high level of sophistication. Injection systems are reliable with a reproducibility of 0.5% (relative standard deviation). There are no severe problems with the delivery of eluent in conventional HPLC. Flow-rate relative standard deviations are less than 0.5%. Problem with solvent delivery are only encountered with micro-HPLC systems (column diameter < 1 mm).

The injection precision of SFC is relatively poor in comparison with HPLC. For the analysis of the excipient cetyl palmitate (Fig. 7), relative standard deviations, on injected amount, of up to 5% were observed, mainly as the result of non-constant splitting ratios or sample precipitation caused by density changes occurring during the injection[18]. The use of an internal standard is therefore recommended. The maintenance of a constant density independent of the flow-rate requires precise restrictors and a sophisticated pressure–flow regulating system. No such systems are commercially available for packed or capillary SFC. The lack of such a device leads to a significant loss of efficiency in capillary SFC during the latter stages of a density gradient, as the flow-rate, and consequently the plate height, increase with increasing density.

In CZE, concentration-dependent detectors, such as UV absorbance of fluorescence types, are 10–20 times less sensitive than their counterparts in HPLC or SFC and the coupling to mass-sensitive detectors is difficult. Depending on the injection method (electromigration, gravitational or pneumatic), relative standard deviations on peak

TABLE III

TECHNICAL FEASIBILITY

Scale from 0 to 10, where 10 = most reliable.

Operation	*HPLC*	*SFC*	*CZE*
Detection	8	8	1
Injection	10	3	6
Delivery of eluent	8	5	10
Pressure limitation	6	2	10
Total	32	18	27

areas of up to 3–4% are typical[19], and bias effects are unavoidable with electrokinetic injection[20]. For this reason in CZE, as in SFC, the use of an internal standard is advisable. If the capillaries are washed with sodium hydroxide between runs, the fluctuations in electroosmotic flow are less than 0.5%.

As shown in Table III, for technical evaluation HPLC is the most reliable technique, followed by CZE, for which fully automated systems are now on the market. To a large extent the detector still represents an unsolved problem in CZE.

Orthogonality of information

The objective of combined analytical separations is to obtain non-redundant information from independent systems[21–23]. In the ideal case different systems can be coupled together to give an on-line multi-dimensional set-up[24]. For comparison of our data, the analysis times for each technique were normalized to give "retention parameters" defined according to the expression

$$\chi_i = \frac{t_i - t_0}{\Delta t}$$

where t_i represents the time for the i_{th} component, t_0 the time for the first component and Δt the total range of analysis times. This procedure was carried out for several drugs and their by-products and degradation products, wich represent a range of substances with vastly different chemical properties. χ_{CZE} and χ_{SFC} are plotted against χ_{HPLC} in Fig. 8. Comparison of HPLC with CZE and HPLC with SFC for several separations suggests that HPLC and CZE are usually orthogonal systems (Figs. 1, 8 and 9). As HPLC and SFC often show only a slight correlation, the on-line coupling of these techniques would be of considerable benefit.

Influence of substance properties on choice of technique

An obvious prerequisite for the analysis of a substance by SFC is an adequate solubility in the supercritical medium. This can often be increased by the addition of an organic modifier. However, this leads to a considerable deterioration of the favourable kinetic properties of the supercritical carbon dioxide when the modifier content exceeds *ca.* 20%. For this reason, substances such as isradipine (calcium antagonist), Sandimmune (immunosupressive agent) or non-polar excipients (waxes, polymers such as cetyl palmitate) (Fig. 7), which are readily soluble in acetonitrile, chloroform

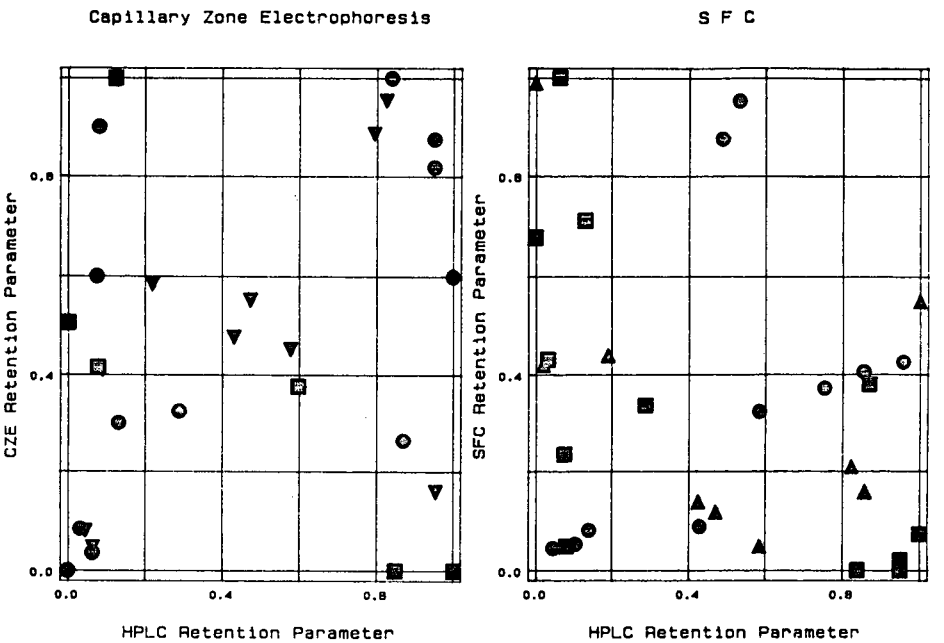

Fig. 8. Demonstration of the orthogonality between HPLC and CZE and between HPLC and SFC. No obvious correlation arises between the retention parameters in HPLC and CZE; some correlation between those of HPLC and SFC may arise (isradipine). All HPLC separations were carried out under reversed-phase conditions, with the exception of isradipine (normal-phase). Compounds: (left) ▼ = terbinafine; ■ = spirapril; ● = AH 21 132; (right) ▲ = terbinafine; ● = isradipine; ■ = AH 21 132.

and similar aprotic solvents (comparable with supercritical carbon dioxide in terms of eluotropic strength), are easily separated, whereby only small amounts of polar modifiers (*ca.* 5%), *e.g.*, methanol, are called for. Moderately basic ionic substances such as alkaloids[25], indole derivatives, α-amino alcohols[7] or barbiturates, and weak acids, *e.g.*, benzoic acid or spirapril[7] and PTH-amino acids[26], can also be separated, although in many instances suitable ion-pairing agents are required. Large peptides such as octreotide and calcitonine are not soluble in carbon dioxide–methanol mixtures.

CZE in its pure form is suitable only for substances that can be ionized in solution, and therefore requires the use of polar eluents of an aqueous nature, although large amounts of organic modifiers can be added if required (Fig. 3). The separation of neutral substances can be achieved using micellar solutions provided that they have an adequate solubility in the buffer mixture. The addition of organic solvents normally increases the critical micelle concentration, which limits the amount of modifier that can be added.

CZE can be applied both for the separation of low-molecular-weight drugs such as terbinafine, propranolol and spirapril and also for peptides and proteins.

Owing to the broad scope of possible eluents and stationary phases, HPLC has the fewest constraints. Polar, non-polar, ionic, small and even large molecules, *e.g.*, antibodies, can be separated. Detection problems arise for molecules without chromophores, because of the lack of a simple mass-sensitive detector.

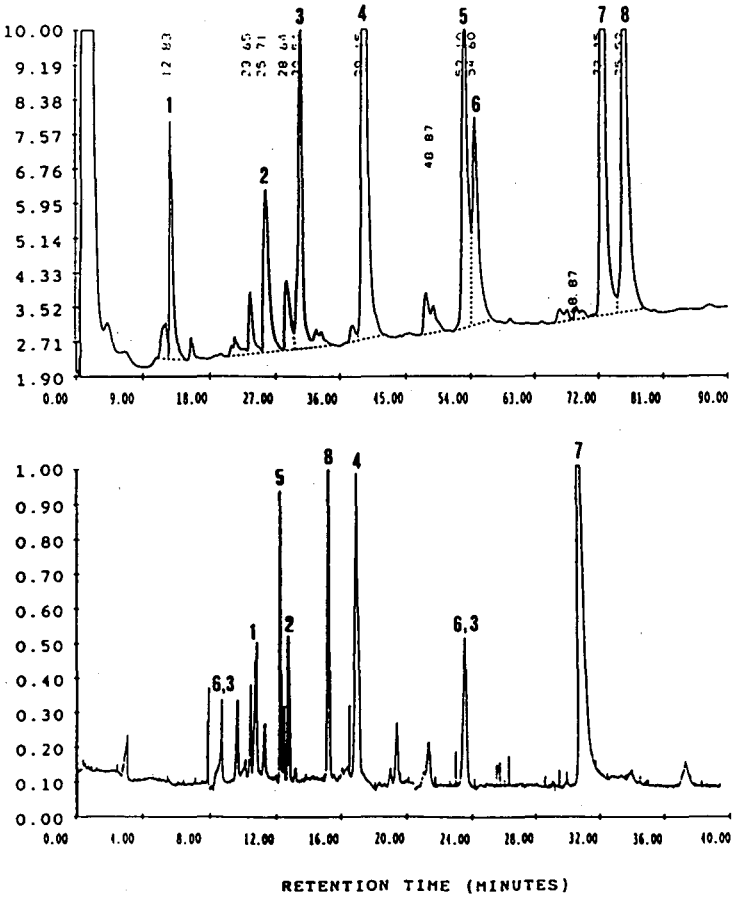

Fig. 9. Comparison of the separation of a protein digest by HPLC (top) and CZE (bottom). HPLC: column, Vydac C_{18} (with Aquapore pre-column); eluent, 0–58% acetonitrile in water in 130 min (0.1% trifluoracetic acid); UV detection at 215 nm. CZE: capillary, 50 cm × 50 μm I.D.; applied voltage, 14 kV ($i = 24$ μA); buffer, 20 m*M* citrate buffer (pH 2.5); UV detection at 200 nm.

Optimum use of HPLC, SFC and CZE

HPLC can be utilized in the determination of drugs in biological matrices, where in addition to a high performance a high sensitivity is required. It can also be implemented for drug stability investigations in galenical forms, where a high performance is required, for the determination of drug purity and in the analysis of biotechnological products (Fig. 9), in which event the use of gradient elution gives rise to a high peak capacity.

CZE is favoured for drug purity control and also for the separation of biotechnological products. It is particularly suitable for the separation of protein digests (Fig. 9) owing to its enormous peak capacity.

Of the three methods, SFC possesses the narrowest range of application in pharmaceutical analysis. Because mass sensitive detection [flame ionization detection (FID)] can be employed, capillary SFC is suitable for the analysis of excipients (Fig. 7).

With a more limited scope than HPLC or CZE, SFC can be used for the purity control of drugs because of its high performance (Fig. 5).

Strengths and weaknesses of HPLC, SFC and CZE

The strength of HPLC is its high technical level, selectivity and versatility according to substance groups and task. The lack of performance and efficiency is partly compensated for by the possibility of using gradient elution. A weak point is the lack of a simple, universal, sensitive method of detection equivalent to FID in gas chromatography and SFC.

CZE displays an enormous efficiency and therefore separation methods can be rapidly developed. The main drawbacks are the poor sensitivity and the fact that elution and extraction buffer have to be similar.

SFC exhibits a higher performance than HPLC and often shorter method development times. An advantage is the possibility of using both modifier and density gradients or a combination of both. Owing to technical problems, SFC with packed columns is far from being at a routine working level. The method is limited to only a small range of eluents and accordingly to a small number of substance groups.

CONCLUSIONS

From the comparison of the three techniques in drug analysis according to the evaluation parameters discussed above, it can be concluded that HPLC can be used successfully in nearly all areas of pharmaceutical analysis. At higher temperatures, performances approaching those of SFC are possible.

CZE has a promising future in drug analysis, where a high number of plates is required within a short time. The method is especially suitable for ionic species. For most applications the detection sensitivity must be improved.

SFC is useful for non-polar and moderately polar compounds or substances for which mass-sensitive detection is required. It is a suitable method for purity control and for the analysis of excipients, although the technical level requires further improvement.

Owing to their orthogonality, CZE and SFC are worth developing, not in competition or as an alternative to HPLC, but as an additional method in order to augment the information obtained from the analysis.

In the future, each of the three techniques will have its place in pharmaceutical analysis, its particular share of application depending on the product range concerned.

APPENDIX

Time optimization under non-ideal conditions: Calculation of optimum time for a given plate number, pressure drop and particle size

The shortest time for a given number of plates with a predetermined particle size will be obtained when the full available pressure is used. Hence the length must be calculated such that the desired number of plates is realized at this pressure drop.

Linear velocity is governed by the equation

$$u = \frac{\Delta P d_p^2}{\varphi \eta L} \tag{1}$$

Substituting $L = Nhd_p$ and $u = vD_m/d_p$ yields

$$vh = \frac{\Delta P d_p^2}{\varphi \eta N D_m} \tag{2}$$

If h is then substituted by the Knox hv curve, following minor rearrangement the equation

$$f(v) = Cv^2 + Av^{4/3} + B - \left(\frac{\Delta P d_p^2}{\varphi \eta N D_m}\right) = 0 \tag{3}$$

is obtained. This equation is then solved for v using a Newton–Raphson iterative scheme in which values of coefficients $A=1$, $B=2$ and $C=0.1$ were assumed:

$$v_{n+1} = v_n - \frac{f(v)}{f'(v)} \tag{4}$$

where $f'(v) = 2Cv + (4/3)Av^{1/3}$

$$v_{n+1} = v_n - \frac{Cv_n^2 + Av_n^{4/3} + B - (\Delta P d_p^2)/(\varphi \eta N D_m)}{2Cv_n + (4/3)Av_n^{1/3}} \tag{5}$$

Successive iterations are carried out until no significant change in v is observed. The reduced velocity obtained from solution of eqn. 3 is then used to calculate h by substitution into eqn. 2. The required column length and the analysis time for an unretained component are given by

$$L = Nhd_p \tag{6}$$

and

$$t_m = Ld_p/vD_m \tag{7}$$

respectively. The time required for the nth component is calculated using the standard expression for the peak capacity:

$$\log\left(\frac{t_n}{t_m}\right) = \frac{n-1}{0.6\sqrt{N}} \tag{8}$$

GLOSSARY OF SYMBOLS

u	Mobile phase linear velocity
d_p	Particle diameter
ΔP	Pressure drop
φ	Dimensionless flow resistance parameter (typically = 500)

η	Mobile phase viscosity
L	Column length
h	Reduced plate heigth
v	Reduced velocity
D_m	Diffusion coefficient
A, B, and C	Knox equation coefficients
N	Number of theoretical plates
v_n, v_{n+1}	(n)th and $(n+1)$th iterates
$f(v)$, $f'(v)$	see eqn. 3
t_m	Column dead time
t_n	Time for the (n)th component

REFERENCES

1 W. Steuer, M. Schindler, G. Schill and F. Erni, *J. Chromatogr.*, 447 (1988) 287.
2 J. H. Knox, *Chromatographia*, 26 (1988) 329.
3 J. M. Davis and J. C. Giddings, *Anal. Chem.*, 55 (1983) 418.
4 M. Martin, D. P. Herman and G. Guiochon, *Anal. Chem.*, 58 (1986) 2200.
5 F. Erni, W. Steuer and H. Bosshardt, *Chromatographia*, 24 (1987) 201.
6 J. H. Knox and M. Saleem, *J. Chromatogr. Sci.*, 7 (1969) 614.
7 W. Steuer, J. Baumann and F. Erni, *J. Chromatogr.*, 500 (1990) 469.
8 P. J. Schoenmakers, in R. M. Smith (Editor), *Supercritical Fluid Chromatography*, Royal Society of Chemistry, London, 1988, Ch. 4, p. 102.
9 J. W. Jorgenson and K. D. Lukas, *J. Chromatogr.*, 218 (1981) 209.
10 F. D. Antia and Cs. Horváth, *J. Chromatogr.*, 435 (1988) 1.
11 P. A. Peaden and M. L. Lee, *J. Chromatogr.*, 259 (1983) 1.
12 D. W. Later, B. J. Bornhop, E. D. Lee, J. D. Henion and R. C. Wiebolt, *LC · GC, Mag. Liq. Gas Chromatogr.*, 5 (1987) 804.
13 S. Fujiwara and S. Honda, *Anal. Chem.*, 59 (1987) 487.
14 S. Terabe, K. Otsuka, K. Ichikava, A. Tsuchiya and T. Ando, *Anal. Chem.*, 56 (1984) 111.
15 J. H. Knox and I. H. Grant, *Chromatographia*, 24 (1987) 135.
16 W. Steuer, M. Schindler and F. Erni, *J. Chromatogr.*, 454 (1988) 253.
17 E. D. Ramsey, J. R. Perkins, D. E. Games and J. R. Startin, *J. Chromatogr.*, 470 (1989) 353.
18 M. L. Lee, B. Xu, E. C. Huang, N. M. Djordjevic, H. C. K. Hang and K. E. Markides, *J. Microcolumn Sep.*, 1 (1989) 7.
19 D. J. Rose and J. W. Jorgenson, *Anal. Chem.*, 60 (1988), 642.
20 X. Huang, M. J. Gordon and R. N. Zare, *Anal. Chem.*, 60 (1988) 375.
21 J. F. K. Huber, E. Kenndler and G. Reich, *J. Chromatogr.*, 172 (1979) 15.
22 H. Vink, *J. Chromatogr.*, 69 (1972) 237.
23 D. L. Massart and R. Smits, *Anal. Chem.*, 46 (1974) 283.
24 F. Erni and R. W. Frei, *J. Chromatogr.*, 149 (1978) 561.
25 J. L. Janicot, M. Caude and R. Rosset, *J. Chromatogr.*, 437 (1988) 351.
26 T. A. Beyer, J. F. Deye, M. A. Khorassani and L. T. Taylor, *J. Chromatogr. Sci.*, 27 (1989) 105.

Journal of Chromatography, 507 (1990) 141–149
Elsevier Science Publishers B.V., Amsterdam — Printed in The Netherlands

CHROMSYMP. 1680

Use of high-performance liquid chromatography in the pharmaceutical industry

F. ERNI
Analytical Research and Development, Pharma Division, Sandoz Ltd., Basle (Switzerland)

SUMMARY

Requirements for new pharmaceutical products and their impact on applications of high-performance liquid chromatography (HPLC) are discussed. The strengths and weaknesses of HPLC in this context are evaluated and compared with current trends and expectation in separation science.

INTRODUCTION

In recent years, a significant change in the techniques available for the chemical analysis of drugs has been observed. More and more sophisticated analytical instrumentation with highly automated sample handling, control and data-processing systems are playing an increasingly important role in analytical laboratories for drug development and quality control. The main goal of this trend is to obtain more reliable results with less effort in a shorter time. This should lead to faster drug development, better quality of the final products and a higher degree of safety for the patient.

This paper reviews the role of high-performance liquid chromatography (HPLC) in the pharmaceutical industry and analyses trends based on new technologies, on new regulatory requirements for new pharmaceutical products and on modern ways of exploring and developing new drugs.

HPLC AS A TOOL IN THE PHARMACEUTICAL INDUSTRY

In the drug discovery process, HPLC is used as both an analytical and a semi-preparative method for the isolation of new natural products. These natural products from plants, fungi and animals are important starting materials ("lead compounds") for chemical modifications which lead to new drugs. In biotechnology, HPLC has many applications for the isolation, characterization and preparation of proteins and peptides. These compounds are thermally and chemically unstable. Therefore, HPLC techniques are ideally suitable. Because of the polarity and the ease of sample preparation, reversed-phase (RP) HPLC is preferred to normal-phase systems in most instances.

0021-9673/90/$03.50

In the course of drug development, HPLC is applied for the characterization of new drugs, especially purity determinations and assays. Automated HPLC is used for the analysis of various dosage forms, for process validation and in process control. HPLC has increasing importance as an analytical technique for raw materials that are used as pharmaceutical excipients for new drug delivery systems, and it will supplement or even replace many simple pharmacopoeial methods. For the determination of drugs, the characterization of metabolites and pharmacokinetic studies HPLC is an important method for the analysis of biological materials. Modern sample preparation methods, precolumn derivatization[1], column switching[2] and the use of robotic systems[3] can simplify complex assay procedures and can improve reproducibility and accuracy.

In the production and quality control of final products and raw materials, HPLC is used as a quality assurance tool. However, HPLC is not only an analytical technique, but it is also applied on a preparatory scale or production scale for the final purification of drugs. HPLC purification is an alternative to multiple crystallization, because the loss of expensive drugs can be minimized by HPLC purification.

In all of these applications, HPLC is found to be a simple and reliable method. The total analysis costs are competitive with those of other analytical methods, *e.g.*, gas (GC) supercritical fluid (SFC) or thin-layer chromatography (TLC) or spectroscopic methods.

CHALLENGES TO THE PHARMACEUTICAL INDUSTRY

The pharmaceutical industry faces challenges in which HPLC plays an important role. It is hoped that modern biotechnology will generate new drugs that fulfil medical needs. New biotechnological products are also important tools for pharmacology. Modern synthetic drugs are no longer marketed as racemates but whenever possible as optically active compounds. Therefore, the optical purity has to be checked[4]. Economic pressure and limiting patent protection call for the fast development of new drugs in order to shorten the time between the discovery of a drug and its introduction into the market. Good manufacturing practice (GMP) and good laboratory practice (GLP) require careful validation of methods and documentation of method development, system suitability[5] and the results of the analysis. All these challenges will lead to a more frequent application of HPLC.

STRONG POINTS OF HPLC

In the pharmaceutical industry, most of the samples are aqueous solutions, which can be analysed efficiently, by RP-HPLC with or without sample preparation. The selectivity of HPLC helps to resolve optically active compounds, *e.g.*, in purity determinations[4] or in pharmacokinetic studies[6]. HPLC is very fast[7]. Automation, including the use of robot samplers, helps to increase the throughput and will be increasingly used in process control.

WEAK POINTS OF HPLC

Most of the currently available HPLC instruments have severe limitations with regard to dead volumes and speed for the use of modern 3-μm HPLC columns. Many

gradient instruments have delay volumes and mixing volumes 10–100 times larger than the column volume of a 3-μm column of 3 cm × 2 mm I.D. This is the main reason why efficient HPLC columns with 3-μm and smaller particles have not yet made a breakthrough. The reliability of HPLC instrumentation is another weak point in routine applications. The mean time to failure (MTF) of samplers and pumps should be increased. The stability and reproducibility of HPLC columns are not yet good enough for complicated separations where the selectivity plays an important role, and finally there is still no sensitive universal detector, such as the flame ionization detector in GC. Compared with other separation techniques, HPLC lacks the separation efficiency of capillary GC, capillary zone electrophoresis (CZE)[8] and capillary SFC[9].

TRENDS IN HPLC

HPLC will be very much influenced by other separation techniques, especially CZE and capillary SFC. These new techniques have boosted instrument development in HPLC. It can therefore be expected that micro-HPLC systems will soon become important. This will help in overcoming the present limitations and open new areas for more efficient LC with smaller particles and shorter columns.

Fig. 1 shows a new development in this respect. The new micro-HPLC UV detector[10] with a capillary flow cell has an optical path length of *ca.* 20 mm and can significantly improve the signal-to-noise ratio, as shown in Fig. 2. On-column fluo-

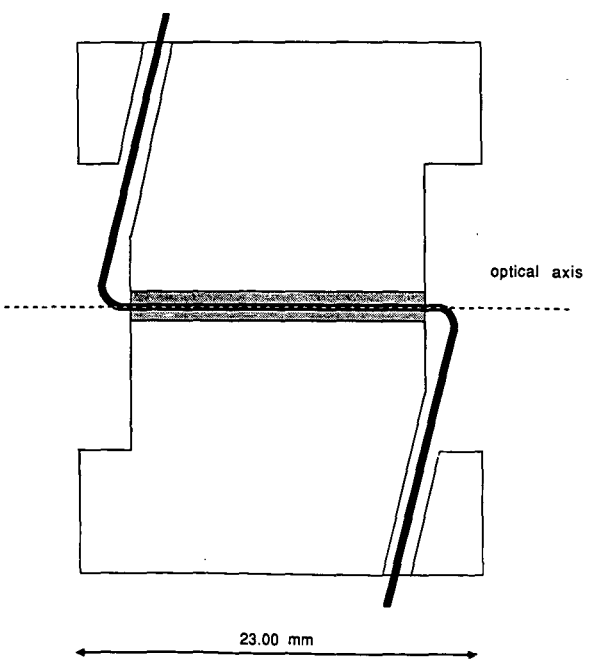

Fig. 1. Cross-sectional view of the logitudinal capillary flow cell (reproduced with permission of LC Packings, Amsterdam).

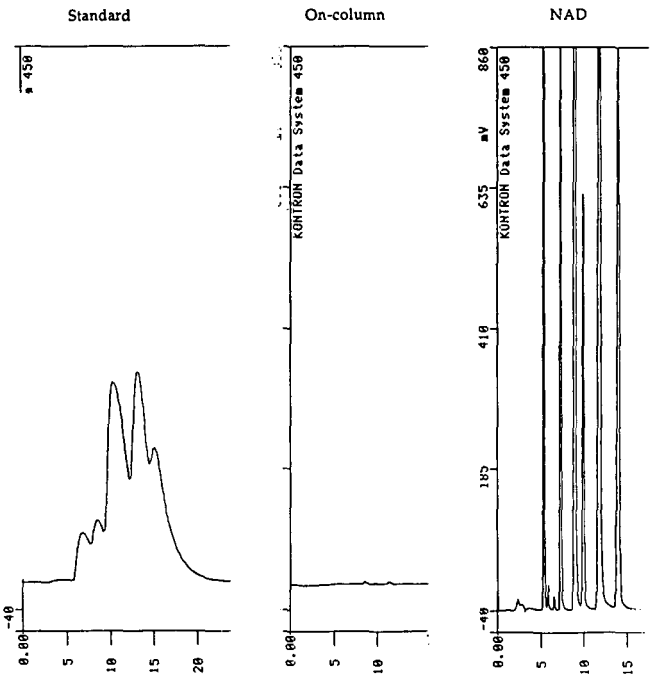

Fig. 2. Resolution and sensitivity in different flow cells (reproduced with permission of LC Packings, Amsterdam, The Netherlands). Test conditions: column, FuC-150, 15 cm × 320 μm I.D.; mobile phase, acetonitrile–water (7:3, v/v); flow-rate, 3 μl/min; temperature, ambient; pressure, 4.6 MPa (46 bar); sample, PAHs; injection volume, 60 nl; detection, UV (254 nm), 0.1 a.u.f.s., t = 2.0 s; chart speed, 0.25 cm/min.

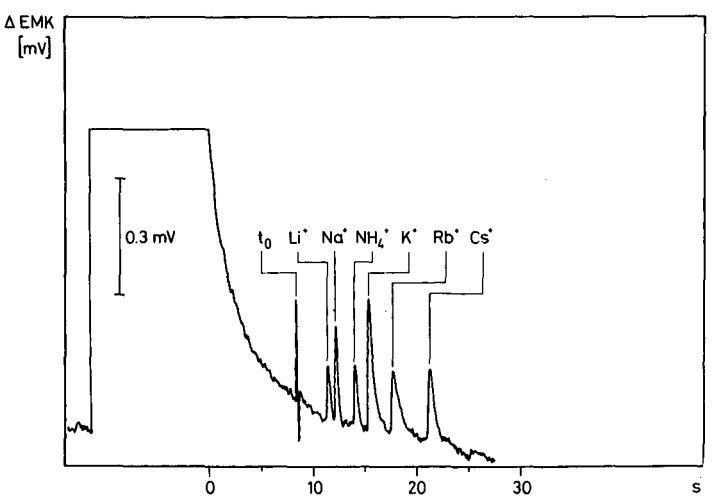

Fig. 3. Separation of ions by open-tubular HPLC (reproduced with permission of Prof. W. Simon, ETH, Zurich, Switzerland). Sample, 10 pl chloride in water, 40–2000 μmol/l; column, 0.33 m × 4.6 μm I.D. coated with 3-sulphopropylsilane; mobile phase, 20 mM formic acid; flow-rate, 10 nl/min.

rescence and UV detectors used in CZE can also be used for open-tubular HPLC systems. Fig. 3 shows an example[11] of electrochemical detection with an ion-selective electrode[12] in an open-tubular LC system for separating ions in a few seconds[13,14].

It is expected that elevated temperature will play an increasingly important role in HPLC. It has been known for years that in packed-column chromatography temperatures above room temperature can improve the performance dramatically, as shown in Fig. 4. From the *H versus u* curve it can be seen that for higher temperatures the minimum shifts to higher flow velocities and also the slope has a much lower value. The loss of efficiency at higher flow-rates is significantly smaller than at room temperature. This is important for the chromatography of large molecules where diffusion can be a limiting factor. As shown by Antia and Horvath[15], elevated temperature also has a beneficial effect on the viscosity and consequently the pressure drop across the column. The elevated temperature is not only beneficial for packed-column chromatography. HPLC in open tubes is feasible at higher temperature even when the inner diameters are 20–100 μm (Fig. 5a). Fig. 5b shows that the strong dependence on k' is much more favourable at higher temperatures. Liquid mobile phases at elevated temperatures have physical properties very similar to those of supercritical fluids and have the same beneficial effects on the kinetics of the separation processes. The question is whether there is any significant difference between high-temperature HPLC and SFC.

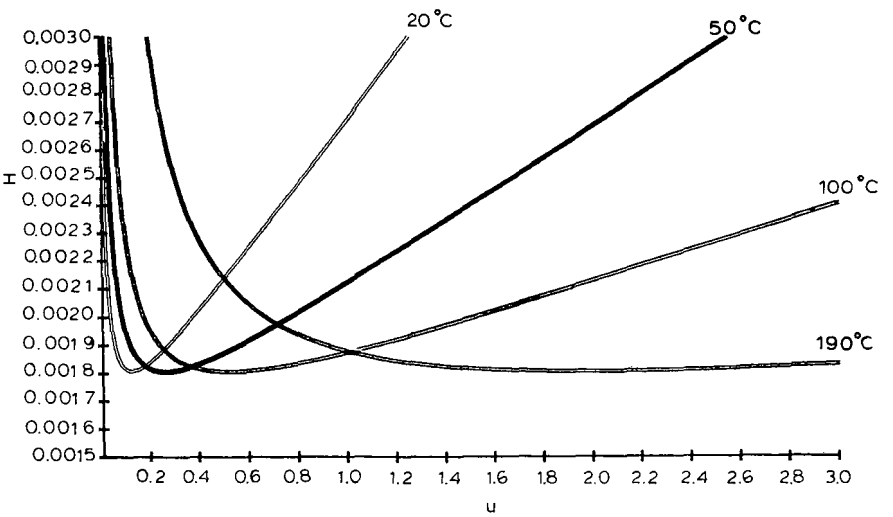

Fig. 4. Simulations of H (cm) *versus* u (cm/s) u curves for packed columns at 20, 50, 100 and 190°C, as indicated. Packed columns. 5 μm.

NEW TECHNIQUES

CZE and SFC are two techniques that have emerged in recent years and will compete with HPLC[16] but are also inspiring new instrumental developments that are important for HPLC techniques. A comparison of SFC, CZE and HPLC techniques in their application to pharmaceutical analysis has been described[16]. In our experi-

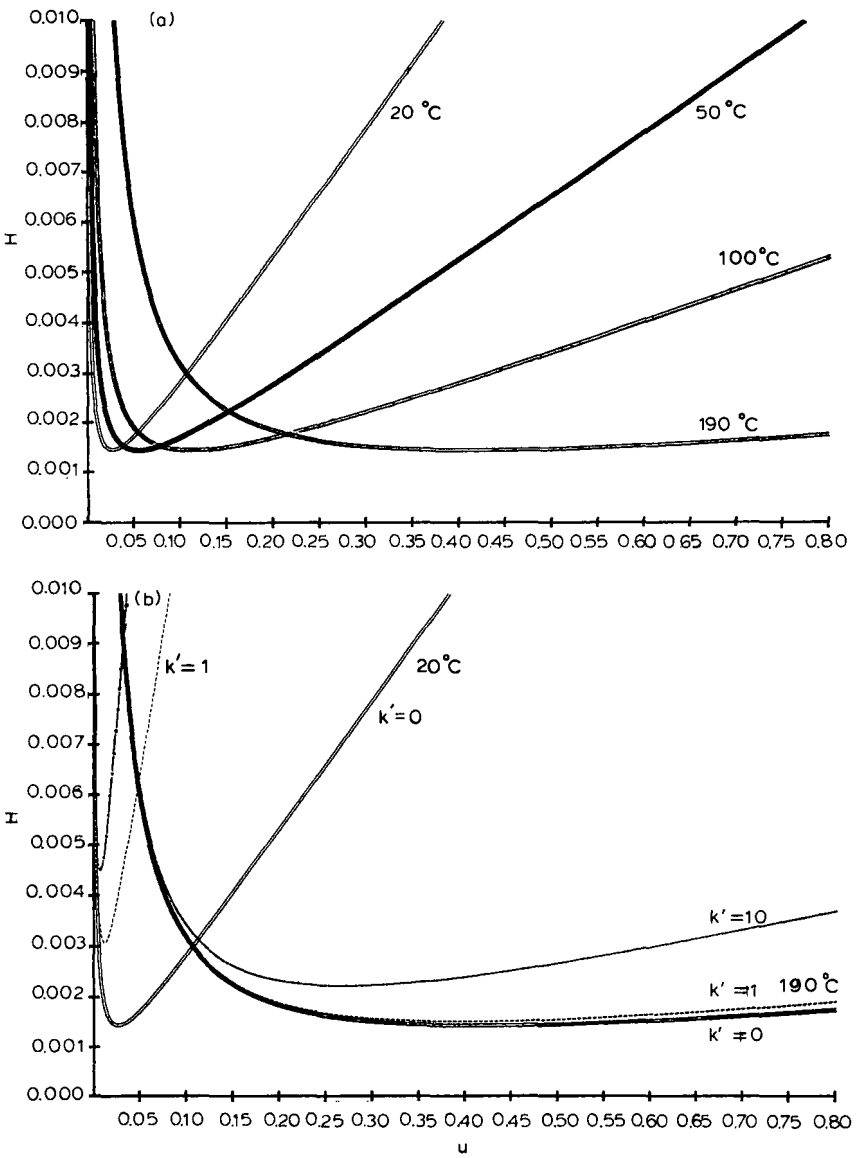

Fig. 5. Simulations of H (cm) *versus* u (cm/s) curves for open-tubular HPLC at 20, 50, 100 and 190°C, as indicated. $k' = 0$. (b) Influence of k' at 20 and 190°C. Capillary, 50 μm I.D.

ence, capillary SFC systems are suitable for the investigation of polymeric excipients for drug delivery systems. These materials, based on natural products, are often complex mixtures that can be analysed of SFC techniques without derivatization or complicated sample preparation.

CZE is a method that has had an important impact not only on the analysis of peptides, proteins and other high-molecular-weight compounds but also on small

molecules[16], as shown in Fig. 6. CZE in open tubes has some limitations, however. The separation of isomeric compounds or, generally, compounds with similar molecular weights and similar structures is often difficult, even with the enormous efficiency of CZE. Secondary interactions, *e.g.*, with gels or micelles, can improve the selectivity of the separations without decreasing the resolution. The development of CZE into electrokinetic chromatographic systems or electroendosmotically driven LC systems (compared with pressure-driven HPLC systems) makes it possible to combine the advantages of HPLC (selectivity) with the advantages of CZE (high efficiency)[8].

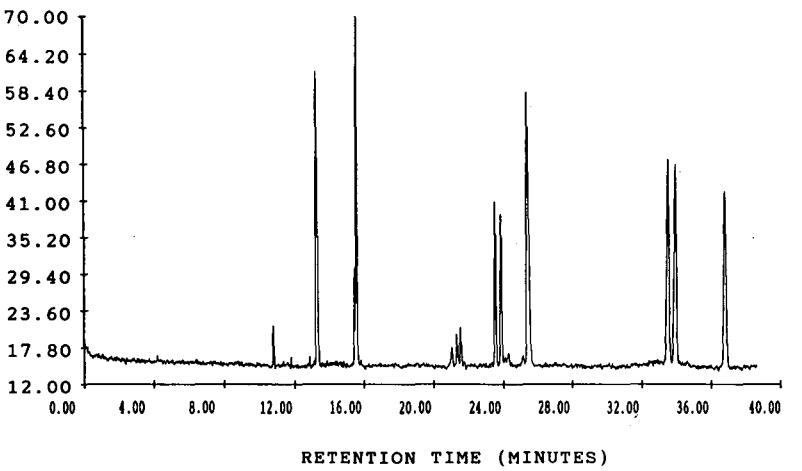

Fig. 6. Separation of terbinafin and its by-products by CZE. Capillary, 87 cm × 50 μm I.D.; buffer, 30 m*M* Na_2HPO_4–40% acetonitrile; voltage, 25 kV; detection, UV on-column (200 nm), 0.006 a.u.f.s.

AUTOMATION

The role of automation in HPLC in saving time, making better use of the instrumentation and obtaining better results has been discussed elsewhere[5]. Automatic sample injectors, intelligent sample processors and the use of robotic systems for sample preparation are part of the mechanization of HPLC systems which dramatically improve the cost efficiency (throughout per instrument) and the quality of the results. Fast LC systems are valuable alternatives to flow-injection analysis (FIA) or continuous flow analysers (CFA) and direct UV determination. The advantage of fast LC systems with very short columns (1–3 cm) compared with FIA, CFA and UV methods is that much less interference and artefacts can be expected and validation of the methods is very simple. More sophisticated HPLC methods for assay and purity determinations can be scaled down to simple and fast HPLC systems by just shortening the columns from 15 cm to 1–3 cm for a high throughput in dissolution-rate testing, content uniformity and process control.

EXPERT SYSTEMS AND METHOD DEVELOPMENT

In addition to automation of sample preparation, sample injection and data evaluation, expert systems are beginning to play a role in HPLC. These expert systems not only help to solve problems efficiently, but are also very useful for training and may become a knowledge base for an organization (knowledge-based expert systems). A few expert systems are already commercially available, *e.g.*, the HPLC Doctor[17] from PiTechnology and DryLab[18] simulation software from LC Resources. The main application of expert systems lies in method development. Many strategies have been discussed in the literature[19]. The most valuable are those which give information about the critical parameters of a separation, also indicating potential problems and the ruggedness of a method[20]. A good documentation of method development also makes method transfer easier from one laboratory to another. Fig. 7 shows an example of DryLab for the optimization of a gradient run with the minimal resolution plot. This and a multi-dimensional presentation of the chromatographic response functions not only give a survey of absolute or local minima but also indicate how sensitive a separation is to variations in separation parameters[5], such as pH, ionic strength or content of organic modifier in reversed-phase systems.

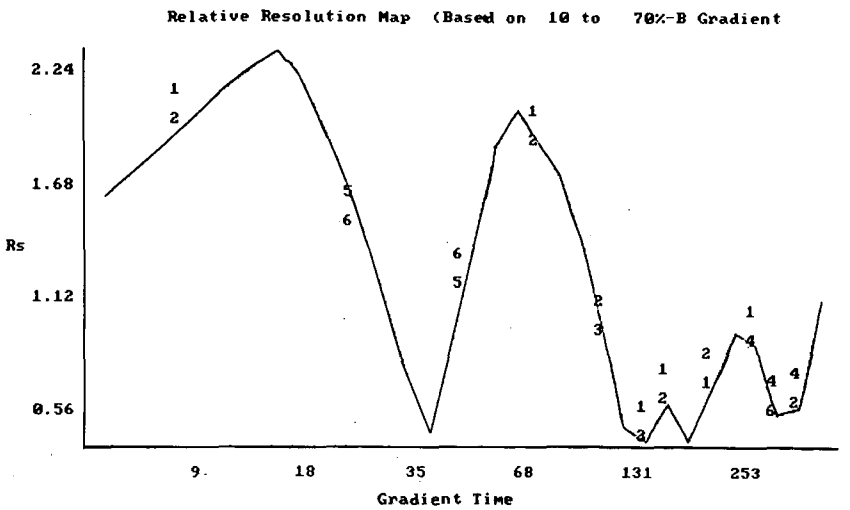

Fig. 7. Simulations of minimal resolution with Drylab.

Electronic data processing (EDP) is playing an increasingly important role in the documentation of HPLC experiments. Laboratory information and managment systems (LIMS) help to organize the work and include office automation systems and scientific spreadsheet programs, such as RS/1[21], statistical evaluation packages, such as SAS[22], and other decision-support software or desk-top publishing tools for making presentations and slides.

CONCLUSIONS

Despite the advent of new techniques, such as SFC and CZE, HPLC is still a growing analytical method in analytical laboratories in the pharmaceutical industry. It can be expected that capillary technology will inspire new developments in HPLC such as smaller, faster and more efficient systems and that future instrument generations will be more reliable and therefore suitable for applications in process control and on-stream analysis. Automation of HPLC systems will continue to make sample preparation easier and method development more efficient. In the future, expert systems will help both in data interpretation and in decision support.

REFERENCES

1 I. F. Lawrence and R. W. Frei, *Chemical Derivatisation in Liquid Chromatography (Journal of Chromatography Library*, Vol. 7), Elsevier, Amsterdam, 1976.
2 F. Erni, H. P. Keller, C. Morin and M. Shmitt, *J. Chromatogr.*, 204 (1981) 65–67.
3 R. Vivilecchia, *LC · GC, Mag. Liq Gas Chromatogr.*, 4 (1986) 94–106.
4 A. Roth, C. Dosenbach and G. Schill, *J. Chromatogr.*, submitted for publication.
5 F. Erni, W. Steuer and H. Bosshardt, *Chromatographia*, 24 (1987) 201–207.
6 W. Lindner, M. Roth, K. Stoschnitzky and H. Semmilrock, *Chirality*, 1 (1989) 10–13.
7 F. Erni, *J. Chromatogr.*, 282 (1983) 371–383.
8 J. H. Knox and I. H. Grant, *Chromatogrpahia*, 24 (1987) 135–143.
9 H. E. Schwartz, P. J. Barthel, S. E. Morning and H. H. Lauer, *LG · GC, Mag. Liq. Gas Chromatogr.*, 5 (1987) 490–497.
10 J. P. Chervet, M. Ursem, J. P. Salzman and R. W. Vannoort, *J. High Resolut. Chromatogr.*, 12 (1989) 278–281.
11 W. Simon and St. Müller, ETH, Zürich, personal communication.
12 A. Manz and W. Simon, *Anal. Chem.*, 59 (1987) 74–79.
13 St. Müller, *Thesis*, ETH, Zürich, (1989) No. 8898.
14 St. Müller, W. Simon, P. Kolla, G. Schomburg, K. Grollimund and H. M. Widmer, *Anal. Chem.*, 61 (1989) 2747–2750.
15 F. D. Antia and Cs. Horváth, *J. Chromatogr.*, 435 (1988) 1–15.
16 W. Steuer, I. Grant and F. Erni, *J. Chromatogr.*, submitted for publication.
17 *The HPLC Doctor*, Pi Technologies, Orinda, CA, 1987.
18 *Drylab Simulation Software*, LC Resources, San Jose, CA, 1987.
19 J. C. Beveridge, *Techniques for the Automated Optimization of HPLC Separations*, Wiley, New York, 1985.
20 E. P. Lankmayr, W. Wegscheider and K. W. Budna, *J. Liq. Chromatogr.*, 12 (1989) 35–58.
21 *RS/1*, BBN Research Systems, Cambridge, MA, 1989.
22 *SAS: Statistical Analysis System*, SAS Institute, Cary, NC, 1987.

Journal of Chromatography, 507 (1990) 151–156
Elsevier Science Publishers B.V., Amsterdam — Printed in The Netherlands

CHROMSYMP. 1705

High-performance liquid chromatographic method for studies on the photodecomposition kinetics of chlorothiazide

VEIKKO ULVI* and SEIJA TAMMILEHTO
Department of Pharmacy, University of Helsinki, Fabianinkatu 35, SF-00170 Helsinki (Finland)

SUMMARY

A simple isocratic high-performance liquid chromatographic method for monitoring the photodecomposition of chlorothiazide in ethanolic solution is described. A 125-mm RP-18 column and an aqueous mobile phase containing 10% methanol and 2% acetic acid were used. The flow-rate was 1.0 ml/min and the UV detector wavelength 265 nm. Samples of 0.2 ml were taken from the reaction vessel and diluted 10-fold. The external standard method was used in the quantitative determinations. The decomposition appeared to proceed according to first-order kinetics. When the solutions were saturated with oxygen, the decomposition was greatly inhibited.

INTRODUCTION

Chlorothiazide (I) was synthesized in 1957 as the first member of the thiazide group[1]. Like the other thiazides, it is used in the treatment of oedema and hypertension[2]. The dose required is larger than that of newer compounds of the group.

The stability of the drug is not a problem in practice, because it is mainly used in tablet form. Hydrolysis of the compound has been studied under various conditions[3–5], but only the structure of the main photolysis product has been elucidated[6]. In ethanolic (ETOH) solution under UV irradiation the free $-SO_2NH_2$ group of the molecule is replaced with a hydrogen atom from the solvent yielding, 6-chloro-2*H*-1,2,4-benzothiadiazine-1,1-dioxide (II).

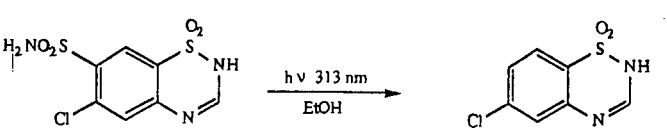

I II

The aim of this study was to develop a suitable high-performance liquid chromatographic (HPLC) method for the quantitative monitoring of II, as the main photolysis product of I. Because of the very low water solubility of the drug, the photolysis reactions were carried out in ethanolic solution.

0021-9673/90/$03.50

EXPERIMENTAL

Materials

Compound I was kindly supplied by Huhtamäki Oy (Turku, Finland). The isolation of the II was described elsewhere[6]. The identity and purity of the compounds were verified by IR, ^{1}H NMR and electron-impact mass spectrometry and by thin-layer chromatography (TLC). TLC examination of II using chloroform–methanol (4:1) as the eluent did not reveal any UV-absorbing impurities. HPLC-grade methanol (Rathburn) and water and Suprapur (Merck) acetic acid were used in the preparation of the mobile phase. All other chemicals were of analytical-reagent grade.

HPLC instrumentation

The HPLC equipment consisted of an LKB 2150 HPLC pump, LKB 2151 variable-wavelength monitor (at 265 nm), Merck-Hitachi D-2000 chromato-integrator and Rheodyne 7125 injector with a 20-μl loop. A 125 mm × 4 mm I.D. Hibar LiChrospher RP-18 column (particle size 5 μm) was used at a flow-rate of 1.0 ml/min. The mobile phase was methanol–water–acetic acid (10:88:2) (pH 2.7).

Irradiation of solutions of I

The four solutions investigated were in the concentration range 0.5–5 m*M*. Three of them were prepared by diluting of the 5 m*M* solution in a 10-ml volumetric flask to yield 0.5, 2.0 and 3.5 m*M* solutions.

The irradiations were carried out using a high-pressure mercury lamp (Original Hanau TQ 150) immersed in a water-bath (MGW LAUDA WB 20, at 25°C). The 313-nm line from the radiation of the lamp was isolated with a chemical filter consisting of potassium chromate and potassium hydrogenphthalate solutions[6]. The filter solutions in two quartz cuvettes (10 mm I.D.) were placed on a stand on the level of the arc of the lamp, aligned between the lamp and a third quartz cuvette (20 mm I.D.) (Fig. 1). The solution to be irradiated (6.5 ml) in the third cuvette was stirred with a small magnetic bar and another larger whirling bar on the side of the reaction vessel. Radiation from the sides was eliminated with small pieces of black plastic that were also used to support the cuvettes with the help of a press. The irradiation period was 30 min, after which the lamp was switched off and a 0.2-ml sample transferred into a 2-ml volumetric flask and diluted to volume. The 0.5 m*M* solution was analysed as such.

As the light stability of the filter solutions proved to be lower than expected, both of them were replaced with fresh solutions after every irradiation period. The lamp was restarted after 15 min.

When the effect of oxygen saturation was investigated, the gas was bubbled through the solution for 60 min before the irradiation and for 10 min after a sample was taken. All the irradiations were carried out twice.

Chromatography

The external standard method was used in the quantitative determinations. Unknown concentrations in the samples were calculated from the peak areas of a standard solution, generally 0.5 m*M* with respect to I and II. At the early stage of the work sulphadiazine was tested as an internal standard, but was found to be unsatis-

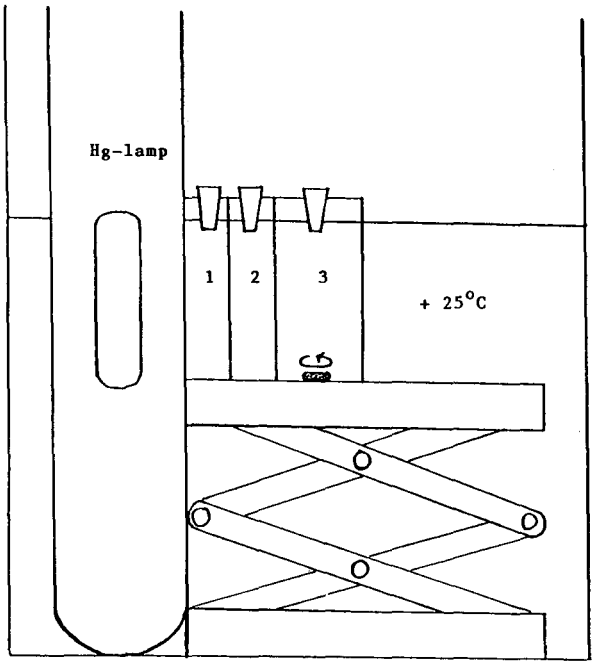

Fig. 1. Schematic representation of the irradiation apparatus used. 1 = Potassium chromate solution; 2 = potassium hydrogenphthalate solution; 3 = reaction vessel.

factory. No other compounds were investigated, as the precision of the peak areas of I and II was good. The injection volume used throughout the study was 3 μl. Before the analysis was started a solution of I was repeatedly injected into the column until the peak area became constant.

The calibration graphs were made with dilutions from 5 mM solutions of I and II over the concentration range 0.1–0.5 mM. The precision of the method was studied by analysing standard solutions of I and II at levels of 0.1 and 0.5 mM six times. In general triplicate injections were made of each sample from the irradiated solutions and an external standard was analysed after every fifth sample.

RESULTS AND DISCUSSION

A typical chromatogram from the irradiated solution is shown in Fig. 2. The retention times for I and II are 3.3 and 21.7 min respectively. The parent compound is well separated from the solvent peaks and from the product. When the flow-rate is 1.0 ml/min, the retention time of the product is relatively long, but it could be shortened by using a higher flow-rate or gradient elution. The calibration graphs were linear over the concentration range studied with correlation coefficients of 0.9995 for I ($n = 21$) and 0.9997 for II ($n = 21$). The equation corresponding to a typical calibration graph for I is expressed as $y = 1.27 \cdot 10^6 x - (5.3 \cdot 10^3)$ and that for II is $y = 1.43 \cdot 10^6 x - (1.78 \cdot 10^4)$, where x is the concentration of the compound injected (mM) and y is the corresponding peak area (integrator units).

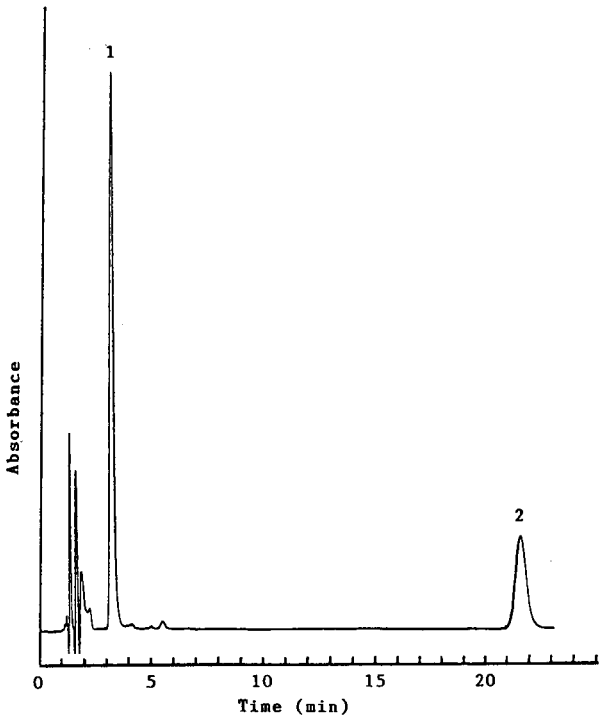

Fig. 2. Typical chromatogram of the irradiated solution. Peak 2 corresponds to II derived from 0.5 m*M* of I (peak 1) after 2 h irradiation exposure.

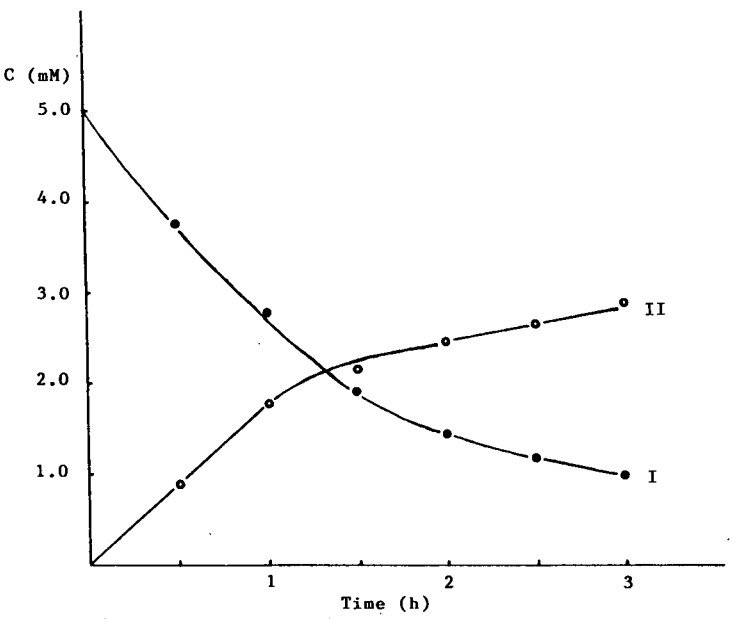

Fig. 3. Time courses for I and II in the photodegradation of a 5 m*M* solution of I.

TABLE I

FIRST-ORDER RATE CONSTANTS FOR THE PHOTODECOMPOSITION OF VARIOUS CONCENTRATIONS OF I IN ETHANOLIC SOLUTION

Concentration (m*M*)	0.5	2.0	3.5	5.0
k_{obs} (min^{-1})	$1.4 \cdot 10^{-2}$	$1.2 \cdot 10^{-2}$	$1.1 \cdot 10^{-2}$	$9.8 \cdot 10^{-3}$

The precision of the peak area expressed as the relative standard deviation was 0.5% ($n=6$) for I and 1.0% ($n=6$) for II at 5 m*M* and 2.1% ($n=6$) for I and 2.4% ($n=6$) for II at 0.1 m*M*. An example of product analysis is shown in Fig. 3. The disappearance of I followed first-order kinetics over the concentration range studied, which is normally the case in photochemical decomposition reactions[7]. The rate constants for the degradation were determined from the slopes of linear plots of the logarithm of residual I against time and are presented in Table I. The decomposition rate was found to be inversely proportional to the initial concentration of the parent compound with a correlation coefficient of -0.998. This can be explained by a greater inner filter effect in concentrated solutions.

The oxygen saturation of the solutions had a similar inhibiting effect on the decomposition of I as for hydrochlorothiazide[8] because of the ability of oxygen gas to quench excited states (Fig. 4).

By using the irradiation method presented it is possible to carry out photolysis reactions under exact and almost monochromatic conditions. As only one solution is

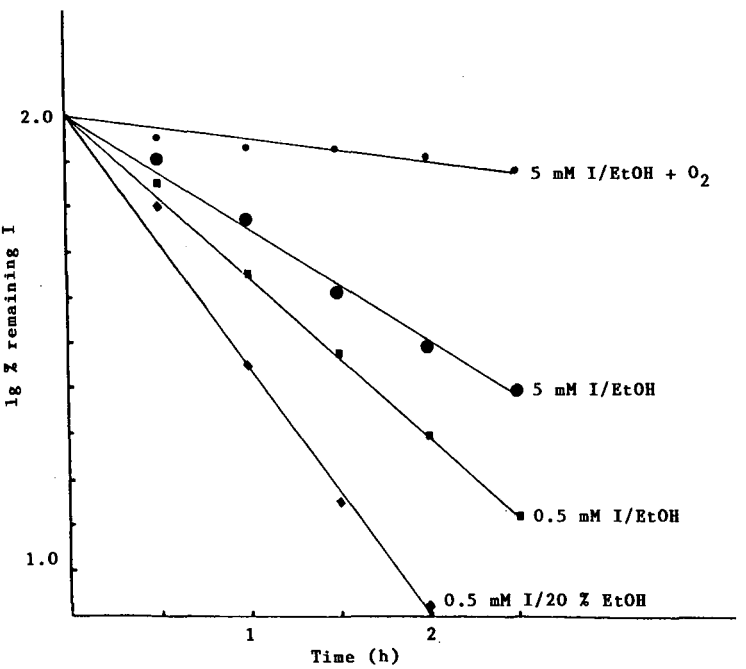

Fig. 4. Effect of concentration, oxygen saturation and solvent composition of the decomposition rate. EtOH = Ethanol.

irradiated at a time, the lamp used should have a relatively constant intensity. The HPLC procedure described is simple and precise and can be modified and used in similar investigations of the photochemical reactions of the thiazides.

REFERENCES

1 F. C. Novello and J. M. Sprague, *J. Am. Chem. Soc.*, 79 (1957) 2028.
2 J. E. F. Reynolds (Editor), *Martindale, The Extra Pharmacopoeia,* Pharmaceutical Press, London, 28th ed., 1982, p. 589.
3 F. C. Novello, S. C. Bell, E. L. A. Abrams, C. Ziegler and J. M. Sprague, *J. Org. Chem.*, 25 (1960) 970.
4 T. Yamana, Y. Mizukami and A. Tsuji, *Chem. Pharm. Bull.*, 16 (1968) 396.
5 T. Yamana, Y. Mizukami and A. Tsuji, *J. Pharm. Soc. Jpn.*, 89 (1969) 422.
6 V. Ulvi and S. Tammilehto, *Acta Pharm. Nord.*, 1 (1989) 195.
7 K. A. Connors, G. L. Amidon and V. J. Stella (Editors), *Chemical stability of Pharmaceuticals, A Handbook for Pharmacists,* Wiley, New York, 2nd ed., 1986, p. 107.
8 S. R. Tamat and D. E. Moore, *J. Pharm. Sci.*, 72 (1983) 180.

Journal of Chromatography, 507 (1990) 157–163
Elsevier Science Publishers B.V., Amsterdam — Printed in The Netherlands

CHROMSYMP. 1744

Quantitative determination of cholesterol in liposome drug products and raw materials by high-performance liquid chromatography

JOHANNA K. LANG
Liposome Technology Inc., 1050 Hamilton Court, Menlo Park, CA 94025 (U.S.A.)

SUMMARY

Most liposomes used as drug delivery systems contain cholesterol as a major structural component. Cholesterol has profound effects on the chemical, physical and metabolic stability of liposomes and lipsome drug products and must be accurately monitored during formulation and processing development, stability testing and manufacturing. Before analyzing their components, the liposomes must be disintegrated and solubilized by dilution with methanol or 2-propanol. This high-performance liquid chromatographic assay is applicable to the resulting lipid-rich matrices and allows a direct quantitative analysis of cholesterol.

Cholesterol separates well from common ingredients of liposome-based drug products and cholesterol oxidation products. Calibration curves are linear over two orders of magnitude and the cholesterol detection limit is 1.5 μl/ml. Method precision for an anticancer liposome drug formulation was 0.9% relative standard deviation. The assay is also useful for measuring cholesterol in phospholipid and cholesterol raw materials.

INTRODUCTION

Liposomes are vesicles composed of single or multiple phospholipid bilayers that form spontaneously when these lipids are exposed to an aqueous environment[1]. They have shown great promise as biocompatible pharmaceutical drug carriers[2]. Liposomes can carry drugs of various compositions. Water-soluble drugs can be carried in the enclosed aqueous space and hydrophobic molecules can be incorporated in the lipid bilayer. The bilayer-forming phospholipids are commonly composed of phosphatidylcholine (PC) and phosphatidylglycerol (PG); cholesterol is also frequently a component in the bilayer structure. Although cholesterol is not essential for the formation and stability of liposomes, it has several beneficial effects, such as increased retention of water-soluble drugs[3,4], prevention of lipid phase transitions[5] and increased resistance to *in vivo* liposome degradation[4]. The phospholipid bilayer can accommodate up to 50 mol% of cholesterol.

0021-9673/90/$03.50

The development of pharmaceutical liposome formulations requires careful monitoring of the key liposomal ingredients during process development and stability testing. Among the various techniques described for the quantitative determination of cholesterol, only chromatographic assays offer the selectivity required for the complex matrices of liposome formulations. Thin-layer chromatography (TLC)[6–8] is labor intensive and of limited reproducibility. Gas chromatography[9,10] generally requires prior derivatization to more volatile compounds. For determining the cholesterol content in liposome formulations, high-performance liquid chromatography (HPLC) is the assay technique of choice, as it is compatible with liquid matrices, requires no derivatization and can be easily automated. While several HPLC methods for the quantitative analysis of cholesterol have been described[11–13], they cannot tolerate the high levels of lipids typically present in liposome drug formulations.

This assay system was developed for the precise quantitative determination of cholesterol in lipid-rich matrices, such as liposome formulations, cholesterol and phospholipid raw materials.

EXPERIMENTAL

Reagents

All solvents were of HPLC grade. Cholesterol external standard was from the National Bureau of Standards (NBS, Gaithersburg, MD, U.S.A.); 7-ketocholesterol, 25-hydroxycholesterol, 7-α-hydroxycholesterol, 7-β-hydroxycholesterol, 3,5-cholestadien-7-one, desmosterol and lanosterol were from Steraloids (Wilton, NH, U.S.A.), 4-cholesten-3-one was from Fluka (Buchs, Switzerland), 5-cholesten-3-one from Sigma (St. Louis, MO, U.S.A.), bulk cholesterol [United States Pharmacopeia (U.S.P.) grade] from Croda (Edison, NJ, U.S.A.), partially hydrogenated egg phospholipids were from Asahi Chemical (Ibarakiken, Japan) obtained through Austin Chemical (Rosemont, IL, U.S.A.).

Chromatography system

The HPLC apparatus was a Hewlett-packard 1090 with a diode-array detector and column heater. A non-endcapped 25 × 0.46 cm I.D. Spherisorb S-5 ODS-1 column was operated at 40°C with 100% HPLC-grade methanol at a flow-rate of 1.0 ml/min. In some instances an Alltech (Deerfield, IL, U.S.A.) ODS guard column was mounted between the injector and the analytical column. Cholesterol was detected with maximum sensitivity at 207 nm. The injection volume was 20 μl.

RESULTS

Sample preparation and the "disintegration-by-dilution" concept

In general, liposome drug formulations are composed of zwitterionic PC and anionic PG, with varying amounts of cholesterol (5–50%) in an aqueous buffer solution. In addition, they may contain antioxidants, such as α-tocopherol, salts, sugars and other excipients. Encapsulated drugs cover a wide spectrum in size and polarity, from small organic molecules to polypeptides and proteins. Liposomes may be viewed as a two-phase system, consisting of the hydrophobic bilayer and the aqueous medium, in which lipids, drugs, and excipients exist in a dynamic equilibrium. Unlike

monomolecular solutions of drugs, the liposome drug formulations require distintegration of the liposomes to form a solution before individual components can be analyzed by HPLC. Frequently, the liposomes are "dissolved" by extracting the liposomal lipids from the aqueous liposome suspension with an organic solvent, *e.g.*, chloroform–methanol mixtures. Usually, multiple extractions are necessary to recover the hydrophilic and/or lipophilic components completely. Extraction procedures are time consuming, error prone, difficult to automate and often produce solvent mixtures that are incompatible with subsequent HPLC analysis. For these reasons, sample preparation procedures which result in a single phase are preferable. Many liposome drug formulations can be "dissolved" to form a single phase by dilution with short-chain alcohols like methanol or 2-propanol. The resulting solvent mixtures (methanol, 2-propanol–water) constitute good solvents for phospholipids, cholesterol and lipid excipients and are sufficiently polar to keep moderate amounts of buffer salts and hydrophilic excipients in solution. By judicious choice of solvents and dilution volumes, the heterogeneous liposome suspension can be diluted with methanol and/or 2-propanol to form a homogeneous solution that can be readily injected into the HPLC system. However, the success of this fast and simple approach requires HPLC conditions in which all sample components are soluble in the mobile phase and do not interfere with the detection of the compound of interest.

Cholesterol in liposome drug formulations

The "disintegration-by-dilution" concept has been successfully applied to the determination of cholesterol in various liposome drug formulations. Fig. 1 shows chromatograms of liposome drug formulations of an anticancer drug (doxorubicin,

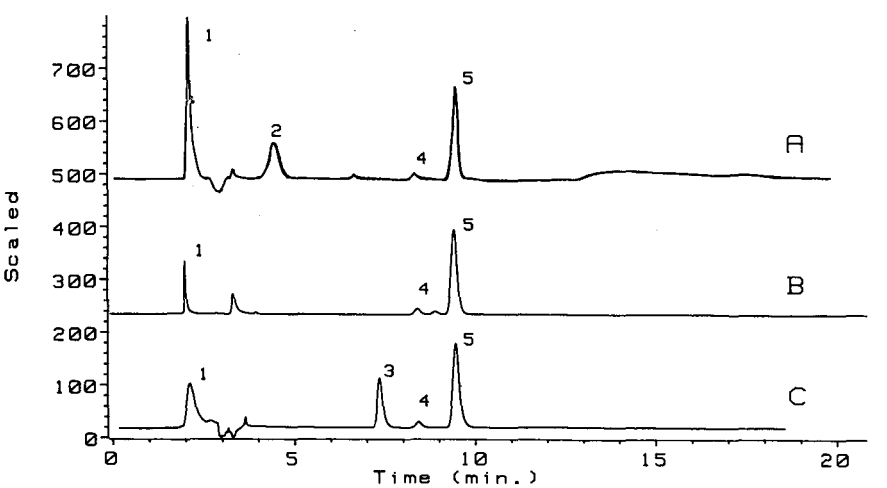

Fig. 1. Chromatograms of liposome drug formulations of doxorubicin, albuterol and an oligopeptide. (A) Doxorubicin liposome formulation was diluted with four volumes of distilled water and solubilized by adding five volumes of 2-propanol; 20 μl of the solution, equivalent to 2 μl of liposome formulation, were injected. (B) Albuterol liposome formulation: 60 mg was dissolved in 10 ml methanol; 20 μl, equivalent to 0.12 mg of liposome formulation, were injected. (C) Liposome formulation of an oligopeptide diluted with an equal volume of 2-propanol; 20 μl, equivalent to 10 μl of liposome formulation, were injected. Peaks: 1 = solvent front and PG; 2 = unidentified; 3 = α-tocopherol; 4 = bulk cholesterol contaminant; 5 = cholesterol.

A), a bronchodilator (albuterol, B) and an oligopeptide (C). The liposome formulations were prepared for cholesterol HPLC analysis by dilution with methanol and/or 2-propanol and were injected into the HPLC system without further treatment. All formulations were composed of PC, PG and cholesterol as major lipophilic liposome-forming components. The polypeptide formulation also contained α-tocopherol, detectable in the cholesterol assay system as a distinct peak between 7 and 8 min. In every case, the cholesterol peak is narrow, symmetrical, and baseline separated. Comparison of diode-array spectra which had been obtained at the leading edge, apex and trailing edge of the cholesterol peak were identical. This peak purity check, made possible by diode-array technology, is a good indication for the absence of interfering peaks. Under the conditions of the cholesterol assay, PG is eluted with or close to the solvent front. PC is eluted with longer retention times, well separated from cholesterol. Depending on its origin, PC may be eluted as a broad, ill-defined peak, (Fig. 1A) as its molecular species are partially separated by chain length and unsaturation. Hydrogenated or saturated synthetic PC may not be visible due to its lower UV absorptivity (Fig. 1B,C). A small peak preceding the cholesterol originates most likely from the cholesterol raw material (Fig. 4).

A partial validation of the cholesterol determination in a doxorubicin liposome formulation showed excellent linearity of the cholesterol response. Calibration curves were established with dilutions of NBS cholesterol from 0.01 to 3.0 mM and based on peak areas. Slope and y-intercept [± standard error (S.E.)] and R^2 were calculated by unweighted linear regression analysis as 2144 ± 38, 16.7 ± 49.7 and 0.9998, respectively. Method precision for a typical doxorubicin liposome sample was 0.9% relative standard deviation (n = 6); the detection limit (defined as signal-to-noise ratio 2) was 1.5 μg cholesterol/ml. There was no measurable interference of the sample matrix with the cholesterol response, as determined by adding a known amount of cholesterol standard to a doxorubicin liposome sample.

Cholesterol oxidation in liposomes

The assay has also proven useful for the analysis of cholesterol and its major oxidation products in experimental liposome formulations, incubated at elevated temperature (50°C) in the absence of antioxidants (Fig. 2). All oxidation products are well separated from the main cholesterol peak (Table I, Fig. 2). Major oxidation products, such as isomeric 7-hydroxycholesterols, 7-ketocholesterol and 3,5-cholestadien-7-one, are well resolved and can be quantitated by external standards, with sensitivities around 1 μg/ml. 3,5-Cholestadien-7-one, 4-cholesten-3-one and 5-cholesten-3-one are eluted with very similar retention times but can be distinguished by their UV spectra. Some oxidation products, like 7-ketocholesterol and 3,5-cholestadien-7-one, can be determined with higher sensitivities by additional monitoring at 240 nm (Fig. 2).

Cholesterol in phospholipid raw materials

Most bulk phospholipids used in the manufacture of liposome drug products are isolated from egg yolk and are contaminated by varying amounts of cholesterol. The sensitivity of the cholesterol determination in phospholipid raw materials is determined by the solubility of the phospholipid in methanol, which, in turn depends on the phospholipid type (PC, PG) as well as the chain length and unsaturation of its

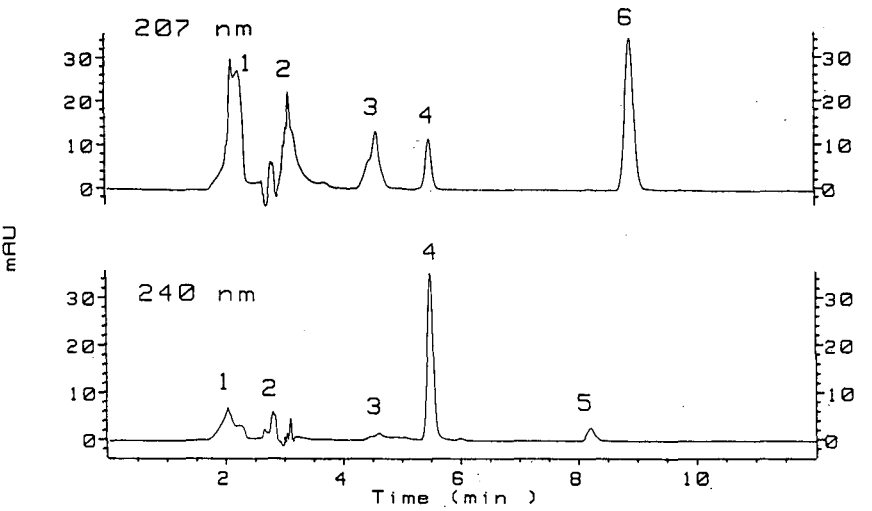

Fig. 2. Chromatogram of a thermally stressed experimental liposome formulation, recorded at 207 and 240 nm. A PC–PG–cholesterol formulation after 2 months incubation at 50°C. Liposomes were dissolved by adding nine volumes of 2-propanol; 20 μl, equivalent to 2 μl of formulation, were injected. Peaks: 1 = solvent front; 2 = unidentified; 3 = 7-α- and 7-β-hydroxycholesterol; 4 = 7-ketocholesterol; 5 = 3,5-cholestadiene-7-one; 6 = cholesterol.

fatty acids. Detection limits for cholesterol are in the best case (native egg PC) 0.1 mg/g, in the worst case (fully hydrogenated PG) *ca.* 2 mg/g. PG and PC are well separated from the cholesterol peak, PG is eluted with or close to the void peak, PC is eluted with longer retention times as a large cluster of convoluted peaks, due to the partial separation of the molecular species varying in chain length and unsaturation of the fatty acids. The phospholipid peak response increases with unsaturation of the phospholipid, because the double bonds of unsaturated fatty acids contribute to the UV absorbance. Fig. 3 shows a typical chromatogram of egg-derived PC raw material.

TABLE I

RETENTION TIMES OF CHOLESTEROL AND CHOLESTEROL AUTOXIDATION PRODUCTS

Compound	*Retention time (min)*
7-α-Hydroxycholesterol	4.55
7-β-Hydroxycholesterol	4.69
25-Hydroxycholesterol	4.76
7-Ketocholesterol	5.45
5-Cholesten-3-one	7.95
3,5-Cholestadien-7-one	8.12
4-Cholesten-3-one	8.16
Cholesterol	8.80

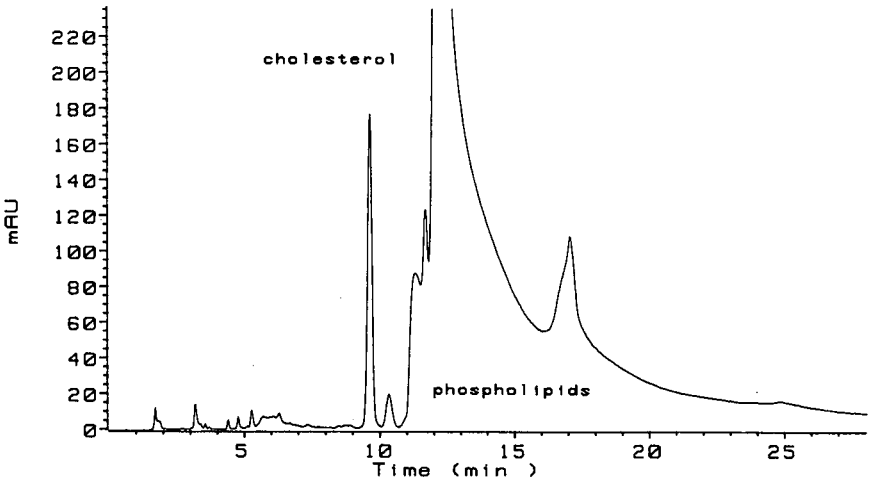

Fig. 3. Chromatogram of an egg-derived PC raw material. A 560-mg amount of egg-derived, partially hydrogenated PC raw material was dissolved in 10 ml of methanol and 20 μl, equivalent to 1.12 mg PC, were injected.

Bulk cholesterol raw material

Bulk cholesterol is frequently contaminated with precursors of its biosynthesis, such as desmosterol or lanosterol[14] and may also contain cholesterol autoxidation products[15]. Cholesterol, desmosterol, lanosterol and cholesterol autoxidation products are well separated from the cholesterol peak (Table I, Fig. 4). The cholesterol content (purity) of the raw material can be determined by external standardization with NBS cholesterol. As cholesterol is quite soluble in methanol, large quantities of

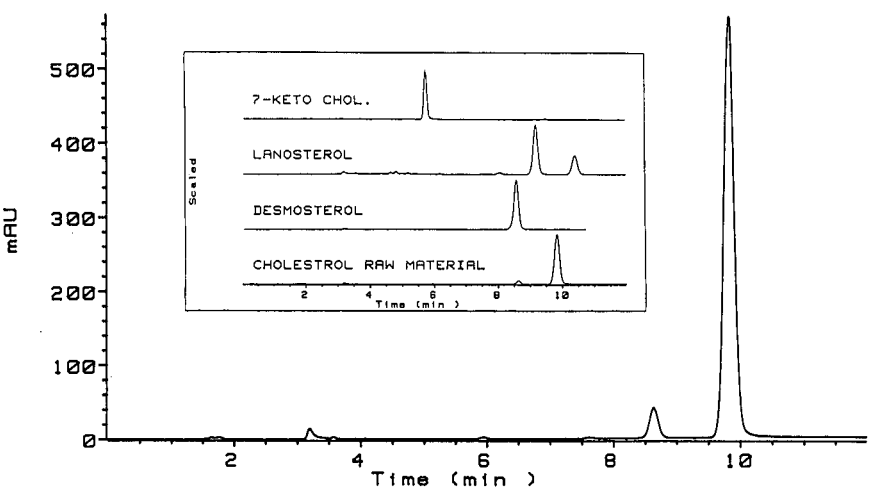

Fig. 4. Chromatogram of a cholesterol raw material. A 116-mg amount of U.S.P.-grade cholesterol raw material was dissolved in 100 ml methanol; 20 μl of the solution, equivalent to 0.023 mg cholesterol, were injected.

the bulk material can be injected to achieve excellent sensitivities for the contaminating compounds.

CONCLUSIONS

The major advantages of this assay system are its versatility, ruggedness, good linearity over a wide concentration range and its tolerance of lipid-rich matrices, common in liposome formulations. Retention time shifts, as often seen with assays operating at ambient temperature, are avoided by controlling the column temperature. The assay does not require mobile phase preparation. The 'disintegration-by-dilution' approach to sample preparation is faster and more reproducible than conventional lipid extraction procedures. This is reflected by the precision of the cholesterol determination in doxorubicin liposomes. The system efficiently separates cholesterol from phospholipids, common liposome ingredients (*e.g.*, α-tocopherol), raw material contaminants, and oxidation products of cholesterol. This allows an accurate quantitative measurement of cholesterol in a wide variety of liposome drug products and raw materials.

REFERENCES

1 A. D. Bangham, M. M. Standish and J. C. Watkins, *J. Mol. Biol.*, 13 (1965) 238.
2 P. Cullis, M. J. Hope, M. Bally, T. Madden, L. Mayer and J. Janoff, in M. J. Ostro (Editor), *From Biophysics to Therapeutics*, Vol. I, Marcel Dekker, New York, Basel, 1987, p. 39.
3 C. Kirby, J. Clarke and G. Gregoriadis, *Biochem. J.*, 186 (1980) 591.
4 J. Senior and G. Gregoriadis, *Life Sci.*, 30 (1982) 2123.
5 D. Papahadjopoulos, K. Jacobson, S. Nir and T. Isac, *Biochim. Biophys. Acta*, 311 (1973) 330.
6 L. L. Smith, W. S. Matthews, J. C. Price, R. C. Bachmann and B. Reynolds, *J. Chromatogr.*, 27 (1967) 187.
7 K. Morris, J. Sherma and B. Fried, *J. Liq. Chromatogr.*, 10 (1987) 1277.
8 V. Damman, G. Donnevert and W. Funk, *J. Planar Chromatogr. — Mod. TLC*, 1 (1988) 78.
9 U. J. Krull, M. Thompson and A. Arya, *Talanta*, 31 (1984) 489.
10 J. R. van Delden, J. L. Cozijnsen and P. Folstar, *Food Sci.*, 7 (1981) 117.
11 G. A. S. Ansari and L. L. Smith, *J. Chromatogr.*, 175 (1979) 307.
12 H. S. Kim, C. K. Choi and Y. H. Park, *J. Chromatogr.*, 398 (1987) 372.
13 W. J. Hurst, M. D. Aleo and R. A. Martin, Jr., *J. Assoc. Off. Anal. Chem.*, 67 (1984) 698.
14 J. W. Apsimon, H. Beierbeck and J. K. Saunders, *Can. J. Chem.*, 51 (1973) 3974.
15 L. L. Smith, *Cholesterol Autoxidation*, Plenum Press, New York, London, 1981, p. 190.

Journal of Chromatography, 507 (1990) 165–170
Elsevier Science Publishers B.V., Amsterdam — Printed in The Netherlands

CHROMSYMP. 1770

High-performance liquid chromatography of the drug fosinopril

JOEL KIRSCHBAUM*, JOYCE NOROSKI*, ANNETRIC COSEY, DON MAYO and JOHN ADAMOVICS[a]

Squibb Institute for Medical Research, One Squibb Drive, P.O. Box 191, New Brunswick, NJ 08903-0191 (U.S.A.)

SUMMARY

High-performance liquid chromatography was used to determine the purity and impurities of fosinopril, an angiotensin-converting enzyme inhibitor used to treat hypertension. Purity values are determined using a silica column and usually are above 99%. All known possible impurities, including stereoisomeric impurities, can be resolved and quantified by injecting solutions of fosinopril onto three separate columns; silica, strong anion exchange and phenyl. Typical impurity contents total 0.5%. Validation data and a study of properties of fosinopril in solution is included.

INTRODUCTION

High-performance liquid chromatography (HPLC) methods were developed for the separation of the angiotensin-converting enzyme inhibitor[1] fosinopril, (compound I, Fig. 1), from its precursors and hypothetical impurities. Fosinopril[2] is a prodrug. The active agent is compound II[3], which is formed *in vivo*. HPLC was chosen because of its prior, successful application to the selective assays of this new class of antihypertensive agents[4,5]. Although most of the possible impurities were separated from the analyte on a silica column, a second separation on a strong anion-exchange (SAX) column was necessary to resolve two possible, stereoisomeric impurities; the *R,R,S,S* and *S,R,S,R* enantiomers. A third system was needed to both resolve a phenyl impurity (IV) and to achieve a low limit of detection of compound V (Fig. 1), another possible impurity.

In this paper, the details of the separations are described.

EXPERIMENTAL

Materials

Fosinopril sodium and related compounds were synthesized at the Squibb In-

[a] Present address: Cytogen, Princeton, NJ 08540, U.S.A.

0021-9673/90/$03.50

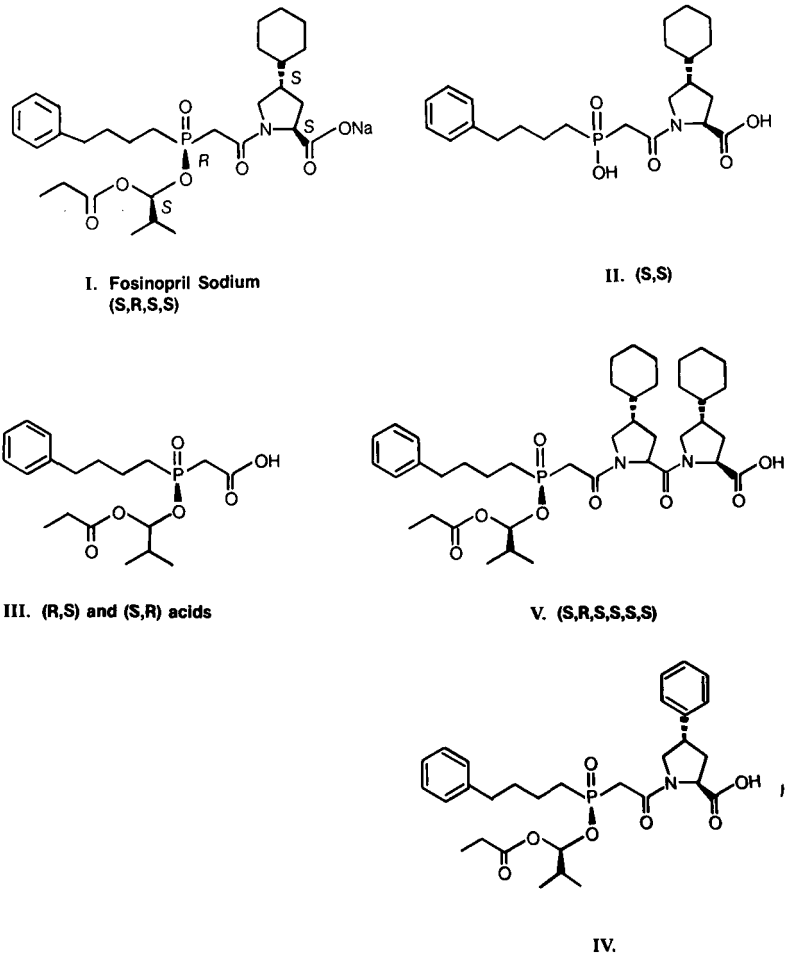

Fig. 1. Structures of fosinopril and its possible, related impurities.

stitute for Medical Research. All solvents were of HPLC grade (American Scientific Products, Edison, NJ, U.S.A.).

The modular HPLC apparatus consisted of a Perkin-Elmer Model 420B, LC-600 or ISS-100 autoinjector (Perkin-Elmer, Norwalk, CT, U.S.A.), a Beckman Model 110B pump (Beckman Instruments, Fullerton, CA, U.S.A.), a SYS-TEC column temperature control system (SYS-TEC, Minneapolis, MN, U.S.A.) and a Kratos-A.B.I. variable-wavelength detector Model 783 (Applied Biosystems, Ramsey Analytical Division, Ramsey, NJ, U.S.A.). Signals were processed with the aid of a Hewlett-Packard laboratory computer, Model 3357 (Hewlett-Packard, Palo Alto, CA, U.S.A.) and monitored using a Kipp & Zonen two-pen recorder, Model BD-41 (Rainen Instrument, Woburn, MA, U.S.A.).

Methods

The silica column separation utilized a Water RESOLVE column, (15 cm × 3.9 mm I.D., 5 μm, Waters, Milford, MA, U.S.A.) thermostated at 32°C, a mobile phase of acetonitrile–water–ortho-phosphoric acid (4000:15:2) with a flow-rate of 1 ml/min and detection at 205 nm. Prior to use, the column was conditioned with about 100 ml of methanol. The SAX separation utilized a Whatman PartiSphere packing (5 μm) in a 25 cm × 4.6 mm I.D. column (Whatman, Clifton, NJ, U.S.A.) thermostated at 40°C, and the same mobile phase (flow-rate, 0.8–1.0 ml/min) and wavelength as the silica assay. The third separation system consisted of an alkyl phenyl column, 5 μm (ES Industries, Marlton, NJ, U.S.A.), a mobile phase of acetonitrile–0.2% aqueous phosphoric acid (80:20) with a flow-rate of 0.5 ml/min and a detector set to 205 nm. The column temperature was 45°C. All three columns were protected by saturator columns packed with 37-μm silica located between the pump and the autoinjector. All injection volumes were 20 μl (nominal). Best separations were found using the given column temperatures.

RESULTS AND DISCUSSION

Fig. 2 is a chromatogram, obtained using a silica column, of fosinopril (0.1 mg/ml mobile phase) and added potential impurities. Because of the lack of separation between fosinopril and the possible *R,R,S,S* impurity, a second, SAX system was used to resolve these compounds, as shown in Fig. 3. (Structures of compounds III, IV and V, are depicted in Fig. 1.) Fig. 3 shows resolution of the fosinopril (0.1 mg/ml mobile phase) from added *R,R,S,S* and *S,R,S,R* possible stereoisomeric impurities using the strong anion-exchange column. The phenyl column separation of fosinopril sodium (0.1 mg/ml mobile phase) from the possible phenyl (IV) and double-proline (V) impurities is depicted in Fig. 4.

Assay validation involved repetitive injections of solutions of 0.1 mg/ml fosinopril in mobile phase. The relative standard deviations of six sets of injections, on two days using two chromatographic systems, were 0.8% and 0.5% using peak areas.

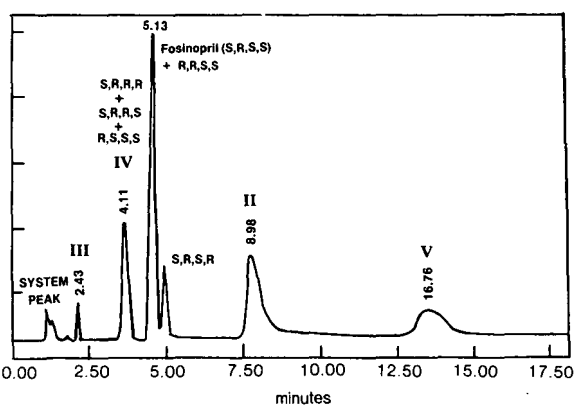

Fig. 2. Silica column chromatogram of fosinopril and added possible impurities. The mobile phase consists of acetonitrile–water–ortho-phosphoric acid (4000:15:2) with a flow-rate of 1 ml/min and detection at 205 nm. The column temperature is 32°C.

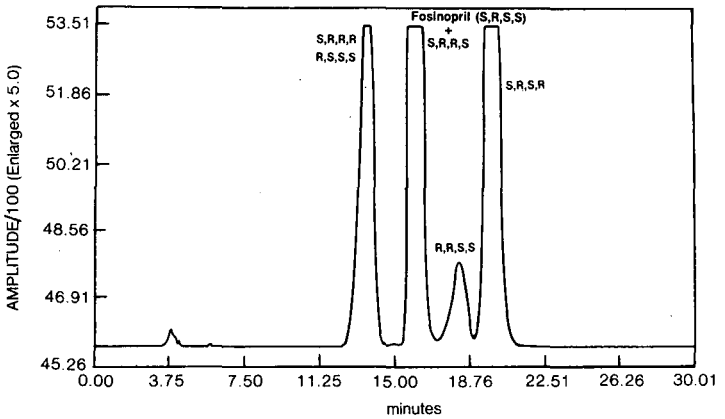

Fig. 3. Strong anion-exchange (SAX) HPLC for the separation of fosinopril from two possible stereoisomers added to the analyte. The SAX used the same mobile phase and flow-rate as the silica column. The column temperature is 40°C.

Chromatography, on different days, of three sets of solutions of fosinopril from 0.02 to 0.2 mg/ml gave linear responses (all correlation coefficients >0.9999), that, when plotted and extrapolated, showed that the lines passed through the origin.

A typical batch of the prodrug contains about 0.1% of impurity III, 0.2–0.3% of the stereoisomer triplet consisting of *S,R,R,R*, *R,S,S,S* and *S,R,R,S*, and about 0.1% of the *S,R,S,R* stereoisomer. None or trace quantities of the other possible impurities, including the active drug and the hydrolysis product (compound II), were seen. The HPLC systems have limits of detection of about 0.02 to 0.04% (three times the signal-to-noise ratio) and minimum quantifiable concentrations of about 0.1% (relative to the concentration of fosinopril) under the conditions described in the experimental section. Accuracy of the silica method was verified by chromatograph-

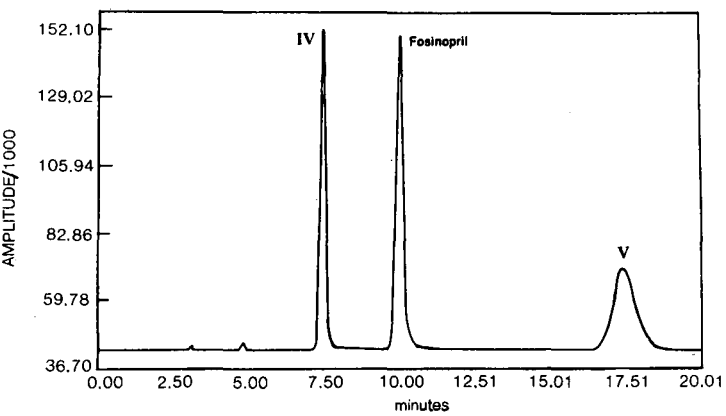

Fig. 4. Phenyl column chromatogram showing the resolution of fosinopril from added quantities of the possible phenyl (IV) and double-proline (V) impurities. The mobile phase consists of acetonitrile–0.2% aqueous phosphoric acid (80:20) with a flow-rate of 0.5 ml/min. Detection was at 205 nm and the column temperature was 45°C.

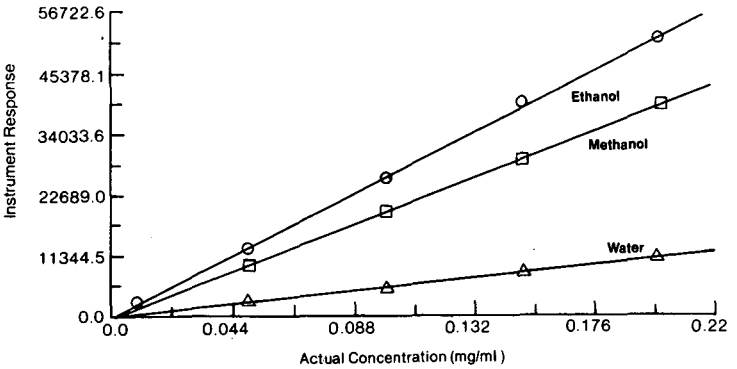

Fig. 5. Dependence of instrument response (peak area) on injection solvent. Linearity plots of various concentrations of fosinopril dissolved in either methanol, ethanol or water and injected into an identical HPLC system using the silica column. All injection volumes were 20 μl (nominal) and the chromatographic conditions were identical to those described in the text and for Fig. 2. The only variation was the solvent used to dissolve the fosinopril.

ing a solution of 0.00500 mg/ml of compound II and 0.09500 mg/ml fosinopril. After assay, 0.00503 mg/ml of compound II was found (n = 7, relative standard deviation = 2.7%) and 0.09504 mg/ml of fosinopril (n = 7, relative standard deviation = 0.4%). This also indicates no hydrolysis product to be present.

The same weight of fosinopril sodium dissolved in various quantities of either water, methanol or ethanol, and injected into an identical LC system with respect to autoinjector, pump, mobile phase, flow-rate, detector, wavelength and data reduction system, gave different peak responses using the silica column. Fig. 5 shows linearity plots for fosinopril in water, methanol and ethanol of concentration *vs.* instrument response (peak area). The correlation coefficients were all <0.9999. The hydrolysis product, compound II, also exhibited this property of peak area being dependent on injection solvent. Void volume effects were not responsible since the retention time of fosinopril was 5 min and that of its hydrolysis product was about 9 min. Injection of the solvents gave a straight baseline, with no negative or positive peaks visible. This phenomenon of the peak response being dependent on the injection solvent has been discussed previously for captopril[6,7] vancomycin[8], vinblastine[8], aztreonam[7] and several other drugs[7]. Since the solvents and fosinopril are over 99.5% pure, the dependence of peak area on injection solvent used to dissolve the fosinopril appears to be a chromatographic phenomenon.

In summary, HPLC systems are presented for quantifying the angiotensin-converting enzyme inhibitor, fosinopril, and its possible isomeric and non-isomeric impurities.

ACKNOWLEDGEMENTS

The authors thank Drs. Berry Kline and Glenn Brewer for their helpful comments and thoughtful criticism. We are grateful to Drs. John Grosso and William Winter for supplying many of the compounds used in these studies, to Mrs. Maria Berrios and Ms. Kim Shields who assisted in this work, and to Mrs. Nancy Garside

Thompson who obtained independent evidence for the varying peak responses of the analyte in various solvents.

REFERENCES

1 Z. P. Horovitz (Editor), *Angiotensin Converting Enzyme Inhibitors,* Urban & Schwarzenberg, Baltimore-Munich, 1981.
2 J. Krapcho, C. Turk, D. W. Cushman, J. R. Powell, J. M. DeForrest, E. R. Spitzmiller, D. S. Karanewsky, M. Duggan, G. Rovnyak, J. Schwartz, S. Natarajan, J. D. Godfrey, D. E. Ryono, R. Neubeck, K. S. Atwa and E. W. Petrillo, Jr., *J. Med. Chem.,* 31 (1988) 1148.
3 M. A. Ondetti, *Circulation,* 77 (1988) 174.
4 S. Perlman and J. Kirschbaum, *J. Chromatogr.,* 206 (1981) 311.
5 J. Kirschbaum and S. Perlman, *J. Pharm. Sci.,* 73 (1984) 686.
6 S. Perlman and J. Kirschbaum, *J. Chromatogr.,* 357 (1986) 39.
7 J. Kirschbaum, *J. Pharm. Biomed. Anal.,* 7 (1989) 813.
8 E. L. Inman, A. M. Maloney and E. C. Rickard, *J. Chromatogr.,* 465 (1989) 201.

Journal of Chromatography, 507 (1990) 171–176
Elsevier Science Publishers B.V., Amsterdam — Printed in The Netherlands

CHROMSYMP. 1804

High-performance liquid chromatographic method for the simultaneous assay of a new synthetic penem molecule and its salt-forming agent in injectable formulations

MARINA FARINA*, GIORGIO FINETTI and VIRGINIO BUSNELLI
Galenical Research and Development, Farmitalia Carlo Erba, Via Carlo Imbonati 24, 20159 Milan (Italy)

SUMMARY

A rapid, stability-indicating, reversed-phase high-performance liquid chromatographic method for the direct and simultaneous determination of a new β-lactam molecule and its salt-forming agent in finished dosage forms was studied for the development of injectable formulations.

INTRODUCTION

threo-*trans*-(*R*)-6-Hydroxyethyl-2-carbamoyloxymethyl-2-penem-3-carboxylic acid, laboratory code FCE 22101 (Fig. 1), is a synthetic β-lactam antibacterial agent[1] belonging to the penem class, with a broad antibacterial spectrum which includes both aerobic and obligate anaerobic species[2–4]. FCE 22101 is designed for parenteral administration in the treatment of infections of the urogenital and upper respiratory tracts.

The injectable formulations of this active drug substance and of all the similar synthetic β-lactam molecules on the market need the presence of a salt-forming agent to allow a rapid reconstitution of the pharmaceutical preparation.

On the basis of its good stability and compatibility with the drug, L-arginine was chosen as the salt-forming agent for FCE 22101; these two components are present in the finished dosage form in the molar ratio 1:1.

The determinations of similar active drug substances and of their salt-forming agents were previously carried out by different time-consuming methods[5]. This study

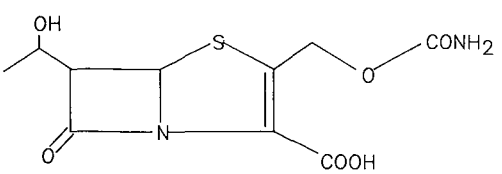

Fig. 1. Structural formula of FCE 22101.

0021-9673/90/$03.50

was aimed at setting up a rapid and stability-indicating high-performance liquid chromatographic (HPLC) assay method allowing the simultaneous determination of FCE 22101 and L-arginine.

EXPERIMENTAL

The trials were carried out with a Spectra-Physics Model SP8770 liquid chromatograph equipped with a Whatman PartiSphere C_{18} column (110 × 4.6 mm I.D., average particle size 5 μm), a Rheodyne 7125 injection valve, a Knauer variable-wavelength UV detector and a Spectra-Physics Model SP4270 integrating recorder. The chromatographic column was kept at 25 ± 1°C by means of a water jacket. High-precision glassware was used for all the sampling operations.

The analytical wavelength was set at 206 ± 1 nm, which gave the best results for

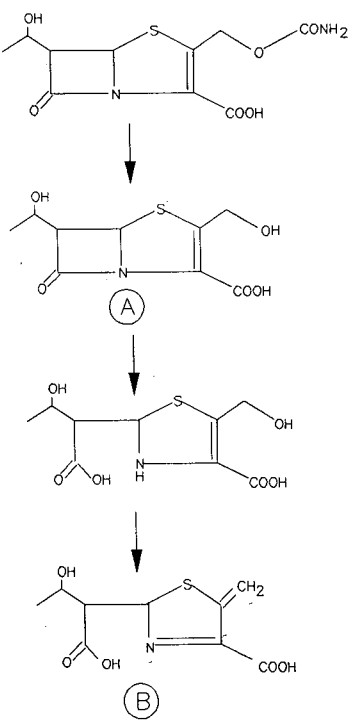

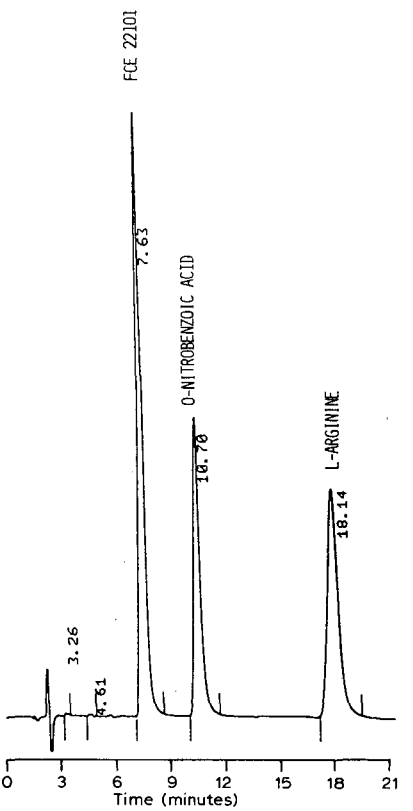

Fig. 2. Degradation pathway of FCE 22101, showing the formation of its more probable degradation products (A and B).

Fig. 3. Typical chromatogram of FCE 22102, L-arginine and *o*-nitrobenzoic acid (internal standard) obtained with a Whatman PartiSphere C_{18} column (110 × 4.6 mm I.D.; average particle size 5 μm) using as the mobile phase phosphate buffer (pH 2.5)–acetonitrile (92.5:7.5, v/v) containing 0.01 *M* heptanesulphonic acid. Analytical wavelength: 206 ± 1 nm.

the statisfactory simultaneous detection of the components of the pharmaceutical preparations and of the most probable degradation products, indicated as products A and B[6], which arise from hydrolytic cleavage of the FCE 22101 molecule (Fig. 2).

FCE 22101 was supplied by Carlo Erba and L-arginine by C.F.M. (USP grade). Acetonitrile was of HPLC grade. All other reagents were analytical-reagent grade.

Phosphate buffer (pH 2.5) was prepared by dissolving 2.722 g of potassium dihydrogenphosphate in distilled water, adjusting the pH to 2.5 with phosphoric acid and diluting to 1000 ml with distilled water.

The mobile phase was phosphate buffer (pH 2.5)–acetonitrile (92.5:7.5, v/v), containing 0.01 *M* sodium heptanesulphonate. The mobile phase flow-rate was 0.7 ml/min and the chart speed 0.5 cm/min.

The integrator attenuation was set at 32 for FCE 22101 and *o*-nitrobenzoic acid and then switched to 8 for L-arginine, during the same run, after about 13–14 min of analysis. For all the analyses a solution containing about 0.1 mg/ml of FCE 22101, about 0.06 mg/ml of L-arginine and 0.2 mg/ml of *o*-nitrobenzoic acid (internal standard) was prepared using as the solvent the HPLC mobile phase. In this way the molar ratio between FCE 22101 and L-arginine was identical with that present in the finished dosage form submitted to HPLC analysis.

Under these conditions, FCE 22101, *o*-nitrobenzoic acid and L-arginine showed retention times of about 8, 10 and 19 min, respectively, and were efficiently separated from the most common related substances present (Fig. 3).

RESULTS AND DISCUSSION

In order to effect the simultaneous elutions of the two component peaks under isocratic conditions, the mobile phase composition was studied and optimized.

Phosphate buffer was chosen as the aqueous component of the mobile phase; the pH for optimum resolution of the compounds under analysis was 2.5. A satisfactory separation was obtained with a mobile phase consisting of a phosphate buffer (pH 2.5)–acetonitrile (92.5:7.5, v/v).

In order to obtain an optimum column retention capacity for L-arginine, an ion-pairing agent was added to the mobile phase, otherwise the retention time of L-arginine would have been very close to the solvent front (Fig. 4). The ion-pairing agents tested were sodium alkanesulphonates salt with a carbon chain length from C_5 to C_8 (Fig. 5). On the basis of the results obtained, sodium heptanesulphonate salt was chosen as it allowed a good separation of L-arginine from the solvent front together with a suitable retention time for FCE 22101. The optimum concentration of this ion-pairing agent was determined from a plot of log k' *versus* sodium heptanesulphonate concentration for the determination of L-arginine (Fig. 6). This plot shows that an increase in ion-pairing agent concentration was followed by a significant increase in the retention time of L-arginine. The best compromise between a good resolution of the L-arginine peak and a practicable analysis time was obtained when sodium heptanesulphonate was added to the mobile phase at a concentration of 0.01 *M*.

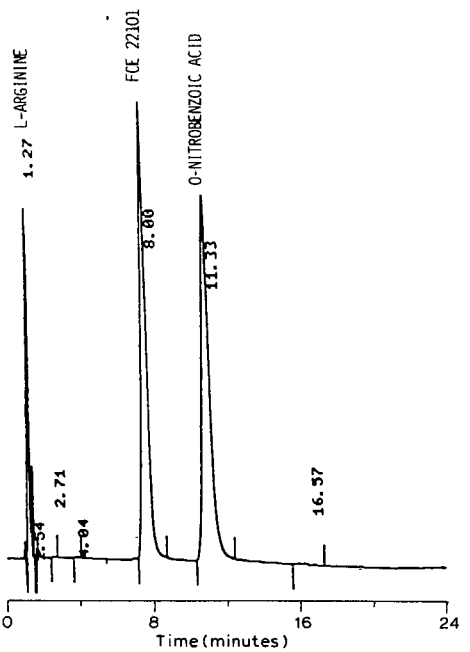

Fig. 4. Typical chromatogram obtained injecting FCE 22102, L-arginine and *o*-nitrobenzoic acid (internal standard) in the absence of the ion-pairing agent.

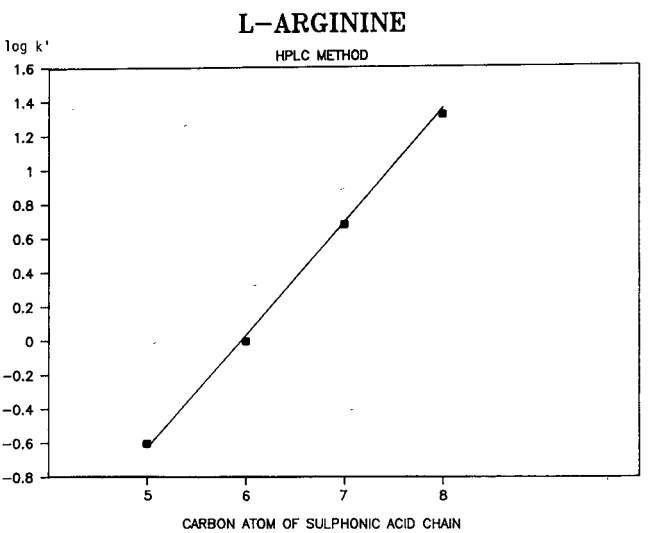

Fig. 5. Choice of the optimum ion-pairing agent: sodium alkanesulphonates with a carbon chain length from C_5 to C_8, at 0.01 *M* concentration.

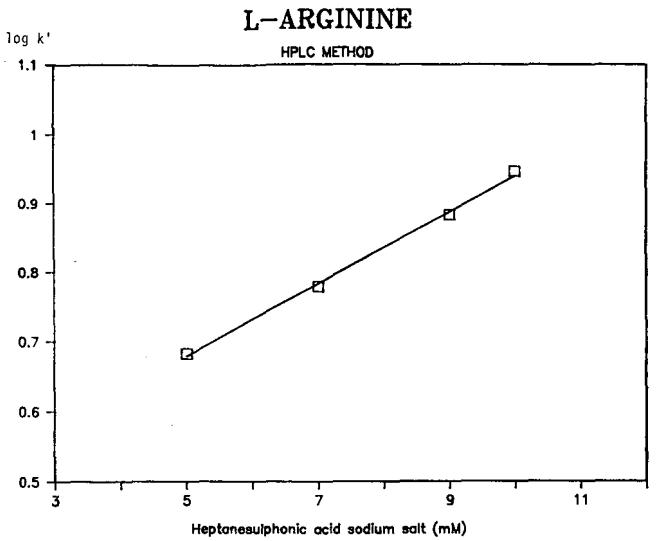

Fig. 6. Determination of the ideal concentration of the ion-pairing agent in the mobile phase.

CONCLUSIONS

The proposed method allowed the simultaneous determination of the active drug substance (FCE 22101), its salt-forming agent L-arginine and the prevalent related substances and degradation products, permitting very detailed stability trials on pharmaceutical preparations during their development to be carried out (Fig. 7),

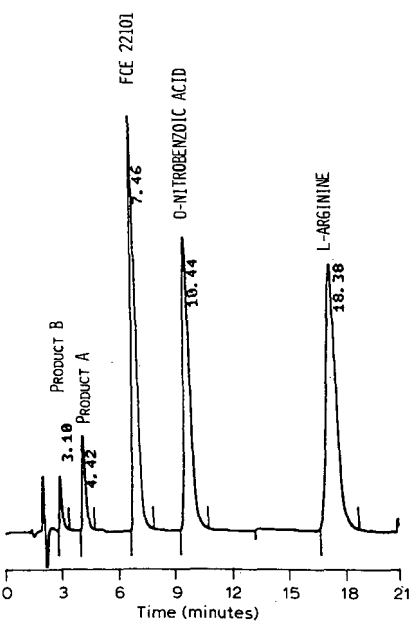

Fig. 7. Chromatogram obtained by injecting a mixture of FCE 22101, L-arginine, *o*-nitrobenzoic acid and the most probable degradation products (A and B) under the optimized analytical conditions.

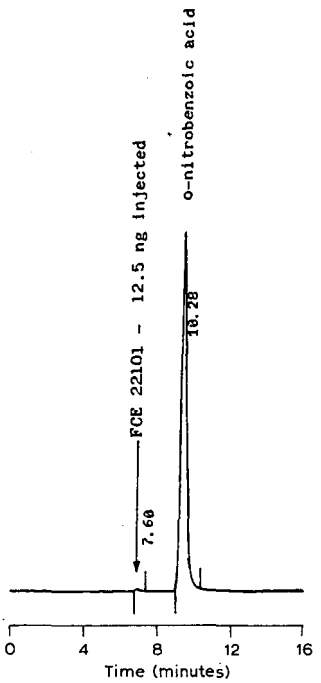

Fig. 8. Sensitivity for FCE 22101: limit of determination without changing the integrator attenuation.

and showed very satisfactory performances for both components of the injectable dosage form.

The method was linear in a concentration range from 25–200% of the amount usually injected ($r = 0.999$ for FCE 22101 and $r = 0.9949$ for L-arginine). The accuracy was 99.58 ± 0.32% for FCE 22101 and 98.06 ± 0.88% for L-arginine (both 95% confidence limits for a mean of twelve determinations at 90% and 110% of the label amounts). The precision (relative standard deviation) was 0.901% for FCE 22101 and 0.507% for L-arginine ($n = 6$).

The method allowed us the detection of about 12.5 ng of FCE 22101 and 60 ng of L-arginine injected (corresponding to about 0.5% and 3.5%, respectively, of the amounts usually injected for a typical sample) (Fig. 8).

The method permitted the determination of FCE 22101 in samples degraded under acidic and basic conditions, under intense white light and in the presence of a strong oxidizing agent, without interference from the side-products formed.

Repeated analyses of six different samples of FCE 22101 showed a relative standard deviation of 3.32% (at a total impurity level of about 3%).

REFERENCES

1 G. Franceschi, M. Foglio, M. Alpegiani, C. Battistini, A. Bedeschi, E. Perrone, F. Zarini, F. Arcamone, C. Della Bruna and A. Sanfilippo, *J. Antibiot.*, 36 (1983) 938–941.
2 C. E. Nord, A. Lindmark and I. Person, *Antimicrob. Agents Chemother.*, 5 (1987) 831–833.
3 H. C. Neu, *Scand. J. Infect. Dis., Suppl.*, 42 (1984) 7–16.
4 D. Reeves, D. Spiller, R. Spencer and J. P. Daly, *J. Antimicrob. Chemother., Suppl. C*, 23 (1989).
5 A. M. Wahbi, M. A. Abounassif, E. A. Gad-Kariem and M. E. Ibrahim, *J. Assoc. Off. Anal. Chem.*, 71 (1988) 31–33.
6 G. Cassinelli, R. Corigli, P. Orezzi, G. Ventrella, A. Badeschi, E. Perrone, D. Borghi and G. Franceschi, *J. Antibiot.*, 41 (1988) 984–987.

Journal of Chromatography, 507 (1990) 177–185
Elsevier Science Publishers B.V., Amsterdam — Printed in The Netherlands

CHROMSYMP. 1714

Determination of penicillin G in milk by high-performance liquid chromatography with automated liquid chromatographic cleanup

W. A. MOATS
U.S. Department of Agriculture, Agricultural Research Service, Bldg. 201, BARC-East, Beltsville, MD 20705 (U.S.A.)

SUMMARY

Specific confirmatory tests are needed to identify and quantify β-lactam antibiotic residues detected in milk at levels of < 10 parts per 10^9 (ppb) by screening tests. A liquid chromatographic method for penicillin G was developed using the liquid chromatography system for cleanup as well as analysis. Milk was deproteinized with two volumes of acetonitrile. The acetonitrile was extracted with hexane–methylene chloride (1:1) and the remaining water layer was concentrated by evaporation. The water layer (2 ml = 5 ml milk) was injected onto a Polymer Laboratories PLRP-S column using a WISP autosampler with the solvent, 0.01 *M* pH 7.0 phosphate buffer (A). Penicillin G was eluted with acetonitrile (B) gradient A–B (100:0) (0–3 min)–(40:60) (25 min). Penicillin G eluted as a narrow band in < 0.5 min. A narrow fraction containing penicillin G was collected and rechromatographed on the same type of column at low pH (1.96). This effectively separated penicillin G from interferences. Recoveries were 92 ± 9% with a sensitivity limit near 2 ppb. The approach used is applicable to determination of other β-lactam antibiotics but specific conditions for analysis must be determined for each one. The cleanup procedure can be automated using an autosampler, gradient controller, and fraction collector.

INTRODUCTION

A number of sensitive screening tests have been described for detection of β-lactam antibiotic residues in milk. These include microbiological tests[1], immunoassays[2,3], competitive binding[1,4,5], and enzyme inhibition (Penzym)[6]. These are all capable of detecting residues at levels of 10 ppb[a] or less. With he possible exception of immunoassays, none of the screening procedures can distinguish β-lactam antibiotics from one another. False positive tests may occur. Specific physico-chemical confirmatory tests for β-lactam antibiotics are needed for identification and quantitation of

[a] Throughout this article, the American billion (10^9) is meant.

suspect residues. However, development of methods of adequate sensitivity has proven difficult. The author described a procedure suitable for determination of β-lactam antibiotics with neutral side-chains at about 5–10 ppb in milk which used a partitioning cleanup with UV detection[7]. Meetschen and Petz[8] described a method using gas–liquid chromatography sensitive to < 1 ppb for β-lactams with neutral side-chains which required a lengthy partitioning cleanup and derivatization. Wiese and Martin[9] described a high-performance liquid chromatography (HPLC) procedure for penicillin G in milk sensitive to < 1 ppb which used electronic subtraction of chromatograms before and after treatment with β-lactamase. This procedure also used a partitioning cleanup and derivatization and required very precise reproducibility of chromatograms. Other published chromatographic methods do not achieve the required sensitivity[10–12].

Many β-lactam antibiotics cannot be partitioned between buffers and organic solvents. Studies in our laboratory have demonstrated that analytes can be concentrated directly on an analytical column from filtrates and eluted with a solvent gradient. This approach was used successfully for determination of novobiocin[13], virginiamycin[14] and tetracyclines[15]. If too much interference is present for direct determination, a narrow fraction containing the analyte of interest can be taken, using a procedure sometimes termed "heart-cutting"[16], and rechromatographed under different conditions. The application of this approach to determination of penicillin G in milk is described in the present paper. The approach is applicable in principle to other β-lactam antibiotics and has been successfully used for determination of lincomycin residues in milk and tissue[17].

EXPERIMENTAL[a]

Chemicals and reagents

Acetonitrile, HPLC grade, other chemicals, analytical-reagent grade. The sodium salt of penicillin G was obtained from Sigma (St. Louis, MO, U.S.A.). A stock solution of 1 mg/ml of sodium penicillin G was prepared fresh weekly in deionized water. Working solutions of 10, 5, and 1 μg/ml were prepared by diluting the stock solution with deionized water or 0.01 *M* pH 7.0 buffer as required.

Apparatus

Glassware required included 125-ml conical flasks, 50-ml graduated cylinders, 250-ml separatory funnels with PTFE stopcocks, 250-ml glass-stoppered side-arm flasks, 75-mm funnels, and 15-ml graduated conical centrifuge tubes. All glassware was cleaned by soaking overnight at room temperature or a few minutes at 50–70°C in special detergent (Micro International Products, Trenton, NJ, U.S.A.). The glassware was rinsed in deionized water, then in *ca.* 0.01 *M* HCl and then in deionized water again.

The Waters chromatographic system consisted of an automatic gradient controller, two Model 510 pumps, a WISP autosampler with a 2000-μl loop and either a Model 481 UV detector or a Model 990 diode array detector (Waters, Milford, MA,

[a] Mention of specific items or trade names is for identification purposes only and does not imply endorsement by the U.S. Department of Agriculture over similar items not specifically mentioned.

U.S.A.) with an ISCO (Lincoln, NE, U.S.A.) FOXY fraction collector. A Varian system (Varian, Sugarland, TX, U.S.A.) consisting of an LC-5000 chromatograph, a 9090 autosampler and a Waters Model 481 UV detector was used for analysis.

Chromatographic columns used were, with matching guard cartridges a Supelcosil LC-18-DB, 150 × 4.6 mm, 5 μm particle size (Supelco, Bellefonte, PA, U.S.A.), and a Polymer Labs (Amherst, MA, U.S.A.) PLRP-S column, 150 × 4.6 mm, 5 μm particle size, 100 Å pore diameter.

A Buchler Rotary Evapomix® (Buchler, Ft. Lee, NJ, U.S.A.) was used to evaporate samples under reduced pressure in centrifuge tubes.

Extraction and cleanup procedures

A 20-ml volume of milk was measured into a 125-ml conical flask and 40 ml of acetonitrile was added slowly with vigorous swirling. After standing for 5 min, the clear suprenatant was decanted through a plug of glass wool in the stem of a funnel and 30 ml filtrate collected. The filtrate was transferred to a separatory funnel, 30 ml methylene chloride and 30 ml hexane or light petroleum (b.p. 30–60°C) were added and the mixture was allowed to separate 5 min. The water layer was collected in a 250-ml side-arm flask. The organic layer was washed with 5 ml water. The combined water layers were evaporated under reduced pressure in the side-arm flask in a 40-50°C water bath to 1–2 ml. The residue was rinsed into a 15-ml graduated centrifuge tube with small (0.5 ml) portions of water. The sample solution was diluted to 4 ml and filtered through a very small plug of glass wool in the stem of a funnel to remove any coarse particles. Slight turbidity if present was not a problem. The filtrate was transferred to 4-ml autosampler vials.

HPLC cleanup

Sample and standards were loaded into 4-ml vials in the WISP. The column was equilibrated with 0.01 *M* pH 7.0 phosphate buffer, flow-rate 1 ml/min. The autosampler automatically started the gradient and the fraction collector. A gradient program of buffer (A)–acetonitrile (B), (100:0) (0–3 min)–(40:60) (25–30 min)–(100:0) (31 min) was used. Loading of the next sample was started 40 min after injection of the previous sample. Two 2-μg standards were injected first, one in 200 μl and one in 2000 μl, to establish the retention time and to make sure that the operation was stable. Fractions were collected in 15-ml conical graduated centrifuge tubes (calibrated in the 0.5–1 ml range). The fraction collector was set to collect a 1.2-min (1.2-ml) fraction centered on the retention time of penicillin G with 0.1 min delay. The gradient controller was programmed to flush the column and shut itself off after elution of the last sample was completed. The fraction was concentrated to $\leq$0.5 ml in the Buchler Rotary Evapomix under reduced pressure and the volume was adjusted to 0.5 ml and transferred to autosampler tubes (1 ml inserts for the WISP).

HPLC analysis

Analysis was done under isocratic conditions using a Polymer Labs, PLRP-S column identical to that used for cleanup, flow-rate 1 ml/min, solvent 0.01 *M* pH 1.96 phosphate buffer–acetonitrile (66:34) using the Varian system. The injection volume was 100 μl (1 ml original milk). Detection was at 200 or 210 nm using either a UV or diode array detector (Waters 990). The response was linear at least to 1 μg. Standards

of 0.1, 0.4 and 1 μg were run with each set of samples to correct for minor changes in response.

Spiked samples and confirmation with penicillinase

An appropriate amount of penicillin G solution was added to the milk prior to carrying out the extraction procedure. For confirmation, 0.2 ml of penase concentrate Bacto (Difco Labs., Detroit, MI, U.S.A.) was added to 20 ml of milk and allowed to stand 15 min before carrying out the procedure.

RESULTS AND DISCUSSION

For the present procedure, the approach adopted was to determine penicillin G by UV absorption thus avoiding lengthy derivatization procedures. Sensitivity was improved over the previous procedure[7] by using absorption at 200 or 210 nm rather than at 220 nm (Fig. 1). Baselines were less noisy at 210 nm. In general, 5–10 ng were required for adequate quantitation although less could be detected. For quantitation at 5–10 ppb, it was therefore necessary to inject the equivalent of 1 ml of milk. This required considerable concentration and cleanup. The practical limit of cleanup which could be achieved by partitioning between organic solvents and buffers was achieved in a procedure described previously[7].

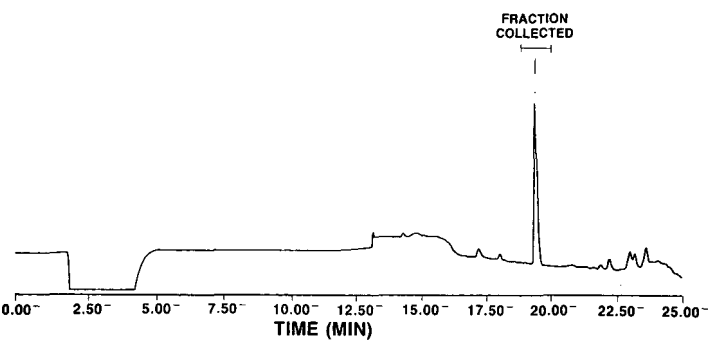

Fig. 1. Penicillin G, 2-μg standard, in 2000 μl, gradient elution, 0.01 *M* pH 7.0 phosphate buffer (A)–acetonitrile (B), 100:0 (0–3 min)–40:60 (25 min); flow, 1 ml/min, detection, UV at 200 nm; Polymer Labs. PLRP-S column, 150 × 4.6 mm, 5-μm packing, 100 Å pore size.

Our previous studies[7] demonstrated that extraction/deproteinization of milk with two volumes of acetonitrile was rapid and gave essentially quantitative recoveries of penicillins in the filtrate. Since the concentration in the filtrate was the same as in the mixture before filtration, an aliquot of the filtrate could be taken as representative. Therefore, no tedious washing of precipitates was required. We explored concentration and cleanup approaches using solid-phase extraction on short laboratory-packed colums and also pre-packed absorbent cartridges widely sold for cleanup. Our labaratory-packed columns somtimes worked well but we were unable to reproduce our results with different lots of the same absorbent. This approach could therefore not

be recommended. The results with pre-packed absorbent cartridges were scarcely more promising. Some disadvantages of the pre-packed cartridges were:

(1) They usually required tedious prewashing with solvents to "activate" them.

(2) Contaminants were frequently eluted from the cartridges.

(3) Analytes either were not fully retained or did not elute sharply. This is well illustrated by data of Terada *et al.*[12] and Terada and Sakabe[11] who found that 10–20 ml of eluent were required to recover penicillins from Sep-Pak™ C_{18} cartridges.

We therefore concluded that a more rigorous approach using an analytical HPLC column would be required to achieve the concentration and rigorous fractionation necessary for determination at <10 ppb.

If the analyte is immobile under the chromatographic conditions used to load it on the column, then the shape of the peak obtained by subsequent gradient elution is not affected by the volume in which the sample is injected. Penicillin G is immobile on reversed-phase packings when injected in water at pH 7 but is readily eluted by acetonitrile. For concentration by solid-phase extraction, it was therefore first necessary to get rid of the organic solvents from the filtrates prepared with acetonitrile. The water layer was separated by adding methylene chloride and petroleum ether to the filtrate. The penicillins were essentially quantitatively recovered in the water layer. This layer was concentrated to <4 ml under reduced pressure and diluted to 4 ml prior to concentration by solid-phase extraction and fraction collection. When penicillin G is loaded on the column in water and eluted with a gradient, the peak height and shape are not affected by the volume of solvent in which the sample is injected.

The Waters WISP autosampler with a 2-ml loop will inject a larger amount of sample than other available autosamplers. However, it took 27 min to load the loop. Injection of an even larger amount of more dilute sample would be preferable. As it is, the sample extract must be concentrated considerably by evaporation in order to load the desired amount onto the analytical column. A polymeric HPLC column (Polymer Labs., PLRP-S), 5 μm particle size, was used with the pH 7 buffer. We found that the polymeric columns were more stable than silica-based reversed-phase columns in the pH range 7–8. Column efficiencies of the PLRP-S columns closely approached those of bonded silica packings of comparable particle size. We found that at least under our conditions the polymeric packing was very unstable above pH 8. The columns developed excessive back pressures indicating that the packing swelled. This could result in permanent damage to the packing even after the column was flushed with buffer of lower pH. This is contrary to the manufacturer's claims that these packings are stable to pH 13. Penicillins eluted as a sharp band (Fig. 1) in <0.5 ml (0.5 min). However, a slightly wider (1.2 ml) fraction was collected to allow for slight variation in retention in successive runs. Fig. 2 shows the chromatogram of a milk sample containing 1 ppm of penicillin G using the fraction collection procedure. The penicillin peak is visible at this concentration.

Use of the HPLC system for cleanup offers a number of advantages over the use of cartridges:

(1) Reproducibility —since the same column was used repeatedly, results were reproducible and were not dependent on the quality control of the manufacturer.

(2) No special washing or activation was required since the column was flushed and reequilibrated between each run.

(3) Fractionation was sharper. Analytes were usually completely recovered in 0.2–0.5 ml.

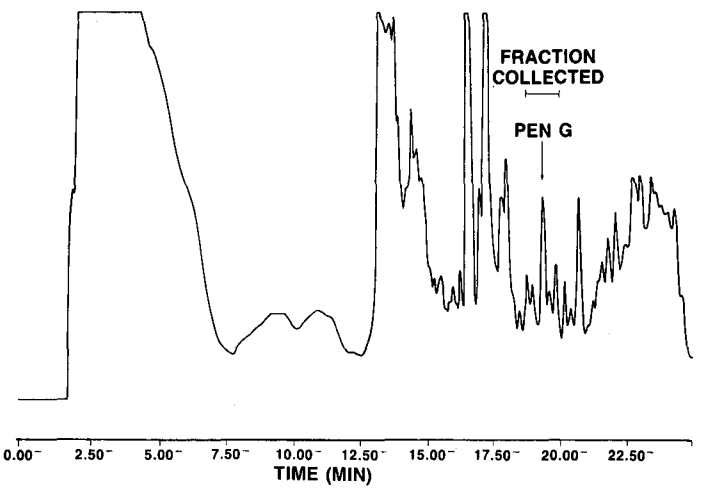

Fig. 2. Milk filtrate, 5 ml equiv. concentrated to 2 ml, 1 ppm penicillin (PEN) G. Conditions as in Fig. 1.

(4) The system could be automated with standard HPLC equipment.

The cleanup required about an hour per sample but was fully automated. Samples were loaded into the autosampler in the afternoon and the machine was run overnight. pH 7-Buffer was used because penicillin G is most stable at that pH and showed little deterioration during holding of samples prior to final analysis.

For analysis, the fraction collected was rechromatographed under conditions which would separate penicillin G from interferences in the fraction. There are several ways of changing the retention of an analyte both absolutely and relative to other compounds:

(1) Change the concentration of organic modifier. This usually does not change the relative retentions very much.

(2) Change the organic modifier. In the present case, only acetonitrile could be used with UV determination at 200 nm.

(3) Add ion-pairs such as quaternary ammonium compounds or alkyl sulfonates.

(4) Change the pH to convert the compound from the salt (ionized) to acid (non-ionized) form. This produce a much larger change in retention on a reversed-phase column than ion-pairing.

(5) Use a different chromatographic mode such as ion-exchange or normal-phase chromatography on silica.

Table I shows the effect of pH and ion-pairs (tetraethylammonium and heptanesulfonate) on retention of penicillin G on polymeric and bonded reversed-phase packings of comparable particle size. An identical solvent gradient was used in all cases to facilitate comparison. At pH 7.0 and 4.6, addition of tetraethylammonium chloride increased retention of penicillin G. The tetraethylammonium chloride had little effect in 0.01 *M* orthophosphoric acid as would be expected. The acid form of penicillin G was much more strongly retained than the salt form and this is the basis of the separation used in the present procedure. The heptanesulfonate anion interfered

TABLE I

EFFECT OF pH, ION-PAIR AND COLUMN PACKING ON RETENTION OF PENICILLIN G

Gradient elution: buffer (A)–acetonitrile (B), 100:0 (0–3 min)–40:60 (25 min). Column packings 5 μm particle size, columns 150 × 4.6 mm. SHS = Sodium heptane sulfonate.

Buffer	*Retention time (min)*	
	Column type	
	Styrene–divinylbenzene (Polymer Labs. PLRP-S)	*Bonded C_{18} (Supelco LC-18-DB)*
0.01 *M* Phosphate (pH 7.0)		
Buffer only	18.97	19.80
0.005 *M* $(C_2H_5)_4NCl$	19.47	20.15
0.005 *M* SHS	16.97	17.13
0.01 *M* $NH_4H_2PO_4$ (pH 4.6)		
Buffer only	19.30	19.98
0.005 *M* $(C_2H_5)_4NCl$	19.86	20.69
0.005 *M* SHS	20.78	21.42
0.01 *M* H_3PO_4 (pH 1.6)		
Buffer only	24.53	25.25
0.005 *M* $(C_2H_5)_4NCl$	24.52	25.21
0.005 *M* SHS	21.48	21.47

with retention of the anion of penicillin G at pH 7 but not at pH 4.6. Retention was also reduced at low pH relative to buffer alone.

The fractions collected at pH 7.0 were rechromatographed in acid buffers under isocratic conditions. The best separations from interferences were obtained with pH 1.96 buffer with a mobile phase composition buffer–acetonitrile (72:28). Better separations were obtained if the same type of column was used for both fraction collection and analysis. Both bonded and polymeric columns were stable at least to the pH of 0.01 *M* orthophosphoric acid. Although penicillin G is unstable at low pH, there was no evidence of decomposition during the analysis procedure or even when longer gradients were used with 0.01 *M* orthophosphoric acid. No suitable internal standard is known for this procedure because of the rigorous fractionation used. In practice use of an external standard in the same sample series is adequate to correct for any variation in instrument performance.

Fig. 3 shows a milk blank and milk spiked with 10 ppb and 100 ppb penicillin G. Penicillin was readily quantitated at 10 ppb. There is little noise in the baseline at the sensitivity used. Table II shows recoveries which averaged 92% at three levels of spiking. Results at 10 ppb were less precise as would be expected. The detection limit at which the penicillin peak can be clearly detected usually above baseline noise is about 2 ppb, comparable to the most sensitive screening procedures.

The procedure is intrinsically simple although not particularly fast, requiring 4–5 h for an individual sample. For multiple samples run, add 1 h per sample since cleanup must be done sequentially. In practice, we ran the chromatographic cleanup unattended overnight so that the time factor was irrelevant.

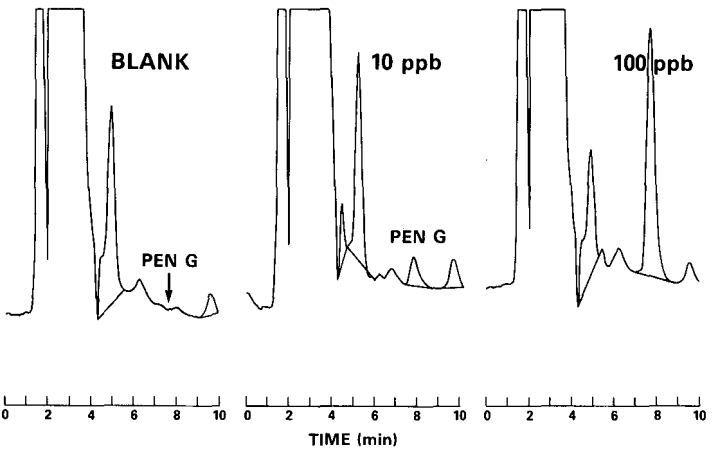

Fig. 3. Analysis of penicillin G, 100 μl injected = 1 ml milk. Blank, 10 ppb and 100 ppb. Isocratic elution, 0.01 *M* pH 1.96 phospate buffer–acetonitrile (66:34). PLRP-S column; detection, UV at 210 nm. Arrow indicates retention time of penicillin G.

TABLE II

RECOVERIES OF PENICILLIN G FROM MILK

Amount added (ppb)	*Found (ppb)*			
	1	*2*	*3*	*Mean ± S.D.*
10	8.9	7.8	11	9.2 ± 1.4
100	98	93	86	92 ± 5
1000	940	960	850	920 ± 48
Mean recovery from all (%)				92 ± 9
Milk from treated cow (32 h)	93	109		

Since the penicillin G was well isolated from interfering peaks in the blank milk, the presence of a peak with the retention time of penicillin G gave a presumptive test for its presence and provided good quantitation. The absence of any peak clearly established that penicillin G was not present above the sensitivity limits of the procedure. Further confirmation of the penicillin G may be based on the UV spectrum obtaind by using a diode array detector and/or by repeating the analysis after treating the sample with penicillinase.

The general approach of using the LC system for cleanup should be applicable to determination of low levels of other β-lactam antibiotics or other residues where rigorous cleanup is required. Conditions for the cleanup and analysis steps which give good separation of analytes from interferences must be established. The approach can be automated to considerable extent.

ACKNOWLEDGEMENTS

The author thanks Miau Huang for technical assistance and Mike Thomas, FDA/CVM, Beltsville, MD, U.S.A., for providing milk samples from treated cows.

REFERENCES

1 D. M. MacCauley and V. S. Packard, *J. Food Prot.*, 44 (1981) 696–698.
2 J. J. Ryan, E. E. Wildman, A. H. Duthie, H. V. Atherton and J. J. Aleong, *J. Dairy Sci.*, 69 (1986) 1510–1517.
3 P. Rohner, M. Schaellibaum and J. Nicolet, *J. Food Prot.*, 48 (1985) 59–62.
4 S. E. Charm and R. Chi, *J. Assoc. Off. Anal. Chem.*, 71 (1988) 304–316.
5 D. L. Collins-Thompson, D. S. Wood and I. Q. Thomson, *J. Food Prot.*, 51 (1988) 632–633.
6 S. A. Thorogood and A. Ray, *J. Soc. Dairy Technol.*, 37 (1984) 38–41.
7 W. A. Moats, *J. Agric. Food Chem.*, 31 (1983) 880–883.
8 U. Meetschen and M. Petz, *J. Assoc. Off. Anal. Chem.*, in press.
9 B. Wiese and K. Martin, *J. Pharm. Biomed. Anal.*, 7 (1989) 95–106.
10 R. K. Munns, W. Shimoda, J. E. Roybal and C. Vieira, *J. Assoc. Off. Anal. Chem.*, 68 (1985) 968–971.
11 H. Terada and Y. Sakabe, *J. Chromatogr.*, 348 (1985) 379–387.
12 H. Terada, M. Asanoma and Y. Sakabe, *J. Chromatogr.*, 318 (1985) 299–306.
13 W. A. Moats and L. Leskinen, *J. Assoc. Off. Anal. Chem.*, 71 (1988) 776–778.
14 W. A. Moats and L. Leskinen, *J. Agric. Food Chem.*, 36 (1988) 1297–1300.
15 W. A. Moats, *J. Chromatogr.*, 358 (1986) 253–259.
16 J. Carlqvist and D. Westerlund, *J. Chromatogr.*, 344 (1985) 285–296.
17 W. A. Moats, unpublished results.

Journal of Chromatography, 507 (1990) 187–198
Elsevier Science Publishers B.V., Amsterdam — Printed in The Netherlands

CHROMSYMP. 1684

Determination of the monoamine oxidase B inhibitor Ro 19-6327 in plasma by high-performance liquid chromatography using precolumn derivatization with fluorescamine and fluorescence detection

R. WYSS* and W. PHILIPP
Pharmaceutical Research, Department of Drug Metabolism, F. Hoffmann-La Roche Ltd., PF/MET, 68/121A, CH-4002 Basle (Switzerland)

SUMMARY

A specific high-performance liquid chromatographic (HPLC) method using precolumn derivatization and fluorescence detection was developed for the determination of the monoamine oxidase B inhibitor Ro 19-6327 in human plasma. After extraction of the basified plasma with *tert.*-butyl methyl ether–1-butanol (8:2, v/v) and back-extraction into dilute phosphoric acid, the solution was neutralized with phosphate buffer and the drug derivatized with fluorescamine. The derivative was chromatographed on a reversed-phase C_8 column, using phosphate buffer–acetonitrile (68:32, v/v) as mobile phase, and fluorescence detection (excitation 370 nm, emission 485 nm). The limit of quantification was 1 ng/ml using 1 ml of plasma. The recovery was 79% in the range 5–200 ng/ml and the inter-assay precision was 3.1–7.9% in the range 2–500 ng/ml. The compound proved to be stable in human plasma. Moderate instability was found in rat plasma and, surprisingly, severe instability in dog plasma. Measures for handling unstable dog plasma samples are described. An HPLC method with UV detection was used for the analysis of dog and rat plasma samples, which is also described briefly. The fluorescence method, which was five times more sensitive than the UV method, was successfully applied to a human tolerance study.

INTRODUCTION

Ro 19-6327, a pyridine carboxamide derivative with a primary amino group in the side-chain (**1**, Fig. 1), is the most potent and selective inhibitor of monoamine oxidase type B (MAO B) reported so far[1], and is very well tolerated at doses that inhibit MAO B 24 h per day[2]. The drug, which has no structural analogy to known MAO B inhibitors, is currently under clinical development as a therapeutic agent in Parkinson's disease. Because of its polar structure (*n*-octanol–water partition coefficient *ca.* 0.1, pK_a of the amino group 8.9), **1** is difficult to extract from plasma with

0021-9673/90/$03.50

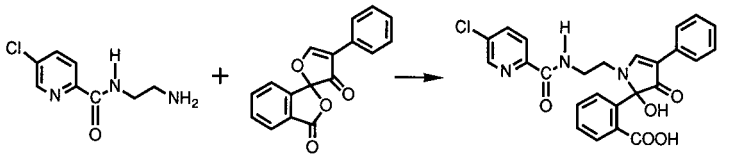

1: Ro 19-6327 2: Fluorescamine 3

Fig. 1. Structures of (1) Ro 19-6327, (2) fluorescamine and (3) their reaction product.

organic solvents, and also shows the typical chromatographic problems with amines in high-performance liquid chromatography (HPLC), as reported, *e.g.*, for moclobemide[3].

Initially, a reversed-phase ion-pair HPLC method with UV detection was developed for the determination of **1** in human, dog and rat plasma[4]. This method, with a limit of quantification of 5 ng/ml, proved to be sensitive enough for use in animal pharmacokinetic and toxicokinetic studies. However, a more sensitive method was needed for pharmacokinetic studies in man after the administration of therapeutic doses. Therefore, precolumn derivatization of the primary amino group was tried.

This paper describes this method, which consists of extraction of the basified plasma with *tert.*-butyl methyl ether–1-butanol (8:2, v/v) and back-extraction into dilute phosphoric acid followed, after neutralization with phosphate buffer, by precolumn derivatization with fluorescamine, HPLC separation and fluorescence detection.

EXPERIMENTAL

Materials and reagents

tert.-Butyl methyl ether (distilled in glass, Burdick and Jackson), orthophosphoric acid (*ca.* 85%) and sodium decanesulphonate monohydrate (both puriss. p.a. grade) were obtained from Fluka (Buchs, Switzerland), and acetonitrile (HPLC grade S) from Rathburn (Walkerburn, U.K.). 1-Butanol (Uvasol), 1-hexanol (for synthesis), disodium hydrogenphosphate dihydrate and sodium dihydrogenphosphate monohydrate (both p.a. analytical-reagent grade) and sodium hydroxide (Titrisol) were purchased from E. Merck (Darmstadt, F.R.G.). Water was distilled twice from an all-glass apparatus. Helium was obtained from PanGas (Lucerne, Switzerland). Compound **1** (as its hydrochloride) and fluorescamine (Fluram) were provided by Hoffmann-La Roche (Basle, Switzerland). Disposable 14-ml polypropylene tubes (100 × 17 mm I.D.; Huber, Reinach BL, Switzerland) were first washed with 5 ml of *tert.*-butyl methyl ether–1-butanol (8:2, v/v) for 20 min on a rotating shaker (Heidolph, Keilheim, F.R.G.), and 5-ml polypropylene tubes (75 × 12 mm I.D.; Semadeni, Ostermundingen, Switzerland) were rinsed beforehand with 1 ml of acetonitrile for 5 s on a Vortex mixer.

Plasma standards were prepared using fresh frozen plasma from sodium citrated human blood, which was obtained from a blood bank (Blutspendezentrum SRK, Basle, Switzerland).

Solutions and standards

Dilute phosphoric acid was prepared by diluting 1 ml of 85% orthophosphoric acid to 500 ml with water, and neutralization buffer by making up 30 g of disodium hydrogenphosphate and 24 ml of 1 *M* sodium hydroxide to 1000 ml with doubly distilled water. A 0.5-mg amount of fluorescamine was dissolved in 10 ml of acetonitrile (this solution was freshly prepared every day).

A stock solution of **1** was prepared by dissolving 5.92 mg of the hydrochloride in 100 ml of doubly distilled water (= 0.05 mg/ml free base). Appropriate amounts of the stock solution were diluted with water to give solutions in the range 50–0.1 μg/ml. These solutions were used as plasma standards by diluting 0.1 ml with blank plasma to 10 ml. For greater accuracy, volumes greater than 4 ml were weighed, taking into account the density of plasma (d_{20} = 1.027 g/cm^3). The plasma standards, containing 500, 200, 50, 20, 5, 2 and 1 ng/ml, were divided into aliquots of 1.3 ml and stored at −20°C (for no more than 2 months). The aqueous solutions were freshly prepared prior to use.

Sample preparation and derivatization

A 1-ml volume of plasma and 50 μl of sodium hydroxide (0.4 *M*) were vortex mixed in a polypropylene tube (14 ml) and 10 ml of *tert.*-butyl methyl ether–1-butanol (8:2, v/v) were added. After extraction for 20 min at 30 rpm on a rotating shaker and centrifugation (5 min, 2000 *g*), 9 ml of the organic phase were transferred to a polypropylene tube (14 ml) containing 0.5 ml of dilute phosphoric acid. After back-extraction (20 min) and centrifugation (5 min), the acidic phase was transferred quantitatively, but without organic phase, to a polypropylene tube (5 ml). After addition of 0.5 ml of neutralization buffer (final pH 7.5), 0.5 ml of fluorescamine solution were slowly added under constant vortex mixing. Subsequently, the acetonitrile portion was evaporated *in vacuo* (Speed Vac Concentrator SVC 200H; Savant Instruments, Farmingdale, NY, U.S.A.; evaporation time exactly 10 min, pre-heating time 10 min). All samples produced in one day (calibration standards, quality control samples and unknowns) must undergo this evaporation step simultaneously. After vortex mixing to dissolve ice and salt crystals, which were sometimes formed, the solution was transferred to the autosampler vial, and 100 μl were injected.

Chromatographic system

A modular HPLC system was used, consisting of a Model 420 HPLC pump and Model 460 autosampler (run time 9 min) (both from Kontron, Zurich, Switzerland), a Model F 1000 fluorescence detector (Merck) (excitation wavelength 370 nm, emission 485 nm), a Model SP 4200 integrator with Kerr minifile 4100D (Spectra-Physics, San Jose, CA, U.S.A.) (sensitivity 8 mV, chart speed 0.5 cm/min) working with a modified version of a BASIC program described earlier for the SP 4100 integrator.

A LiChroCART Superspher 60 RP-8e cartridge (125 × 4 mm I.D.) (Merck) was used as an analytical column. The mobile phase was water–acetonitrile (68:32, v/v), containing 100 m*M* sodium dihydrogenphosphate and 5 m*M* disodium hydrogenphosphate (pH 5.9 ± 0.1, not adjusted), and was degassed with helium prior to use. The flow-rate was 1.0 ml/min.

HPLC method with UV detection

This previously developed method consisted of addition of 50 μl of sodium hydroxide (4 *M*) to 1 ml of plasma. After vortex mixing, the mixture was applied to an Extrelut 1 column (Merck) and, after 15 min, eluted twice with 5 ml of *tert.*-butyl methyl ether–1-hexanol (1:1, v/v). The eluate was collected in a centrifuge tube containing 0.4 ml of dilute phosphoric acid. After extraction (15 min) and centrifugation (5 min, 2000 *g*), the acidic phase was directly injected (40 or 100 μl). The analytical column (125 × 4 mm I.D.) (Merck) contained Nucleosil 5 C_{18} (Macherey, Nagel & Co., Düren, F.R.G.), and the mobile phase was water–acetonitrile (705:295, v/v), containing 3 g/l sodium dihydrogenphosphate and 2 g/l sodium decylsulphonate. The flow-rate was 1.0 ml/min, and the detection wavelength was 233 nm, using a Spectroflow 773 UV detector (Kratos, Ramsey, NJ, U.S.A.).

Calibration and calculation

Together with the unknown and quality control samples, seven plasma standards were processed as described above. The calibration graph ($y = a + bx$) was obtained by a weighted linear least-squares regression (weighting factor $1/y^2$) of the peak height y *versus* the concentration x. The calibration graph was used to interpolate unknown concentrations in the biological samples from measured peak heights.

RESULTS AND DISCUSSION

Extraction

Compound **1**, a primary amine with a polar structure, is difficult to extract from plasma with common solvents. *n*-Butyl chloride, chloroform, diethyl ether or ethyl or butyl acetate gave low recoveries even after the addition of alcohol. Many interferences, due to various biogenic amines which occur in plasma, prevented a specific determination using these solvents. The use of liquid–liquid extraction in combination with solid-phase extraction with a strong cation exchanger gave no improvement. Therefore, back-extraction into dilute phosphoric acid was considered for the HPLC method with UV detection, allowing the possibility of direct injection of the extract onto the column. In this way, time-consuming evaporation of the extraction solvent, which would be difficult with polar solvents and could lead to loss of the drug in the case of amines, could be avoided. Several extraction solvent mixtures were tested. Finally, *tert.*-butyl methyl ether–1-hexanol (1:1, v/v), in combination with Extrelut columns, and dilute phosphoric acid for back-extraction were selected.

However, when these extraction conditions were tried for the method using precolumn derivatization, many interfering substances prevented the determination of **1**. Therefore, cleaner reagents and solvents had to be used in order to avoid impurities from these sources. 1-Butanol (Uvasol quality) gave rise to far less interference than 1-hexanol (for synthesis grade). The latter was preferred during the development of the UV method because it was much less soluble in the phosphoric acid used for back-extraction and gave better chromatograms. The injection of traces of butanol was avoided by using a vacuum evaporation step in the precolumn derivatization method.

Another source of problems was the 4 *M* sodium hydroxide used for adjusting

the pH before extraction, which sometimes resulted in a large tailing front peak in the chromatograms; 0.4 *M* sodium hydroxide gave the same recovery without this problem. Instead of glass tubes, which lead to memory effects, disposable polypropylene tubes were used for the extraction. However, these tubes had to be prewashed with the extraction solvent to prevent interferences.

Derivatization

In a first attempt, 9-fluorenylmethyl chloroformate (FMOC-Cl) was tried as a derivatization reagent. FMOC-Cl reacts with both primary and secondary amino acids or amines to form highly fluorescent and stable derivatives[6]. However, this approach did not provide sufficient sensitivity. Using an excitation wavelength of 220 nm (emission 315 nm), relatively small peaks were obtained, and at 260 nm the high background noise prevented sensitive detection. The frequently used reagent *o*-phthalaldehyde (OPA)–mercaptoethanol[7,8] was also investigated. Surprisingly, the OPA derivative of **1** was about 1000 times less fluorescent than that of glycine or octylamine. The reason for this phenomenon is not known and was not investigated further.

Fluorescamine (Fluram), which is non-fluorescent, reacts rapidly with primary amines to give highly fluorescent pyrrolinone derivatives[9]. Excess of the reagent is rapidly hydrolysed to non-fluorescent products. Precolumn derivatization of **1** with fluorescamine resulted in a sensitive method. The reaction scheme is shown in Fig. 1. However, the exact conditions of the reaction and the detection had to be optimized. First, the pH of the substance solution, which is normally in the range 8–9.5[9], had to be established; pH 7.5 was found to be most suitable for **1**. Other parameters that had to be optimized were the concentration and the solvent of the reagent solution. An excess of the reagent was required owing to hydrolysis in aqueous solution. Fig. 2 shows the dependence of the formation of the derivative **3** on the pH of the reaction solution and the fluorescamine concentration. At concentrations significantly above 0.3 mg/ml, De Bernardo *et al.*[9] observed fluorescence quenching. This effect was only observed at pH 8 using a 0.8 mg/ml concentration. On the other hand, a fluorescamine concentration of 0.8 mg/ml or a pH higher than 7.5 resulted in an increase in plasma interferences. Therefore, a concentration of 0.05 mg/ml at pH 7.5 was found to be optimum. Fluorescamine has to be added in a water-miscible, non-hydroxylic solvent which should contain no fluorogenic impurities. Acetonitrile, acetone, tetrahydrofuran and dioxane were described by De Bernardo *et al.*[9]. Acetonitrile was used in this study, although acetone also gave good results. The instability of the derivative was not investigated in detail, because less than 5% degradation occurred over 12 h at 22°C, or over 24 h at 4°C, and, therefore, was considered unproblematic for overnight automatic injections.

After derivatization, the solution was concentrated in a vacuum concentrator by removing the acetonitrile and a minor part of the aqueous portion. An injection solution without acetonitrile resulted in on-column concentration and, therefore, sharper peaks. However, as no internal standard was used, all samples from one working day had to be treated in one batch, and the evaporation time had to be controlled closely. Interestingly, this procedure appeared to have no negative influence on the precision of the method, provided that the inner diameter of the evaporation tubes was larger than 11 mm.

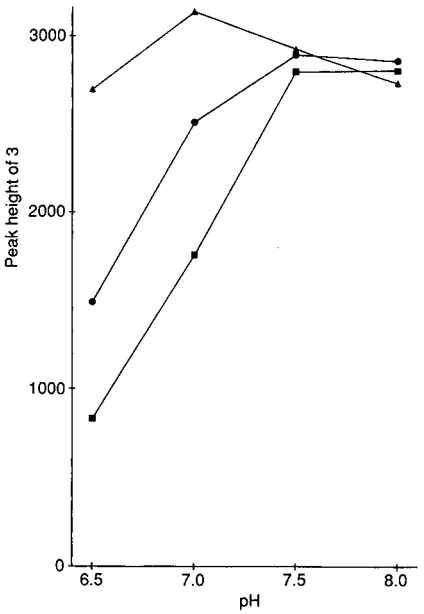

Fig. 2. Dependence of the formation of derivative **3** on the pH of the reaction solution and the fluorescamine concentration (■ = 0.05; ● = 0.2; ▲ = 0.8 mg/ml).

Chromatographic system

The fluorescamine derivative of **1** was strongly retained. Therefore, an ion-pairing agent, as used in the method with UV detection, was no longer necessary. At first, Nucleosil C_{18}, which had proved suitable for **1** in the HPLC method with UV detection, was tried as the stationary phase. However, as with Nucleosil C_8 and Spherisorb C_6, the separation of the fluorescamine derivative **3** from interferences was inadequate. Finally, Superspher C_8 proved to be the best material under these conditions. The composition of the mobile phase also had to be optimized, not only to obtain a good separation, but also to optimize the fluorescence intensity. Concerning the latter, De Bernardo *et al.*[9] mentioned pH, organic modifier content and concentration of reagent and analyte as important factors.

Under the conditions used, the retention time was about 3.7 min. Chromatograms of a blank and a spiked plasma sample are shown in Fig. 3. Investigations with an internal standard (bromine instead of chlorine in the pyridine ring) led to a decrease in the precision of the assay; therefore, the external standard method was preferred[10].

Selectivity

As already mentioned, selectivity was the main problem after extraction and derivatization of plasma samples, because of the many biogenic amines with structures similar to **1**. After derivatization with fluorescamine, separation became even more difficult. However, more than 30 human blank plasma samples have been analysed and more than 90% showed either no interference or a peak corresponding to less than 0.25 ng/ml of **1**. One of these blank plasma samples is shown in Fig. 3.

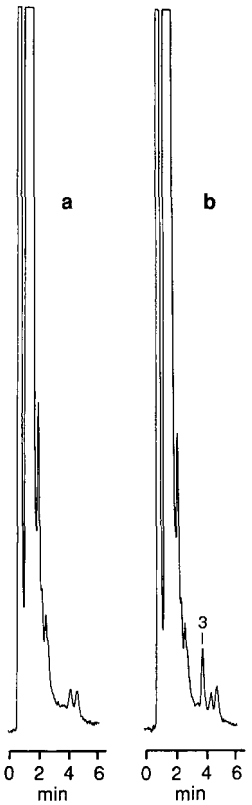

Fig. 3. Chromatograms of human plasma samples. (a) Blank plasma sample; (b) blank plasma sample spiked with 5 ng/ml of **1**. **3** is the fluorescamine derivative of **1**.

Levodopa, benserazide and other decarboxylase inhibitors, which could appear in the plasma of patients with Parkinson's disease, did not interfere with **1**. Dopamine at endogenous levels was well separated. After the administration of levodopa, higher levels of dopamine are expected because this substance is a metabolite of levodopa. Up to a few hundred ng/ml, no interference was observed. However, very high plasma levels of dopamine (μg/ml) would disturb the baseline during chromatography and prevent the determination of **1**.

For dog and rat plasma, the endogenous component eluting directly after **3** caused greater interference than for human plasma. Even though this interference affected quantification adversely only at concentrations below 5 ng/ml, the use of the HPLC method with UV detection for animal plasma determinations is recommended.

Care must be taken to follow the experimental conditions described exactly. Interfering peaks could also be generated by the use of impure solvents, reagents, tubes or by rubber or plastic stoppers.

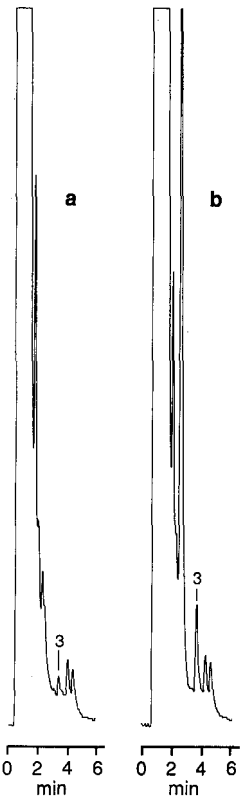

Fig. 4. (a) Chromatogram showing the quantification limit: human blank plasma sample, spiked with 1 ng/ml of **1**. (b) Chromatogram of a volunteer's plasma sample taken 4 h after a single dose of 10 mg of **1**. Measured concentration: 4.71 ng/ml.

Limit of quantification

The limit of quantification of **1** in plasma was 1 ng/ml using a 1-ml sample. A chromatogram of a spiked plasma sample at this concentration is shown in Fig. 4a. The inter-assay ($n = 8$) relative standard deviation (R.S.D.) at this concentration was 17.7% (see Table II). The detection limit, defined by a signal-to-noise ratio of 3:1, was *ca.* 0.5 ng/ml. However, at this concentration the calibration intercept and the precision of the method were found to be unacceptable.

Linearity

The correlation between peak height and concentration of **1** was linear over at least the range 0.5–500 ng/ml. The coefficients of determination (r^2) were better than 0.99, using the weighting factor $1/y^2$.

Recovery

The recovery (extraction yield) of **1** from human plasma was established as follows. Three concentrations of spiked plasma samples were analysed as described

TABLE I

RECOVERY OF 1 FROM HUMAN PLASMA (n = 5)

Concentration (ng/ml)	*Recovery (%)*	*R.S.D. (%)*
5	79.9	2.3
20	78.6	4.7
200	78.0	2.7

above, each in quintuplicate. A second series of samples was analysed simultaneously by extraction and back-extraction of blank plasma, and then adding **1** to the final extract. Recovery was calculated by comparing the peak heights for back-extracted spiked samples with those for the samples to which **1** had been added after back-extraction. The results are presented in Table I.

Reproducibility

The precision (defined as R.S.D. of replicate analyses) and the accuracy (defined as the difference between found and added concentrations) of the method were evaluated in inter-assay studies. In a first study, using calibration standards measured against an independent calibration set, one specimen was analysed on eight days over a period of 3 weeks. The results are given in Table II. Using quality control samples over 2–3 months, similar results were obtained, as shown in Table III. A precision of 3–8% in the concentration range 2–500 ng/ml is acceptable considering the rather extensive extraction and derivatization procedure.

Stability

The stability of **1** in human plasma was investigated by adding the drug to blank plasma at three different concentrations and storing it for 3 and 9 months at −20°C. The results of these stability tests, which were carried out according to our established method[11], are presented in Table IV. The data indicate that **1** is stable in human plasma for 9 months at −20°C, with the exception of the 500 ng/ml concentration, where a decrease of 10.2% after storage for 9 months was found. This corre-

TABLE II

INTER-ASSAY REPRODUCIBILITY FROM PLASMA STANDARDS (n = 8)

Concentration (ng/ml)		*R.S.D. (%)*	*Difference between found and added (%)*
Added	*Found*		
1	1.00	17.7	0.0
2	2.06	7.9	+3.0
5	5.00	7.7	0.0
20	19.6	4.7	−2.0
50	48.5	3.1	−3.0
200	199	3.5	−0.5
500	496	3.1	−0.8

TABLE III

INTER-ASSAY REPRODUCIBILITY FROM QUALITY CONTROL SAMPLES

Replicates (n)	*Concentration (ng/ml)*		*R.S.D. (%)*	*Difference between found and added (%)*
	Added	*Found*		
18	4.14	4.15	7.1	+0.2
21	4.16	4.06	7.2	−2.4
21	42.4	41.7	4.4	−1.7
22	42.7	42.1	6.4	−1.4
20	422	425	5.0	+0.7
21	423	418	5.7	−1.2

sponds exactly to the limit of the relevant instability (−10%)[11]. No instability could be observed when the drug was stored in human plasma at 22°C for 24 h (data not shown).

Surprisingly, severe instability was observed with dog plasma, amounting to −99.8% at 22°C after 24 h, and about −15% per month at −20°C. This decrease, which was not found with dog urine, was confirmed in metabolic studies[12], and could be explained by the presence of a plasma amine oxidase, which only exists in dog plasma[13]. The stability of **1** in rat plasma lay between those in human and dog plasma. In rat plasma, a decrease of nearly 10% after storage at 22°C for 25 h was found, whereas at −20°C no instability was observed after 5 weeks. Dog plasma could be stabilized by immediate addition of 1 *M* sodium hydroxide solution (50 µl/ml) to a plasma sample. In this way, the drug remained stable for 2 months at −20°C.

Application of the method to biological samples

The method was successfully applied to the analysis of more than 360 plasma samples from a tolerance study performed on volunteers. Fig. 4b shows a typical chromatogram, and Fig. 5 shows the good correlation between the concentrations of **1** from this study, as determined by the HPLC method with UV detection, and the precolumn derivatization method.

TABLE IV

STABILITY OF **1** IN HUMAN PLASMA ($n = 5$)

Storage conditions	*Concentration (ng/ml)*	*Change in concentration after storage (%)*	*90% confidence interval (%)*
3 months at −20°C	5	−4.0	−9.5 to +1.7
	50	−3.4	−7.7 to +1.1
	500	−0.9	−5.2 to +3.6
9 months at −20°C	5	−7.5	−9.9 to −5.0
	50	−6.1	−7.9 to −4.2
	500	−10.2	−12.1 to −8.2

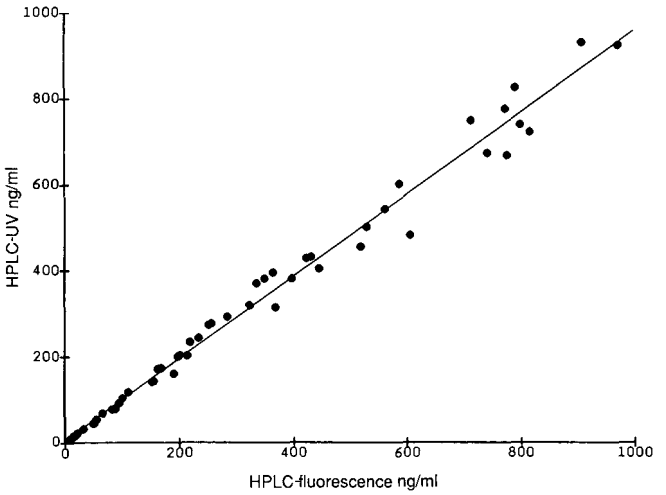

Fig. 5. Correlation between plasma concentrations of **1** as determined by HPLC with UV detection and HPLC with precolumn derivatization and fluorescence detection (n = 53, r^2 = 0.9860, y = 6.9731 + 0.9510x).

CONCLUSION

A specific HPLC method for the determination of **1** in human plasma was developed using precolumn derivatization with fluorescamine and fluorescence detection. The limit of quantification (1 ng/ml) was improved by a factor of five compared with the HPLC method with UV detection[4]. This should be sufficient to study the pharmacokinetic profile after the administration of therapeutic doses, and is much better than other methods using precolumn derivatization with fluorescamine for the determination of drugs in plasma, for which a quantification limit 10 ng/ml[14,15] or greater[16] has been reported. Whereas **1** proved to be stable in human plasma, severe instability was observed in dog plasma. Measures to overcome this instability have been presented.

ACKNOWLEDGEMENTS

The authors thank Mr. B. Maurer for the drawings and Drs. D. Dell and J. Burckhardt for correction of the manuscript.

REFERENCES

1 M. Da Prada, R. Kettler, H. H. Keller, E. Kyburz and W. P. Burkard, *Acta Pharm. Toxicol.*, 60 (1987) 10.
2 R. Zimmer, R. Kettler, K. Bauer and H. M. Thiede, unpublished results.
3 R. Geschke, J. Körner and H. Eggers, *J. Chromatogr.*, 420 (1987) 111.
4 R. Wyss and W. Philipp, unpublished results.
5 U. Timm, D. Dell and D. A. Ord, *Instrum. Comput.*, 3 (1985) 29.
6 S. Einarsson, B. Josefsson and S. Lagerkvist, *J. Chromatogr.*, 282 (1983) 609.

7 P. Lindroth and K. Mopper, *Anal. Chem.*, 51 (1979) 1667.
8 D. Dell, G. Wendt, F. Bucheli and K.-H. Trautmann, *J. Chromatogr.*, 344 (1985) 125.
9 S. De Bernardo, M. Weigle, V. Toome, K. Manhart, W. Leimgruber, P. Boehlen, S. Stein and S. Udenfriend, *Arch. Biochem. Biophys.*, 163 (1974) 390.
10 P. Haefelfinger, *J. Chromatogr.*, 218 (1981) 73.
11 U. Timm, M. Wall and D. Dell, *J. Pharm. Sci.*, 74 (1985) 972.
12 R. Jauch and P. Schmid, unpublished results.
13 A. P. Beresford, P. V. Macrae and D. A. Stopher, *Xenobiotica*, 18 (1988) 169.
14 G. J. de Jong, *J. Chromatogr.*, 183 (1980) 203.
15 M. Abrahamsson, *J. Pharm. Biomed. Anal.*, 4 (1986) 399.
16 A. J. Sedman and J. Gal, *J. Chromatogr.*, 232 (1982) 315.

Journal of Chromatography, 507 (1990) 199–220
Elsevier Science Publishers B.V., Amsterdam — Printed in The Netherlands

CHROMSYMP. 1696

Simultaneous analysis of theophylline, caffeine and eight of their metabolic products in human plasma by gradient high-performance liquid chromatography

TIMOTHY E. B. LEAKEY
Joint Academic Department of Child Health, Queen Elizabeth Hospital for Children, Hackney Road, London E2 8PS (U.K.)

SUMMARY

A method has been developed for the simultaneous determination of methylxanthines and many of their metabolites in plasma. Specially developed extraction columns (Celute-MX) were used and the extracts were separated on a 25-cm ODS column (particle size, 3 μm) at 50°C with a mobile phase gradient. The compounds were detected with a diode array detector at two analytical wavelengths. The value of drug to metabolite ratios has been explored and elevated ratios have been found when metabolic clearance was impaired by disease or co-administered drugs. Large concentrations of pharmacologically active metabolites have been found in renal failure. The assay has proved to be reliable and valuable in the elucidation of therapeutic and metabolic problems involving the methylxanthines.

INTRODUCTION

Caffeine (1,3,7-trimethylxanthine) and its demethylated metabolites paraxanthine (1,7-dimethylxanthine), theobromine (3,7-dimethylxanthine) and theophylline (1,3-dimethylxanthine) are ubiquitous in human plasma due to the almost universal dietary intake of coffee, tea and many soft drinks[1,2]. In addition, theobromine may be present as a consequence of chocolate consumption[2]. The presence of these pharmacologically active dietary methylxanthines may influence patient compliance with theophylline therapy which is frequently used in the treatment of asthma and chronic obstructive pulmonary disease; they may also complicate the evaluation and interpretation of theophylline therapeutic drug monitoring (TDM).

The methylxanthines are extensively metabolised by the hepatic microsomal mixed function oxidase (cytochrome P_{450}) system so that, for example, less than 10% of administered theophylline and less than 2% caffeine are excreted unchanged in the urine[3–6]. Many of these metabolites are pharmacologically active and the importance of considering their contribution to the total biological effect in TDM has been suggested, especially in cases of renal insufficiency or failure[7–9].

The hepatic clearance by the premature new-born of theophylline and caffeine,

0021-9673/90/$03.50

administered for the prevention of apnoea and bradycardia, is poor in comparison with children and adults[10]. A significant proportion of administered theophylline is N_7-methylated to caffeine which accumulates in plasma so that it may account for about a third of the total plasma methylxanthines in this group of patients[11].

Other co-administered drugs impair hepatic theophylline clearance and result in toxicity[12–14]; reduced clearance of drugs is a common complication of some forms of liver disease[15–18]. Fasting plasma caffeine concentrations and the determination of caffeine clearance may provide clinically valuable information for assessing the severity of hepatic dysfunction[19–21] because the routine biochemical liver function tests do not directly indicate cytochrome P_{450} status[16,22], which may provide clinically important indications of potentially abnormal drug metabolism.

The interrelationships of administered methylxanthines and their metabolic products that can be expected to occur in plasma are indicated in Fig. 1. This is very similar to the scheme which was proposed by Cornish and Christman[4] on the findings of their urine studies. 1,3-Dimethyluric acid is now recognized as the principal normal metabolite of theophylline in plasma[23] as well as in urine[4], and does not undergo any further metabolic conversion to 1-methyluric acid[24].

The present method had been developed with the aim of establishing the normal disposition of the administered methylxanthines and their metabolites in human plasma. The determination of the relationships between the drug and its metabolites should permit the identification of abnormal metabolism with more precision, and provide an explanation for toxic symptoms not resolved by results from less comprehensive, routine methylxanthine TDM assays.

EXPERIMENTAL

Equipment for high-performance liquid chromatography (HPLC)

A Perkin-Elmer series 2/2 pump unit (Perkin-Elmer, Beaconsfield, U.K.) was run in the gradient mode. The settings were optimized for each column with 250 × 4.5 mm I.D. 3-μm ODS Apex I columns [100 000 to 120 000 plates per meter (Jones Chromatography, Hengoed, CF8 1QA, Wales, U.K.)] were typically: flow-rate, 0.8 ml/min; gradient starting conditions, 0% A/(A + B); gradient rate, 2.1% A/min. The

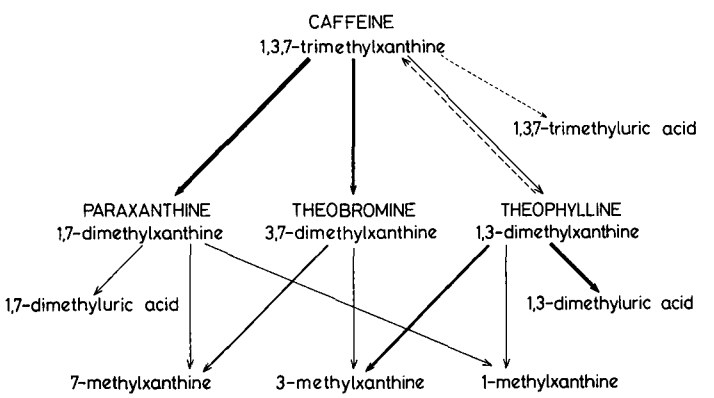

Fig. 1. Interrelationships of the methylxanthines and methyluric acids determined in plasma.

analytical column was maintained at 50°C with an HPLC column block heater (Jones Chromatography). To minimise the isocratic element at the start of the chromatograms the reconstituted extracts were injected 2.5 min after the gradient started. An ISS-100 autosampler (Perkin-Elmer) was used in the slave mode and controlled by the chromatography workstation (see below).

The methylxanthines and methyluric acids were determined with a UV absorbance detector. A Perkin-Elmer LC-75 set at 273 nm (with the absorbance range set at × 0.04) was used throughout the development of the method. Recently it was replaced with an LC-135 diode array UV detector (Perkin-Elmer). This has been used as a dual-wavelength detector so that the methyluric acids could be monitored closer to their λ_{max} (285 nm) without any loss of detector sensitivity for the methylxanthines (λ_{max} 273 nm). Channel 1 was set to 270 nm (band-width 15 nm) and channel 2 set to 285 nm with the same band-width.

The timed events for HPLC (gradient start, reset and autosampler start) were controlled by a Maxima™ chromatography workstation [software version 2.1, Dynamic Solutions Co. Ventura, CA, U.S.A. (purchased from Jones Chromatography] run on an IBM PC-AT (IBM, Basingstoke, U.K.) which was used for storing raw chromatographic data and all subsequent processing. The detector auto-zero was activated by the autosampler 2.4 min after the injection of the sample. Chromatographic data acquisition was started 2 min after sample injection and terminated after the last peak of interest (caffeine) at 25 min, to conserve space on the hard disk. A Hitachi 672-XD plotter (Jones Chromatography) was used to produce the chromatograms from data stored in Maxima™ that illustrate this work.

All the pipetting steps in the sample preparation were performed with a Hamilton Microlab-M equipped with a 250-μl syringe (1725 TLL) (V.A. Howe & Co., London, U.K.) except for reconstitution of the dried extracts, where a 1000-μl syringe (1001 TLL) was used.

All the water that was used to prepare the mobile phase and other aqueous solutions that were injected into the HPLC system was 'polished' before use with a Barnstead Water I apparatus (Gallenkamp, Loughborough, U.K.). This treatment effectively removed contaminants that accumulate in HPLC-grade water during storage. These were responsible for elevated back pressures which compromised the successful prolonged use of 25-cm 3-μm columns.

Reagents

Pure [purum grade >98% (HPLC)] 1-methylxanthine, 3-methylxanthine, 7-methylxanthine, 1-methyluric acid, 3-methyluric acid, 7-methyluric acid, 1,7-dimethylxanthine, 1,7-dimethyluric acid, 1,3-dimethylxanthine, 1,3-dimethyluric acid, 3,7-dimethylxanthine, 3,7-dimethyluric acid, caffeine and 1,3,7-trimethyluric acid were purchased from Fluka (Fluorochem, Glossop, U.K.). β-Hydroxyethyltheophylline from Sigma (Poole, U.K.). 3-Ethylxanthine was a gift from Napp Laboratories. (Cambridge, U.K.). HPLC-grade acetonitrile, methanol, water, tetrahydrofuran stabilised with butylated hydroxytoluene (BHT), dichloromethane and isopropanol from Rathburn (Walkerburn, U.K.). Sodium acetate (Aristar), acetic acid (Aristar), orthophosphoric acid (Analar) and triethanolamine (Analar) were supplied by BDH (Poole, U.K.).

The specially developed sample preparation columns (Celute-MX tubes) were

supplied by Jones Chromatography and Nucleopore 0.4-μm polyester filter membranes were from Sterilin (Hounslow, U.K.).

Glass test tubes (50 × 6 mm and 75 × 10 mm) and other glassware were purchased from Philip Harris Scientific (London, U.K.). Micro sample vials were supplied by Chromacol (London, U.K.).

Preparation of mobile phases

Stock acetate buffer was prepared by adjusting 20 m*M* sodium acetate to pH 4.0 with concentrated acetic acid[25]. Before storage, it was vacuum filtered through a 0.4-μm polyester membrane. For use it was diluted 1:1 with water.

The mobile phase for pump A was composed of 25% acetonitrile and 2.0% tetrahydrofuran (THF) in 10 m*M* acetate buffer, while that for pump B was 0.01% THF in 10 m*M* acetate buffer (all v/v). This latter solution was also used for the reconstitution of the plasma extracts and in the rinse reservoir of the ISS-100 autosampler. The ready mixed mobile phases were vacuum filtered through a 0.4-μm polyester membrane filter before use and degassed by maintaining under reduced pressure for a few minutes.

Preparation of internal standard solution

The primary internal standard, 3-ethylxanthine (approximately 2.2 mg) and a second reference compound, β-hydroxyethyltheophylline (approximately 3.4 mg) were dissolved with a few drops (<0.5 ml) triethanolamine in <5 ml water before being made up to 100 ml with stock (20 m*M*, pH 4.0) acetate buffer. Both compounds were designated as reference compounds in the Maxima component list. In addition, β-hydroxyethyltheophylline could be used in post-chromatographic analysis as an alternative internal standard in the event of there being a chromatographic interference with 3-ethylxanthine.

Sample preparation for HPLC analysis

Volumes of 100 μl of plasma or serum were added to 35 μl of internal standard in 50 × 6 mm glass test tubes. After mixing, they were transferred to Celute-MX sample preparation tubes. In each batch of up to 30 samples, the standard calibration plasma was included in quadruplicate. Ten minutes after the last transfer of sample to the Celute tubes the methylxanthines and methyluric acids were eluted with 2 × 1.5 ml isopropanol–dichloromethane (10:90, v:v) into 10 × 75 mm glass tubes. These extracts were evaporated to dryness in a block heater set to <37°C under a gentle stream of oxygen-free nitrogen. When dry, the extracts were reconstituted in 100 μl of mobile phase B, transferred to the injection vials and capped. Before they were loaded into the autosampler they were spun for 5 min in a refrigerated centrifuge (4400 rpm, MSE™ benchtop Chilspin, Fisons plc, Loughborough, U.K.) as a precaution against any small particulate material blocking the top frit of the analytical column. Normally, 20μl of the prepared sample (standard calibration plasma or unknows) were injected.

Preparation of standard calibration serum

The raw material for the standard calibration serum was pooled human serum. It was spun in a refrigerated centrifuge after which the fatty surface layer was re-

moved and the remaining fluid decanted from the pellet of debris. An aliquot of this pool was set aside for analysis.

Stock high concentration (approximately 100 mg/100 ml) aqueous solutions of all the analytes were prepared. These were used to spike the pooled serum to the intended approximate concentrations and the volume of the spiked serum made up to 1.0 l with more of the pooled blank serum. Since there were detectable concentrations of some of the methylxanthines in the blank, the precise concentrations in the calibration standard were determined as follows.

Of the blank serum, 20 aliquots were prepared for HPLC analysis according to the sample preparation method already described. Since the expected peak areas were small, 30 μl of the reconstituted sample were injected. The mean and standard deviation (S.D.) of the peak areas were determined. A further batch of 20 aliquots of the spiked serum were similarly prepared and analysed except that 20 μl were injected.

Using these data the concentration of the methylxanthines and methyluric acids in the spiked serum were determined.

Example for caffeine. The mean peak area for caffeine in the blank serum (determined from 20 × 30 μl injections) is 2.58 area counts (S.D. = 0.094). The volume of spiked serum injected was 20 μl, therefore, the corrected area for the blank is (2.58·20)/30 = 1.72 area counts.

The total volume of aqueous methylxanthines and methyluric acids added was 50 ml, therefore, the peak area for the blank in spiked serum is (1.72·950)/1000 = 1.63 area counts.

The mean peak area for the spiked serum determined from 20 × 20 μl injections was 11.99 area counts (S.D. = 0.54).

The peak area counts in the spiked serum which are due to the added caffeine = (peak area counts in the spiked serum) minus (volume-corrected peak area counts in the blank) = 11.99 − 1.64 = 10.35 area counts; 10 ml aqueous caffeine were added containing 53.03 μM.

Thus 53.03 μM caffeine gives 10.35 area counts. Therefore the total caffeine in the spiked serum is (added caffeine μM·area counts total caffeine)/area counts added caffeine = (53.03·11.99)/10.35 = 61.43 μM.

RESULTS AND DISCUSSION

Sample preparation

During the development of the sample preparation packing, the performance of batches of the Celute-MX tubes was assessed by determining the recoveries for all analytes together with the internal standards. An aqueous solution of the analytes was prepared from the concentrated stock solutions that were used for the preparation of the standard calibration plasma, and diluted to approximately the same concentration. Plasma was avoided because injection of unextracted plasma samples would severely reduce the life-expectancy of the analytical column. Provided that the conditioned Celite had sufficient buffering capacity to adjust the pH of plasma to the optimal value for the extraction, this test gave a valuable indication of how well it would perform with plasma samples.

Internal standard solution (35 μl) was added to each of fifteen 100-μl aliquots of aqueous standard solution. Five of these were transferred directly to injection vials

(the non-extracted standards), capped and were subsequently used to calibrate the analytical method. The remaining ten aliquots were carried through the sample preparation procedure described in the method, but the residues were reconstituted to 135 μl rather than 100 μl so that the dilution was the same as that of the non-extracted calibration standards. Of each of the fifteen samples 25 μl were injected into the HPLC system.

The recoveries of all the compounds including the two internal standards were assessed by external standard analysis calibrated to the mean of the five non-extracted aqueous injections. Internal standard analysis of the same data was also performed, and the results of a typical Celute-MX batch test are shown in Table I. Comparison of the recoveries assessed by internal and external standard analysis provided an indication of the magnitude of the liquid handling losses. The internal standard analysis results of $>100\%$ indicated that the recovery of the internal standard was not as good as that of the dimethylxanthines and caffeine, which was confirmed by the external standard analysis figures.

Initial studies using acetonitrile precipitation[26] or isopropanol–chloroform (10:90)[27] showed that extraction of the monomethylxanthines was poor or non-existent from these neutral conditions. Subsequent studies including the methyluric acids and during evaluation of a bonded phase sample preparation method[28] confirmed these findings. The extraction of the monomethylxanthines and dimethyluric acids was significantly improved when the sample was acidified with a small quantity of orthophosphoric acid prior to extraction with dichloromethane–isopropanol. The bonded phase method could be similarly modified to include all the analytes by the use of acidic water (pH 4.0 with orthophosphoric acid) for the wash steps. Unfortunately, this was accompanied by a serious increase in the number and frequency

TABLE I

CELUTE-MX BATCH TEST

Devised to assess the performance of individual batches of the conditioned celite, Celute-MX. Details in discussion of sample preparation.

Compound	*Internal standard analysis*		*External standard analysis*	
	Mean (μM)	*Yield (%)*	*Mean (μM)*	*Yield (%)*
7-Methylxanthine	14.62	89.7	13.63	83.6
3-Methylxanthine	15.27	96.0	14.25	89.5
1-Methylxanthine	17.02	99.7	15.88	93.0
1,3-Dimethyluric acid	20.34	95.4	18.97	89.0
3,7-Dimethylxanthine	27.87	101.5	26.00	94.7
3-Ethylxanthine (int. std)	(50.00)	(100.0)	46.65	93.3
1,7-Dimethyluric acid	9.78	96.2	9.13	89.7
1,7-Dimethylxanthine	24.82	101.4	23.15	94.6
1,3-Dimethylxanthine	58.40	101.2	54.48	94.4
1,3,7-Trimethyluric acid	9.39	101.0	8.76	94.2
β-Hydroxyethyltheophylline	50.45	100.9	47.07	94.1
1,3,7-Trimethylxanthine	60.28	101.4	58.11	94.6

of chromatographic interferences which seriously reduced the reliability of the method. Other alternatives using bonded phases, suggested by Dr. P. A. Harris (Analytichem)[29] and Professor M. Burk (University of Arizona)[30], were found to be unable to retain the full range of related compounds that are extracted by Celute-MX from plasma.

The efficiency and convenience of the extraction was improved by the use of Chem-Elut™ tubes (formally Clin-Elut, from Analytichem). Celite in these tubes provides a solid support for the liquid–liquid extraction but was found to produce variable recoveries for the metabolites. The pH of damp native Celite was found to be alkaline[31], and the extraction of the metabolites was found to be unreliable if the bed was not acidified throughout the full length. This was improved if the Celite was preconditioned and buffered so that the tubes were homogeneous from top to bottom.

The Celite packing for the Celute-MX tubes has been developed empirically and conditioned to give maximal recoveries of the 10 related compounds. In practice, the Celute Batch Test has provided valuable data for the assessment of extraction performance, and has been found to give a good indication of expected efficiency when used to extract methylxanthines and methyluric acids from plasma, confirming the observations for theophylline, theobromine and caffeine that there is no difference between extraction from water or plasma when the sample is acidified[32]. In addition, each batch was tested with the standard plasma in order to establish that the buffering capacity of the Celute-MX was sufficient to adjust the plasma samples to the optimum pH for the extraction. If this was inadequate, the recovery of the metabolites was inferior, the dimethyluric acids being the most vulnerable.

The recovery of monomethyluric acids was poor using the Celute-MX columns, and attempts to improve their yields were abandoned when it was realised that they were accompanied by a reduction in selectivity; the increased occurrence of chromatographic interferences made the method unreliable. 3,7-Dimethyluric acid was not included as C_8-oxidation of theobromine is not thought to occur in humans[33] and with the present instruments it was not possible to reliably separate it from 3-methylxanthine.

Gradient vs. isocratic elution

The monomethylxanthines were not retained or separated in the isocratic method[25] that was initially employed, and when the concentration of acetonitrile in the mobile phase was reduced to overcome this problem, there was an unacceptable increase in the retention times for theophylline and caffeine. In a detailed study of the retention behaviour of the methylxanthines[2], the capacity factors [$k' = (t_R - t_0)/T_0$, where t_R is the retention time of the compound and t_0 the retention time of an unretained compound] for the analytes included in this assay were shown to range from 1.83 to 29.00 (Table II). A chromatogram of the standard calibration plasma is given in Fig. 2, and shows how the use of a mobile phase gradient enabled adequate retention and separation of the early eluting compounds without unacceptably wide caffeine and theophylline peaks. The k' in this gradient system (k'_{grad}) at 50°C are given in Table II and range from 0.87 to 3.43.

Maintaining the analytical column at 50°C ensures reproducible separations and requires lower concentrations of organic solvent[34]. Separation of paraxanthine

TABLE II

CONCENTRATION AND RETENTION DATA FOR CHROMATOGRAM OF THE STANDARD CALIBRATION PLASMA (FIG. 2).

Capacity factors for each compound separated at 50°C by gradient elution (k'_{grad}) were calculated from the equation $(t_R - t_0/t_0)$. The capacity factors determined in isocratic conditions at room temperature[2] are included for comparison.

Peak label	*Compound*	*Concentration (μM)*	t_R *(min)*	k'_{grad} *(50°C)*	k' *(ref. 2)*
7-mx	7-Methylxanthine	16.3	8.52	0.87	1.83
3-mx	3-Methylxanthine	15.9	9.42	1.07	2.46
1-mx	1-Methylxanthine	17.1	10.13	1.23	3.00
1,3-di m-ua	1,3-Dimethyluric acid	21.3	11.87	1.61	2.95
Theobromine	3,7-Dimethylxanthine	27.5	12.48	1.74	5.21
3-ex (int.std.)	3-Ethylxanthine	–	13.64	2.00	–
1,7-di m-ua	1,7-Dimethyluric acid	10.2	14.19	2.12	3.39
Paraxanthine	1,7-Dimethylxanthine	24.5	15.20	2.34	8.00
Theophylline	1,3-Dimethylxanthine	57.7	15.60	2.43	9.16
1,3,7-tri m-ua	1,3,7-Trimethyluric acid	9.3	16.95	2.73	7.78
β-OH-et (ref.)[a]	β-Hydroxyethyltheophylline	–	17.61	2.87	–
Caffeine	1,3,7-Trimethylxanthine	61.4	20.17	3.43	29.00

[a] ref. = Reference compound in Maxima component list. This and the int. std (also designated ref.) are used to determine the relative retention times of the component peaks and ensures correct peak indentification.

from theophylline was achieved by the addition of the polar modifier THF to mobile phase A, and this also helped the separation of 1,3-dimethyluric acid from theobromine.

The main reason for continuation of the gradient so long after caffeine has eluted is to ensure the elution of trimethoprim and sulphamethoxazole (the constituents of Septrin and Bactrim). If these late eluting compounds remain on the column at the end of the gradient they come off in the following chromatograms as very wide peaks. The ability to use a purge step (of mobile phase A or stronger solution of acetonitrile) would permit a considerable reduction in the full cycle time, thereby increasing the throughput of samples.

Method validation

Within-run (n = 20) and between-run (n = 26) precision studies were conducted on pools of low (P0), medium (P3), high (P2) and very high (P1) spiked human serum and the results using the LC-75 UV detector are given in Tables III and V. The between run data were acquired over a period of six months; every time a batch of standards and samples was set up for analysis the set of four precision test samples was included and the results set aside until a sufficient number had been acquired. Four different batches of Celute-MX packing were used during this period. The precision tests have been repeated with the recently acquired diode array detector, and the results are given in Tables IV and VI.

The within-run and between-run precision tests using the LC-75 UV detector were mediocre for the methylxanthines, the lower concentrations of acceptable preci-

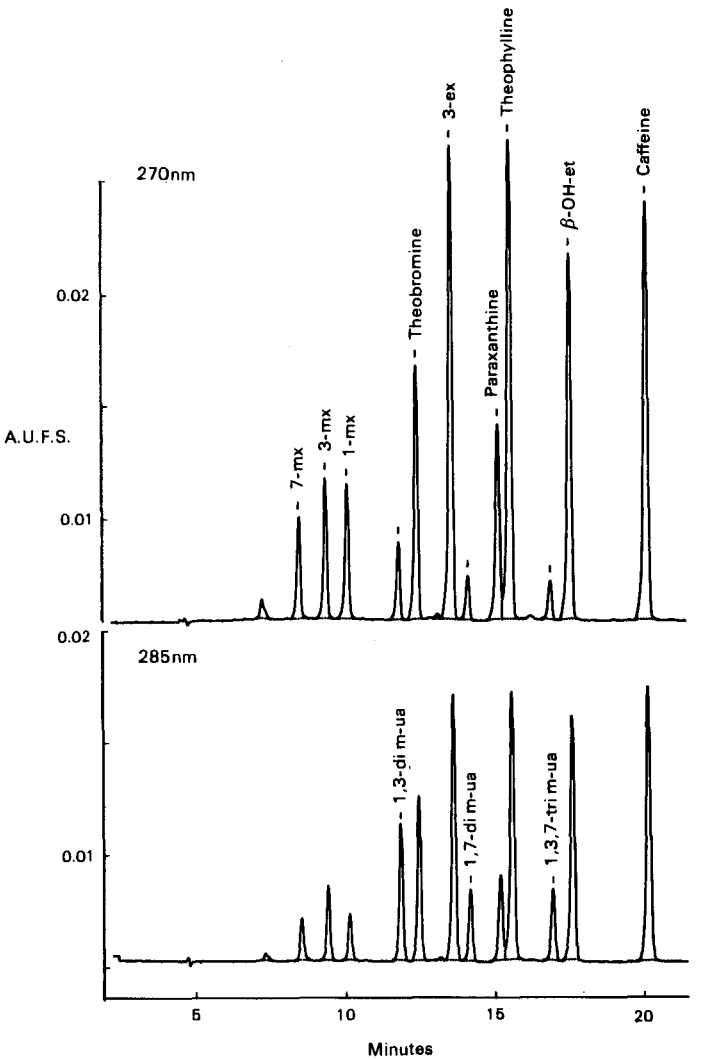

Fig. 2. Chromatogram of the current standard calibration plasma. Concentrations, abbreviations and retention data are given in Table I.

sion being in excess of 3.0 μM and rather higher for the methyluric acids where these latter were being detected well away from their maximum absorption wavelength (λ_{max} = 285 nm). The use of a second detector set to the λ_{max} of the methyluric acids improved the precision for low concentrations of these compounds.

The minimum concentration for acceptable precision [coefficient of variation (C.V.) = 5%] with the present instruments and an injection volume of 20 μl is 1.5–2.0 μM and is linear to 500 μM. At 285 nm the internal standard (3-ethylxanthine) is not being detected at its λ_{max}, but as this is a consistently large peak, the errors are less significant than those resulting from determination of low concentrations of methyluric acids at 273 nm. The performance is critically dependent upon the sample prep-

TABLE III

WITHIN-RUN PRECISION STUDY WITH LC-75 DETECTOR (n = 20)

Compound	*P0*	*P3*	*P2*	*P1*
7-Methylxanthine				
Mean (μM)	0.20	6.43	28.83	55.13
S.D.	0.11	0.28	1.56	1.45
C.V. (%)	55.1	4.4	5.4	2.6
3-Methylxanthine				
Mean (μM)	2.51	8.36	28.06	53.66
S.D.	0.16	0.21	0.56	1.10
C.V. (%)	6.5	2.5	2.0	2.0
1-Methylxanthine				
Mean (μM)	0.31	5.50	23.67	48.80
S.D.	0.14	0.17	0.38	0.81
C.V. (%)	44.5	3.0	1.6	1.6
1,3-Dimethyluric acid				
Mean (μM)	4.47	20.84	45.39	64.21
S.D.	0.40	0.30	0.80	1.75
C.V. (%)	9.0	1.4	1.8	2.7
Theobromine				
Mean (μM)	3.17	28.45	77.53	216.62
S.D.	0.22	0.15	0.79	6.86
C.V. (%)	6.9	0.5	1.0	3.1
1,7-Dimethyluric acid				
Mean (μM)	4.25	7.89	11.37	12.25
S.D.	0.39	0.23	0.34	0.65
C.V. (%)	9.2	3.0	3.0	5.3
Paraxanthine				
Mean (μM)	2.59	13.05	33.68	92.26
S.D.	0.33	0.18	0.32	3.22
C.V. (%)	12.6	1.4	0.9	3.5
Theophylline				
Mean (μM)	39.21	67.38	123.46	283.06
S.D.	0.43	0.43	0.96	10.60
C.V. (%)	1.1	0.6	0.8	3.7
1,3,7-Trimethyluric acid				
Mean (μM)	3.86	7.87	13.02	22.10
S.D.	0.46	0.21	0.40	0.57
C.V. (%)	11.9	2.7	3.1	2.5
Caffeine				
Mean (μM)	6.47	32.12	80.59	223.61
S.D.	0.43	0.39	0.80	11.45
C.V. (%)	6.4	1.2	1.0	5.1

aration and a better understanding of the mechanism might lead to more uniform yields and improved precision. However, this group of compounds exhibits a wide range of polarity and other chromatographically important parameters, so the necessity for some compromise should be anticipated. In the latter case, priority should be

TABLE IV

WITHIN-RUN PRECISION STUDY WITH LC-135 DETECTOR (n = 20)

Compound	*P0*	*P3*	*P2*	*P1*
7-Methylxanthine				
Mean (μM)	0.55	6.75	30.98	56.54
S.D.	0.77	0.33	1.32	1.21
C.V. (%)	11.9	4.9	4.3	2.1
3-Methylxanthine				
Mean (μM)	2.61	8.52	25.83	55.36
S.D.	0.11	0.18	0.56	0.85
S.V. (%)	4.1	2.1	2.2	1.5
1-Methylxanthine				
Mean (μM)	0.81	5.64	22.98	49.04
S.D.	0.05	0.09	0.18	0.60
C.V. (%)	6.8	1.5	0.8	1.2
1,3-Dimethyluric acid				
Mean (μM)	4.85	21.44	47.17	66.10
S.D.	0.16	0.47	1.46	1.23
C.V. (%)	3.2	2.2	3.1	1.9
Theobromine				
Mean (μM)	3.66	29.06	83.85	209.79
S.D.	0.09	0.39	1.03	3.10
C.V. (%)	2.5	1.4	1.2	1.5
1,7-Dimethyluric acid				
Mean (μM)	3.85	8.25	11.84	12.87
S.D.	0.26	0.23	0.34	0.26
C.V. (%)	6.8	2.8	2.9	2.0
Paraxanthine				
Mean (μM)	3.01	13.31	33.90	87.43
S.D.	0.11	0.19	0.33	1.22
C.V. (%)	3.7	1.4	1.0	1.4
Theophylline				
Mean (μM)	40.67	68.12	123.34	270.27
S.D.	0.59	0.92	1.13	2.66
C.V. (%)	1.4	1.4	0.9	1.0
1,3,7-Trimethyluric acid				
Mean (μM)	4.47	7.94	13.22	21.22
S.D.	0.22	0.13	0.16	0.21
C.V. (%)	4.9	1.6	1.2	1.0
Caffeine				
Mean (μM)	7.72	32.54	80.48	212.33
S.D.	0.20	0.58	1.06	3.33
C.V. (%)	2.6	1.8	1.3	1.6

given to the major metabolites of caffeine and theophylline, namely paraxanthine and 1,3-dimethyluric acid, since these have been found to be the most valuable in the investigation of abnormal cases.

The occurrence of co-chromatographic interferences with the analytes and in-

TABLE V

BETWEEN-RUN PRECISION STUDY WITH LC-75 DETECTOR (n = 26)

Compound	*P0*	*P3*	*P2*	*P1*
7-Methylxanthine				
Mean (μM)	0.65	7.52	29.13	56.28
S.D.	0.81	0.66	1.58	3.42
C.V. (%)	124.0	8.7	5.4	6.0
3-Methylxanthine				
Mean (μM)	2.52	8.39	28.31	53.87
S.D.	0.29	0.37	0.75	1.39
S.V. (%)	11.6	4.4	2.7	2.6
1-Methylxanthine				
Mean (μM)	0.49	5.87	23.75	47.91
S.D.	0.35	0.77	1.01	1.76
C.V. (%)	71.8	13.0	4.3	3.7
1.3-Dimethyluric acid				
Mean (μM)	4.78	21.17	47.38	64.46
S.D.	0.74	1.24	1.01	2.92
C.V. (%)	15.4	5.8	2.1	4.5
Theobromine				
Mean (μM)	3.60	28.95	79.30	206.63
S.D.	0.52	0.65	1.22	3.31
C.V. (%)	14.5	2.3	1.5	1.6
1,7-Dimethyluric acid				
Mean (μM)	3.67	7.50	11.63	12.66
S.D.	0.54	0.58	0.70	0.96
C.V. (%)	14.8	7.8	6.0	7.6
Paraxanthine				
Mean (μM)	2.71	13.40	34.50	88.02
S.D.	0.47	0.59	0.55	1.65
C.V. (%)	17.2	4.4	1.6	1.9
Theophylline				
Mean (μM)	39.86	68.62	125.30	268.33
S.D.	0.97	1.35	1.78	3.52
C.V. (%)	2.4	2.0	1.4	1.3
1,3,7-Trimethyluric acid				
Mean (μM)	4.17	7.94	13.57	22.93
S.D.	0.77	0.81	1.05	1.46
C.V. (%)	18.5	10.2	7.7	6.4
Caffeine				
Mean (μM)	7.20	32.43	82.44	208.20
S.D.	0.66	1.09	1.45	5.52
C.V. (%)	9.2	3.4	1.8	2.7

ternal standards have been found to be rare, but may occasionally be suspected from the peak shape or from unusual drug to metabolite ratios. An example of an interference with the internal standard is given in Fig. 5. In this case β-hydroxyethyltheophylline was used as the internal standard to overcome the problems arising from

TABLE VI

BETWEEN-RUN PRECISION STUDY WITH LC-135 DETECTOR (n = 14)

Compound	*P0*	*P3*	*P2*	*P1*
7-Methylxanthine				
Mean (μM)	0.66	7.11	29.35	57.80
S.D.	0.58	0.89	1.50	2.83
C.V. (%)	86.9	12.5	5.1	4.9
3-Methylxanthine				
Mean (μM)	2.77	8.57	29.07	56.22
S.D.	0.19	0.36	1.47	1.80
C.V. (%)	7.0	4.2	5.1	3.2
1-Methylxanthine				
Mean (μM)	0.69	5.67	23.91	49.51
S.D.	0.32	0.25	0.51	1.71
C.V. (%)	45.6	4.5	2.1	3.5
1,3-Dimethyluric acid				
Mean (μM)	5.00	21.38	47.57	66.85
S.D.	0.44	1.40	1.77	2.60
C.V. (%)	8.9	6.6	3.7	3.9
Theobromine				
Mean (μM)	4.05	30.03	81.23	214.07
S.D.	0.29	0.84	2.87	8.27
C.V. (%)	7.3	2.8	3.5	3.9
1,7-Dimethyluric acid				
Mean (μM)	3.97	7.94	11.49	12.21
S.D.	0.27	0.55	0.88	1.07
C.V. (%)	6.9	6.9	7.7	8.7
Paraxanthine				
Mean (μM)	3.17	14.02	34.88	89.71
S.D.	0.35	0.49	1.35	3.33
C.V. (%)	10.9	3.5	3.9	3.7
Theophylline				
Mean (μM)	42.13	70.41	127.76	275.03
S.D.	1.62	2.36	4.75	11.32
C.V. (%)	3.8	3.4	3.7	4.1
1,3,7-Trimethyluric acid				
Mean (μM)	4.48	8.04	12.78	21.16
S.D.	0.55	0.50	1.05	1.99
C.V. (%)	12.4	6.2	8.2	9.4
Caffeine				
Mean (μM)	8.40	34.18	84.83	217.78
S.D.	0.65	1.24	3.34	9.14
C.V. (%)	7.8	3.6	3.9	4.2

the inadvertent installation of a column requiring a different composition of mobile phase in order to achieve acceptable separation. Examination of the maximum absorption wavelength, peak purity indices (both available from the LC-135 print-out) and the peak area absorption ratios (Table VII) may be used to confirm or refute

these suspicions. Metronidazole, paracetamol (Fig. 6) and some of the cephalosporin antibiotics are frequently observed in the chromatograms. The major reason for the use of an alternative internal standard was the increasing occurrence of the cephalosporins since many of these antibiotics had similar retention times to β-hydroxyethyltheophylline which was the only internal standard used at that time.

There has been good correlation between plasma theophylline levels determined by this method and other commercial assays including Abbot's TDX® (Abbot Laboratories, Maidenhead, U.K.) and Syva's EMIT™ (Syva U.K., Maidenhead, U.K.). A small number of samples that produced higher theophylline levels by the Ames Seralyzer® (Miles Laboratories, Slough, U.K.) than by TDX, EMIT and HPLC[35], were found by this method to contain exceptionally high levels of theophylline metabolites, principally 1,3-dimethyluric acid (>100 μM) and the chromatograms were typical of renal failure patients being treated with theophylline (Fig. 4)[36].

Early in the development of this method the recovery of caffeine was extremely unreliable. The temperature (>60°C) used for evaporation of the organic extracts was found to be responsible and reduction of the temperature of the hot block to <37°C improved the precision to values similar for other compounds in the assay. The explanation is thought to be that caffeine, unlike theophylline, sublimes (178°C)[37], and care should therefore be taken with the evaporation step. Examination of the precision tests with the LC-75 indicate that this might be a contributory factor in the inferior reproducibility for caffeine in comparison with dimethylxanthines.

Clinical applications

For patients with normal hepatic cytochrome P_{450} and renal function the concentration of plasma methylxanthine metabolites has been found to depend upon the concentration of the parent drug. A numerical expression of the relationship was required to establish the normal ranges that had been observed and to accommodate

TABLE VII

MAXIMUM ABSORPTION WAVELENGTHS AND PEAK AREA ABSORBANCE RATIOS

Compound	*Maximum absorption wavelength (nm)*[a]	*Peak area ratio (270 nm to 285 nm)*[b]
7-Methylxanthine	269	2.27
3-Methylxanthine	271	1.81
1-Methylxanthine	268	2.94
1,3-Dimethyluric acid	287	0.56
3.7-Dimethylxanthine	274	1.53
3-Ethylxanthine (int std.)	271	1.77
1,7-Dimethyluric acid	285	0.62
1,7-Dimethylxanthine	270	2.28
1,3-Dimethylxanthine	271	1.78
1,3,7-Trimethyluric acid	289	0.58
β-Hydroxyethyltheophylline	274	1.48
1,3,7-Trimethylxanthine	274	1.51

[a] Determined with a Perkin-Elmer LC-135 diode array detector.

[b] Determined from the peak of the within-run test plasma P2 (Table V), band-width for both wavelengths = 15 nm (*i.e.*, 262.5–277.5 nm for the 270 nm channel, and 277.5–292.5 nm for the 285 nm channel).

the considerable range of drug concentrations that were encountered. Molar ratios were the most obvious and the convention 'drug to metabolite' was chosen because the whole numbers normally obtained were considered to be more convenient to assess than the reciprocal values.

Some metabolites may be formed from two compounds (Fig. 1). For example, 3-methylxanthine is a demethylated product of both theobromine and theophylline and therefore a ratio for theophylline to 3-methylxanthine in the presence of significant concentrations of (dietary) theobromine would not accurately reflect either the demethylation of theophylline or the clearance of 3-methylxanthine. This difficulty is overcome to some extent by inclusion of both possible sources of the metabolite; in this case (theobromine + theophylline) to 3-methylxanthine. However, this is not a complete solution because the demethylation of both compounds is uneven[4,33].

The drug to metabolite ratios have been determined on a large number of samples, and values for the normal ranges of the main groups of patients that are served by this laboratory are given in Table VIII. These should be regarded as preliminary since the majority of the samples used to obtain these data was apparently taken at random with respect to dose and time. Other studies have shown that these ratios vary depending upon the dose-to-sample interval[38] and better documentation is necessary to establish the normal ranges with more precision. In practice, the most valuable ratios have proved to be caffeine to paraxanthine and theophylline to 1,3-dimethyluric acid. That is, ratios including metabolites which have no other source in plasma than the cytochrome P_{450} mediated conversion of the parent compound.

The drug to metabolite ratios have been extremely useful for the interpretation of results on exceptionally toxic samples from patients who have deliberately taken an overdose of theophylline. For example, a theophylline to 1,3-dimethyluric acid ratio

TABLE VIII

PRINCIPAL DRUG TO METABOLITE MOLAR RATIOS DETERMINED IN PLASMA OF FOUR GROUPS OF PATIENTS

Ratio	*Mean*	*S.D.*	*Suggested normal range (mean ± S.D.)*
Group I: neonates treated with caffeine (n = 186)			
Caffeine to paraxanthine	57.4	21.6	35.8–79.0
Caffeine to theobromine	52.4	21.5	30.9–73.9
Caffeine to theophylline	39.6	13.7	25.9–53.3
Group II: neonates treated with theophylline (n = 221)			
Theophylline to caffeine	3.7	2.7	1.0–6.4
Theophylline to 1,3-dimethyluric acid	22.2	9.0	13.2–31.2
Group III: children treated with theophylline (n = 159)			
Theophylline to 1,3-dimethyluric acid	15.2	6.8	8.4–22.0
(Theophylline + theobromine) to 3-methylxanthine	31.0	17.7	13.3–48.7
Caffeine to paraxanthine	2.1	1.8	0.3–3.9
Group IV: adults treated with theophylline (n = 50) (small group investigated as part of a correlation study)			
Theophylline to 1,3-dimethyluric acid	11.3	3.5	7.8–14.8
Caffeine to paraxanthine	2.0	0.9	0.3–3.9

within the normal range has been demonstrated for a plasma theophylline concentration of 736 μM (132 mg/l), indicating that the ratios are to a great extent independent of concentration. In other situations they may be used to estimate the quantity of metabolite that would be expected for a given concentration of parent drug and hence gauge the magnitude of metabolic impairment.

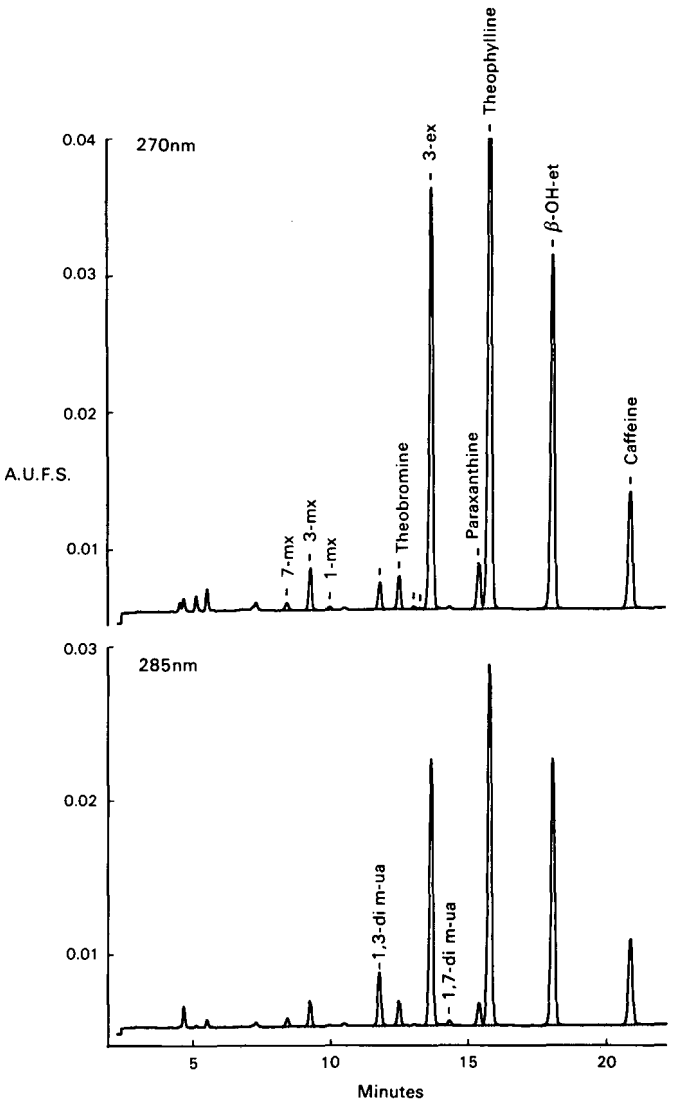

Fig. 3. Theophylline within the recommended therapeutic range, moderate caffeine intake and a normal plasma methylxanthine profile. For abbreviations, see Table II. Concentrations: 7-methylxanthine, 1.0 μM; 3-methylxanthine, 4.8 μM; 1-methylxanthine, 0.4 μM; 1,3-dimethyluric acid, 6.7 μM; theobromine, 3.9 μM; 1,7-dimethyluric acid, 0.6 μM; paraxanthine, 6.6 μM; theophylline, 78.0 μM; 1,3,7-trimethyluric acid, 0.0 μM; caffeine, 19.0 μM. Drug to metabolite ratios (suggested normal reagents in parenthesis): theophylline to 1,3-dimethyluric acid, 11.7 (7.8–14.8); (theophylline + theobromine) to 3-methylxanthine, 17.2 (15.0–50); caffeine to paraxanthine, 2.9 (0.3–3.9); paraxanthine to 1,7-dimethyluric acid, 11.0 (8.0–20).

EXAMPLES

The normal adult plasma methylxanthine profile has been included for comparison with the abnormal examples which demonstrate situations when this assay has been of value and should result in a revision of the therapeutic management.

Theophylline within the recommended therapeutic range, moderate caffeine intake and a normal plasma methylxanthine profile (Fig. 3)

This shows a typical plasma methylxanthine profile for an adult with a moderate dietary caffeine intake and who is receiving theophylline therapy for asthma. The plasma concentration of theophylline, 78.0 μM (15 mg/l), is within the recommended therapeutic range of 55–110 μM (10–20 mg/l) and 1,3-dimethyluric acid is present at the expected concentration for normal theophylline C_8-oxidation and renal clearance. The majority of the 3-methylxanthine is the product of N_1-demethylation of theophylline. The paraxanthine and theobromine concentrations are consistent with normal hepatic clearance of caffeine and no dietary theobromine. The presence of 1,7-dimethyluric acid in samples from caffeine-consuming adults is normal. A value for the paraxanthine to 1,7-dimethyluric acid ratio similar to that of the other C_8-oxidation ratio (theophylline to 1,3-dimethyluric acid) is a common finding.

Gross accumulation of theophylline metabolites in renal failure (Fig. 4)

It is shown here that the theophylline concentration of 213 μM (38 mg/l) is well above the recommended therapeutic range and would be expected to cause serious clinical symptoms of theophylline toxicity. In addition, the gross accumulation of both principal theophylline metabolites is consistent with renal failure[36]. Both compounds are pharmacologically active and contribute significantly to the toxic condition[8,9]. The accumulation of 1,3-dimethyluric acid confirms the report that it does not undergo further demethylation to form 1-methyluric acid[24]. 1,3,7-trimethyluric acid was detected and its identity confirmed by the 270 to 285 nm absorbance ratio.

The probable reason for the toxic level of theophylline in this case is clinical overdose because the hepatic clearance of theophylline is not affected by renal failure[39]. Theophylline toxic symptoms occur in renal failure cases even when the plasma concentration is below the therapeutic range[36] and therefore its use in this condition should only be considered when the metabolites can be monitored to establish that the form of renal support employed (*e.g.*, haemodialysis) is able to remove them from plasma.

Theophylline toxicity due to hepatic clearance impaired by another drug (Fig. 5)

The theophylline concentration of 262 μM (47 mg/l) (Fig. 5) confirmed the clinical diagnosis of theophylline toxicity. The mean adult theophylline to 1,3-dimethyluric acid ratio of 11.3 (Table VIII), indicates that the expected concentration for 1,3-dimethyluric acid would be 23 μM. The level of 1.8 μM is $<10\%$ of the expected concentration and suggests that C_8-oxidation is seriously impaired causing theophylline accumulation through diminished hepatic clearance. The possibility of an adverse drug reaction was suspected and subsequently it was confirmed that the patient had recently completed a ten-day course of erythromycin.

Experience has shown that in cases of theophylline overdose, caffeine to paraxanthine ratios in the range 5 to 9 are not unusual and are thought to reflect caffeine

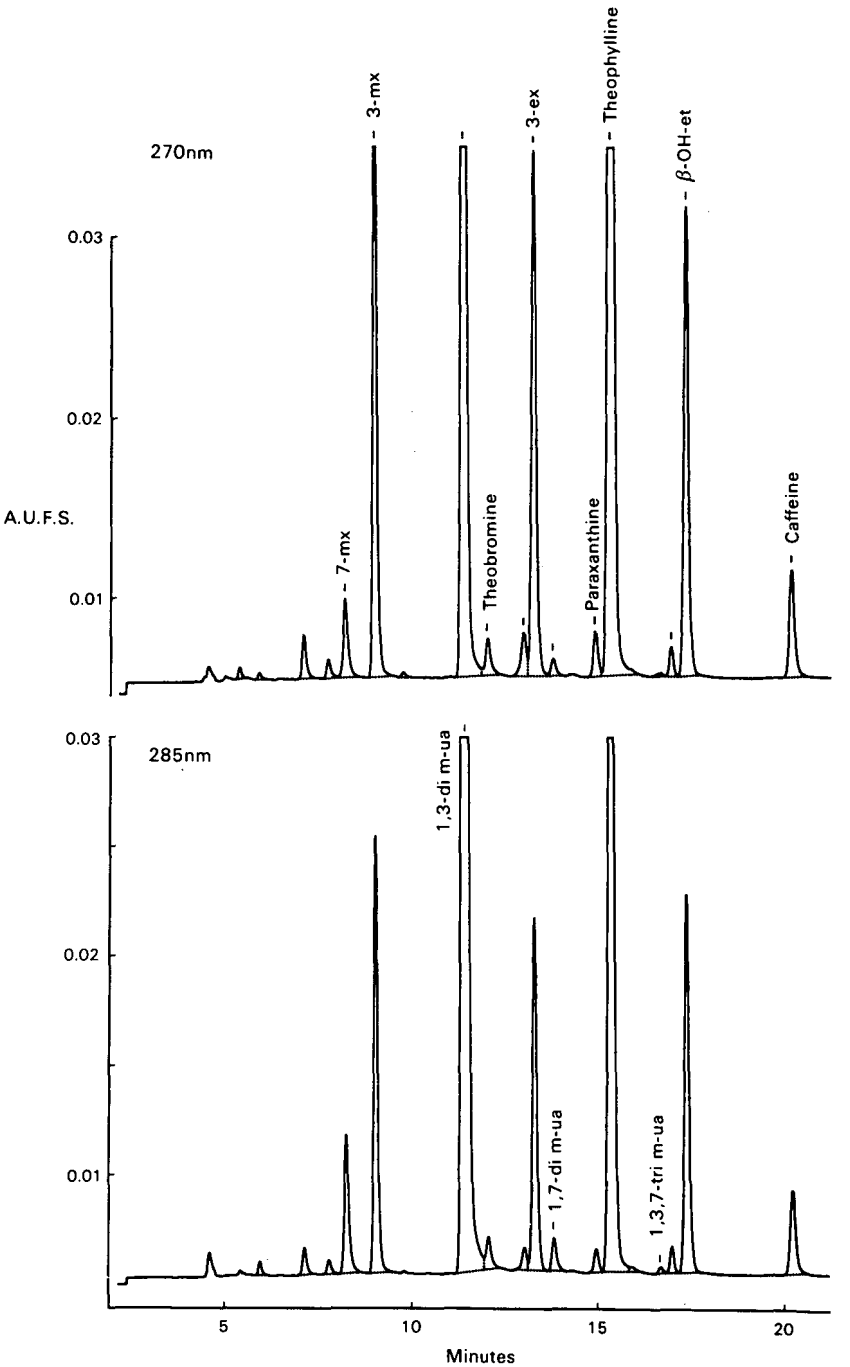

Fig. 4. Gross accumulation of theophylline metabolites in renal failure. For abbreviations, see Table II. Concentrations: 7-methylxanthine, 0.0 μM; 3-methylxanthine, 61.4 μM; 1-methylxanthine, 0.4 μM; 1,3-dimethyluric acid, 522.4 μM; theobromine, 4.5 μM; 1,7-dimethyluric acid, 4.6 μM; paraxanthine, 5.0 μM; theophylline, 213.2 μM; 1,3,7-trimethyluric acid, <1.0 μM; caffeine, 13.7 μM. Drug to metabolite ratios (suggested normal ranges in parenthesis): theophylline to 1,3-dimethyluric acid, 0.4 (7.8–14.8); (theophylline + theobromine) to 3-methylxanthine, 3.6 (15–50); caffeine to paraxanthine, 2.7 (0.3–3.9); paraxanthine to 1,7-dimethyluric acid, 1.1 (8.0–20).

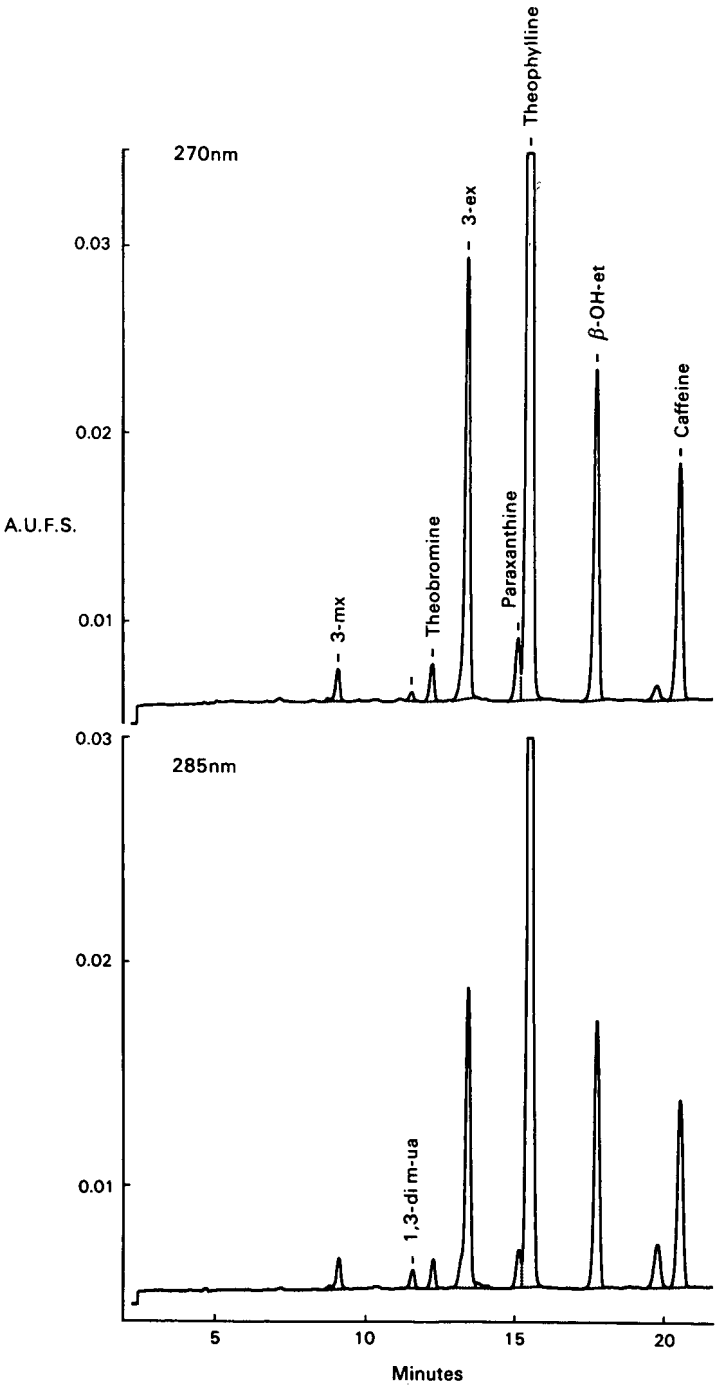

Fig. 5. Theophylline toxicity due to hepatic clearance impaired by another drug. For abbreviations, see Table II. Concentrations: 7-methylxanthine, 0.0 μM; 3-methylxanthine, 2.4 μM; 1-methylxanthine, 0.0 μM; 1,3-dimethyluric acid, 1.8 μM; theobromine, 4.1 μM; 1,7-dimethyluric acid, 0.0 μM; paraxanthine, 8.2 μM; theophylline, 262.5 μM; 1,3,7-trimethyluric acid, 0.0 μM; caffeine, 40.9 μM. Drug to metabolite ratios (suggested normal ranges in parenthesis): theophylline to 1,3-dimethyluric acid, 145.8 (7.8–14.8); (theophylline + theobromine to 3-methylxanthine, 111.1 (15–50); caffeine to paraxanthine, 5.0 (0.3–3.9).

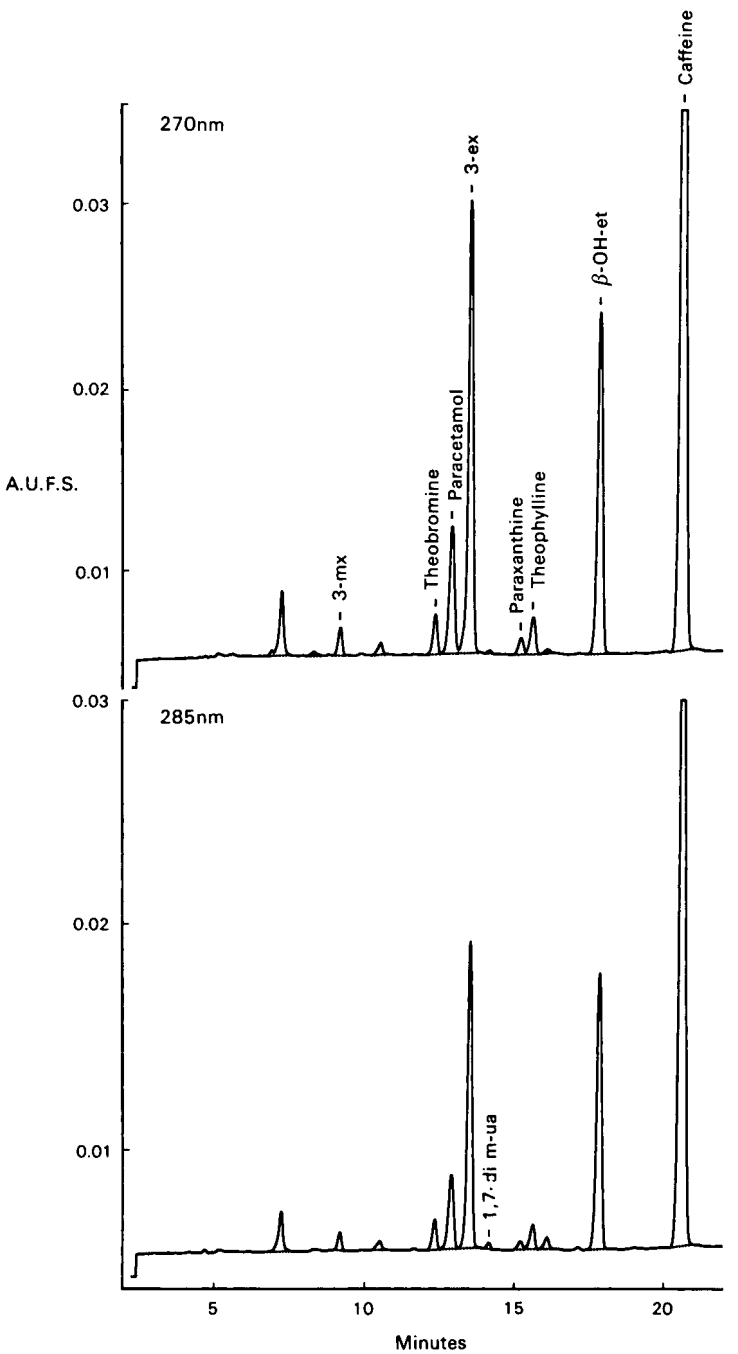

Fig. 6. Impaired demethylation in liver disease causing accumulation of dietary caffeine in plasma. For abbreviations, see Table II. Concentrations: 7-methylxanthine, 0.6 μM; 3-methylxanthine, 3.6 μM; 1-methylxanthine, 0.2 μM; 1,3-dimethyluric acid, 0.0 μM; theobromine, 4.0 μM; 1,7-dimethyluric acid, 1.7 μM; paraxanthine, 2.0 μM; theophylline, 4.1 μM; 1,3,7-trimethyluric acid, 0.0 μM; caffeine, 161.1 μM. Drug to metabolite ratios (suggested normal ranges in parenthesis): (theophylline + theobromine) to 3-methylxanthine, 2.3 (14–50); caffeine to paraxanthine, 80.6 (0.3–3.9); paraxanthine to 1,7-dimethyluric acid, 1.2 (8.0–14.0).

synthesis by N_7-methylation of theophylline[15,36,40]. While this phenomenon cannot be excluded, in this sample the high value of the (theophylline + theobromine) to 3-methylxanthine ratio of >100 implies some impairment of demethylation.

Impaired demethylation in liver disease causing accumulation of dietary caffeine in plasma (Fig. 6)

The expected paraxanthine concentration for an adult plasma caffeine level of 161 μM (31 mg/l) with normal cytochrome P_{450} function would be approximately 80 μM (14 mg/l) (Fig. 6). The level of 2.0 μM is about 2.5% of that expected and indicates a serious impairment of demethylation causing an accumulation of dietary caffeine in the plasma.

The frequent occurrence of high plasma caffeine levels in some forms of liver disease[15,16] was the basis of the suggestion that determination of fasting caffeine concentration could provide a guide to the severity of chronic liver disease[21]. The co-determination of paraxanthine and consideration of the caffeine to paraxanthine ratio would be less dependent upon patient compliance and enable those at risk to be identified with more precision even with low caffeine levels[36,41].

The presence of theobromine and theophylline at concentrations slightly above paraxanthine may reflect a dietary component from the consumption of tea and coffee. The presence of 3-methylxanthine could reflect some renal impairment since it would not be expected for these concentrations of parent compounds, and the (theophylline + theobromine) to 3-methylxanthine ratio of 2.3 is consistent with this interpretation.

CONCLUSIONS

A reliable assay has been developed which enables the simultaneous determination of caffeine, theobromine, theophylline and most of their N-demethylated and C_8-oxidized metabolites in plasma. It has been used to identify abnormal metabolism in several cases of unexpected theophylline toxicity. Toxicity due to impairment of cytochrome P_{450} mediated methylxanthine metabolism by disease or another drug was identified by reduced concentrations of some or all of the metabolites and a corresponding increase of the molar drug to metabolite ratios. Reduced ratios due to excessive metabolite concentrations have been found in renal failure. The use of the drug to metabolite ratios compensates for large differences in concentration and aids the distinction between toxicity due to failures of metabolism and toxicity due to overdose. Therefore, this assay will elucidate impaired hepatic cytochrome P_{450} mediated clearance of methylxanthines caused by disease or other co-administered drugs.

ACKNOWLEDGEMENTS

The author is especially grateful to Dr. D. J. Berry (The Poisons Unit, New Cross Hospital) for his help and advice. Mr. V. G. Oberholzer [Principal Biochemist (retired), Queen Elizabeth Hospital for Children] and Dr. B. J. Houghton (Department of Chemical Pathology, The London Hospital) also provided valuable support and advice. The help and provision of the Celute-MX tubes by Mr. W. C. Jones and

the staff of Jones Chromatography, the support of Professor C. B. S. Wood (Head of the Joint Academic Department of Child Health) and the help from the Queen Elizabeth Hospital Research Appeal Trust are gratefully acknowledged.

REFERENCES

1 A. B. Becker, K. J. Simons, C. A. Gillespie and F. E. R. Simons, *N. Engl. J. Med.*, 310 (1984) 743.
2 T. B. Vree, L. Riemens and P. M. Koopman-Kimenai, *J. Chromatogr.*, 428 (1988) 311.
3 W. J. Jusko, M. J. Gardner, A. Mangione, J. J. Schentag, J. R. Koup and J. W. Vance, *J. Pharm. Sci.*, 68 (1979) 1358.
4 H. H. Cornish and A. A. Christman, *J. Biol. Chem.*, 228 (1957) 315.
5 J. W. Jenne, H. T. Nagasawa and R. D. Thompson, *Clin. Pharmacol. Ther.*, 19 (1976) 375.
6 M. J. Arnaud and C. Welsch, in N. Rietbrock, B. G. Woodcock and A. H. Staib (Editors), *Methods in Clinical Pharmacology No. 3: Theophylline and Other Methylxanthines*, Vieweg, Braunschweig, Wiesbaden, 1982, p. 135.
7 J. M. McDonald, J. H. Ladenson, D. N. Dietzler, J. Turk and N. Weidner, *Clin. Chem.*, 24 (1978) 1603.
8 C. G. A. Persson and K.-E. Andersson, *Acta. Pharmacol. Toxicol.*, 40 (1977) 529.
9 J.F. Williams, S. Lowitt, J. B. Polson and A. Szentivanyi, *Biochem. Pharmacol.*, 27 (1978) 1545.
10 M. Bonati, R. Latini, G. Marra, B. M. Assael and R. Parini, *Pediatr. Res.* 15 (1981) 304.
11 F. N. Takieddine, K.-Y. Tserng, K. C. King and S. C. Kalhan, *Semin. Perinatol.*, 5 (1981) 351.
12 J. H. G. Jonkman, *J. Allergy Clin. Immunol.*, 78 (1986) 736.
13 W. J. A. Wijnands, T. B. Vree, A. M. Baars and C. L. A. van Herwaarden, *Drugs*, 34 (suppl. 1) (1987) 159.
14 A. H. Staib, W. Stille, G. Dietlein, P. M. Shah, S. Harder, S. Mieke and C. Beer, *Drugs*, 34 (suppl. 1) (1987) 170.
15 S. A. Iversen, P. G. Murphy, T. E. B. Leakey, A. Rydlewski, R. D. Levy and D. Gertner, *Human Toxicol.*, 3 (1984) 509.
16 B. E. Statland and T. J. Demas, *Am. J. Clin. Pathol.*, 73 (1980) 390.
17 M. H. Jacobs and R. M. Senior, *Am. Rev. Respir. Dis.*, 110 (1974) 342.
18 J. W. Jenne, *J. Allergy Clin. Immunol.*, 78 (1986) 727.
19 E. Renner, A. Wahllander, P. Huguenin, H. Wietholtz and R. Preisig, *Schweiz. Med. Wochenschr.*, 113 (1983) 1074.
20 E. Renner, H. Wietholtz, P. Huguenin, M. J. Arnaud and R. Preisig, *Hepatology*, 4 (1984) 38.
21 A. Wahllander, E. Renner and R. Preisig, *Scand. J. Gastroenterol.*, 20 (1985) 1133.
22 K. M. Piafsky, D. S. Sitar, R. E. Rango and R. I. Ogilvie, *N. Engl. J. Med.*, 296 (1977) 1495.
23 D. D.-S. Tang-Liu, R. L. Williams and S. Riegelman, *Clin. Pharmacol. Ther.*, 31 (1982) 358.
24 D. J. Birkett, J. O. Miners and J. Attwood, *Br. J. Clin. Pharmacol.*, 15 (1983) 117.
25 J. J. Orcutt, P. P. Kozak, S. A. Gillman and L. H. Cummins, *Clin. Chem.*, 23 (1977) 599.
26 G. W. Peng, M. A. F. Gadella and W. L. Chiou, *Clin. Chem.*, 24 (1978) 357.
27 S. J. Soldin and J. K. Hill, *Clin. Biochem.*, 10 (1977) 74.
28 R. Hartley, I. J. Smith and J. R. Cookman, *J. Chromatogr.*, 342 (1985) 105.
29 P. A. Harris, personal communication.
30 M. Burke, personal communication.
31 V. G. Oberholzer, personal communication.
32 T. Foenander, D. J. Birkett, J. O. Miners and L. M. H. Wing, *Clin. Biochem.*, 13 (1980) 132.
33 D. J. Birkett, R. Dahlqvist, J. O. Miners, A. Lelo and B. Billing, *Drug Metab. Dispos.*, 13 (1985) 725.
34 J. R. Gant, J. W. Dolan and L. R. Snyder, *J. Chromatogr.*, 185 (1979) 153.
35 D. J. Berry, personal communication.
36 A. C. Elias-Jones, T. E. B. Leakey, P. E. Coates and K. J. Smith, in preparation.
37 *The Merck Index*, Merck, Rahway, NJ, 9th ed., 1976.
38 A. C. Elias-Jones, V. F. Larcher, T. E. B. Leakey and P. N. Shaw, in preparation.
39 L. A. Bauer, S. P. Bauer and R. A. Blouin, *J. Clin. Pharmacol.*, 22 (1982) 65.
40 D. D.-S. Tang-Liu and S. Riegelman, *Res. Commun. Chem. Pathol. Pharmacol.*, 34 (1981) 371.
41 S. A. Iversen, P. G. Murphy and T. E. B. Leakey, in preparation.

Journal of Chromatography, 507 (1990) 221–225
Elsevier Science Publishers B.V., Amsterdam — Printed in The Netherlands

CHROMSYMP. 1758

Determination of mephenesin in plasma by high-performance liquid chromatography with fluorimetric detection

P. GUINEBAULT*, C. COLAFRANCESCHI and G. BIANCHETTI
Synthélabo-Recherche (L.E.R.S.), 23–25 Avenue Morane Saulnier, 92366 Meudon-la-Fôret Cédex (France)

SUMMARY

A procedure for the determination of the CNS-active muscle-relaxant mephenesin in plasma samples is described. The method involved a single-step extraction with diethyl ether followed by high-performance liquid chromatography separation and fluorimetric detection. Linearity of the detection response was observed between 1 ng/ml, which is the limit of determination, and 500 ng/ml. Inter-day assays, including quality-control samples, performed over a 4-month period, showed the method to be reproducible and precise, and suitable for routine analysis in pharmacokinetic studies.

INTRODUCTION

Decontractyl is used for the symptomatic relief of muscular spasms. The two main components are mephenesin and methyl nicotinate. Mephenesin is a muscle relaxant and a minor tranquilizer acting centrally at the medullary level. Methyl nicotinate is a revulsant agent with a local vasodilatory effect, which is associated with mephenesin in the percutaneous formulation. A method for the determination of mephenesin was developed in order to obtain pharmacokinetic data on this compound.

EXPERIMENTAL

Materials

Mephenesin and cicloprolol (Fig. 1) were provided by Synthelabo (Paris, France). Methyl nicotinate was purchased from Aldrich-Chemie (Steinheim, F.R.G.). Analytical-reagent grade potassium dihydrogenphosphate, sodium hydrogenphosphate and sodium hydroxide were purchased from Merck (Darmstadt, F.R.G.). RS-ACS grade (for UV spectroscopy) methanol and isopropyl alcohol (IPA) and RPE-grade unstabilized diethyl ether were purchased from Carlo Erba (Milan, Italy) and HPLC-grade acetonitrile from Baker (Deventer, The Netherlands).

The chromatographic system consisted of a Constametric III high-pressure

0021-9673/90/$03.50

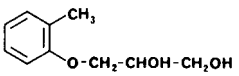

MEPHENESIN

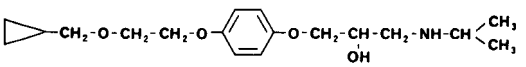

CICLOPROLOL (internal standard)

Fig. 1. Structures of mephenesin and the internal standard, cicloprolol.

pump (Milton Roy, Riviera Beach, FL, U.S.A.), an automatic sampler, either a Sedere 100 (Sedere, Vitry/Seine, France) or a Wisp 710B (Waters–Millipore, Milford, MA, U.S.A.), a spectrofluorimeter, either a Jasco FP210 (Japan Spectroscopic, Tokyo, Japan) or a Kontron SFM23 (Kontron, Zurich, Switzerland), and an SP4270 data station (Spectra-Physics, San Jose, CA, U.S.A.).

Methods

The HPLC column was a stainless-steel tube (15 cm × 4.6 mm I.D.), packed with Spherisorb hexyl, 5 μm (Phase Separations, Queensferry, U.K.). The mobile phase was KH_2PO_4 (0.025 *M*, pH 4.6)–methanol–IPA (56:20:11, v/v/v) at a flow-rate of 1 ml/min. The excitation and emission wavelengths of the fluorimeter were set at 275 and 300 nm, respectively, without using a filter.

A 1-ml volume of plasma was spiked with 200 ng of cicloprolol, the internal standard (I.S.) (Fig. 1), then 1 ml of 0.5 *M* Na_2HPO_4 solution, adjusted to pH 11.5 by addition of sodium hydroxide, was added and the mixture was shaken on a vortex mixer. The final aqueous phase was extracted with 7 ml of diethyl ether on a Sibron Thermolyne shaker for 10 s. After centrifugation at 1000 *g* for 5 min at −20°C, the aqueous phase was discarded and the organic phase evaporated to dryness at 37°C under a gentle stream of nitrogen. The dry extract was dissolved in 250 μl of the injection liquid, KH_2PO_4 (0.025 *M*, pH 4.6)–methanol (70:30, v/v). A 200-μl volume of this solution was injected onto the chromatographic column.

Extraction recovery

Peak heights obtained from the extraction of drug-free plasma samples spiked with 50 ng/ml each of mephenesine and methyl nicotinate were compared with those obtained from an injection solution spiked with the same amount of both drugs and injected directly. Three determinations of the peak-height ratio were made after extraction and after direct injection. Assays were carried out at pH 2.5 and 11.5.

Calculation

Quantification of the drug was performed using peak-height ratios of mephenesin to the internal standard obtained from plasma extracts plotted against concentration. Results for spiked samples were used to generate a linear regression curve. The concentration of the drug in unknown samples was determined by interpolation from

the calibration graph. All these calculations were performed automatically by an SP4270 data station.

Linearity

Linearity was tested against a calibration graph obtained by plotting the peak-height ratios of mephenesin to the internal standard *versus* the theoretical concentration of spiked plasma samples in the range of 1–500 ng/ml.

Reproducibility

A regression curve was obtained by plotting the theoretical concentrations of the spiked plasma samples used for the calibration *versus* their calculated concentrations found using the calibration graph. This regression curve should have a slope as close as possible to 1. Reproducibility was tested by checking such curves from day to day, and the percentage of the residual values was obtained according to the following equation:

$$\% \text{ of residual value} = [(CC - TC)/TC] \cdot 100$$

where CC = calculated concentration and TC = theoretical concentration.

Precision

Quality control samples were made by spiking two batches of drug-free plasma with 8 and 70 ng/ml of mephenesin. Together with each series of analyses, a pair of quality control samples were analysed in the same way as the other samples. Precision was tested by observing the results obtained over a 4-month period.

Stability

Stock solutions, the sample medium and the injection liquid were checked for stability.

Stock solutions (0.1 and 1.0 μg/ml in methanol) were stored in the dark at 4°C. An aliquot of both solutions was injected at time zero (just after preparation of the solution), and then 1.5 months later, after being spiked with 50 ng of an I.S. solution prepared extemporaneously. Peak-height ratios of mephenesin to the I.S. were measured.

Drug-free plasma samples spiked with 20 ng/ml of mephenesin and 50 ng/ml of I.S. were left on the bench or incubated in a water-bath at 37°C. Aliquots of these solutions were sampled at 0, 0.25 and 24 h and then injected. Peak heights were measured.

A 250-μl volume of injection liquid spiked with 20 ng of mephenesin and 50 ng of I.S. was injected immediately and 70 h later. Peak heights were measured.

RESULTS

Selectivity

Fig. 2 shows chromatograms obtained after injection of a drug-free sample (A), spiked plasma samples (B and C) and clinical plasma samples (D and E). Mephenesin and cicloprolol were well resolved from endogenous peaks present in the plasma samples, and their retention times were 4.9 and 5.8 min, respectively.

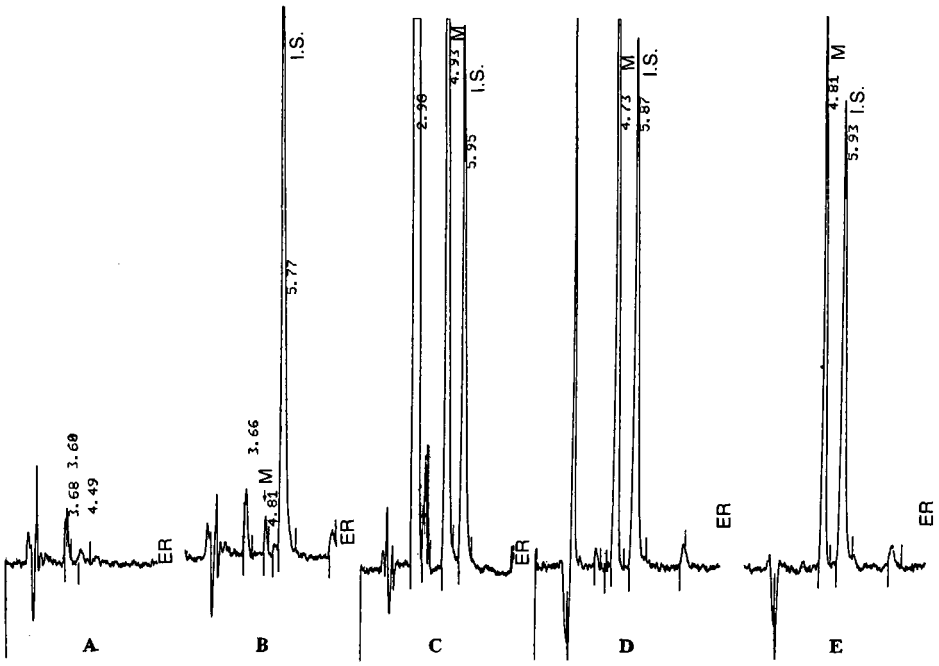

Fig. 2. Chromatograms obtained from (A) drug-free plasma sample; (B) drug-free plasma sample spiked with 1 ng/ml of mephenesin and 200 ng of I.S.; (C) drug-free plasma sample spiked with 75 ng/ml of mephenesin and 200 ng of I.S.; (D) plasma sample obtained from a healthy volunteer 4 h after oral administration of 500 mg of mephenesin; peak height and ratio correspond to a plasma concentration of 36 ng/ml; (E) plasma sample obtained from a healthy volunteer 2 h after percutaneous administration of 500 mg of mephenesin; peak height and ratio correspond to a plasma concentration of 27 ng/ml. M = mephenesin; I.S. = internal standard (cicloprolol). For chromatographic conditions, see text.

Extraction recovery

The average results of three determinations gave recoveries of mephenesin and methyl nicotinate of 84% and 40% respectively, at pH 2.5, and 97% and 0%, respectively, at pH 11.5.

Linearity

The peak-height ratios were linear with theoretical mephenesin concentrations in spiked plasma samples between 1 and 500 ng/ml.

Reproducibility

Fifteen daily regression lines obtained over a 4-month period were tested. The slopes of these curves were found to be between 0.96 and 1.03. The percentage of the residual values obtained between these back-calculated and theoretical concentration values over the 4-month period were mainly found to be less than 10%. Only nine values out of the 122 determinations were found to be more than 10% and all were less than 16%.

Precision

Thirty-two pairs of quality control samples were analysed over a 4-month period. The mean values (±2 standard deviations) for the low-and high-level quality control samples were 7.7 ng/ml (±2 · 0.5 ng/ml) and 70.4 ng/ml (±2 · 2.9 ng/ml), respectively.

Stability

Stock solution. After an extemporaneous injection of 10-μl volume of the stock solution of 0.1 and 1.0 μg/ml of mephenesin in methanol, the peak-height ratios were found to be 0.062 and 0.559, respectively. The same injection 1.5 months after the preparation of these solutions gave peak-height ratios of 0.058 and 0.575, respectively.

In plasma. Solutions of drug-free plasma samples spiked with mephenesin and cicloprolol were left on the bench or in a water-bath at 37°C. They did not show any significant variation of the peak-height ratios over 24 h.

In injection liquid. The peak heights of mephenesin and I.S.-spiked samples left for 70 h in the injection liquid inside a non-refrigerated Wisp injector did not show any significant variations over 70 h.

DISCUSSION

The method, using a single-step extraction and a chromatographic analysis time of 9 min, was linear from 1 ng/ml (which is the limit of determination) to 500 ng/ml, with good reproducibility and precision suitable for pharmacokinetic studies. After administration of the percutaneous formulation, the methyl nicotinate was not extracted under the optimum operating conditions.

Stock solutions of mephenesin in methanol remain stable in the dark at 4°C for at least 1.5 months. No significant degradation was observed for either mephenesin or the I.S. after 24 h in plasma at room temperature on the bench or at 37°C. No significant degradation was observed for mephenesin and the I.S. in the injection liquid stored in a non-refrigerated Wisp autosampler for 70 h.

Journal of Chromatography, 507 (1990) 227–234
Elsevier Science Publishers B.V., Amsterdam — Printed in The Netherlands

CHROMSYMP. 1826

High-performance liquid chromatographic determination of the mucoregulatory drug CO/1408 in rat plasma and urine

M.A. GIROMETTA*, L. LOSCHI and P. VENTURA
Department of Biochemistry and Pharmacokinetics, Camillo Corvi SpA, Stradone Farnese 118, 29100 Piacenza (Italy)

SUMMARY

A sensitive and selective high-performance liquid chromatographic (HPLC) method was developed for the determination of the mucoregulatory drug CO/1408 in plasma and urine. Samples containing an internal standard were prepared for analysis using a simple clean-up procedure based on Extrelut solid-phase extraction and chromatographed using a reversed-phase analytical column. Isocratic elution with a mobile phase consisting of 25 m*M* phosphate buffer (pH 2.5)–acetonitrile–methanol [85:10:5 or 87:9:4 (v/v) for plasma or urine analysis, respectively] was effected at a flow-rate of 0.8 ml/min. The eluate was monitored with an ultraviolet–visible variable-wavelength detector at 200 nm. The limit of quantification for the assay of CO/1408 was 80 ng/ml for plasma and 1 per 0.1 ml for urine samples. In spite of the high solubility of CO/1408 in water, the recovery from plasma and urine was very good and reproducible. The method was found to be applicable to pharmacokinetic studies of the drug in the rat.

INTRODUCTION

CO/1408, (−)-6(*S*)-hydroxy-4(*R*)-(1-hydroxy-1-methylethyl)-1-cyclohexene-1-ethanol (D, Fig. 1), is a synthetic mucoregulatory drug. Changes in mucociliary transport rate, modifications of rheological properties and biochemical composition of

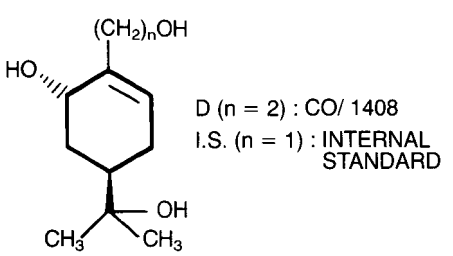

Fig. 1. Structures of CO/1408 and the internal standard.

0021-9673/90/$03.50

mucus have been studied in different animal species and are assumed to be involved in its action (unpublished results).

In order to investigate its pharmacokinetic profile in rats, a sensitive and selective assay for the determination of CO/1408 in plasma and urine was required. Taking into account the preliminary results of the biotransformation of this drug in rats (unpublished results), we have developed a high-performance liquid chromatographic (HPLC) method that is sufficiently rapid, reproducible, selective and suitable for the determination of the unchanged drug in rat plasma and urine after its administration at the active dose level.

EXPERIMENTAL

Chemicals and reagents

CO/1408 and the internal standard, (−)-6(*S*)-hydroxy-4(*R*)-(1-hydroxy-1-methylethyl)-1-cyclohexene-1-methanol (I.S., Fig. 1) were in-house reference standards (purity ⩾ 98.5%). Acetonitrile and methanol were of HPLC grade (Merck, Darmstadt, F.R.G.). All other chemicals were of analytical-reagent grade (Merck) and were used without further purification. Columns for extraction were prepared filling glass columns (13.5 × 1 cm I.D.) with about 1.2 g of granular support material (Extrelut, Merck), with a 1-cm round filter placed into the bottom of the column body.

Standard solutions

Stock standard solutions (1 mg/ml) of CO/1408 and I.S. were prepared in methanol. Working standards of CO/1408 (0.5, 1, 2, 3, 4, 10, 20, 30, 40, 50, 60, 80, 120, 160 and 200 μg/ml in water) and of I.S. (3, 12 and 50 μg/ml in water) were prepared from these stock solutions. The stock and working standard solutions were stored at −20°C and +4°C, respectively, and used within 1 month of preparation.

Chromatographic conditions

The HPLC apparatus consisted of a Model 5020 solvent metering instrument (Varian, Warrington, U.K.) and a Varian Model 2050 variable-wavelength UV detector operating at 200 nm with a sensitivity of 0.08 or 0.02 a.u.f.s. Samples (20 μl) were injected with an automatic injection system (WISP 710B; Waters Assoc., Milford, MA, U.S.A.) onto a guard column (20 mm × 4 mm I.D.) packed with Perisorb RP-8 (30–40 μm particle size) (Merck) in series with a Supelcosil LC-8 (5 μm) column (250 mm × 4.6 mm I.D.) (Supelco, Bellefonte, PA, U.S.A.). Isocratic elution was performed at room temperature (24 ± 2°C) at a flow-rate of 0.8 ml/min. The mobile phase was 25 m*M* phosphate buffer (pH 2.5)–acetonitrile–methanol [85:10:5 and 87:9:4 (v/v) for plasma and urine assay, respectively]. Analyte peak heights were digitized and integrated using a Maxima 820 Chromatography Workstation (Waters Assoc.) running on an APC IV personal computer (NEC, Boxborough, MA, U.S.A.).

Extraction procedure

Plasma. Plasma samples (0.1–1 ml) were adjusted to 1.25 ml with distilled water and 0.25 ml of I.S. solution (3 or 10 μg/ml), 0.5 ml of 0.1 *M* glycine buffer (pH 2) and 0.75 g of sodium chloride were added. Each sample was vortex mixed for 2 min and

applied directly to an Extrelut column. After an equilibration period of 5–10 min, elution was carried out with 13 ml of chloroform–2-propanol (90:10, v/v). The eluate was collected and evaporated to dryness under a stream of nitrogen at 40°C in a water-bath. The residue was dissolved in 0.2–0.5 ml of the HPLC mobile phase and analysed.

Urine. Aliquots of 1 ml of biological samples, obtained by diluting urine with distilled water in the range 10–50-fold, were mixed with 0.25 ml of distilled water and 0.25 ml of I.S. solution (10 or 50 μg/ml), 0.5 ml of 0.1 *M* glycine buffer pH 2 and 0.75 g of sodium chloride were added. Each sample was vortex mixed and then processed as described for plasma.

Drug administration to rats

Male Wistar rats (180–200 g) were used for the preliminary kinetic study of the drug at the active dose level of 25 mg kg^{-1}. CO/1408 was administered both intravenously (bolus) and orally (by gavage) and animals were killed at various times over the following 24 h. Blood was collected from the abdominal artery using heparinized syringes and plasma was immediately separated. The total urine output was collected from each animal during 0–8, 8–24 and 24–48 h after administration. All samples were stored at −20°C until analysis.

RESULTS

Typical elution profiles from extracts of rat plasma and urine are shown in Figs. 2 and 3, respectively. The method provides good resolution of CO/1408 and I.S. from endogenous compounds in both plasma and urine samples. The method has been successfully applied to the determination of CO/1408 concentrations in plasma and urine after intravenous and oral administration of the drug to rats at an active dose of 25 mg/kg.

Stability

The stability of CO/1408 in rat plasma and urine, under the conditions chosen for sample storage until analysis, was investigated. Samples spiked at different concentrations (0.514, 1.028 and 5.140 μg/ml pre-dose plasma and 2.525, 5.050 and 10.100 μg per 0.1 ml pre-dose urine were prepared, stored at −20°C for 1 month, thawed and analysed together with freshly spiked samples. The results are reported in Table I. The plasma and urine standards were shown to be stable for at least 1 month, the deviations from the nominal value being $< 10\%$ in all samples.

Recovery

The recoveries of CO/1408 and I.S. were calculated by preparing plasma and urine samples at different concentrations (Table II). Six replicates of each plasma and urine standard were extracted and analysed. Recoveries were calculated by comparing the observed analyte concentrations with those obtained from the direct injection of unextracted standards containing the same amounts of CO/1408 and I.S. The average overall recoveries of CO/1408 and I.S. were 84% and 77% from plasma and 88% and 74% from urine, respectively. The recovery ratio of CO/1408 to I.S. was very reproducible in both plasma and urine.

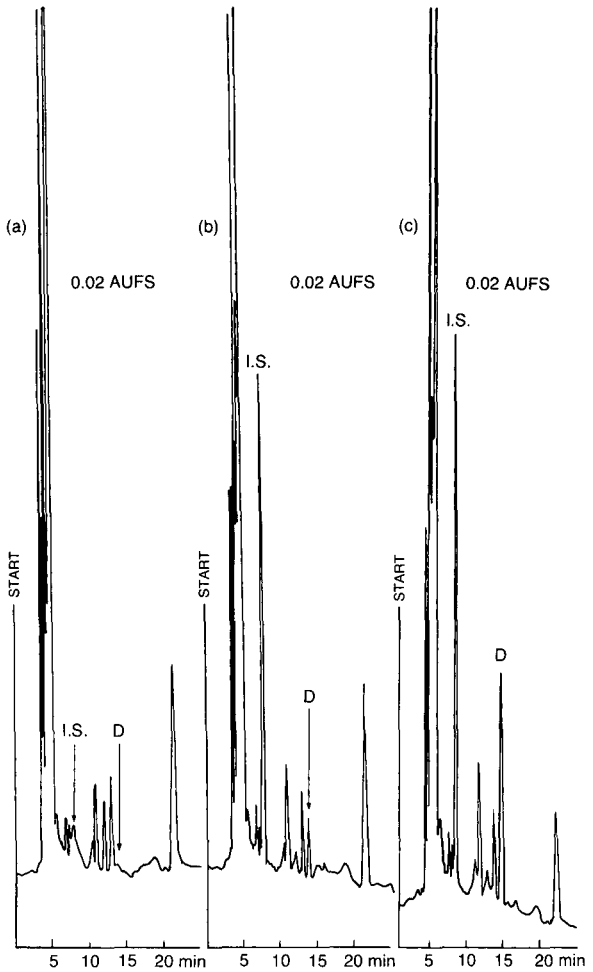

Fig. 2. Chromatogram of (a) a 1-ml plasma blank, (b) a 1-ml plasma blank spiked with 0.129 μg of CO/1408 and 0.787 μg of I.S. and (c) a 1-ml plasma sample containing 0.517 μg of CO/1408 10 h after oral administration of 25 mg kg^{-1} to a rat.

Calibration graphs

Calibration graphs were obtained using drug-free biological samples spiked with standard amounts of CO/1408 at concentration ranges expected to include the unknowns. Two plasma calibration graphs were used, one from 0.125 to 1 μg/ml of CO/1408 and 0.75 μg/ml of I.S. and the other from 1 to 10 μg/ml of CO/1408 and 3 μg/ml of I.S. Two urine calibration graphs were generated, one from 1 to 10 μg of CO/1408 and 3 μg of I.S. and the other from 10 to 50 μg of CO/1408 and 12.5 μg of I.S. Standards were extracted and analysed for each set of unknown samples. The standard daily responses were collected each day and cumulated with the previous graph to calculate the respective daily cumulative least-squares linear regression of the peak-height ratios of CO/1408 to I.S. *versus* drug concentrations[1].

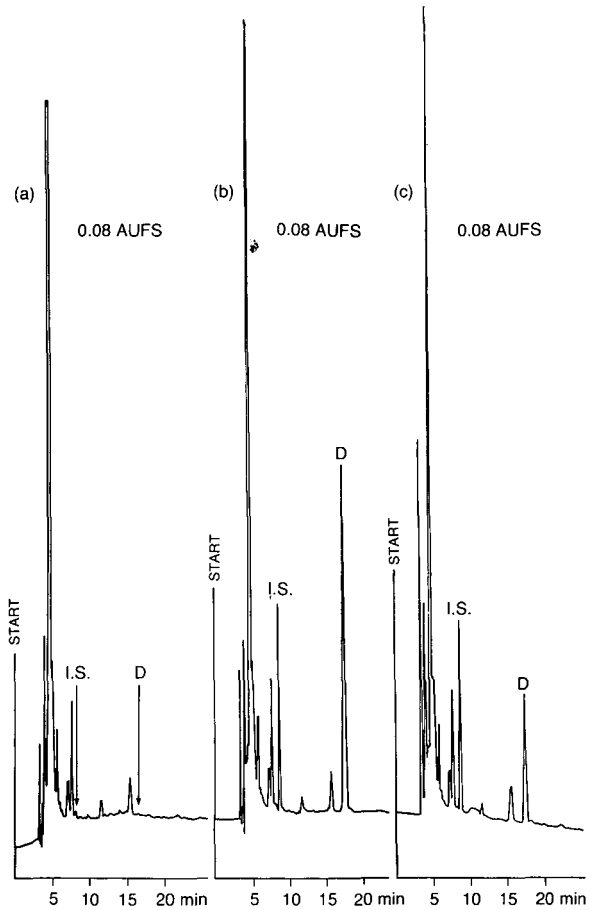

Fig. 3. Chromatograms of (a) a 0.1-ml urine blank, (b) a 0.1-ml urine blank spiked with 6.060 μg of CO/1408 and 2.79 μg of I.S. and (c) a 0.1-ml urine sample containing 2.468 μg of CO/1408 in the interval 8–24 h after oral administration of 25 mg kg^{-1} to a rat.

The analysis of variance (ANOVA) with an *F*-test ($\alpha = 0.05$) and lack of fit[2] were used to confirm the significance of the obtained regression and the adequacy of the linear model. CO/1408 concentrations in plasma and urine samples were calculated from the respective daily cumulative calibration graph[3].

An example of a day-by-day overall least-squares linear regression with the ANOVA, calculated in the drug concentration range 1–10 μg/ml in plasma, is reported in Table III.

Precision and accuracy

The intra-assay precision and accuracy were evaluated by measuring replicate spiked samples ($n = 6$ for each concentration of the drug used). The inter-assay precision and accuracy were calculated by analysing on each day, for five consecutive days, spiked samples ($n = 2$ every day for each concentration). The results are summarized in Table IV.

TABLE I

STABILITY OF CO/1408 IN RAT PLASMA AND URINE AT −20°C FOR 1 MONTH (n = 4)

Sample	*CO/1408 added (μg)*	*Mean CO/1408 observed (μg)*	*Intra-assay relative standard deviation[a] (%)*	*Deviation from amount added[b] (%)*
Plasma (1 ml)	0.514	0.502	4.2	−2.3
	1.028	0.960	3.7	−6.6
	5.140	4.985	5.7	−3.0
Urine (0.1 ml)	2.525	2.533	9.1	+0.3
	5.050	5.070	3.0	+0.4
	10.100	10.648	2.6	+5.4

[a] Relative standard deviation calculated as $(s/\bar{x}) \cdot 100$, where $\bar{x}$ is the mean amount found and s is its standard deviation.

[b] Calculated as $[(\bar{x}-\mu)/\mu] \cdot 100$, where μ is the amount added.

TABLE II

RECOVERIES OF CO/1408 AND INTERNAL STANDARD FROM PLASMA AND URINE (n = 6)

Sample	*CO/1408 added (μg)*	*I.S. added (μg)*	*Recovery (mean ± S.D.) (%)*		*CO/1408/I.S. recovery ratio (mean ± S.D.)*
			CO/1408	*I.S.*	
Plasma (1 ml)	0.514	0.787	81.79 ± 4.8	76.33 ± 4.5	1.071 ± 0.034
	1.028	0.787	77.45 ± 3.2	72.65 ± 4.7	1.066 ± 0.043
	2.570	5.245	84.26 ± 6.1	75.82 ± 5.9	1.111 ± 0.128
	7.710	5.245	90.87 ± 10.1	83.12 ± 9.4	1.093 ± 0.092
Urine (0.1 ml)	3.030	2.790	89.63 ± 6.6	77.25 ± 3.9	1.160 ± 0.046
	6.060	2.790	87.82 ± 5.5	72.86 ± 6.7	1.208 ± 0.049
	12.120	2.790	86.54 ± 8.7	72.81 ± 8.5	1.191 ± 0.030

TABLE III

DAY-BY-DAY CUMULATIVE REGRESSION LINE WITH THE RESPECTIVE ANALYSIS OF VARIANCE (ANOVA)

Day	*n[a]*	*Slope*	*y-Intercept*	*Correlation coefficient*	F_{ratio}	
					ANOVA[b]	*Lack of fit[c]*
1	10	0.198	−0.021	0.9990	4060.673	0.476
2	13 (10+3)	0.197	−0.004	0.9990	5438.352	0.662
3	16 (13+3)	0.197	−0.007	0.9989	6609.719	1.428
4	19 (16+3)	0.195	−0.003	0.9985	5525.609	0.866

[a] Number of standards (previous standards + daily cumulant) of the regression line.

[b] Regression is significant, F_{ratio} is always greater than the tabulated F value.

[c] Lack of fit is not significant, F_{ratio} is always less than the tabulated F value.

TABLE IV

INTER- AND INTRA-ASSAY PRECISION AND ACCURACY OF THE DETERMINATION OF CO/1408 IN RAT PLASMA AND URINE

Sample	*Amount added (μg)*	*Intra-assay*		*Inter-assay*	
		Relative standard deviation[a] *(%)*	*Accuracy*[b] *(%)*	*Relative standard deviation*[c] *(%)*	*Accuracy*[d] *(%)*
Plasma (1ml)	0.257	6.1	−2.7	4.7	+2.9
	0.771	1.9	−2.1	2.6	+0.8
	2.570	3.3	+1.0	2.9	+0.6
	7.710	1.8	+1.3	1.5	+1.5
Urine (0.1 ml)	3.030	2.5	−2.6	7.6	−2.4
	6.060	0.6	+1.9	2.4	+2.9
	12.120	1.0	−0.9	3.5	+1.3

[a] Calculated as $(s/\bar{x}) \cdot 100$, where $\bar{x}$ is the mean amount found ($n = 6$) and s is its standard deviation.
[b] Calculated as $[(\bar{x}-\mu)/\mu] \cdot 100$, where μ is the amount added.
[c] Calculated as in the first footnote but $\bar{x}$ is the between-days mean amount found ($n = 10$) and s is its standard deviation.
[d] See the second and third footnotes.

All relative standard deviations for the intra- en inter-assay precision were below 6.5% in plasma and 8% in urine. The intra- and inter-assay accuracies were also found to be good; the observed means ranged from (−)2.7 to 2.9% in plasma and from (−)2.6 to 2.9% in urine.

Limit of quantification

The limit of quantification (LOQ) was defined as the amount of CO/1408 per ml of plasma or per 0.1 ml of urine giving a signal-to-noise ratio of 10 (ref. 4). The LOQ in plasma was 80 ng/ml and that in urine was 1 μg per 0.1 ml.

DISCUSSION

Owing to the high water solubility of CO/1408 (42%, w/v), we have not been able to develop a reproducible and efficient procedure for the liquid–liquid extraction of this compound from biological media. As an alternative, a number of different types of solid-phase extraction columns and eluting systems have been investigated. Of the many phases tested, only the Extrelut type yielded good recoveries when the biological medium was saturated with sodium chloride and the column was eluted with chloroform–2-propanol (90:10, v/v). Further, the biological sample was sufficiently purified to permit the resolution of CO/1408 and the I.S. from endogenous plasma and urine components during HPLC at 200 nm. We selected HPLC with UV detection even though the products shows only UV end absorption, because degradation of CO/1408 under gas chromatographic (GC) conditions precluded GC analysis of the drug without derivatization. On the other hand, the HPLC analysis was sufficiently rapid; using isocratic elution with a mobile phase buffered to pH 2.5 the

retention times for CO/1408 and the I.S. were 7.2 and 13 min for plasma and 8.5 and 17.5 min for urine, respectively, with a total analysis time for each sample of 20 min.

In addition, this HPLC method yielded a limit of quantification for CO/1408 as low as 80 ng when using 1 ml of plasma or 1 μg when using 0.1 ml of urine. Therefore, this method is sufficiently selective, rapid, sensitive, precise and accurate to be applicable to pharmacokinetic studies of the drug in rats.

REFERENCES

1 M. Schiavi, E. Rocca and P. Ventura, *Chemometr. Intell. Lab. Syst.*, 2 (1987) 303.
2 N. Draper and H. Smith, *Applied Regression Analysis,* Wiley, New York, 2nd ed., 1981, Ch. 1.
3 M. A. Girometta, L. Loschi and P. Ventura, *J. Chromatogr.*, 487 (1989) 117.
4 ACS Committee on Environmental Improvement, *Anal. Chem.*, 52 (1980) 2242.

Journal of Chromatography, 507 (1990) 235–239
Elsevier Science Publishers B.V., Amsterdam — Printed in The Netherlands

CHROMSYMP. 1725

Note

High-performance liquid chromatographic assay of ampicillin and its prodrug lenampicillin

A. MARZO*, N. MONTI and M. RIPAMONTI
Real SRL, Via Milano 7/9, 22079 Villaguardia, Como (Italy)
and
E. ARRIGONI MARTELLI and M. PICARI
Sigma Tau SpA, Via Pontina km 30.400, 00040 Pomezia, Rome (Italy)

Ampicillin (AP), D(−)-α-aminobenzylpenicillin, is a widely used semisynthetic penicillin-like drug (Fig. 1). A series of AP derivatives, produced by esterification of the carboxyl group at C-3, have been developed to improve its oral bioavailability. These include pivampicillin, talampicillin, bacampicillin (BAP) and the novel prodrug lenampicillin (LAP), obtained by esterification of AP with an oxodioxolone (acetoin) group. In previous investigations, this prodrug has yielded a systemic bioavailability higher than that after administering AP as such[1,2]

In this work, two methods were standardized in order to investigate the *in vitro* stability of LAP and the comparative bioavailability of AP after the oral administration of LAP and BAP to twelve healthy volunteers, according to the cross-over design.

EXPERIMENTAL

Materials

Solvents and chemicals, all of analytical-reagent of high-performance liquid chromatographic (HPLC) grade, were supplied by Merck (Bracco, Milan, Italy). Ampicillin and its two esters investigated were supplied by Sigma Tau (Pomezia, Rome, Italy). A Varian Model 5020 liquid chromatograph, a Model 2050 variable-wavelength detector UV (Varian, Sunnyvale, CA, U.S.A.) and a 50-μl fixed loop (Rheodyne, Cotati, CA, U.S.A.) were used for all analyses. The column was a μBondapak C_{18}, 5 μm (300 × 3.9 mm I.D.) supplied by Waters Assoc. (Milford, MA, U.S.A.). The statistical computations were performed on a Macintosh Plus personal computer (Apple Computer, Cupertino, CA, U.S.A.).

Methods

A 0.5-ml sample of plasma was deproteinized with 1 ml of methanol. After stirring for 5 min and centrifuging at 2400 *g* for 10 min, 1 ml of the supernatant was separated and 2 μg of cefazolin as internal standard (in the pharmacokinetic method)

0021-9673/90/$03.50

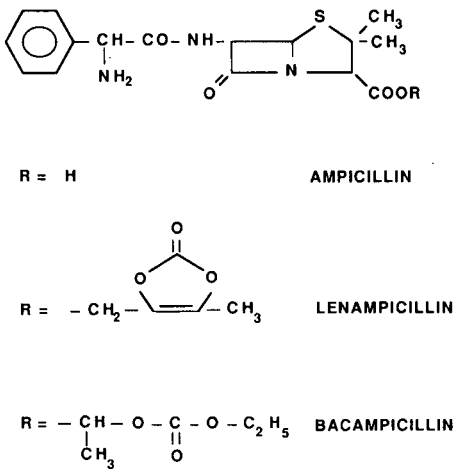

Fig. 1. Structures of ampicillin and its two prodrugs studied.

was added. The mobile phase used consisted of methanol–0.067 *M* KH_2PO_4 in ratios of 35:65 in the stability investigation and 20:80 in the bioavailability study. The flow-rate was 1.5 ml/min and absorbance was monitored at 225 nm in both methods. As internal standards, (I.S.) *o*-tolylpiperazine and cefazolin, respectively, were used. Figs. 2 and 3 show typical chromatograms of the analytical substances under the HPLC conditions validated for the stability and bioavailability investigation, respectively.

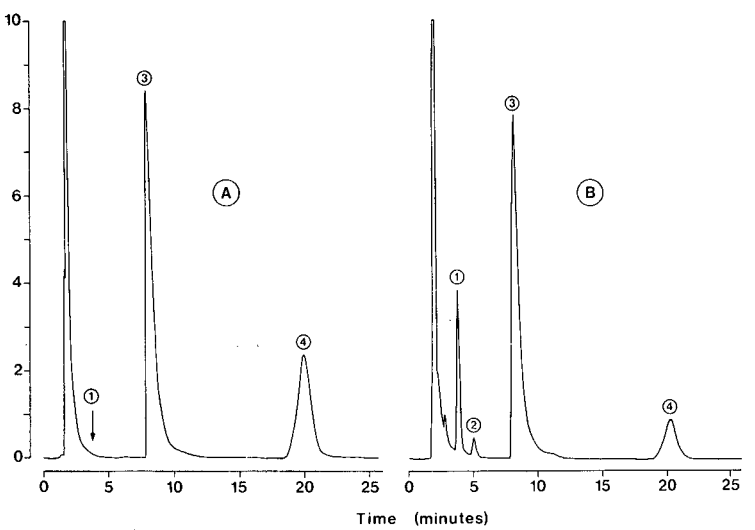

Fig. 2. Chromatograms of (1) ampicillin, (2) unknown, (3) *o*-tolylpiperazine (I.S.) and (4) lenampicillin. Column, μBondapak C_{18}, 5 μm (300 × 3.9 mm I.D.); mobile phase, methanol–0.067 *M* KH_2PO_4 (35:65); flow-rate, 1.5 ml/min; detection, UV, 225 nm. (A) Incubation with phosphate buffer (pH 7.4) at time 0; (B) after 4 h of incubation.

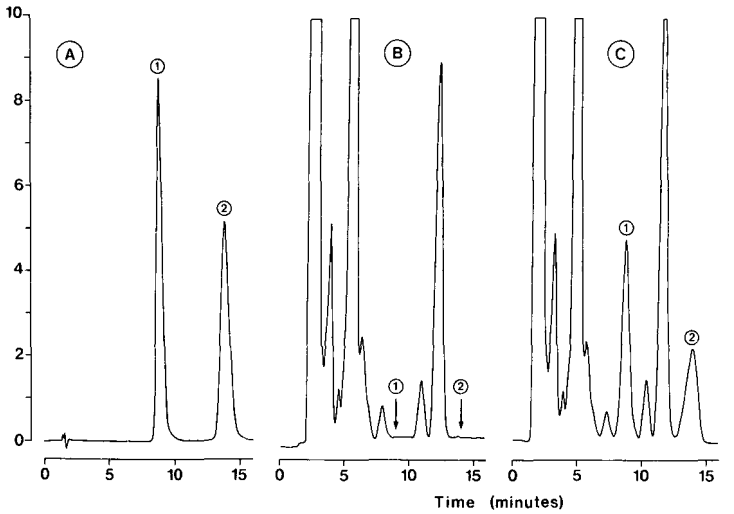

Fig. 3 Chromatograms of (1) ampicillin and (2) cefazolin (I.S.). Column as in Fig. 2; mobile phase, methanol–0.067 *M* KH_2PO_4 (20:80); flow-rate, 1.5 ml/min; detection, UV, 225 nm. (A) Authentic standards; (B) blank plasma; (C) plasma from a volunteer treated with lenampicillin (18.7 μg/ml plasma).

The bioavailability investigation of the two AP prodrugs was carried out on twelve healthy volunteers of both sexes, ranging in age from 18 to 40 years, to whom LAP and BAP (800-mg tablets in both instances) were administered by the oral route according to a randomized cross-over design. The AP concentrations were evaluated in serial plasma samples and in urine excreted over 0–3, 3–6, 6–12 and 12–24-h periods following administration.

RESULTS AND DISCUSSION

Both methods were validated in terms of linearity, reproducibility, specificity and sensitivity. The method used in the stability trial proved to be linear in the range 0.5–10 μg with an inter-assay coefficient of variation (%C.V.) of 0.43 and a detection limit of 1.5 μg/ml.

The other method, used in the bioavailability investigation of the two ampicillin prodrugs, allowed AP to be evaluated with a more favourable signal-to-noise ratio and hence greater sensitivity, the detection limit being 0.5 μg/ml. The linearity of this method was verified in the range 0.1–10 μg of AP and cefazolin as I.S., injected at drug-to-internal standard ratios of 1:1 (C.V. = 0.80%) and 1:4 to 4:1 (C.V. = 0.48%), respectively. The recovery of AP from plasma was 97.6%, linear in the range of 0.5–25 μg/ml, with a correlation coefficient $r = 0.9997$ (Table I).

As ampicillin is a hydrophilic molecule, it could not be extracted by solvent partition. The plasma deproteinization with methanol did not completely clean the sample, as shown in the blank plasma chromatogram (Fig. 3). In any case, a good signal-to-noise ratio was achieved when the ampicillin peak was at 9.00 min and cefazolin was selected as the I.S. The latter is eluted at 14.00 min, where no interfering base peaks are present, and showed a detection limit of 0.5 μg/ml. This method can

TABLE I

RECOVERY OF AMPICILLIN FROM PLASMA IN QUADRUPLICATE TRIALS

The linear regression method gave the correlation $y = 0.062 + 0.959x$; $r = 0.9997$.

Ampicillin added (x) (μg/ml)	*Ampicillin recovered (y)*		*Recovery (%)*
	Mean (μg/μl) (n = 4)	*C.V. (%)*	
–			
0.5	0.5	2.52	100.0
1	1	0.62	100.0
2	1.93	2.88	96.5
5	4.85	1.43	17.0
7.5	7.15	2.96	95.3
10	10.1	4.21	101.0
15	14.25	5.01	95.0
25	24.02	1.49	96.1
			Mean: 97.6 ± 2.36
			%C.V. 2.42

therefore be used in pharmacokinetic and bioavailability investigations as an alternative to the microbiological assay[3] for either ampicillin or cefazolin.

When stored at 37°C for 30 min in blood samples, ampicillin proved to be stable and lose about 2–3% of its titre in 2 h. Hence serum can be used instead of blood.

Ampicillin proved to have poor stability in aqueous solution, mainly in the presence of perchloroacetic acid. For this reason, methanol was used instead for deproteinizing plasma, with injection into the column just after the extraction, thus achieving good stability. When stored in a freezer at −20°C, ampicillin in plasma samples proved to be stable for *ca.* 10–15 days.

When administered to healthy volunteers, both LAP and BAP proved to be

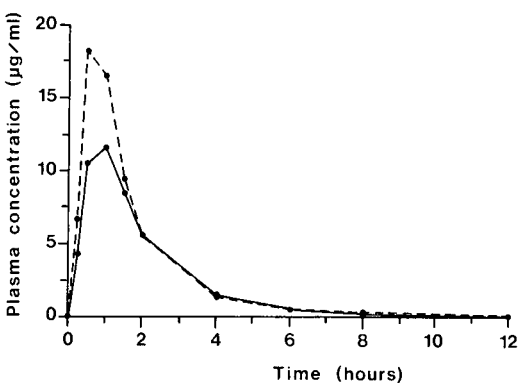

Fig. 4. Plasma concentration of ampicillin *vs.* time after oral administration of lenampicillin (dashed line) and bacampicillin (solid line) tablets (800 mg per subject in both instances) to healthy volunteers. Values lower than the detection limit (0.5 μg/ml) were taken as zero with respect to the mean; other values are means of twelve results.

well absorbed through the intestine, giving plasma concentrations of AP measurable over a 6-h period with BAP and an 8-h-period with LAP (Fig. 4). The cumulative urinary excretion of AP in the 0–24-h period was 561 mg (39%) after administration of LAP and 203 mg (36%) after administration of BAP.

When evaluated from the area under the curve, the systemic bioavailability of ampicillin in healthy volunteers after administration of LAP proved to be 26% higher than after administration of BAP (Fig. 4), the greatest difference being observed in the absorption phase and demonstrated by the C_{max} (peak concentration) values 18.14 and 11.65 μg/ml for LAP and BAP administration, respectively (Table I).

REFERENCES

1 J. Guibert, M. D. Kitzis, S. Yamabe and J. F. Acar, *Chemioterapia*, 4 (1985) 293.
2 N. Neuman, *Drugs Exp. Clin. Res.*, 12 (1987) 115.
3 A. Wildfener, U. Schwiersch, K. Engel, E. Castell, A. Schilling, J. Potempa and H. Lenders, *Arzneim.-Forsch. Drug Res.*, 38 (1988) 1640.

Journal of Chromatography, 507 (1990) 241–245
Elsevier Science Publishers B.V., Amsterdam — Printed in The Netherlands

CHROMSYMP. 1726

Note

Determination of aliphatic amines by gas and high-performance liquid chromatography

A. MARZO*, N. MONTI and M. RIPAMONTI
Real SRL, Via Milano 7/9, 22079 Villaguardia, Como (Italy)
and
S. MUCK and E. ARRIGONI MARTELLI
Sigma Tau SpA, Via Pontina km 30.400, 00040 Pomezia, Rome (Italy)

Aliphatic amines, such as mono-, di- and trimethylamine (MMA, DMA, TMA) and trimethylamine N-oxide (TMAO), are produced by bacterial degradation of trimethylalkylammonium compounds, such as choline, acetylcholine, carnitine and γ-betaines. This degradation can be environmental, intestinal or faecal[1,2].

This paper describes an analytical investigation by gas chromatography (GC) with flame ionization detection (FID) or thermionic specific detection (TSD) and by high-performance liquid chromatography (HPLC) with conductimetric, refractive index (RI) and electrochemical detection (ED) for the simultaneous determination of the above amines, mainly applied to biological samples such as urine, and an assay procedure adopted consisting in chemical reduction of TMAO to TMA, followed by evaluation of the latter by GC in order to determine the TMAO.

EXPERIMENTAL

Materials

Solvents and chemicals were supplied by Merck (Bracco, Milan, Italy). The apparatus used was a Model 3400 gas chromatograph (Varian, Sunnyvale, CA, U.S.A.) equipped with FID and TSD instruments and a Model 4000i and Model BIO LC 4000 liquid chromatographs (Dionex, Sunnyvale, CA, U.S.A.).

Gases of high purity were supplied by SIAD (Cinisello Balsamo, Milan, Italy). The apparatus used for the TMAO reduction consisted of a dynamic thermal stripper and a Supelco thermal unit, from Supelco (Supelchem, Milan, Italy).

GC

A glass column (375 cm × 2 mm I.D.) packed with 4% Carbowax 20M + 0.8% KOH on Carbopack B (60–80 mesh), TSD, nitrogen at 40 p.s.i. as carrier gas, temperatures of 100°C for the column, 160°C for the injector and 250°C for the detector and monoisopropylamine (MIPA) as internal standard (I.S.) were used.

0021-9673/90/$03.50

Retention times were 1.76 min for MMA, 2.63 min for DMA, 3.24 min for TMA and 5.07 min for the I.S. (Fig. 1).

HPLC with conductimetric detection

A Dionex Ionpac NS 1 (10 μm) column (250 × 4 mm I.D.) was used. The mobile phase was 2 m*M* hexanesulphonic acid (HSA) at a flow-rate of 1 ml/min. Retention times were 9.6 min for K^+, 13.1 min for MMA, 18.8 min for DMA and 27.5 min for TMA (Fig. 2).

HPLC with RI detection

A μBondapak C_{18} (7 μm) column (300 × 4.6 mm I.D.) (Waters Assoc, Milford, MA, U.S.A.) was used. The mobile phase was 0.05 *M* ammonium acetate in water–methanol (95:5) at a flow-rate of 1 ml/min. RI detection was used.

HPLC with electrochemical detection

A Dionex HPIC-CS3 (10 μm) cationic column (250 × 4 mm I.D.) was used. The mobile phase was 30 m*M* hydrochloric acid at a flow-rate of 1 ml/min. ED was

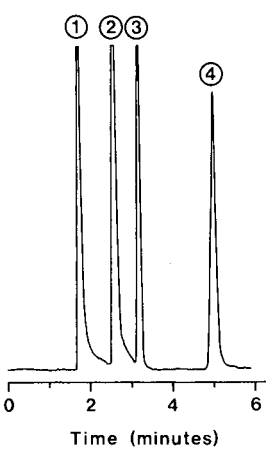

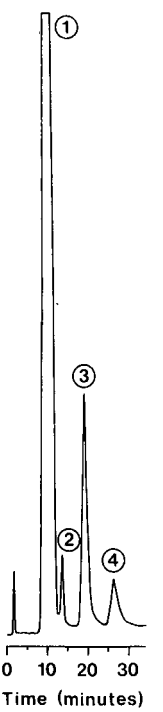

Fig. 1. GC of MMA, DMA and TMA. Column, 4% Carbowax 20 M + 0.8% KOH on Carbopack B, 60–80 mesh (375 cm × 2 mm I.D.); carrier gas, nitrogen at 40 p.s.i.; column temperature, 100°C; injector temperature, 160°C; detector temperature, 250°C; detection, TSD. Peaks: 1 = MMA; 2 = DMA; 3 = TMA; 4 = MIPA (I.S.).

Fig. 2. HPLC of aliphatic amines, with conductimetric detection. Column, Ionpac NS1 (250 × 4 mm I.D.); mobile phase, 2 m*M* HSA; flow-rate, 1 ml/min. Peaks: 1 = K^+; 2 = MMA; 3 = DMA; 4 = TMA.

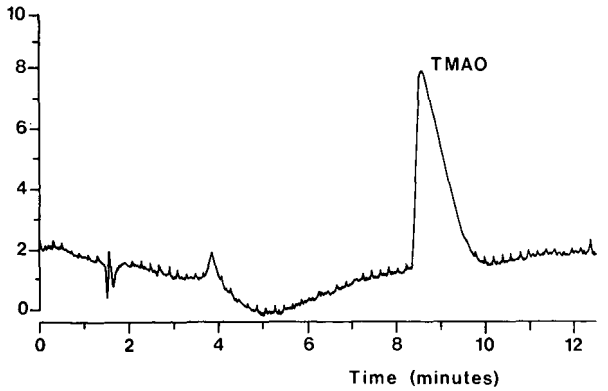

Fig. 3. HPLC of TMAO obtained with ED. Column, HPIC-CS3 (250 × 4 mm I.D.); mobile phase, 30 m*M* HCl; flow-rate, 1 ml/min.

effected with a pulsed amperometric detector from Dionex (PAD-2, Series 883818) equipped with a gold electrode (Dionex). The retention time of TMAO was 8.56 min (Fig. 3).

Chemical reduction of TMAO

Two approaches were attempted. The first, proposed by Lin and Hurng[3], consists in using 0.3% titanium(III) chloride in 10% (w/v) hydrochloric acid at 80°C as reducing agent. The other was reduction by hydrogen–palladium with a 5% Pd on charcoal catalyst, stripped under a flow of hydrogen at 100 ml/min for 30 min at 30°C. The gases were trapped on a Supelco Carbotrap 200 tube by using the dynamic thermal stripper. The tube, now containing TMA as a reduction product of TMAO, was transferred to the Supelco thermal unit to desorb the trapped compound into the

TABLE I

LINEARITY OF DETECTOR RESPONSE FOR MMA, DMA AND TMA WITH A FIXED ANALYTE-TO-INTERNAL STANDARD RATIO, ASCERTAINED BY A CONSTANT DETECTOR RESPONSE FACTOR (D.R.F.) FOR THE GC–TSD METHOD

Trials in quadruplicate for each amount; S.D. = standard deviation; C.V. = coefficient of variation.

Amount injected (ng)	*D.R.F. (mean ± S.D.)*		
	MMA	*DMA*	*TMA*
0.25	0.667 ± 0.012	0.443 ± 0.026	0.406 ± 0.134
0.5	0.617 ± 0.029	0.430 ± 0.023	0.389 ± 0.070
1	0.663 ± 0.012	0.459 ± 0.014	0.410 ± 0.036
2.5	0.634 ± 0.025	0.442 ± 0.032	0.406 ± 0.039
5	0.598 ± 0.024	0.427 ± 0.022	0.390 ± 0.023
10	0.625 ± 0.006	0.432 ± 0.004	0.417 ± 0.019
20	0.638 ± 0.011	0.440 ± 0.008	0.410 ± 0.034
Mean	0.634	0.439	0.404
S.D.	0.024	0.011	0.011
C.V. (%)	3.86	2.46	2.61

TABLE II

LINEARITY OF DETECTOR RESPONSE FOR MMA, DMA AND TMA WITH A VARIABLE ANALYTE-TO-INTERNAL STANDARD RATIO (1:4 → 4:1), ASCERTAINED BY A CONSTANT DETECTOR RESPONSE FACTOR (D.R.F.) FOR THE GC–TSD METHOD

Amine/I.S. (ng)	*D.R.F*		
	MMA	*DMA*	*TMA*
0.25/1	0.652	0.487	0.400
0.5/1	0.672	0.447	0.416
1/1	0.620	0.505	0.436
2/1	0.662	0.452	0.412
4/1	0.666	0.457	0.410
Mean	0.654	0.470	0.415
S.D.	0.021	0.025	0.013
C.V. (%)	3.14	5.36	3.19

TABLE III

RECOVERY OF TMA CONSIDERED AS EXPRESSION OF TMAO, AFTER HYDROGEN-PALLADIUM REDUCTION

TMAO added (μg)	*TMA theoretical (μg)*	*TMA recovered (μg)*	*Recovery (%)*
27.775	14.75	13.39	90.78
55.55	29.50	26.40	89.49
111.1	59.0	53.80	91.19
166.65	88.5	73.21	82.72
222.2	118.0	115.91	98.22
277.75	147.5	135.03	91.86
555.50	295.0	224.0	82.37
1111.0	590.0	522.21	88.51
Mean			89.39
S.D.			5.124
C.V. (%)			5.73

GC column. TMA was determined before and after reduction, the difference representing the TMAO originally present.

RESULTS AND DISCUSSION

HPLC with RI detection allowed all the amines to be evaluated but some interference from endogenous parent substances was observed.

The HPLC–ED technique produced negative results, because the potential needed for the TMAO reduction was very high (between -0.65 and -0.85 V) and the sensitivity was poor. The other approaches for the evaluation of TMAO as such proved to be unsatisfactory. GC and HPLC with conductimetric detection allowed the satisfactory simultaneous determination of MMA, DMA and TMA but not of TMAO.

Chemical reduction of TMAO to TMA appeared to be the only approach able to lead to the detection of all the amines. The method proposed by Lin and Hurng[3] was discarded because it also produced demethylation products (DMA and TMA). The hydrogen–palladium reduction of TMAO proved to give TMA as the only product.

GC with FID or TSD of the aliphatic amines carried out before and after hydrogen–palladium reduction of TMAO allowed TMA, DMA, MMA and TMAO to be determined in biological samples, such as urine, with satisfactory results in terms of linearity, reproducibility, specificity and recovery, as shown in Tables I–III and Fig. 1.

REFERENCES

1 M. Al Waiz, S. C. Mitchell, J. R. Idle and R. L. Smith, *Xenobiotica*, 17 (1987) 551.
2 S. H. Zeisel, J. S. Wishnok and J. K. Blusztayn, *J. Pharmacol. Exp. Ther.*, 225 (1983) 320.
3 J. K. Lin and D. C. Hurng, *Food Chem. Toxicol.*, 23 (1985) 579.

Journal of Chromatography, 507 (1990) 247–251
Elsevier Science Publishers B.V., Amsterdam — Printed in The Netherlands

CHROMSYMP. 1694

High-performance liquid chromatographic determination of propylthiouracil in plasma

M. T. ROSSEEL* and R. A. LEFEBVRE
Heymans Institute of Pharmacology, University of Gent Medical School, De Pintelaan 185, B-9000 Ghent (Belgium)

SUMMARY

A high-performance liquid chromatographic method for the determination of the antithyroid drug propylthiouracil in dog plasma has been developed. Propylthiouracil and the internal standard, methylthiouracil, are extracted from plasma with methylene chloride at pH 6 and the organic layer is evaporated to dryness. The residue is chromatographed on a Chromspher C_{18} reversed-phase column using Pic B-7 (0.005 *M* 1-heptanesulphonic acid in water)–1% acetic acid–methanol (40:45:15, v/v/v) as the mobile phase. Quantification is achieved by monitoring the UV absorbance at 300 nm. The response is linear (0.1–15 μg/ml) and using 100 μl of plasma the detection limit is 50 ng/ml. The within-run coefficient of variation is $\leqslant 5\%$ and the accuracy is within 10% of the theoretical value at concentrations between 0.1 and 15 μg/ml plasma.

INTRODUCTION

Propylthiouracil (PTU) (Fig. 1) is an antithyroid drug. In humans less than 10% of the drug is excreted unchanged in the urine, and about 60% is excreted as a glucuronic acid conjugate of PTU (for references, see ref. 1).

Serum or plasma concentrations of propylthiouracil were first measured by Ratliff *et al.*[2] by spectrophotometry, which lacks specificity and sensitivity. This problem was solved by the development of a gas chromatographic (GC) method[3] using alkylation of propylthiouracil. Several high-performance liquid chromatographic (HPLC) methods were later developed, using an ion-exchange column with UV detection[4] or a reversed-phase column with UV detection, without or with addition of an internal standard after extraction[5,6]. McArthur and Miceli[7] used reversed-phase chromatography with UV detection and an internal standard incorporated in the extraction solvent. Another reversed-phase HPLC method[8] requires a lengthy deproteinization step for the determination of blood concentrations of PTU. A sensitive radioimmunoassay has also been published[9].

We have developed a sensitive HPLC method using ion-pair reversed-phase chromatography with UV detection at 300 nm. A structurally related compound,

0021-9673/90/$03.50

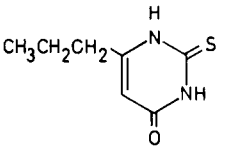

PROPYLTHIOURACIL

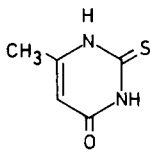

METHYLTHIOURACIL
(internal standard)

Fig. 1. Structures of propylthiouracil and the internal standard methylthiouracil.

methylthiouracil (Fig. 1) is used as an internal standard. The method was applied to dog plasma, as the dog is a suitable model for propylthiouracil disposition in man[10].

EXPERIMENTAL

Reagents and standard solutions

Propylthiouracil and the internal standard, methylthiouracil, were kindly supplied by Sanders Pharma (Brussels, Belgium). Methanol (HPLC grade) was obtained from Alltech Europe (Eke, Belgium) and Pic B-7 from Waters Assoc. (Milford, MA, U.S.A.). All other reagents were of analytical-reagent grade from Merck (Darmstadt, F.R.G.). Water doubly distilled in glass was passed through a 0.45-μm filter (Type HA, Millipore, Bedford, MA, U.S.A.).

Stock solutions of propylthiouracil (5 mg/ml) and methylthiouracil (5 mg/ml) were prepared by dissolving accurately weighed samples in methanol. These solutions were stable for at least 1 month when stored at 4°C. Working standard solutions of propylthiouracil and the working solution of methylthiouracil were made by diluting the stock solutions with water.

Analytical procedure

A 100-μl plasma sample was pipetted into a 7-ml brown, glass-stoppered, silanized centrifuge tube and adjusted to pH 6 with 0.1 *M* hydrochloric acid. To this were added 25 μl of internal standard solution (10 μg/ml in water) and 3 ml of methylene chloride. The mixture was shaken horizontally for 10 min, followed by centrifugation at 3015 *g* for 5 min. The organic phase was transferred into a 6-ml brown, silanized conical tube, evaporated to dryness under nitrogen and reconstituted in 50 μl of water in the dark. An aliquot (20 μl) of this solution was injected onto the column.

Chromatography

Measurements were made using a Spectra-Physics 8700 high-performance liquid chromatograph equipped with a Perkin-Elmer LC 235 diode-array detector. A

Chromspher C_{18} reversed-phase column (250 × 4.6 mm I.D.) (Chrompack, Antwerp, Belgium) was maintained at 40°C.

The mobile phase was Pic B-7 (0.005 *M* 1-heptanesulphonic acid in water)–1% acetic acid–methanol (40:45:15, v/v/v). The flow-rate of the helium-degassed mobile phase was 1 ml/min. The column temperature was 45°C. The samples were injected into the chromatograph via a Rheodyne (Berkeley, CA, U.S.A.) Model 7125 injector equipped with a 20-μl loop. Chromatographic separation was monitored by UV detection at 300 nm. Peak heights were measured with an HP 3390 A integrator.

Calibration graphs

Standards for the calibration graph were prepared by adding known amounts of propylthiouracil to blank dog plasma to provide concentrations from 0.1 to 15 μg/ml. Calibration graphs were obtained by plotting the peak-height ratio of propylthiouracil to the internal standard (y) against the concentration (x) of propylthiouracil in plasma and calculating the regression line by least-squares linear regression analysis.

Stability of propylthiouracil

The stability of propylthiouracil in dog plasma (5 μg/ml) was studied for various storage times at −20 and −80°C.

RESULTS AND DISCUSSION

Extraction

Using methylene chloride, the recovery of propylthiouracil from plasma was highest at pH 6. The extraction yield (mean ± S.D.) was 77.3 ± 4.6, 80.0 ± 1.8 and 81.6 ± 2.3% for propylthiouracil at concentrations of 0.1, 5 and 15 μg/ml, respectively (n = 5 for each concentration), and 52.1 ± 3.2% for methylthiouracil at a concentration of 2.5 μg/ml (n = 5).

Chromatography

Propylthiouracil has a UV absorbance peak maximum at 275 nm. However, at this wavelength there is a peak of an endogenous substance which nearly coelutes with the PTU peak and with a UV absorbance peak maximum at about the same wavelength (272 nm). This peak was also observed with blank plasma, but it was absent if water was used instead of plasma. Therefore, a detection wavelength of 300 nm was selected, which resulted in a diminished absolute sensitivity for PTU, but the interference was avoided.

Fig. 2 shows sample chromatograms of extracts of (A) blank dog plasma, (B) blank dog plasma spiked with PTU and methylthiouracil and (C) a plasma sample from a dog that had received a 300-mg oral dose of PTU. Under the chromatographic conditions used, the retention times for the internal standard and PTU were 3.9 and 10.8 min, respectively.

The limit of detection was 50 ng/ml, with a signal-to-noise ratio of 3:1, using 100 μl of plasma. This detection limit is comparable to that of the micro-HPLC method[7] and is better than that of the method of Kim[8]. Other HPLC methods[4–6] require relatively large volumes of plasma (1–3 ml).

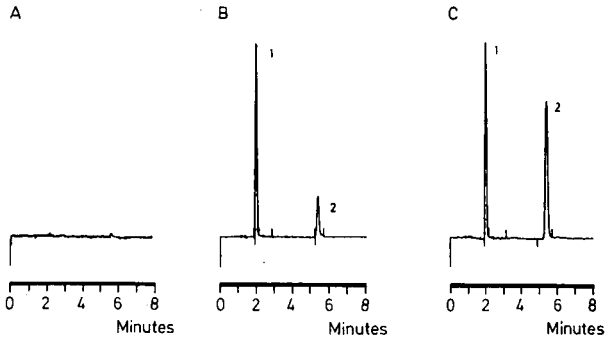

Fig. 2. Representative HPLC traces for extracts of 100 μl of dog plasma. (A) Blank plasma; (B) blank plasma spiked with 1 = internal standard (2.5 μg/ml) and 2 = PTU (0.5 μg/ml); (C) plasma from a dog 8 h after on oral dose of 300 mg of PTU: 1 = internal standard (2.5 μg/ml); 2 = PTU (1.20 μg/ml).

Calibration graphs

The calibration graphs for PTU showed a linear response over the range evaluated (0.1–15 μg/ml). A typical calibration graph gives a regression of $y = -0.0028 + 0.3145x$, $r = 0.9993$, where y = peak-height ratio, x = concentration of propylthiouracil and r = correlation coefficient.

Within-run precision and accuracy

The within-run precision and accuracy were evaluated from the analyses of five plasma samples for each of five PTU concentrations (range 0.1–15 μg/ml). The within-run coefficient of variation (C.V.) was $\leqslant 5\%$. The accuracy was within 10% of the theoretical value at each concentration (Table I).

Stability

Propylthiouracil was observed to be stable for at least 14 days at $-20°C$ and for at least 1 month at $-80°C$ (stability is defined as $\geqslant 95\%$ of the initial amount remaining).

In conclusion, the proposed HPLC method is sufficiently sensitive and selective for monitoring unchanged propylthiouracil in pharmacokinetic studies.

TABLE I

WITHIN-RUN PRECISION AND ACCURACY FOR THE DETERMINATION OF PROPYLTHIOURACIL IN PLASMA (n = 5)

Concentration added (μg/ml)	*Precision (C.V.) (%)*	*Accuracy (%)*
0.1	2.5	110.0
0.5	3.7	90.8
1.0	2.3	110.5
5.0	3.5	100.6
15.0	2.6	98.1

ACKNOWLEDGEMENTS

The authors thank Sanders Pharma for financial support. R.A.L. is a Senior Research Associate of the National Fund for Scientific Research (Belgium).

REFERENCES

1 J. P. Kampmann and J. M. Hansen, *Clin. Pharmacokinet.*, 6 (1981) 401.
2 C. R. Ratliff, P. F. Gilliland and F. F. Hall, *Clin. Chem.*, 18 (1972) 1373.
3 D. Schuppan, S. Riegelman, B. V. Lehmann, A. Pilbrant and C. Becker, *J. Pharmacokinet. Biopharm.*, 1 (1973) 307.
4 D. S. Sitar and D. B. Hunninghake, *J. Clin. Endocrinol. Metab.*, 40 (1975) 26.
5 H. G. Giles, R. Miller and E. M. Sellers, *J. Pharm. Sci.*, 68 (1979) 1459.
6 H. P. Ringhand and W. A. Ritschel, *J. Pharm. Sci.*, 68 (1979) 1461.
7 B. McArthur and J. N. Miceli, *J. Chromatogr.*, 278 (1983) 464.
8 C. Kim, *J. Chromatogr.*, 272 (1983) 376.
9 D. S. Cooper, V. C. Saxe, F. Maloof and E. C. Ridgway, *J. Clin. Endocrinol. Metab.*, 52 (1981) 204.
10 P. Ringhand, H. R. Maxon, W. A. Ritschel, I.-W. Chen and D. H. Bauman, *J. Clin. Pharmacol.*, 20 (1980) 91.

Journal of Chromatography, 507 (1990) 253–258
Elsevier Science Publishers B.V., Amsterdam — Printed in The Netherlands

CHROMSYMP. 1698

Direct injection high-performance liquid chromatographic assay of morphine with electrochemical detection, a polymeric column and an alkaline eluent

F. TAGLIARO* and G. CARLI
Institute of Forensic Medicine, University of Verona, Policlinico di Borgo Roma, 37134 Verona (Italy)
R. DORIZZI
Laboratory of Clinical Chemistry, Legnago Hospital, Legnago (Italy)
and
M. MARIGO
Institute of Forensic Medicine, University of Verona, Policlinico di Borgo Roma, 37134 Verona (Italy)

SUMMARY

A simple method is described for the direct determination of morphine in untreated plasma or serum, using reversed-phase high-performance liquid chromatography with amperometric electrochemical detection. A basic eluent [0.05 mol/l phosphate buffer–isopropanol–tetrahydrofuran (88:10:2) (pH 9.5)] allows both reversed-phase chromatography of morphine under ionization control conditions and its detectability at an unprotected thin-layer glassy carbon electrode at a potential of 350 mV (*vs.* an Ag/AgCl reference electrode). In addition, the alkaline mobile phase promotes the ionization of serum proteins, which, being poorly retained by the hydrophobic column packing [poly(styrene–divinylbenzene) copolymer], elute early in the chromatogram, leaving a clean baseline. Up to 50 μl of simply filtered plasma can be injected. The absolute limit of detection is 0.75 ng on-column. No interferences were observed from more than 80 opiate and non-opiate drugs. The intra- and inter-assay relative standard deviations (n = 5) were 3.2 and 6.6%, respectively, at a morphine concentration of 100 ng/ml in plasma and 0.09 and 4.2%, respectively, at the level of 500 ng/ml.

INTRODUCTION

The ability of modern liquid chromatographic systems to handle samples containing large amounts of proteins has prompted the direct high-performance liquid chromatographic (HPLC) analysis of biological fluids, such as blood plasma and serum. Although devised in the late 1970s[1], this approach has until recently been regarded as little more than a curiosity. However, given the great interest in coupling the specificity and reliability of chromatography with the operative simplicity and high sample throughput typical of the newest clinical chemistry assays, in recent times

0021-9673/90/$03.50

much effort has been put into the development of HPLC methods suitable for plasma or serum injection.

Yoshida *et al.*[2] proposed the use of 'protein-coated ODS' and later Hagestam and Pinkerton[3] introduced the concept of the internal surface reversed phase. More recently, Shihabi and co-workers used either silica-based wide-pore[4] or polymeric columns[5] for the direct determination of carbamazepine and pentobarbital, respectively, with injections of a few microlitres of serum. A silica support with a polymeric surface in which hydrophobic pockets are shielded by a hydrophilic network (shielded hydrophobic phase) was later reported by Gisch *et al.*[6]. A different approach to the same problem was developed by Arunyanart and co-workers by using micellar mobile phases[7] and cyano or C_{18} derivatized silica columns[8]. Recently, excellent reviews on this subject were published by Westerlund[9] and Shihabi[10].

All of these different approaches proved useful particularly in therapeutic drug monitoring (TDM). Direct assays have been reported of therapeutic and potentially toxic drugs present at relatively high concentrations (>1 μg/ml) with a high molar absorptivity above 250 nm; lower wavelengths are usually precluded by interfering compounds present naturally in the serum.

Until now, there have been very few reports concerning methods for the direct HPLC assay of basic drugs, particularly morphine. It is well known that silica-based column packings are in general problematic for the reversed-phase chromatography of basic compounds, because of the residual silanols. Numerous remedies such as adjustment of the pH of the mobile phase and addition of organic amines have been proposed, often achieving limited results in terms of improvements in peak shape[11]. Moreover, in our opinion, the 'silanol effect' is a difficult point in systems dedicated to the direct injection of plasma and serum, in which the mobile phase composition (pH, ionic strength, organic modifiers) is strongly limited by the need to allow solubility in the eluent of large protein fractions throughout chromatography. In addition, as the molar absorptivity of morphine is poor above 210–220 nm and its potentially lethal levels are fairly low (ca. 0.1–1 μg/ml), 'direct injection' HPLC methods with UV detection are in practice unsuitable. The only examples of direct morphine determination in untreated biological fluids were reported by Nelson *et al.*[12] and, more recently, by Arunyanart and Cline Love[8]; however both appear ill-suited for practical use. The former, adopting a reversed-phase system with off-line analysis of the collected fractions of the eluate by immunoassay, is too complex and time consuming; the latter, using micellar chromatography with fluorescence HPLC detection, has limited sensitivity (300 ng/ml).

Recently, we developed an HPLC assay for morphine using an alkaline mobile phase (pH 9.5) and a poly(styrene–divinylbenzene) column (PLRP-S) with amperometric electrochemical detection (ED) at an oxidation potential of 350 mV[13]. Because of the high selectivity of such a low voltage, the injection of biological samples required only simple and rough extraction procedures.

Hux *et al.*[14] and Shihabi *et al.*[5] reported the use of polymeric packings (Amberlite XAD-2 and PRP-1) for achieving the direct injection of blood plasma and serum into HPLC systems. They observed that, as most plasma proteins have their isoelectric point close to neutral pH, in alkaline media they are highly charged and therefore unretained by the hydrophobic, pH-stable stationary phase. In addition polymeric matrices for basic compounds allow work in reversed-phase chromatogra-

phy under ionization control conditions, and intrinsically lack any 'silanol effect'.

On this basis, we devised the possibility of developing a 'direct injection' HPLC assay of morphine by simple adjustments of the above-mentioned HPLC–ED method, which just used a polymeric column and an alkaline mobile phase. In addition, taking advantage of the low potential (350 mV) required to oxidize morphine at basic pH, the use of highly sensitive amperometric detection seemed not to be precluded, notwithstanding the risks of electrode passivation because of the amounts of proteins injected.

EXPERIMENTAL

Apparatus

The isocratic HPLC system consisted of a Model 880 PU high-pressure pump (Jasco, Tokyo, Japan), a Model 7125 sample injector with a 50-μl loop (Rheodyne, Cotati, CA, U.S.A.), a Clar 055 column oven (Violet, Rome, Italy) and an electrochemical detector (Bioanalytical Systems, West Lafayette, IN, U.S.A.) with a glassy carbon thin-layer transducer cell (LC-17A) with an Ag/AgCl reference electrode, and an LC-4B controller. An on-line 0.5-μm filter frit (Rheodyne) following the injection valve protected the column from particle contamination. The column used was a PLRP-S 300 Å, 8 μm (250 x 4.6 mm I.D.) from Polymer Labs. (Church Stretton, U.K.), packed with spherical macroporous poly(styrene–divinylbenzene) particles. A 150 x 4.6 mm I.D. column packed with 100 Å 5 μm resin from the same producer was also used in early experiments.

Reagents, standards and samples

HPLC-grade solvents, analytical-reagent grade chemicals and morphine hydrochloride from Carlo Erba (Milan, Italy) were used.

Standards of therapeutic drugs and drugs of abuse, supplied desiccated on glass microfibre discs impregnated with silicic acid (Toxi Disc Library) were purchased from Analytical Systems (Laguna Hills, CA, U.S.A.).

A stock solution of morphine (1 mg/ml) was prepared in water; working standard solutions were prepared in human plasma over the range 31–500 ng/ml.

Human blood plasma (sodium citrate) serum and 'cadaveric serum' were obtained by centrifugation for 10 min at 1500 *g*. The supernatant was stored at −20°C for assay later (within 1 month).

Control samples were preliminarily checked by a commercially available radioimmunoassay (RIA) for morphine (Diagnostic Products, Los Angeles, CA, U.S.A.) with a sensitivity of 2.5 ng/ml.

Spiked plasma samples were assayed after allowing them to stand for at least 1 h in order to allow protein binding equilibration. However, a comparison study with samples incubated for 24 h showed no differences.

Procedure

Sample preparation was limited to filtration through 0.45-μm disposable cellulose acetate filters. Frozen and/or 'dirty' samples (*e.g.*, cadaveric blood, sera containing residues of clotting or precipitates) were clarified by centrifugation, before filtration. The volume of plasma and serum injected varied from 25 to 50 μl.

Chromatographic separation was carried out with a mobile phase composed of 0.05 mol/l phosphate buffer–isopropanol (IPA)–tetrahydrofuran (THF) (88:10:2) at pH 9.5. The eluent mixture was filtered under reduced pressure through a 0.45-μm nylon 66 membrane filter (Alltech, Eke, Belgium) prior to use. The flow-rate was 1 ml/min. The column oven was set at 65°C. Under these conditions the pressure on the top of the column was in the range 80–90 kg/cm^2.

Detection was by electrochemical oxidation at a thin-layer carbon electrode using a potential of 350 mV *vs.* Ag/AgCl. Sensitivity ranges down to 1 nA full-scale were used, still with an acceptable baseline noise.

Because no extraction procedures requiring the monitoring of the recovery were involved, we used external standardization, interpolating the concentrations of unknown samples from a plot of peak height of morphine standards diluted in plasma *vs.* concentration in the range 31–500 ng/ml.

RESULTS AND DISCUSSION

Serum and plasma samples showed no evidence of precipitation when mixed with the mobile phase at pH 9.5; however a slow increase in pressure was observed after serveral injections of real samples into the HPLC system, but it was always possible to restore normal levels by replacing the on-line frit filter between injector and column. Frits were recycled by boiling in 65% nitric acid for 20 min and thoroughly rinsing with distilled water.

No evidence of protein precipitation or adsorption on the top of the column was observed, even after more than 200 injections. So far, the procedure of column regeneration by reversing the flow direction or by removing and replacing the first few millimetres of the resin, as reported by Shihabi *et al.*[5], has not been required. However, the column was always flushed overnight and during weekends with mobile phase at 0.01 ml/min, without recycling.

Under the described conditions, proteins and other endogenous compounds eluted with the 'solvent front' of the chromatogram within 9 min, allowing a clean baseline for the morphine peak. The morphine peak ($k' \approx 4$) was resolved well from matrix components and showed an acceptable asymmetry factor of 1.3 at 10% of the peak maximum, but was fairly broad. No relevant differences in the chromatographic pattern were observed when serum instead of plasma was injected. Typical chromatograms of control and spiked human plasma are shown in Fig. 1.

Sharper peaks were obtained by using acetonitrile (15%) as the organic modifier, but in this instance the solvent front was broad enough to overlap the morphine peak at the highest sensitivities. The observed poor efficiency may be dependent on both the particle size (8 μm) and pore size (300 Å) of the resin. On the other hand, Shihabi and Dyer[4,10] reported some advantages of wide-pore over narrow-pore packings when used for direct serum injection. Our experience with a 100 Å, 5 μm resin, packed in a 150 x 4.6 mm I.D. column, confirmed problems with matrix components and worsening peak shapes. Progressive clogging of the particle pores at the top of the column by the largest proteins injected, with related disturbances to band formation, could tentatively be suggested.

Possible interferences from as many as 82 opiate and non-opiate drugs at concentrations of 20 μg/ml were excluded. It should be noted that hydromorphone was

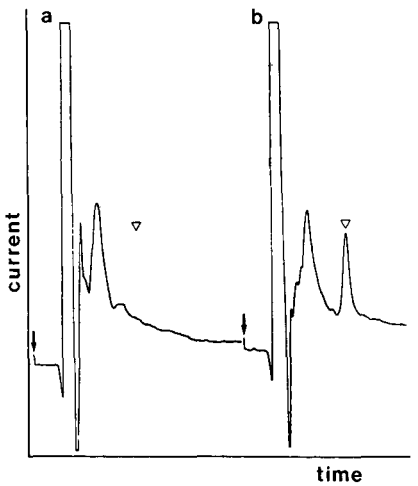

Fig. 1. Chromatograms of (a) blank plasma and (b) plasma spiked with 250 ng/ml of morphine. Injection volume, 25 μl; sensitivity range, 2 nA full-scale deflection; chart speed, 0.5 cm/min. Other conditions as in the text. The triangles indicates morphine retention time (13.4 min) and the arrows indicate injection.

not completely resolved from morphine (α = 1.2). Complete resolution was achieved by omitting THF from the mobile phase. However, in this instance the morphine peak shape was much poorer. Also, the use of acetonitrile (15%) in place of IPA and THF in the eluent (at the same pH of 9.5) achieved a baseline separation between morphine and hydromorphone but, as noted above and elsewhere[5], this solvent did not fit well with the need for protein solubility. Nevertheless, in case of any doubt, both of these eluent mixtures can actually be used for resolving the two compounds.

Oxidation potential was chosen on the basis of a previous study on the hydrodynamic electrochemical behaviour of morphine at different pH which showed a marked cathodic shift of the voltammographic curve at increasing pH[13]. Although not fully understood, this phenomenon could be attributed to the favoured ionization of the morphine phenolic group, which would promote the oxidation of the molecule. In practice, in alkaline media electrochemical detection of morphine is possible at fairly low potentials; +350 mV was chosen as the best compromise between the morphine signal and the matrix-related noise. Under these conditions, detector selectivity and ruggedness are substantially improved, allowing relatively large amounts of proteins and other endogenous compounds, such as found in 'direct injection' methods, to be handled. No evidence of electrode passivation was observed even after 20–30 serial plasma injections per day. Electrode cleaning was intentionally omitted for 1 month without any appreciable decay of response. The background current was always in the range 2–5 nA.

The relative limit of detection (LOD) signal (= three times the noise, measured with plasma blanks) was 30 ng/ml and the absolute LOD was 0.75 ng on-column. The linearity of the assay within the range 31–500 ng/ml was described by the equation $y = -0.182 + 0.0371x$; $r = 0.99996$, where x is morphine concentration (ng/ml) and y is peak height (cm). The intra-assay relative standard deviation (R.S.D.) (n = 5) was 4.3, 3.2, 1.6 and 0.09% at morphine levels of 50, 100, 200 and 500 ng/ml in

plasma, respectively. The inter-assay R.S.D. ($n = 5$), evaluated at concentrations of 100 and 500 ng/ml, was 6.5 and 4.2%, respectively.

Eleven sera from patients admitted to a first-aid station with symptoms of heroin overdose were assayed by the presented method and the results were compared with those obtained by RIA. A good correlation was obtained ($r = 0.98$).

CONCLUSION

Reversed-phase HPLC at basic pH coupled with electrochemical detection at a low potential has proved able to deal with the direct injection of plasma and serum samples. Polymeric wide-pore column packings seem suitable for this purpose. On this basis, a very simple and rugged HPLC–ED method for morphine determination was developed, which seems particularly useful in clinical toxicology. Although less sensitive than other methods requiring liquid–liquid or solid–liquid extractions[15], the present method is by far the most sensitive of those without any extraction step.

This work strongly supports the ability of amperometric electrochemical detection, in flow systems, to deal with untreated body fluids, which too often are considered incompatible with electrodes. This approach could provide 'direct injection' HPLC methods with the sensitivity the lack of which is claimed to be their main disadvantage. The use of unprotected electrodes seems possible only for compounds amenable to electrolysis at relatively low potentials, such as morphine. Otherwise, electrode protection with size-exclusion membranes could be adopted, although this would cause a significant loss of signal. Of course, these considerations apply particularly to thin-layer electrodes; 'coulometric' detectors seem intrinsically less suitable for these purposes, as endogenous proteins are more likely to foul porous electrodes by irreversible adsorption.

REFERENCES

1 D. J. Popovich, E. T. Butts and C. J. Lancaster, *J. Liq. Chromatogr.*, 1 (1978) 469–478.
2 H. Yoshida, I. Morita, G. Tamai, T. Masujima, T. Tsuru, N. Takai and H. Imai, *Chromatographia*, 19 (1984) 466–472.
3 H. Hagestam and T. C. Pinkerton, *Anal. Chem.*, 57 (1985) 1757–1763.
4 Z. K. Shihabi and R. D. Dyer, *J. Liq. Chromatogr.*, 10 (1987) 2383–2391.
5 Z. K. Shihabi, R. D. Dyer and J. Scaro, *J. Liq. Chromatogr.*, 10 (1987) 663–672.
6 D. J. Gisch, B. Feibush and R. Eksteen, poster at the *17th International Symposium on Chromatography, Vienna, September 25–30, 1988*, Abstracts, I P 30.
7 F. J. DeLuccia, M. Arunyanart and L. J. Cline Love, *Anal. Chem.*, 57 (1985) 1564–1568.
8 M. Arunyanart and L. J. Cline Love, *J. Chromatogr.*, 342 (1985) 293–301.
9 D. Westerlund, *Chromatographia*, 24 (1987) 155–164.
10 Z. K. Shihabi, *J. Liq. Chromatogr.*, 11 (1988) 1579–1593.
11 D. Chan Leach, M. A. Stadalius, J. S. Berus and L. R. Snyder, *LC·GC Int. Mag. Liq. Gas Chromatogr.*, 1 (1988) 22–30.
12 P. E. Nelson, S. M. Fletcher and A. C. Moffat, *J. Forensic Sci. Soc.*, 20 (1980) 195–202.
13 F. Tagliaro, G. Carli, F. Cristofori, G. Campagnari and M. Marigo, *Chromatographia*, 26 (1988) 163–167.
14 R. A. Hux, H. Y. Mohammed and F. F. Cantwell, *Anal. Chem.*, 54 (1982) 113–117.
15 F. Tagliaro, D. Franchi, R. Dorizzi and M. Marigo, *J. Chromatogr.*, 488 (1989) 215–228.

Journal of Chromatography, 507 (1990) 259–265
Elsevier Science Publishers B.V., Amsterdam — Printed in The Netherlands

CHROMSYMP. 1695

Measurement of 5-fluorouracil and its active metabolites in tissue

THEODORE A. STEIN*, GERARD P. BURNS, BEVERLY BAILEY and LESLIE WISE
Department of Surgery, Long Island Jewish Medical Center, Clinical Campus for the Albert Einstein College of Medicine, New Hyde Park, NY 11042 (U.S.A.)

SUMMARY

The 5-fluorouracil content of serum, bile, pancreatic juice, liver, pancreas and muscle was measured by reversed-phase high-performance liquid chromatography using a mobile phase of 5 m*M* 1-heptanesulfonic acid in 5 m*M* acetic acid. Free or unmetabolized 5-fluorouracil was extracted from samples with a mixture of light petroleum–*n*-propanol (40:60). The active metabolites of 5-fluorouracil were hydrolyzed with hot perchloric acid to free 5-fluorouracil and the combined 5-fluorouracil content was extracted. The active metabolite fraction was calculated from the difference between the combined and the free fractions. A straight line plot of the peak areas against concentration was achieved and the detection limit was 50 ng/ml. Five minutes after stopping an intravenous infusion of 15 mg/kg of 5-fluorouracil in a dog, the serum contained only the free form, but other body fluids and tissues contained both free and metabolite fractions. The method may be useful to determine the amount of total drug in patient samples.

INTRODUCTION

5-Fluorouracil (5FU) has been used for the chemotherapeutic treatment of various solid tumors for more than twenty years[1,2]. The antineoplastic effects of 5FU are caused by its metabolites, 5-fluoro-2′-deoxyuridine monophosphate (5FdUMP) which inhibits thymidylate synthetase activity and the synthesis of DNA, and 5-fluorouridine triphosphate (5FUTP) which forms fraudulent RNA[3]. Adequate recoveries of these and other metabolites of 5FU are difficult from small amounts of tissue. 5FdUMP forms a tightly binding covalent bond with thymidylate synthetase and 5,10-methylenetetrahydrofolate, and is a competitive inhibitor of deoxyuridine monophosphate (dUMP) binding[4]. 5FUTP incorporates primarily into nuclear RNA, and smaller quantities also incorporate into other RNA[3]. Methods which determine these active metabolites in cell culture use radioactive 5FU, and are not suitable for application to patients[5,6]. Other methods which determine only the free or unmetabolized fractions of 5FU in plasma or serum may be a poor measure of the active metabolites, since 5FdUMP forms an irreversible bond and the elimination kinetics of

0021-9673/90/$03.50

5FU are non-linear which is consistent with a two-compartment metabolic model[7,8]. Steady state plasma levels of 5FU may or may not be achieved depending on the dose administered and the metabolic status of the patient[7,9]. The purpose of this investigation was to devise a means by which 5FU and its active metabolites can be measured in tissue and body fluids.

EXPERIMENTAL

Materials

All chemicals and reagents were either analytical or spectroquality grade. Hydrochloric acid, perchloric acid and light petroleum (b.p. 37.2–57.8°C) were obtained from Mallinckrodt (St. Louis, MO, U.S.A.). Potassium hydroxide, sodium sulfate, sodium acetate, 5FU, 5-fluorocytosine (5FC), 5-fluorodeoxyuridine (5FdU) and 5-fluorodeoxyuridine monophosphate were purchased from Sigma (St. Louis, MO, U.S.A.). Water and *n*-propanol were of HPLC-grade and were obtained from Burdick & Jackson Labs. (Muskegan, MI, U.S.A.). Zetopar® membrane filters, 13-mm diameter, 0.45-μm pore size were purchased from Rainin (Woburn, MA, U.S.A.), high-purity dry nitrogen from T. W. Smith (Brooklyn, NY, U.S.A.) and polypropylene test tubes from Sarstedt (Princeton, NJ, U.S.A.).

Apparatus

The high-performance liquid chromatography (HPLC) system was purchased from Waters-Millipore (Milford, MA, U.S.A.) and consisted of an automatic injector (Model 712), an automatic gradient controller (Model 680), a pump (Model 510), a 300 × 2 mm I.D. μBondapak C_{18} column, a LC spectrophotometer (Model 481) and the data integrator (Model 730). The mobile phase, 1-heptanesulfonic acid (PIC B7) was also obtained from Waters-Millipore. One vial was dissolved in 1 l of water resulting in a solution of 5 m*M* 1-heptanesulfonic acid in 5 m*M* acetic acid.

Chromatographic conditions

The column was equilibrated at room temperature with the mobile phase at a flow-rate of 0.5 ml/min. The injection volume of the samples and standards was 20 μl and the elution of 5FU and 5FC, the internal standard, were detected at 254 nm. Samples and standards were analyzed in triplicate.

Standards

Two sets of standards of 5FU were prepared. 5FU and 5FC concentrations in serum were compared to similar levels in water. Aqueous standards were prepared at a concentration of 1 mg/ml and stored at −70°C. Dilutions with water were made daily for assay and determination of the standard curve which had a range from 0.01 to 1000 μg/ml. Serum concentrations varied from 0.05 to 200 μg/ml of 5FU. In all dilutions the concentration of 5FC was brought to 5 μg/ml. The volume of the aqueous standards or the spiked serum used for assay was 0.2 ml. After extraction and evaporation of the solvent, the recovered 5FU and 5FC was redissolved in 0.2 ml of water.

Sample extraction

The optimal method for extracting 5FU and 5FC from the body fluids and tissues was determined. Since preliminary studies indicated that ethyl acetate extracted substances from the samples that coeluted with 5FU, a light petroleum–*n*-propanol mixture was used to minimize the extraction of the contaminant. In order to determine the appropriate solvent mixture, the recoveries of 1 μg of 5FU and 50 μg of 5FC in 0.2 ml of serum were determined after extraction with 2 ml of light petroleum–*n*-propanol mixtures at ratios of 100:0, 80:20, 60:40, 40:60, 20:80 or 0:100 (v/v), and compared to the unextracted aqueous control. The pH of samples was adjusted to 4.8 with 0.5 ml of 0.8 *M* sodium sulfate and 0.05 ml of 1.5 *M* sodium acetate buffer. The solution was extracted three times with 2 ml of the same petroleum ether–*n*-propanol mixture. The upper organic layers were pooled and evaporated with nitrogen. The residue was dissolved in 2 ml of water. The amount of 5FU and 5FC recovered with each solvent mixture were compared to the unextracted standard.

In order to determine the time required to completely hydrolyze the 5FU active metabolites to free 5FU, two experiments were performed. Amounts of 10 μg of 5FU and 5FdU were brought into separate tubes, and were then incubated in 1 ml of 70% perchloric acid at 85°C for 0, 1, 2, 3 and 4 h. The amount of 5FU obtained from 5FdU hydrolysis was determined for each time. After cooling to room temperature 2.8 ml of 4 *M* potassium hydroxide was added and the tubes were centrifuged at 3000 *g* for 10 min. The supernatant was acidified with 2 *M* hydrochloric acid to pH 3, and then extracted using 30 ml of light petroleum–*n*-propanol (40:60). After two additional extractions the pooled organic layers were evaporated with nitrogen. The residue was dissolved in 2 ml of water. The amount of 5FU produced was compared to the appropriate control tube. In a second experiment 10 μg of 5FU, 5FdU, 5FdUMP and 5FC were dissolved in separate tubes containing 0.2 ml of serum. Then 1 ml of 70% perchloric acid was added to each tube and samples were incubated at 85°C for 2 h. Samples were extracted as before. The amount of 5FU recovered after hydrolysis of each metabolite was compared to control tubes containing unhydrolyzed but extracted metabolites.

Animals

A healthy mongrel dog weighing 20 kg was obtained from Biomedical Assoc. (Friedenburg, PA, U.S.A.). In order to condition the dog to the laboratory environment, a standard laboratory chow was fed (Ralston Purina, St. Louis, MO, U.S.A.) and the animal was housed in a U.S. Department of Agriculture approved facility for at least one week before the experiment.

Following an overnight fast, the dog was anesthetized with an intravenous injection of sodium phenobarbital at a dose of 35 mg/kg and intubated with an endotracheal tube, allowing spontaneous air breathing. A laparotomy was performed. The common bile duct, pancreatic duct and a foreleg vein were cannulated for sample collection. Approximately 1 ml of bile and pancreatic juice, and 3 ml of blood were obtained. Then 1 to 2 g of liver, pancreas and *rectus abdominus* muscle were resected. Samples were placed on ice.

Using another intravenous cannula placed in a second leg, 15 mg/kg of 5FU was administered over 10 min. Five minutes after stopping the infusion, samples of fluids and tissues were again collected. Sera were obtained after centrifugation.

Samples of liver, pancreas and muscle weighing from 150–300 mg and 0.2 ml of serum, bile and pancreatic juice were placed in separate tubes and 5FC was added to concentrations of 5 μg/ml or μg/g. In order to determine the content of free 5FU, tissues were homogenized in 2 ml of the buffered light petroleum–*n*-propanol mixture (40:60, v/v), at pH 4.8 with a Polytron homogenator set at position 7 for 20 s; body fluids were extracted in a similar solution. The aqueous layer was extracted two additional times, and the organic layers were pooled. After evaporation with nitrogen the residue was dissolved in 0.2 ml of water.

Similar quantities of samples were hydrolyzed for 2 h by incubating in 1 ml of 70% perchloric acid at 85°C. After cooling to room temperature 2.8 ml of 4 *M* potassium hydroxide were added, and mixed to precipitate potassium perchlorate. Following centrifugation at 3000 *g* for 10 min the supernatant was acidified with 2 *M* hydrochloric acid to pH 3. 5FU was extracted three times with 30 ml of the buffered petroleum ether–propanol extraction solution. The organic solvent was evaporated with nitrogen and the residue was dissolved in 0.2 ml of water and assayed. The amount of the active 5FU metabolites was calculated from the combined 5FU content minus the free 5FU.

RESULTS AND DISCUSSION

Standard curve

A plot of the 5FU to 5FC area ratio against serum concentration was linear from 0.05–200 μg/ml. The coefficients of variation (C.V.) of the data points were 1 to 3%. A standard curve of 5FU diluted in water was also linear but the C.V. was 0.5 to 1%. Since little 5FU is bound to plasma protein[7], the slightly greater variation seen in the plasma standards can be attributed to the small variation in the recovery of 5FU by the extraction method. The sensitivity of the method is similar to previous reports[10,11]. Other investigators using radioactive 5FU as an internal standard have reported more sensitive methods[12,13].

Extraction and hydrolysis

While light petroleum did not extract any detectable 5FU or 5FC, *n*-propanol extracted 95–97% of the 5FU and 5FC present in serum (Table I). *n*-Propanol,

TABLE I

EXTRACTION OF 5-FLUOROURACIL AND 5-FLUOROCYTOSINE FROM SERUM

Concentrations of 5-fluorouracil and 5-fluorocytosine were 5 μg/ml and 250 μg/ml, respectively. Values are from two experiments.

Light petroleum–n-propanol	*5-Fluorouracil (%)*	*5-Fluorocytosine (%)*
Unextracted aqueous control	100	100
100:0	0; 0	0, 0
80:20	0; 0	2.5; 3.1
60:40	54.7; 58.7	20.5; 25.3
40:60	62.6; 65.6	63.8; 65.2
20:80	83.1; 87.9	88.9; 91.7
0:100	94.4; 99.2	91.4; 98.0

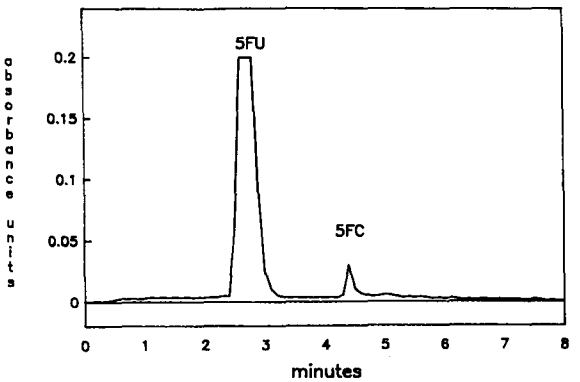

Fig. 1. Chromatogram of a 0.2-ml serum sample which contained 100 μg/ml of 5-fluorouracil (5FU) and 5 μg/ml of 5-fluorocytosine (5FC), and extracted with a mixture of light petroleum–*n*-propanol (40:60, v/v). Retention times for 5FU and 5FC were 2.70 and 4.40 min, respectively. The elution solvent was 5 m*M* 1-heptanesulfonic acid in 5 m*M* acetic acid.

however, also extracts contaminating substances which coelute with 5FU. With a light petroleum–*n*-propanol mixture (40:60) the contaminant was not extracted from serum which contained no 5FU or 5FC. Using this extraction mixture, 64–75% of the 5FU and 5FC was recovered. In Fig. 1 a serum sample containing 100 μg/ml of 5FU and 5 μg/ml of 5FC had retention times of 2.70 and 4.40 min, respectively.

The time required to completely hydrolyze the active metabolites of 5FU was determined. When 5FdU was hydrolyzed, only 1 h was required to achieve near complete conversion to 5FU (Table II). Under the conditions of hydrolysis, the amount of 5FU was stable for at least 4 h. At zero time only 5FdU was present and eluted with a retention time of 3.60 min, whereas only 5FU was detected with a retention time of 2.70 min after hydrolysis.

Hydrolysis of 5FU, 5FdU, 5FdUMP and 5FC with 70% perchloric acid at 85°C for 2 h and extracted as before resulted in the complete conversion of 5FdUMP to 5FU and 93.1% of the 5FdU to 5FU. The amount of 5FU recovered in each tube was

TABLE II

PERCENTAGE OF 5-FLUOROURACIL PRESENT AFTER HYDROLYSIS OF 5-FLUORODEOXYURIDINE

Amounts of 10 μg of 5FU and 5FdU were hydrolyzed in 1 ml of 70% perchloric acid at 85°C from 0 to 4 h. After stopping the reaction with potassium hydroxide and extraction, the amount of 5FU was determined. The percent of 5FU converted from 5FdU was calculated by adjusting for the amount of 5FU lost after extraction of the time-control tubes which contain only 5FU.

Time (h)	*5-Fluorodeoxyuridine (%)*	*5-Fluorouracil (%)*
0	100	0
1	2	98
2	4	96
3	6	94
4	4	96

adjusted by correcting for the proportion of 5FU lost from hydrolysis and extraction in the control tube. Treatment of 5FC with perchloric acid did not result in any 5FU generation. Since 5FdUMP rapidly dissociates from the thymidylate synthetase–5,10-methylenetetrahydrofolate–5FdUMP complex at temperatures greater than 60°C[14], and free bases are liberated from RNA by hydrolysis with hot perchloric acid[15], the method for hydrolysis and extraction is suitable for converting the chemotherapeutic active metabolites in tissue to free 5FU.

Animal experiments

With our extraction methodology no contaminating substances eluted from zero time serum, bile or pancreatic juice with the retention times of 5FU and 5FC. Liver, pancreas and muscle, however, contain substances that elute very near to the 5FU peak. At a light petroleum–*n*-propanol ratio of 40:60, the extraction of the interfering substances was reduced, and as little as 0.1 μg of 5FU in 1 g of tissue can be measured. The chromatogram of the elution of the combined 5FU present in the liver 5 min after stopping the 5FU infusion is shown in Fig. 2. The 5FU content of the liver was 16 μg/g. Although 5FdU was detected in extracted tissues, it was not present after hydrolysis and not in serum.

The content of 5FU in the combined fraction containing free 5FU plus the 5FU obtained after hydrolysis of the active metabolites, the free 5FU fraction and the metabolite fraction in serum, bile, pancreatic juice, liver, pancreas and muscle obtained 5 min after stopping 5FU infusion is listed in Table III. In the serum 5FU was present only in the free form, and the level, 21.0 μg/ml, was similar in magnitude as found by others[16,17]. The concentration of the combined 5FU in bile and pancreatic juice was 70% and 30% respectively of that in the serum. Although 20% of the combined 5FUin the bile was from active metabolites, it comprised only 4% in the pancreatic juice. The concentration of the combined 5FU in bile was 91% of the liver content, suggesting that 5FU was easily excreted by the liver. 5FU secretion in the pancreatic juice was less. The pancreas contains a large proportion of the combined 5FU in the active metabolite fraction, compared to the liver and the muscle.

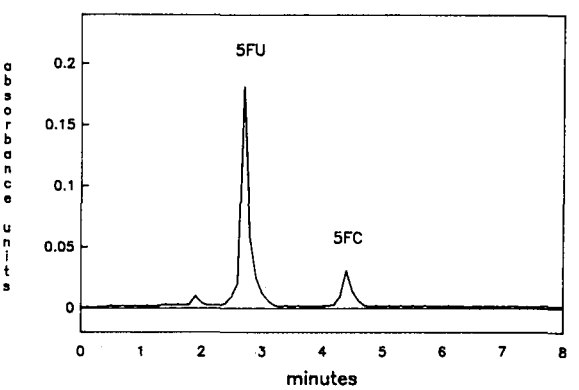

Fig. 2. Chromatogram of a 0.2-g liver sample which was obtained 5 min after cessation of the intravenous infusion of 15 mg/kg of 5-fluorouracil (5FU). The tissue was hydrolyzed with 70% perchloric acid at 85°C for 2 h and extracted with a mixture of light petroleum–*n*-propanol (40:60, v/v). The specimen contained 16 μg/g of 5FU; 5 μg/g of 5-fluorocytosine (5FU), the internal standard, was added.

TABLE III

5-FLUOROURACIL CONTENT IN FLUIDS AND TISSUES

The combined fraction contained free 5FU plus the 5FU obtained after hydrolysis of the active metabolites. The free fraction contained only the unmetabolized 5FU. The active metabolite fraction was calculated by substracting the free from the combined fraction.

Sample	*Combined*	*Free*	*Active metabolites*
Serum	21.0 μg/ml	21.0 μg/ml	0.0 μg/ml
Bile	14.6 μg/ml	11.6 μg/ml	3.0 μg/ml
Pancreatic juice	6.4 μg/ml	6.0 μg/ml	0.4 μg/ml
Liver	16.0 μg/g	14.8 μg/g	1.2 μg/g
Pancreas	23.6 μg/g	13.2 μg/g	10.4 μg/g
Muscle	10.5 μg/g	9.0 μg/g	1.5 μg/g

Reducing 5FU active metabolites, which may be covalently bound to enzymes and RNA, to free 5FU provides a means by which normally unattainable 5FU can be easily measured. Since the chemotherapeutic forms of 5FU can be measured as the free form after hydrolysis, determining the proportion of 5FU in the free and metabolite fractions in samples from biopsies or catheters could be a means by which the penetration of the drug in tissues and body fluids can be evaluated.

REFERENCES

1 C. Heidelberger and F. J. Ansfield, *Cancer Res.*, 23 (1963) 1226.
2 G. E. Moore, I. D. J. Bross, R. Ausman, S. Nadler, R. Jones, Jr., N. Slack and A. A. Rimm, *Cancer Chemother. Rep.*, 52 (1968) 641.
3 H. M. Pinedo and G. J. Peters, *J. Clin. Oncol.*, 6 (1988) 1653.
4 P. V. Danenberg, *Biochim. Biophys. Acta*, 473 (1977) 73.
5 A. L. Pogolotti, Jr., P. A. Nolan and D. V. Santi, *Anal. Biochem.*, 117 (1981) 178.
6 J.-P. Sommadossi, D. A. Gewirtz, R. B. Diasio, C. Aubert, J.-P. Cano and I. D. Goldman, *J. Biol. Chem.*, 257 (1982) 8171.
7 J. G. Wagner, J. W. Gyves, P. L. Stetson, S. C. Walker-Andrews, I. S. Wollner, M. K. Cochran and W. D. Ensminger, *Cancer Res.*, 46 (1986) 1499.
8 J. L.-S. Au, J. S. Walker and Y. Rustum, *J. Pharmacol. Exp. Ther.*, 227 (1983) 174.
9 J. E. Byfield, S. S. Frankel, C. L. Hornbecak, T. R. Sharp, F. B. Callipari and R. A. Floyd, *Am. J. Clin. Oncol.*, 8 (1985) 429.
10 N. Christophidis, G. Mihaly, F. Vajda and W. Louis, *Clin. Chem.*, 25 (1979) 83.
11 P. L. Stetson, U. A. Shukla and W. D. Ensminger, *J. Chromatogr.*, 344 (1985) 385.
12 A. R. Buckpitt and M. R. Boyd, *Anal. Biochem.*, 106 (1980) 432.
13 C. Finn and W. Sadee, *Cancer Chemother. Rep.*, 59 (1975) 279.
14 D. V. Santi, C. S. McHenry and H. Sommer, *Biochemistry*, 13 (1974) 471.
15 G. R. Wyatt, in E. Chargoff and J. N. Davidson (Editors), *The Nucleic Acids*, Vol. 1, Academic Press, New York, 1955, p. 243.
16 L. A. Celio, G. J. DiGregorio, E. Ruch, J. N. Pace and A. J. Piraino, *J. Pharm. Sci.*, 72 (1983) 597.
17 L. J. Schaaf, D. G. Ferry, C. T. Hung, D. G. Perrier and I. R. Edwards, *J. Chromatogr.*, 342 (1985) 303.

Journal of Chromatography, 507 (1990) 267–276
Elsevier Science Publishers B.V., Amsterdam — Printed in The Netherlands

CHROMSYMP. 1681

Optimization of multidimensional high-performance liquid chromatography for the determination of drugs in plasma by direct injection, micellar cleanup and photodiode array detection

JOSEPH V. POSLUSZNY* and ROBERT WEINBERGER
Applied Biosystems, Inc., 170 Williams Drive, Ramsey, NJ 07446 (U.S.A.)
and
ERIC WOOLF
Berlex Laboratories, 110 East Hanover Avenue, Cedar Knolls, NJ 07927 (U.S.A.)

ABSTRACT

Improvements in a multidimensional liquid chromatography system for the direct determination of drug substances in blood plasma are reported. The system employs an on-line micellar chromatographic cleanup followed by a reversed-phase analytical separation. The limit of detection of propanolol is improved by a factor 10 compared to previously reported work. The technique is applied towards the determination of a multicomponent mixture of tricyclic anti-depressants in blood plasma. A protocol for optimization is described.

INTRODUCTION

Direct injection of biological fluids into the liquid chromatograph is advantageous from the standpoints of speed, cost, safety, sample identification and analytical recovery. This subject was recently reviewed[1]. The problems encountered here generally include shortened column life, lack of trace enrichment and interferences, both exogenous and endogenous. Many of these problems are addressed by column switching[2–10]. More recently, the use of micellar reagents for the first dimension of the column switching procedure has been shown to have certain advantages[11–12]. These advantages include prolongation of column life through solubilization of proteins, extraction of protein-bound drugs and the ability to finely control the elution pattern on the cleanup column.

The advantages of this micellar–reversed-phase system are exploited and applied to the determination of a multicomponent mixture of a structurally related series of anti-depressant drugs. Guidelines for the selection and optimization of the cleanup or extraction column are provided. A high-sensitivity photodiode array de-

0021-9673/90/$03.50

tector is shown to enhance methods development as well as to be capable of trace analysis (ng/ml) of drugs in biological fluids.

The routine use of this direct sample injection (DSI) technology is demonstrated by the analysis of 450 samples over a three-week time frame. Data are presented for precision and accuracy among days. Fifty assays per day were typical for determining propranolol in blood plasma.

EXPERIMENTAL

Apparatus

The high-performance liquid chromatography (HPLC) and related column switching equipment was described in ref. 11. The system was modified with a second low-pressure solenoid valve, to facilitate solvent switching, as indicated in Fig. 1. In addition, an Applied Biosystems (ABI; Ramsey, NJ, U.S.A.) 1000S Photodiode array detector was employed for multiwavelength chromatographic detection and spectral acquisition.

Reagents and columns

The tricyclic anti-depressant drugs, imipramine (IMI), desipramine (DES), amitriptyline (AMI), and nortriptyline (NOR) were obtained from Sigma (St. Louis, MO, U.S.A.). Doxepin was obtained as a 1-mg/ml solution in methanol from Supelco (Bellfonte, PA, U.S.A.). Sequanal-grade sodium dodecyl sulfate (SDS) was obtained from Pierce (Rockford, IL, U.S.A.). All other reagents and solvents were from sources described in ref. 11. Precise reagent compositions are given in individual figure captions as appropriate.

All of the chromatographic columns were obtained from ABI (formerly Brownlee Labs.).

Detection

Propranolol was measured with fluorescence by using an ABI 980 fluorescence

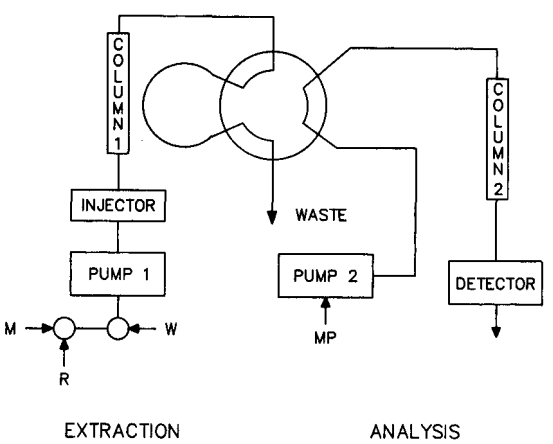

Fig. 1. System configuration. Key: M = micellar mobile phase; R = recovery mobile phase; W = wash mobile phase; MP = analytic mobile phase.

detector with excitation at 240 nm. The emission wavelengths were selected with a 360-nm bandpass filter. The flow cell volume was 25 μl. The photomultiplier tube voltage was 650 V with a range of 0.1 μA full scale.

The tricyclic anti-depressants were determined by absorbance with a photodiode array absorbance detector. The detector wavelength was set at 239 nm unless otherwise specified.

Procedure

Plasma samples were prepared by filtration through 0.45-μm Centrex disposable centrifuge filtration units (nylon membrane) obtained from Schleicher and Schuell prior to loading the autosampler (WISP, Waters Assoc., Milford, MA, U.S.A.).

RESULTS AND DISCUSSION

Improving sensitivity and selectivity

Improvements in sensitivity in column switching procedures can be realized by simply increasing the sample size and trace enrichment on-line provided there is appropriate selectivity. The problem of selectivity was the limiting factor in our earlier work[11]. Interferences from endogenous and exogenous material limited the ultimate limit of detection (LOD) that was attainable. That work employed a 3 × 1 cm I.D. enrichment column packed with 5-μm porous reversed-phase material. While the column lifetime was in the hundreds of injections, the dispersion caused by the large frits required opening the cut window thereby allowing the admission of potential interferences to the analytical column. Narrower I.D. frits (*e.g.* 2 mm) substantially reduced column lifetime.

A more optimal solution is to employ 4.6 or 3.2 mm I.D. columns with the length tailored to the individual application (usually 15–40 mm). These small columns provide less dispersion than those with larger diameters. This results in sharper peaks. Therefore, the extraction/cleanup column and the analytical column can be kept in series for a shorter period of time. These miniature columns are inexpensive enough such that they can be discarded every hundred injections.

Exogenous interferences from reagents, primarily SDS, can also limit detectibility. Since the micellar mobile phase has relatively weak eluting power, hydrophobic contaminants are retained at the head of the analytical column. These contaminants may be subsequently eluted during mobile phase switching. The degree of interference was related to the grade of the raw material employed. Interferences were evident for both absorbance and fluorescence detection. Sequanal-grade SDS provided the lowest interferences. Since this column switching procedure employs trace enrichment, the purity of all reagents is especially critical.

Selective recovery from the extraction column

In our previous work, the drug was cut onto the analytical column with micellar mobile phase as it eluted off the tail of the exclusion front. This style of recovery, illustrated in Fig. 2, has three significant disadvantages that markedly impact selectivity: (i) endogenous serum substances are eluted onto the analytical column; (ii) the micellar mobile phase is drastically different from the analytical mobile phase result-

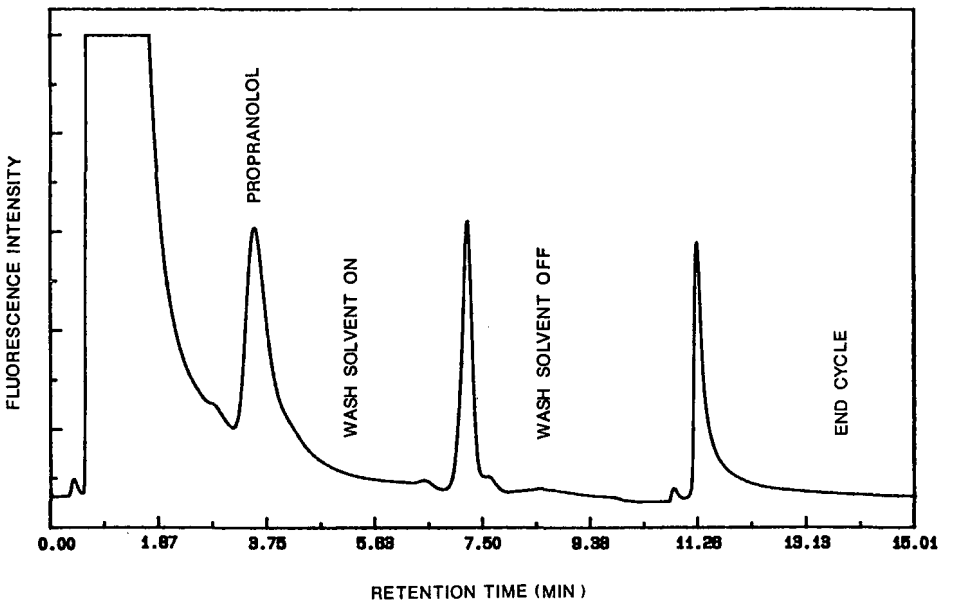

Fig. 2. Extraction column chromatogram of propranolol in blood plasma, 400 ng/ml with a common extraction and micellar recovery solvent. Column: 30 × 10 mm I.D. (cyanopropyl bonded phase on 5 μm porous silica). Injection size: 100 μl. Extraction mobile phase: acetonitrile–water (8:92, v/v) containing 40 m*M* SDS, 10 m*M* sodium dihydrogenphosphate, 10 m*M* sodium hydrogenphosphate; flow-rate: 2 ml/min. Wash mobile phase: acetonitrile–water (70:30, v/v) containing 40 m*M* SDS and 10 m*M* sodium dihydrogenphosphate; flow-rate: 2 ml/min.

ing in a large baseline shift since as much as 4 ml may be cut onto the analytical column; and (iii) the relatively weak eluting power of the micellar mobile phase results in the retention and buildup of hydrophobic substances on the analytical column.

These disadvantages were overcome by providing for a more selective elution of the extraction column. This was achieved in the following stepwise manner: (i) inject a plasma sample under micellar conditions; (ii) select the micellar solvent and column to ensure significant retention of the drug; (iii) after clearance of the proteinaceous material, elute the drug with a non-micellar recovery mobile phase; (iv) the extraction and analytical columns are placed in series and the drug recovered onto the analytical column; (v) switch to the analytical mobile phase and perform the separation on the analytical column; and (vi) simultaneously with step (v) wash and re-equilibrate the extraction column with micellar mobile phase.

Following this protocol results in the ordering of mobile phases flowing through the extraction column as follows: (i) micellar solution (extraction solution; the solvent that washes endogenous material off the column while permitting analyte retention); (ii) recovery solution (the solvent that elutes the analyte off the extraction column onto the analytical column); (iii) wash solution (a strong solvent employed to clean-up the extraction column).

A chromatogram of the extraction column run under the above conditions is shown in Fig. 3. Compared to Fig. 2, the drug is further removed from the proteinaceous front and the peak is considerably sharpened. Two hundred separate cycles were

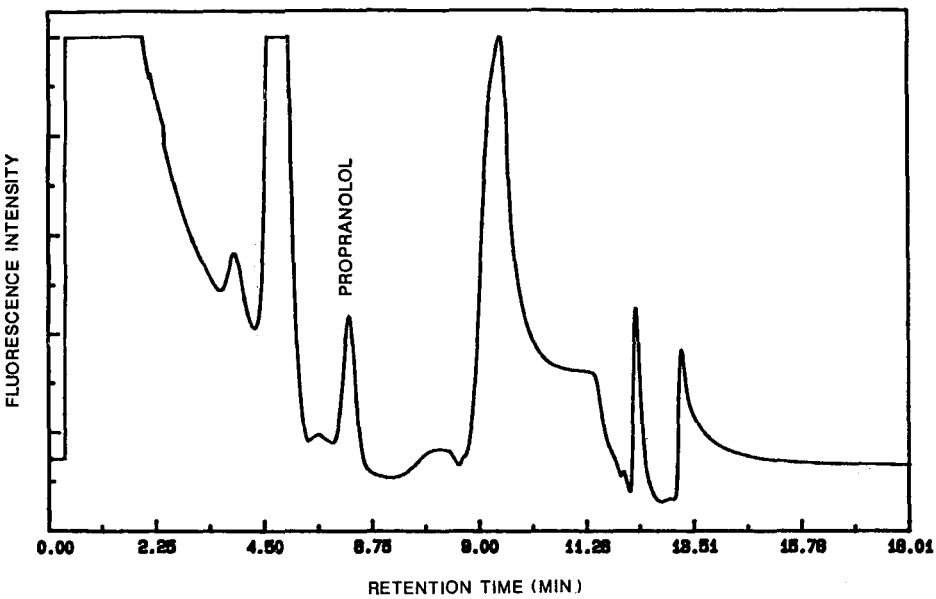

Fig. 3. Extraction column chromatogram of propranolol in blood plasma, 100 ng/ml with a selective recovery solvent. Column: 40 × 4.6 mm I.D. (phenylpropyl bonded phase on 5 μm porous silica). Injection size: 200 μl. Extraction mobile phase: aceonitrile–water (8:92, v/v) containing 60 m*M* SDS, 10 m*M* sodium dihydrogenphosphate, 10 m*M* sodium hydrogenphosphate; flow-rate: 2 ml/min. Recovery mobile phase: acetonitrile–water–acetic acid–triethylamine (42:58:0.2:0.04, v/v); flow-rate: 2 ml/min. Wash mobile phase: acetonitrile–water (70:30, v/v) containing 60 m*M* SDS and 10 m*M* sodium dihydrogenphosphate; flow-rate: 2 ml/min.

performed while monitoring the retention time of propranolol on the extraction column. No significant shifts in retention time were found. The cut window remained constant over a span of 200 injection cycles, a requirement for this form of analytical procedure.

The qualifications of the recovery solvent are straight forward. The solvent is usually an aqueous dilution of the analytical mobile phase. This measure generally provides for solvent focusing on the head of the analytical column.

The end result of all of these measures is a dramatic sharpening of the peak or peaks of interest both on the extraction as well as the analytical column. Both sensitivity and selectivity are improved. The chromatogram of propranolol, Fig. 4, is substantially improved compared to previous work[11]. The LOD, conservatively estimated at 0.5 ng/ml, is improved by a factor ten.

Routine operation of the method

The method was applied towards the determination of propranolol in blood plasma from nine subjects receiving a single oral dose of 80 mg propranolol hydrochloride. Plasma samples were drawn just prior to dose and at 0.5, 1, 2, 3, 4, 5, 6, 8, 10 and 12 h post dose. The mean observed peak drug level was 31 ng/ml. The limit of quantitation (LOQ) was set at 1.0 ng/ml where the relative standard deviation (R.S.D.) approached 10%. The complete results of the pharmacokinetic studies will be published elsewhere.

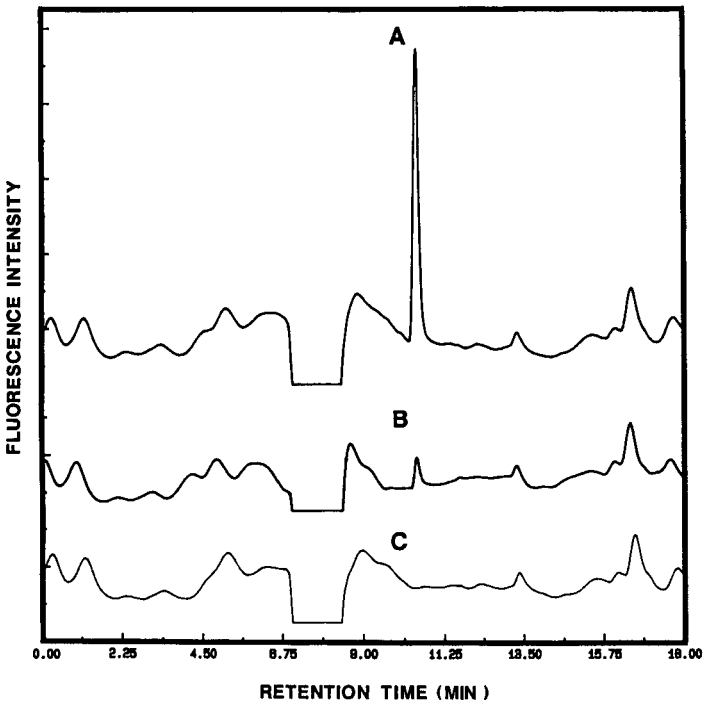

Fig. 4. Multidimensional chromatograms of propranolol. (A) 10 ng/ml; (B) 1 ng/ml; and (C) blank, all in blood plasma. Extraction column, extraction mobile phase, recovery mobile phase and wash mobile phase as in Fig. 3. Injection size: 200 μl. Analytical column: Spheri-5, RP-18, 22 cm × 4.6 mm I.D. cartridge column. Analytical mobile phase: acetonitrile–water–acetic acid–triethylamine (58:42:0.5:0.1, v/v); flow-rate: 1.5 ml/min.

A typical overnight automated run consisted of 25 plasma samples, 16 spiked plasma standards, and 4 spiked plasma quality control samples. All samples and controls were randomized and bracketed by randomized standards.

While extraction columns could be used for 200 analyses, the volume of plasma available for analysis was limited. In order to eliminate the possibility of sample loss due to column failure, the extraction column was changed every two days or 100 injections. The cost of the 40 cm × 4.6 mm I.D. extraction column was U.S.$ 0.90/injection. The same analytical column was used throughout these studies with no measurable deterioration.

The concentration of each sample was calculated from a least-squares regression plot of an eight-point standard curve. A standard curve was run in duplicate with each automated run. The precision and accuracy of the assay are shown in Table I. At propranolol concentrations above 25 ng/ml, the assay precision was found to be less than 1.7% R.S.D. At the LOQ, the R.S.D. was 9.3%.

Same day precision was assessed in two ways. Thirty percent of all samples were run in duplicate on each day. The average R.S.D. values for duplicates on a single day ranged from 0.7 to 11.7% (mean 3.8%) for nine days of experiments. On one partic-

TABLE I

STANDARD CURVE STATISTICS OF PROPRANOLOL IN PLASMA

Predicted concentrations from regression analysis.

Day	*Actual concentration (ng/ml)*							
	1.00	*2.00*	*5.00*	*10.0*	*25.0*	*50.0*	*75.0*	*100*
1	1.05	2.06	4.88	9.71	25.3	50.2	75.2	99.8
2	1.09	1.83	5.20	9.69	24.6	49.5	76.1	100
3	1.02	2.02	4.96	9.89	25.0	50.1	75.1	
10	0.85	2.23	5.40	9.48	24.5	50.2	75.4	99.9
11	1.00	2.01	5.10	9.78	25.2	50.1	72.9	102
14	1.03	2.00	4.98	9.77	24.8	50.1	75.5	
15	1.09	2.00	4.74	9.71	24.5	49.8	75.8	101
18	1.00	2.12	5.14	9.23	24.3	50.7	75.4	100
19	1.21	1.98	4.94	9.25	24.1	50.2	75.8	100
Mean (ng/ml)	1.04	2.03	5.04	9.61	24.7	50.1	75.2	100
R.S.D. (%)	9.3	5.3	3.9	2.5	1.7	0.65	1.2	0.7
Accuracy (%)	3.8	1.5	0.7	−3.9	−1.1	0.3	0.2	0.4
Same day[a] R.S.D. (%)	1.5	7.4	0.3	2.9	2.6	2.2	0.6	1.6

[a] Calculated from triplicate runs of each plasma standard during a single day.

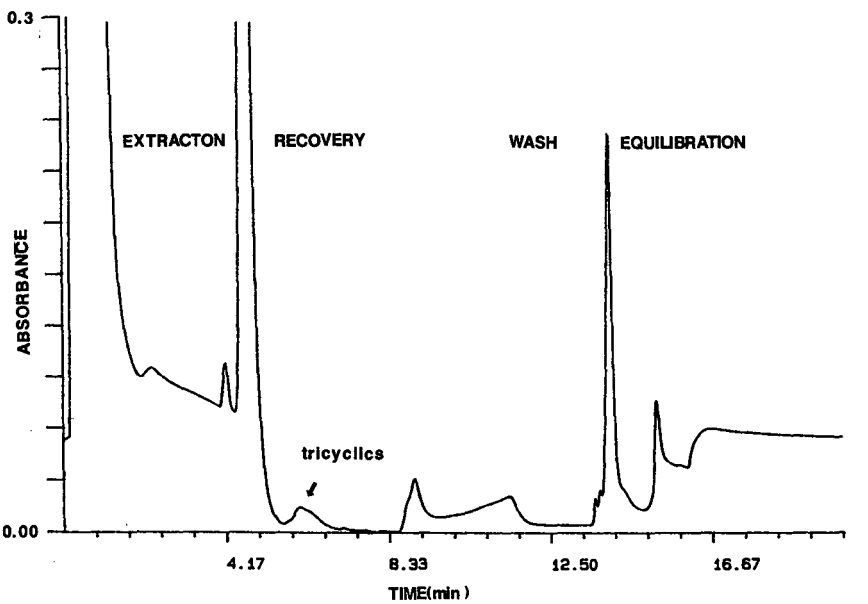

Fig. 5. Extraction column chromatogram of tricyclic anti-depressants in plasma. Extraction column: 40 × 4.6 mm I.D. polystyrene–divinylbenzene, 10 μm spherical polymer). Extraction mobile phase: acetonitrile–water–triethylamine (8:92:0.2, v/v) containing 60 m*M* SDS, 10 m*M* sodium dihydrogenphosphate and 10 m*M* sodium hydrogenphosphate; flow-rate: 2 ml/min. Recovery mobile phase: acetonitrile–methanol–water (56:12:32, v/v) containing 8 m*M* SDS, 8 m*M* sodium dihydrogenphosphate and 1 m*M* phosphoric acid; flow-rate: 2 ml/min. Wash mobile phase: acetonitrile–water (90:10, v/v) containing 60 m*M* SDS; flow-rate: 2 ml/min.

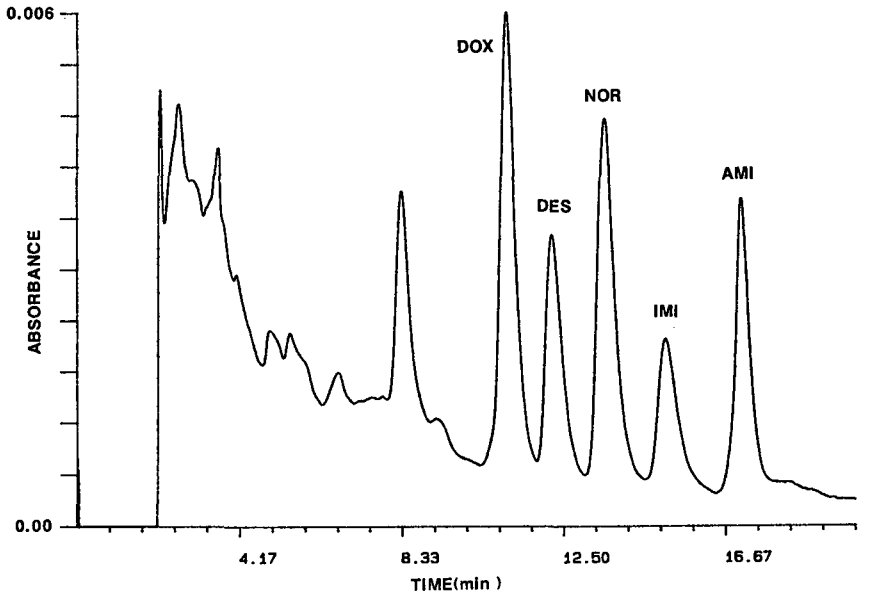

Fig. 6. Multidimensional chromatogram of tricyclic antidepressants (270 ng/ml) in blood plasma. Extraction column, extraction, recovery and wash mobile phases as in Fig. 5. Analytical column: Spheri-5, RP-18, 22 cm × 4.6 mm I.D. cartridge column. Analytical mobile phase: acetonitrile–methanol–water–triethylamine (56:12:32:0.08, v/v) containing 8 m*M* SDS, 8 m*M* sodium dihydrogenphosphate and 1 m*M* phosphoric acid. DOX = doxepin; DES = desipramine; NOR = nortriptyline; IMI = imipramine; and AMI = amitriptyline.

ular day, the entire eight-point calibration curve was run in triplicate. These data are also reported in Table I.

No carryover between sample injections was observed for the concentration range studied (0–100 ng/ml).

MULTICOMPONENT ANALYSIS

Multicomponent analysis is facile under a set of well defined conditions: (i) the compounds elute off the extraction column in a single band; (ii) the compounds are separable on the analytical column; (iii) ideally, the mechanism of separation differs in each of the columns; and (iv) detection is optimized.

For the determination of tricyclic anti-depressants, the pH of the mobile phase could be exploited along with various mobile phase additives to accomplish the first three conditions. Previous reports[13] for the solid phase extraction of these compounds from blood plasma used high pH. In that off-line sample preparation procedure, the extraction columns are discarded after only one use. For our application, multiple cycles are required so polymeric phases were used.

The selective recovery of the tricyclics from a polymeric extraction column is illustrated in Fig. 5. The five components are separated as a single peak from the solvent front of the recovery mobile phase. The recovery is accomplished by a pH

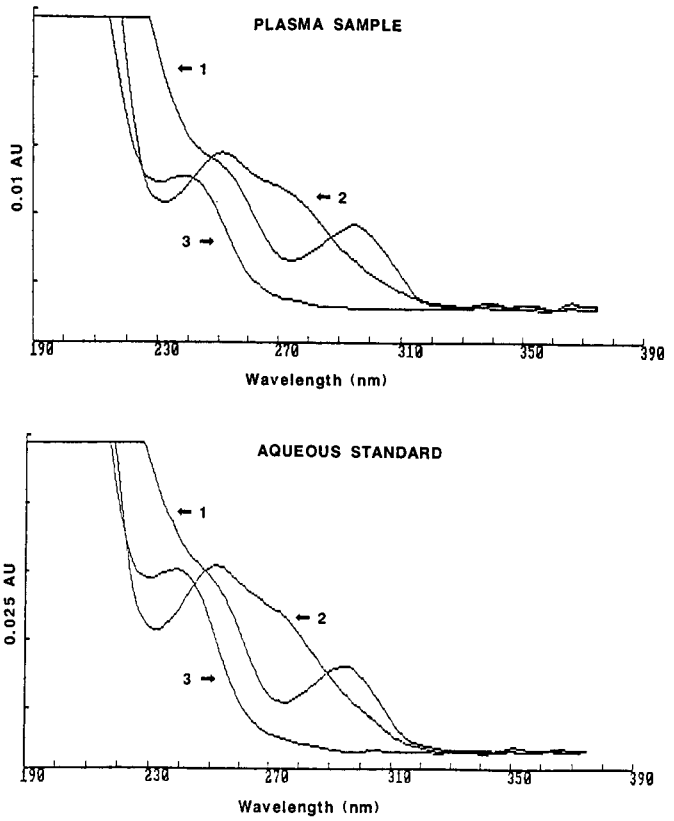

Fig. 7. UV spectra of (1) doxepin, (2) imipramine and (3) amitriptyline captured on-the-fly at the peak maxima from multidimensional chromatograms of the drugs from plasma (top) and aqueous spiked samples (bottom).

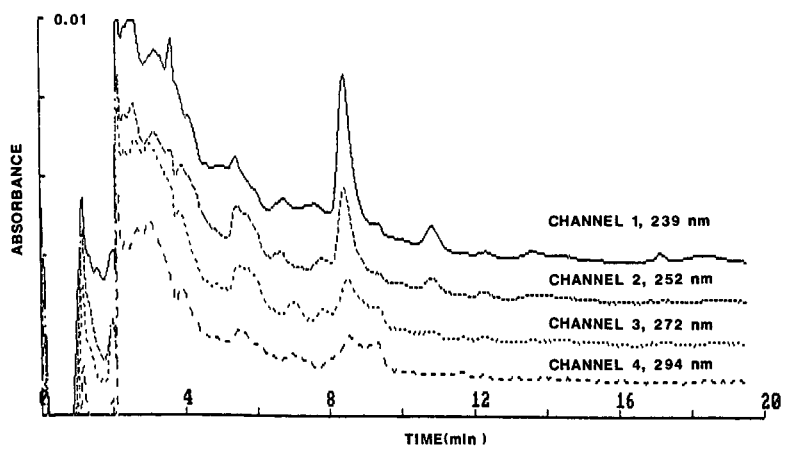

Fig. 8. Blank plasma multidimensional chromatograms obtained under conditions described in Fig. 6.

change; the extraction solvent pH was adjusted to 10 with triethylamine (TEA) while the recovery solvent was formulated without the base. It was important to ensure that none of the high-pH extraction solvent was passed onto the silica-based analytical column. No problems were found here. The selection of the analytical mobile phase was straight forward. TEA was added to minimize peak tailing and facilitate elution at pH 6.0.

A column-switched separation of an injection of 500 μl of blood plasma containing 270 ng/ml of each tricyclic anti-depressant is shown in Fig. 6. Monitored at a compromised wavelength of 239 nm, doxepin and desipramine showed positive interferences of 18 and 10%, respectively. The other drugs gave recoveries of 100%. The UV spectra of the tricyclics and their metabolites (Fig. 7) indicate opportunities for monitoring at wavelengths other than 239 nm. Indeed, using 294 nm for doxepin gives a 100% recovery. The same holds true for desipramine monitored at 272 nm. Examination of the blank plasma runs (Fig. 8) at four selected wavelengths clearly indicates these interferences at 8.5 and 10.3 min. That information, coupled with the spectroscopic data, provides a ready and simple solution. With diode array technology, timed programmed-wavelength switching is simple and gives no baseline shifts. It becomes simple to optimize the wavelength for selective and sensitive results. Opportunities to further reduce matrix interferences through chemometric techniques like spectral suppression[14] present challenges for future studies.

REFERENCES

1 Z. K. Shihabi, *J. Liq. Chromatogr.*, 11 (1988) 1579.
2 R. Wyss and F. Bucheli, *J. Chromatogr.*, 456 (1988) 33.
3 J. W. Veals and C. C. Lin, *Am. Lab. (Shelton, CT)*, 20 (1988) 42.
4 U. R. Tjaden, H. Lingmann, H. J. E. M. Reeuwijk, E. A. de Bruijn, H. H. Keizer and J. van der Greef, *Chromatographia*, 25 (1988) 806.
5 M. J. Czejka and A. Georgopoulos, *J. Chromatogr.*, 424 (1988) 182.
6 J. Schmidt and W. Roth, *Drug. Metab. Mol. Man*, (1987) 213.
7 D. J. Gmur, P. Meier and G. C. Yee, *J. Chromatogr.*, 425 (1988) 343.
8 K. Matsumoto, H. Kikuchi, H. Iri, H. Takahasi and M. Umino, *J. Chromatogr.*, 425 (1988) 323.
9 D. Dadgar and A. Power, *J. Chromatogr.*, 416 (1987) 99.
10 J. W. Cox and R. H. Pullen, *J. Pharm. Biomed. Anal.*, 4 (1986) 653.
11 J. V. Posluszny and R. Weinberger, *Anal. Chem.*, 60 (1988) 1953.
12 M. J. Koenigbauer and M. A. Curtis, *J. Chromatogr.*, 427 (1988) 277.
13 P. Ni, F. Guyon, M. Caude and R. Rosset, *J. Liq. Chromatogr.*, 11 (1988) 1087.
14 B. J. Clark, A. F. Fell, H. P. Scott and D. Westerlund, *J. Chromatogr.*, 286 (1984) 261.

Journal of Chromatography, 507 (1990) 277–292
Elsevier Science Publishers B.V., Amsterdam — Printed in The Netherlands

CHROMSYMP. 1670

Liquid chromatographic investigation of quinoxaline antibiotics and their analogues by means of ultraviolet diode-array detection

THOMAS V. ALFREDSON* and AUGUST H. MAKI
Department of Chemistry, University of California, Davis, CA 95616 (U.S.A.)
MARYE E. ADASKAVEG and JEAN-LOUIS EXCOFFIER
Varian Instrument Division, Walnut Creek, CA 94598 (U.S.A.)
and
MICHAEL J. WARING
Department of Pharmacology, University of Cambridge, Hills Road, Cambridge CB2 2QD (U.K.)

SUMMARY

Numerical formats for evaluation of spectral purity and for spectral comparison of ultraviolet diode-array detector data, together with library search routines, were applied to the liquid chromatographic analysis of echinomycin, triostin A and their synthetic and biosynthetic analogues. Samples of monoquinoline and bisquinoline analogues of echinomycin were found to contain echinomycin and the other respective analogue. Triostin A and its undermethylated synthetic analogues, des-N-tetramethyltriostin A (TANDEM) and [$MeCys^3$,$MeCys^7$]-TANDEM, were each composed of two or more components. Triostin A primarily consisted of a major chromatographic component and a minor component with very similar ultraviolet spectral features. TANDEM exhibited three chromatographic components with nearly identical ultraviolet spectral characteristics. Apparent conformational interconversion of at least two forms of the [$MeCys^3$,$MeCys^7$]-TANDEM analogue was observed by reversed-phase liquid chromatography. An activation energy of 15 kcal/mol was estimated for the interconversion based upon an Arrhenius plot of the data.

INTRODUCTION

Quinoxaline antitumor antibiotics are produced by several species of *Streptomycetes* and are characterized by two planar quinoxaline rings linked by a cross-bridged, cyclic octadepsipeptide. Two families of quinoxaline antibiotics are known, the triostins and the quinomycins, which differ in their respective cross-bridge structure. The quinomycins, of which echinomycin is the most prominent member, contain a thioacetal cross-bridge while the triostins, of which triostin A has been most widely studied, contain a disulfide cross-bridge (Fig. 1). Olsen[1] has reviewed the quinoxaline depsipeptide antibiotics. Their biological activity has been extensively documented by

0021-9673/90/$03.50

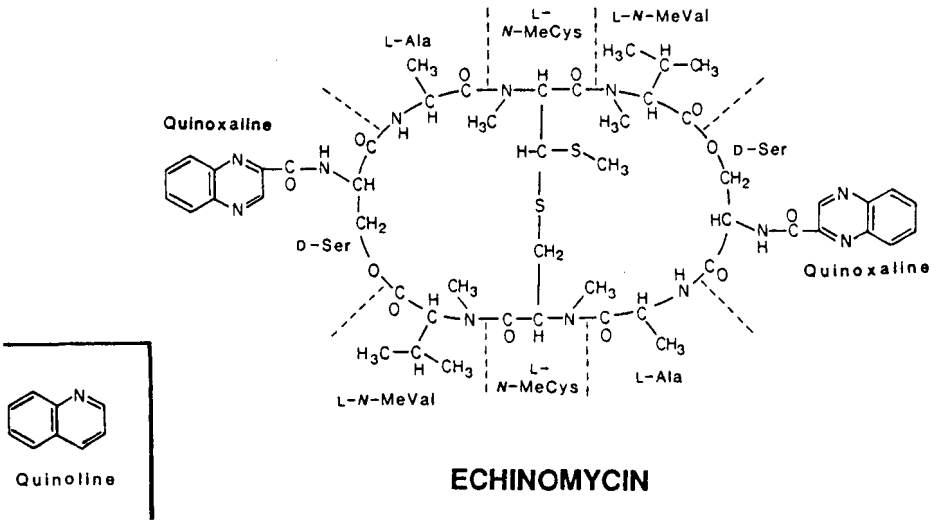

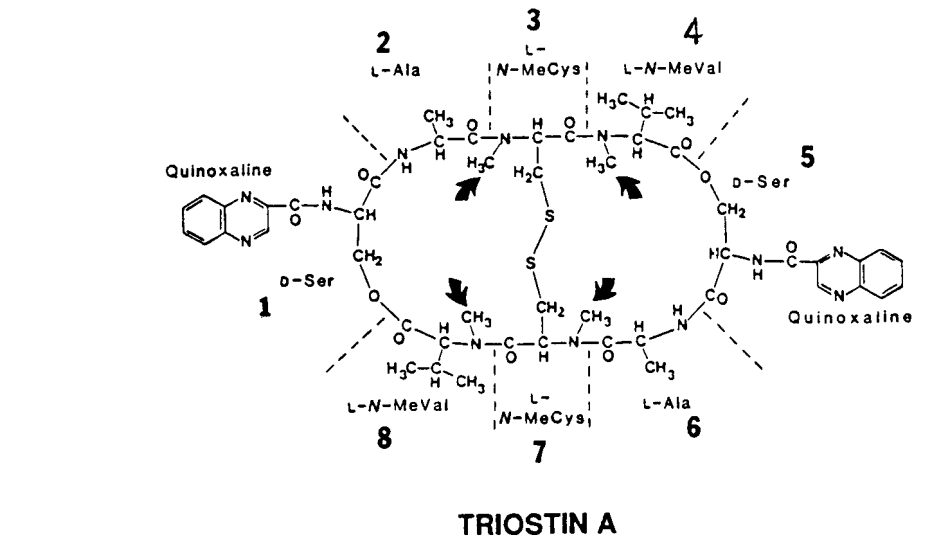

Fig. 1. Structures of echinomycin and triostin A. In the quinoline analogue of echinomycin (1QN) one quinoxaline ring is replaced by a quinoline ring. In the bisquinoline analogue of echinomycin (2QN) both quinoxaline rings are replaced by quinoline rings. The arrows in the triostin A structure represent locations at which the N-methyl groups are replaced by H atoms in the des-N-tetramethyltriostin A (TANDEM) analogue. In the [MeCys^3,MeCys^7]-TANDEM analogue of triostin A, only the N-methyl groups at the 4-MeVal and 8-MeVal positions are replaced by H atoms (see peptide ring numbering scheme for residue positions 1–8).

Katagiri *et al.*[2] and recent developments with respect to their mode of action have been reviewed by Waring[3].

Waring and Wakelin[4,5] proposed over ten years ago that echinomycin interaction with DNA occurs via a bifunctional intercalation (bisintercalation) mode of binding. Recent crystallographic investigations by Wang and co-workers[6,7] and

Quigley *et al.*[8] of the structure of echinomycin and triostin A, complexed with duplex oligonucleotides, have corroborated the earlier findings. These quinoxaline antibiotics were found to bind to the minor groove of the double helix where the quinoxaline rings sandwich a CpG base sequence. Several studies have demonstrated that changes in the peptide ring structure[9,10] and in the aromatic ring moiety[11,12] of these antibiotics affect DNA binding specificity. Directed biosynthesis efforts by Fox *et al.*[13] and Gauvreau and Waring[14] along with synthetic work by Ciardelli *et al.*[15], Chakravarty and Olsen[16], Shin *et al.*[17] and Helbecque *et al.*[18] have yielded a wide variety of depsipeptide drug analogues. Echinomycin and its monoquinoline (1QN) and bisquinoline (2QN) biosynthetic analogues, along with triostin A and its synthetic analogues TANDEM (des-N-tetramethyltriostin A) and [MeCys^3,MeCys^7]-TANDEM, were investigated in this liquid chromatographic study. The quinoxaline and quinoline rings of the drugs were utilized as intrinsic probes for UV spectroscopic diode-array detection.

UV spectral features of a compound have been exploited by liquid chromatography photodiode-array detectors to confirm peak identification and to determine peak homogeneity. The high spectral acquisition rates of diode-array detectors (up to *ca.* 25 Hz) have been a driving force in the development of computer-aided strategies for signal processing, data reduction and data manipulation. Developments in photodiode-array detection for liquid chromatography and spectral data interpretation techniques have been recently reviewed[19].

Conceptually, the numerical formats for spectral data interpretation employed in this study treat spectra as vectors in order to utilize scalar functions for evaluation and comparison of data sets. The numerical technique employed for evaluation of spectral purity, labeled the purity parameter format, has been described previously[20,21]. White[22] has recently reported a detailed comparison of the purity parameter format with the absorbance ratio technique for spectral discrimination between compounds with similar UV spectra. The purity parameter format makes use of an absorbance-weighted mean wavelength to describe a spectrum by a single number. Absorbance-weighting minimizes the effect of noise in the calculation. The purity parameter value ($\bar{\lambda}_w$) of a spectrum is mathematically defined by the following algorithm:

$$\bar{\lambda}_w(\vec{A})_{(\lambda_i,\lambda_f)} = \frac{\sum_{n=i}^{f} a_n^2 \lambda_n}{\sum_{n=i}^{f} a_n^2}$$

where $\vec{A}$ is a spectrum that has absorbance values a_0 at λ_0, a_1 at $\lambda_1,\ldots$, a_n at $\lambda_n,\ldots$, etc. and (λ_i,λ_f) is the wavelength interval included in the calculation. The wavelength range over which $\bar{\lambda}_w$ is calculated can be selected to focus on characteristic spectral features of a chromophore or to enhance discrimination between the spectrum of a compound of interest and that of an impurity.

Spectral comparison was accomplished in this study by treating two spectra as vectors and measuring the differences by means of correlation coefficients [similarity (SIM) and dissimilarity (DISSIM) coefficients] which, together with library search

routines, were used to confirm peak identification. A similar approach was taken by Hill *et al.*[23] who utilized a goodness of fit value in a computerized library search routine for matching UV spectra of unknown drugs to UV spctra of reference drugs.

The SIM and DISSIM coefficients employed in this work for comparison of two spectra can be mathematically defined as follows:

$$\mathrm{SIM}(\vec{A},\vec{B})_{(\lambda_i,\lambda_f)} = \frac{\sum_{n=i}^{f} a_n b_n}{\sqrt{\sum_{n=i}^{f} a_n^2 \sum_{n=i}^{f} b_n^2}} = \cos\theta$$

$$\mathrm{DISSIM}(\vec{A},\vec{B})_{(\lambda_i,\lambda_f)} = \sin\theta = \sqrt{1 - \cos^2\theta}$$

where $\vec{A}$ is a spectrum as defined previously, $\vec{B}$ is a spectrum that has absorbance values b_0 at λ_0, b_1 at λ_1,..., b_n at λ_n,..., etc. and θ is the angle between the vectors $\vec{A}$ and $\vec{B}$.

The SIM coefficient (correlation coefficient) is simply the dot product between two normalized vectors. Excoffier *et al.*[24] have demonstrated that for purity determination the DISSIM coefficient is more linearly related to the amount of impurity present, and thus offers a greater advantage than the SIM coefficient.

The purpose of this study is to apply library search routines that utilize SIM and DISSIM coefficients and the purity parameter numerical format to the confirmation of peak identity and peak homogeneity in the liquid chromatographic analysis of quinoxaline antibiotics and their analogues. The apparent interconversion between two forms of [MeCys^3,MeCys^7]-TANDEM was also investigated using reversed-phase column temperature studies in conjunction with UV photodiode-array detection.

EXPERIMENTAL

Materials

A Varian Series 9010 solvent delivery system, a Polychrom 9065 diode-array detector, with the LC Star 9021 workstation and Polyview spectral processing software, and a 9095 autosampler (Varian, Walnut Creek, CA, U.S.A.) were employed for all chromatographic separations and data collection. The autosampler was equipped with a Rheodyne (Cotati, CA, U.S.A.) 7125 automated loop-valve injector and 20-μl sample loop. A Spark-Holland (Amsterdam, The Netherlands) high-performance liquid chromatography (HPLC) column heater was used for temperature studies. Collected fractions were concentrated or evaporated to dryness in a Pierce (Rockford, IL, U.S.A.) Model 18780 Reacti-Vac evaporator using high-purity nitrogen gas. All measurements of drug concentration were made using a Hewlett-Packard 8450 UV spectrophotometer.

Acetonitrile, methanol and HPLC-grade water were B&J Brand high-purity solvents obtained from Baxter Healthcare, Burdick & Jackson Division (Muskegon, MI, U.S.A.). Buffers were prepared from HPLC-grade potassium dihydrogen-phosphate (Fisher, Pittsburgh, PA, U.S.A.).

Echinomycin was a gift from the National Cancer Institute (Bethesda, MD,

U.S.A.). A sample of echinomycin was also kindly supplied by Drs. H. H. Peter and K. Scheibli of Ciba-Geigy (Basle, Switzerland). 1QN and 2QN samples were products of directed biosynthesis studies[14]. Triostin A samples were generously provided by Drs. J. Shoji and K. Sato of Shionogi Research Laboratories (Osaka, Japan). Samples of TANDEM and [MeCys^3,MeCys^7]-TANDEM were a gift from Dr. R. K. Olsen, Department of Chemistry and Biochemistry, Utah State University (Logan, UT, U.S.A.). All quinoxaline drugs were stored in a dessicator in the dark at −20°C. Quinoxaline and quinoline were obtained from Aldrich (Milwaukee, WI, U.S.A.).

Sample preparation and chromatography

All quinoxaline antibiotic and analogue samples were dissolved in methanol at 100–800 μM concentrations and centrifuged prior to injection. Solutions were freshly prepared whenever possible. No precipitates were observed in the sample solutions. Quinoxaline drug concentrations were determined spectrophotometrically (echinomycin, $\varepsilon_{315} = 11\,500$; 1QN, $\varepsilon_{315} = 8700$; 2QN, $\varepsilon_{315} = 6000$; triostin A, $\varepsilon_{316} = 12\,100$; TANDEM, $\varepsilon_{316} = 12\,400$; [MeCys^3,MeCys^7]-TANDEM, $\varepsilon_{316} = 12\,400$) from standards obtained by collection of the major chromatographic band of each sample and verified by NMR and other spectroscopic techniques. Extinction coefficients of the standards were calculated from methanol solutions using a 1-cm light path quartz cuvette.

A MicroPak SP C-8 IP-5 (Varian) column (150 mm × 4 mm I.D.) with a 0.05 M phosphate buffer (pH 7.0)–acetonitrile (1:1) mobile phase at a flow-rate of 1.2 ml/min was employed for all chromatographic separations. Detection was performed at 239 nm and the raw data were collected for subsequent chromatographic and spectral processing. Fraction collection of [MeCys^3,MeCys^7]-TANDEM components was performed manually using a short piece (4 in.) of 0.009 in. I.D. stainless-steel tubing connected to the detector outlet to minimize band-broadening.

Data reduction

Purity parameter, SIM and DISSIM calculations were performed by using 38 fixed-wavelength values across the UV region (190–367 nm) from which a subset could be defined. The library search routines and attendant spectral processing software employed in this report have been described recently by Sheehan *et al.*[25]. Basically, the library search utilizes a settable wavelength range, purity parameter ($\bar{\lambda}_w$) window, and retention time window as primary search criteria. An activated search routine calculates $\bar{\lambda}_w$ values for all library spectra and compares all $\bar{\lambda}_w$ values and retention data to the search windows. SIM and DISSIM values are then calculated for the unknown and for each selected library spectrum that falls within the search parameter windows. The top five library matches are listed in a search report.

RESULTS AND DISCUSSION

The low solubility of the quinoxaline antibiotics in aqueous solutions (*ca.* 1–6 μM) precluded direct dissolution of the drug samples in the mobile phase solvent at the concentrations desired for analysis[26]. Methanol, in which the antibiotics are freely soluble, was employed for sample dissolution in order to ensure that the drugs were in true solution prior to chromatographic separation. Column plugging or back-pressure

problems were not experienced using this methodology. Studies with quinoxaline and echinomycin dissolved in the mobile phase solvent and in methanol revealed no differences in peak shape or position upon chromatographic analysis.

Echinomycin and its biosynthetic quinoline analogues

Reversed-phase liquid chromatographic separation of echinomycin and its 1QN and 2QN analogues is displayed in Fig. 2. Substitution of the quinoxaline ring with quinoline enhances retention. Consistent with these results, it was observed that quinoline is more highly retained than quinoxaline. Although the echinomycin sample displays only one chromatographic band, the samples of 1QN and 2QN analogues exhibit two and three principal bands, respectively, as well as some evidence of other minor constituents.

Fig. 3 displays the UV spectra and purity parameter values ($\bar{\lambda}_w$) for echinomycin,

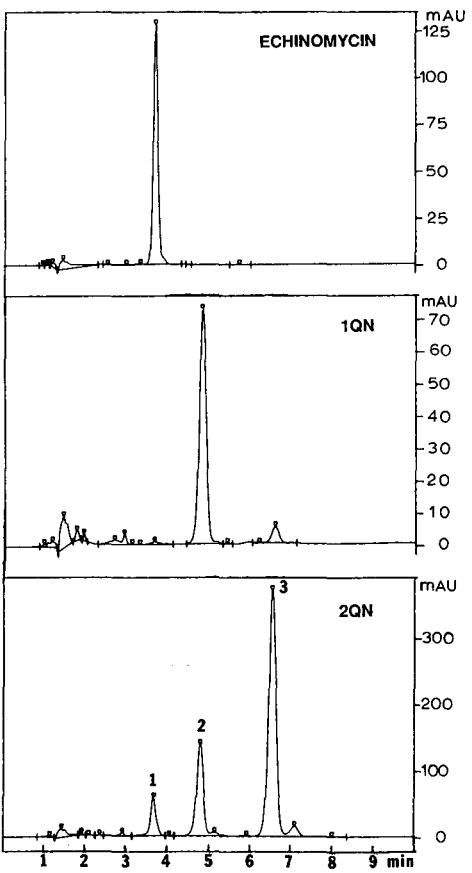

Fig. 2. Reversed-phase HPLC analysis of echinomycin and its 1QN and 2QN analogues. Chromatographic conditions are described in the text. The 1QN sample contains 5% of the 2QN analogue. The 2QN sample contains 8.1% echinomycin (component 1) and 21% of the 1QN analogue (component 2) in addition to 59.7% (by area percent at 239 nm) of 2QN (component 3).

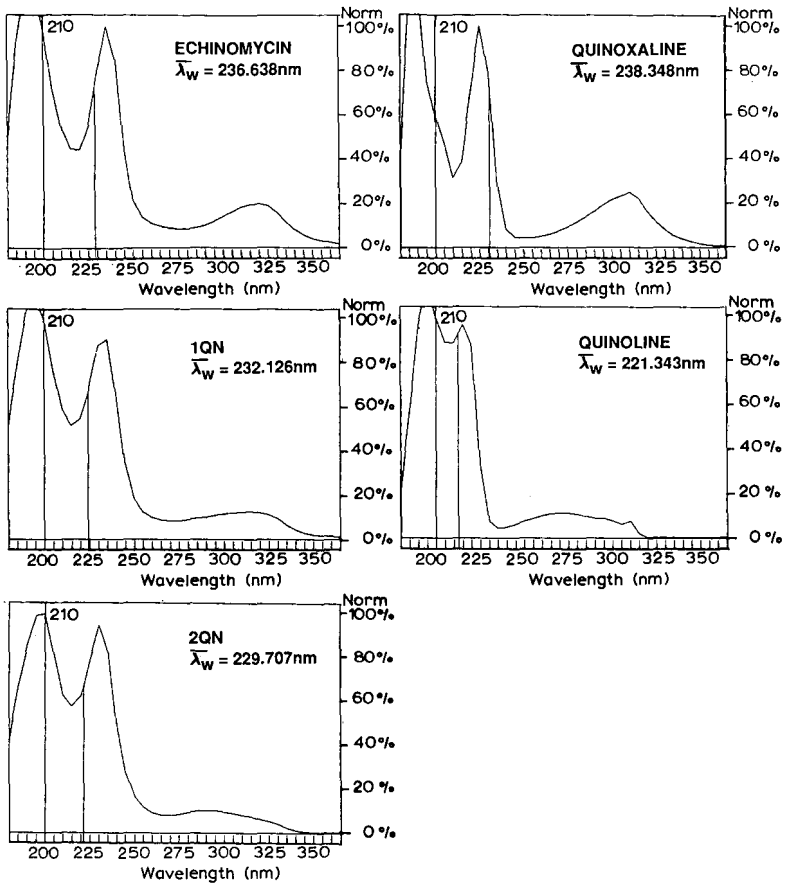

Fig. 3. UV spectra of echinomycin, 1QN, 2QN, quinoxaline and quinoline standards. λ_i values listed in the spectra (starting wavelength for calculation) and $\bar{\lambda}_w$ (purity parameter value) are denoted by solid vertical lines in each spectrum. See text for chromatographic conditions.

1QN and 2QN standards as well as for quinoxaline and quinoline. Table I lists the $\bar{\lambda}_w$ values and their standard deviations calculated over a broad wavelength range (210–367 nm) and over an optimized range (263–344 nm) for enhanced spectral discrimination of echinomycin and its analogues. As can be seen, the $\bar{\lambda}_w$ values calculated over the broad wavelength range (210–367 nm) for echinomycin, 1QN and 2QN differ by *ca.* 7 nm and reflect the spectral differences of the chromophores. However, an optimized spectral range (263–344 nm) yields $\bar{\lambda}_w$ values for echinomycin and its analogues that differ by over 17.5 nm, again reflecting chromophore spectral features. Based upon statistical comparison (*t*-test) of $\bar{\lambda}_w$ values acquired at several points (upslope inflection point, apex, downslope inflection point) across the peak elution profile, the major chromatographic components of each sample were found to exhibit a high degree of homogeneity.

A spectral reference library was constructed by acquiring spectra at several

TABLE I

ECHINOMYCIN, 1QN, 2QN, QUINOXALINE AND QUINOLINE PURITY PARAMETER VALUES ($\bar{\lambda}$)

Standard deviations (σ) were calculated on the basis of spectra acquired from different chromatographic experiments over a six-month period. See text for chromatographic conditions.

Compound	*Wavelength range 210–367 nm*		*Optimized range 263–344 nm*	
	$\bar{\lambda}_w$ *(nm)*	σ $(n = 5)$	$\bar{\lambda}_w$ *(nm)*	σ $(n = 5)$
Echinomycin	236.638	0.052	310.788	0.024
1QN	232.126	0.197	302.656	0.469
2QN	229.707	0.016	293.285	0.019
Quinoxaline	238.348	0.094	309.395	0.151
Quinoline	221.343	0.084	286.206	0.055

points across the elution profile of each quinoxaline depsipeptide in addition to quinoxaline and quinoline (over 100 spectra in all). A library search was then conducted in order to confirm identification of the major chromatographic components of the 1QN and 2QN analogues. Results from a library search report for the 2QN analogue of echinomycin are summarized in Table II. Component 1 of the 2QN sample (t_R = 3.6 min) was matched to echinomycin (DISSIM = 0.01523); component 2 (t_R = 4.7 min) was matched to 1QN (DISSIM = 0.00324); and component 3 (major component with t_R = 6.4 min) was matched to 2QN (DISSIM = 0.00091). About 2% of an unidentified component (t_R = 6.9 min) was present, having spectral features nearly identical with those of 2QN. In an analogous manner, the 1QN sample was found to consist of about 5% 2QN plus a few other components (including 12% of a poorly retained material) in addition to the 1QN analogue (67% by area percent at 239 nm).

TABLE II

LIBRARY SEARCH REPORT SUMMARY FOR 2QN

See Fig. 2 for a representative chromatographic separation from which spectra were acquired. Library search parameters: λ_w value interval, ±2.00 nm; wavelength range, 210–367 nm; retention time range, 1.00–9.99 min; retention time interval, ±5.00%; minimum peak height, 5 mA.U.

	Peak No.		
	1	*2*	*3*
Peak retention time (min)	3.613	4.706	6.396
λ_w value (nm)	236.007	232.188	229.678
Library match identification	Echinomycin	1QN	2QN
Library match retention time (min)	3.679	4.835	6.562
Library match λ_w value (nm)	236.565	232.245	229.695
SIM coefficient	0.99988	0.99999	1.00000
DISSIM coefficient	0.01523	0.00324	0.00091

Due to the asymmetric nature of the quinomycin cross-bridge structure, the 1QN analogue of echinomycin is composed of two positional isomers in which one quinoline ring is substituted for a quinoxaline ring at each respective quinoxaline moiety position. Based upon a lack of any observed resolution, the two 1QN isomers were not apparently separable under the chromatographic conditions used in this study. Williamson *et al.*[27] have reported that although not separable by the liquid chromatographic procedures employed in their study, the 1QN isomers were clearly distinguishable by NMR techniques.

Triostin A and its undermethylated synthetic analogues

Fig. 4 displays the chromatograms of triostin A and its undermethylated analogues TANDEM and [MeCys^3,MeCys^7]-TANDEM (TANDEM with additional N-methyl groups present at both cysteine residues at positions 3 and 7 in the peptide ring). Two chromatographic components are evident for the triostin A sample in addition to a few minor peaks. The sample of TANDEM displays three major chromatographic components as well as a poorly retained minor component. The [MeCys^3, MeCys^7]-TANDEM analogue exhibits an unusual chromatographic profile which is characterized by a broad, flat absorbance region linking two well resolved peaks.

Table III lists the purity parameter values at peak apex calculated over a broad wavelength range (210–367 nm) and their standard deviations for each major chromatographic component of triostin A, TANDEM and [MeCys^3,MeCys^7]-TANDEM. The $\bar{\lambda}_w$ values for the components of all three samples are similar, reflecting the fact that the only structural differences among them are the presence or absence of N-methyl groups at the cysteine and valine residues in the peptide ring. However, the major component of triostin A and TANDEM can be spectrally discriminated ($\bar{\lambda}_w$ values of 237.072 and 240.794 nm, respectively). On the other hand, no significant spectral difference seems to exist between the three apparent components of TANDEM or between the two apparent components of triostin A. In contrast, however, the two major components of [MeCys^3,MeCys^7]-TANDEM have statistically different spectral features. Component 1 of this analogue has a $\bar{\lambda}_w$ value of 235.346 and component 2 has a $\bar{\lambda}_w$ value of 238.908 nm.

Several NMR studies[28–30] have determined that triostin A exists in deuteriochloroform solutions as two symmetrical conformers separated by an energy barrier of 20–22 kcal/mol. Based upon solvent effects on conformer equilibrium, one conformer is known to be favored in non-polar solvents while the other is favored in polar solvents. Blake *et al.*[28] designated the conformer predominant in [$^2H_6$]dimethylsulfoxide([$^2H_6$]DMSO) and other polar solvents as the *p* conformer (*p*-triostin A) and the conformer predominant in non-polar solvents as the *n* conformer (*n*-triostin A). They observed that in [^{2}H]chloroform, [$^2H_6$]benzene–[^{2}H]chloroform and [^{2}H]chloroform–carbon tetrachloride solutions *n*-triostin A predominates although both forms of the drug are present. In polar solvents such as [$^2H_6$]DMSO only the *p*-triostin A conformer was apparent. Kyogoku *et al.*[30] have postulated that based upon ^{1}H and ^{13}C NMR studies of the drug and its S-benzyl triostin A analogue, the triostin A conformers result from *cis–trans* isomerism at either the Ala–MeCys or MeCys–MeVal peptide bonds. Since both the mobile phase and sample dissolution solvent employed in this chromatographic study are polar solvents, *p*-triostin A would be

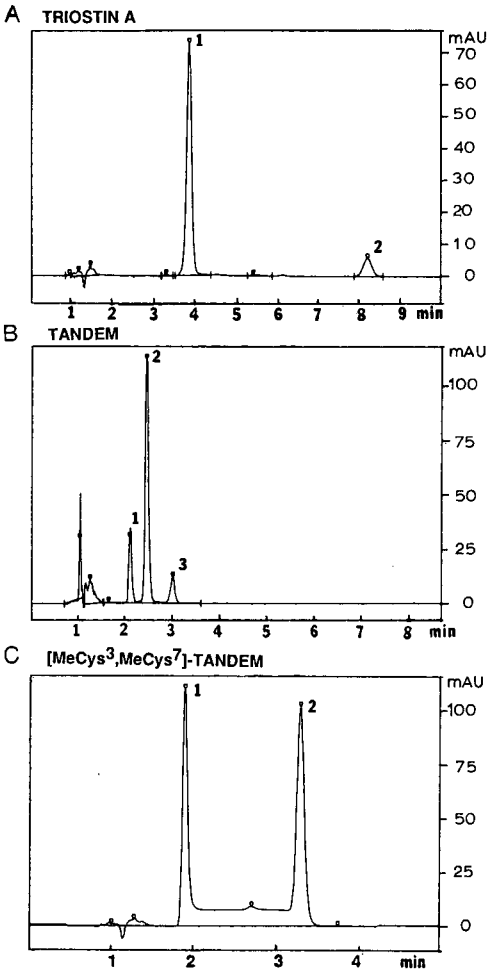

Fig. 4. Reversed-phase HPLC analysis of triostin A, TANDEM and [MeCys^3,MeCys^7]-TANDEM. Chromatographic conditions are described in the text. (A) Triostin A: component 1, t_R = 3.9 min (88.3%); component 2, t_R = 8.25 min (11.7% by area percent at 239 nm). (B) TANDEM: component 1, t_R = 2.1 min (18.7%); component 2, t_R = 2.5 min (71%); component 3, t_R = 3.0 min (10.3%). (C) [MeCys^3, MeCys^7]-TANDEM: component 1, t_R = 2.05 min; component 2, t_R = 3.5 min.

expected to predominate in solution. Triostin A dissolved in DMSO and chromatographed by our reversed-phase methods gave nearly identical results to those shown in Fig. 4A. Although no unequivocal determination of triostin A conformers can be obtained from this work, it is speculated that the major chromatographic band of triostin A (component 1) may be *p*-triostin A. Since both chromatographic components of triostin A have nearly identical UV spectra ($\bar{\lambda}_w$ values of 237.072 and 237.530 nm, respectively), it is likely that both have very similar chromophore environments.

NMR investigations by Hyde *et al.*[31] of the conformation of TANDEM in [^{2}H]chloroform, [$^2H_5$]pyridine and [$^2H_6$]DMSO have shown that, unlike triostin A,

TABLE III

TRIOSTIN A, TANDEM AND [MeCys^3,MeCys^7]-TANDEM PURITY PARAMETER VALUES (λ_w)

Standard deviations were calculated on the basis of spectra acquired from different chromatographic experiments over a six-month period. See text for chromatographic conditions.

Compound	*Wavelength range 210–367 nm*	
	$\bar{\lambda}_w$ *(nm)*	σ $(n = 5)$
Triostin A		
Component 1[a]	237.072	0.069
Component 2	237.530	0.343
TANDEM		
Component 1	240.877	0.375
Component 2[a]	240.794	0.168
Component 3	239.450	1.711
[MeCys^3,MeCys^7]-TANDEM		
Component 1	235.346	0.570
Component 2	238.908	0.409

[a] Major component.

the TANDEM analogue seems to adopt a single conformation in solution. The reversed-phase chromatographic separation of TANDEM (Fig. 4B) reveals three apparent components with very similar UV spectral characteristics. Further work is currently in progress to elucidate the nature of these components.

Of particular interest is the unusual chromatographic profile obtained for the [MeCys^3,MeCys^7]-TANDEM analogue in our reversed-phase study (Fig. 4C). The profile was noted to be similar to the chromatographic profile of the cyclic undecapeptide cyclosporine, reported by Bowers and Mathews[32] and to the profile of the dipeptide L-alanyl-L-proline investigated by Melander *et al.*[33]. Investigation of peak broadening in the reversed-phase chromatography of cyclosporine led to the conclusion that the mechanism involved interconversion of several conformers of the drug. The postulate of solution conformers was supported by NMR spectroscopic results. The L-alanyl-L-proline dipeptide chromatographic study consisted of a detailed analysis of the effects of molecular structure and conformational changes of proline-containing dipeptides. The results were interpreted as evidence for the slow kinetics of *cis–trans* isomerism about the proline amide bond. Due to its smaller hydrophobic surface area, the *trans* conformer of the proline dipeptide eluted faster than the corresponding *cis* conformer. Proline *cis–trans* isomerism in proteins has recently been examined by two-dimensional NMR in the work of Chazin *et al.*[34].

In an attempt to elucidate the nature of our [MeCys^3,MeCys^7]-TANDEM results, the analogue was chromatographed at column temperatures from ambient to 90°C (Fig. 5; chromatogram at 90°C is not shown as it was very similar to that at 75°C). As can be seen, the two sharp major components of the drug vanish and a broad central peak grows as the temperature is increased. A third, sharp component, eluted at a point intermediate to the two major chromatographic bands, is evident in several of these

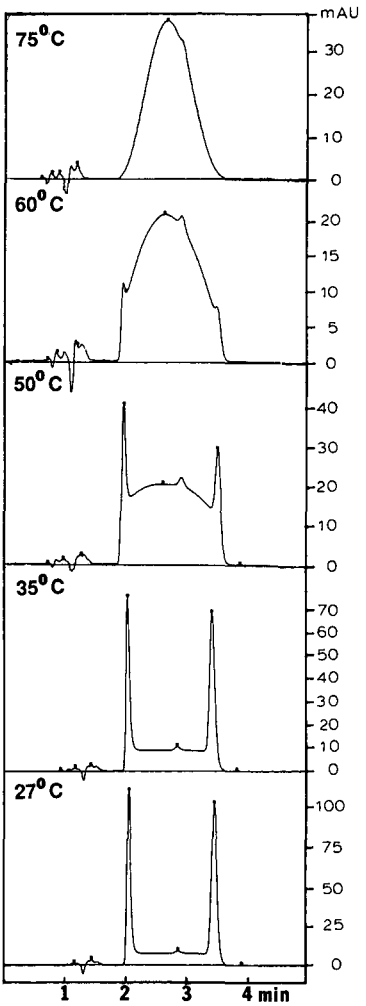

Fig. 5. Reversed-phase HPLC analysis of [MeCys^3,MeCys^7]-TANDEM as a function of column temperature. See text for chromatographic conditions.

chromatograms. Analogy to similar results with the proline dipeptides and cyclosporine seems to indicate that the [MeCys^3,MeCys^7]-TANDEM analogue consists of at least two conformers in polar solutions. Their kinetics are such that interconversion takes place on the chromatographic time scale (a few minutes). Using the height of the broad central peak as a measure of the extent of interconversion, an Arrhenius plot of the column temperature study data was made (Fig. 6). A linear plot is obtained up to about 60°C at which point interconversion may be so rapid that the height of the central peak is no longer a good measure of rate. An activation energy of about 15 kcal/mol was estimated from the slope of a least-squares fit to the linear portion of the data. The activation energy estimated for [MeCys^3,MeCys^7]-TANDEM is lower than that calculated for interconversion of triostin A conformers from NMR results[28], but

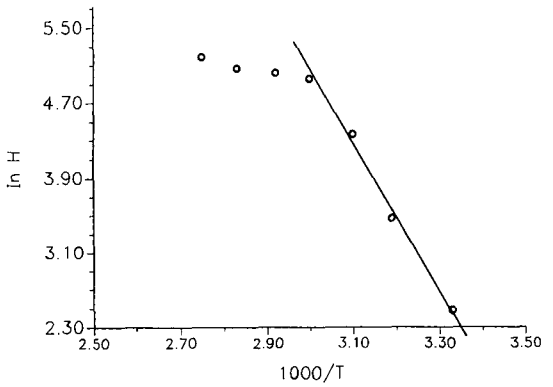

Fig. 6. Arrhenius plot of [MeCys^3,MeCys^7]-TANDEM conformer interconversion data. H is the height of the broad central peak, measured as a function of column temperature (see Fig. 5).

it is similar to the energy barrier calculated for the conformer interconversion of the cyclic tetrapeptide tentoxin[35]. A detailed investigation of conformer content versus time in methanol prior to chromatography is currently in progress to further define the solution kinetics of [MeCys^3,MeCys^7]-TANDEM conformer interconversion.

Fig. 7A shows the chromatogram of the [MeCys^3,MeCys^7]-TANDEM analogue which contains two major components (termed conformer 1 and conformer 2). As previously demonstrated, the two conformers exhibit statistically different spectra indicating a slight difference in chromophore environments. Collection of the conformer 1 fraction followed by concentration in aqueous mobile phase and reversed-phase chromatography gave the results displayed in Fig. 7B. Similar procedures with conformer 2 yielded nearly identical results. Library search results indicated that the major component in the chromatogram matched conformer 1 and the minor peak matched conformer 2. If the conformer 1 fraction of the [MeCys^3,MeCys^7]-TANDEM is collected, evaporated to dryness under a stream of nitrogen and redissolved in methanol for chromatographic reanalysis, the results as shown in Fig. 7C are obtained. In addition to the two conformers observed in the parent compound, a third sharp component eluted between conformers 1 and 2 is obvious in the chromatogram. Spectral characteristics of this component ($\bar{\lambda}_w$ = 239.280 nm) are nearly identical with those of conformer 2 ($\bar{\lambda}_w$ = 238.908 nm), but differ considerably from conformer 1 ($\bar{\lambda}_w$ = 235.346 nm). Apart from the prominence of this intermediate component, the chromatogram is very similar to that obtained for the parent compound (Fig. 7A). Similar procedures carried out with conformer 2 of [MeCys^3,MeCys^7]-TANDEM yielded results comparable to those obtained with conformer 1 but with a slight enhancement of the intermediate component. Assignment of conformers 1 and 2 were again verified by library search methods. The results of this fraction collection study seem to indicate that the ratio of conformers 1 and 2 obtained from reversed-phase chromatography is a function of the sample dissolution solvent. If [MeCys^3,MeCys^7]-TANDEM or its individual conformers are dissolved in methanol, nearly equal amounts of each conformer are obtained upon reversed-phase chromatography with an aqueous buffer–acetonitrile mobile phase

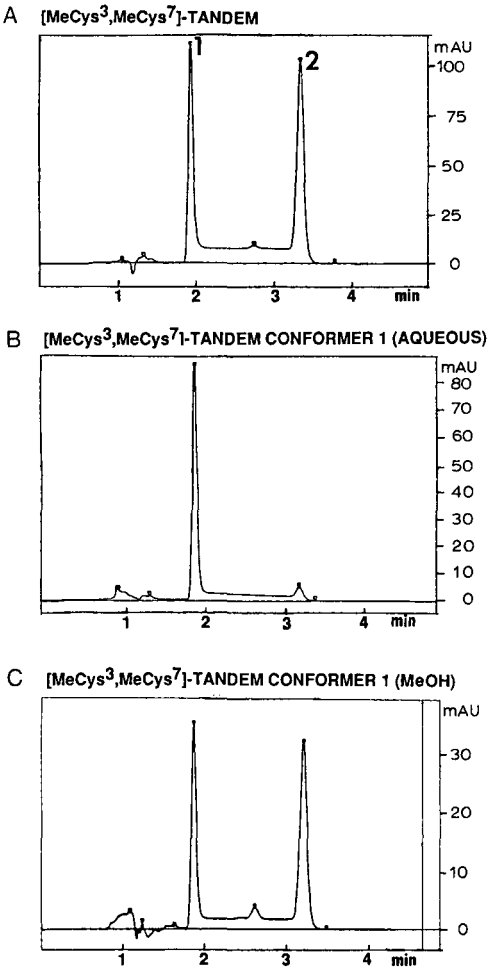

Fig. 7. Reversed-phase analysis of [MeCys^3,MeCys^7]-TANDEM and individual conformer fractions. Chromatographic conditions are described in the text. (A) [MeCys^3,MeCys^7]-TANDEM reversed-phase analysis; (B) HPLC analysis of conformer 1 fraction from (A), concentrated in aqueous mobile phase; (C) HPLC analysis of conformer 1 fraction from (A) evaporated to dryness and redissolved in methanol prior to chromatography.

(see Fig. 7A and C). If conformer 1 or 2 is dissolved in aqueous solvent prior to chromatographic analysis, conformer 1 predominates although both forms of the drug are present (see Fig. 7B). Additionally, if [MeCys^3,MeCys^7]-TANDEM itself is dissolved in the aqueous mobile phase and then chromatographed, conformer 1 is found to predominate over conformer 2. Apparently conformer 1 is favored in aqueous solutions.

Preliminary ^{1}H NMR investigation of [MeCys^3,MeCys^7]-TANDEM reveals, like the TANDEM analogue, one set of resonances for each set of symmetry-related pair of protons in [^{2}H]chloroform. Additional NMR studies of [MeCys^3,MeCys^7]-

TANDEM in methanol and other polar solvents should help elucidate the nature of the conformers and their interconversion in solution.

CONCLUSIONS

Estimation of purity and UV spectral matching of quinoxaline antibiotics and their analogues was greatly aided by numerical formats for evaluation of spectral purity and spectral comparison in conjunction with library search routines. Echinomycin consisted of one major chromatographic component which exhibited a high degree of peak homogeneity based upon UV spectral data. Samples of 1QN and 2QN analogues of echinomycin contained 5 and 21% (by area percent at 239 nm) of the other analogue, respectively. In addition, the 2QN sample contained 8% echinomycin based upon library search results. Analysis of the triostin A sample revealed two apparent chromatographic components (minor component 12% by peak area) with similar spectral characteristics. The TANDEM sample exhibited three apparent components with nearly identical spectral features. The purity parameter format displayed the ability to spectrally discriminate the major component of each depsipeptide drug investigated in this study.

[MeCys^3,MeCys^7]-TANDEM analogue of triostin A was found to consist of about equal amounts of two distinguishable conformers (conformer 1 and conformer 2) when dissolved in methanol prior to chromatography. Conformer 1 appears to be favored in aqueous solutions. Since neither triostin A nor TANDEM display evidence of any interconversion taking place on a chromatographic time scale, it is postulated that the [MeCys^3,MeCys^7]-TANDEM conformers may be the result of *cis–trans* isomerism involving the MeCys peptide bond. UV spectral data suggest that the quinoxaline ring environment is slightly different in the two conformers. An activation energy of about 15 kcal/mol was estimated for the interconversion process.

ACKNOWLEDGEMENTS

Generous gifts of samples are gratefully acknowledged. Thanks are due to Dr. Richard K. Olsen of Utah State University (Logan, UT, U.S.A.) for the [MeCys^3, MeCys^7]-TANDEM and the TANDEM sample (originally to M.J.W.), Drs. H. H. Peter and K. Scheibli of Ciba-Geigy (Basle, Switzerland) and Dr. Matthew Suffness of the National Cancer Institute (Bethesda, MD, U.S.A.) for echinomycin samples and Drs. J. Shoji and K. Sato of Shionogi Research Laboratories (Osaka, Japan) for the triostin A sample. We especially thank Drs. John Robinson, Terry Sheehan and Jim Bennett (Varian, Walnut Creek, CA, U.S.A.) for helpful discussions and support. This work was partially supported by the National Institutes of Health, Grant No. ES-02662, and by a research grant from the University of California, Davis Committee on Research.

REFERENCES

1 R. K. Olsen, in B. Weinstein (Editor), *Chemistry and Biochemistry of Amino Acids, Peptides, and Proteins*, Vol. 7, Marcel Dekker, New York, 1983, p. 1.
2 K. Katagiri, T. Yoshida and K. Sato, in J. W. Corcoran and F. E. Hahn (Editors), *Antibiotics: Mechanism of Action of Antimicrobial and Antitumor Agents*, Vol. III, Springer, Berlin, 1975, p. 234.

3 M. J. Waring, in F. E. Hahn (Editor), *Antibiotics: Mechanism of Action of Leukaryotic and Antivirial Compounds*, Vol. 5, Part 2, Springer, Berlin, 1979, p. 173.
4 M. J. Waring and L. P. G. Wakelin, *Nature*, 252 (1974) 653.
5 L. P. G. Wakelin and M. J. Waring, *Biochem. J.*, 157 (1976) 721.
6 A. H.-J. Wang, G. Ughetto, G. J. Quigley, T. Hakoshima, G. A. van der Marel, J. H. van Boom and A. Rich, *Science (Washington, D.C.)*, 225 (1984) 1115.
7 A. H.-J. Wang, G. Ughetto, G. J. Quigley and A. Rich, *J. Biomol. Struct. Dyn.*, 4 (1986) 319.
8 G. J. Quigley, G. Ughetto, G. A. van der Marel, J. H. van Boom, A. H.-J. Wang and A. Rich, *Science (Washington, D.C.)*, 232 (1986) 1255.
9 J. S. Lee and M. J. Waring, *Biochem. J.*, 173 (1978) 129.
10 C. M. L. Low, K. R. Fox, R. K. Olsen and M. J. Waring, *Nucleic Acid Res.*, 14 (1986) 2015.
11 C. M. L. Low, K. R. Fox and M. J. Waring, *Anti-Cancer Drug Design*, 1 (1986) 149.
12 M. J. Waring and K. R. Fox, in S. Neidle and M. J. Waring (Editors), *Molecular Aspects of Anti-Cancer Drug Action*, Verlag-Chemie, Basle, 1983, p. 127.
13 K. R. Fox, D. Gauvreau, D. C. Goodwin and M. J. Waring, *Biochem. J.*, 191 (1980) 729.
14 D. Gauvreau and M. J. Waring, *Can. J. Microbiol.*, 30 (1984) 439.
15 T. L. Ciardelli, P. K. Chakravarty and R. K. Olsen, *J. Am. Chem. Soc.*, 100 (1978) 7684.
16 P. K. Chakravarty and R. K. Olsen, *Br. J. Pharm.*, 70 (1980) 35.
17 M. Shin, K. Inouye, N. Higuchi and Y. Kyogoku, *Bull. Chem. Soc. Jpn.*, 57 (1984) 2211.
18 N. Helbecque, J. L. Bernier and J. P. Henichart, *Biochem. J.*, 225 (1985) 829.
19 T. Alfredson and T. Sheehan, *J. Chrom. Sci.*, 24 (1986) 473.
20 T. Alfredson and T. Sheehan, *Am. Lab. (Fairfield, Conn.)*, 17 (1985) 40.
21 T. Alfredson, T. Sheehan, T. Lenert, S. Aamodt and L. Correia, *J. Chromatogr.*, 385 (1987) 213.
22 P. C. White, *Analyst (London)*, 113 (1988) 1625.
23 D. W. Hill, T. R. Kelley and K. J. Langner, *Anal. Chem.*, 59 (1987) 350.
24 J. L. Excoffier, J. R. Robinson and M. E. Adaskaveg, paper presented at the *40th Pittsburgh Conference on Analytical Chemistry and Applied Spectroscopy, Atlanta, GA, March 10–15, 1989.*
25 T. L. Sheehan, M. E. Adaskaveg and J. L. Excoffier, *Am. Lab. (Fairfield, Conn.)*, 20 (1989) 66.
26 J. S. Lee and M. J. Waring, *Biochem. J.*, 173 (1978) 129.
27 M. P. Williamson, D. Gauvreau, D. H. Williams and M. J. Waring, *J. Antibiot.*, 35 (1982) 62.
28 T. J. Blake, J. R. Kalman and D. H. Williams, *Tetrahedron Lett.*, 30 (1977) 2621.
29 J. R. Kalman, T. J. Blake, D. H. Williams, J. Feeney and G. C. K. Roberts, *J. Chem. Soc. Perkin Trans. 1*, (1979) 1313.
30 Y. Kyogoku, N. Higuchi, M. Watanabe and K. Kawano, *Biopolymers*, 20 (1981) 1959.
31 E. Hyde, J. R. Kalman, D. H. Williams, D. G. Reid and R. K. Olson, *J. Chem. Soc. Perkin Trans. 1*, (1982) 1041.
32 L. D. Bowers and S. E. Mathews, *J. Chromatogr.*, 333 (1985) 231.
33 W. R. Melander, J. Jacobson and C. Horvath, *J. Chromatogr.*, 234 (1982) 269.
34 W. J. Chazin, J. Kordel, T. Drakenberg, E. Thulin, P. Brodin, T. Grundstrom and S. Forsen, *Proc. Natl. Acad. Sci. U.S.A.*, 86 (1989) 2195.
35 D. H. Rich and P. K. Bhatnagar, *J. Am. Chem. Soc.*, 100 (1978) 2218.

Journal of Chromatography, 507 (1990) 293–302
Elsevier Science Publishers B.V., Amsterdam — Printed in The Netherlands

CHROMSYMP. 1717

Determination of partition coefficients of non-ionic contrast agents by reversed-phase high-performance liquid chromatography

IGNACIO J. ALONSO-SILVA*, JOSE M. CARRETERO, JOSE L. MARTIN and ANTONIO M. SANZ

Research and Development Division, Laboratorios JUSTE SAQF, Julio Camba 7, 28028 Madrid (Spain)

ABSTRACT

Reversed-phase high-performance liquid chromatography was used to measure the lipophilicities of non-ionic contrast agents. Calculated partition coefficients were correlated with the capacity factors extrapolated to zero organic modifier content.

INTRODUCTION

Studies of quantitative structure–activity and structure–toxicity relationships[1,2] have shown that the octanol–water partition coefficient (P) is one of the most important physical parameters related to the biological activities and toxicities of organic compounds. The shake-flask method[3,4] is usually used for the determination of log P. However, this method is tedious and not simple. Reversed-phase high-performance liquid chromatography (RP-HPLC) has also been used to determine log P, as it is simple, rapid and accurate. Octadecylsilica with[5,6] or without[7–11] previous treatment with trimethylsilyl chloride is the most widely used stationary phase.

The method involves:

(a) a linear correlation between capacity factor (log k') and organic modifier volume fraction (φ):

$$\log k' = \log k'_w + S\varphi \quad (1)$$

where

$$\varphi = V_{\text{Org. modifier}}/(V_{\text{Org. modifier}} + V_{\text{water}}) \quad (2)$$

the intercept (log k'_w) is the capacity factor extrapolated to zero organic modifier content and the slope, S, is the slope parameter[12];

(b) a linear regression between log k'_w and log P for several compounds (training

0021-9673/90/$03.50

set) with known partition coefficients, usually determinated by the shake-flask method:

$$\log P = a + b \log k'_w \quad (3)$$

(c) the determination of the $\log k'$ and $\log k'_w$ values for the test compounds by chromatography; the $\log P$ values of the test compounds are obtained from eqn. 3.

In eqn. 3, partition conditions are represented by a value of b close to unity. However, a search for a chromatographic system giving a regression line in which a large change in $\log P$ corresponds to a small modification of $\log k'$ ($b > 1$) is especially important. A value of b of about 2 may be useful[1].

On the other hand, calculation methods[13–17] could be used to avoid the experimental determination of $\log P$.

In connection with our work on non-ionic contrast agents, several 5-amino-2,4,6-triiodoisophthalic and 3,5-diamino-2,4,6-triiodobenzoic acid derivatives have been prepared. As part of a study of the physico-chemical properties of the contrast agents, we report here the determination of their chromatographic parameters $\log k'_w$ and S, and the relationship between $\log k'_w$ and calculated partition coefficients.

EXPERIMENTAL

Materials

HPLC-grade acetonitrile were obtained from Fluka (Buchs, Switzerland). Contrast agents 3–7 (Table I) were prepared by us[18,19]. Compounds 1 (iohexol) and 2 (iopamidol) were isolated from commercially available pharmaceutical products.

Chromatography

The HPLC instrument consisted of a Hewlett-Packard (Waldbronn Analytical Division, Waldbronn, F.R.G.) chromatograph with an autosampler and an

TABLE I

TRAINING SET OF CONTRAST AGENTS

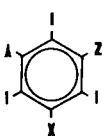

Compound	*X*	*Y*[a]	*Z*[a]
1	$CONHCH_2CH(OH)CH_2OH$	$CONHCH_2CH(OH)CH_2OH$	$N(Ac)CH_2CH(OH)CH_2OH$
2	$CONHCH(CH_2OH)_2$	$CONHCH(CH_2OH)_2$	$NHCOCH(OH)CH_3$ (L)[b]
3	$CONHCH_2CH(OH)CH_2OH$	$N(Ac)CH_2CH(OH)CH_2OH$	$N(Ac)CH_2CH(OH)CH_2OH$
4	$CONHCH_2CH(OH)CH_2OH$	$N(Ac)CH_2CH(OH)CH_2OH$	$N(Ac)CH_3$
5	$CONHC(CH_2OH)_3$	$N(Ac)CH_2CH(OH)CH_2OH$	$N(Ac)CH_3$
6	$CONHCH_2CH_2OH$	$N(Ac)CH_2CH(OH)CH_2OH$	$N(Ac)CH_2CH(OH)CH_2OH$
7	$CON(CH_3)CH_2CH_2OH$	$N(Ac)CH_2CH(OH)CH_2OH$	$N(Ac)CH_2CH(OH)CH_2OH$

[a] Ac = Acetyl.

[b] (L) = Chiral center configuration of the lactoyl group.

HP 1090 A detection system, operating at 254 nm, HP 85 B computer, HP 9121 disc drive and HP Thinkjet printer.

A reversed-phase Novapack C_{18} column (15 cm × 3.7 mm I.D., 4 μm particle size) (Millipore–Waters, Milford, MA, U.S.A.) was used.

Retention times were measured by injecting 5 μl of an aqueous contrast agent solution (1 mg/ml) and eluting under isocratic conditions with several acetonitrile–water volume fractions (eqn. 2). The column temperature was 40°C in order to ensure adequate thermostating and good reproducibility of the chromatographic data. Two flow-rates, 0.5 and 1.0 ml/min, were used. The column dead time, t_0, was determined at each flow-rate and φ used by injecting 3% sodium nitrate solution as the non-retained compound. The capacity factor, k', is defined as

$$k' = (t_R - t_0)/t_0 \tag{4}$$

where t_R is the mean and weighted retention time of the test compound.

The experimental conditions were chosen in order to obtain short retention times (t_R) without losing the discrimination power between the different contrast agents. Hence broad chromatography peaks and thus inaccurate determinations of t_R can be avoided. Fortunately, owing to the high aqueous solubility of the contrast agents, it was possible to work with small t_R and φ values in order to obtain a linear correlation according to eqn. 1.

RESULTS AND DISCUSSION

Log P calculation

The Hansch–Leo method[14] is the most generally used procedure for the calculation of log P values. They suggested a group contribution method based on fragment f_i and corrective factor F_j values:

$$\log P = \sum_i a_i f_i + \sum_j b_j F_j \tag{5}$$

For molecules as complex as the contrast agents, with numerous inter- and intramolecular interactions, the calculated log P values deviated from the experimental results. This was evident when we used the experimental log P values obtained from Haavaldsen *et al.*[20] to evaluate the fit of this parameter using the Hansch–Leo procedure[14] (Table II), the log P values calculated by the Hansch–Leo method being much more positive than the experimental values. This does not mean that this method is invalid but implies that as we can not modify the group contributions f_i in eqn. 5, the F correction factors, especially the proximity factors (F_p), are overestimated and must be corrected.

The modifications made in this work in order to obtain a good correlation between the calculated and experimental values were as follows: (1) F_{p_3} proximity factors were not considered, except for X and/or Y = $CONHC(CH_2OH)_3$; (2) all F_{p_2} factors of the amido and carbamoyl groups with a hydroxyl moiety were considered, except for X and/or Y = $CONHCH(CH_2OH)_2$, where this contribution was divided

TABLE II

CALCULATED AND REPORTED LOG *P* VALUES

Compound	*X*	*Y*	*Z*
1	$CONHCH_2CH(OH)CH_2OH$	$CONHCH_2CH(OH)CH_2OH$	$N(Ac)CH_2CH(OH)CH_2OH$
8	$CON(CH_3)CH_2CH(OH)CH_2OH$	$CON(CH_3)CH_2CH(OH)CH_2OH$	$NHCOCH_3$
9	$CON(CH_3)CH_2CH(OH)CH_2OH$	$CON(CH_3)CH_2CH(OH)CH_2OH$	$N(Ac)CH_2CH_2OH$
10	$CONHCH(CH_2OH)_2$	$CONHCH(CH_2OH)_2$	$NHCOCH_3$
11	$CONHCH_2CH(OH)CH_2OH$	$CONHCH_2CH(OH)CH_2OH$	$N(Ac)CH_2CH_2OH$
12	$CONHCH_2CH_2OH$	$CONHCH_2CH_2OH$	$N(Ac)CH_2CH(OH)CH_2OH$
13	$CONHCH_2CH(OH)CH_2OH$	$CONHCH_2CH(OH)CH_2OH$	$N(Ac)CH_3$
14	$CONHCH(CH_2OH)_2$	$CONHCH(CH_2OH)_2$	$N(Ac)CH_2CH_2OH$
15	$CONHCH(CH_2OH)_2$	$CONHCH(CH_2OH)_2$	$N(Ac)CH_2CH(OH)CH_2OH$

[a] From ref. 20.
[b] Calculated according to the Hansch–Leo method.
[c] $\Delta^* = \log P_{obs} - \log P_{HL}$; $\Delta^{**} = \log P_{obs} - \log P_{CHL}$; $\Delta^{***} = \log P_{obs} - \log P_{calc}$.
[d] Calculated according to the corrected Hansch–Leo method.
[e] From eqn. 7.

by a factor of two; and (3) the hydroxyl–hydroxyl F_{p_2} factors were calculated from the following empirical equation, obtained by a trial and error procedure:

$$F'_{p_2}(OH, OH) = [(A - B)C/N]F_{p_2}(OH, OH) \quad (6)$$

where A is the number of chains with two or more OH groups, B is the number of chains with less than two OH groups, C is the number of chains with OH and N is the total number of hydroxyl groups.

We modified the contribution of the $F_{p_2}(OH, OH)$ factors to consider both the number and the molecular distribution of the OH groups. Hence there are two factors in eqn. 6: (a) C/N can unmodify or decrease the magnitude of the $F_{p_2}(OH, OH)$; and (b) $(A - B)$ can unmodify, increase or decrease the magnitude of the $F_{p_2}(OH, OH)$ and even reverse the sign of this contribution ($A < B$), which is always positive in the Hansch–Leo method.

The following equation shows a good correlation between log P calculated as above and reported experimental values[20]:

$$\log P_{obs} = 0.067 + 1.053 \log P_{CHL} \quad (7)$$

$$n = 9; r = 0.966; SEE = 0.101; F(1,7) = 97.82; p < 0.0001.$$

where SEE = standard error of estimation; n = number of data points (compounds); r = correlation coefficient; F = F-statistic significance test with 1 and 7 degrees of freedom; p = observed significance level of F (probability).

Log P determination

Table III gives the capacity factors at different organic modifier volume fractions (log k'_φ) obtained with flow-rates of 0.5 and 1 ml/min. In the latter instance,

Log P_{obs}[a]	*Log* P_{HL}[b]	Δ^{*}[c]	*Log* P_{CHL}[d]	Δ^{**}[c]	*Log* P_{calc}[e]	Δ^{***}[c]
−3.05	−1.71	−1.34	−2.99	−0.06	−3.08	0.03
−2.17	−0.82	−1.35	−2.10	−0.07	−2.14	−0.03
−2.28	−1.18	−1.10	−2.28	0.00	−2.33	0.05
−2.27	0.10	−2.37	−2.17	−0.10	−2.22	−0.05
−2.47	−1.24	−1.23	−2.34	−0.13	−2.40	−0.07
−1.86	−0.32	−1.54	−1.81	−0.05	−1.84	−0.02
−2.05	−0.81	−1.24	−2.09	0.04	−2.13	0.08
−2.33	−0.25	−2.08	−2.43	0.10	−2.49	0.16
−2.80	−0.73	−2.07	−2.57	−0.23	−2.64	−0.16

the acetonitrile concentration can be decreased to 5% ($\varphi = 0.05$) without increasing the retention times too much.

Fig. 1 shows the linear correlations of φ with log k' obtained at a flow-rate of 0.5 ml/min for compounds 1–7. Table IV gives the linear regression data for the correlations and also the log P values calculated by the corrected Hansch–Leo method. The intercept log k'_w shows the degree of affinity of the compound for the lipophilic phase when aqueous elution occurs. The slope S shows the reduction in the affinity of the compound for the stationary phase with increase in the organic modifier concentration.

The relationship between log k'_w and calculated partition coefficients, log P_{CHL}, is expressed by the following equations:

$$\log P_{CHL} = -2.113 + 1.813 \log k'_w \quad (8)$$

$$n = 7; r = 0.980; SEE = 0.221; F(1,5) = 123.38; p < 0.001$$

and

$$\log P_{CHL} = -2.244 + 2.007 \log k'_w \quad (9)$$

$$n = 6; r = 0.998; SEE = 0.072; F(1,4) = 1098.55; p < 0.001.$$

The data referring to these equations are given in Table IV. Eqn. 9 is obtained from the same data as eqn. 8, excluding the most deviating point (residual = 0.384) corresponding to iopamidol. It is noteworthy that there is an improvement in the quality of the regression on going from eqn. 8 to 9.

The "deviant" behaviour of iopamidol could be explained by its structural dissimilarities with the other compounds in the training set. Moreover, the calculated log k'_w values for iohexol (−0.367) and iopamidol (−0.366) were almost identical and

TABLE III

RP-HPLC CAPACITY FACTORS (LOG k'_{φ}) OF CONTRAST AGENTS

Compound	*Flow-rate 0.5 ml/min*				*Flow-rate 1.0 ml/min*				
	Log $k'_{0.15}$	*Log* $k'_{0.20}$	*Log* $k'_{0.25}$	*Log* $k'_{0.30}$	*Log* $k'_{0.05}$	*Log* $k'_{0.10}$	*Log* $k'_{0.15}$	*Log* $k'_{0.20}$	*Log* $k'_{0.25}$
1	−0.887	−1.100	−1.196	−1.439	−1.221	−1.561	−1.309	−1.201	−1.291
2	−0.917	−1.194	−1.303	−1.524	−0.983	−1.505	−1.353	−1.318	−1.439
3	−0.600	−0.906	−1.009	−1.243	−0.373	−1.196	−1.077	−1.055	−1.047
4	−0.164	−0.509	−0.732	−0.910	0.058	−0.596	−0.484	−0.613	−0.732
5	0.384	0.042	−0.242	−0.460	0.699	0.015	0.096	−0.016	−0.250
6	−0.478	−0.788	−1.044	−1.336	−0.437	−0.974	−0.814	−0.838	−1.064
7	−0.383	−0.647	−0.861	−1.149	−0.166	−0.796	−0.729	−0.824	−0.884

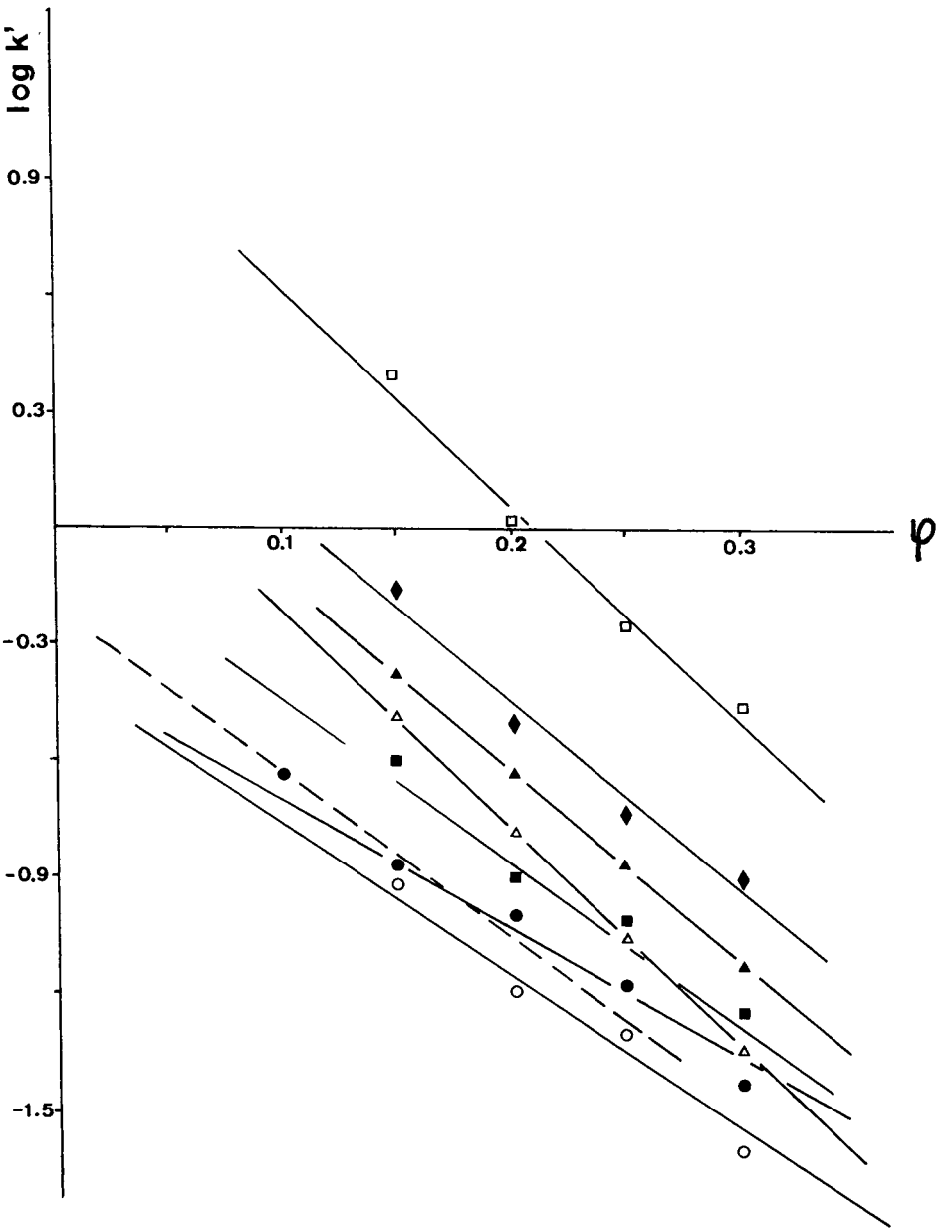

Fig. 1. Relationship between log k' values of CA and acetonitrile concentration (φ) in the mobile phase (flow-rate 0.5 ml/min). The compounds are numbered as in Table I. Key: ○ = 1; ● = 2; ■ = 3; ◆ = 4; □ = 5; △ = 6; ▲ = 7.

hence the partition coefficients calculated by eqn. 8 and 9 were also the same. This result conflicts with the experimental data found by Haavaldsen *et al.*[20] for iohexol (log $P = -3.046$) and by Jacobsen[21] for the iohexol (log $P = -3.000$) and iopamidol

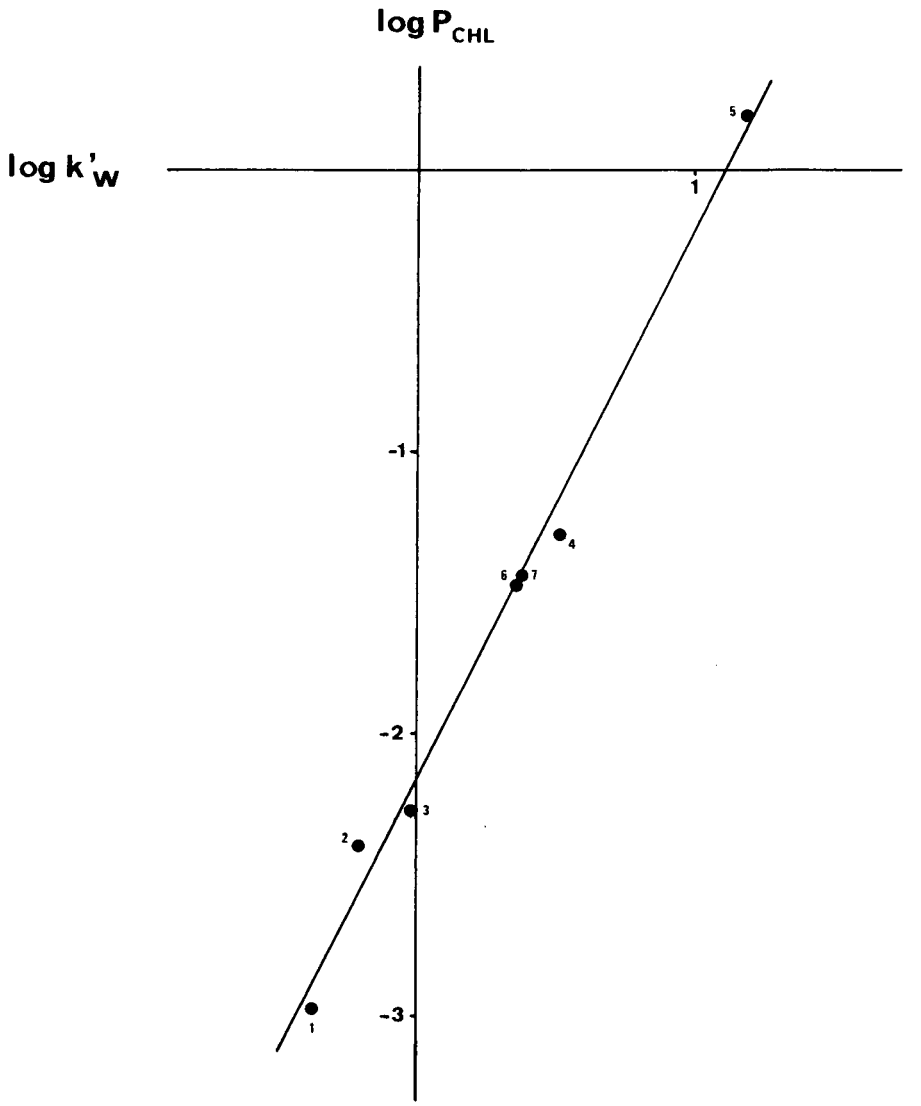

Fig. 2. Correlation of calculated log P_{CHL} with log k'_w. Regression data are given in eqn. 10.

(log $P = -2.699$). To obviate this discrepancy, log k'_w of iopamidol was recalculated using three data points at $\varphi = 0.10$, 0.15 and 0.20, giving log $k'_w = -0.208$. By including this new log k'_w value, the following equation is obtained (Fig. 2):

$$\log P_{CHL} = -2.185 + 1.931 \log k'_w \quad (10)$$

$$n = 7; r = 0.994; SEE = 0.120; F(1,5) = 428.67; p < 0.001.$$

TABLE IV

LOG P_{CHL} VALUES OF THE TRAINING SET AND LINEAR REGRESSION DATA FOR THE CORRELATIONS OF LOG k' AND φ

Compound	*Log* P_{CHL}	*Calculated for* $\log k' = \log k'_w + S\varphi$					
		Log k'_w	*S*	*r*	*SEE*[a]	*F(1,2)*	*n*
1	−2.988[b]	−0.367	−3.504	−0.988	0.043	82.74[d]	4
2	−2.393[c]	−0.366	−3.860	−0.988	0.048	79.19[d]	4
3	−2.267	−0.025	−4.064	−0.984	0.058	60.07[d]	4
4	−1.308	0.529	−4.922	−0.988	0.060	83.32[d]	4
5	0.191	1.198	−5.632	−0.995	0.044	206.12[d]	4
6	−1.484	0.362	−5.660	−0.999	0.016	1647.92[e]	4
7	−1.457	0.370	−5.024	−0.999	0.021	691.30[e]	4

[a] *SEE* = standard error of estimate.
[b] Reported values: −3.046[20]; −3.000[21].
[c] Reported value: −2.699[21].
[d] $p \leq 0.01$.
[e] $p \leq 0.001$.

Log *P* values of compounds 1–7 obtained using eqn. 10 are −2.894 (1), −2.587 (2), −2.233 (3), −1.164 (4), +0.128 (5), −1.486 (6) and −1.471 (7). As can be seen, log *P* for iohexol and iopamidol calculated by the corrected Hansch–Leo method (Table IV) and by eqn. 10 are close to the literature reported values (Table IV).

On the other hand, as can be seen in Table III, the log k' values obtained at a flow-rate of 1 ml/min were poorly correlated with φ. This shows that with highly water-soluble compounds such as the contrast agents, an increase in flow-rate may cause a deviation of the partition phenomenon, probably owing to the poor retention of the compounds under these conditions.

CONCLUSION

The measurement of partition coefficients of highly water-soluble contrast agents by RP-HPLC is a viable alternative to the tedious shake-flask method. It is possible to calculate log *P* values of molecules as complex as the contrast agents by making slight modifications to the Hansch–Leo method. The calculated log *P* values showed a high correlation with experimental log *P* values (eqn. 7) and with log k'_w (eqns. 9 and 10). As Leo reported[22], the deviation between calculated log *P* and values determined by RP-HPLC may be due more to unsuitable experimental conditions than to a formal error in the calculation procedure.

Once it has been verified that the method used for the calculation of log *P* affords accurate results for a set of compounds, the use of calculated log *P* values correlated with log k'_w values for the training set allows experimental log *P* values for compounds not included in that set to be obtained.

REFERENCES

1 H. Terada, *Quant. Struct.–Act. Relat.*, 5 (1986) 81.
2 R. Franke, *Theoretical Drug Design Methods*, Elsevier, Amsterdam, 1984.
3 J. J. Kirchner, W. E. Acree, A. J. Leo and G. Gelli, *J. Pharm. Sci.*, 74 (1985) 1129.
4 M. Kuchar, E. Kraus, M. Jelínková, V. Rejhlee and V. Miller, *J. Chromatogr.*, 347 (1985) 335.
5 M. S. Mirrlees, S. J. Moulton, C. T. Murphy and P. J. Taylor, *J. Med. Chem.*, 19 (1976) 615.
6 J. M. McCall, *J. Med. Chem.*, 18 (1975) 649.
7 T. L. Hafkenscheid and E. Tomlinson, *Adv. Chromatogr.*, 25 (1986) 1.
8 M. Recatanini, *Quant. Struct.–Act. Relat.*, 6 (1987) 12.
9 S. Lembo, V. Sasso, C. Silipo and A. Vittoria, *Farmaco, Ed. Sci.*, 38 (1983) 750.
10 J. E. Garst, *J. Pharm. Sci.*, 73 (1984) 1623.
11 T. Braumann, *J. Chromatogr.*, 373 (1986) 191.
12 D. J. Minick, J. H. Frenz, M. A. Patrick and D. A. Brent, *J. Med. Chem.*, 31 (1988) 1923.
13 R. F. Rekker, *The Hydrophobic Fragmental Constant*, Elsevier, Amsterdam, 1977.
14 C. Hansch and A. Leo, *Substituent Constants for Correlation Analysis in Chemistry and Biology*, Wiley, New York, 1979.
15 A. J. Hopfinger and R. D. Battershell, *J. Med. Chem.*, 19 (1976) 569.
16 P. Broto, G. Moreau and C. Vandycke, *Eur. J. Med. Chem.*, 19 (1984) 71.
17 A. K. Ghose and G. M. Crippen, *J. Chem. Inf. Comput. Sci.*, 27 (1987) 21.
18 J. L. Martin, J. M. Carretero, A. M. Sanz and I. J. Alonso-Silva, *Span. Pat.*, 8 801 664 (1988).
19 J. L. Martin, J. M. Carretero, A. M. Sanz and I. J. Alonso-Silva, *An. Quim. (C)*, in press.
20 J. Haavaldsen, V. Nordal and M. Kelly, *Acta Pharm. Suec.*, 20 (1983) 219.
21 T. Jacobsen, *Farmacoterapi*, 38 (1982) 45.
22 A. J. Leo, *J. Pharm. Sci.*, 76 (1987) 166.

Journal of Chromatography, 507 (1990) 303–310
Elsevier Science Publishers B.V., Amsterdam — Printed in The Netherlands

CHROMSYMP. 1687

Combination of positron emission tomography with liquid chromatography in neuropharmacologic research

PER HARTVIG*
Hospital Pharmacy, University Hospital, S 751 85 Uppsala (Sweden)
and
BENGT LÅNGSTRÖM
Department of Organic Chemistry, University of Uppsala, S-751 21 Uppsala (Sweden)

SUMMARY

Positron emission tomography (PET) is an *in vivo* autoradiographic technique that determines the radioactive distribution and kinetics of a radiolabelled tracer in a tissue. By choice of tracer, it is possible to study physiological processes in living animals and man non-invasively. PET has certain disadvantages such as limited spatial resolution and similtaneous measurement of radiolabelled tracer with the metabolites formed. For an adequate interpretation of the data obtained, complementary techniques such as column liquid chromatography of radioactive composition in blood, plasma, urine and tissue samples have to be used. The prerequisites for any chromatographic technique used for the radioanalysis of substances are speed, high selectivity and high separation efficiency.

Examples from PET studies in combination with chromatographic analysis will be given. The utilitzation of L-dopa in the brain constitutes several steps. Analysis by column liquid chromatography of metabolites in plasma and in monkey brain tissue will make it possible to elucidate different utilization processes of the tracer. Kinetic studies of ^{11}C-labelled neuropeptides such as methionine-enkephalin and substance P revealed high radioactivities in the brain of monkeys. However, simultaneous determination plasma and urine radioactivities using liquid chromatography with radiochemical and photometric detection both indicated that the brain radioactivities emanated to a large extent from ^{11}C-labelled metabolites formed *in vivo*.

Studies with PET using radiotracers having a rapid and extensive metabolism require complementary techniques in the evaluation. High detection selectivity, by combination of photometric and radiochemical detection and rapid and efficient separation, will make liquid chromatography a most important complement in the analysis.

INTRODUCTION

Positron emission tomography (PET) is a non-invasive tracer technique that

0021-9673/90/$03.50

measures the kinetics of a radiolabelled endogenous or exogenous compound in a biochemical process in the tissue of a living animal or man. The technique has found widespread use in clinical oncology for the delineation and classification of tumours and for the evaluation of treatment effects[1]. Measurement of blood flow in the heart and brain and of brain pH are other important clinical applications[2]. Energy metabolism is studied with various tracers in the heart and brain[3]. However, most applications of PET are still in a state of development, and have not been used on a clinical basis.

Studies with PET on receptor binding characteristics have led to great interest in a number of neurological and psychiatric diseases, and studies on the turnover of substrates for transmitter synthesis have been performed. Further, transport of radiolabelled amino acids over the placenta and the transport of radiolabelled drugs in the spinal canal are other applications that have been addressed using PET. In short, PET may visualize any biological event in the body if the choice of radiolabelled tracer and the time perspective are adequate.

The most serious drawback of PET, in addition to limited resolution, is, as in any other radiometric technique, that the detectors will measure any signal irrespective of its emanation from the radiotracer itself or from metabolites formed during the course of the study. This drawback is particularly troublesome in studies of processes that rapidly yield metabolites in high concentrations. Such interferences can be detected only by simultaneous assay of radiolabelled metabolites with the radiotracer in different body fluids by means of rapid and efficient chromatographic techniques. This paper reviews several applications of chromatographic assays combined with PET, the results of which have been essential in understanding the process under study.

PRINCIPLES OF POSITRON EMISSION TOMOGRAPHY

PET involves three main procedures (Table I), as follows.

TABLE I

POSITRON EMISSION TOMOGRAPHY

Activity	*Location*
Radionuclide production	Tandem accelerator
Radiopharmaceutical synthesis	Organic chemical laboratory
Patient investigation	Positron emission tomography

Radionuclide production

The first step is the production of the radionuclide of choice at the Tandem Accelerator Laboratory at the University of Uppsala. Nitrogen gas is bombarded by a proton beam to form ^{11}C. Trace amounts of oxygen in the target gas will yield $^{11}CO_2$.

Synthesis and analysis

The second step is the conversion of $^{11}CO_2$ in a series of steps to a useful ^{11}C-labelled precursor. In many cases, [^{11}C]methyl iodide has been used, which is a valuable alkylating reagent. For example, the corresponding demethylated analogues are reacted with [^{11}C]methyl iodide, using spiperone in an N-alkylation to give N-[^{11}C]methylspiperone or using S-benzylhomocysteine in an S-alkylation to give [^{11}C]methionine. After separation of the product by semipreparative liquid chromatography[3], the preparation and control of the product with respect to chemical and radiochemical purity are performed by analytical liquid chromatography. The half-life of ^{11}C is 20.4 min, which means that only a limited time period is available for production of the radiotracer by rapid organic chemical procedures and for purification. Additional requirements of the tracer administered to the patient are a sterile and pyrogen-free preparation.

Tomography

The third step is the investigation of the patient. The patient lies in a fixed position in the positron emission tomograph. Images from the tomograph are obtained in the following manner (Fig. 1). The radionuclides emit positrons, which, after traversing the tissue for a few millimetres, collide with its antimatter equivalent, the electron. In the annihilation reaction, two antiparallel photons are emitted. The photons are measured by external detectors, and the detector signals are processed and computed to give an exact localization of the annihilation. By measuring sequential images, the change in radioactivity with time in an organ or part of organ can be studied, in addition to its spatial localization. A radioactive uptake, corrected for physical decay of the radiotracer and the radioactive dose per gram of body weight, will characterize the distribution and kinetics of the radiotracer in the region of interest. Using radiolabelled receptor ligands, the difference in radioactivity over time in the receptor-rich region compared with a reference tissue devoid of specific receptors, *e.g.*, cerebellum for dopamine receptor studies, will give information on the number and binding characteristics of the receptor ligand after fitting a model to the data.

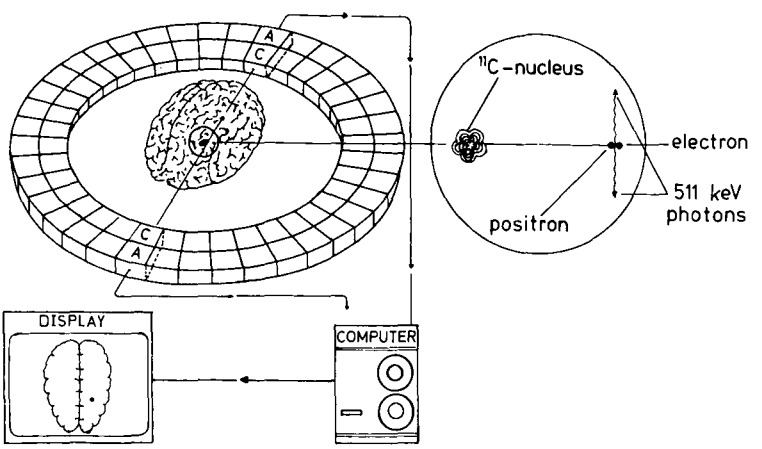

Fig. 1. Principles of positron emission tomography with ^{11}C-labelled tracers.

PHARMACEUTICAL CONTROL

Before administration to man, the radiotracer must fulfill the requirements of a pharmaceutical product to be administered parenterally. The preparation of the product should be achieved in the shortest possible time because of the rapid decay of the radiotracer. Identity, chemical and radiochemical yield, together with sterility and absence of endotoxins, must be ensured in a short time period[3]. In these instances, liquid chromatography is an invaluable tool. A rapid and efficient chromatographic separation, together with the detection selectivity obtained by the combination of radiochemical and photometric detection, are necessary for control of purity and coelution with unlabelled reference compound. The chromatographic analyses are performed using standard conditions frequently employing reversed-phase systems (Fig. 2).

The product is controlled by two independent analyses using liquid chromato-

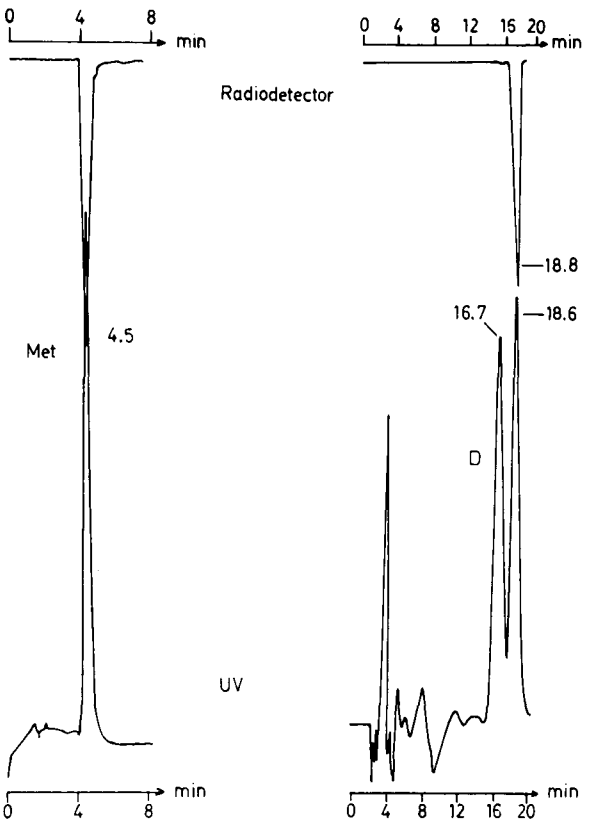

Fig. 2. Qualitative liquid chromatographic determination of [^{11}C]methionine used in clinical oncology for the delineation and classification of tumours and the evaluation of tumour treatment. A photometric detector is used in series with a β-detector as radiodetector. Left: radiochemical analysis on reversed-phase C_8-amino column. Amount injected, 5 MBq of [^{11}C]methionine corresponding to about 0.5 ng and standard addition of methionine. Right: analysis of the optical enantiomers of [^{11}C]methionine on an enantiomeric column packing (Daicel N) after standard addition of unlabelled reference.

graphy, for example one on the preparative scale and one on the analytical scale. Addition of the corresponding reference compound to the radiolabelled compounds and then reanalysis by liquid chromatography will further strengthen the control. Monitoring of the eluate with both radiochemical and photometric detectors will give both the chemical and radiochemical purity of the product, respectively. After dissolving the product in the appropriate buffer, the preparation is thereafter filtered through a 0.22-μm filter in a laminar flow hood to give a sterile product. The control tests are approved by the hospital isotope committee before patient studies. The total time for pharmaceutical preparation does not take more than 10 min.

APPLICATIONS

PET studies of receptor agonists and antagonists

Studies on the alterations of specific receptors in disease are field of great interest in using PET. Symptoms of many psychiatric and neurological disease are successfully relieved by treatment with receptor-active drugs. Any indication of an alteration of receptor binding may be of importance for a further understanding of the etiology. Blockade of dopamine D_2 receptors is the main pharmacological action of antipsychotic drugs. Although still debated, there are now several independent reports of unchanged dopamine D_2 receptor binding in schizophrenic patients. Furthermore, no changes in dopamine D_2 receptor binding have been shown with PET in other disorders such as tardive dyskinesia and in more advanced stages of Parkinson's disease. Although studies on dopamine D_2 receptor binding has been largely negative, other important aspects of specific receptor binding can be addressed with PET.

Clozapine is an atypical antipsychotic drug with a superior clinical effect coupled with a low incidence of extrapyramidal side-effects and the absence of induced tardive dyskinesia. On the other hand, rapidly after termination of clozapine therapy, psychotic symptoms which may have serious consequences may return. PET studies in monkey[4] and man[5] revealed an accumulation of brain radioactivity to the striatal region and cortical areas. Interaction with pharmacological doses of a selective D_2 receptor antagonist, haloperidol, showed part of the striatal binding to be at selective dopamine D_2 receptors. Binding to the serotonin (5HT-2) receptor in the frontal cortex of Rhesus monkey was suggested[4]. Binding to other receptor populations must also be accounted for. The binding of clozapine to several receptor populations, as indicated with PET, might be of significance in the good clinical effect seen in schizophrenic patients[5].

Quantification of the receptor binding characteristics of [^{11}C]clozapine revealed a high dissociation rate from the receptors. In fact, the rate of elimination of radioactivity from the brain was similar to the plasma elimination rate of intact clozapine[4]. Simultaneously with the radioactive dose, a pharmacological dose of unlabelled clozapine was given to the monkey, and blood samples were withdrawn at regular intervals after dosing. After extraction into an organic phase and further purification, clozapine was determined by gas chromatography–mass spectrometry with selected ion monitoring[4]. A loose receptor binding for clozapine may have implications both for the low incidence of extrapyramidal side-effects and the occurrence of psychotic symptoms early after drug withdrawal.

Brain L-dopa utilization studied with PET

Dopaminergic nerve function has been addressed in many PET studies owing to the cumulation of dopamine nerve terminals in the striatum-substansia nigra area in the brain, and to the relative availability of tracers that will selectively measure the processes within the synaptic cleft. [^{18}F]Fluoro-dopa utilization in the brain has been studied both in health and disease for several years. The [^{18}F]fluoro-dopa-derived radioactivity represents a complex system, and several processes in dopamine turnover are visualized. After systemic administration of [^{18}F]-L-dopa, the radioactivity is transferred rapidly over the blood–brain barrier, taken up into the dopaminergic terminals, converted by decarboxylases to dopamine (which is stored in the vesicles) and released eventually to the postsynaptic receptors or metabolized. Metabolic enzymes such as monoamine oxidase and catecholamine-O-methyltransferase yield a complex pattern of radioactive metabolites[6].

Hence, a defective L-dopa brain turnover is difficult to visualize with PET, and several complementary methods have to be used. Recently, Firnau *et al.* used column liquid chromatography to separate the different F-labelled metabolites in both plasma[7] and brain tissue of monkey[6]. Plasma and brain tissue samples were analysed by reversed-phase liquid chromatography. The eluent was collected into fractions, which were measured for radioactivity[6]. The peaks representing ^{18}F radioactivity were identified by comparison of their elution times with those of the authentic ^{18}F-labelled catechol materials chromatographed under identical conditions. A simultaneous detection with both radiochemical and photometric detection would increase the performance of the procedure. From these studies[6,7], it was concluded that about 70% of the radioactivity in the striatum was due to the formation of [^{18}F]dopamine. [^{18}F]-3-O-methyl-dopa constituted a large fraction of the radioactivity in the cortical regions and the cerebellum. This finding is an obstacle for an adequate *in vivo* calculation of dopamine synthesis rate using cerebellum as a reference.

A second way to overcome this problem is to block selectively the metabolic enzymes monoamineoxidase and catecholamine-3-O-methyltransferase one by one in animal experiments[8]; thereby the contribution of each metabolic step to the brain radioactivities can be assessed more adequately.

A third and interesting approach is to label the molecule of interest in different positions[8]. Labelling of L-dopa with ^{11}C in the 1-position in the carboxylic acid group means that the label is lost in the decarboxylation step to dopamine. The $^{11}CO_2$ formed is eliminated from the brain. Hence this tracer gives information on the input rate to the brain and the rate of decarboxylation.

L-Dopa labelled with ^{11}C in the 3-position is transferred to the brain so that the radiolabel is withheld in all metabolic steps. This tracer gives the full information on brain L-dopa utilization.

Only by using a combination of all three approaches can a full understanding of dopamine brain turnover be reached.

Brain kinetics of neuropeptides studied with PET

Many peptides are produced both in the central nervous system and in peripheral tissues: The endogenous agonists for the opioid receptors, the opioid peptides endorphins, are typical examples. There have been discussions as to whether endorphins produced in peripheral tissues cross the blood–brain barrier and induce signifi-

cant central activity. The smallest opioid peptides, the enkephalins, are relatively unstable in plasma, and an extensive metabolism may hamper their transfer to the CNS. Enkephalin analogues that are metabolically stable, on the other hand, are known to be analgesic after systemic administration, indicating passage over the blood–brain barrier.

These issues have also been studied using PET in combination with column liquid chromatography[9]. The enkephalins studied were methionine-enkephalin and three synthetic analogues, Tyr–D-Ala–Gly–Phe–Met–NH_2 (DALA), Tyr–D-Met–Gly–Phe–Pro–NH_2 and Tyr–D-Ala–Ala–Phe–Met–NH_2. They were all labelled with ^{11}C in the methyl group of methionine. The kinetics of the radioactive distribution to the Rhesus monkey brain was visualized with PET and the elimination in Rhesus monkey plasma *in vivo* and *in vitro* were measured by reversed-phase liquid chromatography. At regular intervals, blood samples were collected and the plasma was separated. The plasma was filtered through a Sephadex G-25 PD-10 column. A sample from the low-molecular-weight fraction was injected onto a Spherisorb C_{18} column with a variable-wavelength photometric detector and a β-flow detector. Gradient LVC programmes were carried out using 0.1 *M* aqueous ammonium formate (pH 3.5) and methanol as the mobile phase. Fractions of the eluate were collected, and the radioactivity was measured in *in vivo* studies. Photometric detection of the eluent for the column had sufficient sensitivity for *in vitro* analysis. A chromatogram is shown in Fig. 3.

Analysis with PET showed an increased radioactivity in the monkey brain over the 60–90-min investigation period following intravenous administration of the enkephalin peptides. Highest brain radioactivities were measured for injections of methionine-enkephalin and DALA. However, a large fraction of brain radioactivity derived from these two enkephalin peptides probably emanated from ^{11}C metabolites formed *in vivo*, as evidenced by chromatographic analysis of plasma and urine samples from the monkeys. Methionine-enkephalin was cleared rapidly from plasma *in vitro* with a half-life of less than 2 min, whereas DALA was found to be stable *in vitro*. ^{11}C radioactivity in the brain originated from ^{11}C metabolites formed from methionine-enkephalin and DALA. For the two other enkephalin peptides, only minor concentrations of plasma ^{11}C metabolites were determined.

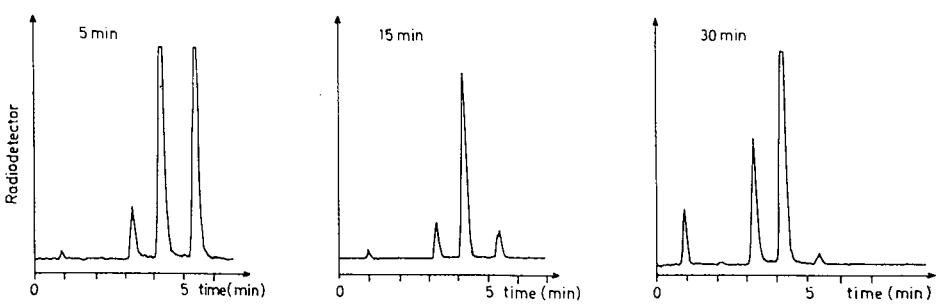

Fig. 3. Analysis of the *in vitro* metabolism of [^{11}C]methionine-enkephalin in plasma using a reversed-phase Spherisorb C_{18} column equipped with a variable-wavelength UV detector, showing the rapid hydrolysis of [^{11}C]methionine-enkephalin to polar ^{11}C-labelled metabolites.

Substance P labelled with ^{11}C in the methyl group of methionine showed similar results with high radioactivities in brain. After analysis of plasma samples by liquid chromatography, high concentrations of ^{11}C metabolites were seen. Hence, in the case of ^{11}C-labelled substance P, the brain radioactivities probably also emanated from radiolabelled metabolites formed.

These conclusions concerning the brain distribution and kinetics of ^{11}C-radiolabelled neuropeptides could only be reached by a careful combination of PET with studies using liquid chromatography on the *in vivo* and *in vitro* metabolism of the peptide.

CONCLUSIONS

The new imaging technique PET visualizes specific biochemical processes in the tissues of a living animal and man, and the information given cannot be obtained with any other method. The results and conclusions obtained with PET have been achieved only by combination with other measurement techniques. The most important and powerful of these other methods is the liquid chromatographic analysis of the radioactive constitution of different body fluids and tissues. Liquid chromatography also plays an important role in the purity control of the radiolabelled product before administration to a patient. The high detection selectivity achieved by the simultaneous use of radiochemical and photometric detection had to be combined with a rapid and versatile chromatographic separation with good selectivity and high separation efficiency.

ACKNOWLEDGEMENTS

These studies were supported by grants from the Swedish Medical Research Council (grants Nos. 7005 and 8645) and the Swedish Natural Reseach Council (K-KU-3463).

REFERENCES

1 A. Lilja, K. Bergström, P. Hartvig, B. Spännare, C. Halldin, H. Lundqvist and B. Långström, *Am. J. Neuroradiol.*, 6 (1985) 505.
2 M. E. Phelps, J. C. Maziotta and H. R. Schelbert (Editors), *Positron Emission Tomography: Principles and Applications for the Brain and Heart*, Raven Press, New York, 1986.
3 P. Hartvig, K. Bergström, A. Lilja, S. M. Aquilonius, S. Å. Eckernäs, H. Lundqvist, G. Antoni, C. Halldin, K. Någren and B. Långström, in S. Lindgren, B. Davidsson and J. Bruhn (Editors), *Topics in Clinical Pharmacy, Acta Pharm. Suec.*, Suppl. 1, (1986) 205.
4 P. Hartvig, S. Å. Eckernäs, L. Lindström, B. Ekblom, U. Bondesson,H. Lundqvist, C. Halldin, K. Någren and B. Långström, *Psychopharmacology*, 89 (1986) 248.
5 T. Lundberg, L. H. Lindström, P. Hartvig, S. Å. Eckernäs, B. Ekblom, H. Lundqvist, K. J. Fasth, P. Gullberg and B. Långström, *Psychopharmacology*, 99 (1989) 8.
6 G. Firnau, S. Sood, R. Chirakal, C. Nahmias and E. S. Garnett, *J. Neurochem.*, 48 (1987) 1077.
7 G. Firnau, S. Sood, R. Chirakal, C. Nahmias and E. S. Garnett, *J. Nucl. Med.*, 29 (1988) 363.
8 P. Hartvig, S. M. Aquilonius, J. Tedroff, L. Reibring, H. Ågren, P. Bjurling, J. Ulin and B. Långström, *Proceedings of Fifth Symposium on the Medical Application of Cyclotrons, Acta Radiol. Scand.*, Suppl., (1990) in press.
9 P. Hartvig, K. Någren, P. O. Lundberg, C. Muhr, L. Terenius, H. Lundqvist, L. Lärkfors and B. Långström, *Regulat. Pept.*, 16 (1986) 1.

Journal of Chromatography, 507 (1990) 311–319
Elsevier Science Publishers B.V., Amsterdam — Printed in The Netherlands

CHROMSYMP. 1789

Interrelation between nucleotide degradation and aldehyde formation in red blood cells

Influence of xanthine oxidase on metabolism: an application of nucleotide and aldehyde analyses by high-performance liquid chromatography

ANDREAS WERNER*, WERNER SIEMS, TILMAN GRUNE and CORNELIA SCHREITER
Institute of Biochemistry, Medical Faculty (Charité), Humboldt University of Berlin, Hessische Strasse 3/4, 1040 Berlin (G.D.R.)

ABSTRACT

The mechanism by which hypoxia leads to irreversible cellular damage is poorly understood. A decrease in purine nucleotides is common to all ischaemic tissues, yielding hypoxanthine as the substrate of the xanthine oxidase reaction. Excessive production of radicals via xanthine oxidase induces peroxidation of unsaturated fatty acids, accompanied with the formation of aldehydes. The nucleotides and aldehydes were determined by high-performance liquid chromatography (HPLC) of red blood cell extracts. Nucleotides and their derivatives were determined by HPLC on an ODS column and elution with 10 m*M* phosphate buffer containing 2 m*M* *tert.*-butylammonium phosphate. The aldehyde production in glucose deprived red blood cells was stimulated by addition of xanthine oxidase and by inhibition of different haemotype enzymes with sodium azide. Aldehydes were analysed by derivatization to dinitrophenylhydrazones, followed by thin-layer chromatographic and HPLC separation with aqueous methanol on an ODS column. The HPLC methods presented are appropriate for the determination of nucleotides, nucleosides and nucleobases, in addition to alkenals and hydroxyalkenals in extracts of oxidatively stressed red blood cells.

INTRODUCTION

There are a wide range of factors relating the metabolic state of erythrocytes to their susceptibility to oxidative stress. It is known that depletion of erythrocyte adenosine triphosphate before incubation under radical-generating conditions favours accumulation of malondialdehyde (MDA)[1]. The peroxidative susceptibility seems to be determined by the metabolic state of the cell and the site of the peroxidized lipids within intracellular pools. A decrease in purine nucleotides is common to all ischaemic tissues[2–4].

0021-9673/90/$03.50

It has been proposed that oxygen radicals are generated via xanthine oxidase reactions in reoxygenated tissues[5,6]. Hypoxanthine, the substrate of the xanthine oxidase reaction, accumulates during oxygen deficiency owing to the breakdown of purine nucleotides[7]. The conversion to uric acid via xanthine oxidase induces lipid peroxidation of polyunsaturated fatty acids[8]. Lipid peroxidation results in a wide range of carbonyl products, some of which are extremely reactive[9,10]. Aldehydes are formed as secondary oxidation products from the primary products of hydroperoxides. It has been known for many years that some of these aldehyde products inhibit energy-requiring processes of the cell[9,10]. An important representative of the aldehydes generated is 4-hydroxy-2-nonenal (4-HNE), occurring in well known biological model systems for oxidative burst (*e.g.*, NADPH oxidation by liver microsomes, carbon tetrachloride intoxication). The aldehyde production could be used for the assessment of the oxidative loading of cells. Under ischaemic and post-ischaemic conditions, radicals are generated via xanthine oxidase by conversion of purine breakdown products. Therefore, under these conditions it is useful to determine both parameters (nucleotides and aldehydes) in order to evaluate the radical-induced changes. Both phenomena, nucleotide degradation and lipid peroxidation, could be analysed by high-performance liquid chromatography (HPLC).

The nucleotides, especially ATP, are of importance for proteolytic pathways occurring in red blood cells (ATP increases the degradation of untreated proteins 4–6-fold in reticulocyte extracts). The share of ATP-independent proteolytic pathways which may give protection against the accumulation of proteins damaged by oxygen radicals or other active oxygen species is to be determined[11]. As a consequence of the production of free radicals ($O_2^{-\bullet}$), haemoglobin in red blood cells is first oxidized to methaemoglobin and then to hemicrome[12]. At the same time, modifications of the membrane proteins, lipids, cell permeabilities and autologous IgG binding have been reported. The final result of these events is cell lysis and/or phagocytosis. Both processes occur *in vivo*. Owing to the heterogeneity of the physico-chemical properties of polar or apolar compounds (nucleotides, nucleosides) and the very different concentrations (low concentration of nucleobases), a reversed-phase (RP) ion-pair HPLC separation was applied to measure the breakdown of nucleotides and the increase in nucleosides and nucleobases in a single run. Red blood cells of rabbits were used in the HPLC methods for the determination of nucleotides and aldehydes. The aldehyde production in red blood cells (RBC) was initiated by addition of xanthine oxidase (XOD) and further stimulated by addition of sodium azide, which inhibits different haemotype enzymes (*e.g.*, catalase), leading to the acceleration of radical generation.

EXPERIMENTAL

Determination of nucleotides

Chemicals. All reference standard of the highest analytical grade available were purchased from Boehringer (Mannheim, F.R.G.) and Sigma (St. Louis, MO, U.S.A.). $NH_4H_2PO_4$ was purchased from Fisher scientific (Fairlawn, NJ, U.S.A.), acetonitrile from Merck (Darmstadt, F.R.G.), TBA (tetratbutylammonium phosphate, PIC reagent A) from Waters Assoc. (Milford, MA, U.S.A.) and XOD from Boehringer.

Cell preparation. Red blood cells were drawn from the ear vein of rabbits, washed twice in an isotonic solution of triethanolamine buffer (pH 7.43) and incubated at 37°C with XOD (0.2 units per 10-ml reaction volume) and sodium azide (2 mmol/l).

Extraction procedure and sample preparation. The samples were deproteinized (6% perchloric acid), centrifuged (8 min 1200 *g*) and neutralized with triethanolamine (1 mol/l)–potassium carbonate (1.3 mol/l) (pH 9). After filtration, 50 μl of the supernatant were analysed by HPLC.

HPLC instrument and chromatographic conditions. A Perkin-Elmer (Norwalk, CT, U.S.A.) liquid chromatograph was used, consisting of a M410 pump system, LC-95 variable-wavelength detector (operated at 254 nm), LCI-100 integrator and a Rheodyne injector. The column was Supelcosil LC-18-S (5 μm) (150 × 4.6 mm I.D.) with 9800 theoretical plates, with a 25 mm × 4.6 mm I.D. precolumn.

Buffer A was 0.01 *M* $NH_4H_2PO_4$ containing 2 m*M* PIC A and buffer B was 80% buffer A containing 20% (v/v) acetonitrile, with the following gradient: 5 min linear gradient from 100% A to 70% B, 8 min isocratic 70% B–30% A, 20 min convex gradient to 100% B (curve 3; this curve leads to 37% B after 10 min and to 65% B after 15 min of this gradient elution), 7 min isocratic 100% B, 2 min to 100% A; at the end the system was switched back by pumping buffer A for 10 min. The flow-rate was 1 ml/min. Peak identification and quantification were performed as described elsewhere[13].

Determination of aldehydes

Chemicals. Aldehyde standards (dinitrophenylhydrazones) were obtained from Professor H. Esterbauer (University of Graz, Austria). The solvents *n*-hexane, dichlormethane and methanol and thin-layer chromatographic (TLC) plates (silica gel 60 F_{254}, 0.2 mm thickness) from Merck (Darmstadt, F.R.G.) were used. 2,4-Dinitrophenylhydrazine (DNPH) was obtained from Union Chimique (Brussels, Belgium), dissolved in a 1 *M* hydrochloric acid, extracted with 15 ml of *n*-hexane, then adjusted to 1.8 m*M* solution by absorbance measurement.

Preparation of 2,4-dinitrophenylhydrazones from biological samples[14,15]. After incubation of 4.5 ml of a suspension of RBC (+ 0.5 ml of EDTA) with 5 ml of DNPH solution for 2 h in the dark with mixing, samples were kept for 1 h in an ice-bath in the dark, then extracted with 7 ml of dichloromethane, centrifuged at 900 *g* (three times), evaporated to dryness and the residue was dissolved in 1 ml of dichloromethane.

Thin-layer chromatography. TLC plates were developed with dichloromethane in comparison with known standards[14]. Two individual fractions were scraped off [zone I, zone III according to ref. 14, containing 4-hydroxyalkenals (I) and alkenals, 2-alkenals and ketones (III)], extracted with 10 ml of methanol (three times), evaporated to dryness and the residue was dissolved in 1 ml of methanol.

HPLC instrument and chromatographic conditions. A Shimadzu LC-6A HPLC pump, a Rheodyne injector and a Hewlett-Packard 104A photodiode-array detector with an HP 9000 Series 300 Workstation (9153A Winchester drive, Think-Jet printer, Color Pro plotter) were used. The eluent was methanol–water (4:1, v/v) at a flow-rate of 0.9 ml/min. The column was Nucleosil $5C_{18}$ (Macherey, Nagel &Co., Düren, F.R.G.) (250 × 4.0 mm I.D.) with a 50 × 4.0 mm I.D. precolumn.

Peak identification was performed using internal standards and comparison

with the spectra of reference compounds. Quantification was achieved by separating authentic standards under identical conditions. Recoveries were determined for all reference compounds following derivatization and TLC.

RESULTS AND DISCUSSION

Nucleotide determination

The gradient RP-HPLC method with ion pairing applied to RBC extracts allowed the separation of hypoxanthine, xanthine, uric acid, inosine, guanosine, adenine, adenosine, NAD, IMP, AMP, GDP, ADP, GTP and ATP (Fig. 1). The separation of nucleotides, nucleosides and nucleobases obtained was comparable to those reported by other workers[16,17]. The low-concentrated hypoxanthine, xanthine and uric acid were eluted in the first few minutes of separation without peak broadening. The method allowed changes in nucleotide metabolism to be monitored during incubation experiments with increased nucleotide catabolism induced by glycose starvation, and also the influence of radical formation on nucleotide metabolism. The radical formation in ischaemic tissues via purine breakdown could be assessed, as radical formation via XOD is the most important source during and following oxygen deficiency[6].

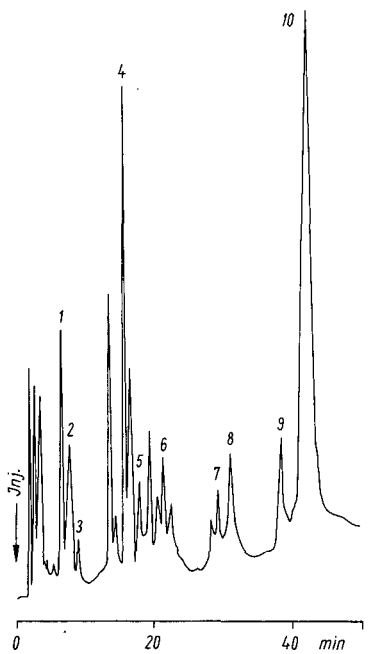

Fig. 1. Ion-pair RP-HPLC separation of nucleobases and nucleotides extracted from RBC using a gradient system (see Experimental). Eluents: (A) 10 mmol/l $NH_4H_2PO_4$ with 2 mmol/l tetrabutylammonium phosphate and (B) eluent A containing 20% (v/v) acetonitrile. Flow-rate, 1 ml/min. A Supelcosil LC-18-S (5 μm) column (150 × 4.6 mm I.D.) was used. Detection wavelength, 254 nm (0.02 a.u.f.s.). Peaks: 1 = hypoxanthine; 2 = xanthine; 3 = uric acid; 4 = NAD^+; 5 = IMP; 6 = AMP; 7 = GDP; 8 = ADP; 9 = GTP; 10 = ATP. Peak identities of the biological sample were confirmed by coelution with reference compounds.

Glucose starvation yielded an increased catabolism of purine nucleotides in red cells[18]. Hypoxanthine accumulated under these conditions. The addition of XOD yielded a radical-generating system and furthermore accelerated the degradation of ATP, ADP and AMP in comparison with controls without addition of XOD to the suspension. RBC in a control experiment with glucose-containing buffer showed no degradation of adenine nucleotides[19]. The addition of sodium azide had no significant effect on nucleotide breakdown but modified the response of the lipid peroxidation in the RBC. A comparison of nucleotide degradation under glucose deprivation and glucose deprivation with added XOD yielded a faster decrease in adenine nucleotides in the latter instance.

The ion-pair RP-HPLC separation of nucleobases, nucleosides and nucleotides is influenced by the interaction of the cationic ion-pair reagent with the ionic nucleotides. The formation and retention of ion pairs causes the sequence of elution of nucleoside monophosphates before nucleoside diphosphates and before nucleoside triphosphates. The buffer salt concentration of 10 m*M* $NH_4H_2PO_4$ allowed no competition with the nucleotides for the ion-pair reagent, and maintained a sufficient amount of free ion pair cations[20].

Aldehyde determination

After derivatization of free aldehydes with 2,4-DNPH, the extraction yielded a separation of polar and non-polar fractions[14]. The non-polar fraction contained *n*-alkenals, 2-alkenals, dicarbonyl compounds and 4-hydroxyalkenals. Zone I contained 4-hydroxynonenal, 4-hydroxyoctenal and 4-hydroxyhexenal. Fig. 2 (bottom) shows the chromatogram of OH-alkenal standards obtained after TLC. The upper panel shows the spectrum of the dinitrophenylhydrazone of 4-hydroxyhexenal and the corresponding standard compound.

Zone III consists of pentanal, 2,4-hexadienal, hexanal, 2,4-heptadienal, octenal, 2,5-nonadienal and 2,4 decadienal. The chromatogram is shown in Fig. 3 (bottom).

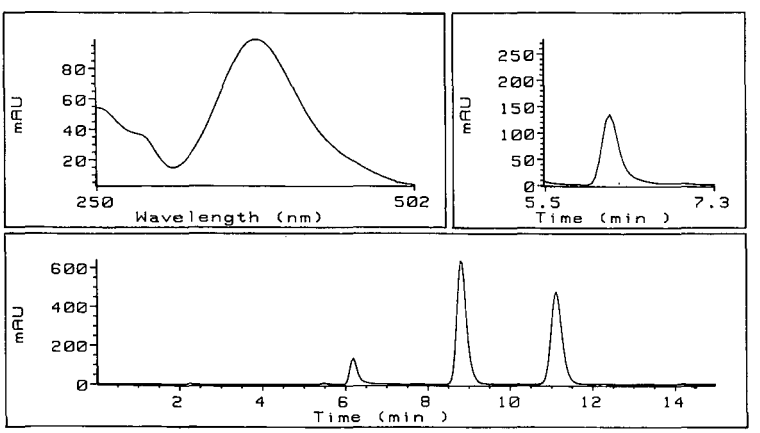

Fig. 2. (Bottom) chromatogram of a standard mixture of 2,4-dinitrophenylhydrazones of hydroxyalkenals (zone I after TLC). Retention times: 6.3 min = 4-hydroxyhexenal (also in the inset in the upper panel, spectrum of 4-hydroxyhexenal), 8.8 min = 4-hydroxyoctenal, 11.3 min = 4-hydroxynonenal. Column, Nucleosil $5C_{18}$ (250 × 4.0 mm I.D.); flow-rate, 0.9 ml/min.

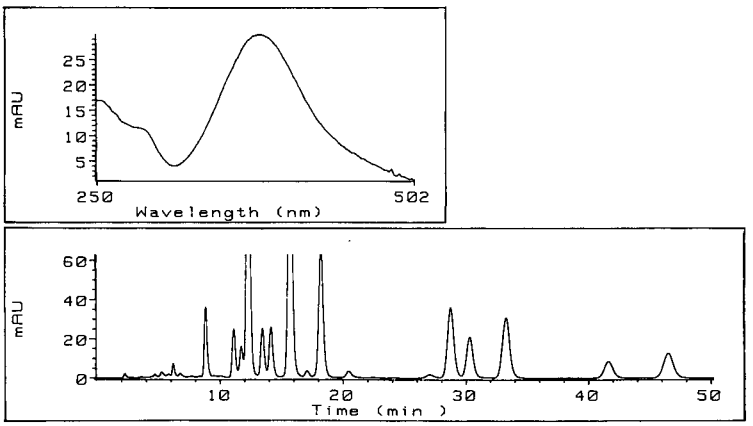

Fig. 3. (Bottom) chromatogram of a standard mixture of 2,4-dinitrophenylhydrazones of aldehydes (zone III after TLC) and (top) spectrum of 2,4-heptadienal. Retention times: 12.5 min = pentanal; 16 min = 2,4-hexadienal; 18.4 min = hexanal; 28.5 min = 2,4-heptadienal; 30.5 min = octenal; 33.5 min = 2,5 nonadienal; 46.5 min = 2,4-decadienal).

In the upper panel the spectrum of the dinitrophenylhydrazone of 2,4-heptadienal is shown. After addition of XOD and hypoxanthine to the red cell suspension containing sodium azide as inhibitor of haemotype enzymes the first sample was taken and prepared for aldehyde analysis (extraction and TLC). Fig. 4 shows the chromatogram of zone I after TLC of the lipid peroxidation products. The chromatogram in Fig. 5 (bottom), was obtained after 60 min of incubation with XOD and hypoxanthine (sodium azide). The upper panel shows the spectra of the dinitrophenylhydrazones of 4-hydroxynonenal from the standard chromatogram and the chromatogram of the biological extract comparison which were used for peak identification in the extracts of the cell suspensions. 4-HNE production was much more pronounced after addition

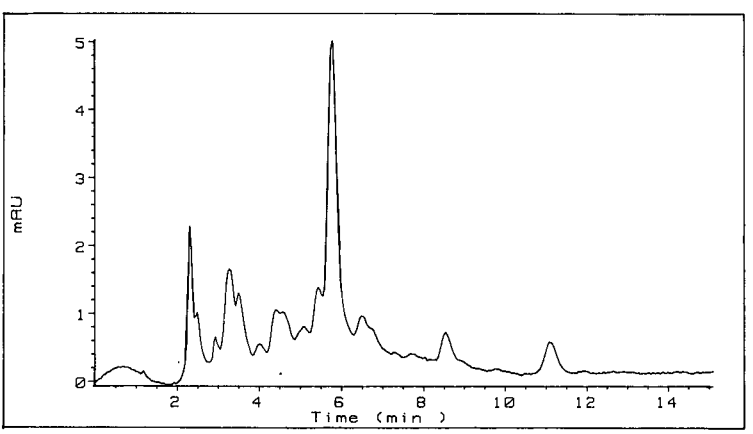

Fig. 4. Chromatogram of zone I after TLC of lipid peroxidation products originating from RBC immediately after addition of XOD to the suspension containing hypoxanthine and sodium azide (initial value of 4-hydroxynonenal at retention time 11 min).

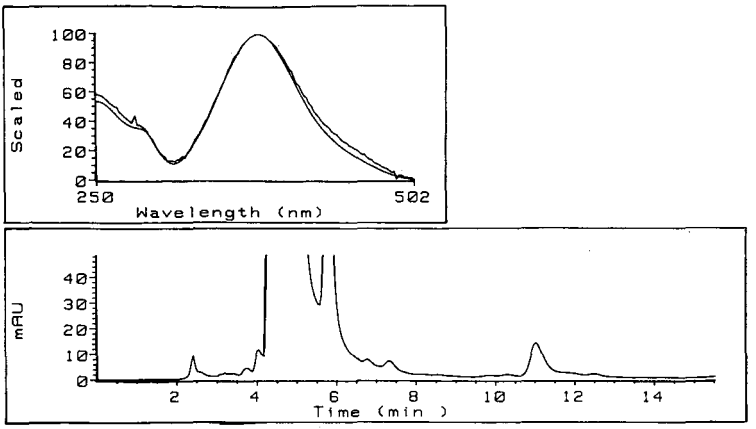

Fig. 5. (Bottom) chromatogram of zone I after TLC of lipid peroxidation products of RBC incubated with XOD, hypoxanthine and sodium azide (after 60 min at 37°C). (Top) spectra for comparison of 4-hydroxynonenal from the biological extract and a standard compound.

of XOD and hypoxanthine (250 μmol/l) compared with the incubation with XOD only, using the hypoxanthine from the ATP degradation under glucose deprivation conditions. Nucleotide analysis indicated an increase in hypoxanthine from 10 μmol/l at the beginning of the incubation experiment (after glucose-free washing of RBC suspension) to 300 μmol/l after incubation for 4 h without glucose. The incubation of the RBC suspension with XOD alone yielded a 25-fold increase in 4-HNE (17.94 ± 2.9 μmol/l) and a 150-fold increase for the glucose-free incubation of RBC with XOD and hypoxanthine (107.6 ± 17.4 μmol/l).

The ATP degradation in RBC was accelerated in comparison with control incubations without detectable 4-HNE formation (glucose-free incubation from 1.3 ± 0.08 to 1.05 ± 0.05 mmol/l, glucose-free + XOD to 0.84 ± 0.06 mmol/l, glucose-free + XOD + hypoxanthine to 0.9 ± 0.08 mmol/l; $n = 4$). Fig. 6 shows the chromatogram of an extract of RBC suspension after 60 min of lipid peroxidation induced by XOD and hypoxanthine. Pentanal, hexanal and 2,4-decadienal were increased (2,4-decadienal is shown in the inset in Fig. 6) in comparison with the initial values 20-, 26- and 15-fold (1.78 ± 0.27, 2.43 ± 0.25, 1.93 ± 0.25 μmol/l), respectively, after incubation of RBC for 4 h with XOD + Hyp. Sodium azide was applied in all experiments to stimulate the lipid peroxidation in RBC containing very active antioxidant enzymes, such as superoxide dismutase, catalase or glutathione peroxidase. Reactive oxygen species could diffuse across the RBC membrane.

In RBC exposed to hypoxanthine and XOD, which generate both superoxide and hydrogen peroxide, the lipid peroxidation and degradation of proteins to free amino acids increase dramatically owing to deterioration of membrane organization and an increase in proteolytic processes induced by aldehyde-mediated reactions[11]. This effect coincides with the appearance of methaemoglobin and other oxidized forms of haemoglobin in the cells. The simplest explanation of these observations is that the major cell protein haemoglobin is damaged either by the oxygen radicals ($HO_2^{\cdot}$, $O_2^{-\cdot}$, $^{\cdot}OH$), or by other activated oxygen species (H_2O_2 or possibly $^1O_2$) generated by hypoxanthine + XOD. For the determination of the radical-induced

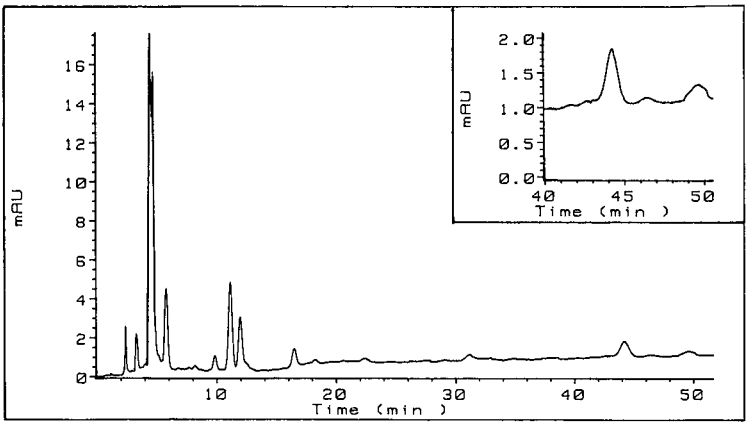

Fig. 6. Chromatogram of zone III after TLC of lipid peroxidation products of RBC incubated with xanthine oxidase, hypoxanthine and sodium azide (after 60 min at 37°C). Retention times: 12.5 min = pentanal; 16.5 min = hexanal; 44.5 min = 2,4-decadienal (detailed in the inset). Peaks were identified by comparison of spectra with standard compounds.

lipid peroxidation the TLC–HPLC determination of aldehydes was applied. The detectable amount of lipid peroxidation measured by generation of 4-HNE increased during the 4 h of the incubation of rabbit erythrocytes at 37°C. The appearance of lipid peroxidation was followed by haemolysis. Glucose could protect against lipid peroxidation by maintaining normal levels of reduced glutathione. The incubation with hypoxanthine and XOD generates larger amounts of urate, which has been shown to protect membrane lipids against peroxidation[21].

The aldehyde detected in the experiments could be generated by cleavage reactions from primary hydroperoxides or from secondary or tertiary oxygenated products. Hexanal can be formed by dismutation of various monohydroperoxides (*e.g.*, 15-hydroperoxyarachidonic acid) and 4-hydroxynonenal in peroxidizing liver microsomes arises exclusively from arachidonic acids of polar lipids[8]. This could also be due to RBC peroxidation. The measured increase in 4-HNE is of interest because of the inhibiting effects on a number of cellular functions (cellular glycolysis, 5'-nucleotidase, adenylate cyclase)[22].

The chromatographic methods presented allow the assessment of radical-induced changes in cells by the determination of changes in nucleotide metabolism and of the generation of lipid peroxidation products, and could therefore be applied to various cells and tissues showing changes after the action of reactive oxygen species.

REFERENCES

1 D. W. Allen and J. J. Cierzan, *J. Lab. Clin. Med.*, 112 (1988) 87.
2 D.A. Hems and J. T. Brosnan, *Biochem. J.*, 120 (1970) 105.
3 M.-F. Vincent, G. van den Berghe and H. G. Hers, *Biochem. J.*, 202 (1982) 117.
4 S. Marubayashi, M. Takenaka, K. Dohi, H. Ezaki and T. Kawasaki, *Transplantation*, 30 (1980) 294.
5 D. N. Granger, G. Rutili and J. M. McCord, *Gastroenterology*, 81 (1981) 22.
6 J. M. McCord and R. S. Roy, *Can. J. Physiol. Pharmacol.*, 60 (1982) 1346.

7 H. Osswald, *Pflügers Arch.*, 371 (1977) 45.
8 A. Benedetti and M. Comporti, *Bioelectrochem. Bioenerg.*, 18 (1987) 187.
9 E. Schauenstein, G. Schatz and G. Benedikt, *Monatsh. Chem.*, 92 (1961) 442.
10 E. Schauenstein and H. Esterbauer, *Monatsh. Chem.*, 94 (1963) 164.
11 K. J. A. Davies and A. L. Goldberg, *J. Biol. Chem.*, 262 (1987) 8227.
12 J. H. Jandl, L. K. Engle and D. W. Allen, *J. Clin. Invest.*, 39 (1960) 1818.
13 A. Werner, W. Siems, G. Gerber, H. Schmidt, S. Gruner and H. Becker, *Chromatographia*, 25 (1988) 237.
14 H. Esterbauer, K. H. Cheeseman, M. U. Dianzani, G. Poli and T. F. Slater, *Biochem. J.*, 208 (1982) 129.
15 G. Poli, M. U. Dianzani, K. H. Cheeseman, T. F. Slater, J. Lang and H. Esterbauer, *Biochem. J.*, 227 (1985) 629.
16 D. R. Webster, G. D. Boston and D. M. Paton, *J. Liq. Chromatogr.*, 8 (1985).
17 V. Stocchi, L. Lucchiarini, F. Canestrari, M. P. Piscentini and G. Fornaini, *Anal. Biochem.*, 167 (1987) 181.
18 F. Bontemps, G. van den Berghe and H. G. Hers, *J. Clin. Invest.*, 77 (1986) 824.
19 A. Werner, I. Rapoport and G. Gerber, *Biomed. Biochim. Acta*, 46 (1987) 324.
20 D. Perrett, in C. K. Lim (Editor), *HPLC of Small Molecules—A Practical Approach*, IRL Press, Oxford, 1986, p. 221.
21 A. Sevanian, S. F. Muakkassah-Kelly and S. Montestruque, *Arch. Biochem. Biophys.*, 223 (1983) 441.
22 H. Esterbauer, in D. C. H. McBrien and T. F. Slater (Editors), *Free Radicals, Lipid Peroxidation and Cancer*, Academic press, London, 1982, p. 101.

Journal of Chromatography, 507 (1990) 321–326
Elsevier Science Publishers B.V., Amsterdam — Printed in The Netherlands

CHROMSYMP. 1817

Monitoring and purification of gluconic and galactonic acids produced during fermentation of whey hydrolysate by *Gluconobacter oxydans*

J. C. MOTTE*, N. VAN HUYNH, M. DECLEIRE, P. WATTIAU, J. WALRAVENS and X. MONSEUR

Ministère de l'Agriculture, Institut de Recherches Chimiques, Museumlaan 5, B-1980 Tervuren (Belgium)

SUMMARY

Because the sugar concentration of whey is low, the substrate conversion must lead to products with a high added value and with the highest possible yields. Deproteinised and hydrolysed whey was found to be an excellent medium for acidic fermentations and both gluconic and galactonic acids were produced in high yields during the growth of *Gluconobacter oxydans* on hydrolysed whey.

The production, the identification by ionic high-performance liquid chromatography and the purification of both acids on ion-exchange columns will be described here.

INTRODUCTION

Usually the whey that is available in large amounts in most European countries is ultrafiltered and the lyophilized proteins are used for cattle feed. The retentate contains up to 5% of lactose and low-molecular-weight peptides and it has been found to be an excellent growth medium for bacteria involved in acidic fermentations[1–3].

The fermentation of sugars to alcohols or acids is well known and is very reliable but, in contrast to studies where sugar had been used at high concentrations, the lactose is present at a maximum level of only 5%. Accordingly, the conversion must lead to products with the highest possible yields. The products must also be easily isolated with a high added value and a high marketing potential. In order to meet all these requirements, acid fermentations leading to gluconic acid and galactonic acid have been assessed.

The use of whey as a culture medium is not very common because many microorganisms are not able to metabolize lactose. For example, less than 12% of yeast strains can assimilate this sugar[4]. This is the reason why hydrolysed whey was used for *Gluconobacter oxydans* fermentations[5].

The products that are obtained are so closely related that different chromatographic methods have been needed to identify and quantify them. The selected

0021-9673/90/$03.50

analytical methods have been high-performance liquid chromatography (HPLC) on a cation-exchange column or on a strong anion-exchange column[6] and capillary gas chromatography (GC) after derivatization of the acids that are produced[7]. The results of the assays are presented here.

EXPERIMENTAL

Instrumentation

The HPLC system consisted of a Model 6000A pump, a WISP intelligent automated injector, an R-401 refractometer and a UV-441 detector (set at 214 nm) (all from Waters Assoc., Milford, MA, U.S.A.). The results were recorded with a Trilab 2500 from Trivector (Sandy, Bedfordshire, U.K.). Two columns were used: a Bio-Rad Aminex HPX-87-H with the corresponding precolumn (elution with $5 \cdot 10^{-3}$ *M* sulphuric acid at 0.7 ml/min and 70°C) and a Dionex HPIC-AS5 fitted with an HPIC-AG5 precolumn (elution with 0.01 *M* sodium hydroxide solution at 0.7 ml/min and 25°C).

Capillary GC was performed with a Carlo-Erba Vega instrument equipped with an OV-17 column (20 m × 0.32 mm I.D.). The column temperature was programmed at 10°C/min from 60 tot 150°C and at 5°C/min from 150 to 300°C.

The sugar derivatization procedure has been described previously[6].

The ultrafiltration system consisted of a Minipuls-2 peristaltic pump (Gilson) and a tangential ultrafiltration module (Amicon) with an effective surface area of 43 cm^2 and a molecular-weight cut-off of 10^4.

The Model C16/100 glass purification columns (Pharmacia, Uppsala, Sweden) with adaptor, having a volume of 175 ml were filled with Amberlite IRC-120 (Rohm and Haas, Philadelphia, PA, U.S.A.) as a cation-exchange resin and Bio-Rad AGMP-1 (Bio-Rad Labs., Richmond, CA, U.S.A.) as an anion-exchange resin.

The Biolafitte(F) 2-L fermenter was thermostated at 30°C and equipped with a automatic pH regulator (Consort, Turnhout, Belgium).

The *Kluyveromyces bulgaricus* IRC 101 used for whey hydrolysis has been described previously[5]. *Gluconobacter oxydans* ATCC 621H was grown on the hydrolysed whey.

RESULTS

The kinetics of both sugar conversion and acid production by the bacteria can be monitored in a single chromatographic run when a strong cation-exchange column is used. The rare infections that occurred during long fermentations can be detected at an early stage by the production of polar acidic or alcoholic metabolites, mainly acetic acid and butyric acid and ethanol, respectively. Typical chromatograms of the standards used for monitoring the whey fermentation are presented in Fig. 1.

As shown in Fig. 2, the gluconic acid production, occurring from hydrolysed whey as described[3], can give ambiguous results because of the overlapping of the glucose and gluconic acid peaks. To overcome this problem, the gluconic acid formation was then monitored without any sugar interferences by UV detection at 214 nm.

Before using the whey hydrolysate to produce gluconic acid, preliminary fermentations were conducted on either glucose or galactose medium. The glucose was

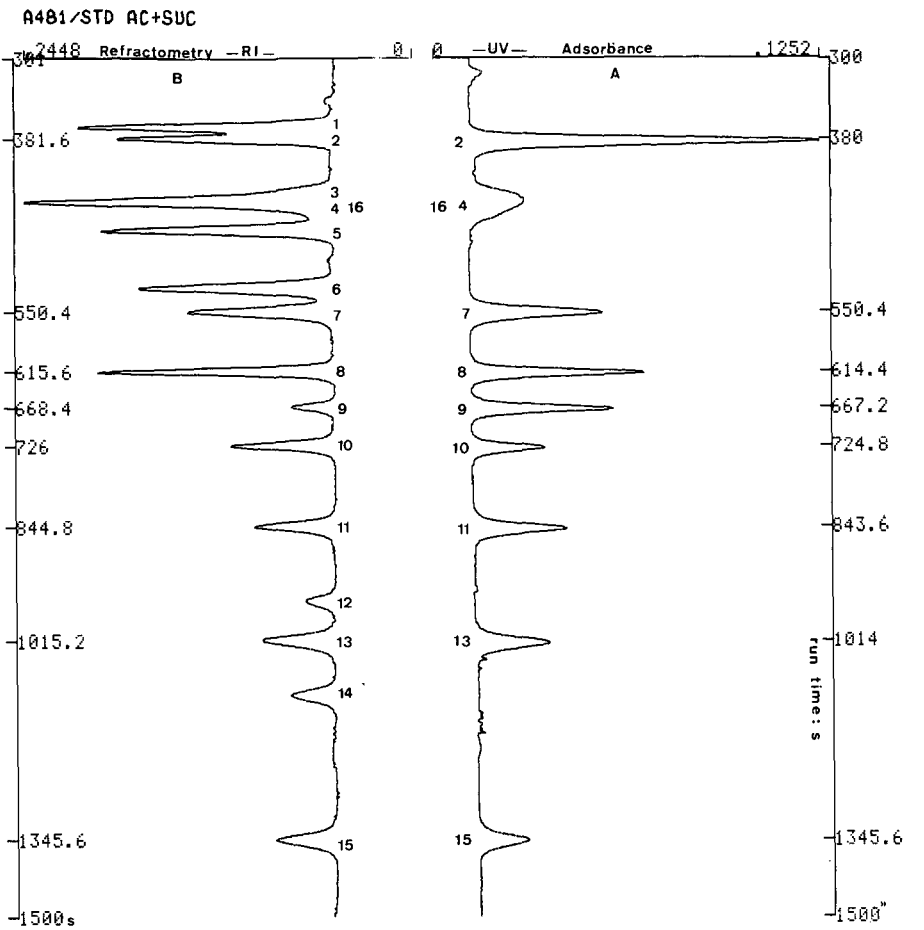

Fig. 1. (A) UV and (B) refractometric determinations of the standards used for the identification of the most important compounds present in whey. Peaks: 1 = citric acid; 2 = lactose; 3 = glucose; 4 = gluconic acid; 5 = galactose; 6 = ribose; 7 = succinic acid; 8 = lactic acid; 9 = formic acid; 10 = acetic acid; 11 = propionic acid; 12 = methanol; 13 = butyric acid; 14 = ethanol; 15 = valeric acid.

completely oxidized to gluconic acid within 24 h and if the reaction was stopped at this stage no ketogluconic acid could be found[9]. Galactose was metabolized at an obviously slower rate. Up to 72 h were needed for its complete conversion into the corresponding acidic molecule that had the same retention time as that of gluconic acid on the cation-exchange column.

In order to try to separate the acids produced, an anion-exchange column was also used. No differences in retention time was observed in either the isocratic mode or the gradient mode using a gradient of sodium hydroxide concentration. While the search for an HPLC method for the separation of these products is being continued and will be published elsewhere, capillary GC was used to identify both metabolites. As shown in Fig. 3, two peaks eluting at 167 and 172°C were observed. After comparison with standards of both acids, it was clearly established that *Gluconobacter ox-*

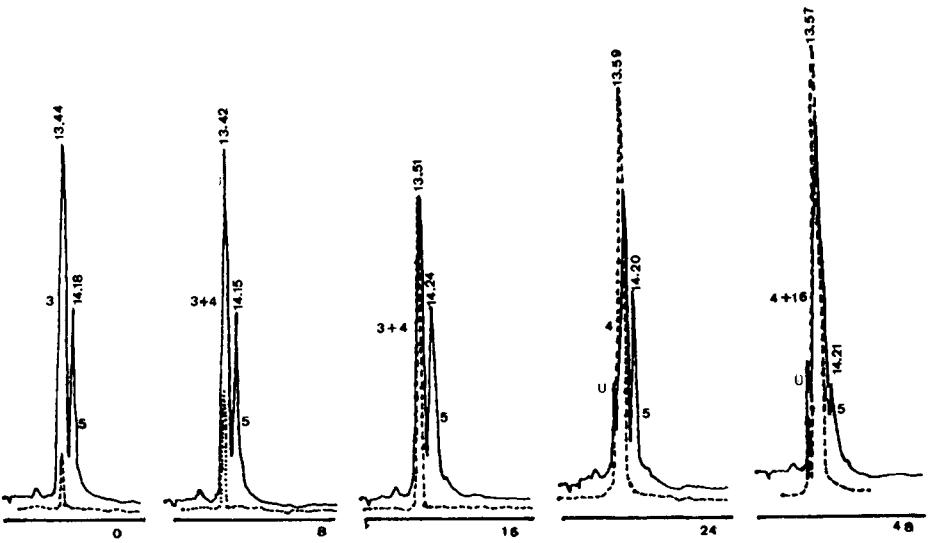

Fig. 2. On-line monitoring of gluconic acid fermentation at 0, 8, 16, 24 and 48 h, as indicated. Peaks: 3 = glucose; 4 = gluconic acid; 5 = galactose; U = unknown; 16 = galactonic acid. Retention time given in min. UV, 214 nm (---) and RI (——) detection.

ydans produces gluconic acid and galactonic acid from glucose and galactose, respectively.

The use of the whey hydrolysate leads rapidly to a broth containing mainly gluconic acid and galactose as sugar. Subsequently, the broth was ultrafiltered and saved. The biomass was concentrated for a further run while the ultrafiltered gluconic acid and galactose were separated by using ion-exchange column. The resulting galactose solution, sterilized by ultrafiltration, was directly oxidized to galactonic acid by *Gluconobacter oxydans* that had grown previously on a galactose medium. Following this, a two-step fermentation was conducted with no cross-contamination of the two acids.

In order to elute the acids produced (gluconic or galactonic acid) from the anion-exchange column, dilute hydrochloric acid was used first. The eluted organic acid contained all the other acids present in the broth. A rapid darkening of the solution was also observed. Moreover, hydrochloric acid could not be removed even after concentration under reduced pressure and the crystallization yields were low.

Better results were obtained by using formic acid, which could also be easily removed by evaporation under reduced pressure while concentrating the eluted acid. These solutions were lightly coloured and pure enough to be used for the crystallization process without any further purification. As shown in Table I, under the conditions used during this study, more than 75% of the total galactonic acid can be eluted with a maximum of 5% (w/w) contamination by formic acid. The fractions that follow the desired acid can be combined and exchanged again on a regenerated column.

Table II shows the different yields of galactonic acid obtained during the fermentation process and from the first crystallization. Further improvements in crystallization are under development.

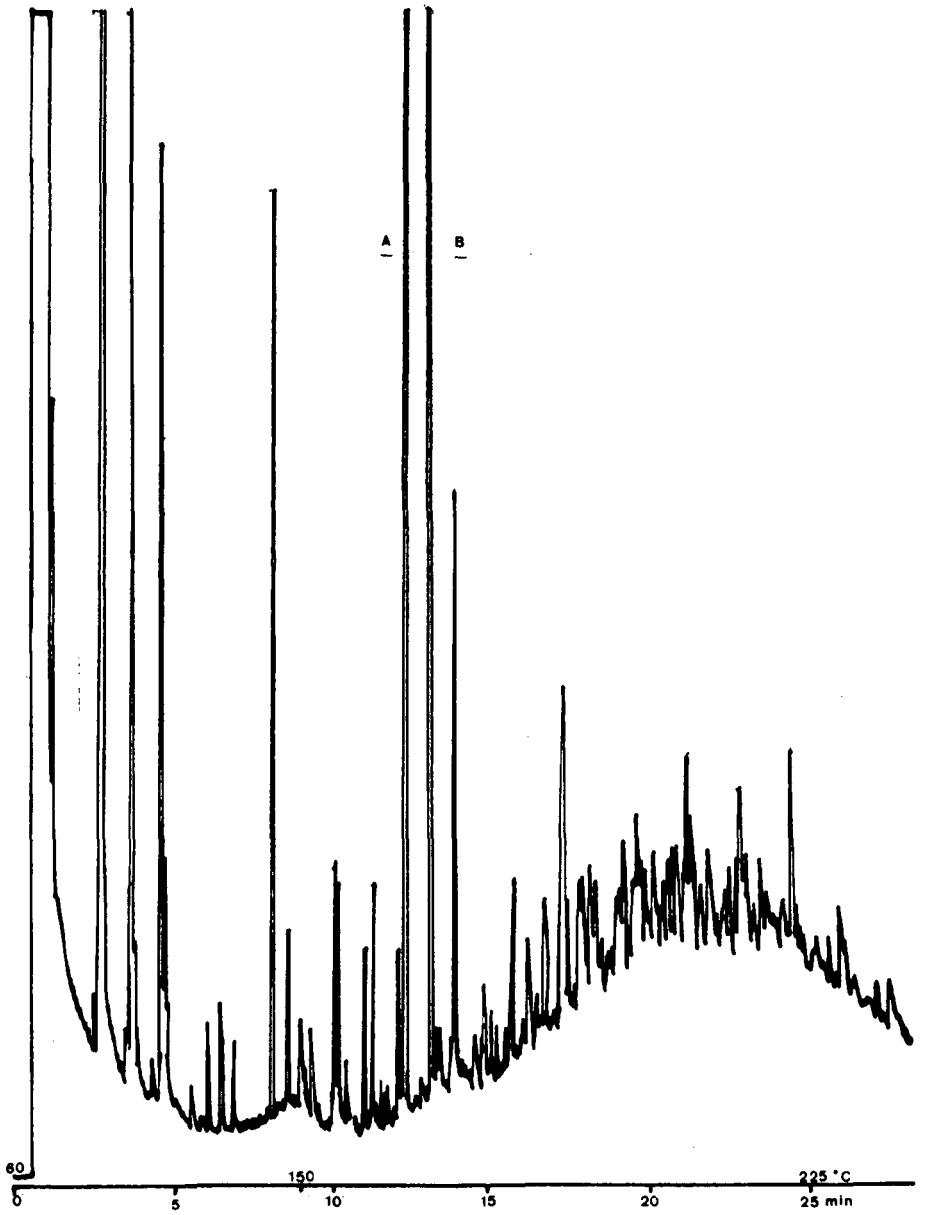

Fig. 3. Capillary GC of the derivatized acids. Peaks: A = gluconic acid; B = galactonic acid.

While galactonic acid is obtained as white crystals, gluconic acid is only concentrated up to a 50% concentrated solution. This solution is comparable to the already commercially available product and it is light yellow, turning to light brown on standing.

In conclusion, the HPLC method with a UV detector set at 214 nm may be used

TABLE I

ELUTION OF GALACTONIC ACID FROM THE ANION-EXCHANGE COLUMN WITH 1 *M* FORMIC ACID

Elution volume (ml)	*Galactonic acid (mg/ml)*	*Formic acid (mg/ml)*
0	0	0
10	0	0
20	0	0
30	0	0
40	0	0
50	5	0
60	26.9	0
70	61.8	1.3
80	60.1	6.7
90	30.5	21.6
100	11.4	32.9
110	4.2	38.3
120	1.3	41.2
130	0.5	45
140	0	45

TABLE II

YIELDS FROM VARIOUS GALACTONIC ACID FERMENTATION

Assay No.	*Yield (%) fermentation*	*Yield (%) purification*	*Total yield after crystallization (%)*
1[a]	90	98	36
2[a]	73	97	32
3[a]	89	99	40
4[b]	57	98	46
5[b]	80	99	69

[a] Hydrochloric acid elution of the galactonic acid produced by fermentation.
[b] Formic acid elution of the galactonic acid produced during fermentation

to monitor the fermentation of the whey hydrolysate, but the simultaneous determination of both gluconic and galactonic acid needs a derivatization of the acidic compounds followed by a gas GC analysis. Highly reproducible yields of both acids were obtained both from the fermentation process and from the purification steps.

REFERENCES

1 J. C. Motte, X. Monseur, M. Termonia, M. Hofman, G. Alaerts,, A. De Meyer, P. Dourte and J. Walravens, *Anal. Chim. Acta,* 163 (1984) 275.
2 M. Decleire, N. Van Huynh and J. C. Motte, *J. Appl. Microbiol. Biotechnol.*, 21 (1985) 103.
3 N. Van Huynh, M. Decleire, A. M. Voets, J. C. Motte and X. Monseur, *Process. Biochem.*, 21 (1986) 31.
4 J. A. Barnett, in R. S. Tipson and D. Horton (Editors), *Adv. Carbohydr. Chem. Biochem.*, 39 (1981) 394.
5 N. Van Huynh and M. Decleire, *Rev. Ferment. Ind. Aliment.*, 37 (1982) 153.
6 R. Schwarzenbach, *J. Chromatogr.*, 251 (1982) 339.
7 S. Hakomori, *J. Biol. Chem.*, 55 (1964) 205.
8 X. Monseur and J. C. Motte, *Anal. Chim. Acta,* 204 (1988) 127.
9 G. Weenk, W. Olijve and W. Harder, *Appl. Microbiol. Biotechnol.,* 20 (1984) 400.

Journal of Chromatography, 507 (1990) 327–332
Elsevier Science Publishers B.V., Amsterdam — Printed in The Netherlands

CHROMSYMP. 1737

Simultaneous determination of ginsenosides and saikosaponins by high-performance liquid chromatography

HIDEKO KANAZAWA, YOSHIKO NAGATA, YOSHIKAZU MATSUSHIMA* and MASASHI TOMODA
Kyoritsu College of Pharmacy, Shibakoen 1-5-30, Minato-ku, Tokyo 105 (Japan)
and
NOBUHARU TAKAI
Institute of Industrial Science, University of Tokyo, Roppongi 7-22-1, Minato-ku, Tokyo 106 (Japan)

SUMMARY

Octadecyl porous glass was used as the packing for reversed-phase high-performance liquid chromatography. A mixture of ginsenosides and saikosaponins (saponins of ginseng and bupleurum root, respectively) were analysed with detection at 203 nm. A well resolved chromatogram of ginsenoside Rb_1, Rc, Rb_2 and Rd and saikosaponin a, b_2 and c was obtained with acetonitrile–water (25.5:74.5) as the mobile phase. The whole separation was achieved in 20 min with a flow-rate of 1.5 ml/min. Calibration graphs for ginsenoside Rb_1, Rc, Rb_2 and Rd and saikosaponin a and c were linear up to 5 μg. Rapid and accurate simultaneous determinations of the saponins are possible by the described method.

INTRODUCTION

Octadecyl porous glass (IPG-ODS) was previously prepared as a packing for reversed-phase high-performance liquid chromatography (HPLC)[1] and rapid and excellent separations and determinations of ginsenosides were achieved with the column[2,3]. Ginsenosides are saponins of ginseng, the roots of *Panax ginseng*, which has log been used in traditional oriental medicine.

In medicine, several crude drugs are generally prescribed in a single formula. Among the important crude drugs often prescribed with ginseng are bupleurum root (the roots of *Bupleurum falcatum*) and glycyrrhiza. Pharmacological studies on these crude drugs have centred on the saponins. Ginsenosides, saikosaponins and glycyrrhizin were isolated from ginseng, bupleurum root and glycyrrhiza, respectively. They are the glycosides of tetracyclic and pentacyclic triterpenes and the sugar moieties contain glucose, fucose, rhamnose, glucuronic acid, arabinose, xylose, etc. Structures are shown in Fig. 1.

As the crude drugs are used in the same pharmaceutical preparations, simultaneous determinations of the saponins are often required. This paper describes

0021-9673/90/$03.50

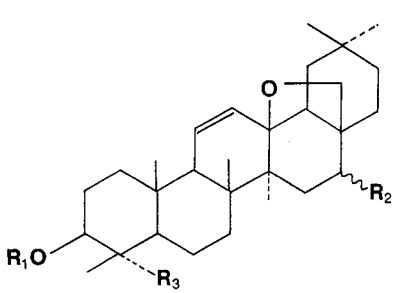

	R_1	R_2	R_3
Saikosaponin a	Fuc^{3}Glc	β-OH	CH_2OH
c	Glc^{4}Rha, Glc^{6}	β-OH	CH_3
d	Fuc^{3}Glc	α-OH	CH_2OH

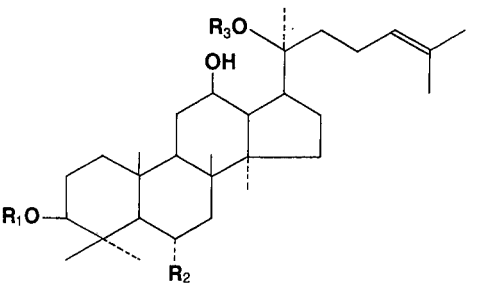

	R_1	R_2	R_3
Ginsenoside Rb_1	Glc^{2}Glc–	H	Glc^{6}Glc–
Rb_2	Glc^{2}Glc–	H	Ara(p)^{6}Glc–
Rc	Glc^{2}Glc–	H	Ara(f)^{6}Glc–
Rd	Glc^{2}Glc–	H	Glc–

Fig. 1. Structures of saikosaponins and ginsenosides.

the simultaneous HPLC determination of the saponins of ginseng and bupleurum root using an IPG-ODS column. The determination of acidic saponins such as glycyrrhizin, ginsenoside Ro and malonyl derivatives of ginsenosides and saikosaponin was also possible by HPLC with an IPG-ODS column, details of which were reported separately[4].

EXPERIMENTAL

The HPLC system consisted of a Tosoh Model CCPM multi-pump, a Rheodyne Model 7125 valve, a Tosoh Model UV-8000 monitor and a Hitachi Model 833A data processor. The system was operated at room temperature.

Octadecylsilyl porous glass (IPG-ODS) was supplied by Ise Chemical Industries (Tokyo, Japan) with a pore size of 550 Å and a particle size distribution of 8–10 μm. IPG-ODS was packed into a stainless-steel column (150 × 4.0 mm I.D.) by the high-pressure slurry technique.

Acetonitrile used as the mobile phase was of HPLC grade (Wako, Tokyo, Japan). Water was deionized and distilled. Other chemicals were of analytical-reagent grade.

Standard samples of ginsenosides were kindly supplied by Prof. J. Shoji of Showa University, Tokyo. The diene-saikosaponins were prepared by treating the parent saponins with 0.1 *M* hydrochloric acid. Standard samples of other saponins, crude drugs and pharmaceutical preparations were obtained from commercial sources.

RESULTS AND DISCUSSION

Chromatograms of a mixture of saikosaponins monitored at 203 and 254 nm are shown in Fig. 2. The C_{13}–C_{28} cyclic ether moieties of saikosaponin a, c and d are labile under acidic conditions and the diene products, saikosaponin b_1, b_2 and h, are derived

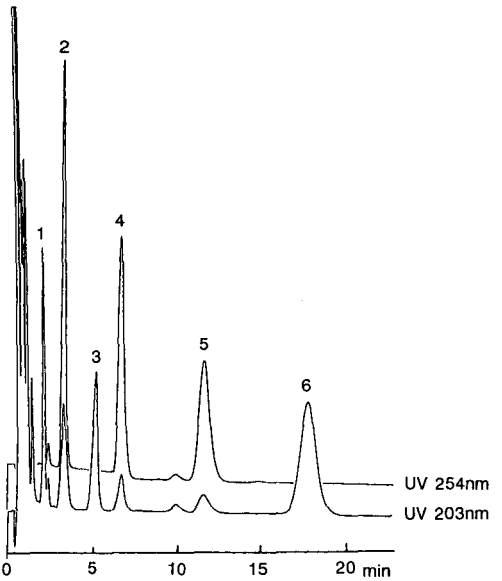

Fig. 2. HPLC of a mixture of saikosaponins. 1 = Saikosaponin c; 2 = saikosaponin h; 3 = saikosaponin a; 4 = saikosaponin b_2; 5 = saikosaponin b_1; 6 = saikosaponin d. Column, IPG-ODS (150 × 4 mm I.D.); eluent, acetonitrile–water (28.0:72.0); flow-rate, 2.0 ml/min; detection, 254 and 203 nm.

from saikosaponin a, d and c, respectively. The diene-saponins have a strong absorption band at *ca.* 250 nm, which is lacking in the parent saponins. Previously reported HPLC methods for the analysis of saikosaponins were based on the absorption at 254 nm after conversion of the ether-saponins into diene-saponins[5,6].

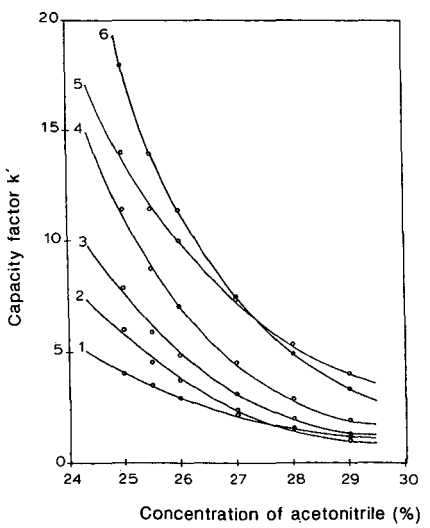

Fig. 3. Effect of acetonitrile concentration in the mobile phase on the capacity factor (k') of saponins. 1 = Saikosaponin c; 2 = ginsenoside Rb_1; 3 = ginsenoside Rc; 4 = ginsenoside Rb_2; 5 = saikosaponin a; 6 = ginsenoside Rd.

Such methods are not suitable for the analysis of samples containing the both types of saponins, such as decocted preparations. The simultaneous determination of saikosaponin a, b, c, d and h was possible by monitoring at 203 nm using the present conditions.

A mixture of ginsenoside Rb_1, Rc, Rb_2 and saikosaponin a and c was chromatographed by monitoring at 203 nm with a flow-rate of 1.5 ml/min with varying concentrations of acetonitrile–water as the mobile phase. The results in Fig. 3 indicate that the six saponins were separated with a mobile phase containing 25% of acetonitrile. A well resolved chromatogram of the six saponins and two diene-saikosaponins was obtained with acetonitrile–water (25.5:74.5) in 20 min, as shown in Fig. 4.

Solutions containing 0–5 μg of the saponin were injected and the corresponding peak areas integrated. The calibration graphs, shown in Fig. 5, were linear and reproducible. Results of the regression analysis and the correlation coefficients (r) were as follows: saikosaponin a, $y = 3.54x - 0.19$ ($r = 0.999$); saikosaponin c, $y = 2.33x - 0.32$ ($r = 0.999$); ginsenoside Rb_1, $y = 3.09x - 0.45$ ($r = 0.999$); ginsenoside Rc, $y = 1.35x - 0.09$ ($r = 0.999$); ginsenoside Rb_2, $y = 0.92x - 0.05$ ($r = 0.999$); and ginsenoside Rd, $y = 1.11x - 0.08$ ($r = 0.999$).

Extracts of bupleurum root and ginseng and of a mixture of the two drugs were analysed using the above procedure. Ginseng was extracted with methanol as described previously[2,3]. Bupleurum root was extracted with weakly alkaline methanol. The extracts were applied to a Sep-Pak C_{18} cartridge, dissolved in the mobile phase and injected into the HPLC system. Separation of the saponin peaks was satisfactory.

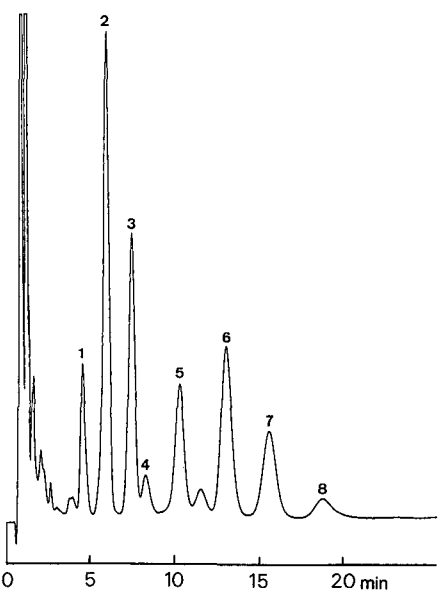

Fig. 4. HPLC of a mixture of saponins. 1 = Saikosaponin c; 2 = ginsenoside Rb_1; 3 = ginsenoside Rc; 4 = saikosaponin h; 5 = ginsenoside Rb_2; 6 = saikosaponin a; 7 = ginsenoside Rd; 8 = saikosaponin b_2. Column, IPG-ODS (150 × 4 mm I.D.); eluent, acetonitrile–water (25.5:74.5); flow-rate, 1.5 ml/min; detection, 203 nm.

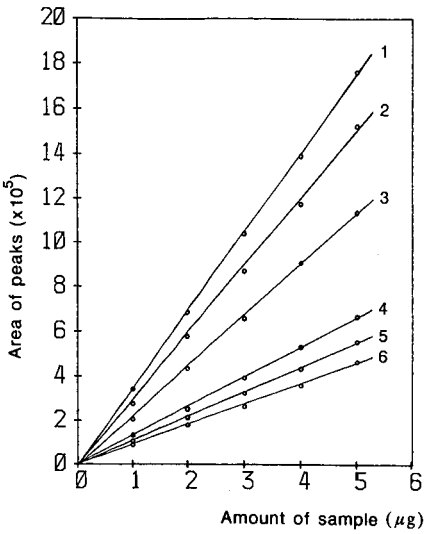

Fig. 5. Calibration graphs for saponins. 1 = Saikosaponin a; 2 = saikosaponin c; 3 = ginsenoside Rb_1; 4 = ginsenoside Rc; 5 = ginsenoside Rb_2; 6 = ginsenoside Rd. Column, IPG-ODS (150 × 4 mm I.D.); eluent, acetonitrile–water (25.5:74.5); flow-rate, 1.5 ml/min; detection, 203 nm.

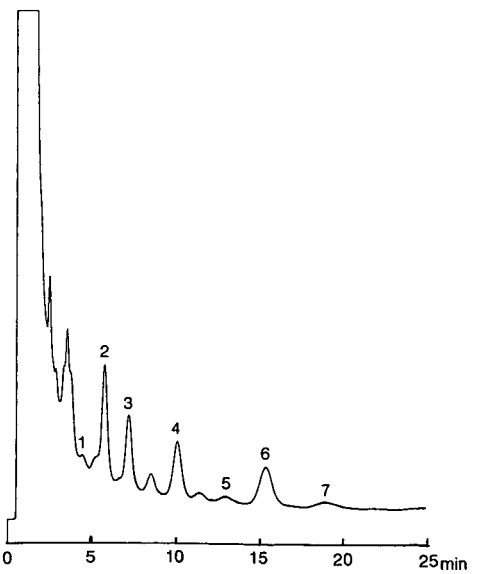

Fig. 6. HPLC of saponins from a commercial product (Shosaiko-to). 1 = Saikosaponin c; 2 = ginsenoside Rb_1; 3 = ginsenoside Rc; 4 = ginsenoside Rb_2; 5 = saikosaponins a; 6 = ginsenoside Rd; 7 = saikosaponin b_2. Column, IPG-ODS (150 × 4 mm I.D.); eluent, acetonitrile–water (25.5:74.5); flow-rate, 1.5 ml/min; detection, 203 nm.

Known amounts of saikosaponins were added to bupleurum root, the crude drug was extracted and saikosaponins in the extracts were determined. The recoveries of the amounts added were in the range 97–101%. The recovery test for ginsenosides has been described previously[2].

A pharmaceutical preparation of commercial origin, Shosaiko-to, was analysed by the above procedure. The analytical sample was prepared in the same way as for the crude drugs. The chromatogram (Fig. 6) indicated the presence of saikosaponin b_2, a diene-saponin. The content of the saponins in the preparation were as follows: ginsenoside Rb_1, 0.11; ginsenoside Rc, 0.13; ginsenoside Rb_2, 0.12; saikosaponin a, 0.03; and ginsenoside Rd, 0.19%. The contents of saikosaponin c and b_2 were too small to be determined exactly.

For the analysis of pharmaceutical preparations containing crude drugs other than ginseng and bupleurum root, the methanol extract was further extracted with butanol. This procedure did not affect the determinations of saikosaponins and ginsenosides. The following crude drugs did not give interfering chromatographic peaks: glycyrrhiza, ginger, atractylodes rhizome, hoelen, jujuba, pinellia tuber, scutellaria root, citrus unshu peel, evodia fruit, coptis rhizome, ophiopogon tuber, non-glutinous rice, cinnamon bark, peony root, Japanese angelica root, cimicifuga rhizome, astragalus root, cnidium rhizome, rehmannia root and magnolia bark.

It is concluded that the simultaneous determination of saikosaponins and ginsenosides is possible by the present method. The determination of the saponins in crude drugs and various pharmaceutical preparations is in progress.

REFERENCES

1 Y. Matsushima, Y. Nagata, K. Takakusagi, M. Niyomura and N. Takai, *J. Chromatogr.*, 332 (1985) 265.
2 H. Kanazawa, Y. Nagata, Y. Matsushima, M. Tomoda and N. Takai, *Chromatographia*, 24 (1987) 517.
3 H. Kanazawa, Y. Nagata, Y. Matsushima, M. Tomoda and N. Takai, *Shoyakugaku Zasshi*, 43 (1989) 121.
4 N. Takai, H. Kanazawa, Y. Matsushima, Y. Nagata and M. Tomoda, *Seisan-Kenkyu*, 41 (1989) 773.
5 H. Kimata, C. Hiyama, S. Yahara, O. Tanaka, O. Ishikawa and M. Aiura, *Chem. Pharm. Bull.*, 27 (1979) 1836.
6 A. Yamaji, Y. Maeda, M. Oishi, Y. Hirotani, H. Kishi, E. Hiraoka and K. Yoneda, *Yakugaku Zasshi*, 104 (1984) 812.

Journal of Chromatography, 507 (1990) 333–337
Elsevier Science Publishers B.V., Amsterdam — Printed in The Netherlands

CHROMSYMP. 1792

Modified high-performance liquid chromatographic determination of diamine oxidase activity in plasma

PIER ANTONIO BIONDI* and FABRIZIO CECILIANI
Istituto di Fisiologia Veterinaria e Biochimica, Via Celoria 10, 20133 Milan (Italy)
CINZIA GANDINI
Istituto di Clinica Chirurgica Veterinaria, Via Celoria 10, 20133 Milan (Italy)
and
CLAUDIO LUCARELLI
Istituto Superiore di Sanità, Viale Regina Elena 299, 00146 Rome (Italy)

SUMMARY

A previous high-performance liquid chromatographic determination of diamine oxidase activity suitable for tissue homogenates was modified in order to adapt it to plasma samples. Simple additional steps were introduced after the enzyme reaction and before the chromatographic separation, both according to the previous method. In this way the sensitivity and the reproducibility of the overall procedure was suitable for routine plasma diamine oxidase estimations.

INTRODUCTION

Diamine oxidase [diamine:oxygen oxidoreductase (deaminating), E.C.1.4.3.6] (DAO), catalyses the oxidation of diamines, such as putrescine and cadaverine, to the corresponding aminoaldehydes, which are in equilibrium with Δ^1-pyrroline and Δ^1-piperideine, respectively. DAO is present in high concentration in the intestinal mucosa of man and other mammalian species[1]. The determination of DAO in this tissue has been considered to be a marker of its integrity in different pathological conditions[2–4]. Further, the determination of DAO activity in plasma has been used to monitor by non-invasive means the severity of injury of the intestinal mucosa in rat[5,6] and man[7].

In order to set up a high-performance liquid chromatographic (HPLC) procedure as an alternative to radiochemical measurements[8], we followed the classical method of Holmstedt *et al.*[9]. The aminoaldehyde obtained from enzymatic oxidation of cadaverine was allowed to react with *o*-aminobenzaldehyde (OAB) to give the 2,3-tetramethylene-1,2-dihydroquinazolinium ion ($4Q^+$); pyrroline was used as an internal standard, giving 2,3-trimethylene-1,2-dihydroquinazolinium ion ($3Q^+$)[10]. Recently, we modified the original method in order to speed it up and make it suitable for routine DAO assays in dog tissue homogenates[11]. $4Q^+$ was analysed directly on

0021-9673/90/$03.50

a reversed-phase column without any other post-enzymatic reaction. When we attempted to apply the modified procedure to plasma sample, some problems arose with regard to terminating the enzyme incubation and sensitivity.

This paper describes the modifications introduced to adapt the procedure to the evaluation of DAO activity in plasma. The modified method was applied to dog plasma.

EXPERIMENTAL

Materials

Dog plasma samples were obtained in heparinized tubes by routine venous puncture from normal healty adult animals and stored frozen until analysis. Other enzyme preparations, reagents and standard solutions were as described previously[11].

Apparatus and chromatographic conditions

The UV spectrophotometer, HPLC system and operating conditions were as described previously[11].

Methods

To 0.5 ml of plasma sample, 0.5 ml of 0.1 *M* phosphate buffer (pH 7.0), 100 μl of saturated aqueous OAB solution and 50 μl of 1 m*M* Δ^1-pyrroline solution were added. After a 10-min preincubation at 37°C, the enzyme reaction was started by the addition of 50 μl of 0.1 *M* cadaverine, buffered at pH 7.0. After 20 min, the incubation was stopped by diluting the mixture with 1 ml of acetonitrile. The suspension was centrifuged, the precipitate was discarded and the supernatant was tranferred into a screw-capped vial; acetonitrile was then evaporated at 37°C under a stream of nitrogen. To the resulting aqueous solution, 1 ml of 0.1 *M* glycine buffer (pH 12) was added; 4 ml diethyl ether were then added and the mixture was shaken well. The organic phase was separated, filtered through anhydrous sodium sulphate and evaporated to dryness under a stream of nitrogen. The residue was finally dissolved in 50 μl of the HPLC eluent and injected.

Quantitative analysis

Different amounts (1–100 nmol) of Δ^1-piperideine in 1 ml of 0.1 *M* phoshate buffer (pH 7.0) were obtained by oxidation of cadaverine with DAO from pea seedlings. These samples were treated according to the procedure described above. The height ratios between the $4Q^+$ and $3Q^+$ peak were calculated in the final chromatograms and plotted against Δ^1-piperideine amounts to prepare a calibration graph. The DAO activity in mU/ml in a plasma sample was obtained from the corresponding amount of $4Q^+$ formed by enzymatic oxidation of cadaverine; 1 mU is defined as the amount of enzyme that catalyses the oxidation of 1 nmol of cadaverine per minute under the described conditions.

The recovery of $4Q^+$ from post-enzymatic steps was studied by comparing the $4Q^+$ HPLC response before and after addition of glycine buffer, extraction, drying and redissolution in the same original volume.

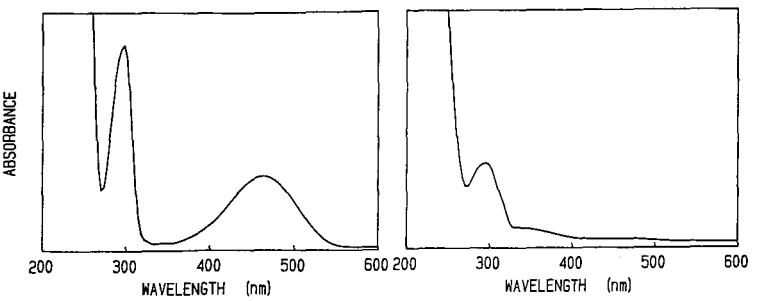

Fig. 1. UV spectra of HPLC eluent mixture of $4Q^+$ (right) and 4QOH (left), obtained from $4Q^+$ purified by HPLC before and after addition of 0.1 *M* glycine buffer (pH 12), respectively.

RESULTS

Fig. 1. shows the UV spectra of $4Q^+$ and its derivative obtained after the pH increase, 2,3-tetramethylene-1,2,3,4-tetrahydro-4-hydroxyquinoline (4QOH). By monitoring the change in the UV spectrum, the progress of the conversion of $4Q^+$ to 4QOH was followed; the absorption at 465 nm disappeared when pH 11 was reached. A similar behaviour was shown by $3Q^+$, obtained from Δ^1-pyrroline used as an internal standard. When the 4QOH solution was again acidified, the original spectrum was obtained, demonstrating the reversibility of hydroxide addition to $4Q^+$. Different amounts of Δ^1-piperideine in the presence of the same amount (50 nmol) of Δ^1-pyrroline were treated according to the described post-enzymatic steps and a linear relationship between $4Q^+/3Q^+$ peak-height ratio (R_h) and piperideine amount was found:

$$R_h = 0.0265 \text{ (nmol } \Delta^1\text{-piperideine)} + 0.0176 \ (r = 0.998)$$

Using the described procedure, $4Q^+$ could be detected in amounts as low as 0.5 nmol, corresponding to 0.025 mU of DAO activity; $4Q^+$ (50 nmol), after conversion to 4QOH, extraction with diethyl ether and evaporation, was recovered with yields of 65 $\pm$ 3.1% ($n = 5$).

The reproducibility of the method was determined by repeated analyses of the same plasma sample. The mean DAO content was 1.35 $\pm$ 0.10 mU/ml ($n = 5$). In ten samples from different normal healthy adult dogs the DAO activity was found to be between 0.18 and 1.41 mU/ml with a mean of 0.62 mU/ml.

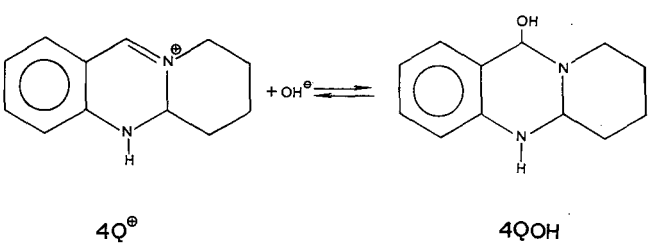

Fig. 2. Equilibrium reaction between $4Q^+$ and 4QOH.

DISCUSSION

With regard to DAO assay, plasma samples appeared to differ from intestinal mucosa homogenates, mainly in two respects, lower DAO activity and higher protein content. When we attempted to adapt our modified HPLC procedure, suitable for tissue homogenates, to plasma, we encountered two difficulties, low sensitivity and poor reproducibility.

In the previous procedure, the incubation mixture was injected directly onto the HPLC column after the inactivation of DAO by heat treatment. When a low content of DAO was present in the sample, the final chromatographic profile did not allow the determination of small amounts of $4Q^+$. However, with plasma specimens the heat treatment always gave rise to a final mixture appearing as a gel because of its high protein content, and the final withdrawal of the supernatant solution was very difficult. The usual method of increasing the sensitivity of a HPLC method is to extract the compound to be analysed into a volatile solvent, evaporate it to dryness and dissolve the residue in a small volume of eluent. As the condensation product of piperideine and OAB is an ionic compound at pH 7, it was not possible to apply this method directly to the final incubation mixture. Nevertheless, a pH increase is known to convert $4Q^+$ to 4QOH according to the equilibrium shown in Fig. 2. By exploiting this reaction, we modified the procedure with simple additional steps: addition of alkaline buffer to pH between 11 and 12 and extraction of QOH with diethyl ether. After evaporation of the organic phase, a final concentrated solution of the analyte is obtained and a higher sensitivity is achieved. It is remarkable that, when 4QOH is dissolved in an acidic eluent solution, $4Q^+$ is again formed. Hence the subsequent HPLC analysis can be performed according to the previous chromatographic procedure[11].

The operating conditions for the conversion of $4Q^+$ to 4QOH were checked. Satisfactory recovery of $4Q^+$ after its hydroxylation and extraction was achieved only when the pH was carefully adjusted to between 11.0 and 12.0 with glycine buffer and extraction was performed immediately. When pH 12 was exceeded or extraction was delayed, only low yields of $4Q^+$ were obtained, demonstrating the instability of this compound in alkaline medium. Despite the poor recovery of $4Q^+$ after conversion to 4QOH, the reduction of the final volume to be analysed and the good reproducibility made the overall procedure convenient for achieving a suitable sensitivity.

For terminating the enzyme incubation, addition of acetonitrile was chosen instead of heat treatment. In this way, precipitated proteins were discarded after centrifugation and a clear aqueous acetonitrile mixture was obtained. However, as in the presence of acetonitrile the reaction between aminoaldehydes and OAB does not occur to a significant extent, the organic solvent was evaporated. It is noteworthy that at neutral pH the rate of formation of $4Q^+$ is clearly higher than that at acidic or slightly alkaline pH. Hence, at the end of the evaporation step, carried out at pH 7.0 and 37°C, the condensation between aminoaldehydes and OAB reached completeness and, at the same time, the sample volume was decreased, making the subsequent extraction step more efficient.

In conclusion, the DAO content of plasma can be determined by direct HPLC of $4Q^+$, provided that additional steps are introduced in the previously described procedure. The sensitivity and reproducibility of this modified method are suitable for routine plasma DAO determinations in both biochemical and clinical experiments.

ACKNOWLEDGEMENT

This work was supported by a grant from Regione Lombardia (project No. 1422).

REFERENCES

1 T. Bieganski, J. Kusche, W. Lorenz, R. Hesterberg, C. D. Stahlknecht and K. D. Feussner, *Biochim. Biophys. Acta,* 756 (1983) 196.
2 J. Kusche, J. A. Izbicki, R. Mennigen, A. Curt and J. V. Parkin, *Cancer Detect. Prevent.*, 9 (1986) 17.
3 R. Mennnigen, M. Gunther, N. Bonninghoff, C. D. Stahknecht, I. Kubitza and J. Kusche, *Agents Actions*, 18 (1986) 38.
4 R. Mennigen, J. Kusche, B. Krakamp, A. Elbers, B. Amoei M. Kessebohm and H. Sommer, *Agents Actions*, 23 (1988) 351.
5 G. D. Luk, T. M. Bayless and S. B. Baylin, *J. Clin. Invest.*, 66 (1980) 66.
6 G. D. Luk, T. M. Bayless and S. B. Baylin, *J. Clin. Invest.*, 71 (1983) 1308.
7 P. Forget, Z. Saye, J. L. Van Cutsem and G. Dandrifosse, *Pedriatr. Res.*, 19 (1985) 26.
8 T. Okuyama and Y. Kobayashi, *Arch. Biochem. Biophys.*, 95 (1961) 242.
9 B. Holmstedt, L. Larsson and R. Tham, *Biochim. Biophys. Acta*, 48 (1961) 182.
10 P. A. Biondi, T. Simonic, C. Secchi, S. Ronchi and A. Manzocchi, *J. Chromatogr.*, 309 (1984) 151.
11 P. A. Biondi, C. Secchi, A. Negri, G. Tedeschi and S. Ronchi, *J. Chromatogr.*, 491 (1989) 209.

Journal of Chromatography, 507 (1990) 339–349
Elsevier Science Publishers B.V., Amsterdam — Printed in The Netherlands

CHROMSYMP. 1699

Separation and determination of molecular species of phosphatidylcholine in biological samples by high-performance liquid chromatography

A. CANTAFORA*, M. CARDELLI and R. MASELLA
Laboratory of Metabolism and Pathological Biochemistry, Istituto Superiore di Sanità, Viale Regina Elena 299, 00161 Rome (Italy)

SUMMARY

A method for determining the molecular species composition of phosphatidylcholine in biological samples by reversed-phase high-performance liquid chromatography with dual-wavelength ultraviolet detection is described. The optimum compromise between analysis time and chromatographic resolution under isocratic and isothermal conditions (0.8 ml/min and 32°C, respectively) was obtained with the mobile phase methanol–ethanol (6:4, v/v) containing 20 m*M* choline chloride–water–acetonitrile (90:7:3, v/v/v). The problems of quantification at 205 nm, due to large differences in the detector response with the degree of unsaturation, were resolved by using the appropriate calibration factors chosen with the ratio of absorbances at 205 and 215 nm. The proposed procedure gave results in good agreement with fatty acid composition in samples of rat bile, liver, liver mitochondria and microsomes determined by gas–liquid chromatography.

INTRODUCTION

The determination of phosphatidylcholine (PC) molecular species is important in lipid micellar biochemistry and in studies of membrane function. However, both the fractionation and quantification of PC still present problems if complex mixtures of molecular species, such as those found in biological samples, must be analysed.

The separation of PC molecular species is typically achieved by reversed-phase high-performance liquid chromatography (RP-HPLC) of either unmodified PC molecules[1–6] or enzymatic hydrolysis products of PC (*e.g.*, phosphatidic acid[7,8], or diacylglycerol[9–12]). In the last instance the hydrolysis product of PC can be derivatized with a strong UV chromophore, which offers some advantages in terms of resolution and quantification. On the other hand, this approach requires some additional steps in the analytical procedure and may be unsuitable for applications in which PC must be recovered from column eluates or in which PC isotopically labelled in the choline must be analysed[13].

The chromatography of intact PC molecules does not have these limitations but

0021-9673/90/$03.50

UV detection in the 200-nm range creates problems for quantification. At that wavelength, the detector response is a function of the number of double bonds and is not the same for the various PC molecular species[3], which causes serious problems for the analysis of biological samples in which each chromatographic peak may contain different molecular species of PC. In a previous paper[5], we reported a method for biliary PC which used calibration factors for each peak to alleviate this problem. These were determined with a standard bile PC and were based on an exact knowledge of the elution profile of the molecular species in this particular type of sample.

In this paper, we report changes to the mobile-phase composition that give results comparable to our previous findings without the need for high column temperatures or a flow programme.

EXPERIMENTAL

Palmitoyloleoyl-, palmitoyllinoleoyl- and palmitoylarachidonoyl-PC were purchased from Sigma (St. Louis, MO, U.S.A.). Oleoyllinoleoyl-, dilinoleoyl- and linoleoyllinolenyl-PC were isolated by preparative HPLC from purified soy lecithin, as previously described[5]. Analogously, palmitoyldocosahexanoyl-, palmitoyldocosapentanoyl-, stearoylarachidonoyl-, stearoyllinoleoyl- and stearoyloleoyl-PC were isolated from purified egg lecithin.

Lipid extracts from samples of whole liver, liver microsomes, liver mitochondria and the bile of male Wistar rats on a standard laboratory diet were prepared with chloroform–methanol (2:1, v/v), according to Folch *et al.*[14]. PC was isolated from lipid extracts by thin-layer chromatography (TLC) with the solvent system chloroform –methanol–acetic acid–water (65:25:15:4, v/v). The TLC scrapings were dissolved in a small volume of mobile phase. Silica gel particles were subsequently removed by centrifugation and an aliquot of 20–50 μl of the sample was injected into the column.

The HPLC apparatus, manufactured by Gilson Medical Electronics (Middleton, WI, U.S.A.), was equipped with a dual-wavelength detector (settings 205 and 215 nm, 0.1 a.u.f.s.) and a dual-channel integrator. The column used in all the experiments was 5-μm Spherisorb ODS-2, 25 cm x 4.6 mm I.D. (Phase Separations, Queensferry, Clwyd, U.K.) which was kept at 32 ± 0.1°C with a Clar-055 electronic thermostat (Violet, Rome, Italy). The mobile phases were prepared by mixing the ion-pair solution [IPS; methanol–ethanol (6:4, v/v) containing 20 m*M* choline chloride] with acetonitrile and water in various proportions. The best analytical result was obtained with IPS–water–acetonitrile (90:7:3, v/v/v) at a flow-rate of 0.8 ml/min.

The total fatty acid (FA) distribution in biological samples and FA quantification in the isolated molecular species were obtained by gas–liquid chromatography (GLC) as described previously[15].

RESULTS AND DISCUSSION

In a previous paper[5], we described the separation of the major molecular species of biliary PC with a mobile phase containing choline chloride, as described by Patton *et al.*[3]. We obtained a three-fold reduction in the time required for the chromatographic separation by using a particular type of column under unusual condi-

tions of high temperature and programmed flow-rate. In this study, we attempted to obtain similar results by using a common reversed-phase column under normal analytical conditions.

We reduced the analysis time by increasing the strength of the eluent, using a methanol–ethanol mixture instead of pure methanol as the mobile phase. Fig. 1 shows the effect of this replacement in our previous[5] mobile phase [methanol containing 20 m*M* choline chloride–water–acetonitrile (90:8:3, v/v/v)] on the retention times of palmitoyllinoleoyl- and palmitoylarachidonoyl-PC molecular species. The results indicate that retention times of 16–17 min can be obtained with a methanol to ethanol ratio of 1.5. Consequently, an analysis time of *ca.* 30 min can be obtained with biological samples, because the above-mentioned species are eluted in the middle of the major PC natural species.

This modification required some further adjustments in the proportions of acetonitrile and water in order to maintaining both the transparency of the mobile phase and the resolution of some critical pairs. This last aspect was studied using a mixture of five molecular species of PC which form a cluster of peaks in the chromatograms of biological samples. This mixture was chromatographed with different water contents in the mobile phase. Fig. 2 shows the significant effect of the water content on the resolution of palmitoyllinoleoyl- and oleoyllinoleoyl-PC and on the length of the analysis time for three of these conditions. The results of these experiments, summarized in Table I, demonstrate that the loss of resolution between palmitoyllinoleoyl-

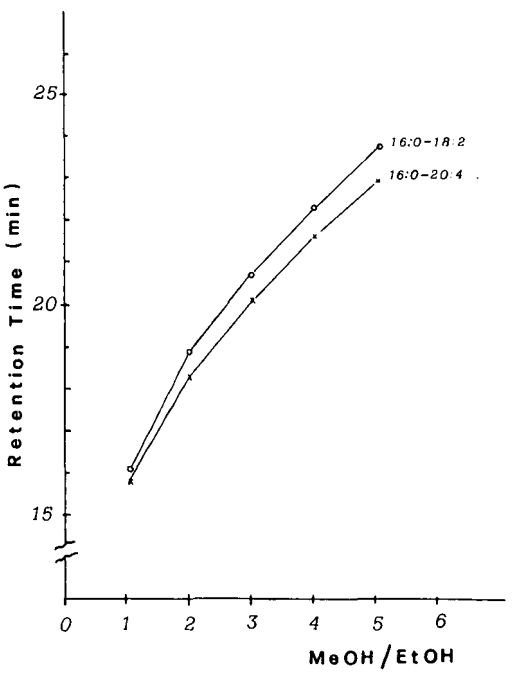

Fig. 1. Changes in retention times of palmitoyllinoleoyl-PC (16:0–18:2) and palmitoylarachidonoyl-PC (16:0–20:4) with increase in methanol to ethanol ratio in the mobile phase. Mobile phases: methanol (MeOH)–ethanol (EtOH) mixtures containing 20 *M* choline chloride–water–acetonitrile (90:8:3, v/v/v).

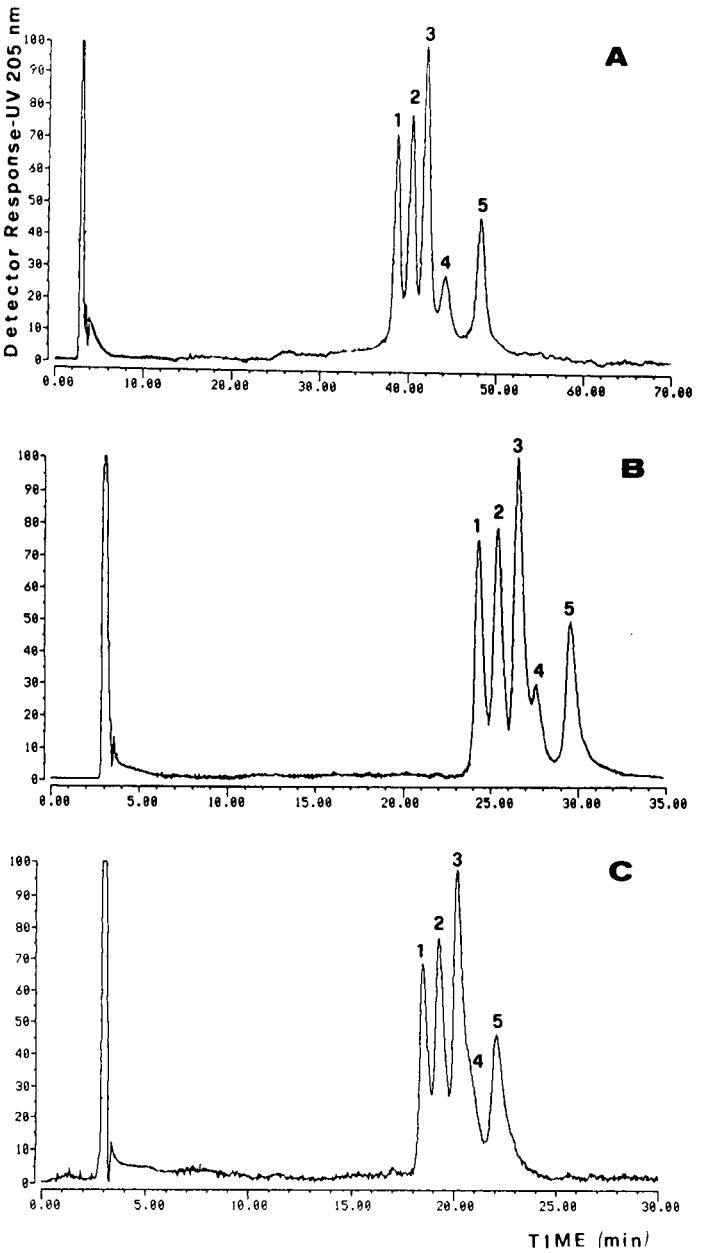

Fig. 2. Chromatography of five molecular species of PC that form a cluster of peaks in biological samples with different water contents in the mobile phase. Mobile phases: methanol–ethanol (6:4, v/v) containing 20 m*M* choline chloride–water–acetonitrile (90:*X*:3, v/v/v); *X* = (A) 9, (B) 7 and (C) 5.6. Peaks (1) 16:0–22:6; (2) 16:0–20:4; (3) 16:0–18:2; (4) 18:1–18:2; (5) 16:0–22:5.

TABLE I

EFFECT OF WATER CONTENT IN THE MOBILE PHASE ON THE NUMBER OF THEORETICAL PLATES *(N)*, CAPACITY FACTOR *(k')* AND MOBILITY OF FIVE MOLECULAR SPECIES OF PC.

Peak numbers and mobile phase compositions (A, B and C) correspond to those in Fig. 2.

Peak No.	*Molecular species*	*Mobile phase A*			*Mobile phase B*			*Mobile phase C*		
		N	*k'*	*RRT*[a]	*N*	*k'*	*RRT*[a]	*N*	*k'*	*RRT*[a]
1	16:0–22:6	3270	15.71	1.00	4500	8.10	1.00	5200	6.02	1.00
2	16:0–20:4	3230	16.48	1.05	4200	8.50	1.04	5150	6.28	1.04
3	16:0–18:2	2500	16.88	1.07	4100	8.93	1.09	5100	6.65	1.10
4	18:1–18:2	2200	18.23	1.15	4000	9.31	1.13	4800	6.90	1.12
5	16:0–22:5	1900	19.94	1.25	3980	10.04	1.21	4500	7.37	1.19

[a] RRT (relative retention time) was calculated by dividing the retention time of each molecular species by the retention time of the 16:0–22:6 species (39.2, 24.4 and 18.8 min with mobile phase A, B and C, respectively).

and oleoyllinoleoyl-PC, observed with a low water content, is attributable to a decrease in selectivity, but not in column efficiency. Consequently, a mobile phase that gave a good compromise between resolution and analysis time was used throughout the study.

TABLE II

VALUES OF ABSORBANCE RATIO (AR) 205/215 nm, RELATIVE CALIBRATION FACTOR (RCF) AND RELATIVE RETENTION TIME (RRT) OBTAINED WITH PHOSPHATIDYLCHOLINE STANDARDS.

Means and standard deviations (S.D.) obtained from five replicate analyses of each molecular species.

Peak No.	*Molecular species*	*Double bonds*	*AR 205/215 nm (mean ± S.D.)*	*RCF*[a] *(mean ± S.D.)*	*RRT*[b] *(mean ± S.D.)*
1	18:2–18:3	5	3.59 ± 0.032	0.09 ± 0.005	0.761 ± 0.001
2	18:2–18:2	4	4.57 ± 0.039	0.13 ± 0.005	0.933 ± 0.002
3	16:0–22:6	6	1.55 ± 0.028	0.07 ± 0.004	1.000
4	16:0–20:4	4	3.48 ± 0.042	0.12 ± 0.007	1.043 ± 0.008
5	16:0–18:2	2	5.70 ± 0.029	0.27 ± 0.002	1.089 ± 0.001
6	18:1–18:2	3	5.19 ± 0.039	0.15 ± 0.004	1.180 ± 0.007
7	16:0–22:5	5	2.32 ± 0.015	0.08 ± 0.004	1.230 ± 0.008
8	16:0–18:1	1	6.22 ± 0.051	1.00	1.328 ± 0.005
9	18:0–20:4	4	3.46 ± 0.034	0.11 ± 0.006	1.478 ± 0.013
10	18:0–18:2	2	5.72 ± 0.028	0.30 ± 0.005	1.554 ± 0.011
11	18:0–18:1	1	6.32 ± 0.039	1.04 ± 0.007	1.811 ± 0.012

[a] RCF was calculated by dividing the calibration factor of each species by the calibration factor of 16:0–18:1-PC.

[b] RRT was calculated by dividing the retention time of each species by the retention time of 16:0–22:6-PC.

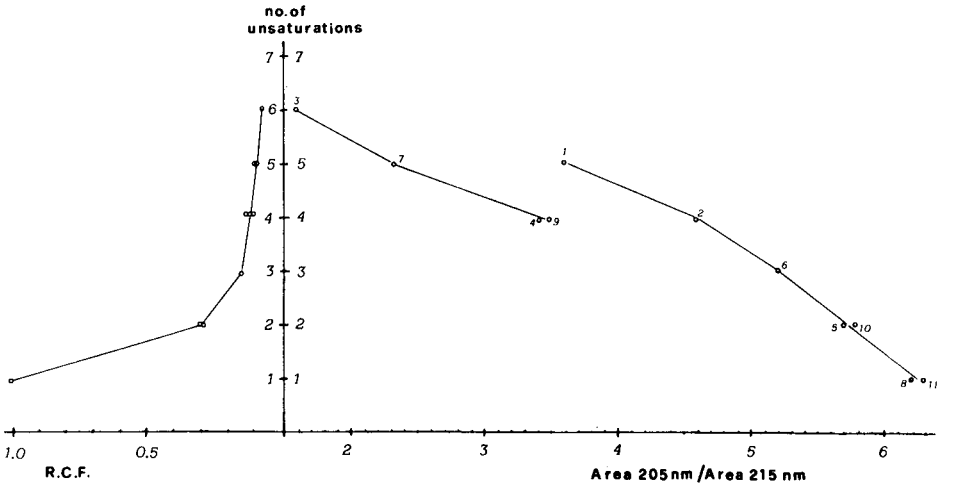

Fig. 3. Values of absorbance ratio (AR), peak-area ratio 205/215 nm and relative calibration factor (RCF) as a function of the degree of unsaturation of PC molecular species. These values were obtained with eleven pure molecular species of PC (see Table I).

TABLE III

MEAN VALUES OF ABSORBANCE RATIO (AR) 205/215 nm, OBTAINED FOR THE 21 PEAKS INTEGRATED IN SAMPLES OF PHOSPHATIDYLCHOLINE FROM RAT BILE, LIVER, LIVER MITOCHONDRIA AND LIVER MICROSOMES.

These values were used to calculate the relative calibration factors (RCF) and the degree of unsaturation by the curve shown in Fig. 3.

Peak No.	*Molecular species*	*AR 205/215 nm (mean ± S.D.)*	*RCF (mean ± S.D.)*	*No. of unsaturations*	
				Theoretical	Found
1	14:0–22:6	1.87 ± 0.87	0.058 ± 0.005	6	5.6
2	18:2–18:3	1.80 ± 0.20	0.058 ± 0.002	5	5.7
3	16:1–18:2	2.03 ± 0.30,	0.063 ± 0.006	3	5.4
4	14:0–16:1	3.55 ± 0.69	0.089 ± 0.013	1	3.8
5	16:0–20:5	1.86 ± 0.35	0.058 ± 0.008	5	5.6
6	18:2–18:2	2.98 ± 0.37	0.078 ± 0.003	4	4.3
7	16:1–18:1 16:0–22:6	2.28 ± 0.21	0.065 ± 0.006	–	5.2
8	16:0–20:4	2.78 ± 0.14	0.073 ± 0.006	4	4.6
9	16:0–18:2	4.77 ± 0.39	0.134 ± 0.023	2	3.6
10	18:1–18:2	3.74 ± 0.47	0.091 ± 0.009	3	4.7
11	16:0–22:5	2.32 ± 0.42	0.068 ± 0.010	5	5.0
12	16:0–20:3	2.80 ± 0.61	0.073 ± 0.009	3	4.4
13	16:0–18:1	4.20 ± 0.57	0.098 ± 0.028	1	4.3
14	18:1–18:1	4.41 ± 0.72	0.098 ± 0.024	2	4.0
15	18:0–22:6	1.90 ± 0.13	0.059 ± 0.002	6	5.6
16	18:0–20:4	2.54 ± 0.20	0.073 ± 0.006	4	4.7
17	18:0–18:2	4.94 ± 0.40	0.165 ± 0.084	2	3.3
18	18:0–22:5	1.68 ± 0.12	0.055 ± 0.000	5	5.8
19	18:0–20:3	2.32 ± 0.16	0.068 ± 0.004	3	5.0
20	18:0–18:1	4.65 ± 0.50	0.100 ± 0.052	1	3.7
21	18:0–22:4	1.86 ± 0.13	0.058 ± 0.002	4	5.6

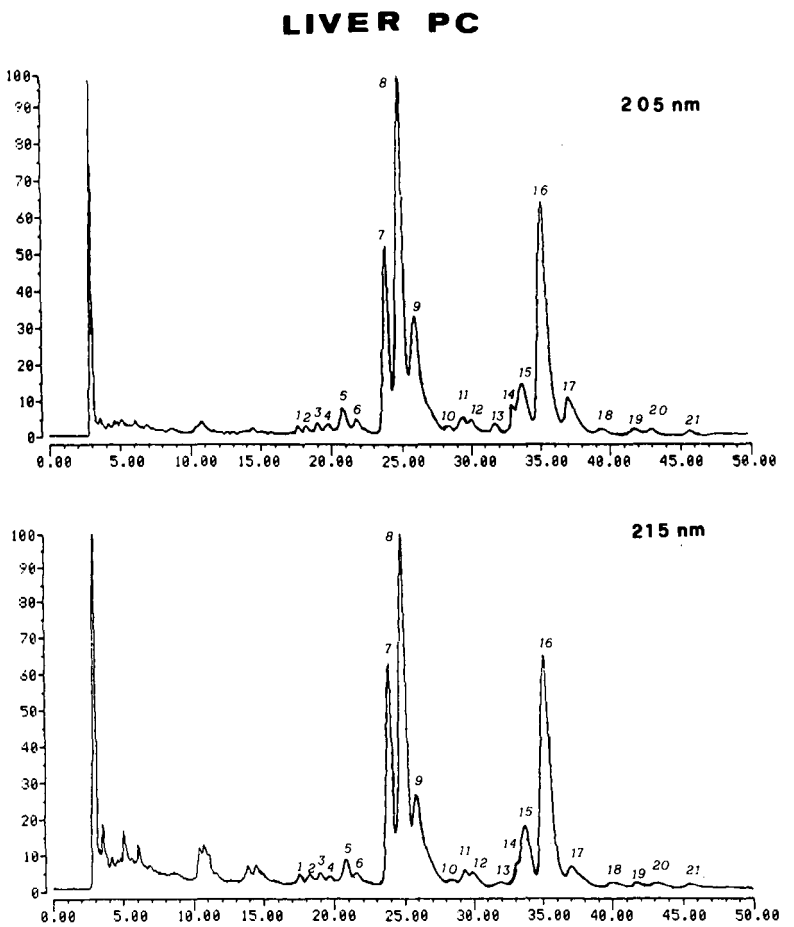

Fig. 4. Chromatograms of liver PC with UV detection at 205 and 215 nm. Peaks as in Table II. For HPLC conditions, see Experimental.

One of the major difficulties in analysing biological samples for intact molecular species of PC is that species with different degrees of unsaturation and, hence, with large difference in absorbance at the analytical wavelength (205 nm) may be not resolved[2]. This led us to investigate whether the absorbance ratio (AR) between the analytical wavelenght and another wavelength could be used for evaluating the average degree of unsaturation of the molecular species eluted in each band. This was made taking into account that UV absorption results primarily from the double bonds in the fatty acid moiety of PC[16] and that species with different degrees of unsaturation have distinct UV spectra[17]. The study was carried out with standard mixtures of eleven molecular species, by evaluating the ARs 205/210, 205/215 and 205/220 nm. The AR 205/215 nm represented a reasonable compromise between unsaturation-discriminating power and sensitivity and was adopted in the subsequent study. The AR 205/220 nm provided more variations with the degree of unsaturation.

However, at 220 nm the less unsaturated species were not integrated because of their lower absorptivity.

These standard mixtures were also used for determining the calibration factors (CF) used for correcting the peak areas at the analytical wavelength on the basis of the average degree of unsaturation of each peak. The CFs were calculated by dividing the molar amount of each molecular species by the area of the relative chromatographic peak.

Table II shows the AR values at 205/215 nm and the CF, expressed as the CF relative (RCF) to palmitoyloleoyl-PC, obtained with standard PC species. These values are plotted in Fig. 3 as a function of the degree of unsaturation of the eleven pure molecular species used for detector calibration. The section of the graph that relates the degree of unsaturation to AR 205/215 nm, a relationship that is fundamental for calculating the RCF, is neither linear nor continuous. In fact, the species containing

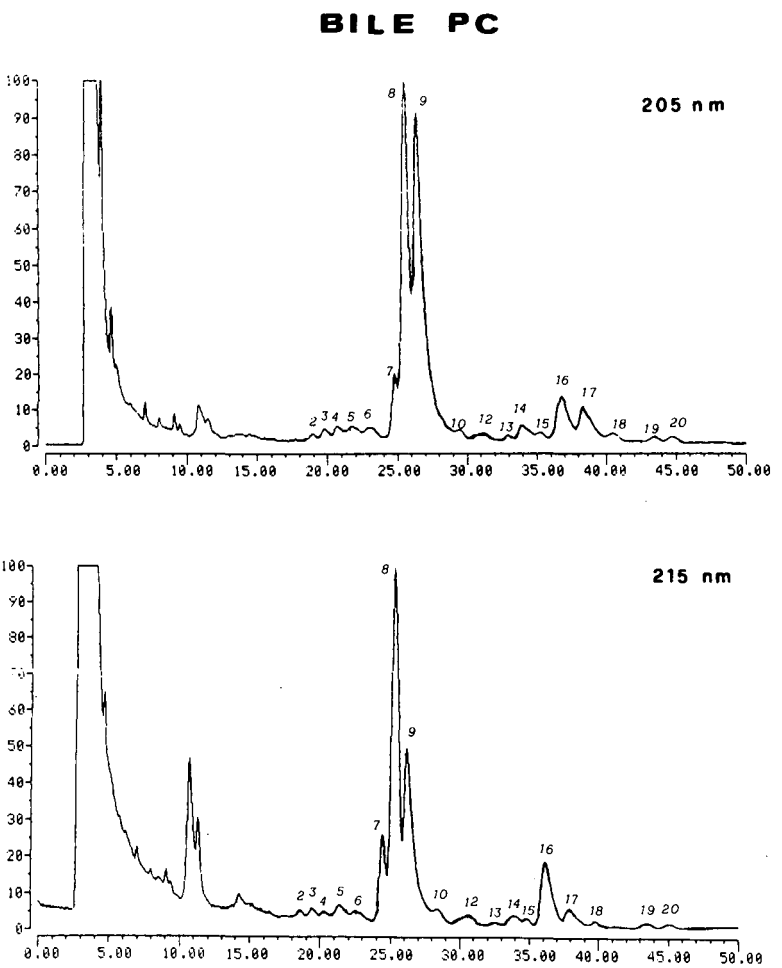

Fig. 5. Chromatograms of bile PC with UV detection at 205 and 215 nm. Peaks as in Table II. For HPLC conditions, see Experimental.

the more polyunsaturated fatty acids appear to lie on a curve separate from that for the species containing fatty acids with less than four double bonds. However, this does not create practical problems, because in biological samples there is an unequivocal correlation between AR and the degree of unsaturation and, hence, between AR and RCF.

The chromatographic pattern of the biological samples analysed in this study had a maximum of 21 peaks, which were identified both by their mobility and the GLC analysis of the species eluted with each peak. Figs. 4 and 5 show the chromatograms of liver and bile PC, obtained at 205 and 215 nm.

Table III reports the mean values of AR, RCF and degree of unsaturation found for the four different types of samples examined. It should be noted that the degree of unsaturation observed is generally higher than the theoretical value expected for the main molecular species in the band. This fact, which is particularly evident with monounsaturated species, indicates that minor polyunsaturated species contaminate other bands. In a case where it is known that a band is composed of two molecular species, *e.g.*, peak 7, it is possible to calculate the distribution of these species from the average degree of unsaturation.

TABLE IV

DISTRIBUTION OF MOLECULAR SPECIES OF PHOSPHATIDYLCHOLINE IN SAMPLES OF RAT LIVER, LIVER MICROSOMES, LIVER MITOCHONDRIA AND BILE OBTAINED WITH THE PROPOSED HPLC METHOD.

The values reported represent the means of three replicate analyses of each sample.

Peak No.	*Molecular species*	*Whole liver (%)*	*Liver microsomes (%)*	*Liver mitrochondria (%)*	*Bile (%)*
1	14:0–22:6	0.15	1.05	0.10	—
2	18:2–18:3	0.31	1.72	0.30	0.14
3	16:1–18:2	0.51	0.73	0.39	0.26
4	14:0–16:1	0.50	0.29	0.44	0.48
5	16:0–20:5	1.13	1.26	1.28	0.16
6	18:2–18:2	0.91	2.11	0.34	0.45
7	16:1–18:1	4.25	5.12	7.36	0.59
	16:0–22:6	3.89	3.72	5.98	1.55
8	16:0–20:4	19.61	21.06	24.42	16.59
9	16:0–18:2	25.40	23.13	21.79	57.73
10	18:1–18:2	0.61	0.86	0.36	0.63
11	16:0–22:5	1.91	1.65	1.18	—
12	16:0–20:3	1.16	0.53	1.01	0.39
13	16:0–18:1	0.67	0.57	0.43	0.30
14	18:1–18:1	5.63	1.85	1.27	1.49
15	18:0–22:6	3.68	2.47	3.29	0.30
16	18:0–20:4	17.50	17.57	21.96	3.48
17	18:0–18:2	10.20	12.72	7.18	14.46
18	18:0–22:5	0.13	0.22	0.10	0.12
19	18:0–20:3	1.07	0.96	0.29	0.13
20	18:0–18:1	0.61	0.23	0.49	0.21
21	18:0–22:4	0.16	0.18	0.07	—

TABLE V

COMPARISON OF TOTAL FATTY ACID DISTRIBUTIONS (%) DEDUCED FROM PC MOLECULAR SPECIES COMPOSITION AND GLC ANALYSIS

Fatty acid	*Microsomes*		*Mitochondria*		*Liver*		*Bile*	
	HPLC	*GLC*	*HPLC*	*GLC*	*HPLC*	*GLC*	*HPLC*	*GLC*
14:0	0.33	0.86	0.67	1.40	0.27	0.60	0.24	0.10
16:0	26.89	30.43	25.14	32.29	28.55	36.75	38.36	39.72
16:1	2.63	3.09	3.07	3.97	4.10	3.20	0.66	1.40
18:0	16.68	19.19	17.78	18.45	17.19	17.79	9.35	9.34
18:1	8.70	9.57	6.06	8.03	5.59	6.85	2.35	4.24
18:2	19.43	16.25	21.68	16.22	14.20	14.75	36.99	33.22
18:3	0.15	0.20	0.86	0.50	0.15	0.40	0.07	0.58
20:3	1.11	0.49	0.75	0.77	0.65	0.30	0.26	0.55
20:4	18.54	16.54	19.31	15.54	23.19	16.36	10.04	9.05
20:5	0.56	0.54	0.63	0.51	0.64	0.50	0.08	0.60
22:4	0.10	0.40	0.10	0.60	0.05	—	—	—
22:5	1.02	0.90	0.93	0.30	0.64	0.30	0.06	—
22:6	3.86	2.04	3.62	1.42	3.04	2.20	0.90	1.20

The results of the HPLC analysis of samples of PC, extracted from rat whole liver, liver microsomes, liver mitochondria and bile samples, are given in Table IV.

The total fatty acid compositions, deduced from HPLC analysis with dual-wavelength detection of these samples, are compared in Table V with the corresponding values of fatty acid composition determined by GLC. The agreement is generally good, except that differences greater than 5% may be observed for palmitic and polyunsaturated acids. This may be caused by the presence of disaturated species which are not detected unless present in large amounts and which may cause the underevaluation of palmitic acid and the overevaluation of polyunsaturated acids.

In conclusion, this method be suitable for the analysis of mixtures of highly unsaturated PC species of reasonably well characterized composition. It cannot be used to measure the more saturated species which present the greater analytical problems to UV detection methods in general.

REFERENCES

1 N. A. Porter, R. A. Wolf and J. R. Nixon, *Lipids*, 14 (1979) 20.
2 M. Smith and F. B. Jungalwala, *J. Lipid Res.*, 22 (1981) 697.
3 G. M. Patton, J. M. Fasulo and S. J. Robinson, *J. Lipid Res.*, 23 (1982) 190.
4 B. J. Compton and W. C. Purdy, *Anal. Chim. Acta*, 141 (1982) 405.
5 A. Cantafora, A. Di Biase, D. Alvaro, M. Angelico, M. Marin and A. F. Attili, *Clin. Chim. Acta*, 134 (1983) 281.
6 W. W. Christie and M. L. Hunter, *J. Chromatogr.*, 325 (1985) 473.
7 J. Y-K. Hsieh, D. K. Welch and J. G. Turcotte, *Lipids*, 16 (1981) 761.
8 Y. Nakagawa and K. Waku, *J. Chromatogr.*, 381 (1986) 225.
9 M. Batley, N. H. Packer and J. W. Redmond, *J. Chromatogr.*, 198 (1980) 520.
10 M. L. Blank, M. Robinson, V. Fitzgerald and F. Snyder, *J. Chromatogr.*, 298 (1984) 473.
11 M. Kito, H. Takamura, H. Narita and R. Urade, *J. Biochem.*, 98 (1985) 327.
12 H. Takamura, H. Narita, R. Urade and M. Kito, *Lipids*, 21 (1986) 356.

13 W. W. Christie, *Z. Lebensm.-Unters.-Forsch.*, 181 (1985) 171.
14 J. Folch, M. Lees and G. H. Sloane Stanley, *J. Biol. Chem.*, 226 (1957) 497.
15 A. Cantafora, M. Angelico, A. Di Biase, M. Pièche, F. Bracci, A. F. Attili and L. Capocaccia, *Lipids*, 16 (1981) 589.
16 F. B. Jungalwala, J. E. Evans and R. H. McCluer, *Biochem. J.*, 155 (1976) 55.
17 W. S. M. Geurts van Kessel, W. M. A. Hax, R. A. Demel and J. de Gier, *Biochim. Biophys. Acta*, 486 (1977) 524.

Journal of Chromatography, 507 (1990) 351–366
Elsevier Science Publishers B.V., Amsterdam — Printed in The Netherlands

CHROMSYMP. 1662

Mechanistic study on the derivatization of aliphatic carboxylic acids in aqueous non-ionic micellar systems

F. A. L. VAN DER HORST*,[a], J. M. REIJN, M. H. POST and A. BULT
Department of Pharmaceutical Analysis, Faculty of Pharmacy, University of Utrecht, Catharijnesingel 60, 3511 GH Utrecht (The Netherlands)
J. J. M. HOLTHUIS
EuroCetus BV, Paasheuvelweg 30, 1105 BJ Amsterdam (The Netherlands)
and
U. A. Th. BRINKMAN
Department of Analytical Chemistry, Free University, De Boelelaan 1083, 1081 HV Amsterdam (The Netherlands)

SUMMARY

A model is proposed for the derivatization mechanism of carboxylic acids with a fluorescent label, 4-bromomethyl-7-methoxycoumarin, in an aqueous non-ionic micellar system with the use of a tetraalkylammonium ion-pairing cation. Using experimentally obtained extraction constants and partition coefficients for aliphatic carboxylic acids in the micellar solution, the model was compared with the observed derivatization rate constants of these acids; this gave a satisfactory correlation. Owing to its similarity with phase-transfer catalysis, the present micelle-mediated derivatization is termed micellar phase-transfer catalysis.

INTRODUCTION

Recently, aqueous micellar systems have been used for the derivatization of carboxylic acids [1,2]. By using micelles, carboxylic acids can be derivatized directly in an aqueous (physiological) matrix with minimum sample pretreatment, *i.e.*, tedious extraction procedures can be circumvented. In a previous paper we reported the influence of micelles on the derivatization of 10-undecenoic acid with the fluorophore 4-bromomethyl-7-methoxycoumarin (BrMMC)[1]. Optimum derivatization rates were obtained in non-ionic micelles in the presence of an ion-pair agent, *e.g.*, tetrahexylammonium bromide. We suggested that the reaction mechanism in the aqueous micellar systems is related to the mechanism known as phase-transfer catalysis (PTC).

[a] Present address: Department of Clinical Chemistry, University Hospital of Leiden, Rijnsburgerweg 10, 2333 AA Leiden, The Netherlands.

0021-9673/90/$03.50

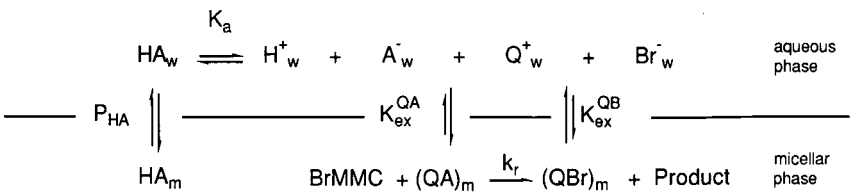

Fig. 1. Model for the MPTC mechanism in a non-ionic micellar system. The symbols are explained in the text.

PTC is based on the principle that an analyte is derivatized in an organic phase directly after it has been extracted from an aqueous phase using an ion-pair agent[3,4]. Because of the observed similarity, the micelle-mediated derivatization reaction is termed micellar phase-transfer catalysis (MPTC). The distinct advantage of using MPTC systems is that the reaction mixture, unlike in traditional PTC systems, can be injected directly into reversed-phase high-performance liquid chromatographic (RP-HPLC) systems without encountering the problem of peak deterioration.

The aim of this study was to investigate further the MPTC mechanism, for which a micellar system was selected composed of an aqueous solution containing Arkopal N-130 as a non-ionic surfactant, tetrahexylammonium bromide as ion-pair agent, several even-numbered saturated aliphatic carboxylic acids as analytes and BrMMC as derivatization reagent. A quantitative model for the MPTC mechanism is proposed which proved to be in satisfactory agreement with the experimental results.

THEORY

Micellar phase-transfer catalysis

The model for the derivatization mechanism of carboxylic acids in a non-ionic micellar system is based on the supposition that the reaction of the acid with the reagent occurs in the hydrocarbonaceous core of the micelle (Fig. 1)[1]. With excess of BrMMC reagent present in the micelles, the derivatization rate, v, can be expressed by

$$v = k_r[(QA)_m] \tag{1}$$

where k_r is the pseudo-first-order rate constant and $[(QA)_m]$ is the concentration of the ion-pair complex of the acid in the micelle. The value of $[(QA)_m]$ is given by[3,4]

$$[(QA)_m] = K^{QA}_{ex}[Q^+_w][A^-_w] \tag{2}$$

where K^{QA}_{ex} is the extraction constant of the acid and $[Q^+_w]$ and $[A^-_w]$ are the concentrations of the tetraalkylammonium cation and of the conjugate base in the aqueous bulk phase, respectively. The extraction of the counter ion of the ion-pair agent, Br^-, into the micelle is expressed by

$$K^{QB}_{ex} = [(QBr)_m]/[Q^+_w][Br^-_w] \tag{3}$$

where K^{QB}_{ex} is the extraction constant of the counter ion. The acidity constant of the acid in the aqueous phase, K_a, is given by

$$K_a = [H^+_w][A^-_w]/[HA_w] \tag{4}$$

The non-dissociated acid HA partitions between the aqueous and micellar phases. The partition coefficient P_{HA} is given by the ratio of the concentrations of HA in the micellar and aqueous phases:

$$P_{HA} = [HA_m]/[HA_w] \tag{5}$$

The partitioning of the conjugate base is not considered, because such a transfer will be restricted electrostatically[5,6]. The partitioning of salts of A^- is also not taken into account, because the partition coefficients are a few decades smaller than those of the non-dissociated acid[7,8]. For reasons of simplification, in the present model the formation of ion pairs in the aqueous phase[9,10] and the dissociation of the ion-pair complex[9,11] or of the acid[12] in the micellar phase and the formation of oligomers of the ion pair[9] and the formation of dimers of the acid[13] in the micellar phase are not taken into account.

The analytical concentration of the acid, $[HA]_t$, is then given by

$$[HA]_t = \varphi_m([HA_m] + [(QA)_m]) + \varphi_w([HA_w] + [A_w^-]) \tag{6}$$

where φ_m and φ_w are the volume fractions of the micelles and the aqueous bulk phase, respectively. φ_m, which is 0.036 at 50 m*M* Arkopal N-130, is equal to CV, where C is the concentration of the surfactant exceeding the critical micelle concentration (CMC = 90 μM, ref. 14), and V (0.9 ml/g, ref. 15) is the specific volume of the surfactant[16]. After substitution of eqns. 2, 4 and 5 into eqn. 6 and rearranging, $[(QA)_m]$ can be expressed as

$$[(QA)_m] = \frac{K_{ex}^{QA}[Q_w^+][HA]_t}{(\varphi_w + P_{HA}\varphi_m)[H^+]/K_a + \varphi_w + K_{ex}^{QA}\varphi_m[Q_w^+]} \tag{7}$$

$[Q_w^+]$ is calculated from the known ion-pair agent analytical concentration, $[Q]_t$. If the analytical concentration of the acid is much smaller than that of the ion-pair agent, then $[(QA)_m]$ is small compared with the other Q-containing species and can be neglected in the calculation of $[Q_w^+]$. In this case, $[Q]_t$ is given by

$$[Q]_t = \varphi_w[Q_w^+] + \varphi_m[(QBr)_m] \tag{8}$$

Provided that $[Q_w^+] = [Br_w^-]$, substitution of eqn. 8 into eqn. 3 results in

$$K_{ex}^{QB}\varphi_m[Q_w^+]^2 + \varphi_w[Q_w^+] - [Q]_t = 0 \tag{9}$$

The physically relevant solution for this equation is

$$[Q_w^+] = -\varphi_w + \frac{\{\varphi_w^2 + 4\varphi_m K_{ex}^{QB}[Q]_t\}^{\frac{1}{2}}}{2K_{ex}^{QB}\varphi_m} \tag{10}$$

In other words, if K_{ex}^{QA}, K_{ex}^{QB} and P_{HA} can be determined, $[(QA)_m]$ can be calculated using eqns. 7 and 10.

Determination of K_{ex}^{QA}, K_{ex}^{QB} and P_{HA}

Data in the literature on extraction constants[3,4,11] and partition coefficients[11,17] could not be used in this study, because they are reported only for traditional two-phase systems and depend on the properties of the two-phase system[3,4,11,17]. The determination of extraction constants or partition coefficients in micellar solutions by simply measuring the concentrations of the species in the two pseudo-phases will be very difficult because of the macro-homogeneity of micellar solutions.

However, previous studies have demonstrated that it is possible to calculate the partition coefficient of an analyte in a micellar solution from the relationship between the observed acidity constant of an acid in the micellar solution, termed K_a^{obs}, and φ_m[5,6,14,18–21]. This approach is based on the supposition that all acid species present in either the micellar or the aqueous bulk phase contribute to K_a^{obs}:

$$K_a^{obs} = \frac{[H^+]([A_w^-]\varphi_w + [A_m^-]\varphi_m)}{[HA_w]\varphi_w + [HA_m]\varphi_m} \tag{11}$$

In this study, the above expression was modified by neglecting the $[A_m^-]\varphi_m$ term (see above) and introducing $[(QA)_m]\varphi_m$ as a species which in this instance contributes to K_a^{obs}:

$$K_a^{obs} = \frac{[H^+]([A_w^-]\varphi_w + [(QA)_m]\varphi_m)}{[HA_w]\varphi_w + [HA_m]\varphi_m} \tag{12}$$

Substitution of eqns. 2, 4 and 5 into eqn. 12 yields

$$K_a^{obs} = \frac{K_a(\varphi_w + K_{ex}^{QA}\varphi_m[Q_w^+])}{(\varphi_w + P_{HA}\varphi_m)} \tag{13}$$

or, in logarithmic form,

$$pK_a^{obs} = pK_a + \log(\varphi_w + P_{HA}\varphi_m) - \log(\varphi_w + K_{ex}^{QA}\varphi_m[Q_w^+]) \tag{14}$$

This equation allows the calculation of the partition coefficient, P_{HA}, and the extraction constant, K_{ex}^{QA}, from the relationship between pK_a^{obs} and $[Q_w^+]$. First, in the absence of the ion-pair agent the value of P_{HA} can be calculated from the difference between pK_a^{obs} in the pure micellar solution and in water. Next, after addition of the ion-pair agent the value of K_{ex}^{QA} can be calculated from the slope of the relationship between K_a^{obs} and $[Q]_t$, which is almost linear. From the deviation of linearity of this relationship, because $[Q_w^+]$ is not directly proportional to $[Q]_t$ (*cf.*, eqn. 10), the value of K_{ex}^{QB} can be deduced. In practice, the above approach was carried out by using a three-parameter (*i.e.*, P_{HA}, K_{ex}^{QA} and K_{ex}^{QB}) non-linear optimization procedure, as will be explained under Experimental.

EXPERIMENTAL

Materials

Milli-Q water (Millipore, Milford, MA, U.S.A.) was used throughout. Except

for the Arkopal N-130 surfactant [a polyoxyethylene(13)nonylphenyl ether], the chemicals were of analytical-reagent grade. The chemicals were used as received. The even-numbered aliphatic carboxylic acids were purchased from Merck (Darmstadt, F.R.G.). Arkopal N-130 was a gift from Hoechst Holland (Amsterdam, The Netherlands). Tetrahexylammonium bromide (THxABr) and tetrabutylammonium bromide (TBuABr) were obtained from Fluka (Buchs, Switzerland) and 4-bromomethyl-7-methoxycoumarin (BrMMC) from Fluka or Sigma (St. Louis, MO, U.S.A.).

The aliphatic carboxylic acids were dissolved in acetone at a concentration of 100 m*M* (titrimetric experiments) or 5 m*M* (derivatization experiments) and stored at 4°C. A saturated solution of the reagent, made by adding 8 mg of BrMMC per millilitre of acetone, was stored at 4°C; it was prepared fresh every week. Prior to derivatization the BrMMC was completely dissolved by heating to *ca.* 40°C.

Derivatization procedure

A summary of the derivatization procedure[1] is as follows. To 965 μl of a 10 m*M* phosphate buffer (pH 7.0) containing 50 m*M* Arkopal N-130 and 36 m*M* THxABr, 10 μl of the carboxylic acid stock solution were added, if not stated otherwise. The incubation was started by the addition of 25 μl of BrMMC stock solution. All incubations were carried out protected from light, in a laboratory-built swerve-water-

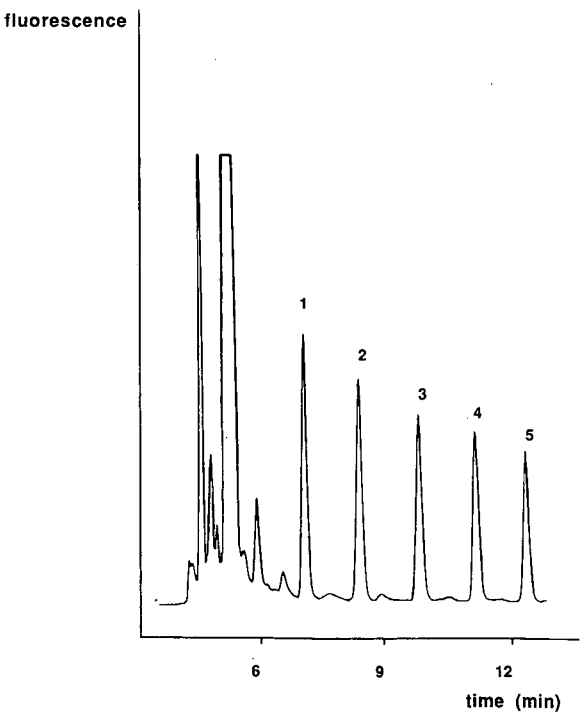

Fig. 2. Reversed-phase HPLC of MMC derivatives of five fatty acids (50 μ*M* each) obtained from an aqueous non-ionic micellar system containing 50 m*M* Arkopal N-130 and 36 m*M* THxABr at 70°C and pH 7.0. Peaks: 1 = decanoyl-MMC; 2 = dodecanoyl-MMC; 3 = tetradecanoyl-MMC; 4 = hexadecanoyl-MMC; 5 = octadecanoyl-MMC.

bath at 70°C. At given times, 75-μl samples were taken and added to 75 μl of acetonitrile.

Chromatographic system

As described previously[1], 20 μl of the diluted sample were analysed using an automated high-performance liquid chromatographic (HPLC) system. A 100 × 3.0 mm I.D. analytical column (5-μm Chromspher C_{18}; Chrompack, Middelburg, The Netherlands) was used. A linear gradient was run in 12 min from methanol–water (60:40, v/v) to 100% methanol. A Model 650 fluorescence detector (Hitachi–Perkin-Elmer, Tokyo, Japan) was used with optimized excitation and emission wavelengths of 330 and 395 nm, respectively. Retention times and peak areas were measured with an SP 4270 integrator (Spectra-Physics, Santa Clara, CA, U.S.A.). The performance of the chromatographic system is illustrated by Fig. 2, which shows that the MMC derivatives of five saturated fatty acids (50 μM) are well separated.

Identification of the derivatives

The product of dodecanoic acid with BrMMC was prepared in acetone and in the micellar system. The derivatization in acetone, using potassium carbonate and 18-crown-6 ether to accelerate the reaction, has been described previously[1,22]. After reaction for 30 min at 60°C, the supernatant was transferred to a clean vial, in which the acetone was evaporated under a stream of nitrogen.

After derivatization in the micellar system for 1 h at 70°C, the derivative was extracted into 1,2-dichloroethane (DCE). Next, the DCE layer was transferred to a clean vial and evaporated under a stream of nitrogen. In both instances the dodecanoyl-MMC derivative was isolated using thin-layer chromatography on silica with toluene–ethyl acetate (75:15, v/v) as the eluent[23]. The HPLC retention times of the purified compounds were the same as before the isolation procedure. The mass spectra, obtained using electron impact ionization with an MS 80 spectrometer (Kratos, Ramsey, NJ, U.S.A.), of the derivatives obtained from acetone and the micellar system were identical; three main peaks occurred, at m/z 388, corresponding to the molecular weight, and at m/z 206 and 190, from the chromophoric label.

Determination of pK_a^{obs}

In general, 250 μl of the carboxylic acid stock solution were added to 20 ml of carbon dioxide-free Milli-Q water in which the surfactant, ion-pair agent and other additives had been dissolved. After acidification with 1 M hydrochloric acid, the pK_a^{obs} values of the acids were determined in duplicate at 25.0 ± 0.2°C, using a glass–calomel pH electrode (Metrohm, Herisau, Switzerland), by titration with 0.1 M sodium hydroxide solution with a 636 Titroprocessor (Metrohm). For the long-chain acids ($\geqslant C_{10}$), the pK_a values could not be determined experimentally because of the poor solubility of the acids. For these acids the pK_a values were obtained from ref. 24.

Calculation of K_{ex}^{QA}, K_{ex}^{QB} and P_{HA}

For the calculation of the extraction constants and the partition coefficients, eqn, 10 was substituted into eqn. 13 and a three-parameter non-linear optimization procedure (Marquardt algorithm[25]) of this equation was performed through the experimental pK_a^{obs} *vs.* $[Q]_t$ data points. To ensure a satisfactory statistical significance

of the fitting procedure, the number of degrees of freedom, *i.e.*, the number of data points minus the number of parameters, P_{HA}, K_{cx}^{QA} and K_{cx}^{QB}, was at least seven in all instances.

For several acids the value of P_{HA} was also determined from the relationship between pK_a^{obs} and φ_m[5,6,18]:

$$(\varphi_w - K_a^{obs}/K_a)\varphi_m^{-1} = P_{HA}(K_a^{obs}/K_a) - P_A \quad (15)$$

which is a different expression for eqn. 11.

RESULTS AND DISCUSSION

First in this section, the effects of additives on the pK_a values of acids in the micellar system are discussed. From these experimental data, the partition coefficients and extraction constants for the acids were calculated, and were subsequently fitted into the proposed model for the derivatization rate in the micellar system. Finally, by comparing the model with experimental reaction rate data, its validity was evaluated.

Determination of acidity constants

Fig. 3 shows the pK_a^{obs} values of the acids in various solutions as a function of their chain length. The pK_a values of the shorter chain homologues ($\leqslant C_8$) are in good agreement with those reported in the literature[24,26]. In aqueous 50 m*M* Arkopal N-130 solution, no significant pK_a^{obs} shift was observed with the short-chain acids ($\leqslant C_4$), indicating that the partition coefficients of these acids are small (*cf.*, eqn. 14). In contrast, in the micellar solution pK_a^{obs} increases for the long-chain acids. This marked

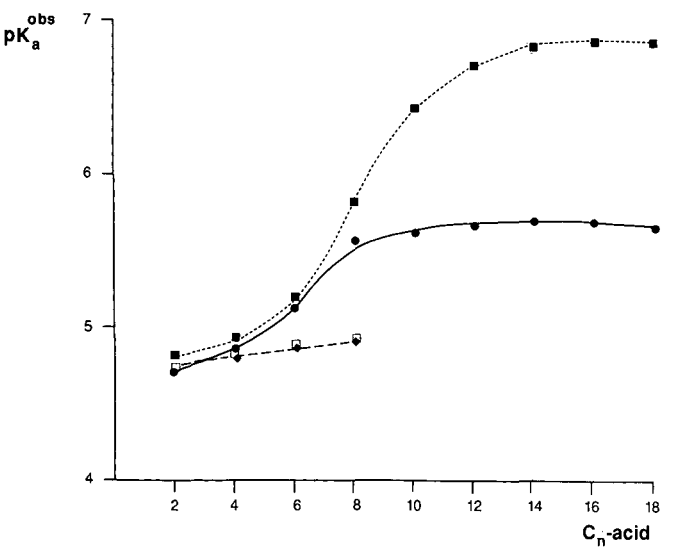

Fig. 3. Dependence of pK_a^{obs} (at 25°C) of aliphatic carboxylic acids with alkyl chain length C_n on the composition of the aqueous micellar system. ◆ = Water; □ = 18 m*M* THxABr; ■ = 50 m*M* Arkopal N-130; ● = 50 m*M* Arkopal N-130 with 36 m*M* THxABr.

shift cannot be attributed to the influence of the micelles on the pH electrode[27,28]. Shifts in the pK_a^{obs} values of ionizable analytes in the presence of micelles are often observed[12,29] and are related to the influence of the low dielectric constant, ε, in the micelle on the acidity constant of the analyte[12,30]; that is, a low ε restricts the dissociation of the non-charged acid. Therefore, the partitioning of the acid from the aqueous bulk phase, with $\varepsilon = 80$[30], to the micelle, with ε(interface) = 25 and ε(core) = 3[30], probably causes the shift in the pK_a^{obs} found in this present study. From the value of pK_a^{obs} of *ca.* 6.85 for the long-chain acids in the pure micellar system (Fig. 3), it can be concluded that the carboxylic moiety mainly resides in an environment with medium polarity, probably the hydrated polyoxyethylene interface of the micelle.

The addition of 36 m*M* THxABr to the micellar solution causes a decrease in the pK_a^{obs} values relative to those observed in pure micellar systems (Fig. 3), whereas with the addition of 18 m*M* THxABr (solubility limit) to an aqueous solution no marked effect on the pK_a^{obs} is found. As is also true for surfactants, it is unlikely that the shift in pK_a^{obs} in the micellar solution originates from an influence of the ion-pair agent on the pH electrode. Probably the anionic species, A^-, is extracted by the ion-pair agent into the micellar phase. This decreases the ratio HA/A^- (Fig. 1) and hence causes a decrease of pK_a^{obs}.

The MPTC mechanism predicts that $[(QA)_m]$ will decrease in the presence of other anions that compete for extraction into the micelle. This obviously depends on both the extraction constant and the concentration of the competitive ions[3,4]. The decrease in $[(QA)_m]$ in the micellar system results in an increase in pK_a^{obs} of the acid and a decrease in the derivatization rate[1]. Fig. 4 shows the influence of perchlorate, bromide and chloride anions on the pK_a^{obs} of dodecanoic acid in an aqueous solution of 50 m*M* Arkopal N-130 and 36 m*M* THxABr. The effect is strongest for the perchlorate

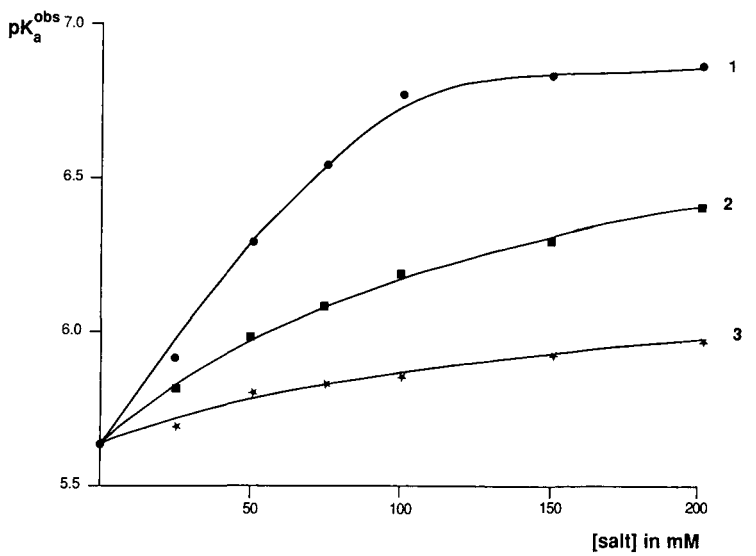

Fig. 4. Influence of 0–200 m*M* (1) $NaClO_4$, (2) KBr or (3) NaCl on the pK_a^{obs} of dodecanoic acid in an aqueous solution of 50 m*M* Arkopal N-130 and 36 m*M* THxABr at 25°C.

TABLE I

COMPILATION OF CALCULATED EQUILIBRIUM CONSTANTS

Acid	*Log K_{ex} using*				*Log P_{HA} using*			
	$THxA^+$		*$TBuA^+$*		*Eqn. 14*		*Eqn. 15*	*Ref. 11*[a]
	A^-	*Br^-*	*A^-*	*Br^-*	*THxABr*	*TBuABr*		
C_6	2.7	1.6	1.9	1.2	1.4	1.3	1.5	0.9
C_8	3.4	1.5	2.3	1.1	2.2	2.2	2.3	2.1
C_{10}	4.0	1.5	2.9	1.0	3.0	3.0	ND[b]	3.3
C_{12}	4.2	1.4	3.5	0.9	3.1	3.2	ND	4.5
C_{14}	4.2	1.3	3.8	0.7	3.2	3.1	ND	5.7
C_{16}	4.2	1.3	4.2	0.8	3.2	3.2	ND	6.7
C_{18}	4.2	1.3	4.2	0.5	3.2	3.2	ND	8.1

[a] P_{HA} determined in a chloroform–water two-phase system.
[b] ND = Not determined.

ion and is in good agreement with the order of the extraction constants of these ions ($ClO_4^- \gg Br^- > Cl^-$[3,4]).

In the absence of the ion-pair agent, the influence of 100 m*M* sodium chloride on the pK_a^{obs} of dodecanoic acid in an aqueous 50 m*M* Arkopal N-130 micellar system is

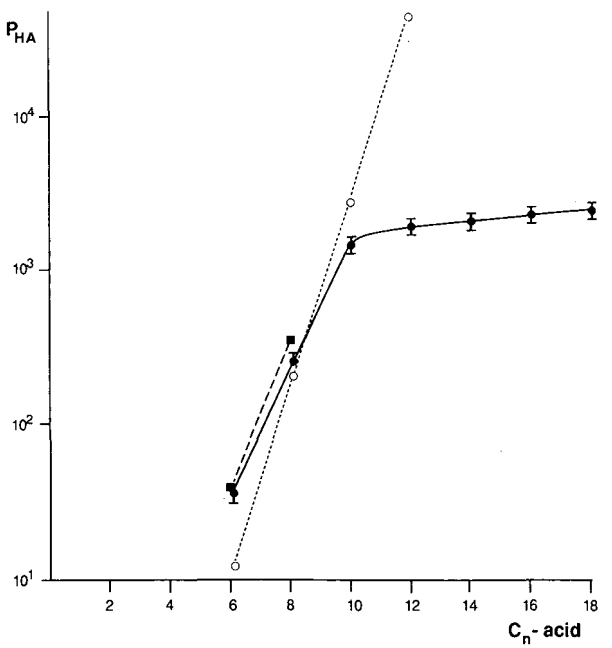

Fig. 5. Partition coefficient, P_{HA}, calculated for fatty acids with chain length C_n. ● = P_{HA} calculated from eqn. 14; ■ = P_{HA} calculated from eqn. 15; ○ = P_{HA} with dichloromethane as the organic phase[11]. The vertical bars indicate the standard deviation of the determined values.

small, *viz.*, *ca.* 0.1 pH unit. Obviously, the partitioning of the carboxylate salts is small; this was an additional argument for neglecting it in the present model.

Determination of P_{HA}

Table I and Fig. 5 show the P_{HA} values calculated for the acids in the micellar solutions using eqn. 14. For acids up to decanoic acid, log P_{HA} increases linearly with increasing carbon number (Fig. 5). A similar relationship has been observed in other two-phase systems[11,17], and is to be expected on the basis of thermodynamic considerations. For the long-chain acids the calculated P_{HA} values abruptly reach a plateau at a value of 1600, which was explained as follows. If the first derivative of eqn. 14 is taken, *i.e.*, dpK_a^{obs}/dP_{HA}, it is evident that the sensitivity of this expression decreases with increasing P_{HA}. Eventually, the sensitivity becomes less then the experimental error of 0.02 pH unit, that is, large P_{HA} values cannot be discriminated by the optimization algorithm, which results in a plateau being reached.

The partition coefficients were determined using the relationship between pK_a^{obs} and φ_m (*cf.*, eqn. 15), as shown in Fig. 6 and Table I. The P_{HA} values for decanoic acid and larger homologues could not be determined because these acids form mixed micelles with the non-ionic surfactant[31]. Even at low surfactant concentrations, this yielded a high and constant pK_a^{obs} of 6.85. For butanoic acid and smaller homologues, the P_{HA} values could not be determined either, because their pK_a^{obs} values turned out to be insensitive to even high surfactant concentrations. The P_{HA} values calculated for hexanoic and octanoic acid using eqn. 15 are in satisfactory agreement with those obtained from eqn. 14. The P_{HA} values determined for the acids in the present micellar and in conventional two-phase systems[11,17] are similar (Fig. 5). This suggests that it may by possible to use the P_{HA} values, which have been extensively reported for common two-phase systems[17], also for micellar systems.

From the influence of the number of carbon atoms in the acid on the partition coefficients of hexanoic acid to decanoic acid, it is possible to calculate the incremental free energy of transfer from water to the micelle per methylene group, n, in the acid[21,32]:

$$d\mu_t^0 = d\mu_x^0 + n d\mu_c^0 = -RT \ln (55.5\,K) \qquad (16)$$

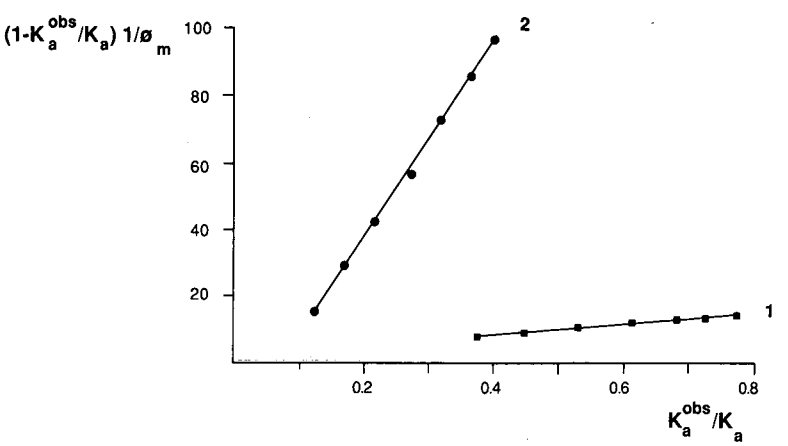

Fig. 6. Plots of $(1 - K_a^{obs}/K_a)/\varphi_m$ *vs.* K_a^{obs}/K_a according to eqn. 13 for (1) hexanoic acid and (2) octanoic acid.

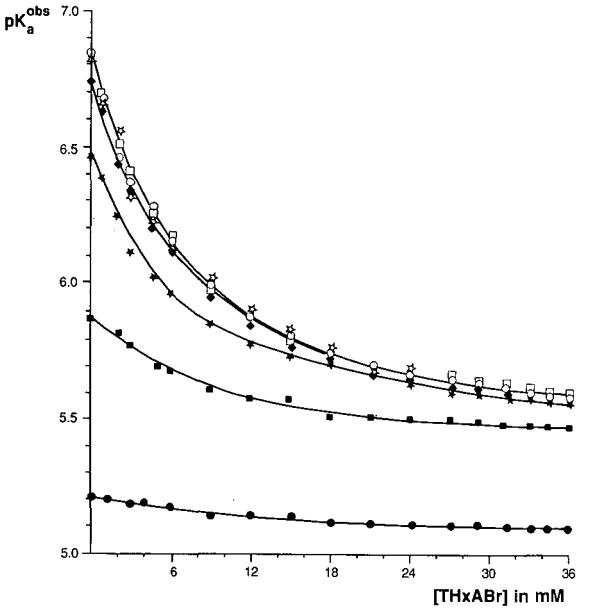

Fig. 7. Dependence of pK_a^{obs} for acids with chain length C_n on the THxABr concentration in an aqueous solution of 50 m*M* Arkopal N-130. ● = Hexanoic acid; ■ = octanoic acid; ★ = decanoic acid; ◆ = dodecanoic acid; ☆ = tetradecanoic acid; □ = hexadecanoic acid; ○ = octadecanoic acid.

where $d\mu_t^0$ is the standard free energy of transfer, $d\mu_c^0$ and $d\mu_x^0$ are the contributions of the methylene group and the residual groups and K is the absolute temperature in Kelvin, respectively. Using eqn. 16, a value for $d\mu_c^0$ of *ca.* -2.3 kJ mol^{-1} is calculated, which is in good agreement which those reported for other micellar systems (-2.4 to -3 kJ mol^{-1})[21,32].

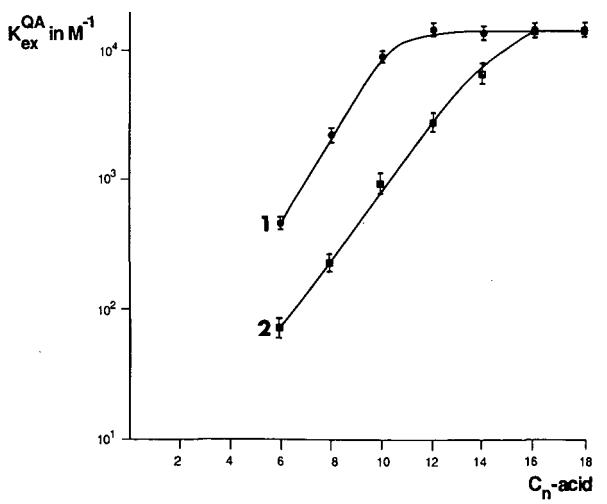

Fig. 8. Extraction constants, K_{ex}^{QA}, for C_n carboxylic acids calculated using eqn. 13, with (1) THxABr and (2) TBuABr. The vertical bars indicate the standard deviation of the determined values.

In conclusion, the partition coefficients determined from hexanoic acid through to decanoic acid in the micellar solution seem to be reliable for use in further calculations.

Determination of K_{ex}^{QA}

Fig. 7 shows the influence of THxABr concentration on the pK_a^{obs} values of several acids in aqueous 50 m*M* Arkopal N-130 solution. From these curves, the K_{ex}^{QA} values for the acids were calculated using eqn. 14; they are shown in Fig. 8 and Table I. Log K_{ex}^{QA} increases linearity with increasing number of carbon atoms in the carboxylic acid from hexanoic acid through to decanoic acid. A similar behaviour in two-phase systems is known from the literature[3,4,11], and is to be expected on the basis of thermodynamic considerations. For dodecanoic acid and larger homologues, log K_{ex}^{QA} reaches a plateau, for reasons mentioned in the discussion on the determination of P_{HA}. The extraction constants for the acids with TBuABr were also determined in the micellar solution. Up to hexadecanoic acid no plateau is reached (Fig. 8). This also suggests that the plateau observed for K_{ex}^{QA} is caused by the inadequacy of eqn. 14 to discriminate between large extraction constants, rather than by factors such as non-ideal behaviour of the extraction equilibrium in the micellar system. The variation in the calculated values of K_{ex}^{QB} for THxABr and for TBuABr is small (Table I), as is to be expected.

The combined results emphasize the reliability of eqn. 14 for calculating extraction constants in micellar solutions if they are not too large.

Effect of pH on the derivatization rate

The influence of the pH on k_{obs} in the micellar system was investigated for the reaction between decanoic acid and BrMMC. Fig. 9 shows that the observed derivatization rate constant is sigmoidally related to the pH with an inflection point at pH 5.5 $\pm$ 0.1, while a conventional sigmoidal titration curve was obtained with a pK_a^{obs}

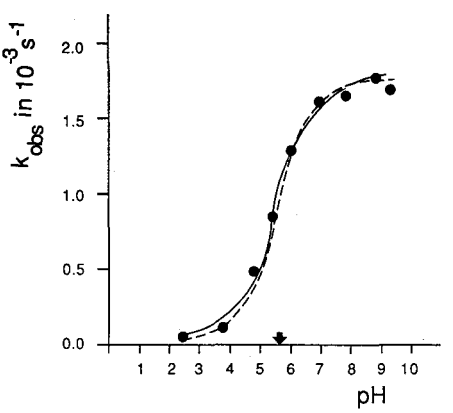

Fig. 9. Dependence of k_{obs} of the reaction of decanoic acid (50 μ*M*) with BrMMC, on the pH of an aqueous solution containing 50 m*M* Arkopal N-130 and 36 m*M* THxABr at 70°C. The arrow indicates the pK_a^{obs} as determined titrimetrically for decanoic acid in the micellar system at 25°C. The dashed line indicates the influence of the pH on $[(QA)_m]$ obtained from eqn. 7.

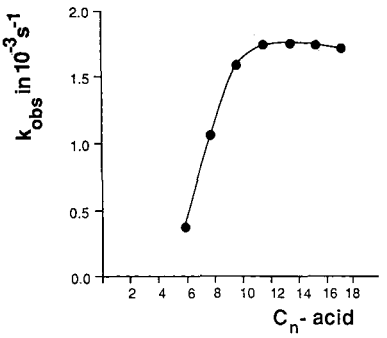

Fig. 10. Dependence of k_{obs} on the number of carbon atoms in the carboxylic acids, C_n. Conditions: aqueous solution containing 50 m*M* Arkopal N-130 and 36 m*M* THxABr at 70°C and pH 7.0.

of 5.64 ± 0.02 (data not shown). The direct proportionality of the derivatization rate and $[A^-]$ is to be expected, as can easily be verified by combining eqns. 1 and 2.

In addition, Fig. 9 includes data on the influence of pH on $[(QA)_m]$ calculated using eqn. 7 and the parameters given in Table I. A good correlation is observed, which supports the validity of the present model.

From the above results, it can be inferred that, as in other micelle-mediated reactions[29], the pH of the micellar solution is an important parameter. From Figs. 3 and 9 it can be deduced that the derivatization of aliphatic carboxylic acids has to be performed at neutral pH, which is *ca.* 1.5 units above pK_a^{obs} in the micellar solution, to ensure optimum reaction rates for these acids.

Effect of the acid chain length on the derivatization rate

Fig. 10 shows the relationship between k_{obs} and the chain length of the aliphatic carboxylic acids. The k_{obs} values of the short-chain acids ($\leqslant C_4$) could not be determined owing to high reagent blanks. Up to decanoic acid, k_{obs} increases, which reflects the expected influence of the increasing extractability of the acids on the derivatization rate. For the long-chain acids the derivatization rate reaches a plateau, because of the complete extraction of the conjugate bases having a large K_{ex}^{QA}. The overall reaction rate is then likely to be limited by the rate constant in the micelle, k_r, which is probably independent of the alkyl chain length of the acid.

For two acids, hexanoic and decanoic acid, the validity of the model for the prediction of their derivatization rate in the micellar solution (eqn. 7) was investigated further. Eqn. 1 shows that, if k_r is constant, the derivatization rate is linearly related to $[(QA)_m]$. The latter parameter was, therefore, used as a measure of the derivatization rate in the micellar solution. Fig. 11 shows the value of $[(QA)_m]$, expressed as a percentage of $[HA]_t$, for hexanoic acid and decanoic acid as a function of the ion-pair agent concentration in aqueous 50 m*M* Arkopal N-130 solution, using the data given in Table I. Fig. 11 shows that the general shape of the calculated extraction curves is in line with expectation[3,4]: first, the curves reflect the influence of the extractibility of the acid on $[(QA)_m]$ and, second, a plateau is reached in $[(QA)_m]$ for decanoic acid owing to its large extraction constant. The model also predicts such a plateau for hexanoic acid; however, this should occur at a much higher ion-pair agent concentration, which is not attainable experimentally, because of the occurrence of phase separation above 36 m*M* THxABr[1].

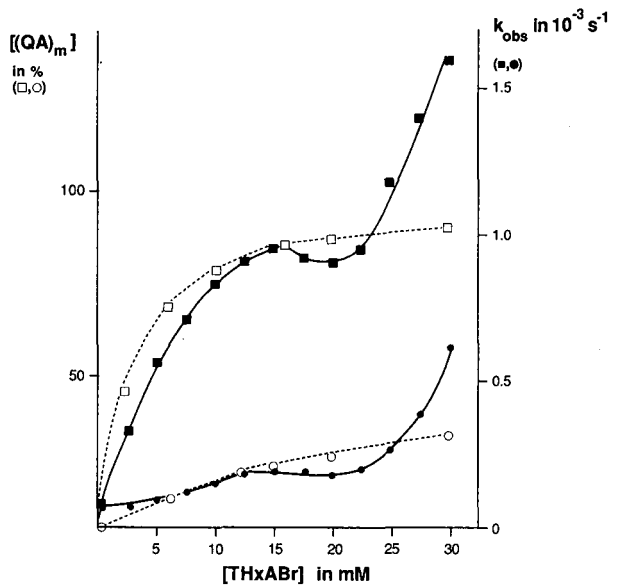

Fig. 11. Effect of THxABr concentration on the calculated concentration of $[(QA)_m]$, expressed as a percentage of $[HA]_t$, using eqn. 7, and on the rate constant, k_{obs} (at 70°C), for hexanoic and decanoic acid in aqueous 50 m*M* Arkopal N-130 solution. ○ = $[(QA)_m]$ calculated for hexanoic acid; □ = $[(QA)_m]$ calculated for decanoic acid; ● = observed rate constant for hexanoic acid; ■ = observed rate constant for decanoic acid.

The observed derivatization rate constants for hexanoic and decanoic acid in aqueous 50 m*M* Arkopal N-130 solution at pH 7.0 and 70°C are also shown in Fig. 11. The calculated $[(QA)_m]$ values are seen to match the actual derivatization profiles fairly well up to *ca.* 20 m*M* THxABr. The similarity indicates that below this THxABr concentration, the observed derivatization rate is likely to be limited by $[(QA)_m]$ (eqn. 1). Above 20 m*M* THxABr the derivatization profiles deviate from the calculated curve, which will be discussed below.

It has been shown that above 20 m*M* thxABr the micellar size increases markedly, which finally results in opaque solutions at the so-called cloud temperature, T_c, at 36 m*M* THxABr[1,33,34]. An increase in the size of micelles is not likely to reduce φ_m significantly and is, therefore, considered not to be the main cause of the deviating derivatization rates observed. The conclusion that changes in the micellar system as such have a small effect on the derivatization rate is further supported by the observation that for the fluorescence reagent 9-bromomethylacridine (BrMAC) the calculated extraction curve is very similar to the actual derivatization profile[35], that is, a plateau in the rate constant is observed above 20 m*M* THxABr.

A likely explanation for the observed derivatization profile is as follows. Next to the micellar size, the physico-chemical properties of the micellar solution also change on approaching T_c, *e.g.*, water is expelled from the micelles[30,36]. Because it has been demonstrated that reactions involving BrMMC are very sensitive to the presence of water[37,38], the latter effect may well be responsible for the optimum in the reaction rate at T_c. These combined results indicate that below *ca.* 20 m*M* THxABr, the increasing

derivatization rate is related to an increase in $[(QA)_m]$, whereas for 20–36 m*M* THxABr the increase is caused by an increase in the reaction rate constant in the micelle.

The decrease in the observed derivatization rate above 36 m*M* THxABr, which occurs for both BrMMC[1] and BrMAC[35], can be attributed to the occurrence of phase separation[1], which probably disturbs the MPTC mechanism.

CONCLUSIONS

The MPTC model presented here is supported well by the experimental results. For example, the influence of the pH on the derivatization rate (Fig. 9) and the derivatization profiles is adequately described (Fig. 11). In addition, the discrepancies can be satisfactorily explained. It is obvious however, that despite the good results, the present model may require refinement.

The major goal of this paper and ref. 1 was to elucidate the derivatization mechanism of carboxylic acids in the micellar system. The main conclusions from these studies and their practical implications are discussed below.

The derivatization in the micellar system exhibits most of the properties that are characteristic for phase-transfer catalysis (PTC) systems, such as the following. In the absence of an ion-pair agent, only low derivatization rates are observed in both ionic and non-ionic micellar systems. In non-ionic micellar systems, the derivatization rate increases with increasing hydrophobicity of the analyte and of the ion-pair agent. This means that lipophilic ion-pair agents such as THxABr should be used to obtain high derivatization rates. The derivatization reaction is inhibited by the presence of anions that can compete for extraction into the micelle. The degree of inhibition is related to the extractability of the anions. This implies that the use of MPTC is not easily compatible with deproteination agents such as perchloric acid.

The pH of the micellar system is of primary importance for the derivatization rate. It should be *ca.* 1.5 pH units above the pK_a^{obs} of the acid in the micellar system to ensure its complete dissociation. With common carboxylic acids the derivatization reaction should therefore be performed at neutral pH.

Factors that affect the properties of the micellar system can also influence the derivatization reaction. The derivatization rate increases with the size of the non-ionic micelles. With BrMMC, unexpectedly high derivatization rates are observed if the micellar system is turbid at the derivatization temperature. An obvious reason for this marked increase in the observed reaction rate is that in these turbid micellar solutions water is expelled from the micelles, which is of significant importance, because reactions that involve BrMMC are very sensitive to the presence of water. The turbid solutions can be obtained with several combinations of non-ionic surfactants and ion-pair agents, *i.e.*, the actual composition of the micellar system is of secondary importance. We selected a micellar system that contains 50 m*M* Arkopal N-130 and 36 m*M* THxABr, because this system performs well with respect to the derivatization rate and with respect to the fact that the maximum derivatization rate is not critically related to the precise composition of the micellar system. The addition of large amounts of organic solvents, *e.g.*, above 10% (v/v) acetone, results in a decrease in the derivatization rate in the Arkopal N-130–THxABr micellar solutions, because micellization is then inhibited. Therefore, when using the Arkopal N-130–THxABr

system, organic solvents cannot be used for the precipitation of proteins. However, it is not obligatory to remove plasma proteins prior to the incubation procedure. This has been demonstrated for the anti-epileptic drug valproic acid (2-propylpentanoic acid), which can be derivatized directly in diluted plasma using MPTC[2].

Finally, one can safely conclude that MPTC will offer a convenient and versatile technique for the derivatization of carboxylic acids in aqueous matrices. As an illustration, in a subsequent paper we shall demonstrate that free fatty acids in plasma can be determined using a fully automated HPLC system with an on-line MPTC unit[39].

REFERENCES

1 F. A. L. van der Horst, M. H. Post and J. J. M. Holthuis, *J. Chromatogr.*, 456 (1988) 201.
2 F. A. L. van der Horst, G. G. Eikelboom and J. J. M. Holthuis, *J. Chromatogr.*, 456 (1988) 191.
3 E. V. Dehmlow and S. S. Dehmlow, *Phase-Transfer Catalysis*, Verlag Chemie, Weinheim, 1980.
4 C. M. Starks and C. Liotta, *Phase-Transfer Catalysis, Principles and Techniques*, Academic Press, New York, 1978.
5 E. Pellizetti and E. Pramauro, *Anal. Chim. Acta*, 169 (1985) 1.
6 I. V. Berezin, K. Martinek and A. K. Yartsimirski, *Russ. Chem. Rev. (Engl. Transl.)*, 42 (1973) 787.
7 W. F. van der Giesen and L. H. M. Janssen, *Int. J. Pharmacol.*, 12 (1982) 231.
8 R. F. Rekker, *The Hydrophobic Fragmental Constant*, Elsevier, Amsterdam, 1977.
9 R. Modin and G. Schill, *Acta Pharm. Suec.*, 4 (1967) 301.
10 C. K. Shim, R. Nishigaki, T. Iga and M. Hanano, *Int. J. Pharmacol.*, 8 (1981) 143.
11 A. Fürangen, *J. Chromatogr.*, 353 (1986) 259.
12 M. S. Fernández and P. Fromherz, *J. Phys. Chem.*, 81 (1977) 1755.
13 R. Modin and A. Tilly, *Acta Pharm. Suec.*, 5 (1968) 331.
14 P. Becher, in M. J. Schick (Editor), *Nonionic Surfactants*, Marcel Dekker, New York, 1967, p. 478.
15 Zs. Bedö, E. Berecz and I. Lakatos, *Colloid Polym. Sci.*, 265 (1987) 715.
16 K. Martinek, A. K. Yatsimirski, A. V. Levashov and I. V. Berezin, in K. L. Mittal (Editor), *Micellization, Solubilization and Microemulsions*, Vol. 2, Plenum Press, New York, 1977, p. 489.
17 A. Leo, C. Hansch and D. Elkins, *Chem. Rev.*, 71 (1971) 525.
18 L. J. K. Tong and M. C. Glesmann, *J. Am. Chem. Soc.*, 79 (1957) 4305.
19 E. Pramauro, G. Saini and E. Pellizetti, *Anal. Chim. Acta*, 166 (1984) 233.
20 P. Rychlovsky and I. Nemcová, *Talanta*, 35 (1988) 211.
21 E. Pramauro and E. Pellizetti, *Anal. Chim. Acta*, 126 (1981) 253.
22 S. Lam and E. Grushka, *J. Chromatogr.*, 158 (1978) 207.
23 W. Dünges, *Anal. Chem.*, 49 (1977) 442.
24 A. L. Underwood, *Anal. Chim. Acta*, 140 (1982) 89.
25 D. W. Marquardt, *J. Soc. Ind. Appl. Math.*, 11 (1963) 431.
26 G. Kortüm, W. Vogel and K. Andrussow, *Dissociation Constants of Organic Acids in Aqueous Solution*, Butterworths, London, 1961.
27 P. Johansson, G. Hoffmann and U. Stefansson, *Anal. Chim. Acta*, 140 (1982) 77.
28 C. A. Bunton and M. J. Minch, *J. Phys. Chem.*, 78 (1974) 1490.
29 F. A. L. van der Horst and J. J. M. Holthuis, *J. Chromatogr.*, 426 (1988) 267.
30 G. G. Warr and D. I. Evans, *Langmuir*, 4 (1988) 437.
31 M. J. Schick (Editor), *Nonionic Surfactants*, Marcel Dekker, New York, 1987.
32 L. Sepulveda, E. Lissi and F. Quina, *Adv. Colloid. Interface Sci.*, 25 (1986) 1.
33 T. Nakagawa, in M. J. Schick (Editor), *Nonionic Surfactants*, Marcel Dekker, New York, 1967, p. 558.
34 N. Furasaki, S. Hada and S. Neya, *J. Phys. Chem.*, 92 (1988) 3488.
35 F. A. L. van der Horst, M. H. Post, J. J. M. Holthuis and U. A. Th. Brinkman, *Chromatographia*, 28 (1989) 267.
36 H. L. Casal, *J. Am. Chem. Soc.*, 110 (1988) 5203.
37 J. H. Wolf and J. Korf, *J. Chromatogr.*, 436 (1988) 437.
38 P. Leroy, S. Chakir and A. Nicolas, *J. Chromatogr.*, 354 (1986) 267.
39 F. A. L. van der Horst, M. H. Post, J. M. M. Holthuis and U. A. Th. Brinkman, *J. Chromatogr.*, 500 (1990) 443.

Journal of Chromatography, 507 (1990) 367–380
Elsevier Science Publishers B.V., Amsterdam — Printed in The Netherlands

CHROMSYMP. 1836

Optimization of the high-performance liquid chromatography of coumarins in *Angelica archangelica* with reference to molecular structure

P. HÄRMÄLÄ* and H. VUORELA
Pharmacognosy Division, Department of Pharmacy, University of Helsinki, SF-00170 Helsinki (Finland)
P. LEHTONEN
Research Laboratories, Alko Ltd., P.O. Box 350, SF-00101 Helsinki (Finland)
and
R. HILTUNEN
Pharmacognosy Division, Department of Pharmacy, University of Helsinki, SF-00170 Helsinki (Finland)

SUMMARY

Molecular connectivity indices were calculated and compared with measured isocratic and gradient (binary gradient and isoselective multi-solvent gradient) reversed-phase high-performance liquid chromatographic retention data of ten coumarins in *Angelica archangelica*. Retention measurements were performed, using organic solvent–water eluents, containing methanol, ethanol, 1-propanol, tetrahydrofuran, dioxane, acetonitrile and their mixtures, according to the "PRISMA" model in the optimization process. The solvent strength values were obtained experimentally. A baseline separation of the ten coumarins was achieved. The elution order of the coumarins varied according to the solvent. Decreasing the volume fraction in many instances increased the separation factor. The compounds were divided into two groups. The path type of the fourth-order and path/cluster type of the fourth-order valence level indices best described the retention. High correlations were observed between the calculated and measured retentions. The retention could be well predicted for different selectivity points in the "PRISMA" using the molecular connectivity indices.

INTRODUCTION

The retention of compounds in high-performance liquid chromatography (HPLC) analyses can be predicted by using molecular connectivity indices[1–3]. The concept of molecular connectivity was introdued by Randic[4] and further developed by Kier and Hall[5]. The molecular connectivity index terms are numerical values which are fundamental in defining and quantitatively describing the adjacency relationships in the molecular structure. When the nature of the atom is not taken into consideration, the index is referred to as the connectivity level, χ; when it is, the index is described as

0021-9673/90/$03.50

the valence level, χ^v. Connectivity indices have been extended to include indices of different orders, in addition to subgraphs composed of paths, clusters and path/clusters, which are described by the subscripts p, c and pc, respectively.

Coumarins usually contain many heteroatoms. The behaviour of heteroatom-containing molecules is sometimes difficult to predict on the basis of molecular connectivity indices. Kier and Hall[5] improved the correlation between the water solubility of oxygen-containing compounds and the corresponding molecular connectivity indices by adding the vertex value, δ, of the oxygen atom to the regression equation for alcohols and ethers. A similar procedure gave a high correlation for boiling points and partition coefficients in the case of primary, secondary and tertiary amines. As shown by Lehtonen[6], the retention of oxygen-containing amines was difficult to predict when analysed together with oxygen-free amines.

The retention behaviour of ten closey related coumarins in *Angelica archangelica* (L.) was studied, using six common solvents in reversed-phase liquid column chromatography. The aim of the study was to compare molecular connectivity indices with the retention measurements. A further aim was to optimize the HPLC separation of ten closely related coumarins by using the "PRISMA" model[7] with reference to molecular connectivity indices describing the molecule structure. The indices were used to study the predictability of the HPLC behaviour and optimization.

EXPERIMENTAL

Apparatus

A Waters Assoc. Model 6000A liquid chromatograph, equipped with a Pye Unicam PU4020 UV detector and a Hewlett-Packard 3390A integrator, was used.

Chemicals

The coumarins (Fig. 1) (+)-oxypeucedanin, ostruthol and isoimperatorin were isolated from *Angelica archangelica* (L.) at the Pharmacognosy Division, Department of Pharmacy, University of Helsinki. Angelicin, bergapten, isopimpinellin, umbelliferon, and xanthotoxin were obtained from Roth (Karlsruhe, F.R.G), imperatorin from Serva (Heidelberg, F.R.G.) and scopoletin from Sigma (St. Louis, MO, U.S.A.). The water used was distilled and deionized. 1,4-Dioxane was of HPLC quality from E. Merck (Darmstadt, F.R.G.) and absolute ethanol from Alko (Helsinki, Finland). All other solvents were of HPLC quality from Rathburn Chemicals (Walkerburn, U.K.).

Chromatographic conditions

The column was a 200 × 4 mm I.D. tube, laboratory-packed with Spherisorb S5 ODS-2 (Phase Separations, Queensferry, U.K.), thermostated at 50.0°C. The mobile phase was prepared from acetonitrile, dioxane, ethanol, methanol, 1-propanol and tetrahydrofuran (THF), each diluted with water, and their mixtures (see Results and Discussion). The flow-rate was 1.5 ml/min and detection was effected at 320 nm. The samples were diluted to give the smallest detectable peaks at 320 nm. The dead volume was determined at 250 nm with 0.2 μl of aqueous sodium nitrite.

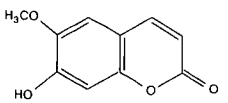

1. Scopoletin

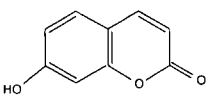

2. Umbelliferon

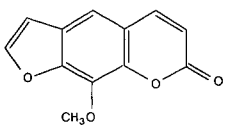

3. Xanthotoxin

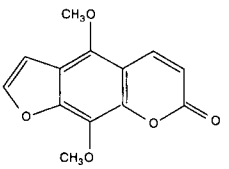

4. Isopimpinellin

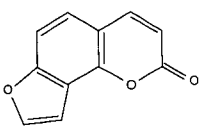

5. Angelicin

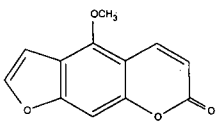

6. Bergapten

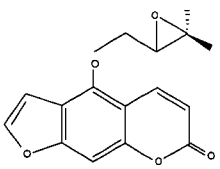

7. (+)-Oxypeucedanin

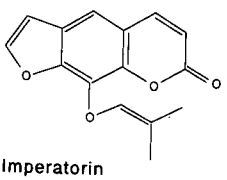

8. Imperatorin

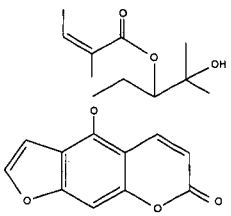

9. Ostruthol

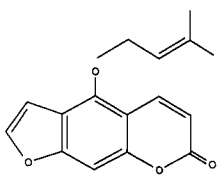

10. Isoimperatorin

Fig. 1. Structures of the coumarins

Calculation of molecular connectivity indices

The molecular connectivity indices for the coumarins were calculated using a BASIC program, as described previously for dansylamides[6]. The following general equation, proposed by Kier and Hall[5], was used for computation of an index of type t and order m:

$$ {}^{m}\chi_t = \sum_{j=1}^{{}^{m}n_s} m_{c_j} = \sum_{j=1}^{{}^{m}n_s} \left[\prod_{i=1}^{m} (\delta_i)_j^{-1/2} \right] $$

where ${}^{m}c_j$ is the subgraph term for mth-order subgraphs, m_{n_S} is the number of mth-order subgraphs and δ is the connectivity level vertex value or the valence level vertex value given to the atoms.

Correlation between retention and molecular connectivity indices

The Macintosh StatView 512+ procedure was used for determining the index best describing retention, using linear regression analysis. The coumarins were divided into two groups according to their retention behaviour with reference to connectivity indices: group I (compounds **3, 6, 8** and **10**; see Fig. 1) and group II (compounds **1, 2, 3, 4, 5, 6, 7** and **9**; see Fig. 1).

RESULTS AND DISCUSSION

Retention measurements were carried out on the closely related coumarins in volume fractions (φ) acetonitrile (54–42%), dioxane (52–42%), ethanol (46–36%), methanol (69–54%), 1-propanol (38–24%) and THF (36–28%), each in six steps, by decreasing the amount of organic solvent in water by 1–4% (v/v).

The retention orders of the eluates in six different organic solvent–water mixtures are presented in Fig. 2 and Table I. The capacity factors (k') in Table I were calculated from the equation $k' = (t_R - t_0)t_0$, where t_R is the retention time of the compound and t_0 is the dead volume. The volume fraction of each organic solvent was chosen such that k' of the last-eluted peak remained nearly the same, irrespective of the solvent used. The retention order of the compounds varied considerably in different solvents; only compound **10** was consistently the last-eluted compound. Acetonitrile showed great opposing shifts for some compounds, *e.g.*, **4** and **7**. Compounds **1** and **2** were unresolved with ethanol but, when injected separately, **2** was eluted first. The same occurred with acetonitrile. With THF and ethanol **4** and **5** were unresolved, whereas **1**, **2** and **3** separated in this order. Compounds **1** and **2**, **4** and **5** and **8** and

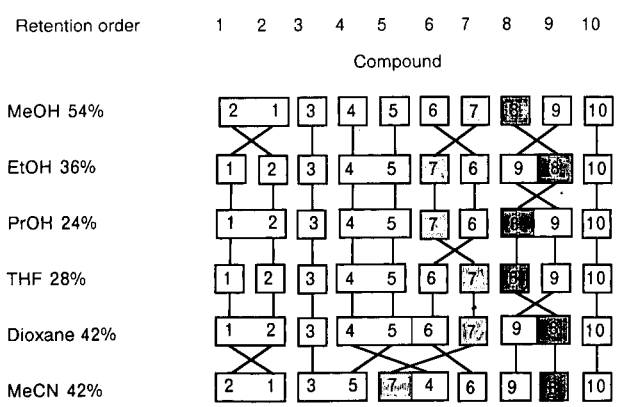

Fig. 2. Retention order of ten coumarins in six organic solvent–water mixtures using isocratic runs with Spherisorb ODS 2 as the stationary phase (compound numbers, see Fig. 1). The concentrations were chosen so that the capacity factor (k') of the last-eluting peak in all mobile phases was *ca.* 25. The compound was regarded to elute in the same peak if the resolution (R_s) was < 1.1. MeOH = Methanol; EtOH = ethanol; PrOH = propanol; THF = tetrahydrofuran; MeCN = acetonitrile.

TABLE I

CAPACITY FACTORS, k', OF THE COUMARINS IN SIX ORGANIC SOLVENT WATER MIXTURES

For compounds see Fig. 1.

Compound	k'					
	Methanol (54%)	*Ethanol (36%)*	*1-Propanol (24%)*	*THF (28%)*	*Dioxane (42%)*	*Acetonitrile (42%)*
1	0.83	0.51	0.55	0.73	0.44	0.53
2	0.55	0.86	0.60	1.13	0.50	0.47
3	2.44	2.08	1.12	1.95	1.45	2.16
4	2.85	2.69	1.90	2.53	1.66	3.00
5	3.55	2.79	2.28	3.02	1.87	2.23
6	4.30	4.69	3.53	4.77	2.11	4.52
7	5.11	3.99	2.73	8.53	3.40	2.95
8	11.86	11.70	9.22	9.67	7.25	9.87
9	15.61	11.60	9.31	10.94	7.18	8.28
10	24.10	22.05	16.23	17.67	16.48	15.35

9 were unresolved with 1-propanol. THF, 1-propanol and acetonitrile were selected as the most interesting solvents for further studies.

The effect of changing φ on the separation factor (α) was investigated in the six solvents. α-1 was defined as k'_2/k'_1, where k'_2 is the capacity factor for the second-eluting peak and k'_1 that for the first-eluting peak, and similarly α-2 = k'_3/k'_2, etc. Fig. 3 shows this effect in THF, 1-propanol and acetonitrile. The change in volume fraction in 1-propanol from 0.24 to 0.27 had the greatest influence on the separation of most of the compounds. However, α-8 and α-5 remained the same or decreased throughout the whole range of φ values. In THF the effect of φ was less than that in 1-propanol, although α-6 and α-5 increased more strongly from 1.4 to 1.7 and from 1.1 to 1.45, respectively. Increasing the amount of acetonitrile improved α to some extent. α-2 remained high throughout the change in φ, *i.e.*, 3.5–4.1.

Table II shows the experimentally obtained solvent strength (S_T) values. S_T values were calculated from observed capacity values using five or six concentrations of the organic solvents (Table I). S_T values were derived from the equation $\log k' = \log k'_w - S_T\varphi$, where k'_w represents the capacity factor of a solute with pure water as mobile phase[8]. The mean S_T values for the solvents varied between 2.8 and 5.3, ethanol having the lowest and THF the highest value. The S_T values obtained here are in good agreement with the values presented elsewhere[6,8–11]. However, the obtained S_T values were strongly dependent on the compounds used in calculating them. The calculated S_T values were used for the solvents when forming the "PRISMA".

As none of the six organic solvents gave a baseline separation in isocratic runs three solvents were selected for further optimization of the mobile phase by the "PRISMA" model[7]. THF, 1-propanol and acetonitrile were chosen on the basis of their effect on the retention order and α for further studies with "PRISMA" (see Fig. 4).

Three selectivity points (P_s), 118, 181 and 811, were chosen for further

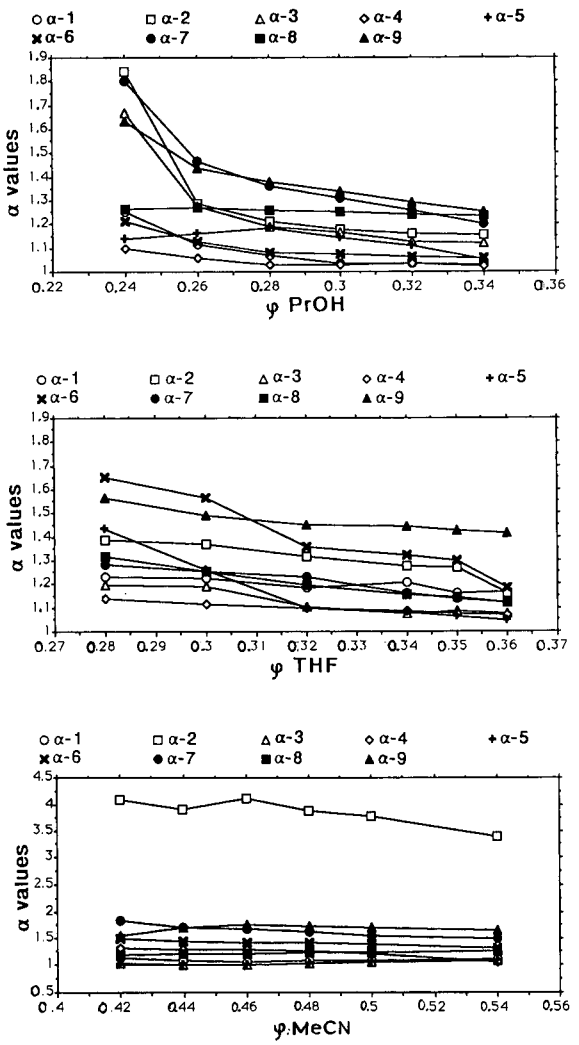

Fig. 3. Effect of the volume fraction (φ) on the separation factor (α).

optimization of isocratic runs according to "PRISMA" with $S_T = 1.4$. The separation in isocratic runs at any of the P_s was not good. The possibility of carrying out gradient runs was therefore studied. In isocratic runs THF alone proved to be the most promising solvent for obtaining an excellent separation (Fig. 5a). THF was therefore tested in a binary linear gradient run (Fig. 5b). The separation was better than that in the isocratic run, but was still not a baseline separation, especially for **4** and **5** [$R_s = 0.82$; $R_s = 2(t_2 - t_1)/(w_2 + w_1)$, where t_2 is the retention time for the later eluting compound and t_1 that for the earlier eluting compound, w_2 is the peak width for the later eluting compound and w_1 that for the earlier eluting compound]. Compound **10** was eluted with some impurities that interfered with the separation and made the

TABLE II

SOLVENT STRENGTH (S_T) VALUES CALCULATED FROM OBSERVED k' VALUES USING 5–6 CONCENTRATIONS OF THE ORGANIC SOLVENTS

S_T values were derived from $\log k' = \log k'_w - S_T\varphi$, where k'_w represents the capacity factor of a solute with pure water as mobile phase.

Compound	S_T					
	Methanol	*Ethanol*	*1-Propanol*	*THF*	*Dioxane*	*Acetonitrile*
1	1.18	0.58	1.95	2.25	1.30	2.11
2	2.17	0.41	1.77	3.12	1.32	2.15
3	2.76	2.00	2.31	3.96	2.94	2.76
4	3.09	2.22	3.43	4.70	3.10	3.04
5	2.95	2.25	3.45	5.05	2.96	2.46
6	2.91	3.16	3.38	7.34	2.97	3.20
7	2.95	3.01	4.22	7.96	3.74	3.25
8	4.19	4.27	6.94	6.32	4.46	3.60
9	4.88	4.59	5.52	6.03	4.67	3.82
10	4.96	5.08	7.17	6.25	5.94	3.54
Mean	3.20	2.76	4.01	5.30	3.34	2.99
Standard deviation	1.18	1.58	1.94	1.83	1.44	0.61

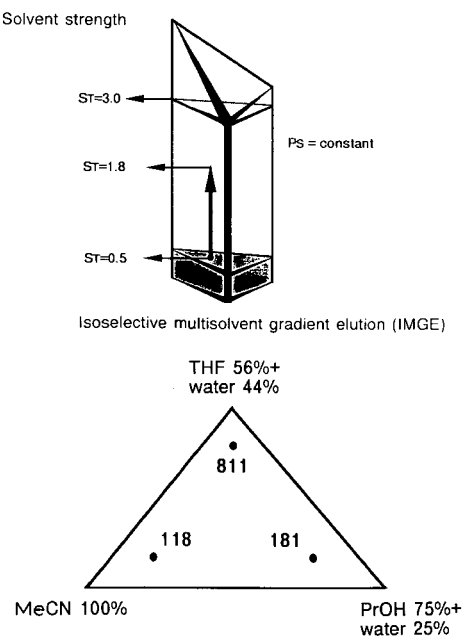

Fig. 4. The "PRISMA" model applied in this study.

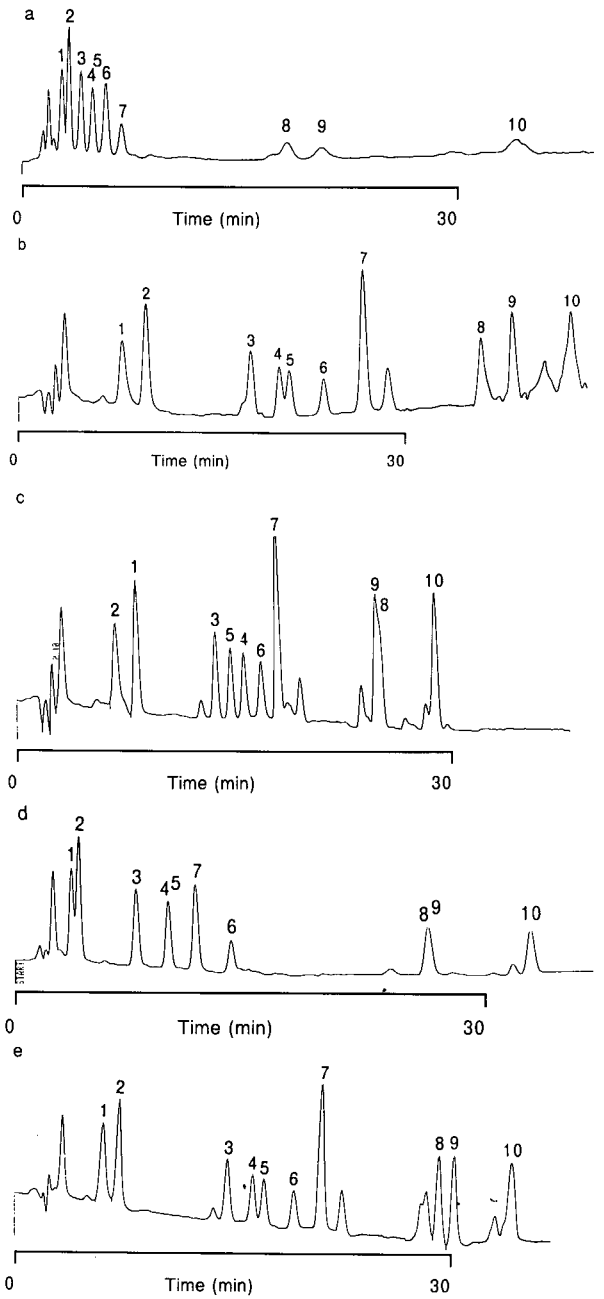

Fig. 5. Separations of the studied coumarins in *A. archangelica*; for compounds, see Fig. 1. Other analytical conditions see Experimental. (a) THF, isocratic run at $S_T = 1.4$; (b) THF, gradient run, S_T from 0.5 to 1.8 in 30 min; (c) IMGE at $P_S = 118$ (THF, 1-propanol, acetonitrile), S_T from 0.5 to 1.8 in 30 min; (d) IMGE at $P_S = 181$, S_T from 0.5 to 1.8 in 30 min; (e) IMGE at $P_S = 811$, S_T from 0.5 to 1.8 in 30 min.

quantitative determination inaccurate. This is the reason why the previously mentioned three P_s values were tested in linear gradient runs (Fig. 5c, d and e). The gradient used here was so-called isoselective multi-gradient elution (IMGE), where the selectivity point remains the same in the gradient run but the solvent strength is changed (Fig. 4)[12]. As can be seen, IMGE at P_s 811 and S_T from 0.5 to 1.8 in 30 min gave an excellent baseline separation of the compounds (Fig. 5e). IMGE was necessary owing to the difference in the polarities of the compounds.

The correlation between indices describing the molecular structure and retention in isocratic and gradient runs was studied. The retention was correlated with the molecular connectivity level (χ_p) and valence level (χ_p^v) indices for the path type through to the sixth order. The connectivity and valence level indices for the cluster (χ_c, χ_c^v) and path/cluster (χ_{pc},χ_{pc}^v) types were calculated to the fourth order. The compounds were divided into two groups on the basis of their different behaviour in HPLC (see Experimental for groups I and II).

The indices best describing the retention in isocratic runs are presented in Table III. The index best describing the retention for group I was ${}^4\chi_p$ (Table IV). Group II was best described in most of the eluents by a valence level index *i.e.*, ${}^4\chi_{pc}^v$ (Table IV). In THF ${}^2\chi^v$ and in acetonitrile ${}^3\chi_p$ were selected as best describing the retention (Table IV). The correlation for the solvents showed r values ranging from 0.93 to 0.98. The regression equations are given in Table IV as $k' = A\chi + B$, where A is the slope and B the intercept of the regression curve. A correlation coefficient of 0.95 ($2p < 0.0001$) was achieved (Fig. 6) when correlating the experimental k' values obtained from the isocratic runs with pure solvents with calculated k' values obtained from the equations in Table IV and indices from Tabe III. In isocratic runs the retention can be well predicted. This has also been shown by Vuorela and Lehtonen[13] for eight furocoumarins.

The correlation between retention and the molecular connectivity indices in gradient runs has not been studied very much. It was investigated here for three solvents, THF, acetonitrile and 1-propanol, with S_T changing from 0.5 to 1.8. The observed k' values are shown in Table V. In all three solvents the index ${}^4\chi_{pc}^v$ showed the

TABLE III

MOLECULAR CONNECTIVITY INDICES BEST DESCRIBING THE RETENTION OF THE CLOSELY RELATED COUMARINS

Compound	${}^3\chi_p$	${}^4\chi_p$	${}^2\chi^v$	${}^4\chi_p^v$	${}^4\chi_{p_c}^v$
1	5.01	4.02	2.82	1.25	0.67
2	4.14	3.36	2.78	1.27	0.43
3	6.20	5.54	3.42	1.79	0.76
4	6.98	6.40	3.73	2.08	0.85
5	5.49	4.79	3.07	1.57	0.67
6	6.20	5.59	3.41	1.83	0.82
7	6.92	6.08	5.32	2.09	1.17
8	7.05	6.12	4.81	2.03	0.98
9	10.07	7.80	7.04	2.65	2.04
10	7.22	6.29	4.80	2.06	1.01

TABLE IV

REGRESSION COEFFICIENTS FOR EQUATIONS OF THE TYPE $k' = A\chi + B$ IN SIX ORGANIC SOLVENTS

Coefficient	*Methanol (54%)*		*Ethanol (36%)*		*1-Propanol (24%)*		*THF (28%)*		*Dioxane (42%)*		*Acetonitrile (42%)*	
	I[a]	*II*[a]	*I*	*II*	*I*	*II*	*I*	*II*	*I*	*II*	*I*	*II*
A	24.40	9.35	22.40	6.69	17.10	5.38	17.19	2.36	16.96	4.28	15.10	1.32
B	−132.93	−4.26	−121.72	−2.55	−93.14	−2.23	−92.64	−5.13	−93.03	−1.64	−80.94	−5.39
r	0.94	0.97	0.95	0.95	0.96	0.94	0.95	0.95	0.93	0.98	0.97	0.93
Index χ	$^{4}\chi_{p}$	$^{4}\chi^{v}_{pc}$	$^{4}\chi_{p}$	$^{4}\chi^{v}_{pc}$	$^{4}\chi_{p}$	$^{4}\chi^{v}_{pc}$	$^{4}\chi_{p}$	$^{2}\chi^{v}$	$^{4}\chi_{p}$	$^{4}\chi^{v}_{pc}$	$^{4}\chi_{p}$	$^{3}\chi_{p}$

[a] Groups I and II (see text).

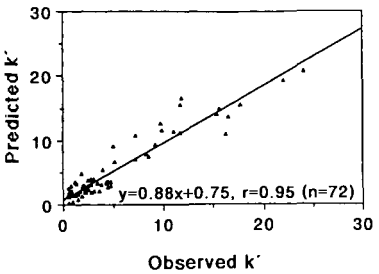

Fig. 6. Plot of the observed and predicted capacity factors (k') for isocratic runs. The predicted values were calculated from equations of the type $k' = A\chi + B$ (see Table IV).

best correlation for group I (Table VI). The indices of the type $^4\chi_p$ best correlated with retention in acetonitrile and 1-propanol for compounds in group II, whereas in THF the $^4\chi_p^v$ indices best described the retention. The correlation for the solvents showed r values from 0.91 to 0.99. The regression equations are given in Table VI as

TABLE V

CAPACITY FACTORS, k', OF THE COUMARINS IN THREE ORGANIC SOLVENT–WATER MIXTURES AND SELECTIVITY POINTS IN GRADIENT RUNS

Compound	k'					
	THF	*1-Propanol*	*Acetonitrile*	$P_s = 811$	$P_s = 181$	$P_s = 118$
1	5.14	0.81	2.87	3.58	1.72	5.87
2	6.56	1.20	2.69	4.51	2.05	4.12
3	12.65	5.64	9.46	10.07	4.82	9.31
4	14.42	7.08	12.17	11.40	6.37	10.79
5	14.88	7.08	9.46	11.98	6.37	10.12
6	16.88	9.00	13.82	13.66	9.43	10.67
7	19.31	7.98	12.17	15.11	7.69	12.53
8	26.19	22.68	17.80	21.14	18.91	17.93
9	23.08	22.68	17.08	22.05	18.91	17.70
10	31.53	25.34	20.74	25.18	23.92	20.80

TABLE VI

REGRESSION COEFFICIENTS FOR EQUATIONS OF THE TYPE $k' = A\chi + B$ IN THE THREE ELUENTS FOR GRADIENT RUNS

Coefficient	*THF*		*1-Propanol*		*Acetonitrile*	
	I[a]	*II*[a]	*I*	*II*	*I*	*II*
A	56.61	12.27	31.64	2.92	39.01	3.40
B	−32.72	−10.47	−15.32	−7.38	−19.16	−8.48
r	0.99	0.94	0.91	0.91	0.97	0.93
Index χ	$^4\chi_{pc}^v$	$^4\chi_p^v$	$^4\chi_{pc}^v$	$^4\chi_p$	$^4\chi_{pc}^v$	$^4\chi_p$

[a] Groups I and II (see text).

TABLE VII

REGRESSION COEFFICIENTS FOR EQUATIONS OF THE TYPE $k' = \Sigma\Pi(A\chi+B)$ AT THREE DIFFERENT SELECTIVITY POINTS IN IMGE RUNS

These equations are calculated on the basis of the equations in Table VI.

Coefficient	$P_s = 118$		$P_s = 181$		$P_s = 811$	
	I[a]	*II*[a]	*I*	*II*	*I*	*II*
A	40.03	10.21	34.87	9.23	52.35	11.70
B	−20.13	− 8.49	−17.44	−7.75	−29.62	− 9.95
r	1.00	1.00	1.00	1.00	1.00	1.00
Index χ	$^4\chi^v_{pc}$	$^4\chi^v_p$	$^4\chi^v_{pc}$	$^4\chi^v_p$	$^4\chi^v_{pc}$	$^4\chi^v_p$

[a] Groups I and II (see text).

$k' = A\chi + B$. A correlation coefficient of 0.91 ($2p < 0.0001$) was achieved when correlating the experimental k' values obtained from the gradient runs with pure solvents (THF, 1-propanol and acetonitrile) with calculated k' values obtained from the equations in Table IV. In the gradient runs the retention could be well predicted. This is in good agreement with results obtained by Lehtonen[14] for amines.

The retention of the coumarins was estimated for the IMGE run at the selectivity points (P_s) 118, 181 and 811 using regressions obtained with pure solvents. The capacity factors were calculated from the regression curves of the type $k' = A\chi + B$ shown in Table VI and it follows at the different selectivity points of $k' = \Sigma\Pi(A\chi + B)$, where Π is the fraction of the solvent used in forming the "PRISMA", when assuming that a linear correlation for retention between different selectivity points exists (Table VII). Fig. 7 demonstrates the efficiency of the method for calculating the k' values at different selectivity points within the "PRISMA" based on the retention information at the "PRISMA" edges, *i.e.*, gradient runs with THF, 1-propanol and acetonitrile only. The correlation between the calculated and measured k' values (Table V) at $P_s = 811$ is highly significant ($2p < 0.0001$) with a correlation coefficient of 0.97 in regression analysis (Fig. 8). The existence of the same relationship at other selectivity points was also tested using factor analysis. Table VIII shows the orthogonal transformation solution varimax with two factors. It shows clearly that when the measured retention of the compounds correlates with the measured retention at

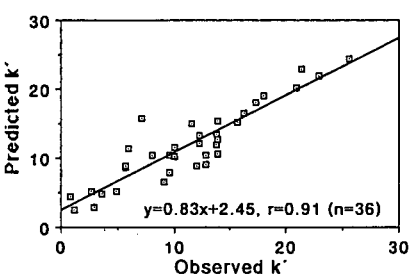

Fig. 7. Plot of the observed and predicted capacity factors (k') for gradient runs. The predicted values were calculated from equations of the type $k' = A\chi + B$ (see Table VI).

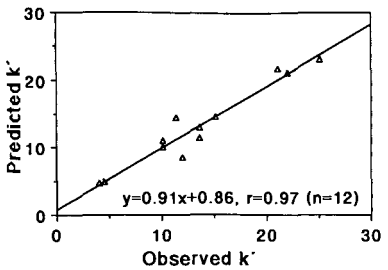

Fig. 8. Plot of the observed and predicted capacity factors (k') for the IMGE runs at P_S = 811 and S_T = 0.5–1.8 in 30 min. The predicted values were calculated from equations of the type $k' = \Sigma\Pi(A\chi + B)$ (see Table VII).

TABLE VIII

DEPENDENCE BETWEEN OBSERVED AND CALCULATED k' VALUES AT THE SELECTIVITY POINTS TESTED WITH FACTOR ANALYSIS USING THE ORTHOGONAL TRANSFORMATION SOLUTION VARIMAX WITH TWO FACTORS

Value[a]	*Factor 1*	*Factor 2*
Obs (P_S = 118)	0.985	0.131
Obs (P_S = 181)	0.964	0.078
Obs (P_S = 811)	0.039	0.996
Calc (P_S = 118)	0.968	0.180
Calc (P_S = 181)	0.963	0.205
Calc (P_S = 811)	0.240	0.967

[a] Obs = Observed k' values, Calc = calculated k' values at the indicated P_S.

different P_S, a correlation also exists between the calculated values at different P_S. When the retention at a certain P_S is not correlated with that at different P_S, then there is only the tie between the measured and calculated retention at a certain P_S.

CONCLUSIONS

A baseline separation between the ten coumarins was achieved using the "PRISMA" model in the optimization of the mobile phase. The retention of coumarins under different HPLC conditions correlated well with the indices describing molecular structure. The retention could be well predicted for the different selectivity points in the "PRISMA" using the molecular connectivity indices.

ACKNOWLEDGEMENTS

We thank Dr. Sz. Nyiredy, Swiss Federal Institute of Technology (ETH), Zürich, for very fruitfull discussions. This work was supported by a grant from the Finnish Cultural Foundation.

REFERENCES

1 P. Lehtonen, *Chromatographia*, 19 (1984) 316.
2 M. J. M. Wells, C R. Clark and R. M. Patterson, *Anal. Chem.*, 58 (1986) 1625.
3 J. Burda, M. Kuras, J. Kriz and L. Vodicka, *Fresenius Z. Anal. Chem.*, 321 (1985) 549.
4 M. Randic, *J. Am. Chem. Soc.*, 97 (1975) 6609.
5 L. B. Kier and L. H. Hall, *Molecular Connectivity in Chemistry and Drug Research*, Academic Press, London, 1976.
6 P. Lehtonen, *Academic Dissertation*, University of Helsinki, Helsinki, 1987.
7 Sz. Nyiredy, *Application of the "PRISMA" Model for the Selection of Eluent Systems in Over-Pressure Layer Chromatography (OPLC)*, Labor MIM, Budapest, 1987.
8 L. R. Snyder, J. W. Dolan and J. R. Gant, *J. Chromatogr.*, 165 (1979) 3.
9 J. W. Dolan, J. R. Gant and L. P. Snyder, *J. Chromatogr.*, 165 (1979) 31.
10 T. Braumann, G. Weber and L. H. Grimme, *J. Chromatogr.*, 261 (1983) 329.
11 S.D. West, *J. Chromatogr. Sci.*, 27 (1989) 2.
12 Sz. Nyiredy and O. Sticher, *J. High Resolut. Chromatogr. Chromatogr. Commun.*, 10 (1987) 208.
13 H. Vuorela and P. Lehtonen, *J. Liq. Chromatogr.*, 12 (1989) 221.
14 P. Lehtonen, *Z. Lebensm.-Unters.-Forsch.*, 183 (1986) 177.

Journal of Chromatography, 507 (1990) 381–387
Elsevier Science Publishers B.V., Amsterdam — Printed in The Netherlands

CHROMSYMP. 1738

Determination of warfarin in drinking water by high-performance liquid chromatography after solid-phase extraction

JOHAN DALBACKE*, IRENE DAHLQUIST and CHRISTIANE PERSSON
Analytical and Quality Development Department, Gacell Laboratories AB, P.O. Box 839, S-201 80 Malmö (Sweden)

SUMMARY

A method for the determination of 0.1 μg/l of warfarin in drinking water involving concentration by solid-phase extraction is described. A 1000-ml volume of drinking water is aspirated through a solid-phase extraction column and warfarin is eluted to 1.0 ml. The eluate is analysed by reversed-phase high-performance liquid chromatography with UV detection. The detection limit is 0.02 μg/l. Recoveries of greater than 90% were obtained when tap water was spiked with warfarin.

INTRODUCTION

Warfarin, 4-hydroxy-3-(3-oxo-1-phenylbutyl)coumarin, is used both as an anticoagulant in man and as a rodenticide. The concentration of warfarin in drinking water must not exceed 0.1 ppb (0.1 μg/l) according to the European Communities guidelines[1]. A method that can detect warfarin at levels down to at least 0.1 ppb was therefore required.

Various techniques have been applied to the determination of warfarin, including gas chromatography[2] and high-performance liquid chromatography (HPLC)[3–9]. HPLC has been used in both normal-phase[3] and reversed-phase modes[4–9]. Wang and Bonakdar[4] used HPLC with electrochemical detection and obtained a detection limit of 40 ppb. Lee *et al.*[5] published an HPLC method with fluorimetric detection. The limit of detection was 18 ppb, and 1.8 ppb when a concentration step was used. Fasco *et al.*[6] described a method for the determination of warfarin and its metabolites in plasma, using solid-phase extraction and HPLC with UV detection. The limit of detection was 30 ppb.

We have developed a method that has a detection limit of 0.02 ppb. Solid-phase extraction with an enrichment factor of 1000 is used prior to analysis by reversed-phase HPLC with UV detection.

0021-9673/90/$03.50

EXPERIMENTAL

Chemicals and reagents

HPLC-grade methanol and acetonitrile were obtained from Labscan (Dublin, Ireland), glacial acetic acid, phosphoric acid (min. 85%) and potassium hydrogenphosphate from Merck (Darmstadt, F.R.G.) and sodium hydroxide from Eka Nobel (Surte, Sweden). The water used to prepare the mobile phase and all aqueous solutions was purified using a Milli-Q water purification system from Millipore (Bedford, MA, U.S.A.). Amorphous sodium warfarin of USP quality was provided as a gift by Chemoswed (Malmö, Sweden).

Extraction columns and vacuum apparatus

Bond-Elut octadecyl-(C_{18}, 200 mg, 3 ml), ethyl-(C_2, 500 mg, 2.8 ml) and phenyl-(PH, 500 mg, 2.8 ml) bonded silica columns were obtained from Analytichem International (Harbor City, CA, U.S.A.). The columns were used with a Vac-Elut 10 sample-processing station from Analytichem International.

Chromatographic equipment

The HPLC system consisted of a Model 590 solvent-delivery pump and a WISP Model 712 autosampler, both from Waters Assoc. (Milford, MA, U.S.A.). A Waters Assoc. Lambda-Max Model 481 variable-wavelength LC spectrophotometer, a Waters Assoc. Model 490 programmable multi-wavelength detector and a Hewlett-Packard (Waldbronn, F.R.G.) Model HP 1046A programmable fluorescence detector were used. A Spectra-Physics (San Jose, CA, U.S.A.) Model SP4270 integrator was used to record chromatograms and calculate peak heights. A Spectra-Physics ChromStation-AT was used for data handling and storage. An HP 79994A HPLC ChemStation was used together with the fluorescence detector.

Standard solution

A solution containing 1 mg/ml of warfarin in deionized water was prepared. This solution was diluted to a concentration of 0.1 μg/ml with acetonitrile–0.04 *M* phosphate buffer (pH 7.4) (1:1).

Extraction procedure

Drinking water and drinking water spiked with 0.1 ppb of warfarin were allowed to stand for 24 h before being acidified to pH 4.3 with acetic acid. Warfarin was extracted from the water using octadecyl-bonded silica columns (Bond-Elut C_{18}, 200 mg, 3 ml). The columns were held in a Vac-Elut 10 processing station operated at 10 in.Hg pressure. The columns were conditioned with 5 ml of acetonitrile followed by 5 ml of water (pH adjusted to 4.3 with acetic acid). A small volume of water was left in each column to prevent the sorbent from drying before the samples were applied. PTFE tubes of 1/8 in. I.D. were immersed in the sample solutions and connected to Bond-Elut adaptors. The siphon effect was used to fill the columns with sample solutions. The Bond-Elut adaptors were connected to the columns and 1000 ml of the sample solutions were aspirated through the columns by vacuum. The columns were washed with 20 ml of acetonitrile–water (pH 4.3) (20:80). Warfarin was eluted with acetonitrile–0.04 *M* phosphate buffer (pH 7.4) (1:1) to 1.0 ml.

Chromatography

The standard solution and the eluates from the solid-phase extraction columns were analysed by reversed-phase HPLC on a 150 × 3.9 mm I.D. Nova-Pak C_{18} (4 μm) column (Waters Assoc.). The mobile phase was prepared by mixing 620 ml of methanol, 380 ml of water and 10 ml of glacial acetic acid. The mixture was filtered through a 0.45-μm nylon-66 membrane filter and degassed before use. The flow-rate was 1.0 ml/min and the column temperature was ambient. The injection volume was 30 μl. Warfarin was detected at both 282 and 306 nm. Quantification was based on peak heights. Before use, a number of suitability tests were performed in order to evaluate the chromatographic system. The standard solution was injected six times. The number of theoreticl plates (n) and the tailing factor (T) were calculated according to USP XXI[10]. Typical values of n were in the range 3000–3100 and of T in the range 1.3–1.6. The relative standard deviation of the peak heights of warfarin from six successive injections was also calculated. Typical values were in the range 1.2–3.0%.

The eluate from the drinking water was injected and the peak height of warfarin was compared with that obtained when the standard solution was injected directly. The peak height of warfarin from spiked drinking water was compared with that obtained when the standard solution was injected directly and with that of the eluate from unspiked drinking water, in order to establish the recovery of warfarin from the drinking water in question.

RESULTS AND DISCUSSION

Solid-phase extraction

Solid-phase extraction columns with different phases (octadecyl-, ethyl- and phenyl-bonded silica) were tested. Use of the ethyl column gave eluates that were as clean as those from the octadecyl column, whereas the eluates from the phenyl column were not as clean. The recoveries were identical with all the columns. Octadecyl-bonded silica columns were used in all subsequent experiments. Washing of the extraction columns prior to elution was necessary in order to obtain suffciently clean eluates. Volumes of 5 ml of different concentrations (10–40%) of acetonitrile in acidified water (pH 4.3) were used to wash the extraction columns after sample application. Warfarin was eluted when an acetonitrile concentration higher than 25% was used. Different volumes (5–20 ml) of 20% acetonitrile in acidified water (pH 4.3) were used for the column washing. All volumes gave the same recovery of warfarin, but the chromatograms were cleaner when 20 ml was used instead of 5 ml.

An additional wash with a mixture of dichloromethane in hexane was tested. The sorbent was dried for 5 min before hexane was sucked through the column and then mixtures of dichloromethane in hexane. A wash with 5 ml of dichloromethane–hexane (5:95) resulted in elution of 50% of the warfarin. It was possible to wash with 1 ml of dichloromethane–hexane (5:95) without warfarin being eluted. However, the eluates were no cleaner when this additional wash was used.

Chromatograms of the standard solution injected directly and of spiked tap water analysed according to the described method are shown in Fig. 1. Chromatograms are shown both with and without the washing procedure. The typical retention time of warfarin was 5.0 min.

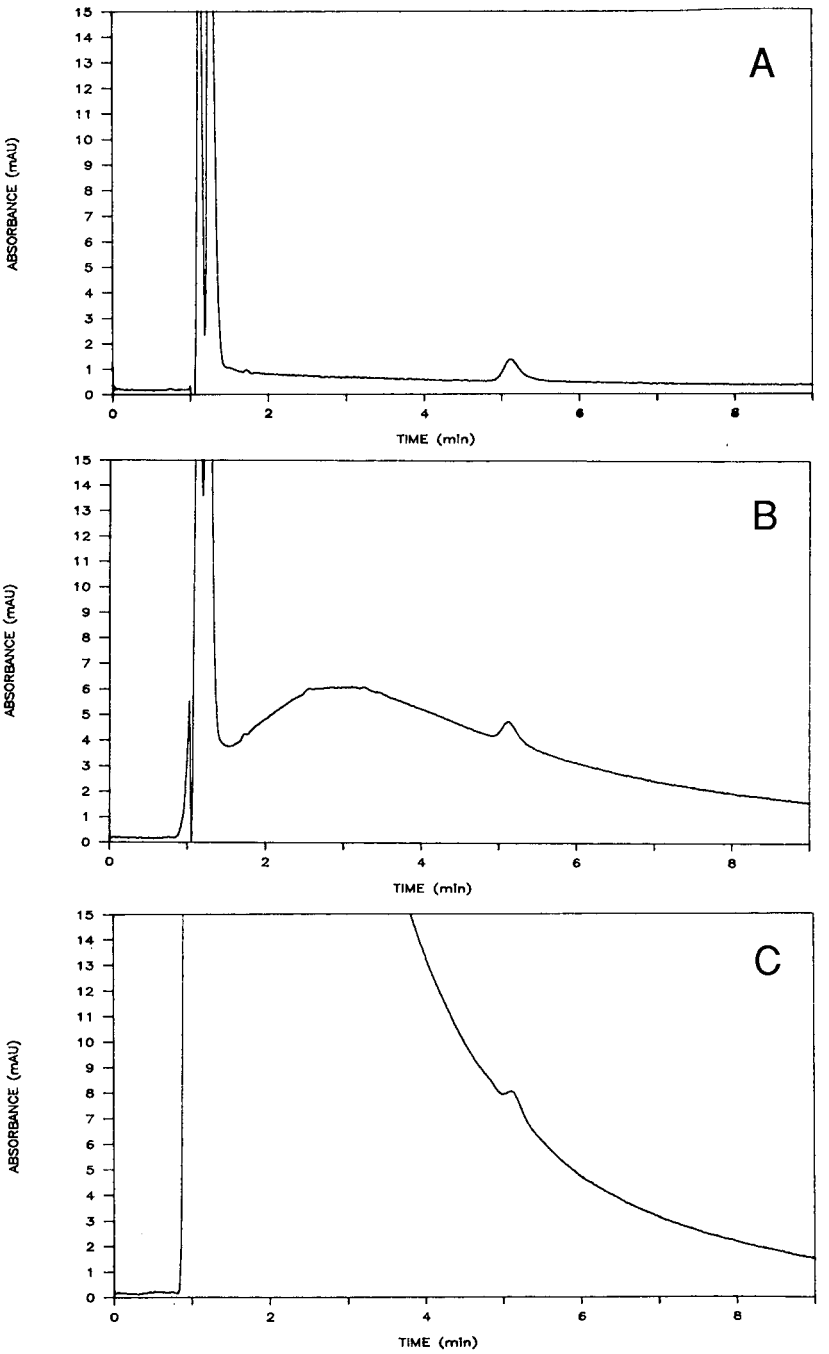

Fig. 1. Chromatograms of (A) the standard solution injected directly and of eluates of tap water spiked with 0.1 ppb of warfarin, (B) with the washing procedure and (C) without washing. Details of the washing procedure for the solid-phase extraction columns and the HPLC conditions are given under Experimental.

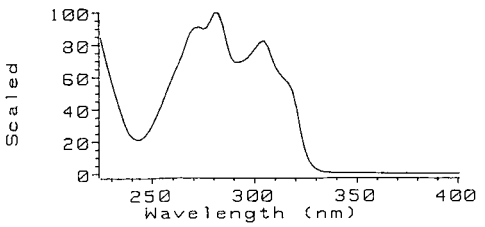

Fig. 2. UV spectrum of warfarin dissolved in mobile phase.

Detection

A UV spectrum of warfarin dissolved in the mobile phase is shown in Fig. 2. Warfarin showed UV absorption maxima at 272, 282 and 306 nm. It was deteced at both 282 and 306 nm and the absorbance ratio was used to confirm the identity of the warfarin peak; the ratio obtained was 1.2.

Fluorimetric detection was tested to see whether a lower detection limit could be achieved. A lower detection limit would mean that smaller volumes of the sample solution could be applied to the solid-phase extraction column. Lee *et al.*[5] reported that the fluorescence of warfarin was quenched under acidic conditions. The mobile phase used in our method was acidic. A post-column acid–base manipulation procedure to enhance the fluorescence of warfarin has been described[5,9]. In order to increase the pH we used a post-column pump that added 1.0 ml/min of methanol–0.5 *M* sodium hydroxide (60:40) to the column effluent through a Valco low-dead-volume T-piece. Warfarin was injected and trapped in the flow cell of the detector by stopping the flow. Excitation and emission scans were collected. Warfarin had three excitation wavelength maxima, at 241, 290 and 328 nm. The emission wavelength maximum was about 386 nm for the three excitation wavelengths. An excitation wavelength of 241 nm gave the highest fluorescence. The limit of detection for warfarin was about the same when fluorimetric detection was used instead of UV detection. It was surprising that fluorimetric detection did not give a lower limit of detection. However, the chromatographic parameters were not optimized for fluorimetric detection. A higher degree of selectivity and a more reliable peak identification are possible advantages of fluorimetric detection.

Validation of the method

The linearity was determined by analysing solutions of warfarin in deionized water with concentrations between 0.02 and 0.30 ppb. Warfarin was concentrated by solid-phase extraction, the eluates were injected onto the HPLC column and the warfarin peak heights were measured. The regression line was calculated by the method of least squares. The results from the linear regression analysis are given in Table I.

The peak height was linear between 0.02 and 0.30 ppb at both wavelengths. A solution of 0.02 ppb of warfarin in deionized water gave a peak with a signal-to-noise ratio of 3. Hence it follows that the detection limit of the method was 0.02 ppb.

The precision and accuracy were determined by spiking tap water with sodium warfarin to give concentrations of 0.05, 0.10 and 0.20 ppb of warfarin and analysing these solutions according to the method on each of three days. The results obtained are

TABLE I

LINEAR REGRESSION ANALYSIS

Parameter	*282 nm*	*306 nm*
Slope	5964	5344
Intercept	5.6	−6.7
Correlation coefficient	0.9995	0.9997

given in Table II. The relative standard deviation of the results for each concentration ranged from 4 to 13%. The highest value was obtained for the lowest concentration. The mean recovery for each concentration ranged from 97 to 103%.

In conclusion, the method was found to be selective, linear, precise and accurate.

TABLE II

PRECISION AND ACCURACY

Concentration (ppb)	*282 nm*			*306 nm*		
	Recovery (%)	*Mean recovery (%)*	*R.S.D.*[a] *(%)*	*Recovery (%)*	*Mean recovery (%)*	*R.S.D.*[a] *(%)*
0.05	92	100	13	92	103	11
	87			114		
	111			102		
0.10	100	100	4	94	97	9
	104			106		
	96			90		
0.20	94	99	5	98	99	5
	104			104		
	99			94		

[a] Relative standard deviation.

ACKNOWLEDGEMENT

The authors thank Göran Oresten for valuable discussions.

REFERENCES

1 *EEC Drinking Water Guideline, 80/778/EEC, No. L229/11–29*, Commission of the European Communities, Brussels, August 30th, 1980.
2 S. Hanna, M. Rosen, P. Eisenberger, L. Rasero and L. Lachman, *J. Pharm. Sci.*, 67 (1978) 84–86.
3 R. A. R. Tasker and K. Nakatsu, *J. Chromatogr.*, 228 (1982) 346–349.
4 J. Wang and M. Bonakdar, *J. Chromatogr.*, 415 (1987) 432–437.
5 S. H. Lee, L. R. Field, W. N. Howald and W. F. Trager, *Anal. Chem.*, 53 (1981) 467–471.

6 M. J. Fasco, M. J. Cashin and L. S. Kaminsky, *J. Liq. Chromatogr.*, 2 (1979) 565–575.
7 L. T. Wong, G. Solomonraj and B. H. Thomas, *J. Chromatogr.*, 135 (1977) 149–154.
8 M. J. Fasco, L. J. Piper and L. S. Kaminsky, *J. Chromatogr.*, 131 (1977) 365–373.
9 J. M. Steyn and H. M. van der Merwe, *J. Chromatogr.*, 378 (1986) 254–260.
10 *United States Pharmacopeia, XXI Revision*, U.S. Pharmacopeial Convention, Rockville, MD, 1985, pp. 1228–1230.

Journal of Chromatography, 507 (1990) 389–398
Elsevier Science Publishers B.V., Amsterdam — Printed in The Netherlands

CHROMSYMP. 1720

Isolation of toxic polychlorinated biphenyls by electron donor–acceptor high-performance liquid chromatography on a 2-(1-pyrenyl)ethyldimethylsilylated silica column

PETER HAGLUND*
Department of Analytical Chemistry, University of Stockholm, S-106 91 Stockholm (Sweden)
and
LILLEMOR ASPLUND, ULF JÄRNBERG and BO JANSSON
Special Analytical Laboratory, National Environmental Protection Board, Box 1302, S-171 25 Solna (Sweden)

SUMMARY

A rapid and simple liquid chromatographic method for the isolation of toxic planar polychlorinated biphenyls from their formulations by electron donor–acceptor high-performance liquid chromatography using a 2-(1-pyrenyl)ethyldimethylsilylated silica column is described. The separation takes less than 15 min and a complete analysis, including quantitation by gas chromatography–mass spectrometry or gas chromatography with electron-capture detection, may be completed in 60 min.

Retention data for 105 individual polychlorinated biphenyl congeners are presented and the retention behaviour, as well as the mechanisms of separation, are discussed.

INTRODUCTION

Increasing attention is being centred on the toxicity of polychlorinated biphenyls (PCBs), especially on the congeners that show the same type of toxicity as polychlorinated dibenzo-*p*-dioxins (PCDDs) and dibenzofurans (PCDFs). The topic has been extensively reviewed by Safe[1]. Certain non-*ortho*-chlorinated PCBs (0-*ortho*-PCBs) show particulary high "dioxin-like" toxicity, *viz.* 3,3′,4,4′-tetrachlorobiphenyl (TeCB, IUPAC 77), 3,3′,4,4′,5-pentachlorobiphenyl (PeCB, IUPAC 126) and 3,3′,4,4′,5,5′-hexachlorobiphenyl (HxCB, IUPAC 169), which all are approximately isosteric with the extremely toxic 2,3,7,8-substituted PCDDs and PCDFs. Considerable toxicity is also attributed to some mono-*ortho*-chlorinated PCBs (1-*ortho*-PCBs), especially 2,3,3′,4,4′-PeCB (IUPAC 105), 2,3′,4,4′,5-PeCB (IUPAC 118) and 2,3,3′,4,4′,5-HxCB (IUPAC 157)[2].

To assess residue levels of these compounds in technical PCB formulations and environmental samples, comprehensive analytical methods are used. Most of the

0021-9673/90/$03.50

methods include activated charcoal columns to isolate toxic 0-*ortho*-PCBs[3–6]. Using the method of Jensen and Athanasiadou[6] it is also possible to isolate the 1-*ortho*-PCBs of interest. However, this method is very laborious since it requires the use of multiple charcoal column chromatography to obtain sufficient purity of the 0- and 1-*ortho* fractions. Furthermore, the activated charcoal columns have some serious drawbacks, such as low efficiency, elution profiles with severe tailing, irreversible adsorption, batchwise variations of the adsorbents, and difficulties in using UV detectors because aromatic mobile phases are used.

Recently, Fischer and Ballschmiter[7] reported that all the toxic 1-*ortho*-PCBs can be analysed in PCB mixtures and environmental samples by gas chromatography–mass spectrometry (GC–MS) using an SB-Octyl 50 fused-silica capillary column (Lee Scientific). However, this method does not allow the quantitation of 0-*ortho*-PCBs in technical PCB formulations, since the 0-*ortho*-PCBs are present at such low levels (μg/g of PCB) that it would be necessary to analyse enormous amounts of PCBs. This would exceed the loading limit of the GC column.

The aim of the present study was to investigate if electron donor–acceptor (EDA) high-performance liquid chromatography (HPLC) on a PYE column could be used to separate toxic 0- and 1-*ortho*-PCBs from PCB mixtures, and thereby make it possible to analyse these PCB congeners accurately and simply.

EXPERIMENTAL

Chemicals

All solvents used were of high purity, hexane was of HPLC grade (Rathburn, Walkerburn, U.K.) and isooctane and *n*-undecane were distilled.

Most of the individual PCB congeners used were provided by Dr. Åke Bergman (Wallenberg Laboratory, University of Stockholm). 2,2′,4,6-TeCB, 2,3′,5′,6-TeCB and 2,3,3′,4,4′,6-HxCB were gifts from Prof. Stephen Safe (Texas A&M University, U.S.A.) and [$^{13}C_{12}$]-labelled 3,3′,4,4′-TeCB, 3,3′,4,4′,5-PeCB and 3,3′,4,4′,5,5′-HxCB were purchased from Cambridge Isotope Laboratories (Woburn, MA, U.S.A.). All PCB congeners were dissolved in isooctane prior to use.

The two technical products investigated, Chlophen A50 and Halowax 1014, were produced by Bayer (F.R.G.) and Koppers Chemical (U.S.A.), respectively.

Liquid chromatography

The HPLC system consisted of a Waters 590 programmable solvent-delivery module, a Rheodyne 7125 injector equipped with a 20- or 50-μl loop, a Hitachi 655A-22 UV-absorbance detector and a 150 × 4.6 mm I.D. Cosmosil 5-PYE column [2-(1-pyrenyl)ethyldimethylsilylated silica gel, particle size 5 μm, Nacalai Tesque, Kyoto, Japan]. A PC-based laboratory data system was used to record, store, process and plot the data.

Gas chromatography

GC analysis was performed on a Hewlett-Packard 5890 equipped with a fused-silica capillary column (50 m × 0.20 mm I.D., 0.33 μm film thickness, 5% phenylmethylsilicone phase; Hewlett-Packard, Ultra 2), an electron-capture detector and a Nelson 2600 laboratory data system. Helium was used as carrier gas at

a flow-rate of 0.3 ml/min. The temperature programme was as follows: 70°C (4 min, 90 s splitless) to 180°C at 30°C/min, hold for 2 min, then to 300°C at 2°C/min, then isothermal for 10 min.

Gas chromatography–mass spectrometry

GC was performed on a Hewlett-Packard HP5890 equipped with the same type of column as above. Helium was used as carrier gas at a head pressure of 13 p.s.i. The oven was temperature-programmed from 90°C (2 min, 1 min splitless) to 200°C at 20°C/min, then to 280°C at 3°C/min, then isothermal for 15 min. A Hewlett-Packard HP5970B mass selective detector was used for the MS determination. It was controlled by a Hewlett-Packard HP59970A work-station. Electron impact (EI) ionization was performed with an electron energy of 70 eV, and an ion source and transfer line temperature of 290°C. The detector was turned in the selected ion monitoring (SIM) mode, and two of the most intense ions in each molecular ion cluster were monitored.

Methodology

Injections of 20 μl, containing 20–200 ng, of the PCB congeners listed in Table I were made within a three-day period. Hexane was used as the mobile phase at a flow-rate of 0.70 ml/min and the UV detector was set at 254 nm. Retention and dead times (measured at the front edge of the baseline dip caused by the injection) were recorded, and capacity factors (k') were calculated. To estimate the reproducibility of the k' measurements, 2,3,3′,4′,6-PeCB (IUPAC 110) was injected every tenth injection.

To investigate if the PYE column could be used to separate PCB mixtures into fractions containing mainly 2–4-*ortho*-PCBs, toxic 1-*ortho*-PCBs and toxic 0-*ortho*-PCBs, a technical PCB product, Chlophen A50, was fractionated.

Prior to fractionation, a window-defining mixture consisting of 2,3′,4,4′,5-PeCB, 3,3′,4,4′-TeCB and 3,3′,4,4′,5,5′-HxCB was injected. In accordance with the chromatogram obtained appropriate cutting points for the fractions were established. Following calibration, the injector was thoroughly rinsed with isooctane to ensure that no residual PCBs remained. Injections of 20 μl, containing 10, 50 and 250 μg of Chlophen A50, respectively, were made and fractions were collected according to Fig. 1.

The identification of the PCB congeners present in the fractions was based on the knowledge of the composition of the technical product and the retention order on the PYE column (fraction 1) as well as on comparisons of retention times and mass spectra with pure reference compounds (fractions 2 and 3).

Quantitative analysis of toxic 0-*ortho*-PCBs present in Chlophen A50 was also performed. A solution of 150 μg of Chlophen A50 in isooctane were spiked with 99.0 ng of [$^{13}C_{12}$]3,3′,4,4′-TeCB, 11.9 ng of [$^{13}C_{12}$]3,3′,4,4′,5-PeCB and 0.405 ng of [$^{13}C_{12}$]3,3′,4,4′,5,5′-HxCB, and 150 μl of *n*-undecane were added as a keeper. The solution was reduced to 150 μl with a gentle stream of nitrogen. The spiking levels corresponded to the indigenous levels of these congeners as reported by Jensen and Athanasiadou[6]. Four 25-μl aliquots of the solution were injected using a 50-μl loop, and fractions were collected as described above. Corresponding fractions were combined and reduced to 50 μl by a gentle stream of nitrogen, and 2-μl aliquots were analysed by GC–MS. The isotope dilution method was used for quantitation.

A technical polychlorinated naphthalene (PCN) product, Halowax 1014, has been characterized by charcoal fractionation on Amoco PX-21A, GC–MS and GC

TABLE I

INDIVIDUAL k' VALUES FOR SOME PCB CONGENERS ON A PYE COLUMN

The lines indicate the positions of the cutting points for the 1- and 0-*ortho*-PCB fractions, respectively. The chromatographic conditions are described under Experimental.

k'	*IUPAC No.*	*Structure*	k'	*IUPAC No.*	*Structure*
0.28	98	2 4 6–23	0.70	64	23 6– 4
0.30	155	2 4 6–2 4 6		135	23 5 –23 6
0.34	29	2 45 –		149	23 6–2 45
0.35	152	23 56–2 6	0.71	58	23 – 3 5
0.36	209	23456–23456		83	23 5 –23
0.37	207	23456–234 6		196	2345 –234 6
	197	234 6–234 6	0.72	84	23 6–23
0.38	10	2 6–	0.73	97	2 45 –23
	1	2 –	0.76	168	2 4 6– 345
0.39	7	2 4 –		201	2345 –23 56
0.40	9	2 5 –	0.77	153	2 45 –2 45
	50	2 4 6–2	0.78	85	234 –2 4
	200	234 6–23 56		171	234 6–234
0.41	2	3 –	0.80	61	2345 –
0.42	202	23 56–23 56		70	2 5 – 34 6
0.44	5	23 –	0.81	174	2345 –23
	12	34 –	0.82	80	3 5 – 3 5
0.46	30	2 4 6–	0.83	132	234 –23 6
	146	23 5 –2 45	0.84	87	234 –2 5
0.48	3	4 –		120	2 45 – 3 5
	69	2 4 6– 3		177	23 56–234
	75	2 4 6– 4		206	23456–2345
0.49	24	23 6–	0.85	82	234 –23
0.50	62	234 6–	0.86	66	2 4 – 34
	176	234 6–23 6	0.87	71	2 6– 34
0.53	102	2 45 –2 6		94	23 5 –2 6
0.54	47	2 4 –2 4	0.88	56	23 – 34
	53	2 5 –2 6	0.89	137	2345 –2 4
	165	23 56– 3 5	0.90	15	4 – 4
0.55	21	234 –	0.92	172	2345 –23 5
	73	2 6– 3 5	0.94	110[a]	23 6– 34
0.57	46	23 –2 6	0.98	107	23 5 – 34
	140	234 –2 4 6		180	2345 –2 45
0.59	49	2 4 –2 5	1.00	106	2345 – 3
0.60	31	2 5 – 4	1.04	122	345 –23
	42	23 –2 4		158	234 6– 34
0.61	28	2 4 – 4	1.09	123	345 –2 4
0.62	14	3 5 –	1.11	118	2 45 – 34
	52	2 5 –2 5	0.94	138	234 –2 45
	144	234 6–2 5	1.12	128	234 –234
0.63	72	2 5 – 3 5	1.19	159	2345 – 3 5
	183	234 6–2 45	1.24	194	2345 –2345
0.64	90	23 5 –2 4	1.26	193	23 56– 345
0.65	187	23 56–2 45	1.28	170	2345 –234
0.66	86	2345 –2	1.31	167	2 45 – 345
0.67	4	2 –2	1.36	105	234 – 34
	44	23 –2 5	1.58	156	2345 – 34
	92	23 5 –2 5	1.74	157	234 – 345
0.68	99	2 45 –2 4	1.84	189	2345 – 345
0.69	40	23 –23	1.99	77	34 – 34
	95	23 6–2 5	2.73	126	345 – 34
	101	2 45 –2 5	3.52	169	345 – 345
	116	23456–			

[a] IUPAC 110; $k' = 0.94 \pm 0.01$, $n = 10$.

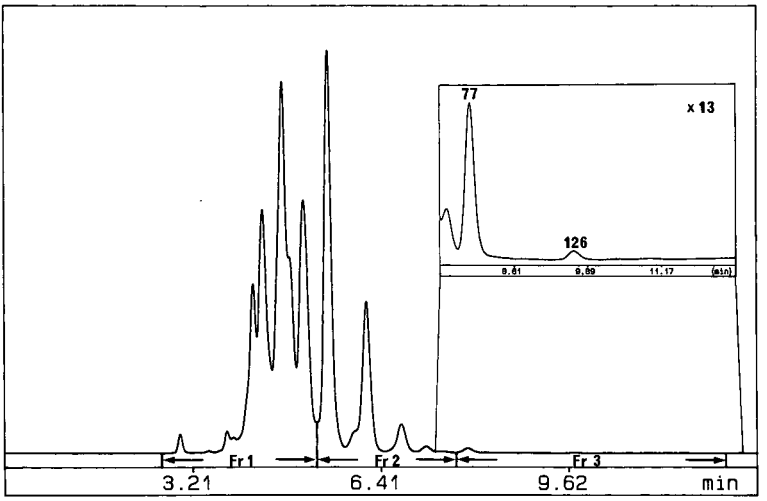

Fig. 1. HPLC chromatogram showing the fractionation of Chlophen A50 on a 150 × 4.6 mm I.D. PYE column. The numbered peaks correspond to 3,3',4,4'-TeCB (IUPAC 77) and 3,3',4,4',5-PeCB (IUPAC 126). The chromatographic conditions are described in Experimental.

with electron-capture detection (ECD), as described elsewhere[8]. To compare the selectivity of the Amoco PX-21A and the PYE phases, 20 μg of Halowax 1014 dissolved in 20 μl of isooctane were injected and fractions were collected according to Fig. 2. GC–ECD analysis of the fractions was performed according to methods described elsewhere[8].

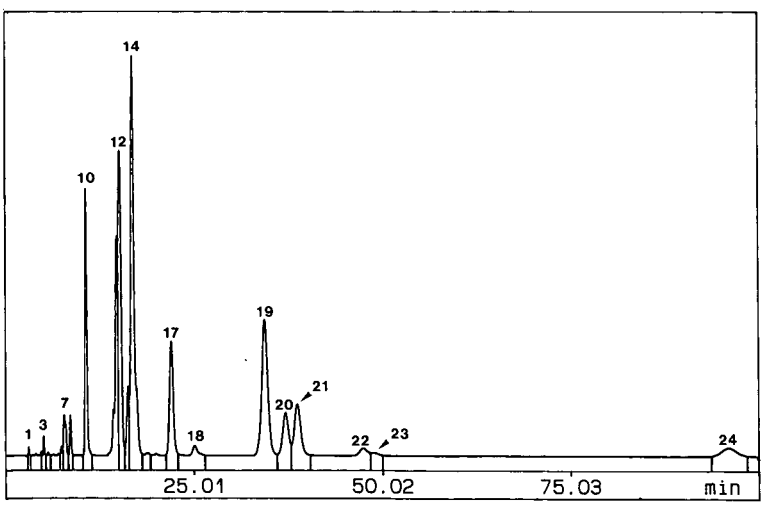

Fig. 2. HPLC chromatogram showing the fractionation of Halowax 1014. The fractions contain the following compounds or compound classes: 1–6, tri-; 7–10, tetra-; 11–16, penta- and early eluting hexa-; 17, 1,2,3,4,5,6,8-hepta-; 18, octa-; 19–23, late eluting hexa- and 24, 1,2,3,4,5,6,7-heptachloronaphthalene. The chromatographic conditions are described in Experimental.

RESULTS AND DISCUSSION

Chromatography of reference compounds

The results of the k' measurements of individual PCB congeners are summarized in Table I. The instrumental error of the k' measurements was *ca.* 1% (IUPAC 110; $k' = 0.94 \pm 0.01, n = 10$). The data in Table I were used to create a three-dimensional plot, in which the k' values were plotted *versus* the number of chlorines and *versus* the number of *ortho* chlorines (Fig. 3). From this plot some general features of the retention on the PYE column become evident. Retention tends to increase with the degree of chlorination and to decrease with increasing number of *ortho* chlorines. The same phenomenon has been described for the retention of PCBs on an activated charcoal (Amoco PX-21) column[3].

Furthermore, since the retention varies considerably between isomers with the same number of total as well as *ortho* chlorines, there must be some other characteristic affecting the retention, probably the substitution pattern. To study the influence of the substitution on the retention, the k' values of biphenyls with the same substitution in one ring and different substitution in the other have been compared. Some trends revealed by the comparison are summarized in Table II. It seems as if half-ring structures with the chlorines close together are more retentive than those with the chlorines spread over the rings, *e.g.*, 2,3,4-substitution is more retentive than 2,3,5-substitution.

The same type of selectivity of the PYE phase has been described for the reversed-phase separation of tetrachlorodibenzo-*p*-dioxins[9].

The selectivity of the PYE phase may be explained by a charge-transfer mechanism, in which electron-density acceptor and donor regions of the PCBs induce a change in the localization of the π-electron cloud of the pyrene moieties of the phase

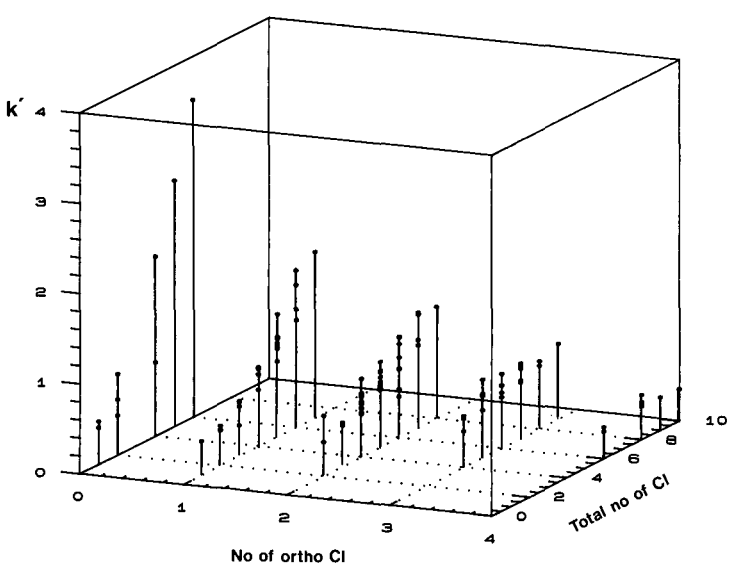

Fig. 3. Plot of k' values from Table I *versus* the number of chlorines and *versus* the number of *ortho* chlorines.

TABLE II

RETENTION ORDER ON A PYE COLUMN OF PCBs SUBSTITUTED IN THE SAME WAY IN ONE OF THE RINGS AND AS BELOW IN THE OTHER

The chromatographic conditions are described under Experimental.

Number of chlorine	*Retention order*
1	$2 < 3 \ll 4$
2	$26 < 25 \approx 24 < 23 \leqslant 35 \ll 34$
3	$246 < 236 \leqslant 235 < 245 < 234 \ll 345$
4	$2346 < 2356 \ll 2345$

so that an EDA complex is formed. This type of mechanism could account for the observed retention behaviour in the following three ways:

(1) Highly chlorinated biphenyls would be expected to form strong EDA complexes with the PYE column because chlorinated compounds are very good electron-density acceptors and polycyclic aromatic hydrocarbons, such as pyrene, are among the most effective electron donors known[10].

(2) PCBs with many *ortho* chlorines should be less retained owing to steric interaction between *ortho* chlorines (or between *ortho* chlorines and *ortho* hydrogens), leading to twisting of the biphenyl σ-bond, an increase in the distance between the biphenyl and the pyrene moieties, and thus to a weaker EDA complex.

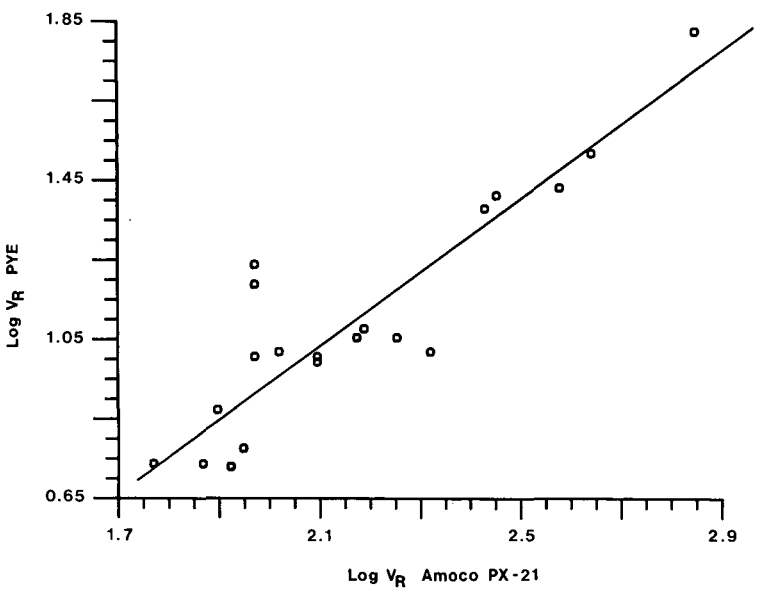

Fig. 4. Graph of log V_R of polychlorinated naphthalenes chromatographed on a 150 × 4.6 mm I.D. PYE column and on a 300 × 4.6 mm I.D. Amoco PX-21 column. The chromatographic conditions for the PYE column are described in Experimental. The chromatographic conditions for the Amoco PX-21 column were the following: mobile phase, toluene; flow-rate, 1 ml/min.

(3) PCBs with half-ring structures with the chlorines close together offer naturally better acceptor pockets for EDA complexing than those that have half-ring structures with the chlorines spread over the rings, and are therefore more retained.

GC analysis of the fractions of the PCN product Halowax 1014 revealed that the elution order, shown in Fig. 2, is much the same from a PYE column as from an activated charcoal column (Amoco PX-21). In Fig. 4 these results are shown in the form of a log V_R (V_R = retention volume) *versus* log V_R plot. This emphasizes further the similarities in retention between the PYE column and activated charcoal columns of the PX-21 type.

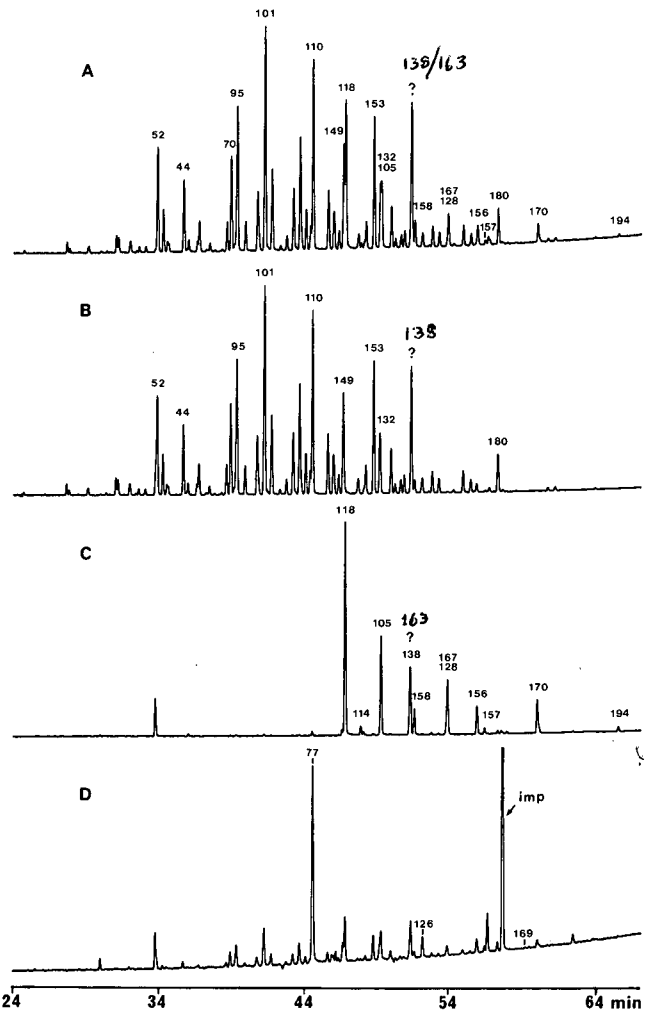

Fig. 5. Gas chromatograms of the fractions from Fig. 1: (A) unfractionated Chlophen A50; (B) fraction no. 1; (C) fraction no. 2; (D) fraction no. 3. The "?" mark denotes a peak of uncertain identity (see Results and Discussion); "imp" means impurity. The chromatographic conditions are described in Experimental.

Fractionation of Chlophen A50

GC chromatograms from the analysis of the Chlophen A50 fractions from the PYE column are shown in Fig. 5.

The peak labelled "?" in the chromatogram of unfractionated Chlophen A50 is generally thought to be 2,2',3,4,4',5-HxCB (IUPAC 138) and is supposed to elute in fraction 2 according to Table I, but since an HxCB isomer with the same retention time also eluted in fraction 2, the peak "?" was suspected to contain two different PCB congeners. Very recently, Roos *et al.*[11,12] reported that an HxCB isomer, 2,3,3',4',5,6-HxCB (IUPAC 163), is present in PCB mixtures and is interfering with the determination of IUPAC 138 when SE-54 type phases are used. However, lack of reference compounds prevented us from identifying the HxCB isomers present in fractions 1 and 2.

According to Fig. 5 the PYE column produces fractions containing toxic 0- and 1-*ortho*-PCBs that are clean enough for GC–ECD analysis, although the second fraction contanis some 2-*ortho*-PCBs in addition to the 1-*ortho*-PCBs. One of these congeners, 2,2',3,3',4,4'-HxCB (IUPAC 128), interferes with the analysis of one of the 1-*ortho*-PCBs, 2,3',4,4',5,5'-HxCB (IUPAC 167). IUPAC 167 has a lower toxicity than the other 1-*ortho*-PCBs and is therefore not of particular interest. If this congener is considered important it could be separatad from IUPAC 128 on an SB-Octyl 50 column (see Introduction). Some carryover of 1-*ortho*-PCBs into the 0-*ortho* fraction can also be seen, which is probably due to deposition of PCBs on the outside wall of the outlet capillary and subsequent washing off into the following fractions. The problem may be avoided by using a fractionation valve and a separate outlet capillary for each fraction, and by washing the tips of the outlet capillaries between runs.

Quantitative analysis of the 0-*ortho* fraction showed that the concentrations of 3,3',4,4'-TeCB, 3,3',4,4',5-PeCB and 3,3',4,4',5,5'-HxCB were 1260 μg, 51.8 μg and 2.72 μg per gram of Chlophen A50, respectively. These results are of the same magnitude as those reported by Jensen and Athanasiadou[6] (660 μg of 3,3',4,4'-TeCB, 79 μg of 3,3',4,4',5-PeCB and 2.7 μg of 3,3',4,4',5,5'-HxCB per gram of Chlophen A50).

No notable effect on the separation could be seen between the different loads of Chlophen A50 studied (10–250 μg).

Comparison of the PYE column and activated charcoal columns for the isolation of toxic PCBs

Although activated charcoal columns seem to separate the compounds covered by the present investigation in almost the same way as the PYE column, there are great differences in efficiency, solvent requirements and consumption, and analysis time.

The PYE columns are highly efficient, *ca.* 45 000 theoretical plates/m, and give sharp peaks with good symmetry (asymmetry factor 1.10), which is in great contrast to the broad elution profiles with severe tailing generally observed with chromatography on activated charcoal. The high efficiency of the PYE column makes it possible accurately to isolate the toxic 1-*ortho*-PCBs, which is not possible by the generally used charcoal methods[3–5].

Toxic 0-*ortho*-PCBs are usually eluted from activated charcoal columns with stepwise gradients of cyclohexane–dichloromethane, benzene in ethyl acetate and toluene[3,4] or increasing percentages of toluene in cyclohexane[5]. In contrast, the PYE column requires only a single solvent, hexane, which provides many advantages: UV detectors can be used to detect the solutes, the fractions become easy to evaporate and the residue can be directly analysed by GC–ECD or GC–MS.

Fractionation of a technical PCB product into three fractions (containing 2–4-*ortho*-PCBs, toxic 1-*ortho*-PCBs and toxic 0-*ortho*-PCBs) takes less than 15 min if the PYE column is used. The fraction volume are only 2–3 ml and are easily reduced to volumes suitable for GC–ECD or GC–MS by a gentle stream of nitrogen. On activated charcoal columns a fractionation of PCB mixtures into two fractions (one containing the bulk of PCB and one containing toxic 0-*ortho*-PCBs) takes at least the same time. Furthermore, the evaporation of the large volumes of aromatic solvents (50–200 ml) used to elute the 0-*ortho*-PCB fraction, is very time-consuming. The risk of contamination is also increased by the use of such large amounts of aromatic solvents.

CONCLUSIONS

The retention behaviour of PCBs on the PYE column can be summarized as follows: a decreasing number of *ortho* chlorines, and thus increasing planarity, gives increasing retention; solutes with continuous acceptor regions are retained through EDA complexing with the pyrene moieties of the stationary phase; highly chlorinated PCBs are retained owing to the high electron affinity of the chlorines.

The PYE column offers a simple and powerful tool for the isolation of toxic 0- and 1-*ortho*-PCBs from technical PCB formulations.

It is worth noting that our method makes it possible to isolate and analyse 1-*ortho*-PCBs, which is not possible by the generally used charcoal methods[3–5].

Further work is needed to adapt and extend the method in such a way that toxic 0- and 1-*ortho*-PCBs can be accurately quantitated in environmental samples.

ACKNOWLEDGEMENTS

We thank Professor N. Tanaka and Nacalai Tesque for making the PYE columns available. Thanks are also due to C. Östman for technical assistance and for fruitful discussions.

The study was supported by a grant from the Research Committee at the National Environmental Protection Board, contract No. 5326168-1.

REFERENCES

1 S. Safe, *CRC Crit. Rev. Toxicol.*, 13 (1984) 319.
2 A. Parkinson, S. Safe, L. W. Robertson, P. E. Thomas, D. E. Ryan, L. M. Reik and W. Levin, *J. Biol. Chem.*, 258 (1983) 5967.
3 D. L. Stalling, L. M. Smith and J. D. Petty, in C. E. van Hall (Editor), *Measurement of Organic Pollutants in Water and Wastewater*, American Society for Testing and Materials, Philadelphia, PA, 1979, p. 302.
4 S. Tanabe, N. Kannan, A. Subramanian, S. Watanabe and R. Tatsukawa, *Environ. Pollut.*, 47 (1987) 147.
5 J. N. Huckins, D. L. Stalling and J. D. Petty, *J. Assoc. Off. Anal. Chem.*, 63 (1980) 750.
6 S. Jensen and M. Athanasiadou, *Ambio*, submitted for publication.
7 R. Fischer and K. Ballschmiter, *Fresenius Z. Anal. Chem.*, submitted for publication.
8 L. Asplund, B. Jansson, G. Sundström, I. Brandt and U. A. Th. Brinkman, *Chemosphere*, 15 (1986) 619.
9 E. R. Barnharth, D. G. Patterson, Jr., N. Tanaka and M. Araki, *J. Chromatogr.*, 445 (1988) 145.
10 L. Nondek, *J. Chromatogr.*, 373 (1986) 61.
11 A. Roos, personal communication.
12 A. H. Roos, P. G. M. Kienhuis, W. A. Traag and L. G. M. Th. Tuinstra, *Int. J. Environ. Anal. Chem.*, in press.

Journal of Chromatography, 507 (1990) 399–402
Elsevier Science Publishers B.V., Amsterdam — Printed in The Netherlands

CHROMSYMP. 1701

Transient changes of mobile phase in the high-performance liquid chromatographic separation of priority pollutant phenols

M. D. ANDRÉS, B. CAÑAS, R. C. IZQUIERDO and L. M. POLO
Departamento de Química Analítica, Facultad de Química, Universidad Complutense de Madrid, 28040 Madrid (Spain)
and
P. ALARCÓN*
Laboratorios del Instituto Tecnológico Geominero de España (ITGE), La Calera 1, 28760 Colmenar Viejo (Spain)

SUMMARY

A study of the effect of cetyltrimethylammonium bromide on the separation of the eleven priority pollutant phenols is presented. Transient changes in a CTAB mobile phase produced by a sodium laurylsulphate solution plug permit the elution of hydrophobic pentachlorophenol.

INTRODUCTION

Phenols are common water pollutants because they are extensively used as pesticides, and also because they may be produced by some industrial activities[1]. The U.S. Environmental Protection Agency (EPA) has included eleven phenols in the list of priority pollutants. The priority pollutant phenols (PPP) are phenol, 2,4-dimethylphenol (24DMP), 4-chloro-3-methylphenol (43CMP), 2-chlorophenol (2CP), 2,4-dichlorophenol (24DCP), 2,4,6-trichlorophenol (246TCP), 2-nitrophenol (2NP), 4-nitrophenol (4NP), 2,4-dinitrophenol (24DNP), 4,6-dinitro-2-methylphenol (46DNOC) and pentachlorophenol (PCP)[2].

In a previous paper[3], the separation of these PPP by high-performance liquid chromatography (HPLC) with isocratic elution was proposed, but this separation may be improved if the capacity factors (k') for 24DNP and 46DNOC are larger than unity. The use of ion-pairing agents increases the k' values of acidic compounds and improves their separation. However, PCP, owing to its acidity and highly hydrophobic character, is strongly retained under these conditions.

The use of transitory mobile phase environments was applied by Gluckman *et al.*[4] to the separation of organic dyestuffs (cationic, non-ionic and anionic). In this work, cetyltrimethylammonium bromide (CTAB) was added to the mobile phase as an

0021-9673/90/$03.50

ion-pairing agent to elute all phenols except PCP. Subsequently, a short plug of mobile phase containing sodium laurysulphate (SLS) was used to elute PCP.

EXPERIMENTAL

Chemicals

The PPP were purchased from Supelco (Bellefonte, PA, U.S.A.) and were of chromatographic grade. HPLC-grade methanol was obtained from Promochem (Wesel, F.R.G.) and HPLC-grade acetonitrile from Mallinckrodt (Paris, KY, U.S.A.). Water was obtained from a Milli-Q (Millipore, Molsheim, France) purification system. CTAB was from Serva (Heidelberg, F.R.G.) and SLS from Carlo Erba (Milan, Italy). All other reagents were of analytical-reagent grade. The mobile phase was 30 m*M* ammonium acetate buffer (pH 5.0)–acetonitrile–methanol (56:34:10), unless indicated otherwise. Before use, all eluents were degassed under vacuum and filtered with an all-glass apparatus through 0.45-μm filters (Millipore, Bedford, MA, U.S.A.).

Apparatus

Analyses were performed with a Milton Roy (Riviera Beach, FL, U.S.A.) liquid chromatograph equipped with a Model CM 4000 multiple-delivery solvent system, a Model SM 4000 programmable-wavelength detector and a Model C14100 computing integrator. The injector was a Model 7125 valve (Rheodyne, Cotati, CA, U.S.A.) with a 20-μl fixed loop. For pH measurements, a Model 501 digital pH meter (Crison Instruments, Barcelona, Spain) with a glass electrode was used. Prepacked analytical columns were a Nucleosil-120, 5 μm (12 cm $\times$ 4 mm I.D.) C_{18} column (Knauer, Berlin, F.R.G.) and a Spherisorb ODS-2, 5 μm (15 cm $\times$ 4 mm I.D.) column (Tecknokroma, Barcelona, Spain).

Methods

The column was equilibrated prior to use with 0.20 m*M* CTAB mobile phase for the Spherisorb packing or 0.15 m*M* CTAB for the Nucleosil packing. The solution was passed through the column for 90 min at a flow-rate of 1.5 ml/min. Equilibrium was reached when the retention time for PPP remained constant. An SLS plug was introduced into the column by a time-programming change in the admission valve of the solvent delivery system after sample injection. The flow-rate was maintained at 1.5 ml/min. The column was reconditioned by passing CTAB mobile phase through it after the plug.

RESULTS AND DISCUSSION

Effect of CTAB concentration

CTAB affects each PPP differently because of their different capacities to form ion pairs; this behaviour is controlled by the pH of the mobile phase, as uncharged phenols do not form ion pairs. For example, phenol is uncharged at pH 5 and therefore, it was used as a reference compound. Fig. 1 shows the effect of the CTAB concentration on this separation. As can be observed, the retention time (t_r) of associated phenols decreases when the CTAB concentration increases. This effect was corroborated by Kastary and Gilpin[5] by increasing the surfactant concentration and

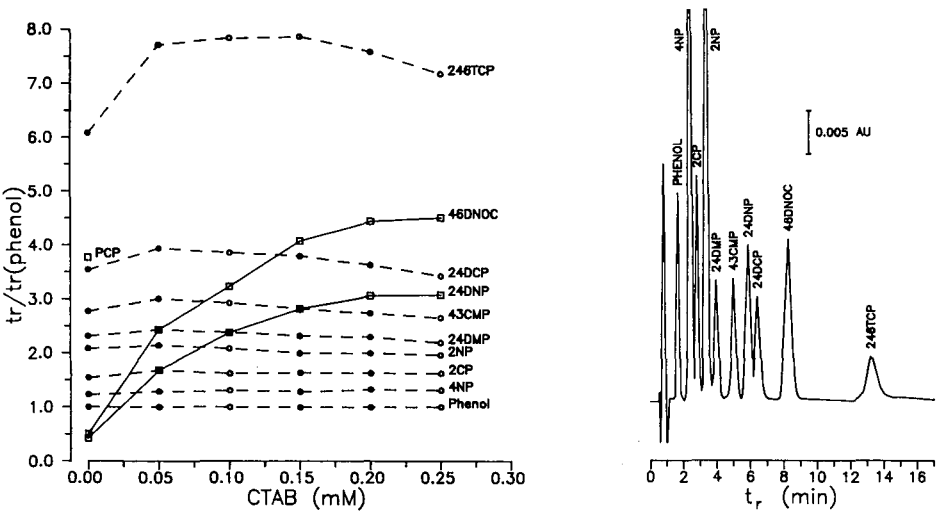

Fig. 1. Effect of CTAB on PPP separation. Column, Spherisorb ODS-2, 5 μm (150 × 4 mm I.D.); flow-rate, 1.5 ml/min; eluent, CTAB in the mobile phase (see Experimental); detection, 280 nm; injection volume, 20 μl; t_r (phenol) = 1.3–1.4 min.

Fig. 2. Separation of PPP with CTAB. Column, Nucleosil-120, 5 μm, C_{18} (120 × 4 mm I.D.); flow-rate, 1.5 ml/min; eluent, 0.15 m*M* CTAB mobile phase (see Experimental); detection, 280 nm; injection volume, 20 μl.

working with uncharged compounds. Under these conditions, PCP is partially ionized and strongly retained, as even at low CTAB concentrations an ion pair ($CTAB^+ \cdot PCP^-$) of high hydrophobic character is formed. The k' values of 46DNOC and 24DNP were also increased owing to ion-pair formation. Thus, better PPP separations were obtained with CTAB concentrations in the range 0.20–0.25 m*M*. A CTAB concentration close to 0.15 m*M* was needed to achieve a similar separation when the Nucleosil column was used (Fig. 2). Nucleosil-120 (5 μm), C_{18} and Spherisorb ODS-5 packings were chosen because of their durability when mobile phases containing CTAB were used[6].

Eluent plugs

The use of transient mobile phases allows the selective elution of strongly retained substances such as, in this instance, PCP. The eluotropic strength of the mobile phase for PCP can be enhanced in two ways, by increasing the methanol concentration or by increasing the ionic strength. When 1.0 *M* sodium chloride or 100% methanol was used, satisfactory results were not obtained. Another possibility is based on establishing a competitive equilibrium between CTAB and a high concentration of another surfactant of a different nature (anionic), which could form an ion pair with CTAB[4]. When a plug containing an excess of anionic surfactant was introduced into the column, the surfactant molecules shifted the ion-pair equilibrium between CTAB and PCP, liberating the ionized PCP. The short-chain surfactant sodium heptanesulphonate was selected in order to facilitate column re-equilibration but, after testing, the need for a more hydrophobic anionic surfactant was evident and SLS was selected. The PCP retention times *versus* the total amounts of SLS in the plug are plotted in Fig. 3 for the two above-mentioned columns. Once the determined amount

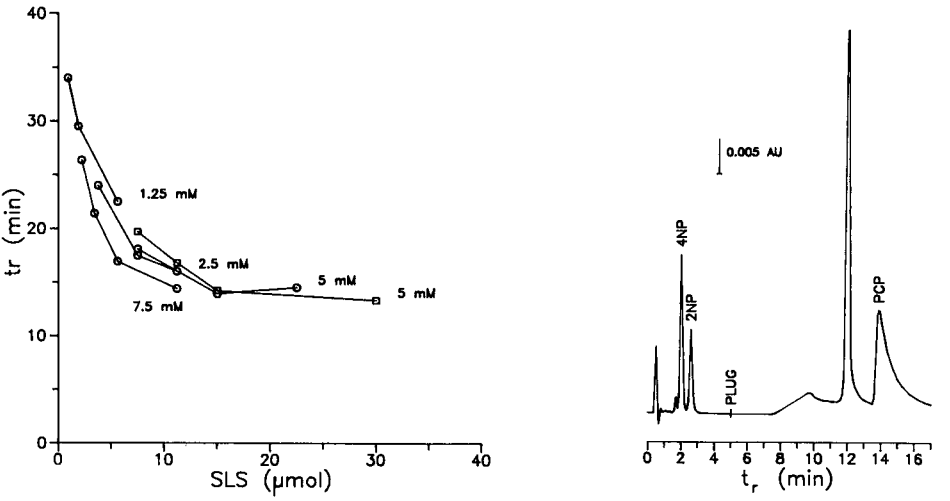

Fig. 3. Effect of the amount of SLS on elution of PCP. Eluent, 0.15 m*M* CTAB mobile phase for the Nucleosil (○) and 0.20 m*M* CTAB mobile phase for the Spherisorb (□) column (see Experimental); plug start time, 5 min; flow-rate, 1.5 ml/min; detection, 254 nm.

Fig. 4. Elution of PCP with CTAB mobile phase and SLS plug. Column, Nucleosil-120, 5 μm, C_{18} (120 × 4 mm I.D.); flow-rate, 1.5 ml/min; eluent, 0.15 m*M* CTAB mobile phase (see Experimental); detection, 254 nm; injection volume, 20 μl; plug volume, 3 ml of 5 m*M* SLS mobile phase.

of SLS had been reached, the retention time of PCP hardly changed. This may be explained as the time necessary for PCP to pass through the column according to a hydrophobic retention mechanism.

A 0.20 m*M* CTAB concentration in the mobile phase and 15 μmol of SLS in the plug were sufficient to separate all PPP and elute PCP when the Spherisorb column was used, whereas a 0.15 m*M* CTAB concentration and 15 μmol of SLS in the plug were needed for the Nucleosil column (Fig. 4). In both instances reconditioning of the column by passing CTAB mobile phase through it was needed. This was monitored by injecting 24DNP or 46DNOC and comparing the retention times with those obtained in the former chromatogram. The time necessary for column reconditioning was directly related to the amount of SLS used in the plug.

REFERENCES

1 A. L. Buikema, Jr., M. J. McGinnis and J. Cairns, Jr., *Mar. Environ. Res.*, 2 (1979) 87.
2 L. H. Keith and W. A. Telliard, *Environ. Sci. Technol.*, 13 (1979) 416.
3 P. Alarcon, A. Bustos, B. Cañas, M. D. Andres and L. M. Polo, *Chromatographia*, 24 (1987) 613.
4 J. C. Gluckman, K. Slais, U. A. Th. Brinkman and R. W. Frei, *Anal. Chem.*, 59 (1987) 79.
5 A. Kastari and R. K. Gilpin, *J. Chromatogr. Sci.*, 25 (1987) 29.
6 B. Cañas, R. C. Izquierdo, P. Alarcón, A. Gonzalez-Menendez and E. Gonzalez-Ortega, unpublished results.

Journal of Chromatography, 507 (1990) 403–407
Elsevier Science Publishers B.V., Amsterdam — Printed in The Netherlands

CHROMSYMP. 1813

Reversed-phase high-performance liquid chromatography applied to the direct analysis of untreated heterophasic systems

A. BETTERO*, A. SEMENZATO and C. A. BENASSI
*Centro di Cosmetologia Chimica, Dipartimento di Scienze Farmaceutiche, Università di Padova, Padova (Italy) and *Istituto di Chimica Farmaceutica e Tossicologica, Università di Milano, Milan (Italy)*

SUMMARY

A simple and rapid approach for the direct analysis of multi-component heterophasic matrices is reported. The procedure is based on sample dilution with tetrahydrofuran–water (9:1) followed by direct reversed-phase high-performance liquid chromatography. The method is suitable for quality control and stability studies of drugs, food and cosmetic products.

INTRODUCTION

Heterophasic systems are non-Newtonian fluids with a thixotropic profile[1,2]. We recently observed that tetrahydrofuran (THF)–water allows the homogeneous dilution of non-ideal fluids suitable for direct investigation of complex matrices such as drugs and cosmetic emulsions[3]. As this polar medium is compatible with the mobile phases usually employed for reversed-phase high-performance liquid chromatography (RP-HPLC), we have studied the analysis of multi-component untreated formulations.

The approach is based on sample dilution with THF–water (9:1) followed by direct RP-HPLC using the standard addition method[4,5]. The procedure is compatible with the precolumn derivatization step before analysis[6,7]. The method allows qualitative and quantitative determinations and the simultaneous evaluation of matrix effects[8–14].

EXPERIMENTAL

Materials and reagents

Prevan [3-acetyl-6-methyl-2*H*-pyran-2,4(3*H*)dione sodium salt], dehydroacetic acid sodium salt, was obtained from Formenti (Milan, Italy), benzalkonium chloride from Sigma (St. Louis, MO, U.S.A.) and formaldehyde and 2,4-dinitrophenylhydrazine (2,4-DNPH) from Carlo Erba (Milan, Italy). Reagents and solvents were of analytical-reagent grade.

0021-9673/90/$03.50

A 0.1% solution of 2,4-DNPH was prepared by dissolving 0.25 g in 40 ml of 32% hydrochloric acid, heating until dissolved and then diluting to 250 ml with water.

Apparatus

A Haake RV-12 absolute rotational viscometer equipped with a PG-142 speed programmer and data station was used. The variable test parameters were set using NV (sensor system) as the measuring head and 0–256 min^{-1} as the speed value (D = shear rate: 0–1384 s^{-1}).

A Perkin-Elmer Series 410 liquid chromatograph equipped with a Rheodyne 7125 valve, LC-235 diode-array UV detector and LC-100 data station was used. LiChrosorb RP-8 (10 μm) and LiChrosorb RP-Select B (5 μm) columns were obtained from Merck (Darmstadt, F.R.G.).

Standards

Prevan was diluted to 1.5 mg/ml with THF–water (9:1) in a screw-capped tube. Benzalkonium chloride was diluted to 0.25–0.002 mg/ml with THF–water (9:1) in a screw-capped tube. Formaldehyde solution (40%, iodimetrically controlled) was diluted to 0.004–0.0001% with THF–water (9:1) in a screw-capped tube.

Samples

About 1 g of each cosmetic emulsion sample, carefully weighed, was diluted to 10 ml with THF–water (9:1) in a screw-capped tube and stirred in a vortex mixer until completely homogeneous.

Derivatization procedure

A 1-ml volume of standard or sample solution was added to 0.4 ml of 0.1% 2,4-DNPH solution, stirred for 60 s in a vortex mixer and allowed to stand for 2 min at room temperature. The solution was then stabilized by adding 0.4 ml of 0.1 *M* phosphate buffer (pH 6.8) and 0.7 ml of 1 *M* sodium hydroxide solution. Aliquots of 6 μl were injected into the HPLC system.

HPLC

Method 1. A LiChrosorb RP-8 (10 μm) column was used with acetonitrile–0.01 *M* phosphate buffer (pH 4.7) (1:1) as eluent at a flow-rate of 1 ml/min and UV detection at 300 nm.

Method 2. A LiChrosorb RP-Select B (5 μm) column was used with acetonitrile–0.02 *M* phosphate buffer (pH 3.5) (0.8:0.2) as eluent at a flow-rate of 1.2 ml/min and UV detection at 210 nm.

Method 3. A LiChrosorb RP-8 (10 μm) column was used with acetonitrile–water (1:1) as eluent at a flow-rate of 1 ml/min and UV detection at 345 nm.

RESULTS AND DISCUSSION

Fig. 1 shows the effect of dilution with THF–water (9:1) on the disappearance of thixotropy in a cosmetic emulsion; a 1:10 dilution allows reticle homogeneity and Newtonian behaviour of the sample, which can be directly injected into the RP-

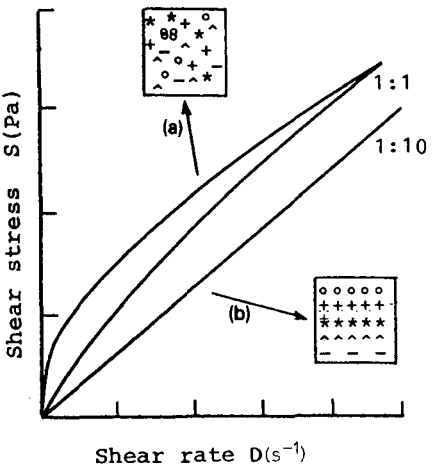

Fig. 1. Rheological behaviour (flow curves) of a typical heterophasic system: effect of dilution with THF–water (9:1) on the disappearance of thixotropy (a) and reticle homogeneity (b) of a commercial cosmetic emulsion sample.

HPLC system and investigated without a memory effect[3]. Fig 2 compared the chromatographic patterns of the cosmetic preservative Prevan obtained from the same emulsion sample, (a) directly injected after THF–water dilution and (b) injected after the usual sample pretreament; chromatographic resolution and the absence of a matrix effect may be seen. The matrix effect can be routinely evaluated by the standard addition method by comparing the slopes of the standard and sample plus standard curves.

The combined action of THF–water and RP-HPLC avoiding sample pretreatment allows more sensitive detection for the study of the modifications that occur in the finished product due to chemical or microbiological effects.

Fig. 3 shows an example of the direct analysis of benzalkonium chloride obtained at 210 nm from a cosmetic product diluted 1:10 with THF–water; the chroma-

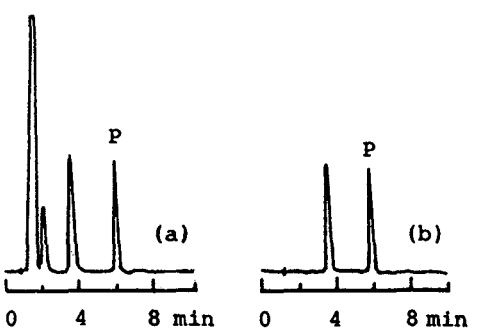

Fig. 2. Chromatographic patterns of cosmetic preservative Prevan (P) obtained from (a) the direct injection of a cosmetic emulsion diluted 1:10 with THF–water (9:1) and (b) the injection of same cosmetic emulsion conventionally pretreated (method 1).

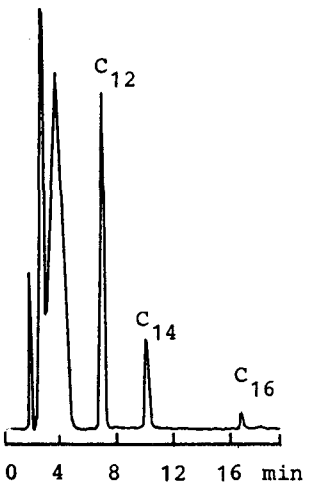

Fig. 3. HPLC resolution of C_{12}, C_{14} and C_{16} alkyl chain components of benzalkonium chloride obtained from an commercial product diluted 1:10 with THF–water (9:1) (method 2).

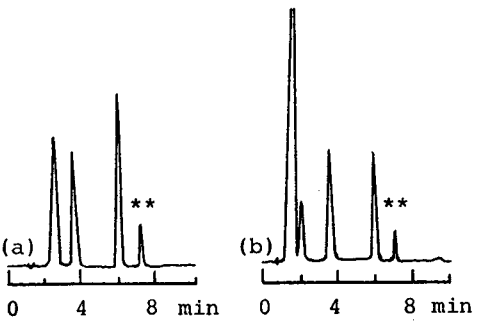

Fig. 4. Chromatographic evidence of an interaction product (peaks with asterisks) formed by the effect of formaldehyde on a typical cosmetic preservative system containing Prevan: (a) aqueous standard solution; (b) cosmetic emulsion. Method 1, UV detection at 300 nm.

tographic pattern reveals not only the C_{12} and C_{14} alkyl chain components but also, at a retention time of 16.8 min, a peak corresponding to the C_{16} alkyl component, which is normally undetected[14].

Fig. 4 shows an example of the appearance at the native level of an interaction product formed in a cosmetic emulsion between the dehydroacetic acid sodium salt (Prevan) and formaldehyde released from preservatives[11].

The procedure may also be employed in conjunction with precolumn derivatization before analysis; Fig. 5 shows the free formaldehyde detected at 345 nm after 2,4-DNPH derivatization of a cosmetic emulsion diluted 1:100 with THF–water (9:1) and injected directly into the HPLC system[7].

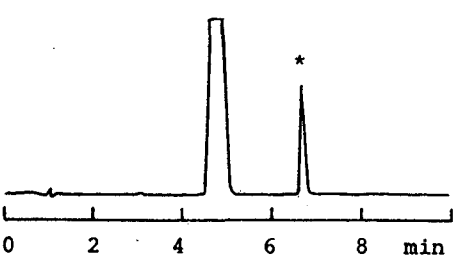

Fig. 5. Chromatographic pattern of formaldehyde (peak with asterisk) obtained after 2,4-DNPH precolumn derivatization of a cosmetic emulsion sample diluted 1:100 with THF–water (9:1) (method 3).

CONCLUSIONS

The combination of THF–water (9:1) dilution of the sample and RP-HPLC allows the direct evaluation of multi-component heterophasic systems such as drug, food and cosmetic products. The long-term effects of direct injections of untreated complex matrices on the chromatographic resolution, evaluated by repeated injections and calibrations, show statistically significant correlations and reproducibility of the data with a mean column lifetime of 100 analyses. The procedure is rapid and sensitive and appears to be a potentially powerful method suitable for quality control and stability studies.

ACKNOWLEDGEMENTS

This work was supported by grants from the Italian CNR Special Project on Fine Chemicals and from the Italian Ministry of Scientific and Technological Research.

REFERENCES

1 J. R. Van Wazer, J. W. Lyons, K. Y. Kim and R. E. Colwell (Editors), *Viscosity and Flow Measurements,* Wiley, New York, London, 1963.
2 J. B. Ward, J. F. Kinney and H. Y. Sand, *J. Soc. Cosmet. Chem.,* 25 (1974) 437.
3 A. Bettero, B. Casetta, F. Galiano, E. Ragazzi and C. A. Benassi, *Fresenius Z. Anal. Chem.,* 318 (1984) 525.
4 A. Bettero and C. A. Benassi, *J. Chromatogr.,* 280 (1983) 167.
5 A. Bettero, *Cosmet. Toilet. Ed. It.,* 2 (1987) 49.
6 A. Bettero, M. R. Angi, F. Moro and C. A. Benassi, *J. Chromatogr.,* 310 (1984) 390.
7 C. A. Benassi, A. Semenzato and A. Bettero, *J. Chromatogr.,* 464 (1989) 387.
8 A. Bettero, *Chim. Oggi,* 5 (1984) 59.
9 F. Galiano, A. Bettero and V. Marin, *Cosmet. Toilet. Ed. It.,* 1 (1985) 10.
10 A. Bettero, A. Semenzato, G. Aversa and C. A. Benassi, *Chim. Oggi,* 11 (1985) 29.
11 C. A. Benassi, A. Semenzato, M. Lucchiari and A. Bettero, *Int. J. Cosmet. Sci.,* 10 (1988) 29.
12 C. A. Benassi, A. Bettero, P. Manzini, A. Semenzato and P. Traldi, *J. Soc. Cosmet. Chem.,* 39 (1988) 85.
13 C. A. Benassi, A. Rettore, A. Semenzato, A.Bettero and R. Cerini, *Int. J. Cosmet. Sci.,* 10 (1988) 231.
14 C. A. Benassi, A. Semenzato, P. Zanzot and A. Bettero, *Farmaco,* 44 (1989) 329.

Journal of Chromatography, 507 (1990) 409–415
Elsevier Science Publishers B.V., Amsterdam — Printed in The Netherlands

CHROMSYMP. 1697

Separation and interconversion of 3-amino-2-cyanoacrylates by high-performance liquid chromatography

Gy. KÖRTVÉLYESSY*, J. KÖRTVÉLYESSY, T. MESTER, G. MESZLÉNYI and G. JANZSÓ
Research Institute for Organic Chemical Industry, P.O. Box 41, H-1428 Budapest (Hungary)

SUMMARY

High-performance liquid chromatography (HPLC) is the preferred method for the resolution of *Z*/*E* isomers. The partly known interconversion of the *Z*/*E* isomers of methyl and ethyl 3-substituted amino-2-cyanoacrylates and amides was observed and quantitatively followed by HPLC analysis. In a solution of alkaline pH and containing methanol instead of acetonitrile, the interconversion is faster. The use of gas chromatography for the analysis of the isomers for unsubstituted aminocyanoacrylates was impracticable owing to the easy interconversion in the sample chamber.

INTRODUCTION

Alkyl 3-amino-2-cyanoacrylates are important intermediates in the synthesis of pyrimidines used in the pharmaceutical industry. Knippel *et al.*[1] measured the *Z*/*E* interconversion of 3-mono- and -disubstituted-amino-2-cyanoacrylates by ^{1}H NMR spectroscopy. Bellanato *et al.*[2] used IR spectroscopy for characterizing these compounds and observed qualitative evidence for the rotation around the C=C double bond in solutions of the N-monosubstituted compounds.

Jacobson *et al.*[3] studied the *cis–trans* isomerization of peptides containing proline by high-performance liquid chromatography (HPLC). They calculated the rate constants of this reaction from the distortion of the peak shapes. Jansen and Both-Miedema[4]. reported the instability of phenylthiohydantoin amino acids in the HPLC mobile phase during automatic HPLC analysis.

Our aim here was to investigate the applicability of the *Z*/*E* isomeric amino-2-cyanoacrylates in the synthesis of some pharmaceutical products. It is known from the work of Knippel *et al.*[1] and Bellanato *et al.*[2] that the interconversion between the isomers is easy. No method has been reported for the quantitative measurement of unsubstituted aminocyanoacrylates. In this paper, the use of HPLC for the analysis of unsubstituted and substituted 3-amino-2-cyanoacrylates is demonstrated.

0021-9673/90/$03.50

EXPERIMENTAL

Apparatus

A Varian (Palo Alto, CA, U.S.A.) Model 5000 liquid chromatograph with a Pye Unicam (Cambridge, U.K.) LC-3 UV detector was used at 272 nm. A 25 cm × 4.6 mm I.D. reversed-phase LiChrosorb RP-8 column (particle size 10 μm) (Merck, Darmstadt, F.R.G.) was used. The mobile phase was acetonitrile–distilled water (40:60, v/v) at a flow-rate of 1 ml/min. Injection was carried out with a Valco 10-μl loop injector.

For gas chromatographic analysis use was made of a Hewlett-Packard (Avondale, PA, U.S.A) Model 5890A gas chromatograph with a flame ionization detector, an HP 3394A reporting integrator and an HP-5 column (5% phenylmethylsilicone, cross-linked; fused-silica capillary column, 25 m × 0.31 mm I.D., 0.52-μm film thickness). The flow-rate of the carrier gas (hydrogen) was 5 ml/min with a splitting ratio of 200.

For structure elucidation of the unknown compounds, NMR, UV and IR spectra were measured using Varian FT80A, Pye Unicam SP 1800 and Perkin-Elmer 783 instruments, respectively.

A Mettler Titriprocessor was used for measuring the pH of the eluents.

Chemicals and materials

Acetonitrile, toluene and chloroform (chromatographic grade) and perdeuterated dimethyl sulphoxide (DMSO-d_6) (spectroscopic grade) were obtained from Merck and methanol and KH_2PO_4 (analytical-reagent grade) from Reanal (Budapest, Hungary). Distilled water was used throughout. Eluent of pH 4 was prepared by dissolving 0.05% KH_2PO_4 in distilled water and adjusting the pH to 4 with phosphoric acid while monitoring the pH with the Mettler titrimeter. Mixing this buffer with acetonitrile in a volumetric ratio of 40:60 gave a mobile phase of pH 4.

UV and IR spectra were measured in acetonitrile solution and as potassium bromide pellets, respectively. 3-Amino-2-cyanoacrylates were prepared by a method similar to that described by Bredereck[5]. The compounds studied are listed in Table I. The isomers were separated by crystallization of the isomer mixture from toluene. The solubility of the *E* isomer is lower. The *Z* isomer can be crystallized from the filtrate. So far only compounds **2** and **3** have been separated.

TABLE I

AMINOCYANOACRYLATES PREPARED AND INVESTIGATED

$R_2NCH=C(CN)COX$

No.	*R*	*X*	*Isomer*
1	H	OCH_3	Mixture
2	H	OC_2H_5	*Z*
3	H	OC_2H_5	*E*
4	H	NH_2	*E*
5	CH_3	NH_2	*E*
6	CH_3	OC_2H_5	*E*

Procedures

For HPLC measurements 4–5 mg of material were weighed on an analytical microbalance and dissolved in 10 ml acetonitrile. A 10-μl volume of the sample was first injected immediately after dissolution. The injection was repeated after given periods of time. The column temperature was 25°C, the same as that for the sample solutions.

For gas chromatography, 1 μl of 1% ethanol solutions was injected into the sample chamber maintained at 220°C. The temperatures of the detector and column were 240 and 140°C (isothermal), respectively.

RESULTS AND DISCUSSION

The IR spectra and the assignments of the prepared and investigate cyanoacrylates are summarized in Table II. The results were found to correspond with those of Bellanato *et al.*[2].

TABLE II

IR ABSORPTIONS (cm^{-1}) AND ASSIGNMENTS (SYMBOLS AS PROPOSED BY SOHÁR *et al.*[6]) OF THE PREPARED COMPOUNDS $R_2NCH=C(CN)COX$

R	*X*	ν_{as} (NH_2)	ν_s (NH_2)	ν (*CN*)	ν (*C=O*)	ν (*C=C*)	β_s (NH_2)	ν (*C–N*)	γ (NH_2)	*Isomer*
H	C_2H_5O	3330	3180	2220	1675	1610	–	1160	730	*E*
H	C_2H_5O	3380	3250	2210	1680	1610	1560	1230	730	*Z*
H	CH_3O	3320	3200	2210	1680	1620	1550	1220	780	
H	NH_2	3350	3150	2210	1670[a]	1620	1560	1180	770	
CH_3	NH_2	3380	3200	2200	1665[a]	1640	–	1140	–	
CH_3	C_2H_5O	–	–	2210	1700	1625	–	1220	–	

[a] Amide I band.

In DMSO-d_6 at room temperature simple ^1H NMR spectra were obtained *e.g.*, for ethyl 3-amino-2-cyanoacrylate; ^{13}C NMR, because of the longer time needed, resulted in duplication of the bands, in the same way as at 80°C with ^1H NMR. We can assign the bands to the isomers, separated by crystallization (Table III).

On injecting either **2** or **3** into the gas chromatograph the same chromatograms were obtained, showing that isomerization takes place in the sample chamber. According to the quantitative evaluation, in the thermodynamic equilibrium the ratio of the *Z*/*E* isomers is 30:70 (w/w). The chromatogram is shown in Fig. 1.

The N,N-disubstituted compounds, *e.g.*, ethyl 3-dimethylamino-2-cyanoacrylate (**6**), showed a single peak under the same chromatographic conditions, owing to the small tendency for rotation around the double bond.

When methyl or ethyl 3-amino-2-cyanoacrylate in methanol or ethanol solution was injected repeatedly into the HPLC column, two peaks appeared and their ratio as a function of time changed as shown in Fig. 2. Thermodynamic equilibrium was attained in neutral solution in 2 h, whereas above pH 7 this happened within a few seconds. In acidic solutions the aminocyanoacrylates are not isomerized; for this

TABLE III

^1H AND ^{13}C NMR BANDS **2** AND **3**

The CH band of isomer **2** could not be assigned because of the near NH_2 bands.

Method	*Band*	*δ(ppm)*	
		E	*Z*
^1H NMR	CH_3	1.20	1.23
	CH_2	4.11	4.14
	CH	8.06	–
^{13}C NMR	C-1	165.21	166.48
	C-2	71.13	69.91
	C-3	158.49	159.25
	CN	116.45	119.21
	CH_2	59.67	59.58
	CH_3	14.36	14.30
	Coupling constant (Hz)		
	^3J(CO,H)	3.36	10.07
	^3J(CN,H)	9.99	4.86

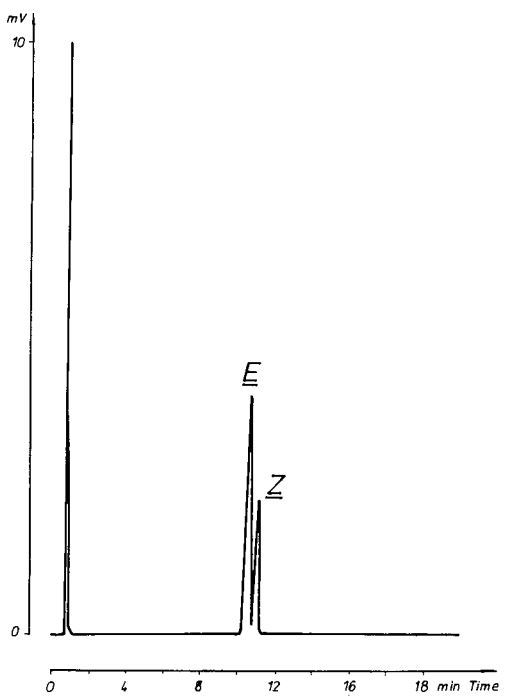

Fig. 1. GC of (*E*)-ethyl 3-amino-2-cyanoacrylate. HP-5 column. Temperature: injector, 220°C; detector, 240°C; oven, 140°C, isothermal.

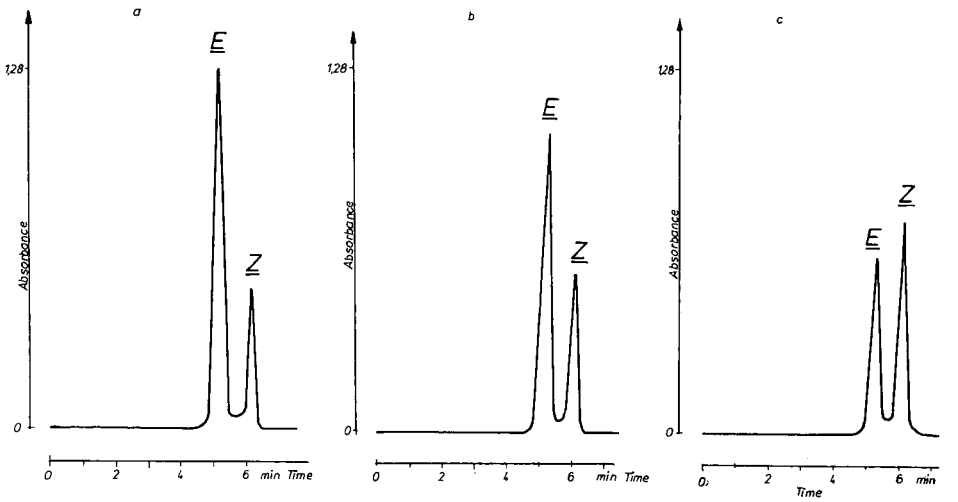

Fig. 2. HPLC of pure *E* isomer of ethyl 3-amino-2-cyanoacrylate. Injection at (a) 20, (b) 40 and (c) 120 min after dissolution in ethanol (5 mg in 10 ml). RP-8 column; mobile phase, acetonitrile–phosphate buffer (40:60, v/v); wavelength, 272 nm.

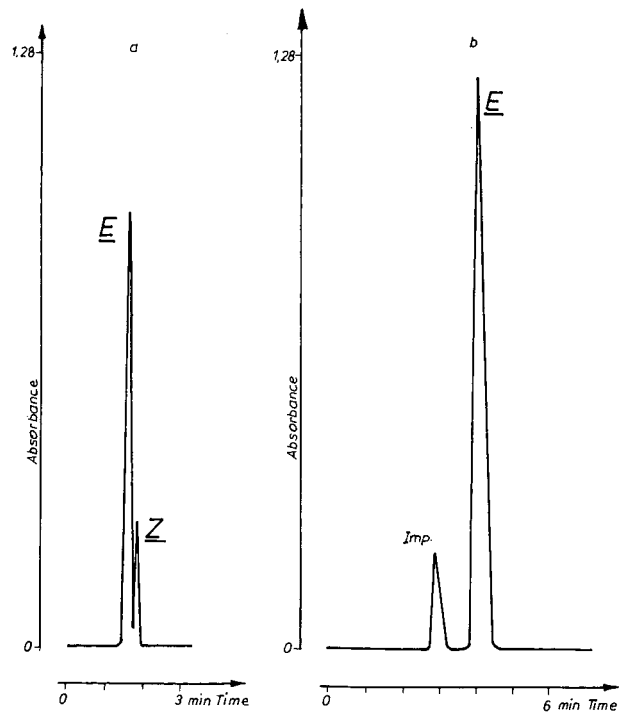

Fig. 3. (a) HPLC separation of 3-amino-2-cyanoacrylamide isomers and (b) HPLC of ethyl 3-dimethylamino-2-cyanoacrylate (*E* isomer). Conditions as in Fig. 2.

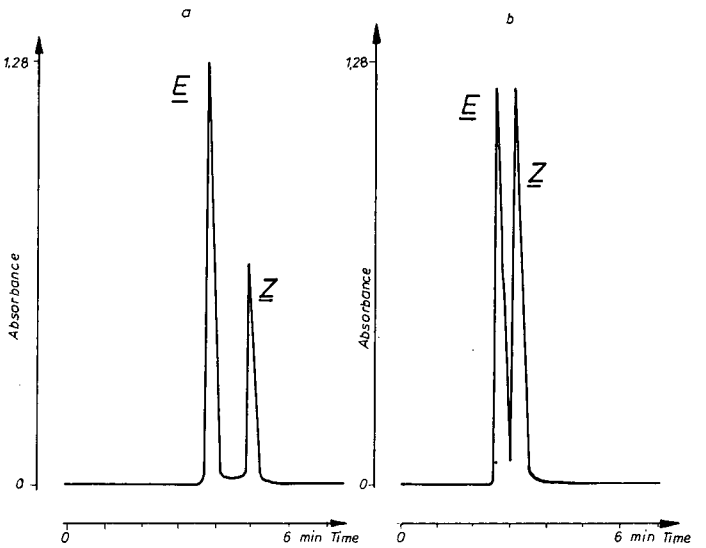

Fig. 4. HPLC separation of (a) ethyl and (b) methyl 3-amino-2-cyanoacrylate isomers. Conditions as in Fig. 2.

reason, we used a mobile phase of pH 4. The retention times of these compounds change very little with the pH of the mobile phase.

It is important to emphasize that an eluent of alkaline pH must not be used in the analysis of these compounds. In an alkaline mobile phase the just separated isomers are immediately reconverted to each other during the elution, resulting in a broad peak. A similar phenomenon was described by Jacobson *et al.*[3] and Jansen and Both-Miedema[4]

HPLC showed that in acetonitrile solution, unlike in alcohols, the unsubstituted compounds do not undergo isomerization for a few hours because of the absence of hydrogen.

Using an RP-18 column the separation was the same as that on the RP-8 column, but the retention times were longer.

TABLE IV

UV ABSORBANCES OF AMINOCYANOACRYLATES IN ACETONITRILE

Compound	*Absorbance maximum (nm)*	$A_{1\,cm}^{1\%}$
1	270	Isomer mixture
2	274	1040
3	276	1260
4	273	1467
5	286	1360
6	285	1285

We also succeeded in resolving the Z/E isomers of 3-amino-2-cyanoacrylamide and methyl 3-amino-2-cyanoacrylate (Figs. 3 and 4).

In Table IV the UV absorbances of aminocyamoacrylates measured in acetonitrile are summarized.

ACKNOWLEDGEMENT

The authors are grateful to the State Office for Technical Development for financial help.

REFERENCES

1 E. Knippel, M. Knippel, M. Michalik, H. Kelling and H. Kristen, *J. Prakt. Chem.*, 320 (1978) 457.
2 J. Bellanato, A. G. Sanchez and P. Borrachero, *An. Quim.*, 72 (1976) 876.
3 J. Jacobson, W. Melander, G. Vaisnys and Cs. Horváth, *J. Phys. Chem.*, 88 (1984) 4536.
4 E. H. J. M. Jansen and R. Both-Miedema, *J. Chromatogr.*, 435 (1988) 363.
5 H. Bredereck, *Chem. Ber.*, 97 (1964) 3397.
6 P. Sohár, S. Holly and Gy. Varsányi, *Kém. Közl.* 31 (1969) 197.

Journal of Chromatography, 507 (1990) 417–420
Elsevier Science Publishers B.V., Amsterdam — Printed in The Netherlands

CHROMSYMP. 1825

Determination of phenol in poly(vinyl chloride)

T. SUORTTI
Technical Research Centre of Finland, Food Research Laboratory, Biologinkuja 1, SF-02150 Espoo (Finland)

SUMMARY

There are strong indications that some poly(vinyl chloride) (PVC) plastics may contain phenol. This would be particularly harmful in the case of PVC used as a raw material for toys. An analytical method for determining phenol in PVC was therefore designed. The method is based on dissolving the whole sample in tetrahydrofuran and precipitating PVC by addition of water. After filtration the solution is ready for injection into an HPLC instrument. For quantitative analysis *p*-cresol is used as internal standard and it is added to the THF solution before precipitation. The method is applicable in the concentration range 50–3000 mg phenol/kg PVC. The detection limit is about 10 mg phenol/kg PVC but may be easily increased ten-fold by gentle removal of tetrahydrofuran from the sample solution and cleaning of the sample with C_{18} cartridge, which allows the injection of larger volumes and thus improves sensitivity.

The method has been submitted for collaborative study in municipal laboratories in Finland.

INTRODUCTION

There are several possible sources of the contamination of poly(vinyl chloride) (PVC) with phenol, *e.g.*, from the residual stabilizer in raw material or from various additives[1]. PVC used for toys is an especially undersirable case of such contamination.

Although there are several high-performance liquid chromatographic (HPLC) methods for the determination of phenol, they are mostly designed for the analysis of environmental samples[2–5] and no method for these kinds of samples has been published. The detection of phenol is normally carried out using UV detection, although fluorescence and electrochemical detection, which offer better selectivity or higher sensitivity, are also applied.

EXPERIMENTAL

The HPLC instrument consisted of an N-6000A pump, an M-710 WISP automatic injector, a Novapak C_{18} column (100 × 8 mm I.D.) in an RCM-100 column chamber and a Maxima 820 data station. The detectors employed were an M-490 UV detector (280 nm), an M-420 fluorescence detector (excitation wavelength 280 nm,

0021-9673/90/$03.50

emission wavelength 305 nm) (all from Millipore and Waters Assoc.) and an ESA 5100A electrochemical detector (0.8 V potential). The mobile phase was methanol–water–acetic acid (40:60:1) at a flow-rate of 1 ml/min.

Sample preparation

A 0.5-g sample of PVC, which had been cut into small pieces, was dissolved in 10 ml of tetrahydrofuran (THF) and 1 ml of *p*-cresol (Aldrich-Chemie) (1000 mg/l in THF) was added as an internal standard. The dissolution normally required overnight shaking. Then 15 ml of water were added to the sample to precipitate PVC. After standing for 15 min, the turbid sample was injected into the HPLC instrument. Standards were prepared by adding 1 ml of internal standard solution to 25 ml of 160, 30 and 5 mg/l phenol standards in THF–water (40:60).

Sample clean-up by solid-phase extraction

THF was released under vacuum from 10 ml of sample solution made as described above. Acetic acid (100 μl) was added to the sample and the mixture was quantitatively transferred into a Sep-Pak C_{18} column (Millipore–Waters) (conditioned with 5 ml of methanol and 10 ml of water). After trapping the fraction, the Sep-Pak column was washed with 5 ml of water and the phenol and *p*-cresol were eluted with 2 ml of methanol–water (60:40). The eluate was transferred into 10-ml measuring flasks, which were filled to the mark. Injections of 50–400 μl of this solution into the HPLC instrument were made.

Preparation of contaminated PVC sample

A 300-mg amount of phenol was accurately weighed and dissolved in 500 ml methanol which was blended with 100 g of PVC powder. The PVC powder was raw material (Neste) intended for the manufacture of toys and, according to the manufacturer and our analysis, was free from phenol and *p*-cresol (< 1 mg/kg), although it did contain ordinary additives. Methanol was released from the slurry under vacuum and the dry cake was thoroughly ground and screened to give a homogeneous sample to be blended with pure PVC to obtain samples with known phenol content for recovery studies and for the laboratory testing of the method.

RESULTS AND DISCUSSION

As THF dissolves PVC samples, it was natural to avoid elaborate and less reproducible extraction of the sample with other solvents. The calibration graphs for both phenol and *p*-cresol were linear ($r^2 = 0.999$) from 150 to 2 mg/l and 25–100 μl. Injection of both compounds dissolved in either the eluent or 40% THF gave peaks of equal height for the same injection volume, so the injection of samples into solvents stronger than the eluent had no reducing effect on the plate count. The peak height for 25–100-μl injections increased linearly, but larger injection volumes made the peak heights less linear, although the peak area naturally still increased linearly. The peak height for the 200-μl injection was only 1.9 times higher than that for the 100-μl injection.

The standards were stable for several weeks when stored in the dark at 4°C, although storage for 2 weeks at room temperature destroyed 15% of both phenol and *p*-cresol.

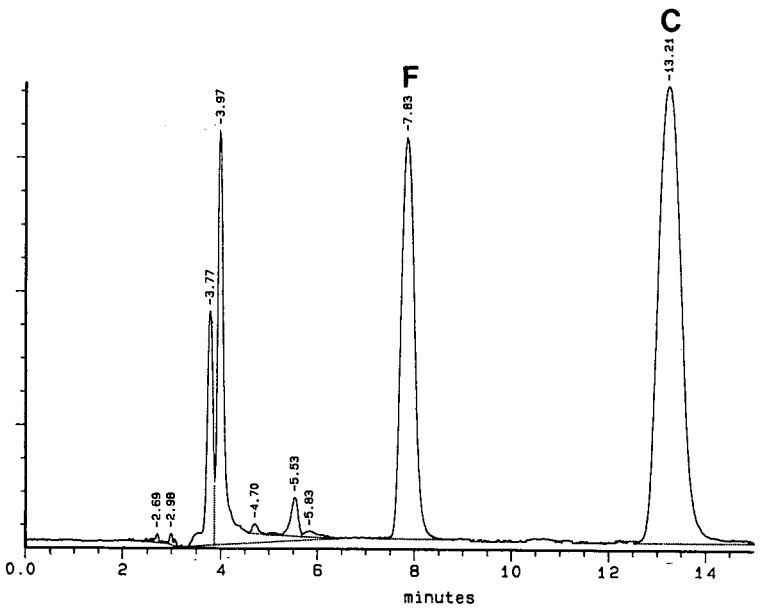

Fig. 1. Chromatogram obtained from a 50-μl injection of sample prepared according to the described procedure. F = phenol; C = *p*-cresol. The starting material was PVC spiked with 600 mg/kg of phenol. For other details see text. Sensitivity, 0.02 a.u.f.s.

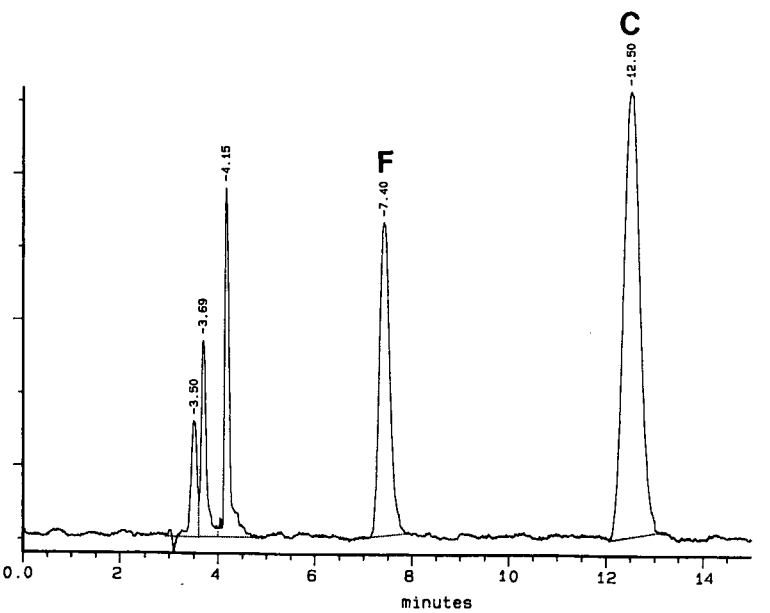

Fig. 2. Chromatogram obtained from a 400-μl injection of sample prepared according to the described procedure with Sep-Pak C_{18} clean-up. F = Phenol; C = *p*-cresol. The starting material was PVC spiked with 60 mg/kg of phenol. The concentration of internal standard (*p*-cresol) was reduced to one tenth. For other details see text.

TABLE I

RESULTS FROM COLLABORATIVE TESTING OF THE METHOD

Nominal	*Observed*	*n*	*R.S.D. (%)*
3000	3060	7	6.1
2700	2717	7	7.0
3000	3050	7	5.8
0	0	7	
600	637	6	7.1
600	625	6	5.4
480	483	6	7.3

No peak at the retention time of *p*-cresol was found in 2000 mg/l phenol standard, nor did the injection of *p*-cresol of equal strength give any peak at the retention time of phenol. None of the PVC samples studied showed any peak at the retention time of *p*-cresol. The recovery for a spiked sample (Fig. 1) containing 600 mg/kg of phenol was 104% for phenol and 101% for *p*-cresol, a relative standard deviation 0.9% ($n=4$) being found for the ratio of phenol to *p*-cresol. For the actual samples in which phenol was found, its identity was confirmed by the use of fluorescence detection in addition to the normally used UV detection, and also by semi-preparative chromatography followed by mass spectrometric identification of the isolated compound[6].

The method was submitted to seven municipal and industrial laboratories for collaborative testing. The results from this study are presented in Table I. As can be seen, the results are very satisfactory and only a few results from one laboratory had to be eliminated on the basis of Grubb's test.

The utilization of trace enrichment to increase sensitivity is not hindered by disturbing peaks, but the injection of samples from which THF was released under vacuum resulted in a rapid increase in back-pressure. Therefore, Sep-Pak C_{18} treatment of samples was applied. The recovery for phenol in this treatment was 97.8% and for *p*-cresol 98.3%. For samples spiked at the 60 mg/kg level, the recovery was 99.6% for phenol and 103.0% for *p*-cresol and the relative standard deviations for four parallel determinations were 4.4 and 2.7%, respectively (Fig. 2). The use of volumetric flasks in sample preparation was needed only for recovery studies, otherwise quantification was based on the internal standard method.

In a limited experiment, electrochemical detection was applied. The concentration of internal standard solution was reduced to one tenth and the recovery for samples spiked at the 30 mg/level was 92.5% for phenol and the standard deviation was 4.2% for four parallel samples made with the sample preparation procedure without Sep-Pak C_{18} clean-up.

The method described provides a simple and reproducible analysis of phenol in PVC with simple sample preparation and with detection at the ppm level.

REFERENCES

1 L. I. Nass, *Encyclopedia of PVC*, Marcel Dekker, New York, Basle, 1976, pp. 29, 102, 288, 357 and 852.
2 K. Ogan and E. Katz, *Anal. Chem.*, 53 (1981) 160.
3 R. E. Shoup and G. S. Mayer, *Anal. Chem.*, 54 (1982) 1164.
4 N. G. Buckman, J. O. Hill, R. J. Masee and M. J. McCormic, *J. Chromatogr.*, 284 (1984) 441.
5 G. Jeanty, J. Massé, P. Bercot and F. Coq, *Beitr. Tabakforsch. Int.*, 12 (1984) 245.
6 Anon., *J. Assoc. Off. Anal. Chem.*, 72 (1989) 694.

Journal of Chromatography, 507 (1990) 421–425
Elsevier Science Publishers B.V., Amsterdam — Printed in The Netherlands

CHROMSYMP. 1732

Note

Determination of fungistatic quaternary ammonium compounds in beverages and water samples by high-performance liquid chromatography

T. SUORTTI*
Technical Research Centre of Finland, Food Research Laboratory, 02150 Espoo (Finland)
and
H. SIRVIÖ
Kaukomarkkinat Oy, 02150 Espoo (Finland)

Fungistatic and fungicidal quaternary alkylammonium compounds are widely used in the prevention of staining of timber. They may also find application in the steeping of barley for restricting the growth of fungi. Although they show only low toxicity, sensitive methods are required for their trace determinations as contaminants in food products and water.

Problems arise with their analysis because they are of low volatility, they do not carry any chromphore and they are difficult to derivatize. The traditional method for their determination has been based on ion-pair extraction followed by photometric detection. Naturally such a system has low selectivity and is therefore most suitable for quality control purposes. Ion-pair extraction has also been applied as a detection system after high-performance liquid chromatographic (HPLC) separation[1], and the other method applied is so-called vacancy chromatography[2]. The former method requires specific equipment and the latter is susceptible to disturbances from the matrix. The use of a refractive index detector, although possible for various formulations[3], is normally affected by other substances in more complicated matrices.

The aim of this study was to develop a simple procedure for the determination of quaternary alkylamines at the μg/ml level.

EXPERIMENTAL

The instrument consisted of an M-6000A pump, a U6K manual injector, a Novapak CN column (100 × 8 mm I.D. packed with 4-μm particles) in an RCM-100 column chamber, an M-411 refractive index detector and Model 820 Maxima chromatographic workstation (all from Millipore/Waters).

Sodium benzenesulphonate (Fluka, Switzerland), sodium *p*-toluenesulphonate (Aldrich, U.S.A.) and sodium *dl*-10-camphorsulphonate (Eastman Kodak, U.S.A.) were dissolved in water to give 0.5 *M* solutions, filtered through a 0.45-μm filter and used as stock solutions from which various dilutions were made.

0021-9673/90/$03.50

As reference compounds didecyldimethylammonium chloride (Lonza, U.S.A.), and dodecyltrimethylammonium bromide (Aldrich) were used as solutions in water for the spiking of samples, and for standard solutions these compounds were diluted with the eluent.

Sample preparation

To 100 ml of decarbonated beer or water, 100 ml of methanol and 10 ml of 50 m*M* benzenesulphonic acid solution were added. The solution was filtered through a medium-fast filter-paper, then through a Sep-Pak C_{18} cartridge (preconditioned with 5 ml of methanol and 10 ml of water) by suction. The quaternary alkylamine–benzenesulphonic acid ion pair was then eluted from the column with 2 × 2 ml of 95% methanol in water and adjusted to 5 ml with water. For wort samples the sample size was restricted to 50 ml because of plugging of the Sep-Pak cardridge. Injections of 50 μl were made into the HPLC instrument.

RESULTS AND DISCUSSION

In Table I the effect of the concentration of benzenesulphonic acid on retention is shown. An increase in the concentration of an ion-pairing agent normally increases the retention, but in this instance for both compounds the opposite trend was observed. The same phenomenon was also reported by Abidi[4] for similar compounds using perchlorate ion pairs and a CN column. This must be the reason for the high selectivity of these quaternary alkylamines for such a complex matrix as beer and wort (Fig. 1). The selectivity between didecyldimethylammonium and dodecyltrimethylammonium is poor, but as these compounds show the expected increase in retention with decreasing methanol content in the eluent, the selectivity may be improved simply by decreasing the methanol concentration (Table I). Experiments with a Novapak C_{18} column showed that the same phenomenon occurs, but is less pronounced. As the

TABLE I

EFFECT OF CONCENTRATION OF BENZENESULPHONIC ACID AND METHANOL ON THE RETENTION OF DIDECYLDIMETHYLAMMONIUM (DE) AND DODECYLTRIMETHYLAMMONIUM (DO)

Column: Novapak CN.

Compound	*Concentration of benzene sulphonic acid (mM)*	*k'*		
		Concentration of methanol in aqueous eluent (%)		
		60	*70*	*80*
DE	10	7.7	6.6	1.2
	30	3.3	1.0	0.6
	50	2.8	0.8	0.5[a]
DO	10	3.4	1.8	1.2
	30	1.8	1.0	0.6
	50	1.5	0.8	0.5[a]

[a] 75% methanol.

capacity factor (k') on a C_{18} column with 80% methanol was five times larger and the solubility of benzenesulphonic acid begins to be a limiting factor with higher methanol concentrations, only a few experiments could be carried out [at benzenesulphonic acid concentrations of 5, 10 and 25 mM, the k' values of didecyldimethylammonium were 1.0, 0.86 and 0.66, respectively, using a Novapak C_{18} column and methanol–water (80:20) as the eluent].

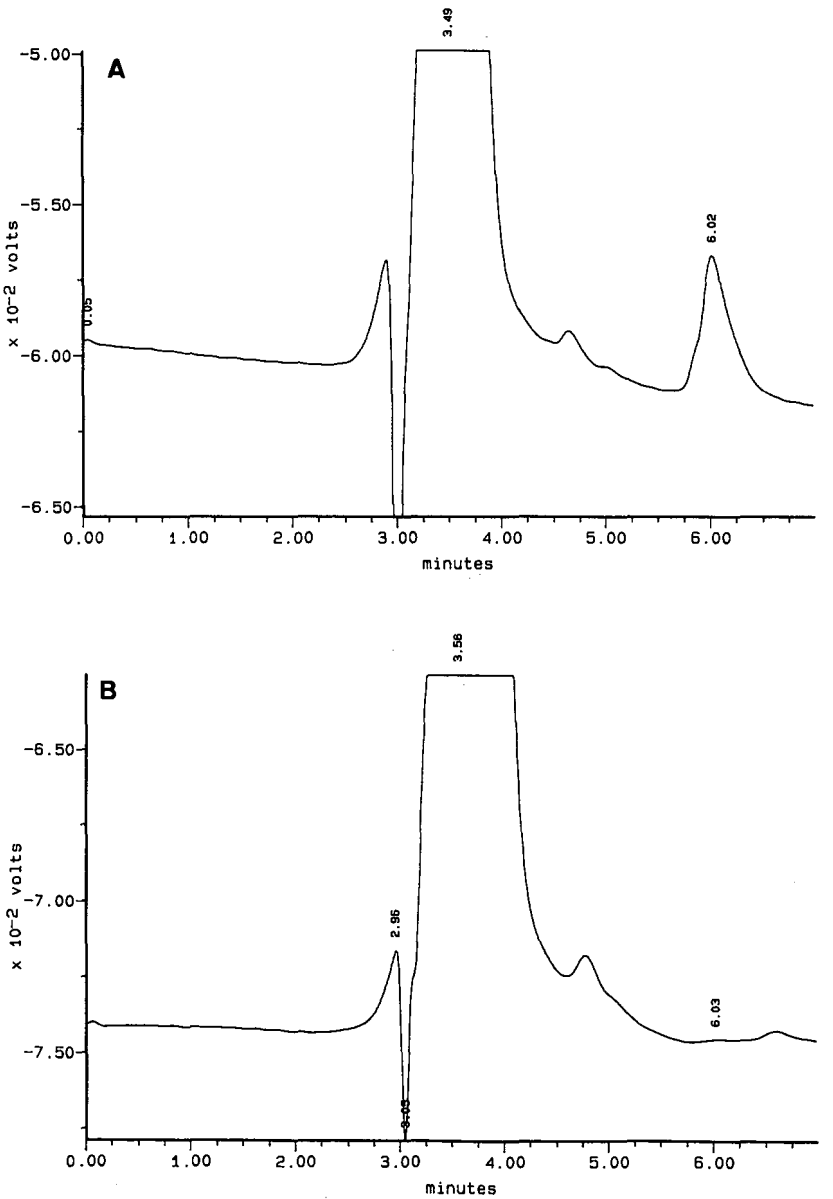

Fig. 1.

(*Continued on p. 424*)

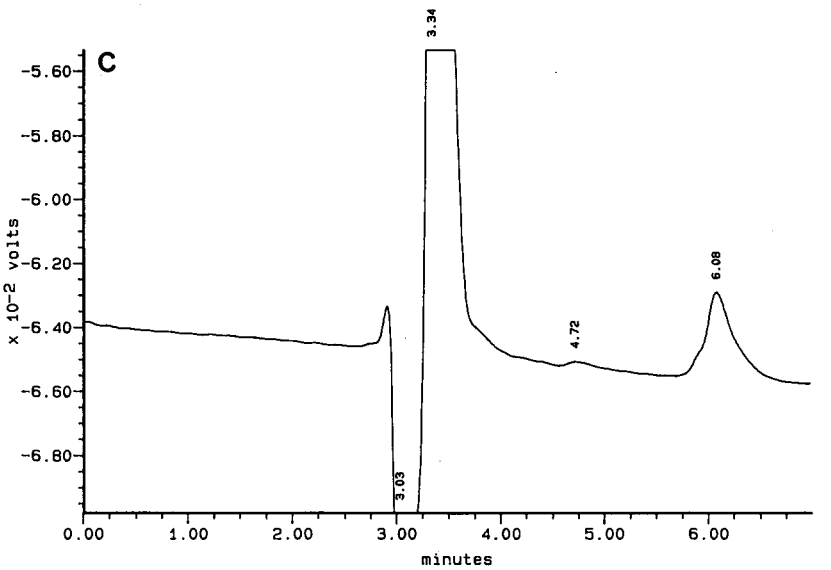

Fig. 1. Chromatograms of (A) a beer sample spiked at the 25 mg/l level with didecyldimethylammonium (B) an unspiked beer sample and (C) a 200 mg/l standard. Eluent, methanol–water (80:20) with 10 m*M* sodium benzenesulphonate.

To clarify this phenomenon further, chromatography with toluenesulphonic acid and camphorsulphonic acids as ion-pairing agents was performed. With an 80% methanol concentration the retention of reference compounds was about 50% shorter using camphorsulphonic acid and about 20% longer using toluenesulphonic acid compared with chromatography using benzenesulphonic acid, so the normal ion-pairing seems to be the effective mechanism in spite of this unusual phenomenon of decreasing retention with increasing concentration of ion-pairing agent.

The calibration graph was linear ($r^2 = 0.97$) from 500 to 50 mg/l. The injection of higher concentrations of standards gave tailing peaks with a sharp front, indicating overloading of the chromatographic system. Spiked samples containing about 10 g/l of quaternary amine showed symmetrical peaks with the same retention as the 500 mg/l standard.

The recovery from three beer samples spiked at the 25 mg/l level was 70% with a relative standard deviation (R.S.D.) of 7%. For three beer samples spiked at the 2.5 mg/l level the recovery was 62% with an R.S.D. of 9%. For three wort samples the corresponding values were 64% with an R.S.D. of 20% at the 25 mg/l level and 45% with an R.S.D. of 23% at the 2.5 mg/l level. The three samples spiked at the 2.5 mg/l level gave peaks that were about 20 times higher than the fluctuation of the baseline, so the detection limit would be about 0.3 mg/l and the determination limit in the 1 mg/l range. For water samples dodecyltrimethylammonium was used for spiking to imitate those fungistatic preparations which are based on cocoa fatty acids. The recovery for a sample spiked at the 50 mg/l level was 68% with an R.S.D. of 23%.

In conclusion, the use of the anomalous effect of the concentration of an

ion-pairing agent on C_{18} and CN columns allows the determination of quaternary alkylammonium compounds in complex matrices with good sensitivity and selectivity.

REFERENCES

1 J. Kawase, Y. Takao and K. Tsuji, *J. Chromatogr.*, 262 (1983) 293.
2 J. Crommen, G. Schill, D. Westerlund and L. Haczell, *Chromatographia*, 24 (1987) 252.
3 S. Sato and Y. Ohno, *Reports of the Central Customs Laboratory*, No. 19, Ministry of Finance, Central Customs Laboratory, Japan.
4 S. L. Abidi, *J. Chromatogr.*, 324 (1985) 209.

Journal of Chromatography, 507 (1990) 427–437
Elsevier Science Publishers B.V., Amsterdam — Printed in The Netherlands

CHROMSYMP. 1767

Liquid chromatography of organotin compounds on cyanopropyl silica gel

A. PRAET
Laboratorium voor Algemene en Anorganische Chemie, Rijksuniversiteit Gent, Krijgslaan 281 S3, B-9000 Ghent (Belgium)
C. DEWAELE*[,a]
Laboratorium voor Organische Chemie, Rijksuniversiteit Gent, Krijgslaan 281 S4, B-9000 Ghent (Belgium)
and
L. VERDONCK and G. P. VAN DER KELEN
Laboratorium voor Algemene en Anorganische Chemie, Rijksuniversiteit Gent, Krijgslaan 281 S3, B-9000 Ghent (Belgium)

SUMMARY

Several stationary phases were evaluated for the liquid chromatography of organotin compounds. Cyanopropyl-derivatized silica gels are the most versatile phases for this type of analysis. In order to reduce stationary phase activity, an iodine chloride "on-column" pretreatment was developed. This leads to very fast quantitative and qualitative separations, as was demonstrated by the analysis of organotin standards, organotin-containing tungsten carbonyl complexes and organotin halides for reaction kinetic studies.

INTRODUCTION

Despite the enormous industrial and environmental interest in organotin compounds, good analytical methodology is still lacking. A few liquid chromatographic (LC) methods have been developed for specific tasks[1–4], the main research work being focused on the detection aspects for trace analysis[5–13]. At present, however, there are still problems with LC phase systems for this type of analysis and reproducing published LC methods is often very tedious.

Organotin compounds have a high reactivity towards oxygen-, nitrogen- and sulphur-containing matrices[1]. Reversed-phase LC used relatively inert stationary phases but polar reactive mobile phases. Normal-phase LC uses non-reactive mobile phases. The stationary phases however, owing to the presence of unreacted silanol groups or other reactive moieties, are not sufficiently inert towards reactive organotin halides. This results in irreversible adsorption and peak tailing in both the reversed-phase and normal-phase modes.

[a] Present address: Bio-Rad RSL, Begoniastraat 5, 9731 Eke, Belgium.

0021-9673/90/$03.50

Several phase systems have been described. Silica gel is not sufficiently inert against the reactive organotin halides[1]. Silanized silica gel, C_8 and C_{18} were tried with both normal[1,2] and reversed[14] mobile phases. Pyrocarbon–silica[1], poly(styrene–divinylbenzene) copolymers[1] and silica-based cation exchangers[3] have also been evaluated. One of the most succesful phases is cyanopropyl silica gel[4,8,15]. However, all these studies used either morin complexes or high concentrations of acetic acid in order to mask hydrogen bonding with remaining silanol groups[4].

In this study, different stationary phases for the analysis of organotin compounds were re-examined. New methods, based on a cyanopropyl phase, in which the addition of acid or modifier to the mobile phase is avoided, are proposed.

EXPERIMENTAL

A Varian 5020 liquid chromatograph equipped with a Varian Vista data system (CDS 401) (Varian, Walnut Creek, CA, U.S.A.) was used as a solvent-delivery system. Injections were made with a Rheodyne 7125 RV valve equipped with a 10-μl loop. The detector was a Varian 2050 variable-wavelength UV detector, a Waters refractive index detector or an LKB diode-array rapid spectral detector (LKB, Bromma, Sweden). The columns were 15 or 25 × 0.46 cm I.D. stainless-steel tubes with Valco fittings. RoSiL and RSiL (RSL, Eke, Belgium), Spherisorb (Phase Separations, Queensferry, U.K.) and Nucleosil (Machery, Nagel & Co., Düren, F.R.G.) packing materials were evaluated. The solvents used were of high-performance liquid chromatography (HPLC)grade (Alltech, Deerfield, IL, U.S.A.). Organotin compounds were purchased from Merck (Darmstadt, F.R.G.) or synthesized in the laboratory[16].

The procedure for "on-column" treatment with iodine chloride (ICl) is as follows. An empty LC column (15 × 0.46 cm I.D.) was filled with 0.5% ICl solution in hexane–tetrahydrofuran (THF) (90:10) and installed between the injector and the analytical column. This solution was pumped into the column at 1 ml/min. During this pretreatment the detector was removed from the column. Subsequently the column was rinsed with about 30 ml of solvent until a stable baseline was obtained. Sometimes a second treatment was necessary.

RESULTS AND DISCUSSION

During this study, different stationary phases were evaluated for the analysis of organotin compounds, including some phases examined previously and some completely new. As the results in the literature are contradictory and difficult to reproduce, our results are summarized as follows.

Octadecyl silica gel: owing to the polarity and reactivity of the methanol– or acetonitrile–water mixtures, reversed-phase LC is unsuitable for the analysis of organotin halides. The applicability is restricted to the analysis of tetraalkyltin compounds. Tetramethyl-, -ethyl-, -propyl-, -butyl- and -phenyltin can easily be separated in the isocratic mode.

Poly(styrene–divinylbenzene): these packing materials, being silanol-free, offer good prospects for organotin separations. Used in the reversed-phase mode, again only the analysis of the tetraalkyltin compounds is possible. In the normal-phase mode with hexane–THF mixtures fairly good separations of the organotin halides

can be achieved. Even the monoalkyltin compounds elute from the column. A disadvantage, however, is the low efficiency of the columns.

Aminopropyl silica gel: this is unsuitable for this analysis. Owing to the free electron pairs on the nitrogen, the compounds are irreversibly adsorbed on the column.

Diol- or polyol-silica gel: these phases seem to be unsuitable for organotin compound analysis. The alcohol group tends to form strong hydrogen bonds and this results in irreversible adsorption or band broadening.

Cyanopropyl silica gel: in our experience and from literature data[4,8,15], cyanopropyl-bonded phases are the best for this type of analysis owing to the good selectivity and efficiency. This phase was chosen for the separation of all the organotin compounds here.

The retention and selectivity were optimized, a new deactivation procedure is proposed and the applicability is demonstrated by the analysis of a variety of organotin compounds.

Retention and selectivity on cyanopropyl-bonded silica gels

Cyano phases, used in the normal-phase mode, separate molecules according to their polarity. Consequently, the phase is less suitable for the separation of tetraalkyltin compounds. However, a separation can be obtained with the elution order (k'): $(C_4H_9)_4Sn < (C_3H_7)_4Sn < (C_2H_5)_4Sn < (CH_3)_4Sn < (C_6H_5)_4Sn$. The system is very selective for the number of R groups in the organotin compound. The elution order (k') is then $R_4Sn < R_3SnX < R_2SnX_2 < RSnX_3$. No separation can be obtained between tin compounds with the same alkyltin group and with different X = Cl, Br, I, acetate, oxide, etc.

Up to now the use of cyanopropyl phases has two major background: the silanol activity and brand-to-brand differences. These points were studied in detail.

Literature data[4] and our own experience show that silanol groups have a negative influence on the chromatographic behaviour or organotin compounds. Different methods for the removal of this silianol activity have been evaluated in our laboratory, *e.g.*, end-capping, dynamic modification with amines. None of the methods proved to be effective or reproducible. The addition of high concentrations of acetic acid (5% in the mobile phase) to mask hydrogen bonding with silanol groups has been proposed[4], but this method is not advisable in, for instance, preparative work.

During the analysis of ICl-containing solutions, a spectacular improvement in the peak shape was observed. Consequently, "on-column" treatment with ICl was optimized as a deactivation method for stationary phases for the analysis of organotin compounds. ICl is considered to form a strong hydrogen bond with the silanol groups. ESCA measurents[17] on ICl-treated silica gels and cyanopropyl silica gels showed a 1:1 ratio of Cl and I, which suggests adsorption and no chemical reaction. This treatment is effective for several weeks of continuous work. The optimized procedure is given under Experimental.

Fig. 1 shows the effect of the ICl treatment on the analysis of tributyltin naphthenate (TBTN) in a commercially available biocide. This treatment always results in a reduction in the retention time and an improvement in the peak shape.

Silica-based cyanopropyl phases can be synthesized by a number of different procedures. This results in brand-to-brand differences and hence different retentions

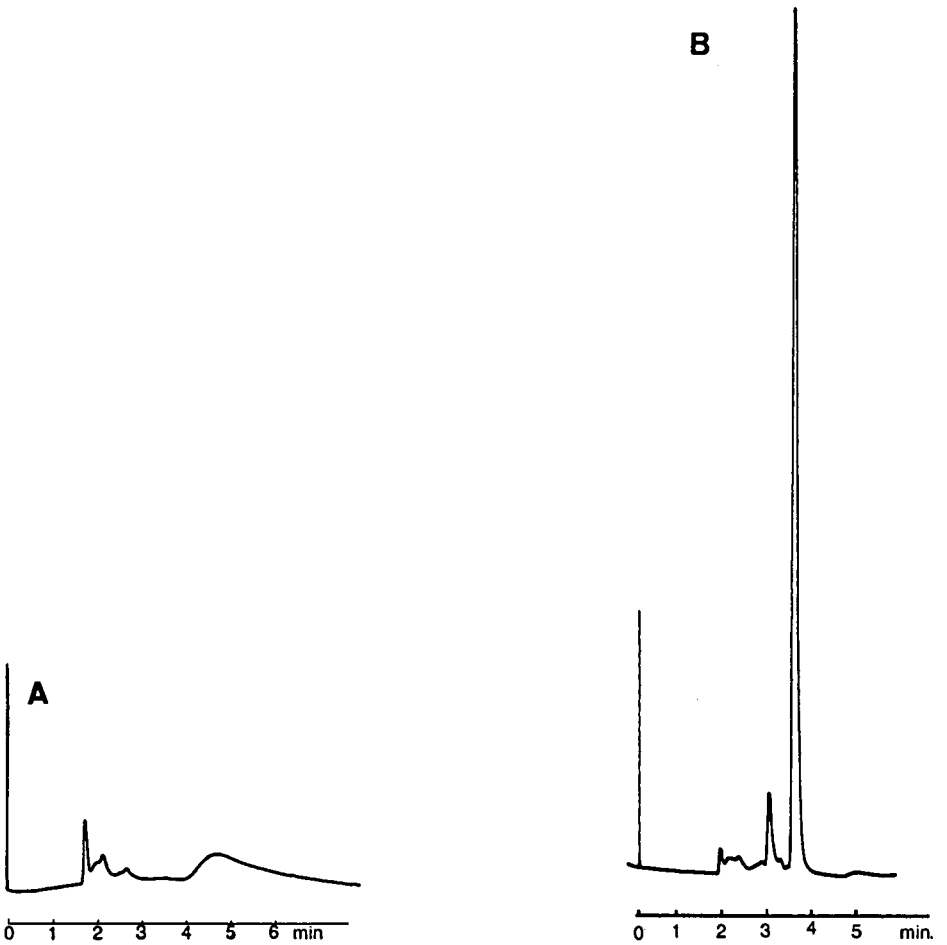

Fig. 1. Effect of ICl preteatment on the analysis of TBTN. Column, 3-μm RoSiL CN (15 × 0.46 cm I.D.); mobile phase, hexane; flow-rate, 1 ml/min; injection volume, 10 μl; detection, UV (220 nm). Sample: commercially available biocide containing TBTN dissolved in mobile phase. (A) Before; (B) after ICl treatment.

and selectivities for organotin compounds. Different laboratory-made and commercially available phases were tested.

In Table I, the capacity factors of some representative organotin halides on different types of cyano phases are shown. As silanol groups are extremely important, cyano phases produced with different silanization procedures on the same base silica gel were compared. The data in Table I were taken after ICl treatment. The following types were used: RoSiL CN prepared with cyanopropyltrichlorosilane and RoSiL $(CH_3)_2CN$ prepared with cyanopropyldimethylchlorosilane. A silica gel prepared with cyanopropyltrichlorosilane (non-end-capped) is expected theoretically to have a 1:2 cyano-to-silanol ratio whereas the cyanopropyldimethylchlorosilane derivative has a 1:0 cyano-to-silanol ratio. The first two RoSiL phases show that the retention

TABLE I

COMPARISON OF DIFFERENT TYPES OF CYANO PHASES FOR THE ANALYSIS OF ORGANOTIN COMPOUNDS

Experimental conditions: columns: 15 × 0.46 cm I.D. or 25 × 0.46 cm I.D. for Nucleosil CN and Spherisorb CN, pretreated with ICl; mobile phase, hexane–THF (90:10); flow-rate 1 ml/min; detection, UV at 220 nm; injection volume, 10 μl.

Compound	*k'*				
	RoSiL CN	*RoSiL $(CH_3)_2$ CN*	*Spherisorb CN*	*Nucleosil CN*	*Deltabond CN*[a]
$(C_4H_9)_3SnCl$	0.17	0.41	0.17	0.26	∞; 0.05[c]
$(C_2H_5)_3SnCl$	0.43	1.24; 0.35[b]	0.40	0.60	∞; 0.18[c]
$(CH_3)_3SnCl$	0.81	2.06	0.73	–	∞; 0.21[c]
$(C_6H_5)_3SnCl$	0.90	2.67; 0.50[b]	0.87	1.13	∞; 0.16[c]
$(C_4H_9)_2SnCl_2$	0.95	1.59[b]	–	2.19	∞; 0.32[c]
$(C_6H_5)_2SnCl_2$	1.83	7.41[b]	1.47	–	∞; 1.37[c]
$(C_2H_5)_2SnCl_2$	2.11	3.11[b]	2.23	∞	∞; 0.66[c]
$(CH_3)_2SnCl_2$	2.76	2.47[b]	2.33	∞	∞; 1.21[c]

[a] No pretreatment with ICl.
[b] Mobile phase: hexane–THF (50:50).
[c] Mobile phase: hexane–THF (75:25).

seems to be governed by the cyano-to-silanol ratio. The highest retention is obtained on the cyanopropyldimethylsilane-derivatized silica gel. Also, the peak shape is better for phases with a high concentration of cyano groups.

Other commercially available cyano phases were tested, such as Spherisorb CN

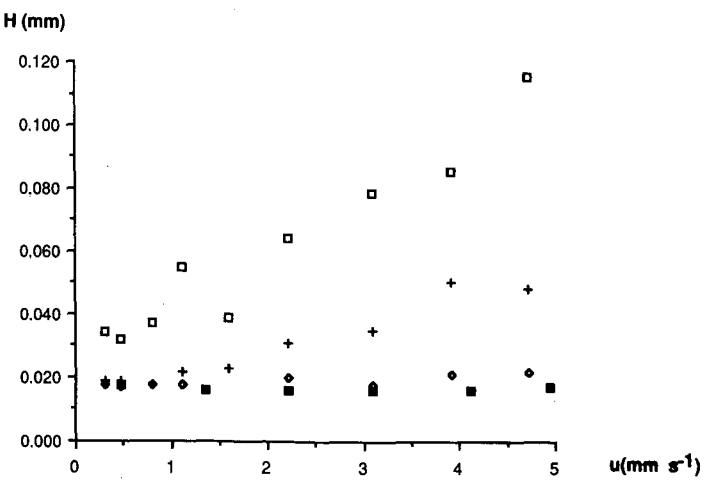

Fig. 2. *H–u* curves for organotin compounds on a cyanopropyl phase. Column as in Fig. 1. (a) Without pretreatment; mobile phase, hexane–THF–acetonitrile (75:18:7). (b) Pretreated with ICl; mobile phase, hexane–THF–acetonitrile (85:10:5). Detection, UV (220 nm). Plate number calculated from band width at half-height. ◇ = $(C_6H_5)_4Sn$ (a); + = $(C_6H_5)_3SnCl$ (a); □ = $(C_6H_5)_2SnCl_2$ (a); ■ = $(C_6H_5)_2SnCl_2$ (b).

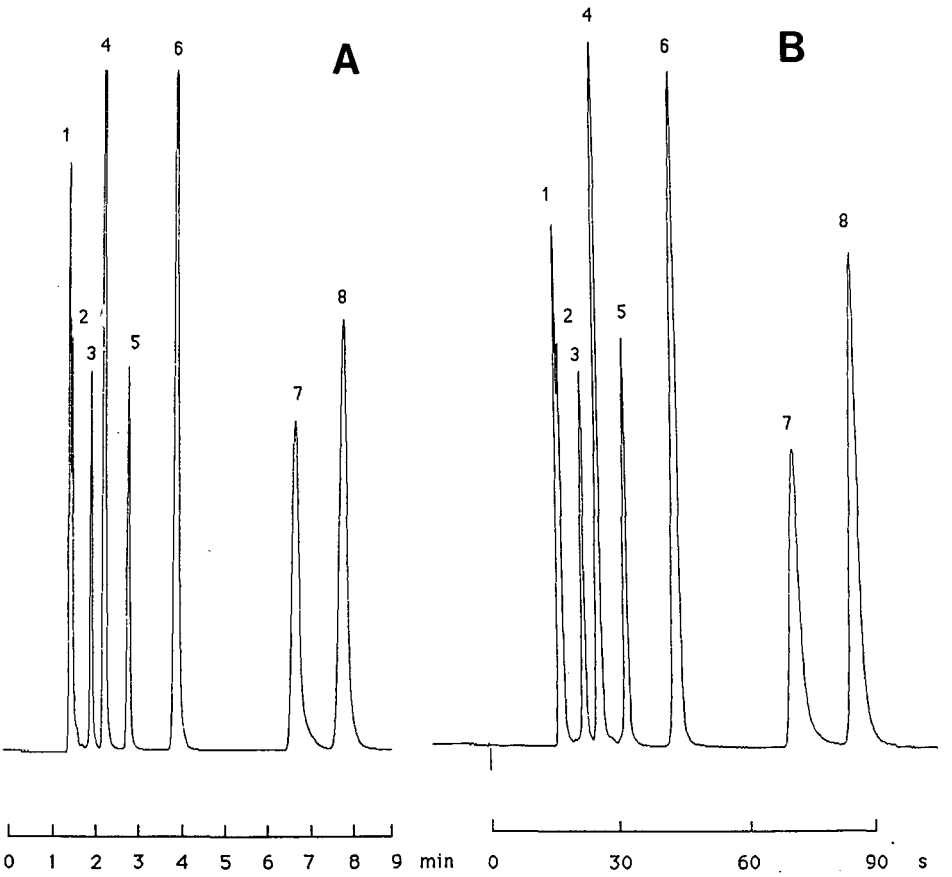

Fig. 3. Fast LC of organotin compounds on a cyanopropyl phase. Column as in Fig. 1. Mobile phase, hexane–acetonitrile–THF (90:4:6). Flow-rate: (A) 1 ml/min; (B) 6 ml/min. Detection, 220 nm (time constant 50 ms). Sample: 1 = $(C_4H_9)_4Sn$; 2 = $(C_2H_5)_4Sn$; 3 = $(C_4H_9)_3SnCl$; 4 = $(C_6H_5)_4Sn$; 5 = $(C_2H_5)_3SnCl$; 6 = $(C_6H_5)_3SnCl$, $(C_4H_9)_2SnCl_2$; 7 = $(C_6H_5)_2SnCl_2$; 8 = $(C_2H_5)_2SnCl_2$.

and Nucleosil CN. All these phases can be readily used for organotin analysis after ICl treatment. Nucleosil CN (see Table I) shows one of the highest retention times.

Finally, a Deltabond CN phase was evaluated. This phase, prepared by polymeric polysiloxane chemistry, is mentioned as being silanol-free[18], which offers good prospects for organotin analysis. Table I shows, however, a very high retention behaviour if tested under the same conditions as for the silane-based cyano phases. Peaks elute from the column on increasing the THF concentration but the peaks are very broad. Apparently this polymeric phase swells in normal-phase eluents and this reduces mass tranfer.

Efficiency

H–u curve. The ICl treatment has a great effect on the efficiency and symmetry of the peaks and also on the shape of the plate height *versus* linear velocity (*H–u*)

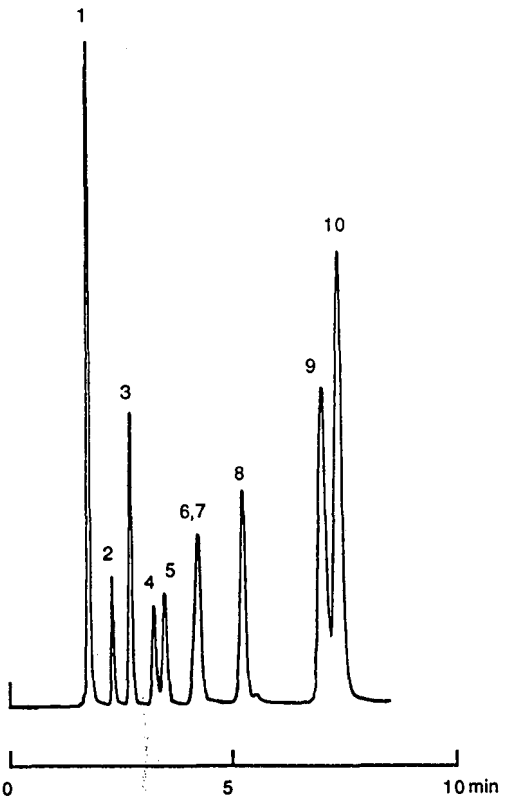

Fig. 4. LC of tungsten carbonyl complexes. Column as in Fig. 1. Mobile phase, hexane–THF (90:10); flow-rate, 1 ml/min; detection, LC–DAD; chromatogram at 220 nm. Sample: 1 = $W(CO)_6$; 2 = $(i\text{-}C_4H_9)_3SnW(CO)_3(\pi\text{-}C_5H_5)$; 3 = $(CH_3)_3SnW(CO)_3(\pi\text{-}C_5H_5)$; 4 = $(i\text{-}C_4H_9)_2ClSnW(CO)_3(\pi\text{-}C_5H_5)$; 5 = $[W(CO)_3(\pi\text{-}C_5H_5)]_2$; 6 = $(i\text{-}C_4H_9)_2Sn[W(CO)_3(\pi\text{-}C_5H_5)]_2$; 7 = $(CH_3)_2ClSnW(CO)_3(\pi\text{-}C_5H_5)$; 8 = $(C_6H_5)_3SnW(CO)_3(\pi\text{-}C_5H_5)$; 9 = $(C_6H_5)_2ClSnW(CO)_3(\pi\text{-}C_5H_5)$; 10 = $ClW(CO)_3(\pi\text{-}C_5H_5)$.

curve[19]. Fig. 2 shows the *H–u* curves for different phenyltin halides before and after this treatment. $(C_6H_5)_4Sn$ is not active towards the stationary phase and shows a relatively low resistance to mass transfer or *C* term (C = 0.2 ms). The *C* term for $(C_6H_5)_3SnCl$ and $(C_6H_5)_2SnCl_2$ is calculated to be 8.1 and 20 ms, respectively. After the ICl treatment all components show ideal chromatographic behaviour and the slope and intercept become comparable to the situation for $(C_6H_5)_4Sn$.

Fast analysis. One of the consequences of the low resistance to mass transfer is the possibility of ultra-fast LC of organotin compounds. This can be useful for routine analysis as the number of analyses per unit time on the same instrument can be increased by a factor of about 5. As can be seen from Fig. 2, the linear velocity can be increased without a decrease in efficiency. This is demonstrated in Fig. 3A and B for a mobile phase velocity of 1 and 6 ml/min. The analysis is completed in about 60 s without a decrease in resolution. Under these conditions, however, it is necessary to reduce the time constant of the detector to its minimum (50 ms).

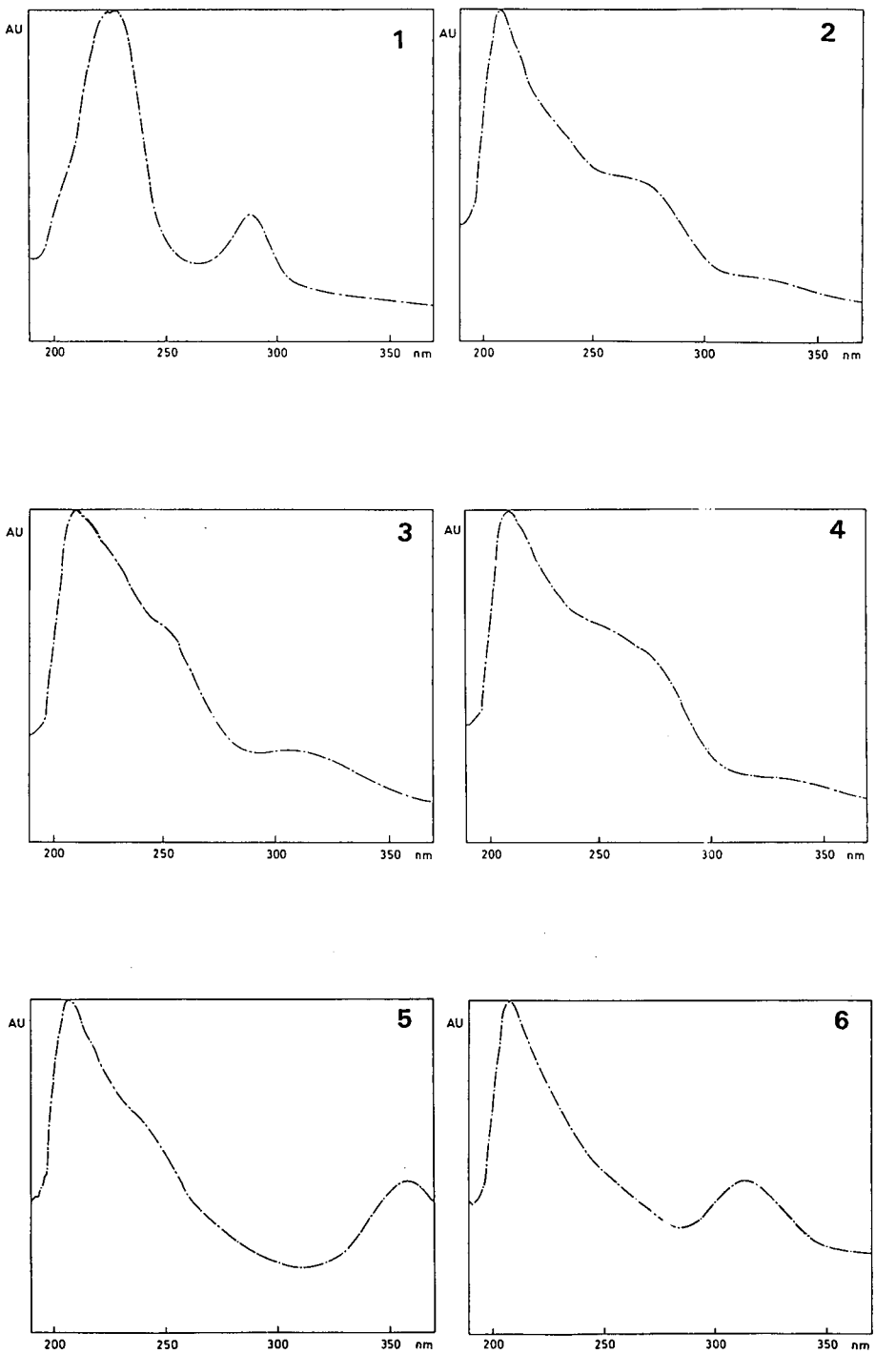
AU
1
200
250
300
350 nm
AU
2
200
250
300
350 nm
AU
3
200
250
300
350 nm
AU
4
200
250
300
350 nm
AU
5
200
250
300
350 nm
AU
6
200
250
300
350 nm

Fig. 5.

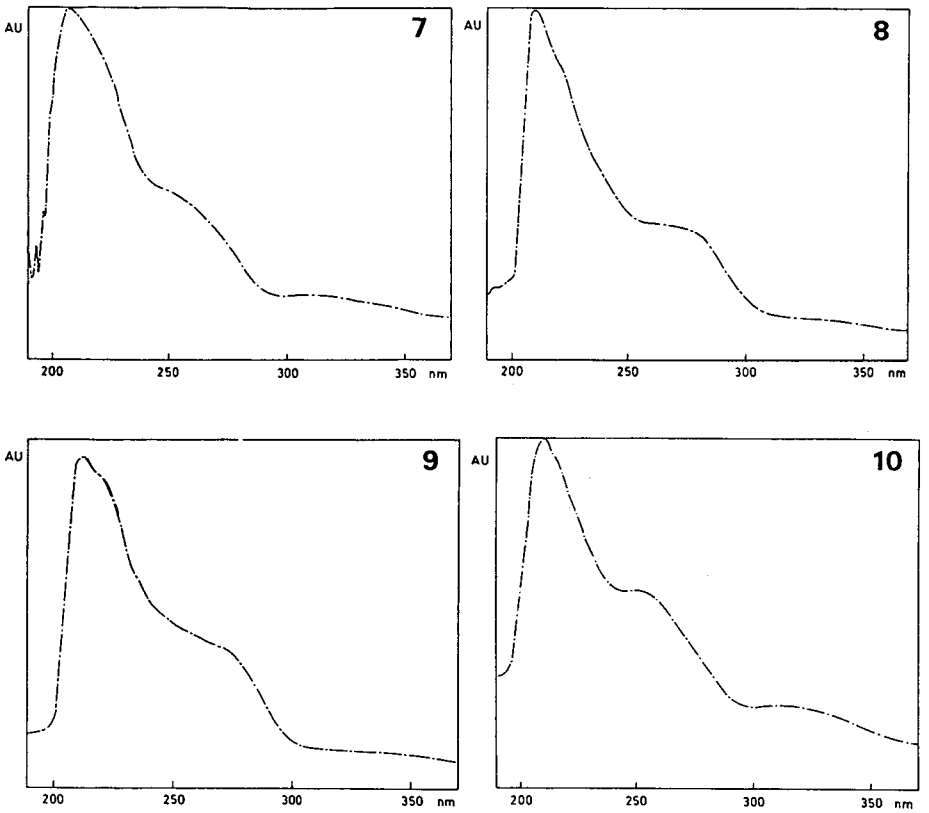

Fig. 5. LC–DAD UV spectra of tungsten carbonyl complexes after separation on an RoSiL CN column. Column as in Fig. 1. 1–10 as in Fig. 4.

Applications

Qualitative analysis of tungsten carbonyl complexes by LC with diode-array detection (DAD). Tungsten carbonyl complexes $LW(CO)_3$ (π-C_5H_5) (L = $R_nCl_{3-n}Sn$, Cl) have been studied as catalysts for the metathesis of olefins[16]. These precursors are activated by (i-C_4H_9)$AlCl_2$ in the presence of oxygen. During this activation process, tungsten carbenes are formed. The influence of the $R_nCl_{3-n}Sn$ substituents (R = CH_3, C_6H_5) on the reactivity as a catalyst was measured. This indicated that the purity of the prepared products has to be carefully checked. Further, for the understanding of the activation process an analysis of the reaction mixture is very helpful.

With this aim, a reference test sample was subjected to LC on a cyanopropyl column. The identification and purity control were performed using diode-array detection. The results are shown in Figs. 4 and 5. This method confirmed the formation of $HW(CO)_3(\pi\text{-}C_5H_5)$ and $ClW(CO)_3(\pi\text{-}C_5H_5)$ during the activation process, already identified by IR spectroscopy. On the other hand, this method showed that (i-C_4H_9)$_2$$ClSnW(CO)_3(\pi\text{-}C_5H_5)$ is always formed, notwithstanding the initial reagent $R_nCl_{3-n}SnW(CO)_3(\pi\text{-}C_5H_5)$ (R = CH_3, C_6H_5) in the reaction mixture.

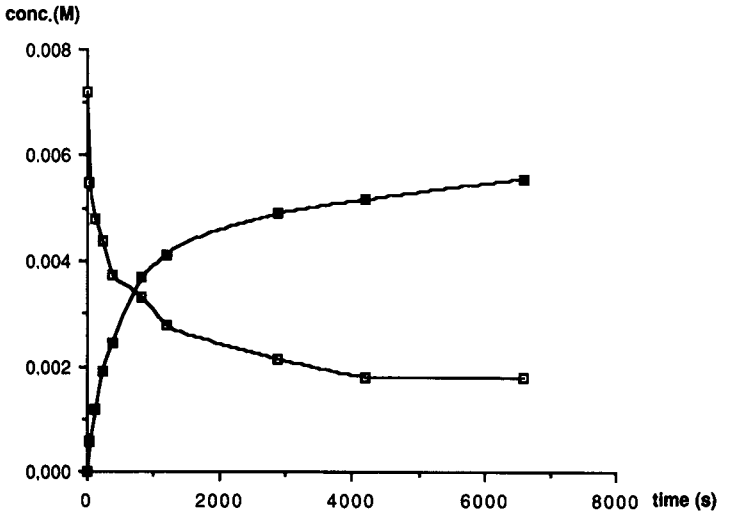

Fig. 6. Concentrations of (□) $(CH_3)_3SnCl$ and (■) $(CH_3)_2SnCl_2$ for the reaction $(CH_3)_3SnCl + ICl \rightarrow (CH_3)_2SnCl_2 + CH_3I$ (solvent, CH_2Cl_2; temperature, 15°C) as a function of time measured by LC.

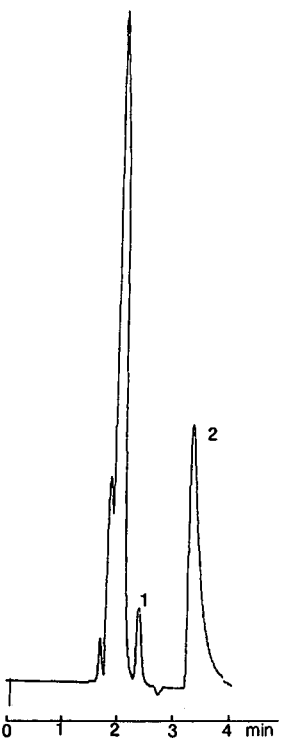

Fig. 7. LC analysis of the reaction mixture 4200 s after mixing the reagents. Column as in Fig. 1. Mobile phase, hexane–THF (75:25); flow-rate; 1 ml/min; injection volume 50 μl; detection, 220 nm. After mixing the reagents, 100-μl samples were taken at different times and dissolved in 1 ml of mobile phase in order to stop the reaction. 1 = $(CH_3)_3SnCl$; 2 = $(CH_3)_2SnCl_2$.

Quantitative analysis of organotin halides for reaction kinetic studies. The influence of solvent and temperature on the reaction rate of the reaction $R_3SnCl + ICl \rightarrow R_2SnCl_2 + RI$ (R = alkyl; solvent = $CHCl_3$, CH_2Cl_2, CCl_4) was evaluated by UV spectrometry, monitoring the ICl band. However, fast LC offers new perspectives for this type of work.

This is illustrated in Fig. 6, where the concentrations of $(CH_3)_3SnCl$ and $(CH_3)_2SnCl_2$ for the above reaction are shown as a function of time, measured by LC. The LC analysis of the reaction mixture after 4200 s is shown in Fig. 7. It has been verified that under, HPLC conditions, no reaction of ICl with the organotin analytes takes place.

CONCLUSION

Cyanopropyl-derivatized silica gels are the most versatile stationary phases for the LC analysis of organotin compounds. In order to reduce stationary phase activity, an ICl "on-column" pretreatment was developed, which results in very fast quantitative and qualitative separations. The applicability was demonstrated by the analysis of organotin standards, organotin-containing tungsten carbonyl complexes and organotin halides for reaction kinetic studies. Qualitative analysis was performed by DAD.

ACKNOWLEDGEMENT

We thank the NFWO (Nationaal Fonds voor Wetenschappelijk Onderzoek) for financial assistance.

REFERENCES

1 E. Jessen, K. Taugbøl and T. Greibrokk, *J. Chromatogr.*, 168 (1979) 139.
2 D. Burns, F. Glocking and M. Harriott, *J. Chromatogr.*, 200 (1980) 305.
3 K. Jewett and F. Brinkman, *J. Chromatogr. Sci.*, 19 (1981) 583.
4 W. Langseth, *J. Chromatogr.*, 315 (1984) 351.
5 T. Vickrey, H. Howell, G. Harrison and G. Ramelov, *Anal Chem.*, 52 (1980) 1743.
6 W. A. MacCrehan, *Anal. Chem.*, 535 (1981) 74.
7 D. Burns, F. Glockling and M. Harriott, *Analyst (London)*, 106 (1981) 921.
8 T. H. Yu and Y. Arakawa, *J. Chromatogr.*, 258 (1983) 18.
9 I. S. Krull and K. W. Panaro., *Appl. Spectrosc.*, 39 (1985) 960.
10 W. R. Blair, E. J. Parks, G. J. Olson, F. E. Brinckman, M. C. Valeiras-Price and J. M. Ballama, *J. Chromatogr.*, 410 (1987) 383.
11 K. S. Epler, T. C. O'Haver, T. C. Turk and W. A. MacCrehan, *Anal. Chem.*, 60 (1988) 2062.
12 O. Nygren, C. A. Nilsson and W. Frech, *Anal. Chem.*, 60 (1988) 2204.
13 C.-W. Whang and L. L. Yang, *Analyst (London)*, 113 (1988) 1393.
14 F. E. Brinckman, W. R. Blair, K. L. Jewett and W. P. Iverson, *J. Chromatogr., Sci.*, 15 (1977) 493.
15 K. Brown, poster presented at the *12th International Symposium on Column Liquid Chromatography, Washington, DC, June 19–24*, 1988.
16 L. M. Vanderyse, T. Haemers, A. R. Bossuyt, L. Verdonck and G. P. Van der Kelen, *Bull. Soc. Chim. Belg.*, 97 (1988) 723.
17 C. Hugelier and A. Praet, unpublished results.
18 M. Ashraf-Korassani, L. Taylor and R. Henry, *Anal. Chem.*, 60 (1988) 1529.
19 J. Kirkland and L. Snyder, *Introduction to Modern Liquid Chromatography*, Wiley-Interscience, New York, 1974.

Journal of Chromatography, 507 (1990) 439–450
Elsevier Science Publishers B.V., Amsterdam — Printed in The Netherlands

CHROMSYMP. 1679

Optimization of electrochemical detection in the high-performance liquid chromatography of lignin phenolics from lignocellulosic by-products

GUIDO C. GALLETTI* and ROBERTA PICCAGLIA
Centro di Studio per la Conservazione dei Foraggi, CNR, Via Filippo Re 8, 40126 Bologna (Italy)
and
VITTORIO CONCIALINI
Dipartimento di Chimica "G. Ciamician", Università di Bologna, Via Selmi 2, 40126 Bologna (Italy)

SUMMARY

Free phenolic acids and aldehydes (*p*- and *o*-hydroxyphenylacetic acid, *p*-hydroxybenzoic acid, *p*-hydroxybenzaldehyde, vanillic acid, vanillin, syringic acid, *p*-coumaric acid, syringaldehyde and ferulic acid) were detected in wheat straw extracts by high-performance liquid chromatography with a dual-cell electrochemical detector operated in the redox mode. Phenolics were oxidized with coulometric efficiency in the first cell (+1.00 V), then detected by reduction in the second cell (−0.20 V). Compared with the oxidative mode, the reductive detection mode has the advantage of being unaffected by large amounts of interferents eluting at the front of the chromatogram that interfere with the detection of small and early eluting compounds. Hydrodynamic voltammograms in the oxidative, reductive and screen-out modes are presented and the corresponding detection limits for real sample are discussed. Perfect linearity of response was found in the range $5 \cdot 10^{-7}$–$5 \cdot 10^{-5}$ *M* and detection limits were of the order of 50–500 fmol injected.

INTRODUCTION

High-performance liquid chromatography with electrochemical detection (HPLC–ED) has been successfully used for the determination of phenolic compounds in various matrices, such as water, vegetable materials and beverages[1–3]. Phenolic acids and aldehydes behave well in ED, being oxidizable at relatively low potentials. Under these circumstances, ED is often more sensitive and selective than the more common UV detection[4].

Recently, we applied HPLC–ED to the determination of phenolics in animal feeds made of lignocellulosic by-products[5], a large and inexpensive source of energy where the characterization of lignin-related phenolics is important owing to their antinutritional properties[6]. A standard method was used to extract different fractions

0021-9673/90/$03.50

of phenolics from lignocellulosics, *viz.*, oxidative hydrolysis with nitrobenzene for the determination of the total content of phenolics (or alkali-resistant lignin), dilute alkali solution for the so-called alkali-labile lignin and pH 7 buffer for the free phenolics. Owing to the selectivity of ED, analyses were carried out by direct injection of the extracts into the HPLC column, without the need for purification from UV-interfering substances (*e.g.*, nitrobenzene)[7]. However, the injection of free phenolic extracts often produced a large and tailing front peak that interfered with the early eluting compounds.

In an attempt to overcome this problem, a dual-cell electrochemical detector was operated in different modes, namely oxidative, reductive, screen-out and differential. This paper compares their application to both standard solutions and real samples, and proposes an experimental approach to the optimization of the detection of phenolics in lignocellulosics. Hydrodynamic voltammograms for several phenolic acids and aldehydes obtained in different modes are presented and other analytical parameters are discussed.

EXPERIMENTAL

HPLC system

A Model 590 pump (Waters Assoc., Milford, MA, U.S.A.) was connected in series to an Model LP 21 damper (Scientific Systems, State College, PA, U.S.A.), a Model 5020 guard cell (ESA, Bedford, MA, U.S.A.) set at +1.10 V, a Waters U6K injector, a Viospher C_6, 5 μm (Violet, Rome, Italy) reversed-phase column (150 × 4.6 mm I.D.) and an ESA 5011 dual-cell detector. The detector was controlled by an ESA Coulochem 5100 A module and chromatographic peaks were displayed on Leeds & Northrup Speedomax XL 681 (Leeds & Northrup Italiana, Milan, Italy) and Model 561 (Perkin-Elmer, Beaconsfield, U.K.) recorders.

The eluent was methanol–0.1% perchloric acid in water (12:88, v/v) at a flow-rate of 1 ml/min under a gentle stream of helium. HPLC-grade methanol (Carlo Erba, Milan, Italy) and laboratory-prepared deionized water were filtered through a 0.22-μm Millipore (Bedford, MA, U.S.A.) filtration unit under vacuum before use.

Hydrodynamic voltammograms (HDVs)

Oxidative mode (ox). Potentials from 0.00 to +1.00 V in increments of 0.05 V were applied to the first working electrode (D1) and the chromatograms of the standard solution (20 μl injected) were recorded at each potential. The current intensity of each peak was plotted against the applied potential, obtaining HDV_{ox} for the various compounds on D1. To obtain the HDV_{ox} on the second working electrode (D2), the first working electrode was fixed at +0.20 V and D2 was scanned from +0.20 to +1.00 V in 0.05 V steps, recording the resultant chromatograms.

Reductive mode (red). D1 was set at +1.00 V and D2 potentials were changed stepwise from +0.90 to −0.40 V in 0.10 V decrements and chromatograms of standard solution (20 μl injected) were recorded at each potential. Current intensity was plotted against the applied potential, obtaining HDV_{red} for the various compounds on D2.

Screen-out mode. D2 was set at +0.90 V and the D1 potential was scanned from +0.00 to +0.90 V in 0.10 V increments. The current intensity of each peak was

plotted against the applied potential, obtaining $HDV_{screen\text{-}out}$ for the various compounds.

Differential mode. The algebraic subtraction of the D2 output was obtained by direct connection of the output labelled CH1–CH2 on the rear of the control module to the recorder.

Standard solution

A working standard solution in the range $5 \cdot 10^{-7}$ *M* was prepared daily by 1:1000 dilution with water from a methanolic stock solution of the following compounds (Sigma, St. Louis, MO, U.S.A.): (1) *p*-hydroxyphenylacetic acid (final concentration $5.6 \cdot 10^{-7}$ *M*); (2) *o*-hydroxyphenylacetic acid ($5.4 \cdot 10^{-7}$ *M*); (3) *p*-hydroxybenzoic acid ($4.8 \cdot 10^{-7}$ *M*); (4) *p*-hydroxybenzaldehyde ($6.1 \cdot 10^{-7}$ *M*); (5) vanillic acid ($5.2 \cdot 10^{-7}$ *M*); (6) vanillin ($8.2 \cdot 10^{-7}$ *M*); (7) syringic acid ($3.6 \cdot 10^{-7}$ *M*); (8) *p*-coumaric acid ($4.4 \cdot 10^{-7}$ *M*); (9) syringaldehyde ($4.3 \cdot 10^{-7}$ *M*); (10) ferulic acid ($7.5 \cdot 10^{-7}$ *M*). The stock solution was stored in a refrigerator and kept for no longer than 1 week.

Calibration

The stock solution was diluted 1:10, 1:100, 1:200, 1:500 and 1:1000 with water to obtain single concentrations of phenolics ranging from $5 \cdot 10^{-5}$ to $5 \cdot 10^{-7}$ *M*. Chromatograms were recorded with both D1 and D2 set at +1.00 V.

Lignocellulose analysis

Sample extraction. A 500-mg wheat straw sample (ground to pass a 0.2-mm sieve) was extracted with pH 7 buffer [containing EDTA disodium salt dihydrate (9.79 g/l), KH_2PO_4 (7.92 g/l) and $Na_2HPO_4 \cdot 2H_2O$ (7.22 g/l)] (20 ml) for 1 h under reflux[8]. After cooling, an aliquot of the supernatant was filtered through a 0.22-μm cartridge filter (Millipore) and injected into the HPLC system. Alternatively, the sample (5 g) was extracted with methanol (40 ml) at room temperature for 1 week with occasional shaking.

Chromatographic analysis. Chromatograms of untreated extracts were obtained in the oxidative mode (D1, +1.00 V), reductive mode (D1, +1.00 V; D2, −0.1 V), screen-out mode (D1, +0.30 V; D2, +1.00 V) and differential mode (D1, +1.00 V; D2, −0.10 V).

RESULTS AND DISCUSSION

The working potential range under the adopted chromatographic conditions was established by monitoring background currents of the flowing mobile phase at different potentials on both D1 and D2 (Fig. 1). Typically for this kind of detector[9], currents ranged from about +2 to about −2 μA for potentials from +1.00 to −0.30 V. Relatively constant currents (± 1 μA) were observed from +0.80 to −0.20 V with sharper slope changes at the extreme potentials. These current values are relatively low and were not affected by the application or non-application of a guard-cell potential, thus indicating that the mobile phase was substantially free from electroactive impurities.

Hydrodynamic voltammograms in the oxidative and reductive modes (HDV_{ox}

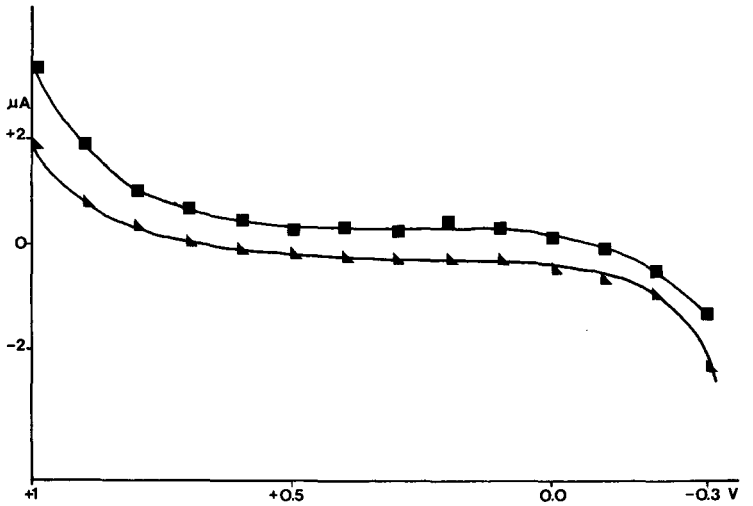

Fig. 1. Mobile phase background current *vs.* applied potential. Chromatographic conditions as under Experimental. ■ = D1; ▲ = D2.

and HDV_{red}, respectively) were recorded for several phenolic acids and aldehydes which are related to the three main monomeric constituents of lignin, namely the hydroxyphenyl moiety (*o*- and *p*-hydroxyphenylacetic acids, *p*-hydroxybenzoic acid, *p*-hydroxybenzaldehyde and *p*-coumaric acid), the coniferyl moiety (vanillic acid, vanillin and ferulic acid) and the sinapyl moiety (syringic acid and syringaldehyde). D1 and D2 showed similar HDV_{ox} curves for the various compounds. The half-wave potential ($E_{1/2}$) of the HDV_{ox} curves was in the range 0.40–0.50 V for the sinapylic, 0.50–0.65 V for the coniferylic and 0.65–0.80 V for the hydroxyphenylic compounds, thus indicating that the latter are less easily oxidizable than the former (Table I). Fig. 2 shows three typical examples of HDV_{ox} (upper curves). This experiment preluded to

TABLE I

HDV_{ox} AND HDV_{red} HALF-WAVE POTENTIALS ($E_{1/2}$) AND DETECTION LIMITS OF PHENOLIC ACIDS AND ALDEHYDES

Compound	$E_{1/2}$ *(V)*		*Detection limit (fmol injected)*
	HDV_{ox}	HDV_{red}	
Syringic acid	+0.40	+0.10	570
Syringaldehyde	+0.50	+0.10	400
Vanillic acid	+0.50	+0.10	65
Vanillin	+0.60	+0.10	75
Ferulic acid	+0.65	+0.10	82
p-Hydroxyphenylacetic acid	+0.65	−0.10	38
o-Hydroxyphenylacetic acid	+0.70	−0.10	40
p-Coumaric acid	+0.70	−0.10	44
p-Hydroxybenzoic acid	+0.80	−0.10	40
p-Hydroxybenzaldehyde	+0.80	0.00	490

the choice of the optimum potential for the oxidative mode detection and for subsequent reductive and screen-out mode operations. It was also useful for identification purposes via comparison of the HDV of the standards with those of the unknowns.

Typical HDV_{red} are reported in Fig. 2 (lower curves). It is interesting that the reductive currents are lower than the oxidative currents and that the hydroxyphenylic

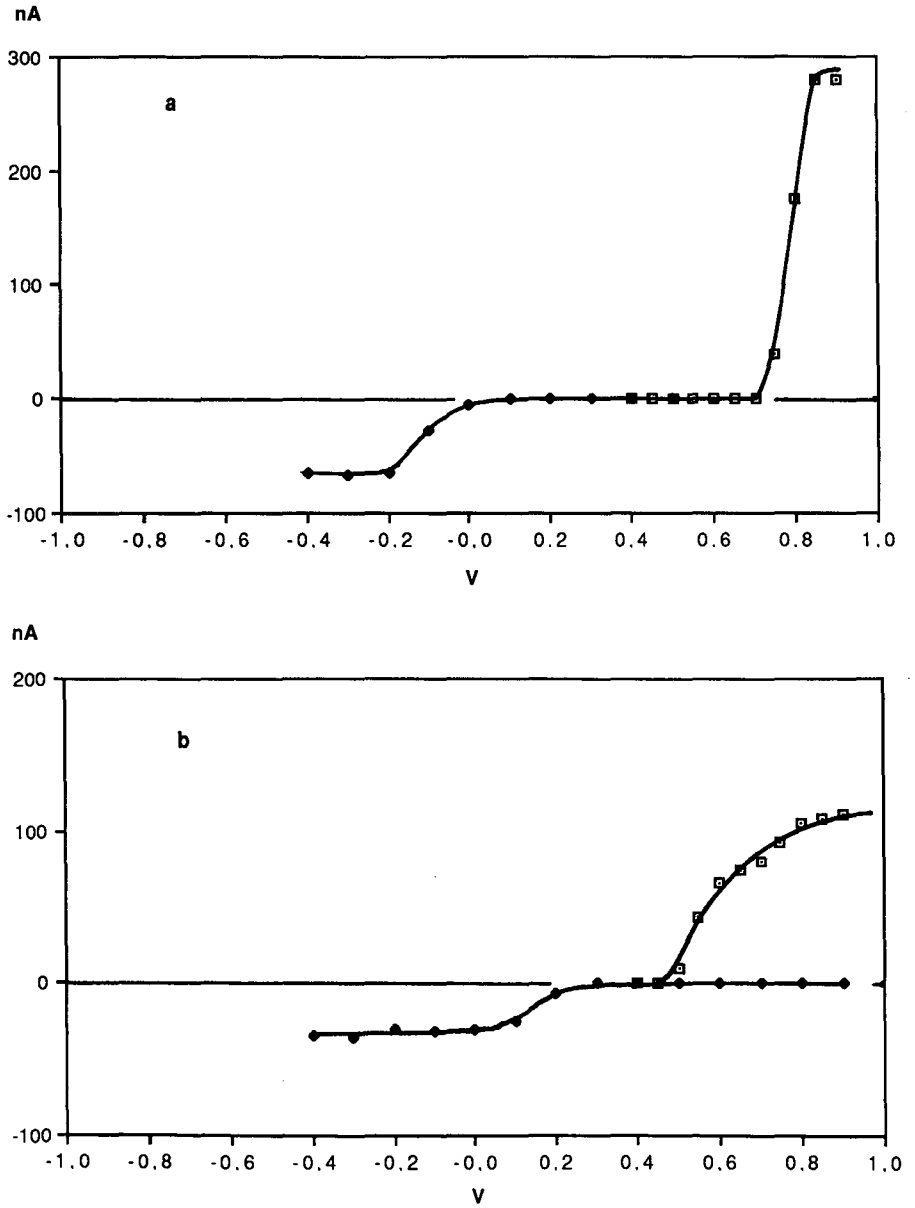

Fig. 2.

(Continued on p. 444)

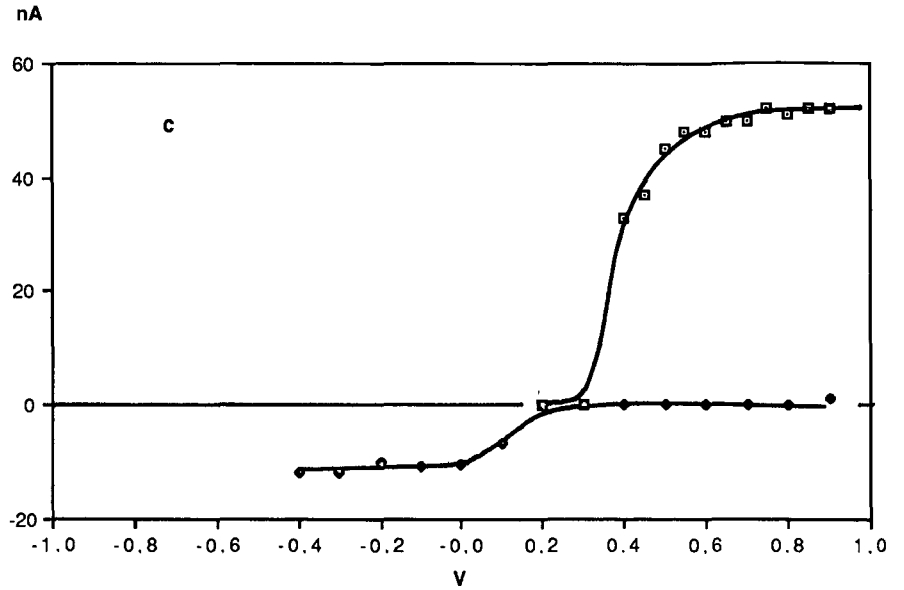

Fig. 2. Hydrodynamic voltammograms in oxidative and reductive detection modes (□ = HDV_{ox}, upper curves; and ◆ = HDV_{red}, lower curves) of representative phenolics: (a) *p*-hydroxybenzoic acid; (b) vanillin; (c) syringic acid. For chromatographic conditions see experimental section.

compounds, which are the more difficult to oxidize, are also the less easily reduced, with $E_{1/2} \approx -0.1$ V.

Detection limits are reported in Table I. These were of the order of 50–100 fmol injected (5–20 pg injected) for all compounds except *p*-hydroxybenzaldehyde, syringic acid and syringaldehyde [400–600 fmol injected (10–60 pg injected)] in reductive mode. These values are about two orders of magnitude lower than those obtainable by UV detection. The oxidative mode can also reach these detection limits, but the detection of the early-eluting peaks at low concentrations is often hindered by a large interfering front peak. In a detailed comparison of UV and electrochemical detection of phenolic compounds, Hayes *et al.*[4] obtained UV detection limits similar to our results, whereas the electrochemical detection limits were about one order of magnitude higher than those reported here, owing to the poorer sensitivity of the amperometric detector used in their work.

D1 can be used to screen out background currents and chromatographic interferents that are oxidized at potentials lower than that for the analyte. In the screen-out mode, detection is carried out at D2, and the D1 potential should be set at a value that is sufficiently high to oxidize impurities, but not so high as to reduce significantly the analyte response. As our compounds covered a fairly wide range of oxidation potentials ($0.4 < E_{1/2} < 0.8$), an optimum screen-out D1 potential was chosen on the basis of the $HDV_{screen\text{-}out}$ of each compound. Relevant examples are shown in Fig. 3. These HDV_{ox} curves were generated by plotting compound responses at D2 (+0.9 V) *vs.* D1 potentials. The maximum allowable D1 potentials for phenolic compounds to be detected at D2 without significant losses of response were +0.2 and +0.3 V for

syringic acid and syringaldehyde (sinapylic compounds), respectively, +0.3 V for coniferylic compounds and +0.4 V for *p*-hydroxyphenylic compounds (+0.6 V for *p*-hydroxybenzoic acid and *p*-hydroxybenzaldehyde).

As a result of these preliminary experiments, it was concluded that, given a useful working potential interval ranging from −0.3 to +1.0 V, optimum detection conditions for the studied phenolic compounds were as follows: D1, +1.00 V (ox-

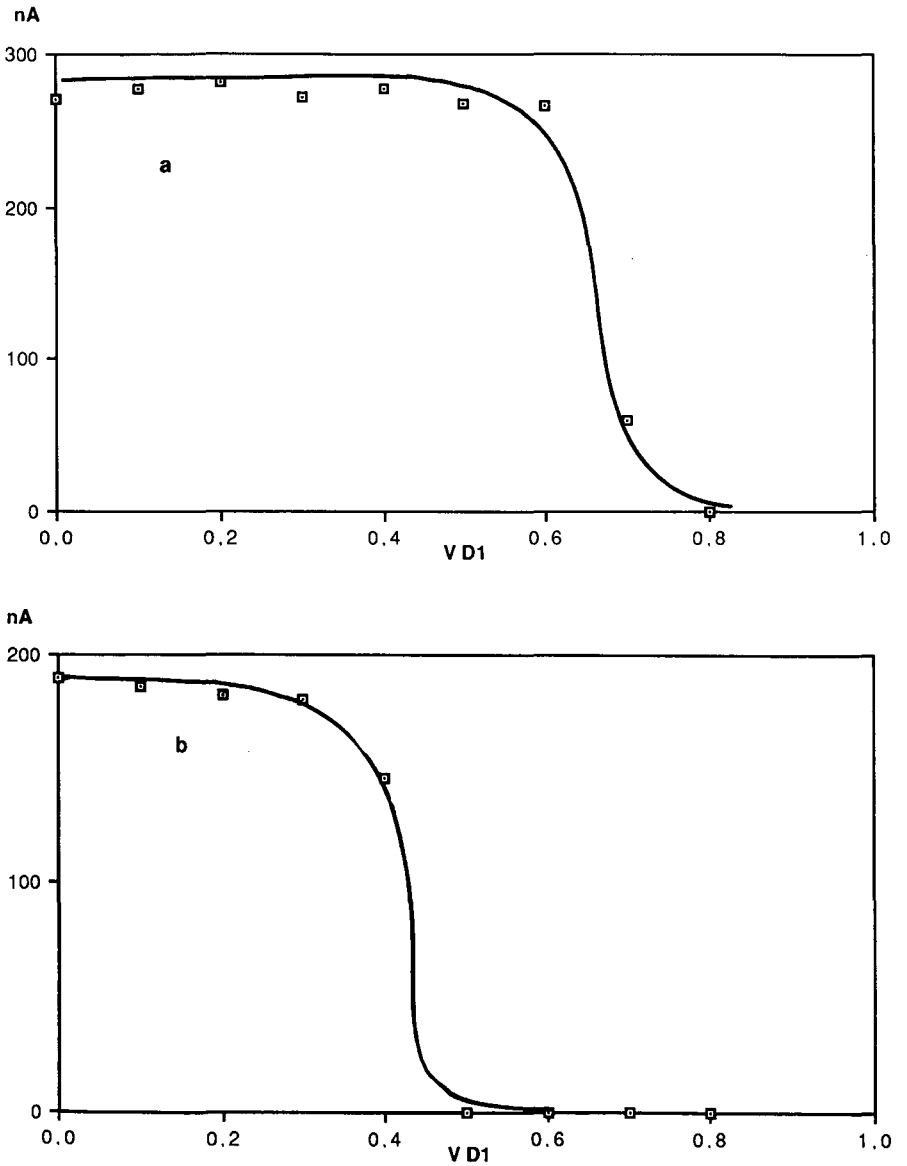

Fig. 3.

(Continued on p. 446)

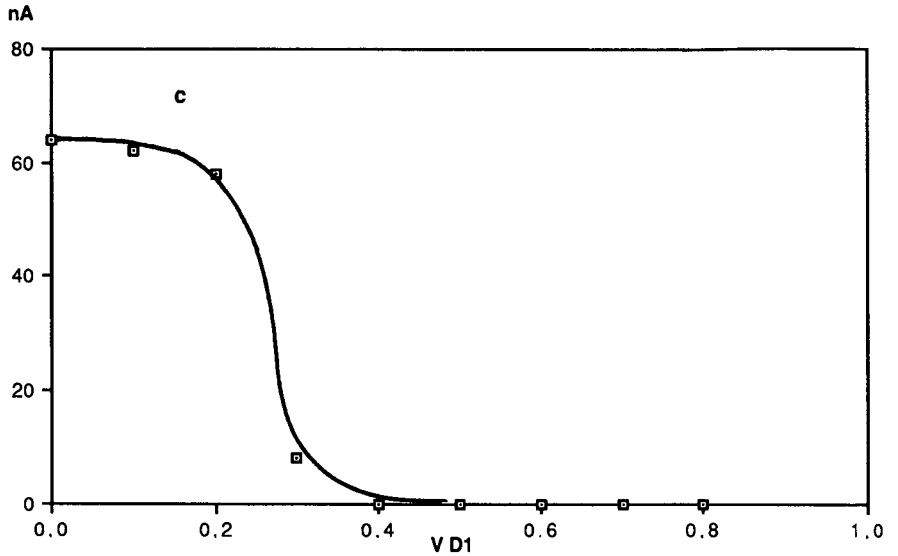

Fig. 3. HDV screen-out of (a) *p*-hydroxybenzoic acid, (b) vanillin and (c) syringic acid. Chromatographic conditions as under Experimental.

idative mode) (Fig. 4); D2, −0.20 V and D1, +1.00 V (reductive mode) (Fig. 4); D2, +1.00 V and D1, +0.3 V (screen-out mode).

The detection response was linear over the range of concentrations ($5 \cdot 10^{-7}$–$5 \cdot 10^{-5}$ *M*) used for the calibration ($R = 1.00$). The oxidative efficiency of D1 was more than 90%, regardless the concentration of the analyte.

The free phenolic extract from straw was firstly run in the oxidative mode. Because detection at +1.00 V resulted in excessive current limits, the detection potential was lowered to +0.80 V, where all the compounds still have good responses (Fig. 5). A large and tailing front peak made detectable only major peaks with retention times longer than 7 min. This peak was present also in the chromatograms with UV detection. Any option taken into consideration to improve the chromatogram would mean either changing the extraction classical method (by changing the buffer composition or concentration or by using another solvent) or changing the detection mode. However, neutral buffers are reported to have better extraction efficiencies for phenolics from forages than other solvents[10] and, hence, can be considered as a standard extraction procedure. On the other hand, simple dilution of the extract was not possible as minor peaks would fall below the detection limit. Examination of the electrochemical behaviour of the front peak showed that its response was almost zero at +0.30 V, reaching a maximum at +0.80 V, thus ruling out the possibility of using the screen-out detection mode. Reductive mode detection resulted in an improved chromatogram (Fig. 5), with a fairly horizontal baseline and minor peaks detectable from retention times of *ca.* 3 min. Differential mode detection (subtracting the D2 reductive output from the D1 oxidative output) resulted in an increase in peak height ranging from 14 to 51% of the original oxidative peaks (Table II). The D2 gain was a compromise between increasing the peak height while minimizing the noise and base-

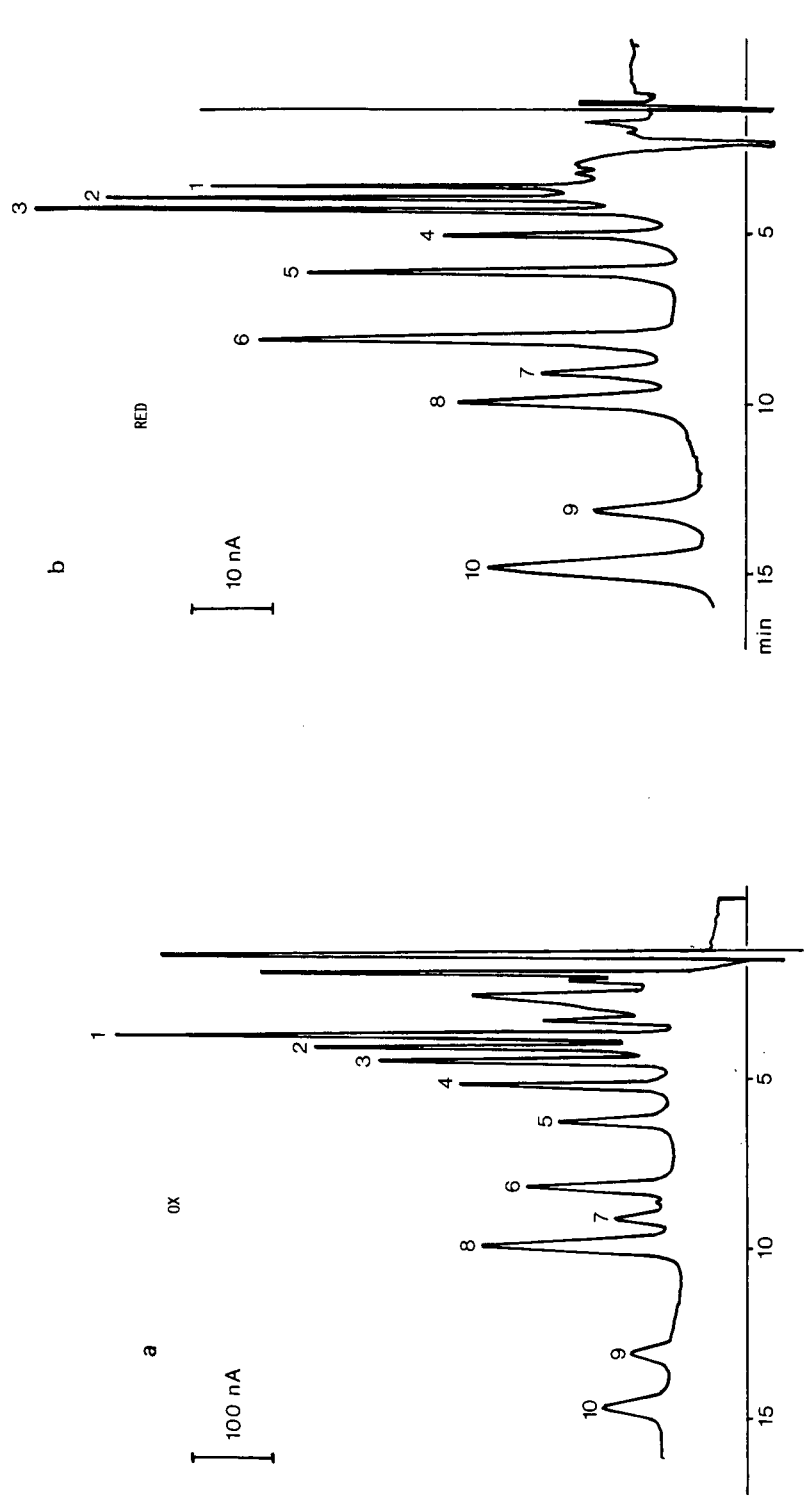

Fig. 4. Standard phenolics (*ca.* $5 \cdot 10^{-7}$ *M*) detected in (a) oxidative (first working electrode, D1 = +1.00 V) and (b) reductive mode (second working electrode, D2 = −0.20 V, D1 = +1.00 V). Chromatographic conditions and peak numbering as under Experimental.

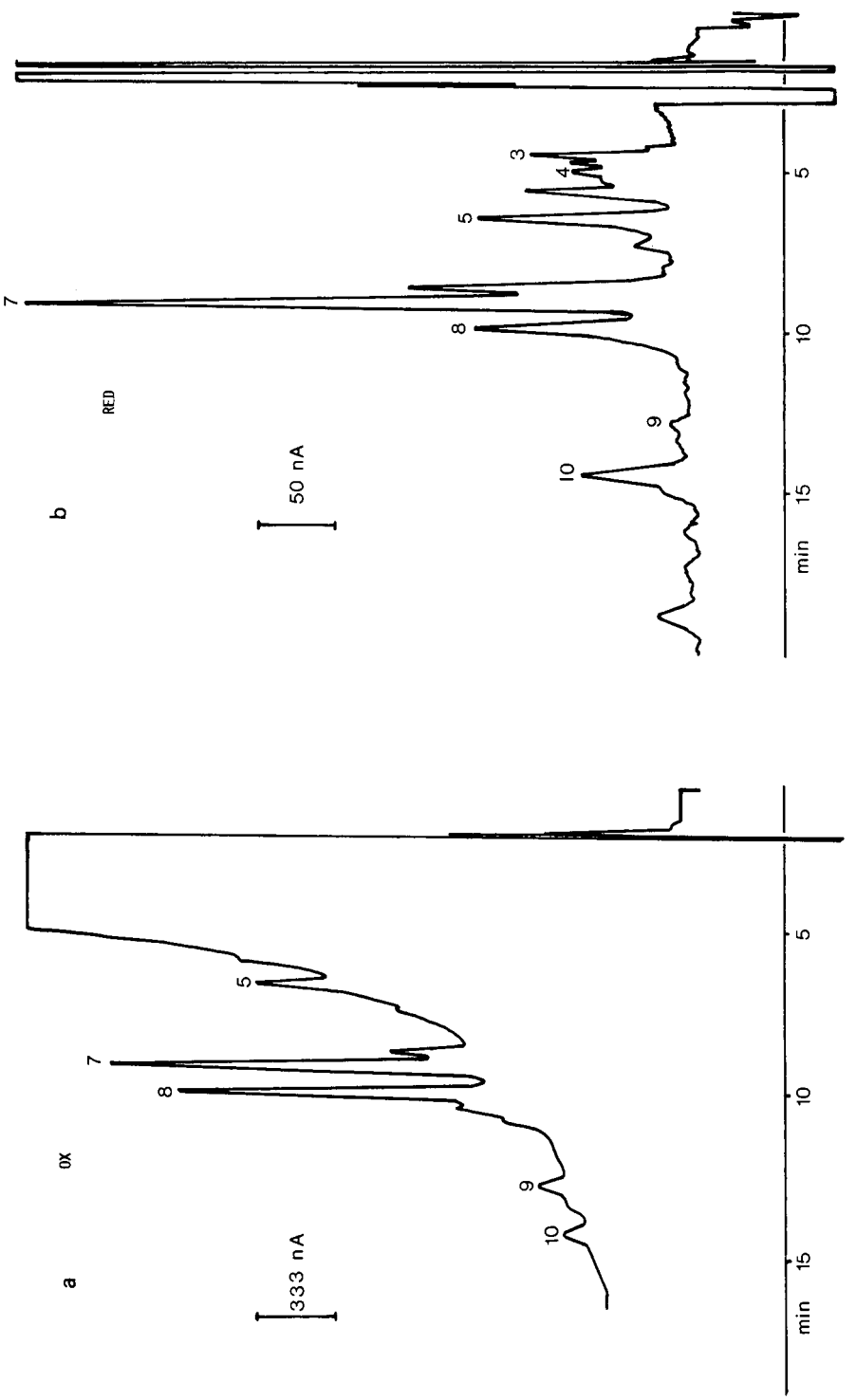

Fig. 5. Wheat straw buffer extract. (a) Oxidative (D1 = +0.80 V) and (b) reductive (D2 = −0.20 V, D1 = +1.00 V) mode detection.

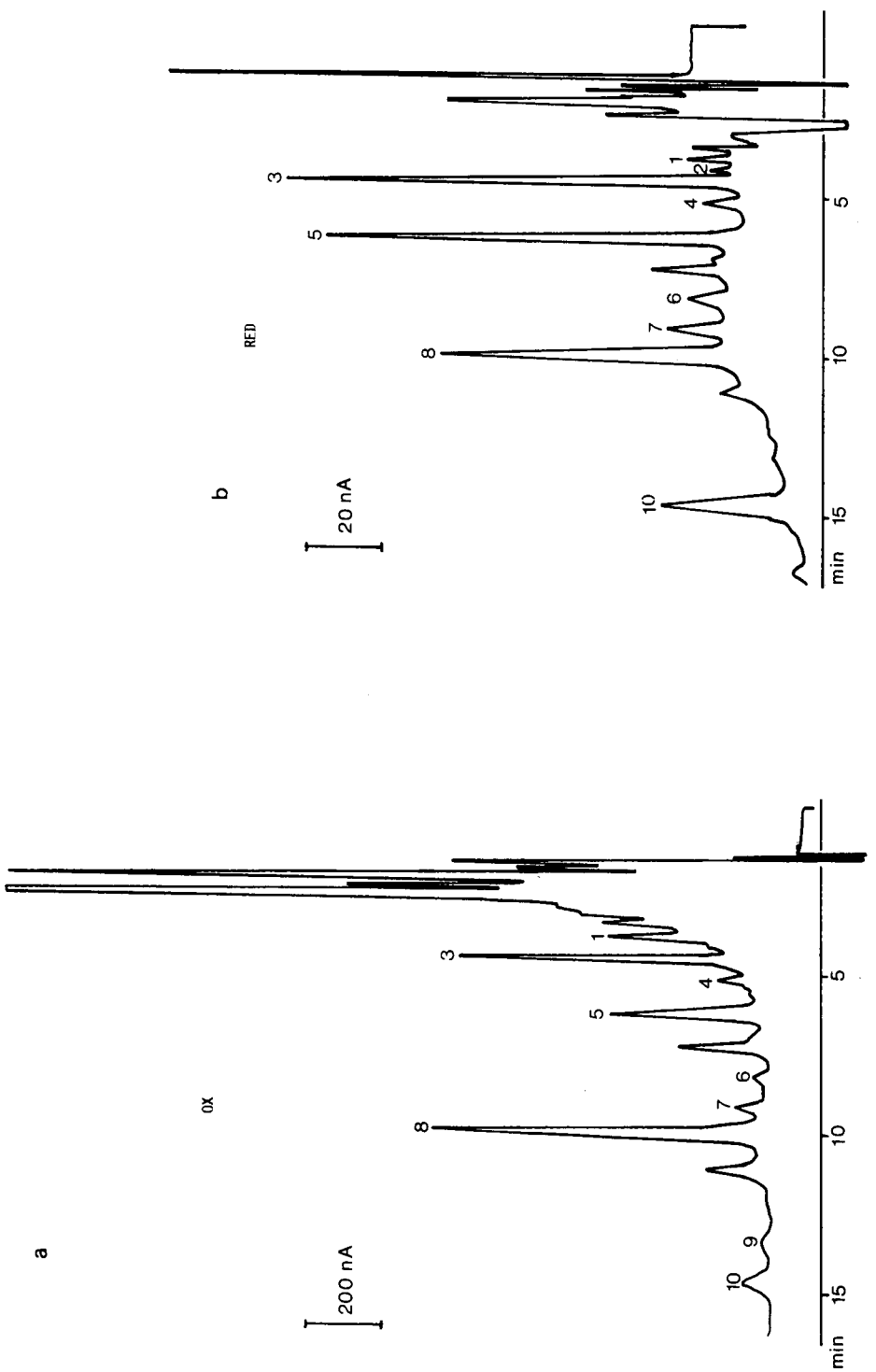

Fig. 6. Wheat straw methanol extract. (a) Oxidative (D1 = +0.80 V) and (b) reductive (D2 = −0.20 V, D1 = +1.00 V) mode detection.

TABLE II

PEAK HEIGHTS (mm) OF STANDARD PHENOLICS ($5 \cdot 10^{-8}$ *M*) DETECTED IN OXIDATIVE (D1, +1.00 V, GAIN ×10 × 50), REDUCTIVE (D2 −0.20 V, GAIN ×100 × 10) AND DIFFERENTIAL MODES (D1 − D2) WITH % INCREASE IN D1 − D2 WITH RESPECT TO D1

Compound	*D1*	*D2*	*D1 − D2*	*Increase (%)*
p-Hydroxyphenylacetic acid	85	10	98	15
o-Hydroxyphenylacetic acid	55	16	75	36
p-Hydroxybenzoic acid	70	28	102	46
p-Hydroxybenzaldehyde	32	9	40	25
Vanillic acid	37	17	56	51
Vanillin	25	14	38	52
Syringic acid	11	5	16	45
p-Coumaric acid	37	8	42	14
Syringaldehyde	9	4	13	44
Ferulic acid	12	7	18	50

line drift. In an attempt to reduce the front peak, a differential mode was operated by setting D1 at +0.80 V (where both the front peak and the phenolics are detectable) and D2 also at +0.80 V (where the front peak only is visible, because it is too large to be coulometrically oxidized at D1, whereas the phenolics are not detectable). The result was unsuccessful, because it was impossible to obtain algebraically zero values from the subtraction of a peak exceeding the current limits.

The other approach to improvement, that is, changing the extracting solvent, was also tested, replacing pH 7 buffer with methanol and diluting the extract with water (1:10) before injection. The front peak was smaller than with buffer extraction, but smaller peaks were detectable better in the reductive mode than in the oxidative mode (Fig. 6). Further, the methanolic extract yielded a different chromatographic profile than the buffer extract, which would make a comparison with the standard extraction procedure impossible.

To conclude, the reductive mode detection of free phenolics in lignocellulose offers the advantages of much better sensitivity than UV detection and of a chromatogram unaffected by the large and tailing front peak present in the oxidative mode, allowing the injection of extracts with no need for purification steps.

REFERENCES

1 G. Chiavari, V. Concialini and P. Vitali, *J. Chromatogr.*, 249 (1982) 385.
2 D. K. Roston, P. T. Kissinger, *J. Liq. Chromatogr.*, 5 (Suppl. 1) (1982) 75.
3 O. Friederich and G. Sontag, presented at the *17th International Symposium on Chromatography, Vienna, September 25–30, 1988.*
4 P. J. Hayes, M. R. Smyth and I. McMurrogh, *Analyst (London)*, 112 (1987) 1197.
5 G. C. Galletti, R. Piccaglia, G. Chiavari and V. Concialini, *J. Agric. Food Sci.*, 37 (1989) 885.
6 H. G. Jung and G. C. Fahey, Jr., *J. Anim. Sci.*, 57 (1983) 206.
7 G. Chiavari, V. Concialini and G. C. Galletti, *Analyst (London)*, 113 (1988) 91.
8 M. M. Lau and P. J. Van Soest, *Anim. Sci. Technol.*, 6 (1981) 123.
9 *The Model 5100A Coulochem Detector, Instruction Manual*, ESA Bedford, MA, 1987, p. 4–3.
10 J. H. Cherney, K. S. Anliker, K. A. Albrecht and K. V. Wood, *J. Agric. Food Chem.*, 37 (1989) 345.

Journal of Chromatography, 507 (1990) 451–458
Elsevier Science Publishers B.V., Amsterdam — Printed in The Netherlands

CHROMSYMP. 1667

High-performance liquid chromatographic determination of aliphatic thiols with aroylacrylic acids as fluorogenic precolumn derivatization reagents

RITA GATTI, VANNI CAVRINI* and PAOLA ROVERI
Department of Pharmaceutical Sciences, Via Belmeloro 6, 40126 Bologna (Italy)
and
SERGIO PINZAUTI
Department of Pharmaceutical Sciences, Via G. Capponi 9, 50121 Florence (Italy)

SUMMARY

The use of the methyl ester of 4-(6-methoxynaphthalen-2-yl)-4-oxo-2-butenoic acid as a fluorogenic labelling reagent for the high-performance liquid chromatography (HPLC) of biologically important thiols (glutathione, cysteine, acetylcysteine, homocysteine, cysteamine, sodium 2-mercaptoethanesulphonate and thiola) was investigated. The compound reacts selectively and rapidly (10 min at ambient temperature and pH 7.5) with the thiols to give fluorescent adducts that can be separated by reversed-phase HPLC and detected fluorimetrically (λ_{em} = 450 nm; λ_{em} = 310 nm). Applications to the determination of L-cysteine and mesna in pharmaceutical formulations are described.

INTRODUCTION

High-performance liquid chromatography (HPLC) in conjunction with a pre- or post-column chemical derivatization constitues an effective technique for the sensitive and selective determination of aliphatic thiols of biological importance[1–3]. Maleimides[4,5], bimanes[6,7] and 7-fluoro-2,1,3-benzoxadiazoles[8,9] proved to be useful reagents for the fluorogenic labelling of thiols in HPLC analyses with fluorimetric detection.

To develop additional selective flurogenic reagents for thiols, our attention was directed to compounds having a naphthoylacrylic structure[10] and, recently, 4-(6-methylnaphthalen-2-yl)-4-oxo-2-olutenoic acid (**I**) has been proposed as useful precolumn derivatization reagent for the HPLC analysis of thiol drugs[11]. This reagent, devoid of native fluorescence, displayed good selectivity toward thiol compounds, giving fluorescent derivatives that were separated by HPLC. The sensitivity achieved, however, was not very high, although it was adequate for the analysis of pharmaceutical formulations, and restricted chromatographic conditions were required. In order to enhance the sensitivity, the methoxy analogue of **I** was chosen as reagent potential-

0021-9673/90/$03.50

ly able to give derivatized thiols with high fluorescence quantum yields. This paper describes the applications of 4-(6-methoxynaphthalen-2-yl)-4-oxo-2-butenoic acid (**II**) and its methyl ester (**III**) as precolumn fluorogenic labelling reagents in the HPLC analysis of some biologically active thiols.

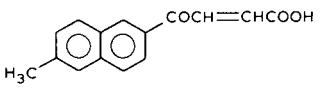

(**I**)

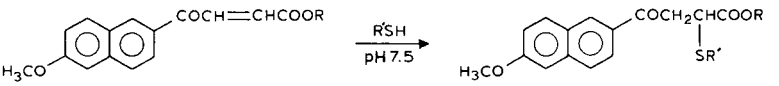

(**II**) R = H
(**III**) R = CH_3
non-fluorescent

(**IIa**) R = H
(**IIIa**) R = CH_3
fluorescent

EXPERIMENTAL

Chemicals

L-Cysteine was purchased from Carlo Erba (Milan, Italy) and N-acetylcysteine, N-(mercaptopropionyl)glycine (thiola), homocysteine, reduced glutathione, sodium 2-mercaptoethanesulphonate (MESNa), penicillamine, cysteine and cysteamine were from Fluka (Buchs, Switzerland). Captopril was kindly supplied by Squibb (Rome, Italy).

Methanol, acetonitrile and tetrahydrofuran (THF) were of HPLC grade from Carlo Erba and water was deionized and doubly distilled. All other chemicals were of analytical-reagent grade. A pH 7.5 borate buffer solution was prepared according to the Italian Pharmacopoeia[12].

As internal standards, 4-(2-naphthyl)-4-oxobutanoic acid[13] and 4-(6-methoxy-2-naphthyl)-4-oxobutanoic acid[14,15] were used.

Apparatus

The liquid chromatograph consisted of a Varian 2010 pump and a Varian 2070 fluorescence detector, operating at λ_{em} = 450 nm with λ_{ex} = 310 nm, connected to a Varian 4720 integrator. Manual injections were carried out using a Rheodyne Model 7125 injection valve (50-μl sample loop). IR spectra were taken in a Nujol mull on a Perkin-Elmer 298 IR spectrophotometer. UV spectra were recorded using a Jasco Uvidec 610 spectrophotometer. ^{1}H NMR spectra were recorded on a Varian EM 390 spectrometer at 90 MHz using tetramethylsilane as internal standard.

*Synthesis of reagents **II** and **III***

4-(6-Methoxynaphthalen-2-yl)-4-oxo-2-butenoic acid (**II**) was synthesized from 6-methoxy-2-acetylnaphthalene (Fluka) and glyoxylic acid (Fluka) as described previously[14]; m.p. = 167–169°C (acetic acid); IR (cm^{-1}), 1705,1655,1615,1180,840; ^{1}H NMR (acetone-d_6), δ 3.95 (3H, s, CH_3O–), 6.85 and 8.05 (2H, q, J = 15.0 Hz, *trans*

–CH=CH–), 7.15–8.6 (6H, m, Ar–H) A solution of the acid **II** ($5.2 \cdot 10^{-4}$ *M*) for analytical applications was prepared in 0.3 *M* phosphate buffer solution (pH 7.4).

The methyl ester **III** was prepared by heating under reflux for 1.0 h a solution of the parent acid (**II**) (0.5 g) and methanol (2.5 ml) in 25 ml of anhydrous benzene in the presence of sulphuric acid (2–3 drops). Water (20 ml) was added and subsequent extractions with 5% sodium hydrogencarbonate (10 ml) and water (20 ml) were performed. The benzene layer was dried over anhydrous sodium sulphate and evaporated *in vacuo*. The residue was purified by flash chromatography on a silica gel column using ethyl acetate–light petroleum (b.p 40–70°C) (4:6) as the mobile phase. A pale yellow compound was isolated; m.p 116–120°C; calculated for $C_{16}H_{14}O_4$,C 71.10,H 5.22; found, C 71.14,H 5.47%; IR (cm^{-1}), 1715, 1665, 1620, 1310, 1165, 850, 840, 825; ^1H NMR ([$^2H_6$]acetone), δ 3.85 (3H, s, –$COOCH_3$), 3.98 (3H, s, CH_3O–), 6,85 and 8.15 (2H, q, J = 15 Hz, *trans* –CH=CH–),7.20–8.80 (6H,m,ArH); UV (ethanol), λ_{max} = 332 nm ($\varepsilon = 1.24 \cdot 10^4$).

A solution of reagent **III** ($5.2 \cdot 10^{-4}$ *M*) was prepared by dissolving 3.5 mg of the compound in 10 ml of THF and diluting to 25 ml with borate buffer solution (pH 7.5).

*Synthesis of N-acetylcysteine adduct with reagent **III***

The methyl ester **III** (150 mg; 0.5 mmol) was dissolved in 30 ml of THF, then 20 ml of borate buffer solution (pH 7.5) and 90.5 mg (0.5 mmol) of N-acetylcysteine were added. The reacton solution was stirred at ambient temperature for 30 min, acidified with 2 *M* hydrochloric acid and then extracted with diethyl ether (2 × 30 ml). The combined extracts were dried over anhydrous sodium sulphate and then evaporated *in vacuo* to give a product homogeneous by thin-layer chromatography (silica gel) using chloroform–methanol–acetic acid (9:1:0.5, v/v/v) as eluent with detection at 254 and 366 nm; m.p. 112–118°C (decomp.); calculated for $C_{21}H_{23}NO_7S$, C 58.05, H 5.33, N 3.22; found, C 57.90, H 5.41, N 3.05%; ^1H NMR (C^2HCl_3), δ 2.0 (3H, s, CH_3CON), 3.75 (3H, s, $COOCH_3$), 3.95 (3H, s, CH_3O), 3.0–3.7 (5H, m, CH_2S + CHS + CH_2CO), 4.80 (1H, m, CHN), 7.10–8.80 (6H, m, Ar–H); UV (ethanol), λ_{max} = 315 nm ($\varepsilon = 1.334 \cdot 10^4$).

Chromatographic conditions

The HPLC separations were performed on a Spherisorb RP-8 (5-μm) column (150 × 4 mm I.D.) or a Hypersil RP-8 (5-μm) column (150 × 4 mm I.D.). For routine analyses of cysteine and MESNa, a mobile phase consisting of methanol–0.05 *M* triethylammonium phosphate (pH 3.0) (53:47) at a flow-rate of 1.0 ml/min was used.

Calibration graphs

Standard solutions of L-cysteine (0.66–2.65 μg/ml) were prepared in EDTA (disodium salt) solution (1 mg/ml); similarly, standard solutions of MESNa (1.34–4.46 μg/ml) were prepared in EDTA (disodium salt) solution (15 μg/ml).

A 1.0-ml volume of thiol standard solution was reacted with 0.3 ml of the reagent **III** solution at ambient temperature for 20 min, then 0.5 ml of 0.3 *M* phosphoric acid solution and 3.0 ml of the appropriate internal standard solution were added. The resulting solution was diluted to 10 ml with water and 50-μl aliquots were

injected into the chromatograph. The peak-height ratio of the thiol adduct to the internal standard was plotted against the corresponding thiol concentration to obtain the calibration graphs. As internal standards, 4-(naphthalen-2-yl)-4-oxobutanoic acid solution (0.24 mg/ml) was used for cysteine determination and 4-(6-methoxynaphthalen-2-yl)-4-oxobutanoic acid solution (4 μg/ml) for MESNa determination.

Sample preparation

Powders. An amount of powder equivalent to about 0.20 mg of cysteine was dissolved in 200 ml of EDTA solution (1 mg/ml).

Tablets. An amount of powdered tablet equivalent to about 7.7 mg of cysteine was treated with 250 ml of EDTA solution (1 mg/ml) under sonication for 5 min. After filtration through paper, a 3-ml aliquot of the clarified solution was diluted to 100 ml with EDTA solution (1 mg/ml).

Solutions. An aliquot of the commercial formulation was diluted with EDTA solution (15 μg/ml) to provide a sample solution containing about 3.2 μg/ml of thiol compound.

Assay procedure. A 1.0-ml aliquot of the sample solutions was subjected to the derivatization procedure with reagent **III** as described under *Calibration graphs*. The determination of the content of thiol compound in each sample was performed by comparison with an appropriate standard solution.

RESULTS AND DISCUSSION

The naphthoylacrylic acid **II** and the corresponding methyl ester **III** were synthesized by standard methods and, according to the NMR spectra, the *E* (*trans*) isomers were obtained. The reaction between **III** and N-acetylcysteine was carried out on a preparative scale and the analytical data for the adduct obtained were consistent with the proposed general structure **IIIa**, according to a Michael-type reaction involving thiol nucleophiles[16].

The fluorescence quantum yield of the N-acetylcysteine adduct in ethanol–triethylammonium phosphate (pH 3.0) (1:1, v/v) was found to be 0.15 by comparison with that of quinine sulphate (0.55 in 0.1 *M* sulphuric acid). This value is significantly higher than that of the corresponding adduct obtained from reagent **I**[10] and meets the requirements for sensitive HPLC analyses.

Chromatography

According to previous experience[11], the naphthoylacrylic acid **II** was first used for the thiol derivatization at pH 7.4 followed by reversed-phase HPLC separation. A representative chromatogram is shown in Fig. 1. As can be seen, biologically active thiols derivatized with **II** can be separated and identified but reagent peaks due to impurities are responsible for some interference. The complete elimination of these fluorescent impurities was attempted by recrystallization and chromatographic procedures, but failed. In addition, when the organic modifier content in the mobile phase was lowered to improve the resolution, splitting of the glutathione peak was observed, probably owing to the separation of the two diastereoisomer adducts from the derivatization reaction. These data led us to prepare the methyl ester **III**, which was obtained in high purity and therefore was chosen for the present study. A typical

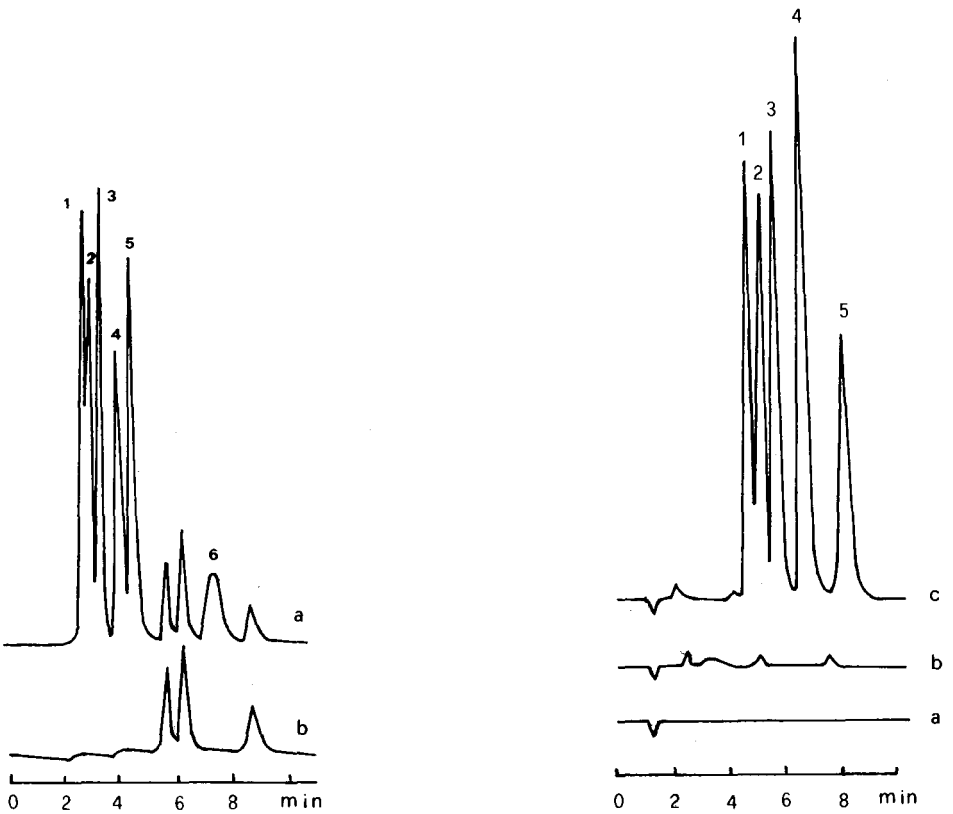

Fig. 1. HPLC of (a) adducts **IIa** from (1) glutathione, (2) L-cysteine, (3) homocysteine, (4) acetylcysteine, (5) thiola and (6) captopril; (b) reagent **II**. Column, Spherisorb RP-8 (5 μm); mobile phase, ethanol–0.05 *M* triethylammonium phosphate (pH 3.0) (40:60) at 1 ml/min. Fluorescence detector: λ_{em} = 450 nm; λ_{ex} = 310 nm.

Fig. 2. HPLC of (a) reagent **III**; (b) reagent **III** after 6 days at 4°C; (c) adducts **IIIa** from (1) glutathione, (2) L-cysteine, (3) MESNa, (4) homocysteine and (5) acetylcysteine. Column, Hypersyl RP-8 (5 μm); mobile phase, methanol–0.05 *M* TEA phosphate (pH 3.0) (53:47) at 1.2 ml/min. Detection as in Fig. 1.

separation of some thiols derivatized with the ester **III** is illustrated in Fig. 2. As shown, interfering reagent peaks were absent and the reagent solution proved to be stable for 3–4 days at 4°C. Using the ester reagent **III**, moreover, more lipophilic thiol adducts were obtained which provided single symmetric peaks under various chromatographic conditions.

The derivatization reaction course was studied with N-acetylcysteine. Using a molar ratio of reagent to analyte of >6, the reaction was completed within 10 min at ambient temperature and pH 7.5 and proved to be quantitative by comparison with an authentic specimen of the adduct. Using reversed-phase HPLC, methanol, acetonitrile and ethanol were found to be equally suitable as organic modifiers in the mobile phase. This represents an improvement with respect to the use of the methyl analogue **I**, which preferentially required ethanol.

The effect of the mobile phase pH on resolution and sensitivity for some biologically active thiols was evaluated and the results can be summarized as follows: (a) thriethylammonium (TEA) phosphate solutions at pH 3.0 and 4.0 were both suitable, whereas at pH 7.0 poorly reproducible separations were observed. (b) The sensitivities achieved at pH 3.0 and 4.0 were comparable but different for the various thiols examined. The highest sensitivity was obtained for glutathione, cysteine and homocysteine. The detection limit (signal-to-noise ratio = 3) was about 0.01 μg/ml. (c) Complete separation between glutathione and cysteine was obtained using a mobile phase consisting of methanol–0.05 *M* TEA phosphate (pH 4.0) (53:47, v/v) or methanol–0.01 *M* KH_2PO_4 (pH 3.0) (53:47, v/v). (d) Shorter retention times were obtained using acetonitrile instead of methanol. A suitable mobile phase was acetonitrile–0.05 *M* TEA phosphate (pH 3.0) (32:68, v/v) (Fig. 3). However, for the separation of more liphophilic thiols such as N-acetylcysteine, captopril, mercaptopropionylglycine and penicillamine, a higher acetonitrile content (42%) in the mobile phase was required.

Analysis of pharmaceutical formulations

The proposed HPLC method, based on precolumn derivatization with **III** and fluorimetric detection, was applied to the determination of L-cysteine and MESNa in commercial pharmaceutical formulations. L-Cysteine is an aliphatic thiol amino acid used as a dietary supplement and in the treatment of leg ulcers and MESNa is used as a mucolytic agent and also to prevent the urotoxic effects of cyclophosphamide or ifosfamide[17]. Under the described chromatographic conditions (Fig. 4), linear calibration graphs were obtained using fluorescent naphthoylpropionic acids (*i.e.*, hy-

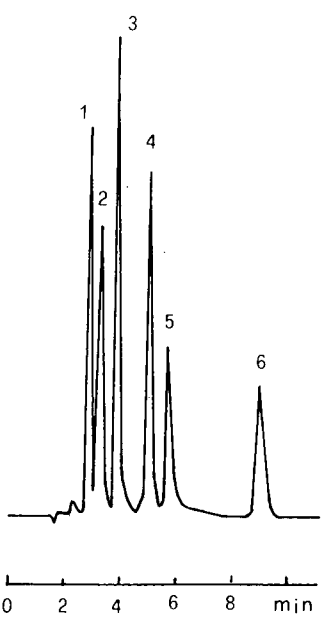

Fig. 3. Typical HPLC separation of adducts **IIIa** from (1) glutathione, (2) L-cysteine, (3) homocysteine, (4) cysteamine, (5) MESNa and (6) acetylcysteine. Column, Spherisorb RP-8 (5 μm); mobile phase, acetonitrile–0.05 *M* TEA phosphate (pH 3.0) (32:68). Detection as in Fig. 1.

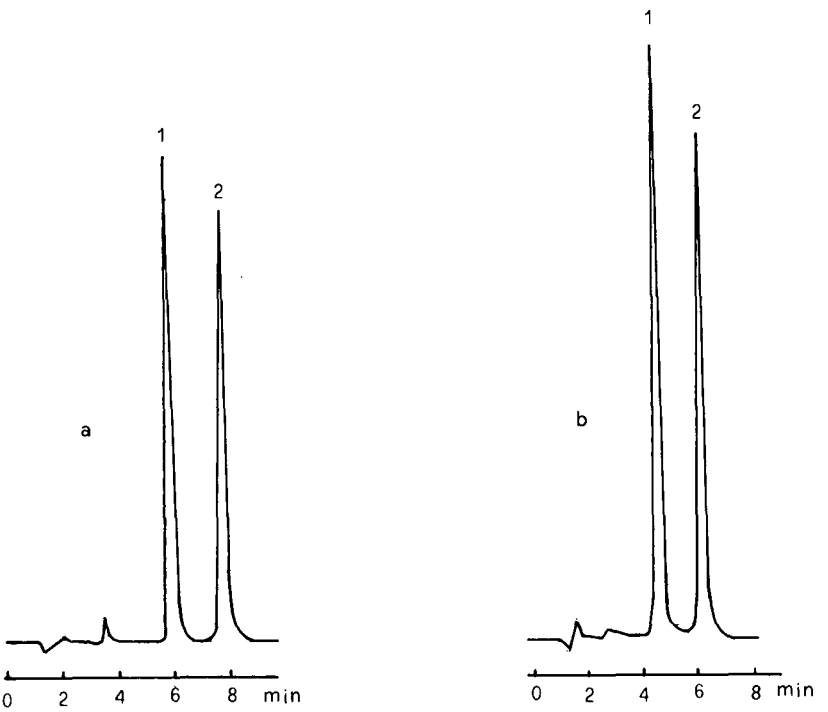

Fig. 4. Typical HPLC separations for quantitative applications: (a) (1) MESNa and (2) internal standard; (b) (1) L-cysteine and (2) internal standard. Column, Spherisorb RP-8 (5 μm); mobile phase, methanol –0.05*M* TEA phosphate (pH 3.0) (53:47) at 1 ml/min. Detection as in Fig. 1.

drogenated naphthoylacrylic acids) as internal standards. A typical calibration graph of the peak-height ratio of derivatized L-cysteine to internal standard (y) *versus* the drug concentration (x) was $y = 1.175x - 0.00276$ ($r = 0.9980$; $n = 6$). For MESNa the calibration graph was $y = 0.368x + 0.0110$ ($r = 0.9956$; $n = 6$). The precision of each method was evaluated by replicate analyses ($n = 8$) of a single standard solution. The relative standard deviation (R.S.D.) of the peak-height ratio of drug to internal standard was 0.6% and 0.85% for cysteine and MESNa, respectively.

TABLE I

ASSAY RESULTS FOR THE HPLC DETERMINATION OF L-CYSTEINE AND MESNa IN COMMERCIAL PHARMACEUTICAL FORMULATIONS

Drug	*Formulation*[a]	*Found (%)*[b]	*R.S.D. (%)*
L-Cysteine	Powder	100.07	0.73
	Tablet	99.50	1.80
MESNa	Solution	100.43	0.65

[a] Other ingredients: powder: neomycin sulphate, bacitracin Zn, glycine, DL-threonine, starch and magnesium oxide; tablet: D,L-methionine, L-cystine, protein hydrolysate, calcium pantothenate, vitamin B_2 phosphate, vitamin B_6, biotin and vitamin E; solution: EDTA disodium salt.

[b] Average of five determinations and expressed as a percentage of the claimed content.

Commercial formulations of L-cysteine and MESNa were analysed. The results obtained are summarized in Table I and were in close agreement with the claimed content. The other ingredients, including amino acids, of the analysed formulations did not interfere. The accuracy of the proposed HPLC method was verified by analysing samples (powders and tablets) spiked with known amounts of the drug; quantitative recoveries were obtained in each instance.

In conclusion, compound **III** proved to be a useful fluorogenic labelling reagent for the HPLC analysis of aliphatic thiols. The compound displayed a good reactivity and selectivity toward the thiol group, giving highly fluorescent derivatives that can be separated by reversed-phase HPLC. The proposed HPLC method exibited good sensitivity and its applications to the determination of bioactive thiols in biological samples are under study.

ACKNOWLEDGEMENTS

We are grateful to Dr. R. Ballardini for the fluorescence quantum yield determinations and to Miss P. Piccardoni for skillful technical assistance. This work was supported by the Ministero della Pubblica Istruzione (40%), Italy.

REFERENCES

1 D. Perret and S.R. Rudge, *J. Pharm. Biomed. Anal.*, 3 (1985) 3.
2 N.D. Danielson, M.A. Targove and B.E. Miller, *J. Chromatogr. Sci.*, 26 (1988) 362.
3 M.A. Martin, B. Lin and B. Del Castillo, *J. Pharm. Biomed. Anal.*, 6 (1988) 573.
4 M. Johansson and D. Westerlund, *J. Chromatogr.*, 385 (1987) 343.
5 K. Nakashima, C. Umekowa, H. Yoshida, S. Nakatsuji and S. Akiyama, *J. Chromatogr.*, 414 (1987) 11.
6 R.M. Maiorino, G.I. Weber and H.V. Aposhian, *J. Chromatogr.*, 374 (1986) 297.
7 W.R.G. Baeyens, G. van der Weken and P. de Moerloose, *Anal. Chim. Acta*, 205 (1988) 43.
8 T. Toyo'ka and K. Imai, *Anal. Chem.*, 56 (1984) 2461.
9 T. Toyo'ka, T. Suzuki, Y. Saito, S. Uzu and K. Imai, *Analyst (London)*, 114 (1989) 413; and references cited therein.
10 V. Cavrini, R. Gatti, P. Roveri and M.R. Cesaroni, *Analyst (London)*, 113 (1988) 1447.
11 V. Cavrini, R. Gatti, P. Roveri and A. Di Pietra, *Chromatographia*, 27 (1989) 185.
12 *Farmacopea Ufficiale della Repubblica Italiana*, Vol. I, Istituto Poligrafico e Zecca Dello Stato, Rome, 9th ed., 1985, p. 749.
13 A. Eirin, F. Fernandez, G. Gomez, C. Lopez, A. Santos, J. M. Colleja, D. Dela Iglesia and E. Cano, *Arch. Pharm. (Weinheim)*, 320 (1987) 1110.
14 V. Cavrini, P. Roveri, R. Gatti, C. Ferruzzi, A. M. Paniço and M. S. Pappalardo, *Farmaco, Ed. Sci.*, 37 (1982) 171.
15 M. Ghosal, *J. Org. Chem.*, 25 (1960) 1856.
16 J. March, *Advanced Organic Chemistry*, Wiley, New York, 3rd ed., 1985, p. 670.
17 E. F. Reynolds (Editor), *Martindale, The Extra Pharmacopoeia*, Pharmaceutical Press, London, 29th ed., 1989.

Journal of Chromatography, 507 (1990) 459–472
Elsevier Science Publishers B.V., Amsterdam — Printed in The Netherlands

CHROMSYMP. 1761

Optimization of the postcolumn hydrolysis reaction on solid phases for the routine high-performance liquid chromatographic determination of N-methylcarbamate pesticides in food products

A. DE KOK*, M. HIEMSTRA and C. P. VREEKER
Governmental Food Inspection Service, Pesticide Analysis Department, Burgpoelwaard 6, 1824 DW Alkmaar (The Netherlands)

SUMMARY

Various solid-phase materials were evaluated as catalysts for the postcolumn hydrolysis of N-methylcarbamate pesticides in a high-performance liquid chromatographic (HPLC) method for food products. Inexpensive magnesium oxide has been used for the first time in HPLC as a very efficient catalyst and as a good alternative for, *e.g.*, expensive anion-exchange resins. The reaction mechanism and kinetics were studied through measurement of the reaction band broadening, which depends on the stationary phase, mobile phase composition and flow-rate, and reaction temperature. Also, relationships between carbamate structure and reactivity were examined. The usefulness of the optimized postcolumn system was thoroughly tested by application to crop sample analysis during an extended period of time. The range of application of the solid-phase reaction was extended to 22 carbamate pesticides and ten of their metabolites. For crop sample analysis, limits of determination in the range 1–10 ppb were obtained.

INTRODUCTION

Postcolumn reaction systems in liquid chromatography[1] have attracted increased interest during the last decade as a means of converting compounds with unfavourable detection properties into derivatives which show enhanced sensitivity and often a higher selectivity towards such specific detectors as fluorescence and electrochemical detectors. For short reaction times, the tubular non-segmented reactors, preferably in the form of PTFE knitted tubes, are by far the most popular postcolumn reactors. However, solid-phase reactors, also called packed-bed reactors, can sometimes be substituted for tubular reactors. In the ideal case, the solid-phase material, normally packed in a short stainless-steel high-performance liquid chromatographic (HPLC) column, acts as a heterogeneous catalyst for the derivatization reaction. The main advantage is that the catalyst material is not consumed during the

0021-9673/90/$03.50

postcolumn reaction. Also, addition of reagent to the column effluent via an extra pump is obviated, thereby reducing the band broadening.

A good example of a possible substitution of a solid-phase reactor for a tubular non-segmented reactor is seen in the postcolumn hydrolysis reaction of N-methylcarbamate pesticides. In routine HPLC analysis for N-methylcarbamates in crops and water samples, the pesticides are first hydrolysed postcolumn in a tubular reactor by addition of a strong base (sodium hydroxide), to yield the common product methylamine, which is converted into a fluorescent derivative in a second, short reactor by addition of *o*-phthalaldehyde (OPA) reagent.

This method is widely used in the U.S.A.[2,3], where it is accepted as an official AOAC method. Recently, our group[4] improved the cleanup method for crop samples by the use of solid-phase extraction cartridges packed with aminopropyl-bonded silica phases. Further, the postcolumn tubular reaction system was optimized and its range of application was extended to include all 22 N-methylcarbamates and ten of their major metabolites. It was also realized that further improvement and/or simplification of the postcolumn reaction could be obtained by the inclusion of a solid-phase reactor acting as a heterogeneous catalyst for the base-catalysed hydrolysis.

Nondek *et al.*[5,6] have demonstrated that a strong anion exchanger, *e.g.*, Aminex A-28, is well suited to catalyse the hydrolysis of N-methylcarbamates when the catalyst bed is maintained at 100–120°C. The reaction band broadening, due to the hydrolysis process in the catalyst column, could be reduced in this way. In other words, the extra-column band broadening for the eluting peaks from the analytical column due to the postcolumn hydrolysis was reduced to negligible values. However, the use of catalytic hydrolysis on solid phases has been evaluated only for six well known carbamates, namely aldicarb, aminocarb, carbaryl, methiocarb, methomyl and propoxur[6]. Application of the complete HPLC method has only been reported for the determination of carbaryl in water samples[6,7].

It was the aim of this work to extend the application of the principle of solid-phase catalysis to a much wider group of N-methylcarbamates, namely 22 parent carbamates and ten of their major metabolites, mainly the sulphoxide and sulphone derivatives. The reaction methanism and kinetics were studied more closely with respect to the influence of mobile phase and stationary phase parameters and also the correlation with the chemical structure of the typical carbamate. Additionally, retention characteristics of reactants and products were determined and reaction band broadening could be indirectly measured. Finally, the total HPLC method was thoroughly tested over 2 years in real crop sample analysis for N-methylcarbamates. Examples of real residues found are presented.

EXPERIMENTAL

Chemicals

HPLC-grade acetonitrile was purchased from Rathburn (Walkerburn, U.K.) and water for HPLC was purified with an Elgastat UHQ water-purification system (Elga, High Wycombe, U.K.). *o*-Phthalaldehyde (for fluorescence analysis), 2-mercaptoethanol and disodium tetraborate (anhydrous) were obtained from Merck (Darmstadt, F.R.G.)

The OPA reagent was prepared as follows: 2.1 g of disodium tetraborate were

placed in a 1-l volumetric flask and dissolved in purified water (*ca.* 500 ml) with heating. A 250-mg amount of *o*-phthalaldehyde was weighed and dissolved in 2 ml of acetonitrile and then added to the flask. Next, 0.25 ml of 2-mercaptoethanol was added and the contents of the flask were made up to volume with water. The mobile phase and OPA reagent were degassed under vacuum prior to use.

Carbamate standards (from the Environmental Protection Agency, Research Triangle Park, NC, U.S.A., or Promochem, Wesel, F.R.G.) were dissolved in pure acetonitrile (1 mg ml^{-1}) and these stock solutions were diluted with the mobile phase solvent to obtain the required concentrations for the HPLC measurements. All other solvents and reagents used in crop sample analysis were as described previously[4].

Apparatus

The HPLC apparatus consisted of a Kratos (Ramsey, NJ, U.S.A.) Model SF 400 pump, a Rheodyne (Berkeley, CA, U.S.A.) Model 7125 injection valve, provided with a 100-μl loop, a Merck LiChroCART 250 × 4.0 mm I.D. cartridge column packed with Supersphere RP-8 (4 μm) and a postcolumn reaction detection system. The postcolumn reactor consisted of a 50 × 4.0 mm I.D. stainless-steel column, packed with various solid phases, and equipped with Valco couplings and 2-μm stainless-steel frits. The reactor column was enclosed in a holder, fitted in a Kratos PCRS 520 postcolumn oven, which could be heated at temperatures up to 150°C. The reactor was packed via a slurry procedure using an HPLC pump with mobile phase solvent at a constant flow-rate of 5 ml min^{-1}. After packing, the reactor column was conditioned at a flow-rate of 0.8 ml min^{-1} and heated at the maximum working temperature for several hours or until reproducible hydrolysis was observed.

The following solid-phase materials were used: (1) alumina N 7-12, neutral (7–12 μm) for HPLC from ICN Biochemicals (Eschwege, F.R.G.); (2) alumina 90, basic (63–200 μm) for column chromatography from Merck; (3) poly-4-vinylpyridine (Reillex 425, 300–900 μm) from Reilly Tar & Chemical (Indianapolis, IN, U.S.A.); (4) anion exchange resin Aminex A-27 (15 $\pm$ 2 μm) with tetraalkylammonium groups in the acetate form, from Bio-Rad Labs. (Richmond, CA, U.S.A.); and (5) magnesium oxide heavy (5–100 μm) from BDH (Poole, U.K.). The ion-exchange resin was allowed to swell in the mobile phase solvent for 24 h before packing the reactor column.

After the catalytic hydrolysis reactor, OPA reagent (0.20 ml min^{-1}) was added to the eluent via a low-dead-volume T-piece (vortex mixer, Kratos). The reaction of methylamine, formed during the hydrolysis of carbamates, with OPA reagent took place in the 20 cm × 0.10 mm I.D. PTFE connection capillary to a Merck–Hitachi (Tokyo, Japan) Model F-1000 double-monochromator fluorescence detector, which was tuned at excitation and emission wavelengths of 340 and 455 nm, respectively. Downstream of the detector cell a back-pressure regulator (*ca.* 10 bar), obtained from Beckman (San Ramon, CA, U.S.A.), was installed to prevent boiling of the mobile phase owing to high temperatures used in the reactor.

For the reaction band-broadening measurements (on both the ion-exchange resin and magnesium oxide reactor column), a Kratos Model 757 UV detector was used with detection at 254 nm, while the analytical column was disconnected. Reaction band-broadening studies were also executed by measurement of methylamine via OPA derivatization and fluorescence detection.

Chromatographic runs were performed isocratically with acetonitrile–water

TABLE I

NAMES, RETENTION TIMES AND OPTIMUM HYDROLYSIS TEMPERATURES OF N-METHYLCARBAMATES ON AMINEX A-27 AND MAGNESIUM OXIDE

Aromatic carbamates				*Aliphatic carbamates*			
Carbamate	t_R *on Aminex (s)*	*Temperature of complete hydrolysis (°C)*		*Carbamate*	t_R *on Aminex (s)*	*Temperature of complete hydrolysis (°C)*	
		Aminex	*MgO*			*Aminex*	*MgO*
Carbofuran	50	100	120	Oxamyl	40	130	120
3-Hydroxycarbofuran	45	100	120	Methomyl	45	>140	>140
3-Ketocarbofuran	42	100	120	Butocarboxim	45	>140	>140
Propoxur	50	100	120	Butocarboxim sulphoxide	34	140	140
Bendiocarb	50	100	120	Butoxycarboxim	42	130	140
Dioxacarb	50	90	110	Aldicarb	45	>140	>140
Ethiofencarb	65	100	120	Aldicarb sulphoxide	34	120	130
Isoprocarb	68	90	120	Aldicarb sulphone	40	120	130
Landrin	78	100	120	Thiofanox	47	>140	>140
Carbaryl	115	90	110	Thiofanox sulphoxide	34	140	140
Carbanolate	n.d.	90	110	Thiofanox sulphone	42	130	140
Methiocarb	115	90	110				
Methiocarb sulphoxide	45	100	110				
Methiocarb sulphone	100	90	110				

(35:65) as the mobile phase at a flow-rate of 0.80 ml min^{-1}. With the reaction-mechanistic experiments the latter solvent, methanol–water (40:60) and pure water were used. Chromatograms were recorded on a Kipp (Delft, The Netherlands) BD 41 recorder.

Methods

Crop sample analysis was carried out as described previously[4] with the improved cleanup method for the HPLC analysis of N-methylcarbamates. Briefly, it consisted of an acetone homogenization/extraction of the chopped sample and subsequent extraction with light petroleum and dichloromethane. An aliquot of the sample extract was evaporated, redissolved in dichloromethane and cleaned up with aminopropyl-bonded silica cartridges. Further details can be obtained elsewhere[4].

RESULTS AND DISCUSSION

Theory

Heterogeneous catalytic hydrolysis of N-methylcarbamates on a solid phase was first studied by Nondek *et al.*[5] using the hydrolysis of carbaryl on an anion exchanger as a model system. In a subsequent paper, Nondek *et al.*[6] studied five more carbamates. They derived some equations for the band broadening due to the solid-phase reaction, the so-called reaction band broadening σ_r, as related to the rate constant of the reaction, k_r, and the capacity factors for reactant and product, k'_R and k'_P:

$$\sigma_r = \frac{c(1 - k'_P/k'_R)}{k_r} \tag{1}$$

where c is a constant. This relationship holds for solid-phase reactions with first-order kinetics, which appeared to be the case in their study of the carbamate hydrolysis. The reaction band broadening could be described by the equation

$$\sigma_r^2 = \sigma_t^2 - \sigma_n^2 \tag{2}$$

where σ_t is the total band broadening caused by the solid-phase reactor and σ_n is the non-reaction band broadening. σ_r can be calculated by measuring the variance of the product peak for the separate injections of product and reactant:

$$\sigma_r^2 = (\sigma_t^2)_{prod} - (\sigma_n^2)_{prod} \tag{3}$$

Solid-phase materials

Included in our routine analysis for the determination of N-methylcarbamates in crop samples[4] are a total of 22 carbamates and ten of their metabolites. This study focused on the application of the solid-phase catalytic hydrolysis for all these compounds. A possible relationship between molecular structure and rate of hydrolysis was determined for five different solid-phase materials. Retention times of the reactant molecules, the parent carbamate and, if possible, the available hydrolysis products were determined. Also, the temperature at which the optimum response of product could be observed was established.

The results for Aminex A-27, a strong-anion exchange resin, and magnesium oxide (MgO) are summarized in Table I. MgO, although never used before in typical HPLC applications, was nevertheless tried, because it is known in organic chemistry as a strongly basic catalyst in batch reactions. In addition, it is a much cheaper and more rigid material for column chromatography than the resin-based anion exchanger Aminex A-27. In practice, MgO fulfilled its expectations and requirements, namely efficiently converting all N-methylcarbamates into their hydrolysis products.

Apart from MgO, aluminium oxide (Al_2O_3) was also studied in two different forms, HPLC grade (neutral Al_2O_3 of particle size 7–12 μm) and classical column chromatographic grade, (basic Al_2O_3 of particle size 70–200 μm). Both forms of Al_2O_3 showed clearly inferior catalytic properties to Aminex A-27 and MgO, which may be explained by the fact that Al_2O_3 is known to act as a weaker basic catalyst and/or anion exchanger. Even at temperatures as high as 150°C, the easiest to catalyse carbamates were hydrolysed by not more than 40%. The same result was obtained with another weakly basic catalyst known from organic catalytic reactions, namely polyvinylpyridine in the form of polymeric beads of particle size 300–900 μm.

The main conclusion that can be drawn from these experiments with five basic catalysts is that the degree of basicity of the catalysts is the predominant factor determining the catalytic activity in the hydrolysis reaction. Although a decrease in particle size increases the degree of catalysis, as was also shown by Nondek *et al.*[5] and Kun She *et al.*[7] for carbaryl, the degree of basicity plays a much more important role than particle size. Neutral Al_2O_3 (7–12 μm) was even less catalytic than basic Al_2O_3 (70–200 μm), which was much less catalytic than 5–100 μm MgO (strongly basic) or 15 μm Aminex A-27 (strong anion exchanger).

More extensive research on the exact mechanism of the catalytic behaviour of the various solid-phase materials was confined to MgO and Aminex A-27. Measurements of reaction band broadening were useless on the Al_2O_3 and polyvinylpyridine phases, because of the low degree of hydrolysis, even at very high reactor temperatures.

Aminex A-27. A closer look at the Aminex A-27 results in Table I reveals that a rough relationship can be discerned between the molecular structure of the carbamate pesticide on the one hand and retention time on Aminex and temperature of maximum response of product on the other. The carbamates may be divided in two typical groups, namely aromatic carbamates and aliphatic carbamates (oxime carbamates). The aromatic carbamates, with retention times (t_R) between 45 and 115 s, invariably have their maximum product response at 90–100°C, whereas the aliphatic carbamates, with distinctly shorter retention times (t_R = 34–47 s) require temperatures of at least 120°C for maximum peak response of the products. The parent carbamates methomyl, butocarboxim, aldicarb and thiofanox even require a temperature slightly above 140°C for complete conversion.

Although Nondek *et al.*[5] had suggested that a certain retention of the parent carbamates on the solid-phase material would be required to undergo catalytic hydrolysis, it can be concluded from Table I that the ease of hydrolysis is definitely not linearly related to the retention on the solid phase.

The assumed reaction equations for the carbamate hydrolysis[6] are as follows:

$$ROC(O)NHCH_3 \rightarrow ROH + CH_3N{=}C{=}O \quad (4)$$

$$CH_3N{=}C{=}O + H_2O \rightarrow CH_3NH_2 + CO_2 \quad (5)$$

By subsequent injection and comparison of retention times of the available standards of the hydrolysis products ROH (oxamyl oxime, methomyl oxime and carbofuranphenol) and the hydrolysed parent compounds, it has been proved that these products are indeed formed.

The first step in the hydrolysis reaction is assumed to be a nucleophilic attack on the carbon atom of the ester group. The speed of this reaction step will be influenced by the fractional charge on the molecule, which will be (extra) induced by the solid-phase catalyst, thereby lowering the activation energy for the nucleophilic substitution. The differences observed in the hydrolysis rate between the various carbamates will probably be influenced by the substituents in the R group. Within the group of aliphatic carbamates, more sequences can be deduced from Table I and additional experiments. For the parent compounds, the hydrolysis rates decrease in the order oxamyl > methomyl > aldicarb > butocarboxim > thiofanox. Note that their respective retention times are 40, 46, 45, 45 and 47 s, which again are apparently not decisive. The hydrolysis rate sequence for the carbamates, which also have sulphoxide and sulphone oxidation products, namely aldicarb, butocarboxim, thiofanox and methiocarb, is invariably sulphone > sulphoxide > parent.

Finally, some general observations are of interest. The retention times of the hydrolysis products (ROH) on Aminex are always higher, than those of the parent compounds, *e.g.*, oxamyl oxime and oxamyl, 138 and 40 s; methomyl oxime and methomyl, 66 and 46 s; carbofuranphenol and carbofuran, 260 and 50 s; and naphthol and carbaryl, >2000 and 115 s. The methylamine, always formed in the hydrolysis reaction of N-methylcarbamates has a retention time of *ca.* 40 s. Methomyl has a strikingly high total band broadening in comparison with the other difficult to hydrolyse carbamates. No explanation can be given for this deviant behaviour.

When critically comparing the results of Nondek's group and this work, some striking differences are revealed. We have never observed any peak in the reaction product formation chromatograms other than those originating from the parent compound and the oxime or phenol. That is, we could not detect any intermediate isocyanate, an extra peak reported by Nondek *et al.* Although Nondek *et al.*[5,6] experienced decomposition of their Animex A-28 ion-exchange material above 120°C, in our study temperatures up to 150°C could be applied without noticeable deterioration of the phase. Surprisingly, the Aminex A-27 (15 $\pm$ 2 μm) used in this study required a *ca.* 20°C higher temperature than the Aminex A-28 (9 $\pm$ 2 μm) used by Nondek *et al.* The small difference in particle size can hardly have such an influence, taking into account the results of Nondek *et al.* when they compared Amberlite CG 400 (70 μm) with Aminex A-28 (9 μm).

There is no other conclusion, then, that the reaction kinetics and possibly also the mechanism appear to be different in our case. This may be caused by differing production batches of the Aminex, due to changed production methods.

Magnesium oxide. Although not commercially available in a small, narrow-ranged particle size as typical HPLC packings, "general-purpose reagent" MgO (particle size 5–100 μm) packed in a catalytic reactor showed surprisingly good catalytic activity. Compared with Aminex A-27, the reactor temperature needed to obtain the optimum product response averaged 20°C higher (see Table I). This could be explained by the differences in basicity and/or available particle sizes of both materials. It is to be hoped that in the near future better defined MgO with a narrow

particle size distribution will become commercially available for our special application. The retention times of all parent carbamates and those of the hydrolysis products (ROH) and methylamine appeared to be identical, namely 40 s. This again underlines the earlier statement that the absolute retention on the solid phase has no relationship with the ease of hydrolysis of the compound. Solute–catalyst interactions at the molecular level must be far more important. With respect to the reaction band-broadening (σ_r) measurements, a significant difference could be seen between the measurements via the methylamine or via the phenol/oxime product with fluorescence and UV detection, respectively. In the latter instance, σ_r appeared to be zero, which would suggest that a first-order reaction takes place (see also eqn. 1). However, with the fluorescence measurements, the peak widths of the hydrolysed reactant and methylamine standard injected differed. In addition, the peak width of the oxime or phenol product (as measured with UV detection) appeared to be equal to the peak width of the injected methylamine standard, but smaller than the peak width of the methylamine product from the injected (carbamate) reactant (as measured with

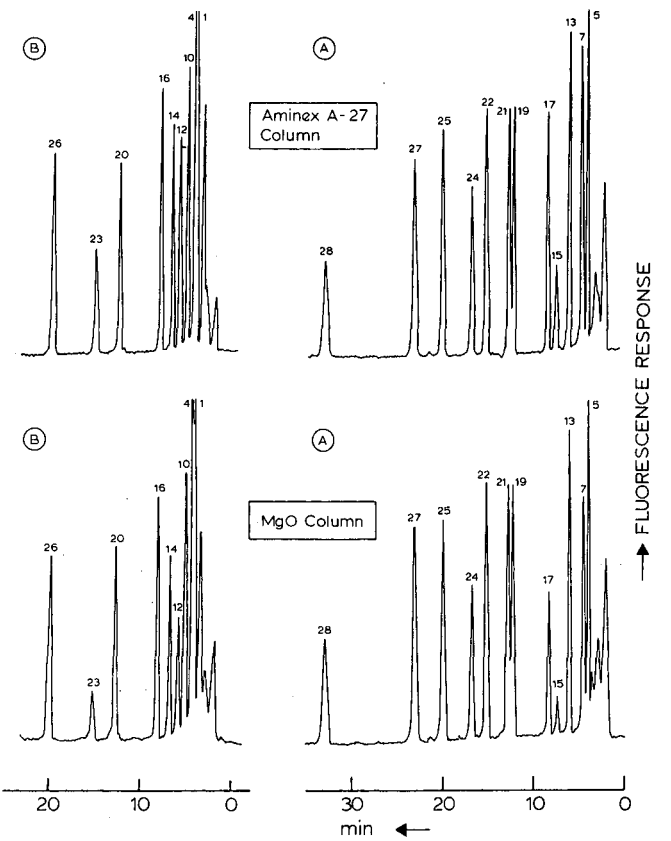

Fig. 1. Comparison of the catalytic hydrolysis efficiency of two mixtures (A and B) of N-methylcarbamate standards on two different solid-phase materials, Aminex A-27 and MgO, at a reactor temperature of 120°C. Mobile phase: acetonitrile–water (35:65); flow-rate, 0.8 ml min^{-1}; injected amounts, 2 ng of each compound. Numbers above the peaks correspond to those in Table III.

fluorescence detection). Apparently, the conversion of methyl isocyanate into methylamine is the rate-determining step, which can only be caused by a certain retention of the intermediate carbamic acid on the MgO. This results in the measured σ_r of methylamine product being unequal to zero. The overall reaction from carbamate to methylamine is thus not of first-order kinetics. Because these differences between σ_r values measured via UV or fluorescence detection did not occur on Aminex A-27, it might be concluded that, if not the reaction mechanism, at least the reaction kinetics of the carbamate hydrolysis are different on the two solid-phase materials. A typical example of chromatograms of two standard mixtures of carbamates hydrolysed on MgO and Aminex A-27 at 120°C is shown in Fig. 1. The absolute response of the aromatic carbamates is identical on both phases, because at 120°C complete hydrolysis has taken place, as can also be seen from Table I. The responses of the aliphatic carbamates, however, are lower with MgO than Animex. Note also that the peak width, at sufficiently high reaction temperatures, is almost identical on both phases. The slightly higher total chromatographic peak width of most carbamates on MgO is simply caused by the higher band broadening of methylamine on MgO compared with Aminex A-27, *e.g.*, 6.5 *versus* 2.6 s, at 120°C.

Reaction band-broadening measurements

Dependence of σ_r on mobile phase. Reaction band broadening, σ_r, on Aminex A-27 and MgO was measured via subsequent injections of the parent compound and oxime/phenol product, directly onto the reactor column, for the model compounds oxamyl, methomyl and carbofuran, followed by UV detection at 254 nm. σ_r could also be measured via subsequent injections of standard methylamine and parent compound, followed by OPA reaction and fluorescence detection.

When oxamyl was tested on Aminex at different flow-rates, σ_r increased when the flow-rate was increased. For, *e.g.*, flow-rates of 0.5 and 1.0 ml min^{-1} of acetonitrile–water (35:65), σ_r was 6.5 and 16 s, respectively. The flow dependence of σ_r means that, in this work, in contrast to the results of Nondek's group[5], the hydrolysis reaction is not first order. The same behaviour was also observed with MgO.

Another interesting feature of the catalytic hydrolysis could be seen when the mobile phase composition was changed. Pure water appeared to give more efficient catalysis and also lower σ_r values than acetonitrile–water (35:65). A methanol–water (40:60) mixture was even less efficient than acetonitrile–water. The influence of the mobile phase is more pronounced the lower the temperature. In practice, the optimum mobile phase is thus an acetonitrile–water mixture with as low as practical a flow-rate for the chromatographic separation of the complete mixture of carbamates.

Dependence of σ_r on retention temperature. In accordance with the expectations, a significant decrease in σ_r with increasing temperature was actually observed on both solid phases. As a typical example, in Table II the dependence of σ_r on reaction temperature is shown for the three model compounds on MgO and Aminex A-27. The absolute values of σ_r are typically higher on Aminex than on MgO. This effect is more apparent as the reaction temperature becomes lower than the temperature for complete hydrolysis. Apparently, σ_r is not necessarily directly related to the ease of hydrolysis. The lower σ_r value of oxamyl compared with the easier to hydrolyse carbofuran also supports this statement. Another example is given by the almost negligible σ_r value (<0.1 s) of methomyl hydrolysed on MgO at 120°C, where the extent of hydrolysis has not yet reached 100%.

TABLE II

DEPENDENCE OF THE CATALYTIC HYDROLYSIS REACTION BAND BROADENING (σ_r) ON REACTION TEMPERATURE ON AMINEX A-27 AND MAGNESIUM OXIDE SOLID PHASES FOR THREE N-METHYLCARBAMATES

Mobile phase, acetonitrile–water (35:65); flow-rate, 0.8 ml min^{-1}.

Solid-phase material	*Carbamate*	*Reaction band broadening, σ_r (s)*			
		80°C	*100°C*	*120°C*	*140°C*
Aminex A-27	Oxamyl	11.4	4.1	0	0
	Methomyl	n.d.	n.d.	8.3	0.8
	Carbofuran	19.1	6.9	0	0
MgO	Oxamyl	5.4	3.1	0	2.7
	Methomyl	6.9	3.8	0.4	0
	Carbofuran	8.1	4.9	0	0

Oxamyl shows a very typical hydrolysis behaviour (see Table II) on MgO. After σ_r has approached zero at 120°C, it increases again towards 2.7 s at 140°C. In the product formation analysis with fluorescence detection, an extra peak with a slightly different retention time indeed appears in the chromatogram. Probably a second reaction route, with a higher activation energy, becomes possible for oxamyl at such high reaction temperatures.

Typical chromatograms of a carbamate standard mixture, catalytical hydrolysed on MgO at various temperatures, are shown in Fig. 2. The decrease in peak width with increase in reactor temperature is clearly visible.

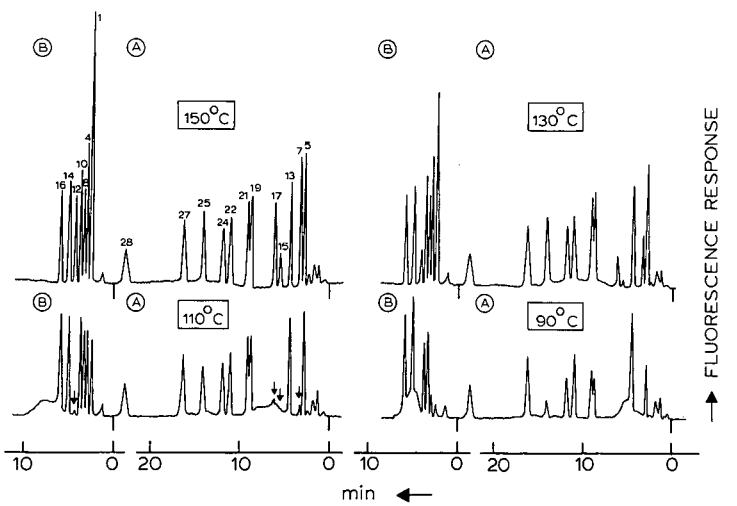

Fig. 2. Dependence of the catalytic hydrolysis effiency on reaction temperature for two standard mixtures of N-methylcarbamates (A and B), separated in the HPLC system Supersphere RP-8 with acetonitrile–water (35:65) at 0.8 ml min^{-1} and hydrolysed on MgO at 90, 110, 130 and 150°C. Injected amounts, 2 ng of each compound (except thiofanox, 20 ng). Numbers above the peaks correspond to those in Table III.

TABLE III

RELATIVE RETENTION TIMES (RRT) AND DETECTION LIMITS OF 22 N-METHYLCARBAMATES AND 10 OF THEIR METABOLITES IN THE REVERSED PHASE HPLC SYSTEM SUPERSPHERE RP-8 (5 μm) WITH ACETONITRILE–WATER (35:65)

Catalytic reactor packed with Aminex A-27 or magnesium oxide (operating temperature, 140°C). Fluorescence detection was performed at excitation and emission wavelengths of 340 and 455 nm, respectively.

No.	*Compound*	*RRT*	*Detection limit (pg)*	*No.*	*Compound*	*RRT*	*Detection limit (pg)*
	Parent compounds:				*Metabolites:*		
5	Oxamyl	0.29	25	1	Aldicarb sulphoxide	0.24	25
7	Methomyl	0.34	25	2	Butocarboxim sulphoxide	0.25	25
9	Ethidimuron	0.39	50	3	Butoxycarboxim	0.28	25
11	Tranid	0.44	50	4	Aldicarb sulphone	0.29	25
13	Dioxacarb	0.46	50	6	Thiofanox sulphoxide	0.31	50
15	Butocarboxim	0.59	50	8	Methiocarb sulphoxide	0.34	50
17	Aldicarb	0.65	50	10	3-Hydroxycarbofuran	0.39	50
18	Cloethocarb	0.93	50	12	Thiofanox sulphone	0.45	50
19	Propoxur	0.94	50	14	Methiocarb sulphone	0.51	50
20	Bendiocarb	0.98	50	16	3-Ketocarbofuran	0.63	50
21	Carbofuran[a]	1.00	50				
22	Carbaryl	1.21	50				
23	Thiofanox	1.25	50				
24	Ethiofencarb	1.31	100				
25	Isoprocarb	1.55	100				
26	Landrin	1.59	100				
27	Carbanolate	1.83	100				
28	Methiocarb	2.58	100				
29	Promecarb	3.05	n.d.				
30	Bufencarb	>4	n.d.				
31	Mexacarbate	>4	n.d.				
32	Aminocarb	>4	n.d.				

[a] Absolute retention time of carbofuran = 10.5 min.

Analytical data

In Table III, relative retention times and detection limits of all the carbamates and their metabolites studied are reported. The retention times were obtained with an isocratic run, using acetonitrile–water (35:65) as the mobile phase at a flow-rate of 0.8 ml min^{-1}. Data for promecarb, bufencarb, mexacarbate and aminocarb are not given, as a different mobile phase would have been required to reduce their high retention. Detection limits, calculated for a signal-to-noise ratio of 3:1, are invariably in the 25–100 pg range for both catalytic solid phases. The only exception is thiofanox, which at a reaction temperature of 140°C displays a 10-fold higher detection limit on MgO compared with Aminex A-27. A further increase in the reactor temperature for MgO drastically improves this situation.

Repeatability studies were performed via repetitive injection of 5 ng of methomyl, carbofuran and methiocarb. For all three compounds a relative standard deviation of *ca.* 2% ($n = 10$) was obtained. No significant differences in repeatability between Aminex A-27 and MgO were observed.

Good linearity ($r = 0.995$) was observed on both solid phases over the practical

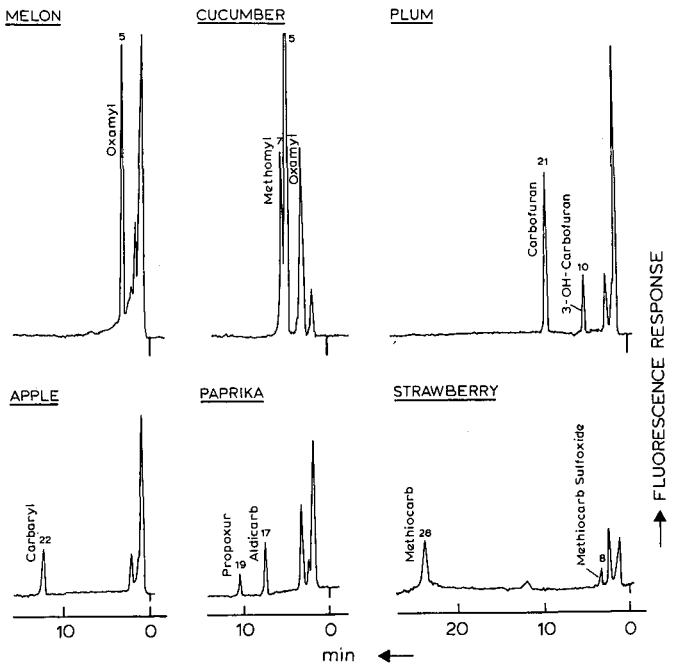

Fig. 3. Examples of HPLC of crop sample extracts containing real residues of various N-methylcarbamates. HPLC system as described under Experimental. Residue concentrations: (melon) 0.04 ppm oxamyl; (cucumber) 0.28 ppm oxamyl and 0.07 ppm methomyl; (plum) 0.02 ppm carbofuran and 0.01 ppm 3-hydroxycarbofuran; (apple) 0.05 ppm carbaryl; (paprika) 0.008 ppm aldicarb and 0.003 ppm propoxur; (strawberry) 0.02 ppm methiocarb and 0.005 ppm methiocarb sulphoxide.

working range of 0.1–10 ng injected amount of the test compounds methomyl, carbofuran and methiocarb. It should be stressed that good linearity was obtained despite the fact that no first-order kinetics were observed for catalytic hydrolysis. This finding is contrary to the expectations which were stated by Nondek *et al.*[5] in their study.

Crop sample analysis

The feasibility of the catalytic solid-phase hydrolysis was tested in crop sample analysis. An HPLC system including the Aminex A-27 reactor has been used routinely over the last 2 years with an annual sample throughput of *ca.* 1000. The catalytic reactor was in use for over 6 months before renewal of the phase was required. Hence no poisoning of the catalyst occurred provided that a guard column was installed in front of the analytical column and solid-phase extraction clean-up of samples was applied as a protective measurement. The catalysis may thus be assumed to be purely heterogeneous.

The carbamate pesticide system now includes the analysis of 22 N-methyl-carbamates and ten of their major metabolites (mostly sulphoxides and sulphones of the oxime carbamates). In the optimized system a flow-rate of 0.8 ml min^{-1} of an acetonitrile–water (35:65) mobile phase and a reactor temperature of 140–150°C (for

Aminex A-27 or, alternatively, MgO) are being used. The major advantages of the use of the solid-phase hydrolysis system developed in this study, compared with the classical sodium hydroxide hydrolysis as used in crop sample analysis by Krause[2,3] and our group[4], are (1) the elimination of a reagent pump and a mixing tee and also reagent costs, (2) the possibility of using higher reaction temperatures with inherent higher hydrolysis efficiencies and thus lower detection limits (which is best illustrated in the case of thiofanox) and (3) reduced reaction band broadening resulting in optimum maintenance of the chromatographic resolution.

Compared with the work of Nondek *et al.*[5,6], the major improvements achieved are (1) the great extension of the range of application of the catalytic reaction to a total of 32 compounds, (2) a further reduction of reaction band broadening to the optimum value zero, (3) the inexpensive solid phase MgO (5–100 μm), compared with their inexpensive anion exchanger Amberlite CG 400 (70 μm), is easier to pack, has a much higher thermal stability and shows negligible retention for both reactant and products, (4) the suitability for application to even difficult crop samples and (5) practical problems with gradient elution due to shrinking and swelling of the Aminex A-27 are obviated with the rigid MgO.

In Fig. 3 chromatograms are shown of six routine crop samples that contained positive residues of various N-methylcarbamates. The clean chromatograms illustrate the selectivity and sensitivity of the method, which is due to the earlier developed improved clean-up method combined with the effective catalytic reaction detection system. Limits of determination are in the range 1–10 ppb when only 400 mg of the original sample is worked up. Owing to the difficult matrix, for citrus fruit products a 10-fold dilution of the original sample extract is recommended, which results in a 10-fold increase in the limits of determination. More results on reproducibility and quantitation, and also residue data from routine analysis, will be given in a subsequent paper.

Future work will be directed towards the extension of the application of solid-phase catalysis to other types of pesticides that might be hydrolysed, *e.g.*, phenylurea herbicides. Also, attention will be paid to the automation of the solid-phase extraction clean-up method, which is still the time-determining step in the whole method.

CONCLUSION

A postcolumn solid-phase reaction system, based on heterogeneous catalytic hydrolysis on a packed-bed reactor, has been optimized for the HPLC analysis of a complete group of 22 N-methylcarbamates and ten major metabolites. Complete hydrolysis was achieved at a reactor temperature of *ca.* 140°C on both the more expensive strong anion exchanger Aminex A-27 and on the inexpensive magnesium oxide. Magnesium oxide showed the additional advantages of lower reaction band broadening, even at lower than optimum temperatures, and the possibility of performing gradient elution analysis.

Reversed-phase HPLC combined with the solid-phase reactor and subsequent OPA derivatization of the resulting methylamine provides a selective and sensitive method for the routine determination of N-methylcarbamates in crop samples. The method has been in operation in our laboratory for more than 2 years, without any significant problems.

Limits of determination in the range 1–10 ppb can be obtained. Future research will be focused on the extension of the catalytic solid-phase reaction principle to other important classes of pesticides.

REFERENCES

1 I. S. Krull (Editor), *Reaction Detection in Liquid Chromatography*, Marcel Dekker, New York, 1986.
2 R. T. Krause, *J. Assoc. Off. Anal. Chem.*, 68 (1985) 726.
3 R. T. Krause, *J. Assoc. Off. Anal. Chem.*, 68 (1986) 734.
4 A. de Kok, M. Hiemstra and C. P. Vreeker, *Chromatographia*, 24 (1987) 469.
5 L. Nondek, U. A. Th. Brinkman and R. W. Frei, *Anal. Chem.*, 54 (1983) 1466.
6 L. Nondek, R. W. Frei and U. A. Th. Brinkman, *J. Chromatogr.*, 282 (1983) 141.
7 L. Kun She, U. A. Th. Brinkman and R. W. Frei, *Anal. Lett.*, 17 (1984) 915.

Journal of Chromatography, 507 (1990) 473–479
Elsevier Science Publishers B.V., Amsterdam — Printed in The Netherlands

CHROMSYMP. 1730

Liquid adsorption chromatography of styrene copolymers of methacrylates and acrylates

SADAO MORI
Department of Industrial Chemistry, Faculty of Engineering, Mie University, Tsu, Mie 514 (Japan)

SUMMARY

Styrene copolymers with methyl, ethyl and *n*-butyl methacrylate and acrylate were prepared by solution polymerization at a low degree of conversion. These copolymers were separated according to composition by gradient elution using silica gel as the stationary phase and chloroform–ethanol as the mobile phase. The initial mobile phase was chloroform–ethanol (99:1, v/v) and the final one (93:7, v/v), the composition changing linearly. Acrylate- or methacrylate-rich copolymers were eluted later and required a higher ethanol content in the mobile phase. The retention volume of the copolymers was influenced by column temperature in such a way that the copolymers tended to be retained in the column longer at high temperatures. The resolution between two adjacent peaks was improved with increase in column temperature. For copolymers having the same styrene content, those having smaller alkyl ester groups tended to be retained in the column longer than those having longer alkyl ester groups at the same column temperature.

INTRODUCTION

Most synthetic copolymers generally have a chemical composition distribution (CCD) in addition to a molecular weight distribution (MWD). Size-exclusion chromatography (SEC) can be used for the determination of the MWD of synthetic polymers, but it is not always easy to obtain accurate molecular weight averages for copolymers by SEC, because the separation of polymers by SEC is achieved according to the sizes of the molecules in solution and the molecular weights of copolymers are not always directly proportional to molecular size[1]. SEC with dual detectors is a well known method for determining the CCD. However, this technique is incapable of determining a real CCD, because components eluted in the same retention volume might have different compositions with the same molecular size. Therefore, only the average composition can be detected[2].

To obtain both the MWD and the CCD, the determination of the MWD independent of composition and the separation of copolymers by composition independent of molecular weight are required. Recent developments in high-performance liquid chromatography (HPLC) have permitted the separation of copol-

0021-9673/90/$03.50

ymers according to their chemical compositions. Styrene–methyl methacrylate[3–5], styrene–acrylate[6], styrene–acrylonitrile[7] and styrene–butadiene[8] copolymers have been separated by HPLC according to their compositions.

In previous papers[4,9–12], the separation of styrene–methyl methacrylate copolymers according to chemical composition by liquid adsorption chromatography (LAC) was reported. A molecular weight dependence on the separation of these copolymers by LAC was not observed. The aim of this work was to apply this LAC technique to the separation of several types of styrene–acrylate and styrene–methacrylate copolymers according to their composition and to explain the usefulness of LAC for the separation of styrene copolymers having carbonyl groups as one component.

EXPERIMENTAL

Apparatus

LAC was performed on a Jasco Trirotar-VI high-performance liquid chromatograph with a Uvidec-100 VI ultraviolet absorption detector operated at 254 nm (Japan Spectroscopic, Tokyo, Japan). The column (50 mm × 4.6 mm I.D.) was packed with silica gel with a pore size of 30 Å and a mean particle diameter of 5 μm (Nomura Chemical, Aichi, Japan). The number of theoretical plates was 1600, obtained by injecting 5 μl of a 0.5% benzene solution in chloroform containing 1% ethanol. The column was thermostated at a specified temperature in a Model TU-100 column oven (Japan Spectroscopic).

Samples

Methyl methacrylate (MMA), ethyl methacrylate (EMA), *n*-butyl methacrylate (BMA), methyl acrylate (MA), ethyl acrylate (EA) and *n*-butyl acrylate (BA) were used as comonomers, and were copolymerized with styrene (S) by solution polymerization at a low degree of conversion. A total volume of 25 ml of a mixture of freshly distilled styrene monomer and methacrylate or acrylate monomer at a specified molar ratio was dissolved in 25 or 50 ml of benzene and 20 or 40 mg of azobisisobutyronitrile (AIBN) were added. Polymerization was performed at 60°C for 10 h under a nitrogen atmosphere. The polymerization products were purified by a solution-precipitation approach by dissolving the products in chloroform, followed by precipitating them in methanol. This approach was repeated twice and the products were dried under vacuum.

The composition of the copolymers was measured by ultraviolet spectroscopy at 260 nm and the results are listed in Table I. A calibration graph was constructed with polystyrene. Polystyrene-equivalent molecular weight averages of the copolymers measured by SEC were between $1.0 \cdot 10^5$ and $3.0 \cdot 10^5$ for the weight-average molecular weight ($\bar{M}_w$) and $0.5 \cdot 10^5$ and $1.5 \cdot 10^5$ for the number-average molecular weight ($\bar{M}_n$), and the values of $\bar{M}_w/\bar{M}_n$ were between 1.6 and 1.7 (Table I).

Gradient elution

The mobile phase was a linear gradient of chloroform–ethanol. The initial mobile phase (A) was chloroform–ethanol (99.0:1.0, v/v) and the final one (B) chloroform–ethanol (93.0:7.0, v/v), the composition changing linearly from 100%

TABLE I

COMPOSITION AND MOLECULAR WEIGHT AVERAGES OF SAMPLE COPOLYMERS

Sample		*Styrene content (mol%)*	*Molecular weight*[a]		*Sample*		*Styrene content (mol%)*	*Molecular weight*[a]	
			$\bar{M}_w \times 10^{-4}$	$\bar{M}_n \times 10^{-4}$				$\bar{M}_w \times 10^{-4}$	$\bar{M}_n \times 10^{-4}$
S–MMA	I	64.6	12.4	6.9	S–MA	I	65.7	10.7	4.9
	II	47.3	12.2	7.0		II	51.3	12.5	7.8
	III	28.7	12.2	7.0		III	35.6	17.8	11.3
	IV	14.7	12.6	7.2		IV	19.0	20.1	12.0
S–EMA	I	69.1	9.5	4.6	S–EA	I	68.6	12.2	6.2
	II	50.2	12.0	7.3		II	52.6	10.9	6.2
	III	30.4	13.5	8.0		III	36.7	20.2	11.9
	IV	15.5	22.9	12.9		IV	20.7	23.8	16.1
S–BMA	I	69.6	9.4	4.6	S–BA	I	75.5	8.7	5.1
	II	50.3	13.8	7.1		II	59.2	10.7	6.4
	III	30.7	14.2	7.2		III	41.0	12.9	8.2
	IV	14.5	18.6	10.3		IV	15.8	22.9	12.8

[a] Polystyrene-equivalent molecular weight.

A to 100% B in 30 min. The flow-rate of the mobile phase was 0.5 ml/min. The sample copolymers were dissolved in solution A at a total concentration of 0.1% (w/v) and the injection volume was 0.1 ml. The sample solutions were injected 1 min after the start of the gradient elution programme.

RESULTS AND DISCUSSION

In the LAC of S–MMA copolymer, the retention volume of the copolymers was affected considerably by the ethanol content in the mobile phase and by the column temperature[9,10]. However, the separation of the copolymers according to composition was not possible with isocratic elution conditions. Gradient elution conditions were required at a constant column temperature. Higher ethanol contents in the mobile phase and lower column temperatures were required to separate MMA-rich copolymers. In the present experiments, several gradient elution conditions, *i.e.*, the initial and the final compositions of the mobile phase and the gradient period, were examined at different column temperatures in order to separate various styrene copolymers with acrylate or methacrylate having different compositions. The optimized gradient elution conditions are given under Experimental.

Figs. 1–3 show examples of the separation of mixtures of S–MMA (Fig. 1), S–MA (Fig. 2) and S–BA (Fig. 3) copolymers at different column temperatures. Peak elution was retarded with increasing column temperature, as observed in previous studies[9,10].

Fig. 1 shows the LAC of a mixture of four S–MMA copolymers of different composition. The mixture was separated into four peaks, indicating the separation was performed according to composition. The gradient elution conditions in the present experiment were different from those used in previous work[10] and the ethanol content in the mobile phase at the retention volume, *ca.* 7–8 ml, was lower in this work than in the previous studies. As a result of the lower ethanol content, the retention volume of

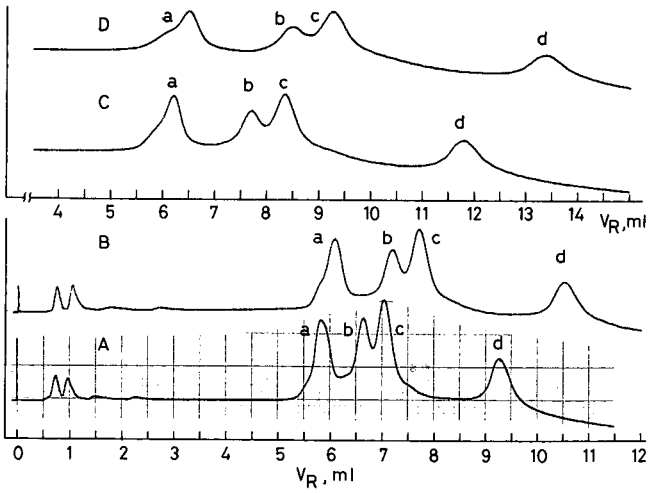

Fig. 1. Chromatograms of S–MMA copolymers. Column temperature: (A) 40; (B) 50; (C) 60; (D) 70°C. S–MMA sample: a = I; b = II; c = III; d = IV. UV attenuation: 0.16 a.u.f.s.

the copolymers increased and the width of the blind zone[10], defined as a space in which no peak appears between V_0 (the interstitial volume of the column) and the point where the most weakly adsorbed solute appears, increased together. As the final ethanol content in the mobile phase was nearly twice that in previous work, sample copolymers with a high MMA content (S–MMA IV, peak d) could be eluted even at high column temperature, such as 70°C. The difference in retention volume between the first two peaks increased with increasing column temperature and the resolution between two peaks, S–MMA I and II (peaks a and b), was improved considerably at

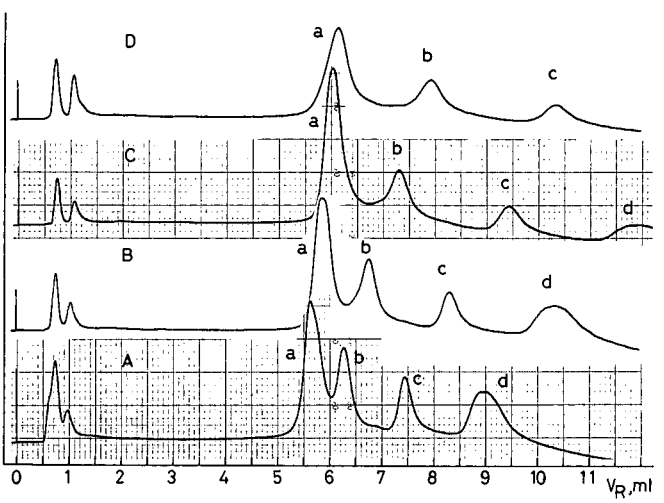

Fig. 2. Chromatograms of S–MA copolymers. Column temperature: (A) 40; (B) 50; (C) 60; (D) 70°C. S–MA sample: a = I; b = II; c = III; d = IV. UV attenuation: 0.16 a.u.f.s.

a column temperature of 70°C. However, the resolution between peaks b and c (S–MMA II and III) was unchanged and the peak widths became broad with increasing column temperature.

The LAC of a mixture of S–MA copolymers at different column temperatures is shown in Fig. 2. The peak retention volume of the copolymers increased and the resolution between adjacent peaks was improved with increasing column temperature. Each of the peaks is symmetrical and the CCD of the sample copolymers is less broad than that for the S–MMA copolymers in Fig. 1. Copolymer S–MA IV (peak d) at a column temperature 70°C eluted at a retention volume of 14.5 ml, and therefore the peak is not shown in Fig. 2D.

Fig. 3 shows examples of the separation of a mixture of S–BA copolymers. Copolymer S–BA I eluted at the interstitial volume (retention volume, V_R = 0.6 ml) even at a column temperature of 70°C. The ethanol content in the initial mobile phase should be lowered to less than 1% in order to retain copolymer S–BA I in the column. The resolution between adjacent peaks of S–BA II, III and IV was improved with increasing column temperature. Peak separation of S–BA III and IV was not observed at column temperatures of 40 and 50°C, but these peaks were separated at 60°C.

The plot of column temperature *versus* retention volume can also explain the separation of a mixture of the copolymers. Fig. 4 and 5 show these plots for S–EMA and S–BMA copolymers. In Fig. 4, the difference in retention volume between two copolymers of different composition increases with increasing column temperature and a corresponding improvement in resolution is observed. The dashed line for

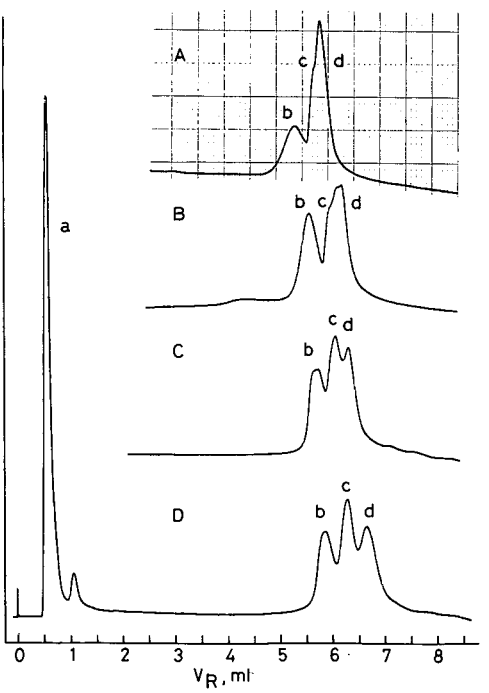

Fig. 3. Chromatograms of S–BA copolymers. Column temperature: (A) 40; (B) 50; (C) 60; (D) 70°C. S–BA sample: a = I; b = II; c = III; d = IV. UV attenuation: 0.16 a.u.f.s.

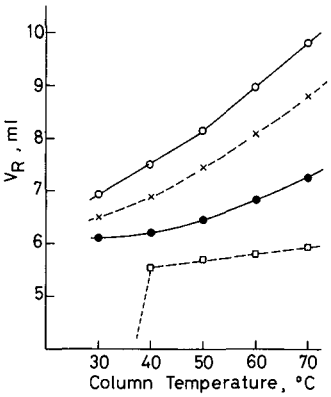

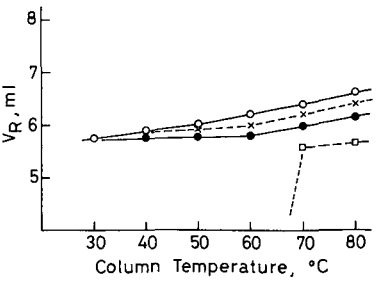

Fig. 4. Plots of retention volume *vs.* column temperature for S–EMA copolymers. S–EMA sample: □ = I; ● = II; × = III; ○ = IV.

Fig. 5. Plots of retention volume *vs.* column temperature for S–BMA copolymers. S–BMA sample: □ = I; ● = II; × = III; ○ = IV.

S–EMA I means that this copolymer eluted at the interstitial volume at a column temperature of 30°C. In Fig. 5, the difference in retention volume between two copolymers of different composition seems to be small, but the resolution was improved at elevated column temperature. Pairs of copolymers S–BMA II and III and S–BMA III and IV were not separated below a column temperature of 60°C but were separated above 70°C. Copolymer S–BMA I eluted at the interstitial volume below a column temperature of 60°C. The plots of column temperature *versus* retention volume for S–EMA and S–BMA demonstrate that, for copolymers with the same styrene content and at the same column temperature, those which have smaller alkyl ester groups (S–EMA in this instance) eluted later than those having larger alkyl ester

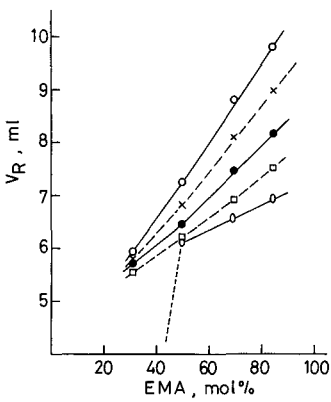

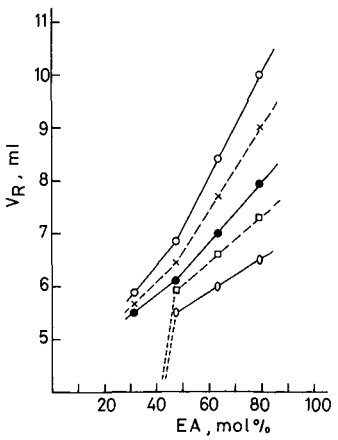

Fig. 6. Plots of retention volume *vs.* EMA content for S–EMA copolymers at different column temperatures. ○ = 70; × = 60; ● = 50; □ = 40; 0 = 30°C.

Fig. 7. Plots of retention volume *vs.* EA content for S–EA copolymers at different column temperatures. ○ = 70; × = 60; ● = 50; □ = 40; 0 = 30°C.

groups (S–BMA). This tendency was generally observed for other styrene copolymers with acrylate and methacrylate.

The relationship between copolymer composition and retention volume at different column temperatures is shown in Figs. 6 and 7 for S–EMA and S–EA copolymers. The retention volume increased both with increasing EMA and EA content in the copolymers and with increasing column temperature. Copolymer S–EMA I at a column temperature of 30°C and S–EA I at 30 and 40°C eluted at the interstitial volume. The plots of composition *versus* retention volume show that, for copolymers with the same styrene content, S–EMA and S–EA were not resolved in most instances. Resolution is observed when the column temperature is 30°C for copolymers having an EA or EMA content of more than 50 mol-% and when column temperature is above 60°C for copolymers having an EA or EMA content of more than 80 mol-%.

CONCLUSIONS

The LAC technique has been applied to the separation of styrene–acrylate and styrene–methacrylate copolymers. These copolymers were separated according to their composition by a gradient elution technique with increasing ethanol content in the ethanol–chloroform mobile phase. As the final ethanol content in the mobile phase was nearly twice that in previous work, sample copolymers with low styrene content could be eluted even at high column temperatures. As observed in previous studies on styrene–methyl methacrylate copolymers, the retention volumes of styrene–acrylate and styrene–methacrylate copolymers were retarded with increasing column temperature and copolymers having more styrene eluted earlier than those having less styrene. The difference in retention volume between two peaks increased with increasing column temperature and a corresponding improvement in resolution was observed. With copolymers with the same styrene content, those having smaller alkyl ester groups eluted later than those having larger alkyl ester groups. Similarly, copolymers of styrene–acrylate and styrene–methacrylate having the same alkyl ester groups and the same styrene content were not resolved in most instances.

REFERENCES

1 S. Mori, *Adv. Chromatogr.*, 21 (1983) 187.
2 S. Mori, *J. Chromatogr.*, 411 (1987) 355.
3 M. Danielewicz and M. Kubín, *J. Appl. Polym. Sci.*, 26 (1981) 951.
4 S. Mori, Y. Uno and M. Suzuki, *Anal. Chem.*, 58 (1986) 303.
5 T. Tanaka, M. Omoto, N. Donkai and H. Inagaki, *J. Macromol. Sci. Phys.*, B17 (1980) 211.
6 S. Teramachi, A. Hasegawa, Y. Shima, M. Akatsuka and M. Nakajima, *Macromolecules*, 12 (1979) 992.
7 G. Glöckner, J. H. M. van den Berg, N. L. J. Meijerink, T. G. Scholte and R. Koningsveld, *Macromolecules*, 17 (1984) 962.
8 H. Sato, H. Takeuchi, S. Suzuki and Y. Tanaka, *Macromol. Chem. Rapid Commun.*, 5 (1984) 719.
9 S. Mori and Y. Uno, *Anal. Chem.*, 59 (1987) 90.
10 S. Mori and Y. Uno, *J. Appl. Polym. Sci.*, 34 (1987) 2689.
11 S. Mori, *Anal. Chem.*, 60 (1988) 1125.
12 S. Mori, *Anal. Sci.*, 4 (1988) 365.

Journal of Chromatography, 507 (1990) 481–486
Elsevier Science Publishers B.V., Amsterdam — Printed in The Netherlands

CHROMSYMP. 1721

Separation of the oligomeric silsesquioxanes $(HSiO_{3/2})_{8-18}$ by size-exclusion chromatography

HERIBERT BÜRGY and GION CALZAFERRI*
Institute for Inorganic and Physical Chemistry, University of Berne, CH-3000 Berne 9 (Switzerland)

SUMMARY

The spherical siloxanes $(HSiO_{3/2})_n$ (n = 8–18) have been separated by size-exclusion chromatography, a technique that allows for preparative separations. These molecules are ideal test-cases for the hard-sphere solute size-exclusion retention theory because of their nearly identical chemical behaviour and their nearly ideal spherical structure.

INTRODUCTION

Spherical siloxanes with the general formula $(RSiO_{3/2})_n$ are called silsesquioxanes and abbreviated as RTn. Frye and Collins[1] reported the synthesis of the simplest silsesquioxane molecules namely HT10–HT16, which always leads to a mixture. For our intentions, however, we need the silsesquioxanes as pure as possible[2–4]. It is difficult to separate them because of their similar properties (solubility, sublimation temperature, etc.).

The appropriate tool for separation seems to be size-exclusion chromatography (SEC), also called gel permeation chromatography.

EXPERIMENTAL

The silsesquioxanes were synthesized as described previously[1]. A solution of 9.5 ml of $HSiCl_3$ in 150 ml of benzene was slowly added to a solution of 200 ml of benzene containing 43 ml of concentrated H_2SO_4 and 31 ml of fuming H_2SO_4. The product was recrystallized in tetrahydrofuran (THF). While the main by-product gelated in THF, the desired products remain in solution. The chromatogram of the products in Fig. 1D shows that the reaction yields not only HT10–HT16 but also HT18.

We tried the same synthesis with toluene as solvent. To our surprise we have obtained not only HT10–HT18 as in the benzene-based synthesis but also HT8. The result of this experiment is illustrated in Fig. 1C.

The separation was performed on a PLGel column (600 × 7.5 mm I.D., 50 Å pore diameter, 5-μm particle size, Polymer Labs., Shropshire, U.K.). The HPLC system consisted of an Erma ERC 3511 on-line degasser, a Merck–Hitachi LC 6200

0021-9673/90/$03.50

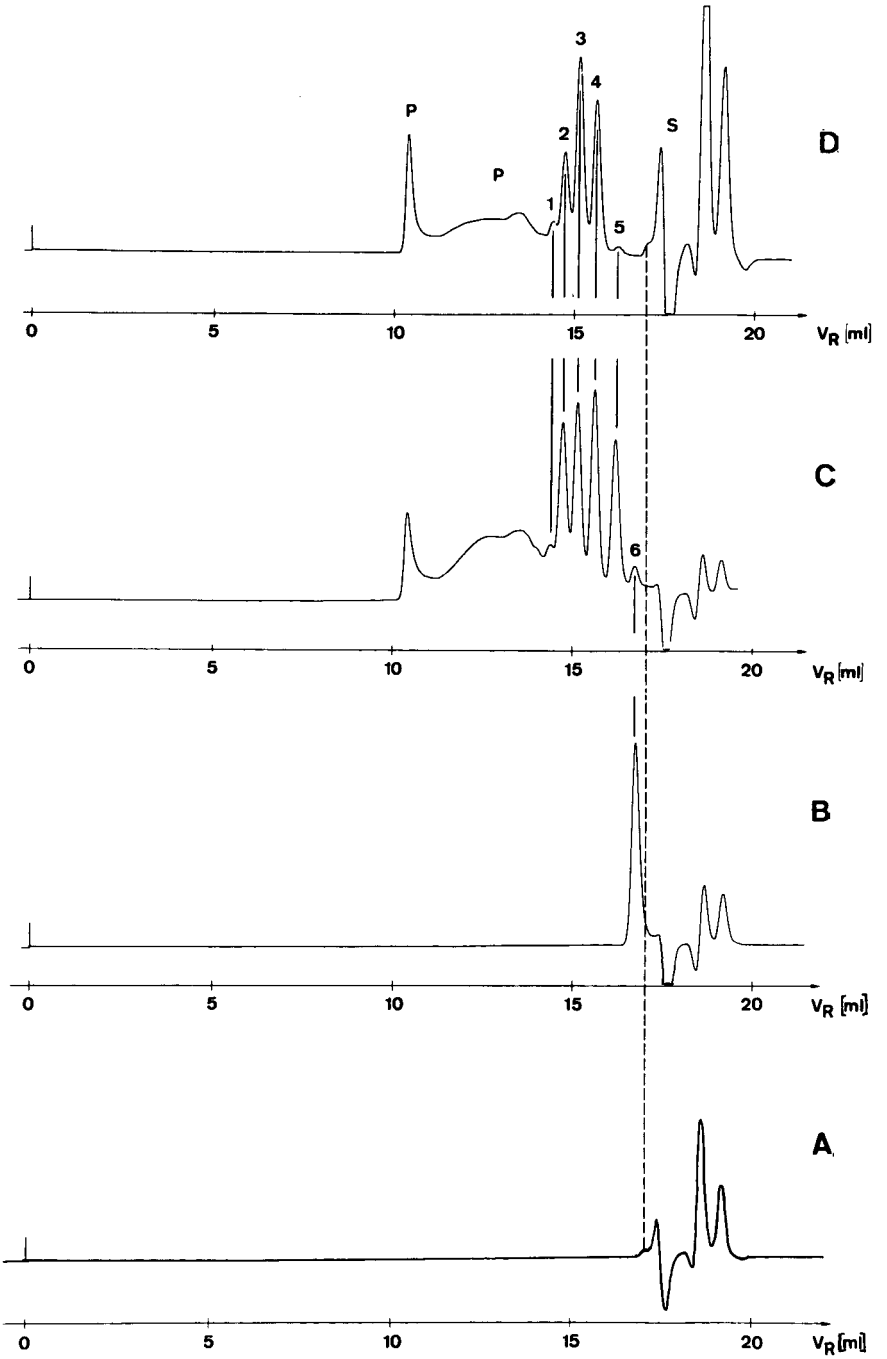

Fig. 1. Comparison of chromatograms in hexane. Peaks: P = polymer; S = solvent; 1 = HT18; 2 = HT16; 3 = HT14; 4 = HT12; 5 = HT10; 6 = HT8. (A) Solvent: hexane fraction that was used as solvent for all samples. (B) Pure HT8; peaks on and to the right of the dashed line belong to the solvent. (C) Products of the synthesis in toluene: peak 6 = HT8 appears. (D) Products of the synthesis in benzene: peak 6 = HT8 is absent.

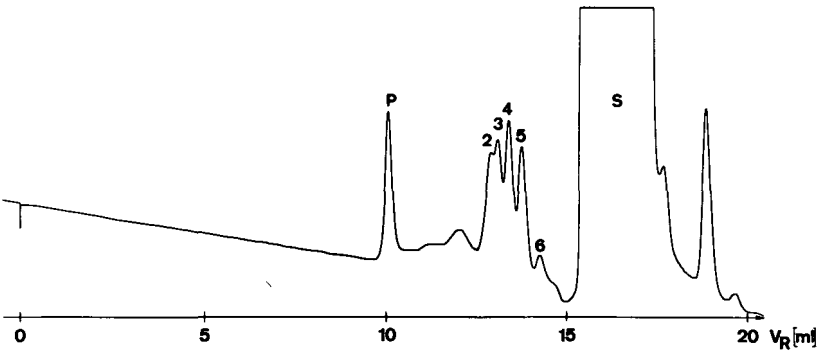

Fig. 2. Chromatogram of the same synthesis products as in Fig. 1D but with toluene as eluent. HT18 does not appear.

pump, the column and an Erma ERC 7512 refractive index detector. The chromatograms were recorded with an HP 3396A integrator. Toluene (Merck p.A.) and hexane fraction for high-performance liquid chromatography (HPLC) (Romil Chemicals) were used as mobile phase. To observe the chromatograms shown in Figs. 1 and 2 the flow-rate was 1 ml/min and the injected sample amount was 20 μl of saturated silsesquioxane solution in hexane.

RESULTS

The chromatograms show significant differences between hexane and toluene as mobile phase (Figs. 1 and 2). The retention volumes for the identified compounds with hexane as mobile phase are listed in Table I.

The peaks were separated and identified by mass spectrometry and infrared and ^1H and ^{29}Si nuclear magnetic resonance spectroscopy.

DISCUSSION

Assuming the absence of adsorption, the SEC retention volume V_R can be expressed[7] as:

$$V_R = V_0 + K_{SEC} V_i \quad (1)$$

where

K_{SEC} = equilibrium constant for the SEC process representing the ratio of the average solute concentration in the pores to that outside the pores.

V_i = stagnant part of the mobile phase (pore volume);

V_0 = moving part of the mobile phase (interstitial volume).

To determine K_{SEC} accurately, one has to set the total exclusion limit and the total permeation limit with $K_{SEC} = 0$ and $K_{SEC} = 1$, respectively. The total exclusion limit is determined by the large polycondensates, the first peak in the chromatograms. The total permeation limit has been determined with hexane (Fig. 1A). Because of differences in temperature and air saturation, it is possible to apply a refractive index detector for the detection of hexane in hexane as mobile phase.

TABLE I

RETENTION VOLUMES IN HEXANE AS MOBILE PHASE

Molecule	*Retention volume (ml)*
HT18	14.23
HT16	14.57
HT14	14.98
HT12	15.45
HT10	16.01
HT8	16.55

Hence the total exclusion limit for our analytical column was determined to be V_R ($K_{SEC} = 0$) = 10.28 ml and the total permeation limit is V_R ($K_{SEC} = 1$) = 18.94 ml. From this we get $V_0 = 10.28$ and $V_i = 8.66$ ml.

Fig. 2 shows a chromatogram obtained with toluene, to illustrate the different behaviour of the two mobile phases toluene and hexane. Comparison of the data in Figs. 1 and 2 illustrates clearly that the resolution is far better in hexane than in toluene.

MOLECULAR GEOMETRY CALCULATIONS

According to the hard-sphere solute model[7], the solute–pore interaction can be described by geometrical considerations. Several relationships for the distribution coefficient K_e can be derived, depending on the pore shape:

$$\text{Cylindrical pores } K_e = \left(1 - \frac{r}{\bar{a}_c}\right)^2 \tag{2}$$

$$\text{Spherical pores } K_e = \left(1 - \frac{2r}{3\bar{a}_s}\right)^3 \tag{3}$$

$$\text{Random-plane pores } K_e = \exp\left(-\frac{2r}{\bar{a}_e}\right) \tag{4}$$

where $\bar{a} = \dfrac{2 \times \text{pore volume}}{\text{pore surface area}}$;

r = radius of a solute molecule;
$\bar{a}_c$, $\bar{a}_s$, $\bar{a}_e$ = radii of the pores.

Neglecting the solute molecule packing interaction, $K_e = K_{SEC}$, it is possible to calculate the radius of every HT*n* molecule by assuming cylindrical pores. The value of r can be calculated from eqn. 2 if we accept the manufacturers' specification of 25 Å for $\bar{a}_c$. K_{SEC} is calcualted from eqn. 1 by applying the experimentally determined values of V_0, V_i and the retention volume V_R and the retention volume V_R (Table I). The radius r_{struct} of HT8 has been determined from X-ray structural data[8,9], assuming the Van der Waals radius of H to be 1.2 Å. For the other molecules r_{struct} was calculated from

TABLE II

VALUES FOR THE EQUILIBRIUM CONSTANTS AND CALCULATED AND STRUCTURAL MOLECULAR RADII

Molecule	K_{SEC}	r (Å)	r_{struct} (Å)
HT8	0.7237	3.7	4.8
HT10	0.6614	4.7	5.5
HT12	0.5968	5.7	6.1
HT14	0.5425	6.6	6.8
HT16	0.4952	7.4	7.5
HT18	0.4559	8.1	8.2

geometrical construction, by applying the same Si–O–Si distances as in HT8. The results are reported in Table II.

The radii calculated for HT8 and HT10 are too small whereas the radii of the other molecules fit perfectly well with r_{struct}. This could be because the smaller molecules "see" a somewhat larger pore size because of non-idealities of the pore-shape.

It is interesting to try the reverse and to calculate the pore size from r_{struct} and K_{SEC} for the different pore-shapes. The results are reported in Table III. HT8 and HT10 lead in each case to a too large pore volume. For cylindrical pores, however, the pore volume converges very well to the expected 25 Å. We conclude that the cylindrical pore-shape model fits best to our data, and that HT8 and HT10 are so small that they "see" the non-idealities of the pores, which means that they "feel" a somewhat larger cage.

TABLE III

VALUES OF THE PORE RADII, CALCULATED FROM r_{struct} AND K_{SEC}

Molecule	$\bar{a}_c$ (Å)	$\bar{a}_s$ (Å)	$\bar{a}_e$ (Å)
HT8	32.1	31.3	29.7
HT10	29.4	28.5	26.6
HT12	26.8	25.7	23.6
HT14	25.8	24.6	22.2
HT16	25.3	23.9	21.3
HT18	25.2	23.7	20.9

CONCLUSION

We have demonstrated that SEC is an appropriate tool for separating the different HTn (n = 8–18). These molecules seem to be ideal test-cases for advancing the SEC retention theory because of their nearly identical chemical behaviour and their nearly ideal spherical structure[5,6]. It is very satisfactory that the simple hard-sphere

solute model seems to work well for describing the separation process of these molecules.

ACKNOWLEDGEMENTS

This work was supported by grant No. 2-5.542 of the Swiss National Science Foundation and grant BEW-EPA 217.307 financed by the Schweizerische Bundesamt für Energiewirtschaft. We thank V. Meyer for her helpful discussion of HPLC techniques.

REFERENCES

1 C. L. Frye and W. T. Collins, *J. Am. Chem. Soc.*, 92 (1970) 5586.
2 R. Beer, H. Bürgy, G. Calzaferri and I. Kamber, *J. Electron Spectrosc. Rel. Phenomena*, 44 (1987) 121.
3 H. Bürgy, G. Calzaferri and I. Kamber, *Mikrochim. Acta (Wien)*, I (1988) 401.
4 P. Bornhauser and G. Calzaferri, *Spectrochim. Acta A*, in press.
5 P. A. Agaskar, V. W. Day and W. G. Klemperer, *J. Am. Chem. Soc.*, 109 (1987) 5554.
6 L. H. Vogt, Jr. and J. F. Brown, Jr., *Inorg. Chem.*, 2 (1963) 189.
7 W. W. Yau, J. J. Kirkland and D. D. Bly, *Modern Size-Exclusion Liquid Chromatography*, Wiley, New York, 1979.
8 K. Larsson, *Arkiv Kemi*, 16 (1960) 215.
9 V. W. Day, W. G. Klemperer, V. V. Mainz and D. M. Millar, *J. Am. Chem. Soc.*, 107 (1985) 8262.

Journal of Chromatography, 507 (1990) 487–496
Elsevier Science Publishers B.V., Amsterdam — Printed in The Netherlands

CHROMSYMP. 1831

Achievements and uses of critical conditions in the chromatography of polymers

A. M. SKVORTSOV
Chemical-Pharmaceutical Institute, Prof. Popova 14, 197022 Leningrad (U.S.S.R.)
and
A. A. GORBUNOV*
All-Union Research Institute for Highly Pure Biopreparations, Pudozhskaya 7, 197110 Leningrad (U.S.S.R.)

SUMMARY

A method for the analysis and separation of macromolecules is proposed, based on the effect of the chromatographic "invisibility" of some chain fragments, namely blocks of a certain type in block copolymers, grafted chains in graft copolymers and linear elements of macromolecules with rings. When certain critical conditions for such fragments of polymer molecules are created neither the length nor the molecules weight distribution of these molecules influences the retention volume, and this effect is treated as a chromatographic "invisibility" of the elements involved.

Results of the modern theory of chromatography and the direct simulation of the equilibrium behaviour of macromolecules in a chromatographic column have been taken into account and conclusion is drawn that this method of "invisibles" provides an efficient separation of macrocycles and linear polymers and the separation of macromolecules according to the number of functional groups. The method of "invisibles" also makes it possible to separate two-block copolymers according to the size of the "visible" block only, and to separate grafted polymers according to the backbone length. The scope of the application of the method to chromatographic analyses of copolymers is discussed.

INTRODUCTION

The fundamental existence of so-called critical conditions is well known in polymer chromatography. Under these conditions, the entropy losses of a macromolecule within a pore and the enthalpic effects due to adsorption of the chain units on the pore walls are exactly compensated. Under the critical conditions, when passing from the solvent volume into the pores, the free energy change for a macromolecule is found to be zero (the distribution coefficient $K = 1$). The first experimental work was published by Tennikov and co-workers[1,2] and subsequently the results were confirmed for different polymers and various adsorbents[3,4] and a theoretical foundation was elucidated[5].

0021-9673/90/$03.50

We use the expression that macromolecules become "invisible", in order to emphasize that, under critical conditions, the retention volumes of homopolymer macromolecules of any molecular weight (MW) become equal to the retention volume of solvent molecules, in such a way as to make them indistinguishable from each other and from the solvent. The idea of chromatographic "invisibility" has been used[6] with the aim of building up a theory of a two-block copolymer separation according to the lengths of one "visible" block only, provided that the copolymer was exposed under the conditions critical for the other "invisible" block. The method of "invisibles" is, in a way, analogous to the well known procedure[7] of copolymer analysis by means of light scattering, where a solvent is chosen that has a refractive index identical with that of one of the copolymer components. This results in the optical invisibility of this component and makes the measurement of the radius of gyration of the visible component possible. In previous work[6] only one case was considered, namely that of a long two-block copolymer with block sizes greater than the pore width; this results in the application limits of the method of "invisibles" in chromatographic analysis being unclear.

Critical conditions can be created experimentally by means of particular choices of mixed eluent, temperature or pH (when aqueous eluents are used) variations, etc. Critical conditions for many polymer–adsorbent–solvent systems have been found experimentally[8]. All operations under conditions of critical chromatography are carried out using standard chromatographic equipment.

The aim of this work was to clarify whether a polymer chain (or its fragment) can be treated as "invisible" when the chromatography is carried out under critical conditions. Further, we shall show that, for this reason, it is necessary for the "invisible" part of the chain to have a free end, as in the cases of end blocks in three-block copolymers, side grafts to the backbone in graft copolymers, etc. However, in general, neither the central block, the backbone of a graft copolymer nor multi-block (both regular and statistical) copolymer fragments can be treated as "invisible" species.

LINEAR BLOCK COPOLYMERS

The distribution coefficient, K, is equal to the ratio of the statistical sum of the chain within the pore to that in the solvent volume. Let one chain end be fixed at a distance x from a certain pore wall and $Z(x)$ this chain statistical sum. For a slit-like pore of width D, we have

$$K = D^{-1} \int_0^D Z(x)\,\mathrm{d}x \tag{1}$$

The function $Z(x)$ can be represented by

$$Z(x) = \int_0^D Z(x, x')\,\mathrm{d}x' \tag{2}$$

where $Z(x, x')$ is the statistical sum of the chain with the two ends fixed at x and x'.

The function $Z(x, x')$ for the Gaussian flexible chain under critical conditions is equal to[9]

$$Z_{cr}(x, x') = D^{-1}\left\{1 + 2\sum_{m=1}^{\infty}\cos\left(\frac{\pi m x}{D}\right)\cos\left(\frac{\pi m x'}{D}\right)\exp\left[-\left(\frac{\pi m R}{D}\right)^2\right]\right\} \quad (3)$$

where $R = (Nb^2/6)^{1/2}$, the average radius of gyration of the chain consisting of N units each of length b.

Under the critical conditions for all values of x with any R and D:

$$Z_{cr}(x) = 1 \quad (4)$$

This becomes evident after the substitution of eqn. 3 into eqns. 2 and 1. Consequently,

$$K_{cr} = 1 \quad (5)$$

Now, let us consider a two-block copolymer, AB, and introduce statistical sums $Z_A(x)$ and $Z_B(x)$ for block A and B, respectively. Then the following is valid for the copolymer distribution coefficient, K_{AB}:

$$K_{AB} = D^{-1}\int_0^D Z_A(x)Z_B(x)\,dx \quad (6)$$

If the critical conditions are attained for block B it follows, from eqn. 4, that $Z_B(x)|_{cr} = 1$ and the distribution coefficient of the copolymer coincides with that of block A:

$$(K_{AB})_{crB} = D^{-1}\int_0^D Z_A(x)\,dx = K_A \quad (7)$$

Hence the block B under critical conditions becomes chromatographically "invisible" in this two-block copolymer. Eqn. 7 is valid and, consequently, the method of "invisibles" applies for two-block copolymers at arbitrary macromolecule and pore sizes and also at any copolymer composition.

The distribution coefficient for a three-block copolymer B_1AB_2 is

$$K_{B_1AB_2} = D^{-1}\int_0^D\int_0^D Z_{B_1}(x)Z_A(x, x')Z_{B_2}(x')\,dx\,dx' \quad (8)$$

Provided that the critical conditions are created for both of the end blocks, B_1 and B_2, using eqn. 4 we obtain

$$(K_{B_1AB_2})_{crB} = D^{-1} \int_0^D \int_0^D Z_A(x, x')\,dx\,dx' = K_A \tag{9}$$

and, consequently, the method of "invisibles" is also valid.

When the critical conditions are created for the inner block, A, the sum $Z_A(x, x')|_{cr}$ is described by eqn. 3. If the block A size is assumed to be greater than the pore width ($R_A > D/\pi$), it is sufficient to take only the first term in the series of eqn. 3, and this leads to $Z_A(x, x')|_{cr} \approx D^{-1}$. The following equation for the distribution coefficient of such a copolymer can be written:

$$(K_{B_1AB_2})_{crA} \approx K_{B_1} K_{B_2} \tag{10}$$

It should be noted that the only characteristics that are present on the right-hand side of eqn. 10 are those of "visible" blocks, B_1 and B_2.

In a similar way, one can write the following equation for the multi-block copolymer $A_1B_iA_2B_2 \ldots A_nB_n$:

$$(K_{multiblock})_{crA} \approx K_{B_1} K_{B_2} \cdot \ldots \cdot K_{B_n} \tag{11}$$

provided that the critical conditions for component A are created and the sizes of the "invisible" blocks A_1, A_2, ... A_n are greater than the value of D. If the sizes of all "visible" blocks B_i also exceed the pore sizes, then the chromatographic behaviour of such copolymers is determined by the total length of all "visible" blocks B only. Note that eqn. 11 is also valid in the case of statistical copolymers with a low content of the "visible" component B.

The method of "invisibles" makes it possible to carry out separations for grafted copolymers according to the backbone length, provided that the critical conditions are created for the grafted copolymer component. This variant of the method is rigorous for the model of flexible chains at any pore width (both narrow and wide). However, when the critical conditions are attained for the backbone units, the chromatographic "invisibility" of these units takes place in narrow pores only. If this condition is satisfied, the distribution coefficients of grafted copolymers are described by eqn. 11 as for linear copolymers. The chromatographic separation in this instance will take place according to the MW of the whole grafted part of the polymer.

MACROMOLECULES WITH FUNCTIONAL GROUPS

One of the important applications of the method of "invisibles" is in the analysis of functionally active polymers by means of critical chromatography. Usually mono- or difunctional molecules are dealt with, one or two end units of which differ in their adsorption properties from the other non-functional units. Problems of the chromatographic separation of such functional molecules, under critical conditions, have been rigorously considered[8–10] and we shall subsequently discuss the scope of application of the method of "invisibles" to these systems and illustrate the efficiency of the method when separation is performed according to the number of functional groups.

When critical conditions are created, normal non-functional units become "invisible"; therefore, for macromolecules without functional groups $K_{cr} = 1$, independent of the pore width, whereas the distribution coefficient of the monofunctional chain coincides with that of the functional group itself and is equal to[9]

$$K_{1_{cr}} = 1 + \frac{2\delta}{D}(q - 1) \tag{12}$$

where δ is the width of the layer near the wall. Getting into this layer causes an energy gain, $-\varepsilon_f$ for a functional unit and $-\varepsilon_{cr}$ for a non-functional unit, and $q = \exp[-(\varepsilon_f - \varepsilon_{cr})]$. Energy values here and further are expressed in units of kT (k = Boltzmann's constant, T = absolute temperature). Note that if there is only one functional group in the polymer molecule, the distribution coefficient of the chain is described by eqn. 12, independent of this group position. This is why non-functional units in monofunctional molecules can be treated under the critical conditions as "invisible" species at any pore width.

According to previous work[10], the following is valid for difunctional molecules in narrow pores:

$$K_2 \approx K_1^2 \tag{13}$$

In a similar way, molecules with S functional groups have been shown[8] to satisfy

$$K_{S_{cr}} \approx (K_{1_{cr}})^S \tag{14}$$

provided that the distance between such groups is greater than the pore size.

Note that macromolecules with functional groups can be treated as a special case of two-block copolymers with the "visible" blocks being very short. Eqns. 13 and 14 are obviously the consequences of eqns. 10 and 11; hence all the conclusions concerning the correctness and the scope of application of the method of "invisibles" given in the above section are still valid for functional macromolecules also.

Fig. 1 shows the theoretical chromatograms calculated for a mixture of equal parts of mono- and difunctional molecules and for molecules without functional groups, their molecular weight distributions (MWD) being the same. The MWD was simulated as a Gaussian function with polydispersity $M_w/M_n = 1.25$. To imitate the experimental conditions, the broadening due to the polydispersity of the samples and the instrumental broadening were taken into account, the latter being assumed to be represented by $\sigma_V = 0.02V_R$. The volumes of both the mobile and stationary phases are assumed to be equal to unity. As can be seen from Fig. 1a, when adsorption-active groups are situated at the ends of the molecule and gel permeation chromatographic (GPC) conditions for the remaining chain units are created, the chromatogram of such a sample looks like a single non-separated peak. An analogous situation also takes place when adsorption of non-functional groups occurs (Fig. 1c). In these instances, macromolecules of different length and functionality are mixed in the exit zone of the chromatographic peak.

Fig. 1b corresponds to the critical conditions created for non-functional chain units. Under these conditions, the retention volume is no longer dependent on MW

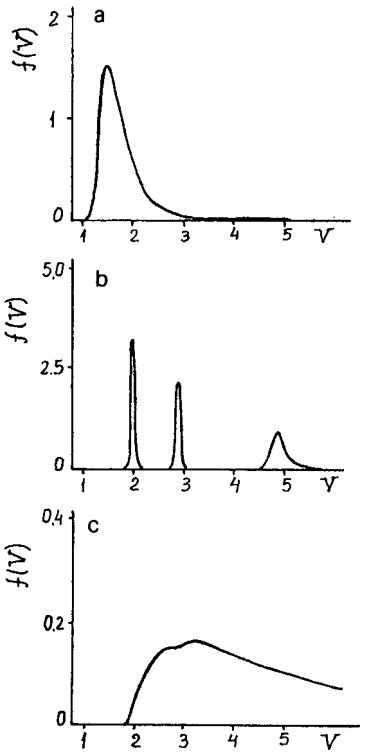

Fig. 1. Pattern of chromatograms for a mixture of equal parts of di-, mono- and non-functional polymers. Polydispersity, $M_w/M_n = 1.25$; ratio of average macromolecular radius to pore width, $R/D = 0.29$; adsorption energy of functional groups, $-\varepsilon_f = 2$. For the internal (non-functional) chain units, the following conditions are attained: (a) GPC conditions, $\varepsilon = 0$; (b) critical conditions, $-\varepsilon = -\varepsilon_{cr} = 0.182$; (c) adsorption conditions, $-\varepsilon = 0.25 > -\varepsilon_{cr}$.

(and consequently on MWD) and separation of macromolecules is carried out exclusively according to the number of functional groups.

RING MACROMOLECULES AND MACROCYCLES

It follows from the theory of the chromatography of ring macromolecules[11,12] that the distribution coefficient of macrocycles is equal to

$$K_{c_{cr}} \approx \begin{cases} 2\sqrt{\pi} \cdot \dfrac{R}{D} & \text{if } R \gg D \\ 1 + \sqrt{\pi} \cdot \dfrac{R}{D} & \text{if } R \ll D \end{cases} \tag{15}$$

As can be seen from eqn. 15, the distribution coefficient of cyclic macromolecules always exceeds unity under critical conditions, and unlike the case with linear chains,

$K_{c_{cr}}$ depends on the ratio of the macromolecule and the pore diameters. Such a dependence is conditioned by specific topology effects, which change the shape of the distribution of polymer chain units near the pore walls of the adsorbent. The density of units of linear macromolecules under critical conditions is known to be constant at any distance from the pore walls[5]. On the other hand, according to the exact theory, the density of units of ring macromolecules near walls is greater than that inside a pore. The increase in distribution coefficient is related to this circumstance. This problem has been treated in detail elsewhere[11,12].

Therefore, even perfectly uniform cyclic macromolecules cannot be considered to be "invisible" when they are exposed under critical conditions. This is why it is possible to separate linear polydisperse chains from ring macromolecules using the method of "invisibles".

In order to demonstrate the efficiency of the method of "invisibles" when separating linear and ring polydisperse polymers let us reconsider our "theoretical chromatograph". Fig. 2 shows the chromatograms calculated for a mixture of equal parts of linear and ring polymers, their average MWs being the same. Their polydispersities are also assumed to be identical and to be $M_w/M_n = 1.25$. In the GPC

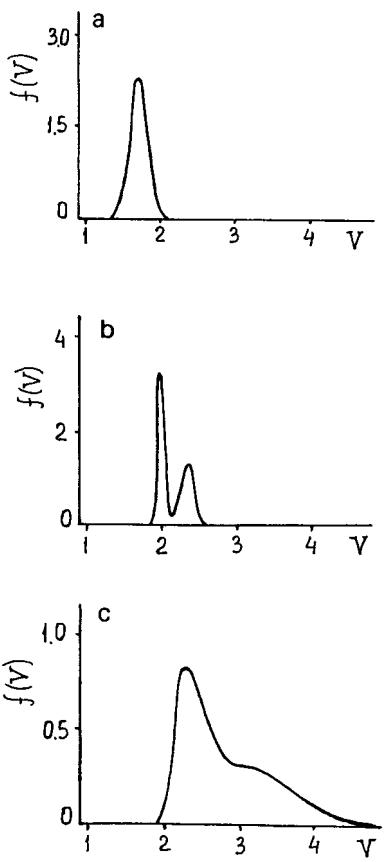

Fig. 2. Chromatograms calculated for a mixture of polydisperse flexible macrocycles with analogous linear molecules. $M_w/M_n = 1.25$; $R/D = 0.2$. (a) $\varepsilon = 0$; (b) $-\varepsilon = -\varepsilon_{cr}$; (c) $-\varepsilon > -\varepsilon_{cr}$.

mode (Fig. 2a), and also under conditions of adsorption chromatography, the separation of macromolecules takes place according to both the sizes and topology of the macromolecules. This results in the presence of a single broadened peak in the chromatogram. Application of the method of "invisibles", *i.e.*, chromatography under critical conditions, allows us to eliminate the broadening due to the linear polymer polydispersity and enables the macromolecules to be separated according to their topology (Fig. 2b). When one part of a chain contains macrocycles, whereas another is linear, the latter becomes "invisible" under critical conditions. In this case, the separation takes place according to the sizes of the cyclic parts of the macromolecule only. The method of "invisibles" for such a system is a rigorous one and could be useful for the problems of the detection and isolation of partially cyclic macromolecules with intramacromolecular cross-linkages.

DISCUSSION

The method of "invisibles" in polymer chromatography is exactly rigorous for a number of polymer systems that contain a single continuous "visible" chain fragment. In particular, monofunctional macromolecules, two-block copolymers, three-block copolymers with the central block being investigated, partially cyclic macromolecules and graft copolymers with "invisible" side-chains (Fig. 3) belong to such systems. The most convenient realization of the method of "invisibles" in such systems would be obtained using wide-pore adsorbents.

For other systems, *e.g.*, copolymers with several "visible" fragments joined together with "invisible" inserts (Fig. 4), the method of "invisibles" becomes rigorous when using narrow-pore adsorbents only, the pore sizes being smaller than those of all the chain elements under the critical conditions. For the realization of the method of "invisibles" in such systems, it is important to have narrow-pore adsorbents with a uniform pore surface, and aslo to be able to select conditions that are both critical for one of the copolymer components and at the same time do not cause strong adsorption of the other "visible" component. This can be achieved by choosing a suitable eluent, variations of temperature and adsorbent surface modification.

The theoretically predicted efficiency of the method of "invisibles" for functionally active macromolecules has been demonstrated experimentally in detail for a large number of polymer systems, and a review was published by Entelis *et al.*[8]. Some other predictions of the theory, in particular the possibility of the application of

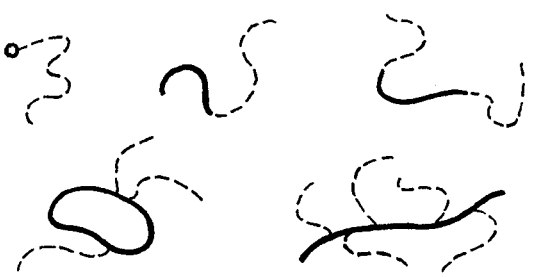

Fig. 3. Types of macromolecules for which the method of "invisibles" is valid in arbitrary pores. Here and in Fig. 4 "invisible" elements under critical conditions are shown as dashed lines.

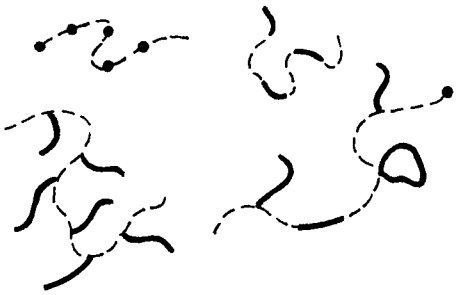

Fig. 4. Types of macromolecules for which the method of "invisibles" is valid only when applied to narrow-pore adsorbents. Dashed lines as in Fig. 3.

the "invisibility" method to the analysis of both block and graft polymers and to the separation of linear and cyclical macromolecules, have not received experimental corroboration to date.

The performance of the model chromatographic experiments according to the method of "invisibles", using well characterized copolymer samples with exactly known structures, and the subsequent comparison of the results of these experiments with the predictions of the theory, seem to be of interest. For example, when there is a series of two-block copolymers differing from each other in the length of one of the blocks, say A-type, whereas the other block, B, is the same, and when the critical conditions are created for the blocks of A-type, all such copolymers leave from the chromatographic column with equal retention volumes; this would be expected according to the theory. In contrast, when block B is made "invisible" in such a system, the copolymers are then separated according to the length of block A.

It would also be of interest to investigate the chromatographic behaviour of both linear and ring polymers with the same chemical structure. It follows from the theory that, under the critical conditions, all linear polymers have a distribution coefficient $K_{l_{cr}} = 1$, independent of their length and polydispersity, whereas for cyclic polymers, according to eqn. 15, $K_{c_{cr}} > 1$ and they are more strongly retained the greater is their molecular weight, *i.e.*, they behave as in adsorption chromatography.

ACKNOWLEDGEMENTS

The authors are grateful to Dr. A. V. Gorshkov, Dr. V. V. Evreinov and Dr. M. B. Tennikov for fruitful discussions.

REFERENCES

1 M. B. Tennikov, P. P. Nefedov, M. A. Lazareva and S. Ya. Frenkel, *Vysokomol. Soedin., Ser. A*, 19 (1977) 657.
2 A. M. Skvortsov, B. G. Belenky, E. S. Gankina and M. B. Tennikov, *Vysokomol. Soedin., Ser. A*, 20 (1978) 678.
3 A. V. Gorshkov, V. V. Evreinov and S. G. Entelis, *Zh. Fiz. Khim.*, 57 (1983) 2665.
4 A. A. Gorbunov, L. Ya. Solovyova, V. A. Pasechnik and A. Ye. Lukyanov, *Vysokomol. Soedin., Ser. A*, 28 (1986) 1859.
5 A. A. Gorbunov and A. M. Skvortsov, *Vysokomol. Soedin., Ser. A*, 28 (1986) 2453.
6 A. M. Skvortsov and A. A. Gorbunov, *Vysokomol. Soedin., Ser. A*, 21 (1979) 339.
7 M. Leng and M. Benoit, *J. Chem. Phys.*, 59 (1962) 929.

8 S. G. Entelis, V. V. Evreinov and A. V. Gorshkov, *Adv. Polym. Sci.*, 76 (1986) 129.
9 A. A. Gorbunov and A. M. Skvortsov, *Vysokomol. Soedin., Ser. A*, 26 (1984) 949.
10 A. M. Skvortsov and A. A. Gorbunov, *Vysokomol. Soedin., Ser. A*, 22 (1980) 2641.
11 A. A. Gorbunov and A. M. Skvortsov, *Vysokomol. Soedin., Ser. A*, 26 (1984) 2062.
12 A. A. Gorbunov and A. M. Skvortsov, *Vysokomol. Soedin., Ser. A*, 28 (1986) 2447.

Author Index

Vol. 507

journal of
chromatography news section

SHORT CONFERENCE REPORT

CLC '89, 13th SYMPOSIUM ON COLUMN LIQUID CHROMATOGRAPHY, STOCKHOLM, JUNE 25–30, 1989

More than a thousand participants gathered in a hot and sunny Stockholm for what turned out to be a really excellent CLC meeting, fully justifying all the work put into it by the organizing committee and its Chairman. The sessions and the social events were enjoyed by all, although the lecture rooms did occasionally become somewhat steamy because of the very warm weather.

Figs. 1 and 2. A wide range of prominent chromatographers can be seen in these views of the audience at the opening session.

Fig. 2.

Fig. 3. Peter Schoenmakers, flanked by Csaba Horváth and Jack Kirkland, somewhat shyly shows the Jubilee Medal Award of the Chromatographic Society he has just received. Another recipient was Lloyd Snyder.

Fig. 4. A general view, from the balcony, of some of the tables and guests at the excellent reception in the historic Town Hall, also well-known because of the Nobel Prize Banquets held there.

Fig. 5. The Symposium Chairman, with Mrs Westerlund. It was no doubt the first moment of relaxation after many months of preparation.

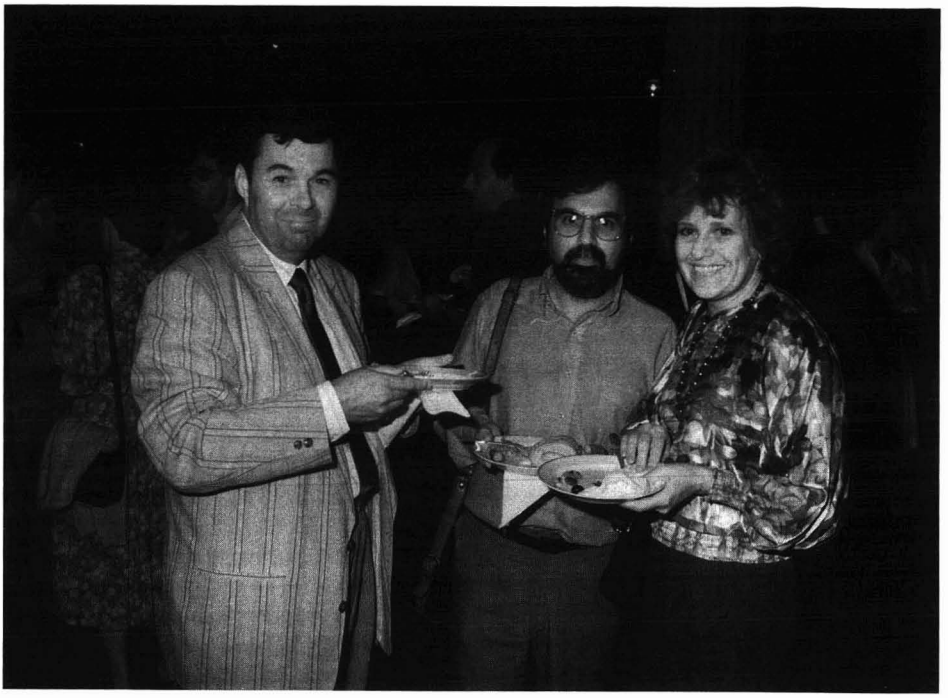

Fig. 6. The Chairman of HPLC '91 (Basel), Fritz Erni, in an animated group with Lois Beaver and Irving Wainer.

Figs. 7, 8 and 9. From these shots taken at another social event, the reader will readily recognise Lloyd and Barbara Snyder, John Haken, Josef Huber, Gerhard Schomburg, Pavel Jandera, Georges Guiochon, Lois Beaver, Csaba Horváth, Karel Macek, Fred Regnier, Peter Schoenmakers, Vadim Davankov, the back of the head of Marc Atkins, and a shadowy Claudia Lipschitz.

Fig. 8.

Fig. 9.

	กำหนดส่ง	
26 ธ.ค. 34		

PUBLICATION SCHEDULE FOR 1990

Journal of Chromatography and Journal of Chromatography, Biomedical Applications

MONTH	J	F	M	A	M	J	
Journal of Chromatography	498/1 498/2 499	500 502/1	502/2 503/1 503/2 504/1	504/2 505/1	505/2 506 507 508/1	508/2 509/1 509/2 510	The publication schedule for further issues will be published later
Cumulative Indexes, Vols. 451–500		501					
Bibliography Section		524/1		524/2		524/3	
Biomedical Applications	525/1	525/2	526/1	526/2 527/1	527/2	528/1 528/2	

INFORMATION FOR AUTHORS

(Detailed *Instructions to Authors* were published in Vol. 478, pp. 453–456. A free reprint can be obtained by application to the publisher, Elsevier Science Publishers B.V., P.O. Box 330, 1000 AH Amsterdam, The Netherlands.)

Types of Contributions. The following types of papers are published in the *Journal of Chromatography* and the section on *Biomedical Applications*: Regular research papers (Full-length papers), Notes, Review articles and Letters to the Editor. Notes are usually descriptions of short investigations and reflect the same quality of research as Full-length papers, but should preferably not exceed six printed pages. Letters to the Editor can comment on (parts of) previously published articles, or they can report minor technical improvements of previously published procedures; they should preferably not exceed two printed pages. For review articles, see inside front cover under Submission of Papers.

Submission. Every paper must be accompanied by a letter from the senior author, stating that he is submitting the paper for publication in the *Journal of Chromatography*. Please do not send a letter signed by the director of the institute or the professor unless he is one of the authors.

Manuscripts. Manuscripts should be typed in double spacing on consecutively numbered pages of uniform size. The manuscript should be preceded by a sheet of manuscript paper carrying the title of the paper and the name and full postal address of the person to whom the proofs are to be sent. Authors of papers in French or German are requested to supply an English translation of the title of the paper. As a rule, papers should be divided into sections, headed by a caption (*e.g.*, Summary, Introduction, Experimental, Results, Discussion, etc.). All illustrations, photographs, tables, etc., should be on separate sheets.

Introduction. Every paper must have a concise introduction mentioning what has been done before on the topic described, and stating clearly what is new in the paper now submitted.

Summary. Full-length papers and Review articles should have a summary of 50–100 words which clearly and briefly indicates what is new, different and significant. In the case of French or German articles an additional summary in English, headed by an English translation of the title, should also be provided. (Notes and Letters to the Editor are published without a summary.)

Illustrations. The figures should be submitted in a form suitable for reproduction, drawn in Indian ink on drawing or tracing paper. Each illustration should have a legend, all the *legends* being typed (with double spacing) together on a *separate sheet*. If structures are given in the text, the original drawings should be supplied. Coloured illustrations are reproduced at the author's expense, the cost being determined by the number of pages and by the number of colours needed. The written permission of the author and publisher must be obtained for the use of any figure already published. Its source must be indicated in the legend.

References. References should be numbered in the order in which they are cited in the text, and listed in numerical sequence on a separate sheet at the end of the article. Please check a recent issue for the layout of the reference list. Abbreviations for the titles of journals should follow the system used by *Chemical Abstracts*. Articles not yet published should be given as "in press" (journal should be specified), "submitted for publication" (journal should be specified), "in preparation" or "personal communication".

Dispatch. Before sending the manuscript to the Editor please check that the envelope contains three copies of the paper complete with references, legends and figures. One of the sets of figures must be the originals suitable for direct reproduction. Please also ensure that permission to publish has been obtained from your institute.

Proofs. One set of proofs will be sent to the author to be carefully checked for printer's errors. Corrections must be restricted to instances in which the proof is at variance with the manuscript. "Extra corrections" will be inserted at the author's expense.

Reprints. Fifty reprints of Full-length papers, Notes and Letters to the Editor will be supplied free of charge. Additional reprints can be ordered by the authors. An order form containing price quotations will be sent to the authors together with the proofs of their article.

Advertisements. Advertisement rates are available from the publisher on request. The Editors of the journal accept no responsibility for the contents of the advertisements.

Discover new solutions

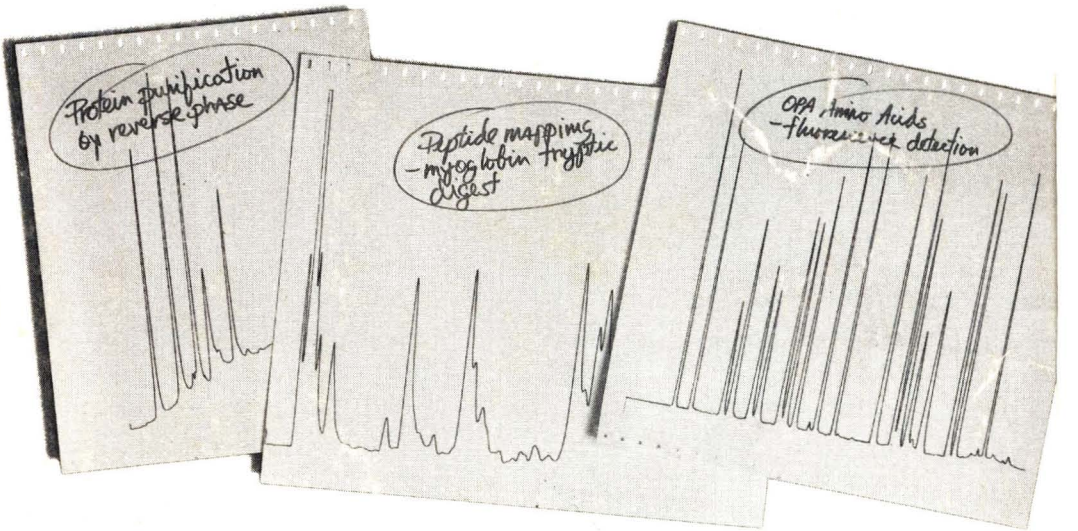

Here are three ways to record success in your biochromatography

Proteins

Isco ProTeam™ LC with proven high-performance macroporous columns offers outstanding speed and flexibility for your protein separations. Choose from a comprehensive selection of columns for SEC, ion exchange, reverse phase, and hydrophobic interaction modes. ProTeam SynChropak columns are available for any separation scale and any molecular size, with a broad range of phases for optimum selectivity. And for added assurance of active protein recovery, Isco ProTeam LC systems are available with fully biocompatible inert construction.

Peptides

For high-resolution peptide mapping by reverse-phase LC, you need precise gradient elution and the right bonded phase for optimum selectivity. ProTeam LC gives you both, with a choice of binary and ternary solvent delivery and packings from C1 to C18. And for sample-limited analyses such as synthetic peptides, you can get the same packings in Isco 2 mm and 1 mm columns.

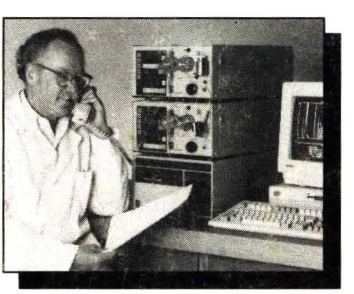

Amino acids

The same ProTeam LC system can also handle your amino acid analyses—in hydrolysates physiological fluids, media, or for sequencing. Modular system design makes it easy to incorporate automated pre-column derivatization. Choose absorbance detection for picomole sensitivity with PITC, dabsyl, or OPA derivatives; or fluorescence for trace analysis with OPA and dansyl derivatives.

Ask today for details.

Isco, Inc., P.O. Box 534
Lincoln NE 68505, U.S.
Tel: **(800)228-425**
Isco Europe AG, Brüschstr.
CH8708 Männedorf, Switzerlar
Fax **(41-1)920 62 0**

ISC

Distributors • **Australia:** Australian Chromatography Co. • **Austria:** INULA • **Belgium:** SA HVL NV • **Canada:** Canberra Packard Canada, Ltd. • **Denmark:** Mikrolab Aarh
Finland: ETEK OY • **France:** Ets. Roucaire, S.A. • **Germany:** Colora Messtechnik GmbH • **Hungary:** Lasis Handelsges. mbH • **Italy:** Analytical Control Italia S.p.A. •
Japan: JSI Co. Ltd. • **Korea:** Sang Chung, Ltd. • **The Netherlands:** Beun-de Ronde B.V. • **Norway:** Dipl. Ing. Houm A.S. • **Spain:** CHEMICONTROL, S.L. •
Sweden: SAVEN AB • **Switzerland:** IG Instrumenten-Gesellschaft AG • **U.K.:** Life Science Laboratories, Ltd. •